



# Durham E-Theses

---

## *The alkali fassalt, andesite association of grenada, lesser antilles.*

Arculus, R. J.

### How to cite:

---

Arculus, R. J. (1973) *The alkali fassalt, andesite association of grenada, lesser antilles.*, Durham theses, Durham University. Available at Durham E-Theses Online: <http://etheses.dur.ac.uk/1310/>

### Use policy

---

The full-text may be used and/or reproduced, and given to third parties in any format or medium, without prior permission or charge, for personal research or study, educational, or not-for-profit purposes provided that:

- a full bibliographic reference is made to the original source
- a [link](#) is made to the metadata record in Durham E-Theses
- the full-text is not changed in any way

The full-text must not be sold in any format or medium without the formal permission of the copyright holders.

Please consult the [full Durham E-Theses policy](#) for further details.

THE ALKALI BASALT, ANDESITE ASSOCIATION  
OF GRENADA,  
LESSER ANTILLES.

Richard John Arculus, B.Sc. (Dunelm)

A thesis submitted for the Degree of Doctor  
of Philosophy in the  
University of Durham

August 1973





**BEST COPY**

**AVAILABLE**

TEXT IN ORIGINAL IS  
CLOSE TO THE EDGE OF  
THE PAGE

**PAGE**

**NUMBERING**

**AS ORIGINAL**

Frontispiece

Concord waterfalls - columnar-jointed transitional  
basalt flow overlying reworked detrital volcanics.







## ABSTRACT

Grenada is the southernmost volcanic island of the Lesser Antilles. A series of volcanic centres ranging from Pliocene to Recent in age are present overlying a folded Lower to Middle Tertiary volcano-sedimentary formation. Eruptions of silica-undersaturated alkali basalt and picrite magmas have occurred repeatedly during the evolution of these centres. Calc-alkaline andesites and dacites show a close field association with the basalts and picrites. Recent activity on the island has been explosive in nature.

A model of variable volumes of Upper Mantle partial melting is proposed to account for the diversity of major, trace and Rare Earth element compositions and strontium isotope ratios of the basalts and picrites. Geochemical, petrographic and mineralogical criteria suggest that the andesites and dacites are related to these basic melts by fractional crystallisation processes. In addition the chemical compositions and strontium isotope ratios of the andesites and dacites reflect the diverse compositions of the parental basalt magmas.

The petrography and mineralogy of the andesites and dacites is similar to calc-alkaline suites elsewhere in the arc. Some of the basalts and picrites contain abundant olivine and sector and oscillatory zoned clinopyroxene phenocrysts. In some basalts, phenocryst amphibole is present.

An origin by partial melting of an Upper Mantle peridotite source is proposed. Alternative sources are examined but partial

melting of a subducted lithospheric plate does not appear to be a significant petrogenetic process in Grenada.

Fractional crystallisation of olivine, clinopyroxene and spinel is mainly responsible for the development of a normal calc-alkaline trend towards increasing silica-saturation in the magmas. Subsequent crystallisation of plagioclase feldspar and then amphibole is also important in the development of a trend towards silica- rather than alkali-enrichment in the residual melts.

The significant feature of the Grenada volcanicity is the occurrence within a restricted geographic range of magmas of contrasted geochemical characteristics. The local volcanic and tectonic history of the southern part of the Lesser Antilles island arc are probably the most important factors in the development of these unusual characteristics.

## ACKNOWLEDGEMENTS

The author gratefully acknowledges the award of an N.E.R.C. Research Studentship and opportunity to participate in a research project in the Lesser Antilles. Research facilities in the University of Durham were made available by Professor M.H.P. Bott.

I am grateful to Dr. H. Sigurdsson and Dr. J.F. Tomblin for their guidance and introduction to Caribbean field relationships and stimulating discussion and hospitality. Mr. and Mrs. A. Dann were also a source of support and assistance in the field. I am particularly grateful for the support and encouragement of my supervisor Professor G.M. Brown. In addition I have benefitted from discussions with the staff and fellow research students of Durham, Edinburgh and Oxford Universities and especially Mr. E.B. Curran, Mr. G.C. Cawthorn, Dr. R.K. O'Nions, Mr. R. Powell and Mr. K.J.A. Wills.

Advice on the use of X-ray fluorescence, electron microprobe equipment and computer programs was received from Mr. E.B. Curran, Dr. J.G. Fitton, Dr. R.C.O. Gill, Dr. J.G. Holland, Mr. J.L. Knight, Dr. A. Peckett and Dr. D. Stephenson.

Thin sections and probe slides were prepared by Mr. L. MacGregor and Mr. G. Randall. Mr. G. Dresser made the necessary photo-reductions of text-figures and printed many of the plates. Mrs. C.L. Mines patiently typed the manuscript.

Finally I would like to thank my wife Patricia, for her encouragement and considerable aid in completing this study.



## CONTENTS

	<u>Page</u>
ABSTRACT	i
ACKNOWLEDGEMENTS	iii
CONTENTS	v
TEXT FIGURES	ix
TABLES IN THE TEXT	xiii
PLATES	xvii
<hr/>	
INTRODUCTION	1
1. THE DURHAM DEPARTMENT OF GEOLOGICAL SCIENCES RESEARCH PROGRAM IN THE WEST INDIES.	3
2. REGIONAL SETTING OF THE LESSER ANTILLES ISLAND ARC.	5
3. GRENADA - GENERAL BACKGROUND	13
4. GRENADA - GEOLOGICAL BACKGROUND	
4:1 Previous work	14
4:2 Volcanic activity	15
4:3 Physiography and bathymetry	15
4:4 Geophysical investigations	20
5. THE GEOLOGICAL HISTORY OF GRENADA - I.	
5:1 Notes on mapping and nomenclature of field units.	23
5:2 Primary rock units.	24
5:2:1 Lava flows and domes	24
5:2:2 Fragmental deposits	26
5:3 Secondary rock units	27
5:4 Discussion of the geological map.	28
6. THE GEOLOGICAL HISTORY OF GRENADA - II	
6:1 Eocene to Miocene	32
6:2 The Northern Domes centre	39
6:3 Southwest Grenada	43
6:4 The South East Mountain centre	49
6:5 Sinai-Mt.Maitland-Mt.Moritz centre	50
6:6 Mt. Granby - Fedon's Camp centre	56
6:6:1 Introduction	56
6:6:2 Details of field exposures	58
6:6:3 Volcanic history	60
6:7 Mt. St. Catherine centre	65
6:7:1 General features of the centre	65
6:7:2 Volcanic history of the centre	71
6:8 Explosion craters	73
6:9 Summary of Grenada vulcanicity	81

	<u>Page</u>
7. GEOCHEMISTRY I	
CLASSIFICATION OF VOLCANIC ROCK SERIES AND THE PICRITES AND BASALTS OF GRENADA.	
7:1 Classification of calc-alkali rock series.	84
7:2 Classification of the Grenada rock series; General Aspects.	88
7:2:1 Calc-Alkaline vs Tholeiitic suites	88
7:2:2 Alkaline vs Tholeiitic basalt	90
7:2:3 High-Alumina vs Tholeiitic basalt.	90
7:3 Classification of the Grenada calc- alkaline series.	96
7:4 The Geochemistry of the Grenada Picrites and Basalts	98
7:4:1 Crystal fractionation	99
7:4:2 Wall-Rock alteration	107
7:4:3 Cumulus enrichment of mineral phases	107
7:4:4 Varying degrees of partial melting	111
7:5 $\text{Sr}^{87}/_{86}$ ratios of the Grenada Calc- Alkaline suite.	118
7:5:1 Isotope equilibration	120
7:5:2 Melts of different Parental Material.	122
7:5:3 Differences imposed at Melting Source.	122
7:6 Notes on the presentation of the Grenada Geochemical Data.	125
8. GEOCHEMISTRY II	
THE BASALT-ANDESITE-DACITE ASSOCIATION OF GRENADA	
8:1 Major oxide variation	127
8:2 Fractional crystallization and trace element variation	130
8:3 Rare Earth element distribtuion and $\text{Sr}^{87}/_{86}$ ratios.	148
8:4 General Geochemical features of the Grenada Calc-Alkaline rock suite.	152
8:5 Discussion.	155
9. THE PETROGRAPHY AND MINERALOGY OF THE GRENADA ROCK SUITE.	
9:1 Introduction	156
9:2 The Picrites and Basalts	156
9:2:1 Inclusions in the Basalts	171
9:2:2 Quartz Xenocrysts	174
9:2:3 Olivine alteration	176
9:2:4 Amphibole phenocrysts in the Basalts	178
9:3 The Andesites and Dacites	185
9:3:1 Variation in texture	188
9:3:2 Mineralogical Distinction between volcanic series.	198

	<u>Page</u>
9:4 The Cumulus Plutonic Blocks of Grenada	204
9:5 Mineralogical variation in the Grenada Rock Series.	208
9:5:1 Olivine	211
9:5:2 Pyroxene	211
9:5:3 The sector and oscillatory zoned clinopyroxenes	223
9:5:4 Feldspars	232
9:5:5 Amphiboles	234
9:5:6 Oxides	240
9:5:7 Minor constituents	242
9:5:8 Summary	243
 10. PETROGENETIC RELATIONSHIPS AMONGST GRENADA MAGMAS	
10:1 Introduction	244
10:2 Island arc tectonics	246
10:2:1 Dehydration of the subducted plate	249
10:2:2 Juvenile water within the Upper Mantle	257
10:2:3 Water in the crust	258
10:3 The origin of the undersaturated magmas of Grenada	260
10:3:1 Partial melting of the subducted lithospheric plate	260
10:4 Composition of the Upper Mantle	262
10:5 Partial melting of the Upper Mantle	266
10:5:1 Dry partial melting	266
10:5:2 Wet partial melting	267
10:6 Evolution of primary melts	273
10:7 Mineral Stability Relationships in Basaltic Melts	283
10:8 Compositional variation in the Basalt-Andesite-Dacite sequence	299
10:9 Discussion	307
 11. MAGMA VARIATION IN ISLAND ARCS	309
 REFERENCES	320
 APPENDIX I	
WHOLE-ROCK ANALYSIS BY X-RAY FLUORESCENCE	
I:1 Sample Preparation	332
I:2 Major Element Analysis	333
I:3 Trace Element Analysis	334
I:4 Whole Rock Analysis	335
 APPENDIX II	
ELECTRON MICROPROBE MINERAL ANALYSIS	
II:1 Techniques and analytical conditions	341
II:1:1 Nepheline Reconnaissance method	345
II:2 Mineral Analyses	347
II:3 X-ray Powder Diffraction Analysis	347

	<u>Page</u>
APPENDIX III	
THE POSSIBILITY OF FURTHER ERUPTIONS ON GRENADA	349



## TEXT FIGURES

	<u>Page</u>
1. Map of the Lesser Antilles island arc.	2
2. Bathymetry of the Eastern Caribbean region.	4
3. Comparison of the velocity structure of Caribbean basins and ridges with those of continents and ocean basins.	6
4. Plate tectonic map of the Middle Americas region.	7
5. Location of possible axes of volcanic activity and of the maximum negative gravity anomaly.	9
6. Cross section perpendicular to the southern Lesser Antilles showing focii of larger earthquakes.	11
7. Bathymetric map of Kick-em-Jenny volcano.	16
8. Surface Geology of Grenada.	17
9. Submarine bathymetry of the southern Lesser Antilles.	19
10. Bouguer Anomaly Map of Grenada.	21
11. A comparison of class divisions used in the present study with those proposed by Robson and Tomblin (1966).	24
12. Locality map of age dated (K-Ar) Grenadan volcanic rocks.	29
13. Lower and Middle Tertiary outcrops of Grenada.	33
14. Outcrop and locality map of northern Grenada.	38
15. Outcrop and locality map of southern Grenada.	45
16. Hot spring localities in northern Grenada.	66
17. Locality map of explosion craters.	74
18. A-F-M diagram for the Mt. Granby - Fedon's Camp volcanic suite.	89

	<u>Page</u>
19. Alkalis-silica plot of Grenada picrites and basalts.	91
20. Plot of weight % $Al_2O_3$ v normative plagioclase content <sup>2</sup> <sub>3</sub> of selected picrite and basalt compositions.	93
21. Normative compositions of selected picrites and basalts projected in Ne-Di-Hy-Ol and Ne-Ol-Hy-Ab diagrams.	94 95
22. Plot of Ce/Y and Rb v Ni of some Grenadan basalts containing less than 48 weight % $SiO_2$ .	100
23. Logarithmic plot of Rayleigh curves for fractional crystallization.	103
24. Experimentally determined silicate phase relationships in the Grenada rock suite.	110
25. Variations in partial melt composition and enrichment factors of incompatible elements as a result of melting of a garnet.	112
26. Rare Earth element distribution in basalts 239 and 476.	117
27. Major oxide variation of the Grenadan rock suite.	128- 129
28a. Major and trace element variations in the Mt. Granby - Fedon's Camp volcanic centre.	132- 135
28b. Major and trace element variations in the Mt. St. Catherine volcanic centre.	136- 139
29. Plot of Sr/Ni v weight % $SiO_2$	141
30a. Projections of normative compositions of the Mt. Granby - Fedon's Camp centre.	142
30b. Projections of normative compositions of the Mt. St. Catherine centre.	143
31. Rare Earth element distribution in andesites 67 and 381, and dacite 214.	149
32. Plot of Ce/Y v weight % $SiO_2$ for Mt. Granby-Fedon's Camp centre.	150
33a. Al/Si relationships in picrite clinopyroxene microphenocrysts.	162

	<u>Page</u>
33b. Al/Ti relationships in picrite clinopyroxene microphenocrysts.	163
34. Comparison of Grenada and St. Vincent cumulus ferromagnesian minerals.	210
35. Mineral variation in the Grenada calc-alkaline rock suite.	212
36. Trends of pyroxene crystallization in the system $\text{CaMgSi}_2\text{O}_6$ (Di)- $\text{CaFeSi}_2\text{O}_6$ (Hed)- $\text{MgSiO}_3$ (En)- $\text{FeSiO}_3$ (Fs).	214
37. Pyroxene compositional in the Grenada calc-alkaline suite.	216
38. $\text{SiO}_2$ v $\text{Al}_2\text{O}_3$ plot of the Grenadan clinopyroxenes.	218
39a. Al/Ti relationships in an oscillatory zoned clinopyroxene phenocryst in transitional basalt 479.	220
39b. Al/Si relationships in an oscillatory zoned clinopyroxene phenocryst in transitional basalt 479.	221
40. Oscillatory and sector zoned clinopyroxenes.	226
41. Al(IV) v A-site occupancy in amphiboles.	239
42. Model of upper 700 km of the Earth showing possible relative motions of lithosphere.	248
43. Model of the structure of oceanic crust generated at mid-ocean ridges.	250
44a. Thermal model for the mantle in a subduction region.	254
44b. Maximum depths to which hydrous materials can be carried in a subduction region.	254
45. Relationship of volcanic front, subducted plate and predicted stability limits of hydrous minerals in an island arc environment.	256
46. Pressure-temperature projection of curves representing the beginning of melting of vapour saturated basalt-water and basalt-water-carbon dioxide ( $P_{\text{H}_2\text{O}} = 0.5 P_{\text{tot}}$ ) compositions.	



	<u>Page</u>
47. Upper Mantle mineralogical stability fields.	265
48. Summary diagrams of basalt fractionation relationships.	268- 269
49. The forsterite-orthopyroxene liquidus boundaries in the system forsterite-nepheline-CaAl <sub>2</sub> SiO <sub>6</sub> -silica-H <sub>2</sub> O at 20 kb under water saturated and dry conditions.	271
50. Pressure-temperature diagram for a lhezolite nodule in the presence of excess water.	267
51. Phase boundary shifts with pressure variation in the C.M.A.S. system.	277
52. Mineral compositional control during the early evolution of the Grenada rock suite.	280
53. H <sub>2</sub> O-saturated melting relations in an olivine tholeiite.	284
54. Pressure-temperature projection of phase stability limits for an anhydrous tholeiitic composition.	285
55. Solubility of water as a function of $P_{H_2O}$ in basalt and andesite melts at 1100°C.	287
56. Pressure-temperature projection of phase stability limits for olivine tholeiite under conditions of $P_{H_2O} = 0.6 P_{tot}$ .	289
57. $T - X_{H_2O}^{fl}$ isobaric projections for pargasite melting relationships.	290
58. Log $f_{O_2}$ - Temperature diagram.	296
59. Plot of Rb/Sr v SiO <sub>2</sub> and K <sub>2</sub> O (wt.%) v Rb (ppm).	303

#### APPENDIX FIGURES

<u>I:1</u> Variation of normative nepheline with increasing oxidation state in the Grenadan picrites and basalts.	336
---	-----



TABLES IN THE TEXT

	<u>Page</u>
1. Classification of pyroclast material.	25
2. Probable order of activity of the volcanic centres of Grenada.	31
3. Recorded temperatures of Hot Springs in Grenada.	67
4. Chemical composition of 'primary' magma types in Japan.	87
5. Major and trace element analyses of selected Grenadan picrites and basalts	97
6. Major and trace element analyses of a picrite and basalts used in the experimental study by Cawthorn <u>et al.</u> (1973) together with a petrographic summary.	109
7. Major analyses of alkali basalts 476 and 239.	115
8. Strontium isotope results for basalts, andesites and a dacite of the Grenada calc-alkaline rock suite, together with major and trace element analyses of the basalts.	119
9. Strontium isotope data for a basanite of southeastern California and individual minerals of a lherzolite inclusion.	121
10. Major and trace element analyses of andesites 67 and 381 and dacite 214.	147
11. Composition of bulk rock and micro-phenocryst minerals of picrite 483.	159
12. Major and trace element analyses of transitional basalts 375 and 468.	165
13. Partial analyses of an olivine, a clinopyroxene and a magnetite phenocryst in transitional basalts 375 and 468.	166
14. Major and trace element analysis of transitional basalt 454 together with estimated modal mineralogy.	168
15. Analysis of phenocryst minerals in transitional basalt 454.	170

	<u>Page</u>
16. Analyses of selected quartz bearing, alkali and transitional basalts, illustrating range of trace element abundances.	175
17. Major and trace element analysis of Kick-em-Jenny basalt (KJO17) together with estimated modal mineralogy.	179
18. Partial analyses of phenocryst minerals in Kick-em-Jenny alkali basalt (KJO17).	180
19. Partial analyses of naturally occurring pargasite in Grenada transitional basalt 40, and amphiboles produced in experiments with natural Grenada compositions ( $P_{H_2O} = P_{tot} = 5 \text{ kb}$ ).	183
20. Analyses of coexisting ferromagnesian minerals in Grenada transitional basalt 40 together with whole rock analysis.	184
21. Major and trace element analysis of dacite 462 together with selected partial analyses of constituent minerals of separate zones.	187
22. Major and trace element analyses of separated zones of contrasted texture in Grenada andesites and dacites.	191
23. Major and trace element analysis of andesite 218 (porphyritic zone only) together with selected partial analyses of constituent minerals of separate zones in the andesite.	194
24. Major and trace element analyses of andesites 337 and 410 together with estimated modal mineralogy.	197
25. Analyses of phenocryst ferromagnesian minerals in andesites 337 and 410.	199
26. Major and trace element analysis of andesite 307 with estimated modal mineralogy.	201
27. Partial analyses of phenocryst ferromagnesian minerals in andesite 307.	203

	<u>Page</u>
28. Major and trace element analyses of Grenada cumulus blocks together with estimated modal mineralogy.	207
29. Partial analyses of cumulus minerals in block x245.	200
30. Partial analyses of several zones of an oscillatory zoned clinopyroxene in transitional basalt 479.	227
31. Analyses of several zones of an oscillatory zoned plagioclase feldspar in dacite 462.	233
32. Partial analyses of oscillatory zoned pargasite phenocryst in andesite 355.	237
33. Partial analyses of oscillatory zoned pargasite phenocryst in dacite 335.	241
34. Velocity structure of the oceanic crust.	251
35. Comparison of oceanic tholeiite and oceanic alkali basalts with a Grenada picrite and alkali basalts.	252
36. Average simple and compound phenocryst/matrix coefficients for Sr, K, Rb and Ba.	301
37. Strontium isotope data for three volcanic centres in the Lesser Antilles island arc.	315.

#### TABLES IN THE APPENDICES

<u>I:1</u> Duplicate X-ray Fluorescence major element analyses.	337
<u>I:2</u> 1971 X-ray Fluorescence major and trace element analyses	338
<u>I:3</u> 1973 X-ray Fluorescence major and trace element analyses	339
<u>I:4</u> List of analysed specimens and their locality.	J

	<u>Page</u>
<u>II:1</u> Optimum analysing conditions and standards used for electron microprobe analysis.	342
<u>II:2</u> Electron microprobe detection limits.	344
<u>II:3</u> Comparison of Na-bearing minerals and picrite groundmass points.	346
<u>II:4</u> Mineral analyses.	348



## PLATES

### Page

#### Frontispiece   Concord Waterfalls

1. Folded and faulted Tufton Hall Formation near Palmiste. 34
2. Neptunian dyke of angular igneous rock fragments in the Tufton Hall Formation, Irvins Bay. 34
3. Folded dyke of clinopyroxene-phyric basalt in south-westerly dipping Tufton Hall Formation, Levera Bay. 35
4. Unfolded clinopyroxene-phyric basalt dyke cutting a south-westerly dipping sequence of Tufton Hall Formation shales and silts, Grenada Bay. 35
5. Breccia of andesite domes fragments and Tufton Hall Formation, northwest of Helvellyn dome. 42
6. Massively jointed andesite forming the dome of Helvellyn. 42
7. Levera Island andesite dome. 44
8. Spheroidally weathered and columnar-jointed clinopyroxene-phyric lava flow, Grand Anse. 44
9. Prickly Point basalt plug overlain by secondary fragmental deposits. 46
10. Cumulus-block bearing conglomerates and gravels unconformably overlying finer reworked volcanics at Prickly Point. 46
11. Channelling and current bedding in reworked volcanics, near Hope Vale, Southwest Grenada. 48
12. Large scale current bedding in reworked volcanic deposits, Canoe Bay. 48
13. Columnar-jointed ultrabasic lava-flow, Mt. Gay. 51

	<u>Page</u>
14. Northern scarp face of Sinai-Mt. Maitland from Richmond.	51
15. The Southern Annandale Falls formed of southerly dipping Tufton Hall Formation.	53
16. Indurated reworked volcanics at Snug Corner, west of Annandale Falls.	53
17. Sheared and jointed clinopyroxene-phyric lava flows, Flamingo Bay.	54
18. Current-bedded reworked volcanics, Dothan.	57
19. Andesitic and basaltic air-fall material, Dothan.	57
20. Steeply dipping clinopyroxene-phyric lava flows overlying autobrecciated material, Concord.	59
21. Massive andesite flow, 60 m thick, near Richmond.	59
22. The Grand Roy valley. Massive andesite flows cap the ridges and overlie scarp-forming basalt lava flows.	61
23. The andesite dome forming the summit of Fedon's Camp.	63
24. Panorama of Mt. St. Catherine from South East Mountain	64
25. Slump features in clay grade, plant-bearing, reworked volcanic deposits, Belmont.	69
26. Mud-flow deposits on the western summit scarp of Mt. St. Catherine.	69
27. Interior of Lake Antoine explosion crater.	72
28. The Queen's Park explosion craters.	77
29. Alkali basalt homb, High Cliff Point.	77
30. Ash scoria, High Cliff Point.	78
31. Contorted ash beds, High Cliff Point.	78
32. Horizontal calcite sheets containing worm casts interleaved with volcanic ash and scoria, High Cliff.	80

	<u>Page</u>
33. Photomicrograph of picrite 483, a loose block in the upper Concord Valley.	158
34. Photomicrograph of transitional basalts 375 and 468.	164
35. Photomicrograph of transitional basalt 454.	167
36. Stained forsteritic olivine phenocryst in transitional basalt 468.	172
37. Quartz xenocryst in alkali basalt 33.	173
38. Photomicrograph of alkali-basalt scoria, Kick-em-Jenny volcano.	177
39. Photomicrograph of twin-textured dacite 462.	186
40. Photomicrograph of andesite 212.	189
41. Photomicrograph of twin-textured andesite 218.	193
42. Photomicrographs of andesites 337 and 410.	196
43. Photomicrograph of andesite 307.	200
44. Photomicrograph of clinopyroxene-plagioclase-magnetite-amphibole cumulus block 521.	205
45. Photomicrograph of transitional basalt 479.	222
46. Photomicrograph of oscillatory and sector-zoned clinopyroxene phenocrysts in transitional basalt 479.	224
47. Photomicrograph of andesite 355.	236

\*Footnote: The length of the hammer used as a measure of scale in the field photographs is 80 cms.

## INTRODUCTION

The island of Grenada is the southernmost volcanic island of the Lesser Antilles island arc (Fig.1). This study is based on the results of two field seasons spent on the island comprising a total of 20 weeks during 1971 and 1972. Reconnaissance-style mapping of the separate volcanic centres and a synthesis of the volcanic history of the island was completed. Rocks dated by K-Ar methods by Dr. J. Briden and Dr. D. Rex (Leeds University) (Fig.12 ) were used to determine the absolute ages of some of these centres.

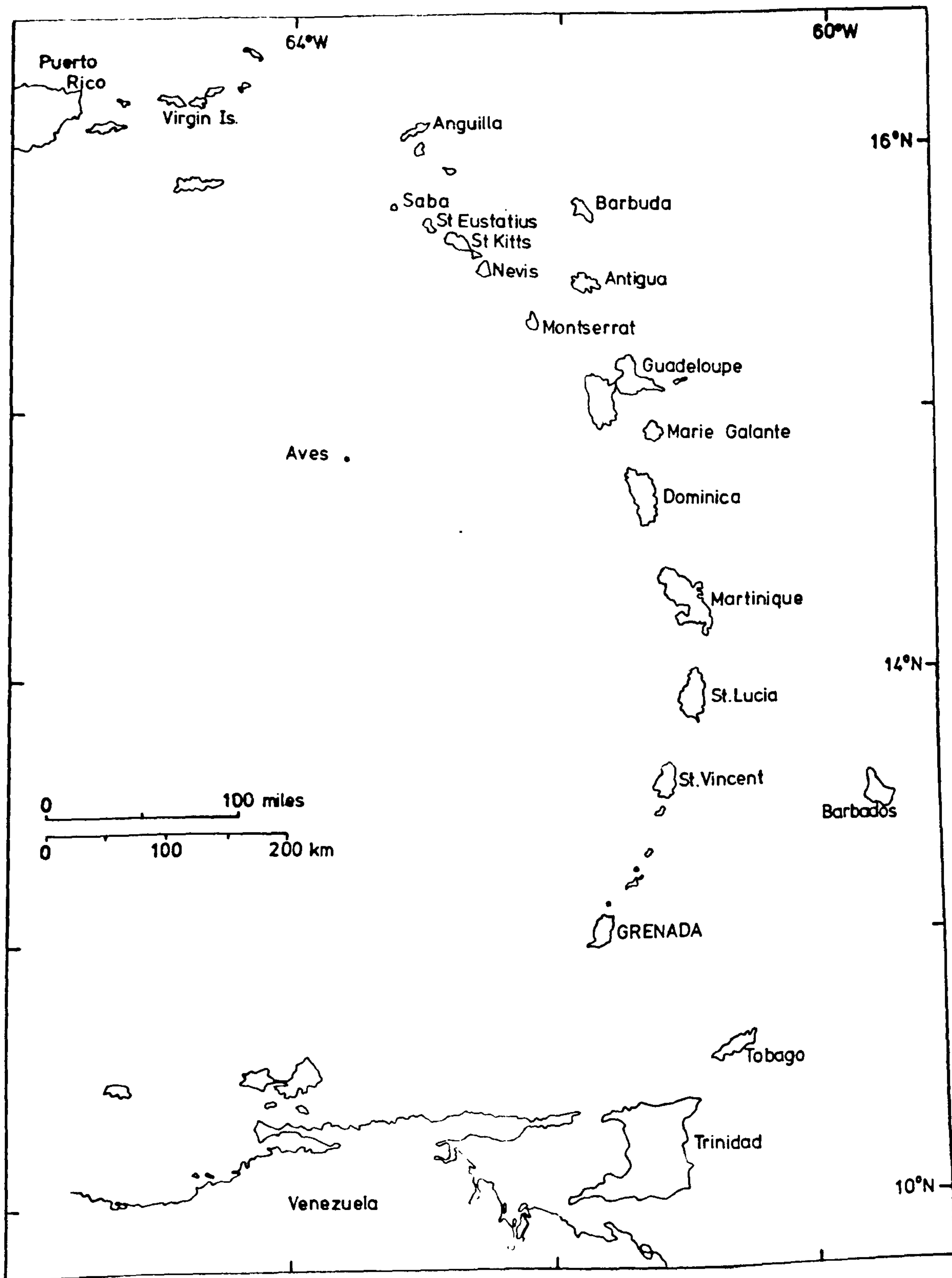
Laboratory study of the samples was carried out mainly at Durham University. Some experimental studies were completed at the Grant Institute of Geology, Edinburgh (Cawthorn et al., 1973). Rare Earth element and strontium isotope ratios were determined at the Department of Geology and Mineralogy, Oxford University (O'Nions et al. in MS).





Fig.1

Map of the Lesser Antilles island arc.  
(After Robson and Tomblin, 1966).



## CHAPTER 1

### THE DURHAM DEPARTMENT OF GEOLOGICAL SCIENCES RESEARCH PROGRAM

#### IN THE WEST INDIES

A program of research into the problems of island arc volcanology, petrology and geochemistry was initiated in 1960 by the late Professor L.R. Wager and Dr. G.M. Brown of Oxford University together with Dr. G.R. Robson of the Seismic Research Unit, University of West Indies, Trinidad.

Regional Studies of St. Kitts (Baker, 1963), St. Lucia (Tomblin, 1964) and Montserrat (Rea, 1970) were carried out by research students at Oxford together with a petrological and mineralogical examination of the plutonic blocks of the Soufriere volcano (St. Vincent) by Lewis (1964).

The program of research has continued under the leadership of Professor G.M. Brown at Durham University where this study of the volcanic geology of Grenada has been completed. In addition, Mr. E.B. Curran has studied aspects of the ferromagnesian mineral assemblages of St. Kitts, Montserrat, St. Lucia and St. Vincent and Mr. K.J.A. Wills has completed a regional study of southern Dominica, and is currently engaged in an inter-island comparison of the plutonic blocks.

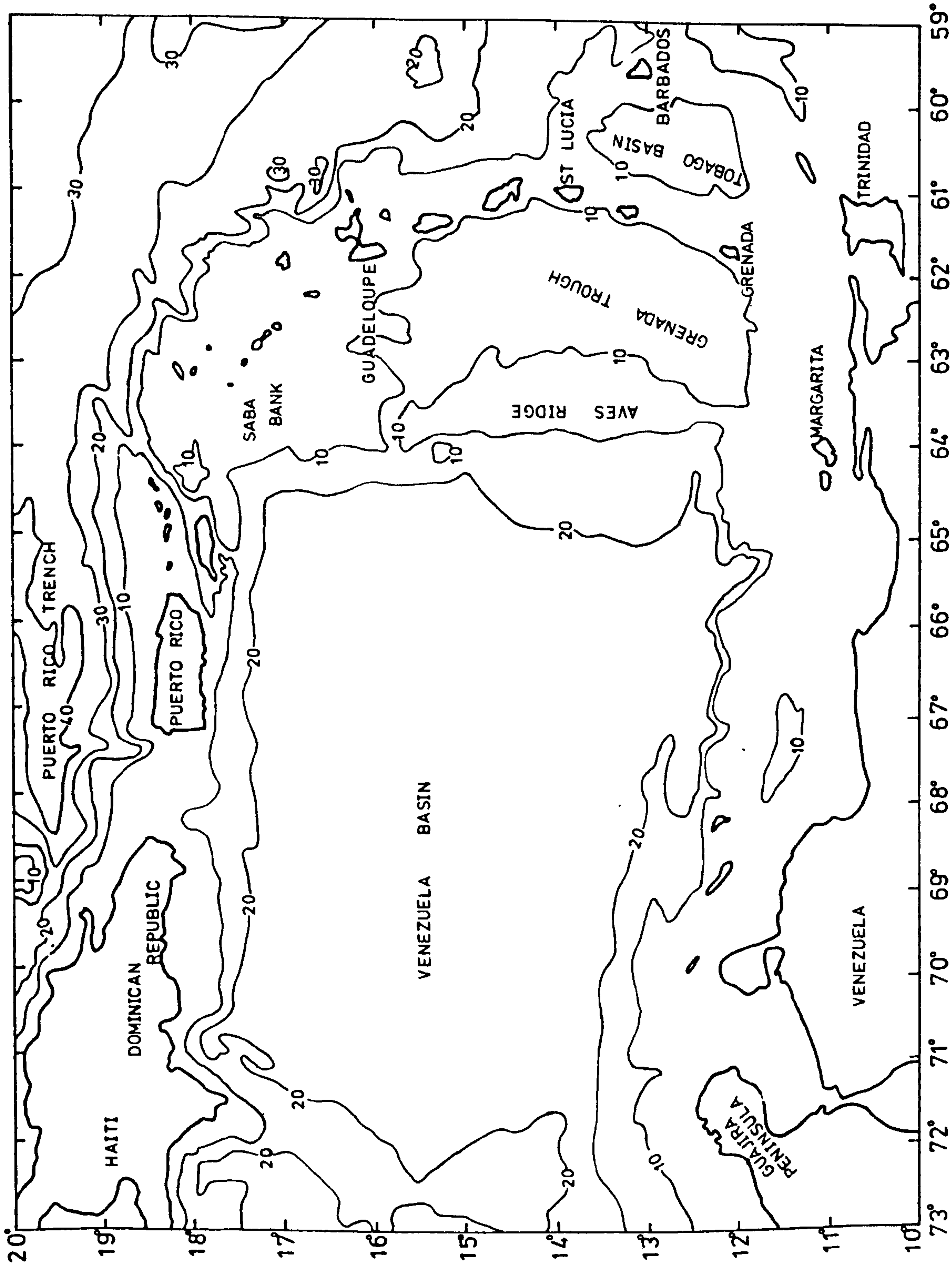
A program of geophysical research in the Eastern Caribbean is in progress under Professor M.H.P. Bott (Department of Geological Sciences, Durham) and the results of these studies combined with data obtained by geological investigations of the islands of the Lesser Antilles may hopefully lead to an integrated analysis of the evolution of the island arc.

Fig.2

Bathymetry of the Eastern Caribbean region.

(After Hess, 1966).

Submarine contour interval every 1000 fathoms





## CHAPTER 2

### REGIONAL SETTING OF THE LESSER ANTILLES ISLAND ARC

The Lesser Antilles island arc forms an arcuate ridge separating the Caribbean Sea to the west from the Atlantic Ocean on the east. The main features of the submarine bathymetry are shown in Fig. 2 and the division of the Caribbean into a series of ridges and basins can be seen. The overall crustal structure is atypical of normal oceanic crust but comparable to that found in many areas of the western Pacific (Edgar et al., 1971). In general the crust is thicker with additional layers of intermediate velocity in comparison with oceanic crust (Fig. 3 ).

The theory of plate tectonics (Isacks et al., 1968) suggests that the Caribbean forms an isolated lithospheric plate between the Americas, Cocos and Nazca Plates (Fig. 4 ). Seismic evidence suggests that different types of structural boundary form the margins of the Caribbean Plate (Molnar and Sykes, 1969; Tomblin, 1971). Along the northern margin (Cayman Trough - Puerto Rico Trench) there is transform faulting. Active underthrusting of the Cocos Plate beneath the Middle America arc and the Americas Plate beneath the Lesser Antilles arc forms the western and eastern boundaries respectively. The relationship of the Caribbean and Americas Plates along the southern margin is more complex. Alternative models of temporary absence of movement and hinge faulting have been proposed (Ball et al., 1969; Molnar and Sykes, 1969; Ball and Harrison, 1970; Tomblin, 1971).

The volcanic ridge of the Lesser Antilles extends northwards

Fig.3

Comparison of the velocity structure of Caribbean basins and ridges with those of continents and ocean basins.

(After Edgar et al. 1971).

(p-wave velocities)

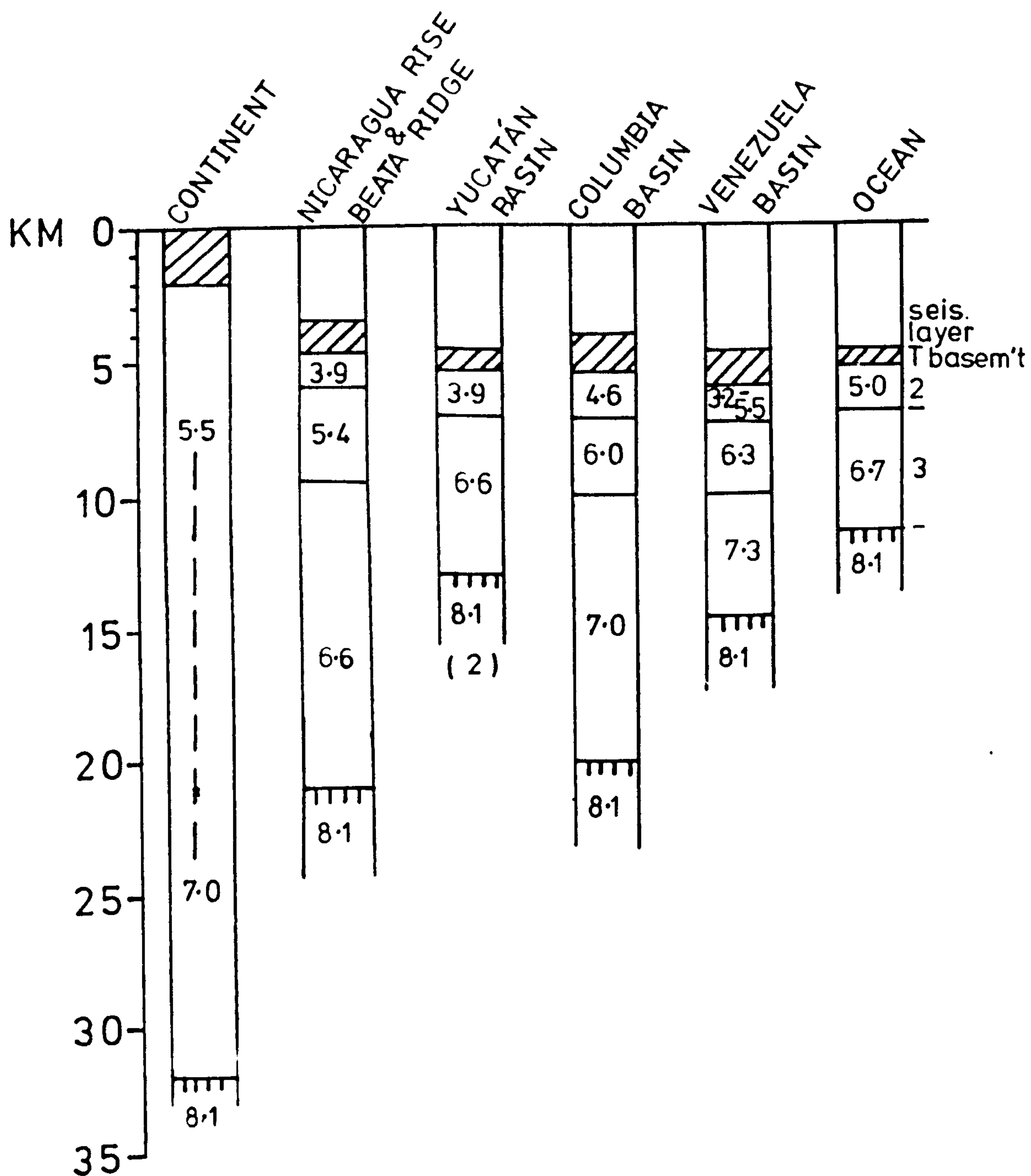
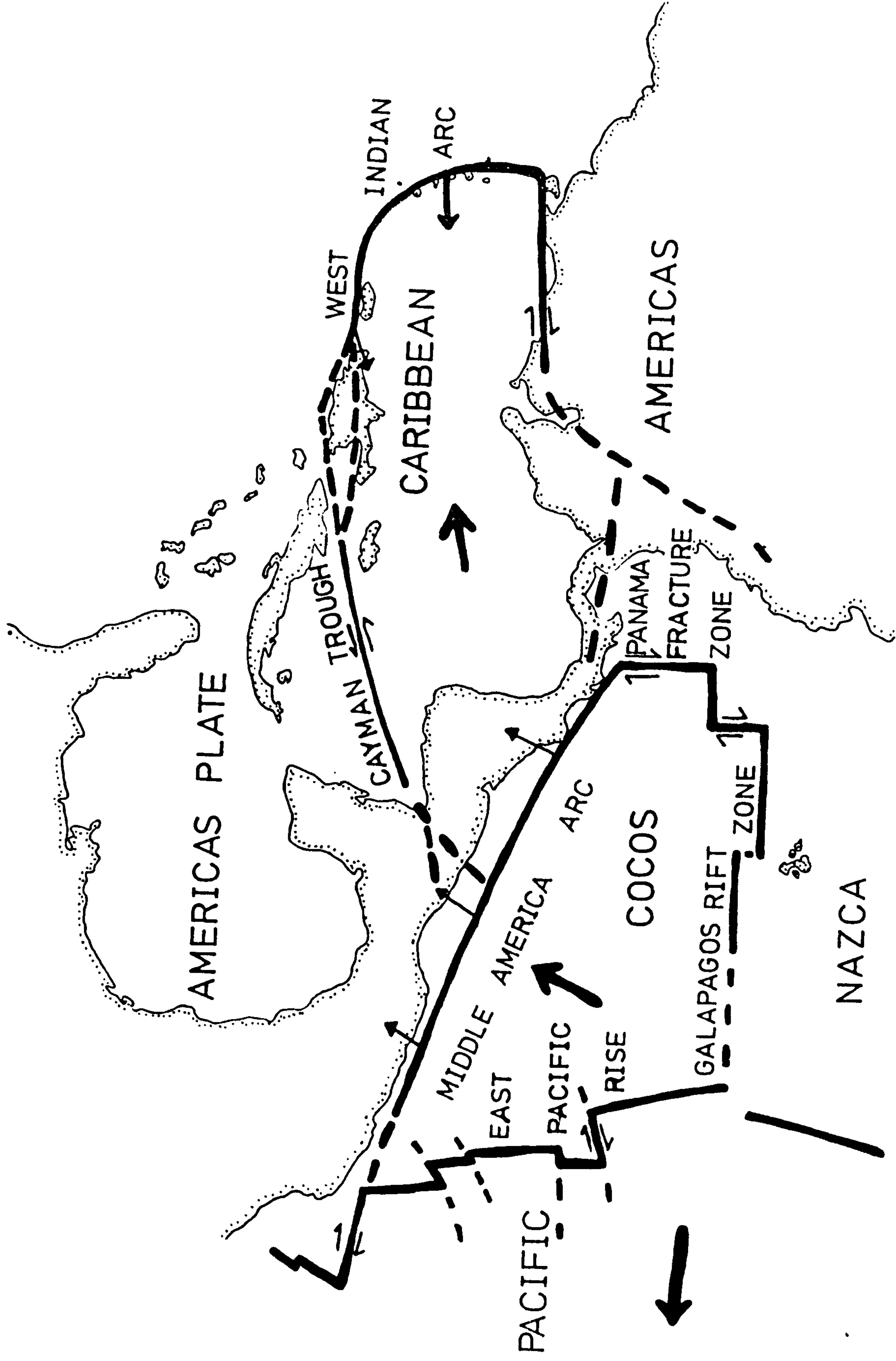




Fig.4

Plate tectonic map of the Middle Americas region.  
(After Molnar and Sykes, 1969).

Bold arrows show direction of motion of the plates relative to the Americas Plate. Fine arrows show possible direction of relative plate motion at boundaries.

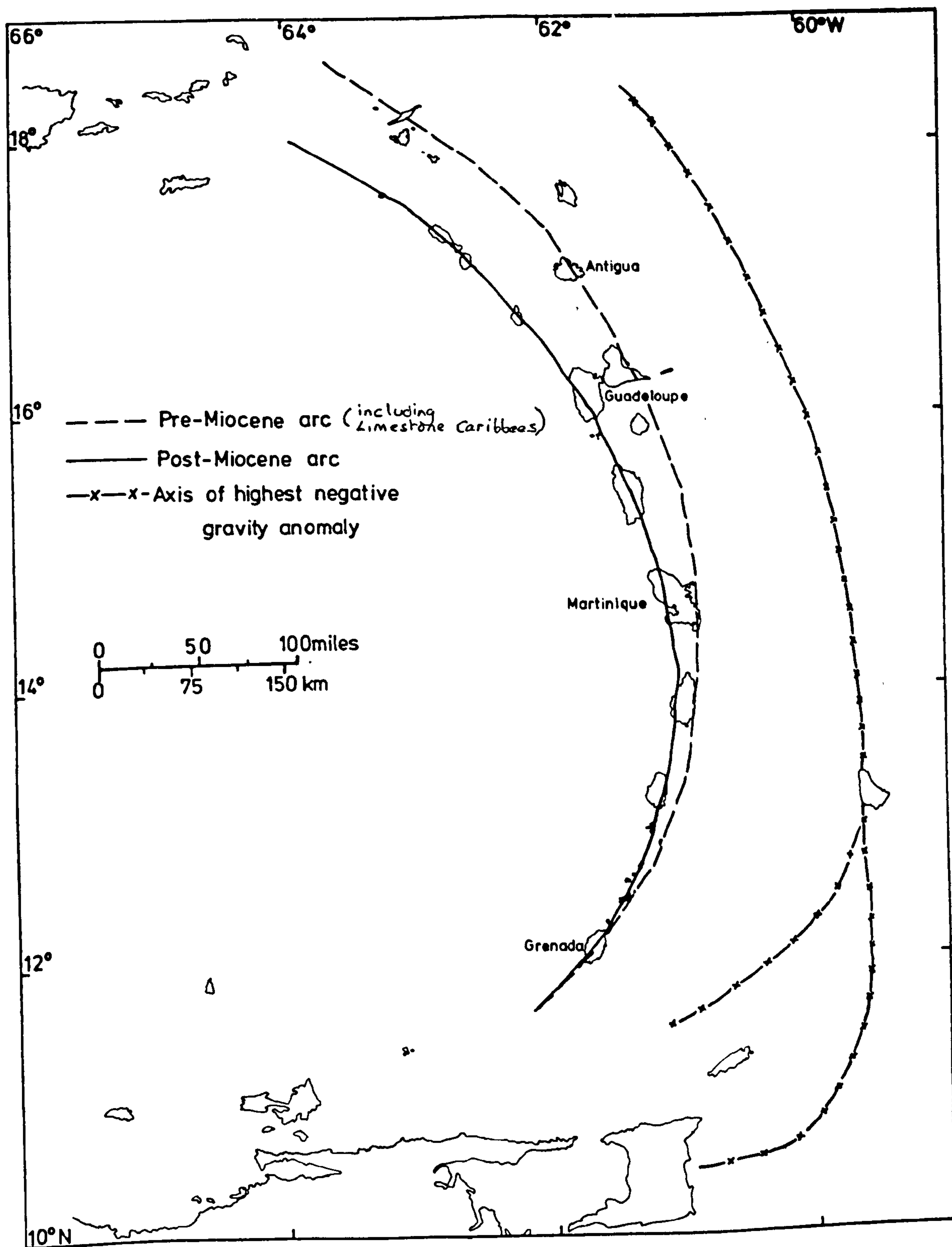


from the continental slope of South America to the Anegada Trough. West of the arc, a depth of 3300 m is attained in the Grenada Trough which is isolated from the Venezuela Basin by the north-south striking Aves Ridge. One of the characteristic features of island arcs, a deep frontal trench, is only present east of the northern half of the Lesser Antilles. However, the belt of negative gravity anomaly associated with the Puerto Rico Trench continues southwards along the deformed sediments of the Barbados Ridge (Chase and Bunce, 1969) before bifurcating nearer the South American continent (Fig. 5 ). Major submarine features (scarps and troughs) transverse to the axis of the Lesser Antilles have been recognised. Fink (1972) has suggested that transverse faulting north of Dominica has taken place and Westbrook (Ph.D. thesis, Durham, in prep'n) has recognised a transverse tectonic lineament east of St. Lucia on the basis of bathymetric, gravity and magnetic evidence. It is suggested that some differential movement of segments of the arc may have taken place (Fink, 1972).

The Lesser Antilles have been divided into the Limestone and Volcanic Caribbees on the basis of the prominent surface rock exposure in the islands north of Dominica (e.g. Martin-Kaye, 1969). The exposed basement of the Limestone Caribbees is formed of Lower Tertiary (Eocene to Oligocene) calc-alkaline volcanics (Christman, 1953; Martin-Kaye, 1969). Erosion, truncation and late Oligocene-early Miocene transgression followed with deposition of a thin sequence of shallow-water marine facies units. In the late Miocene, this part of the arc was uplifted with minor faulting and folding.

Fig.5

Location of possible axes of volcanic activity (after Martin-Kaye, 1969) and of the maximum negative gravity anomaly (after Sigurdsson et al., 1973).





In the Volcanic Caribbees to the south of and including Dominica, late Miocene to Recent calc-alkaline volcanics are exposed. At the southern end of the arc in Grenada and the Grenadines, the Lower Tertiary history appears to be similar to the Limestone Caribbees (Martin-Kaye, 1969). However, in the Volcanic Caribbees north of Dominica, only the Late Miocene to Recent volcanism appears to be present. Thus, in general two major periods of vulcanicity appear to have formed the Lesser Antilles island arc. The axis of the Miocene to Recent activity appears to have migrated westwards in the north but in the south the centres of Tertiary and Quaternary volcanism appear to coincide (Fig. 5 ). The periods of volcanic activity may be related to the major changes occurring in the spreading rate of the Mid-Atlantic Ridge and resultant changes in relative velocity of collision of the Caribbean and Americas Plates (Vogt et al., 1969). Thus the Lesser Antilles appear to be predominantly of Tertiary origin, but the discovery of a late Jurassic (142 m.y.) volcanic sequence on Desirade, east of Guadeloupe (Fink, 1968) may indicate structural continuity of the northern half of the arc at least, with the Greater Antilles.

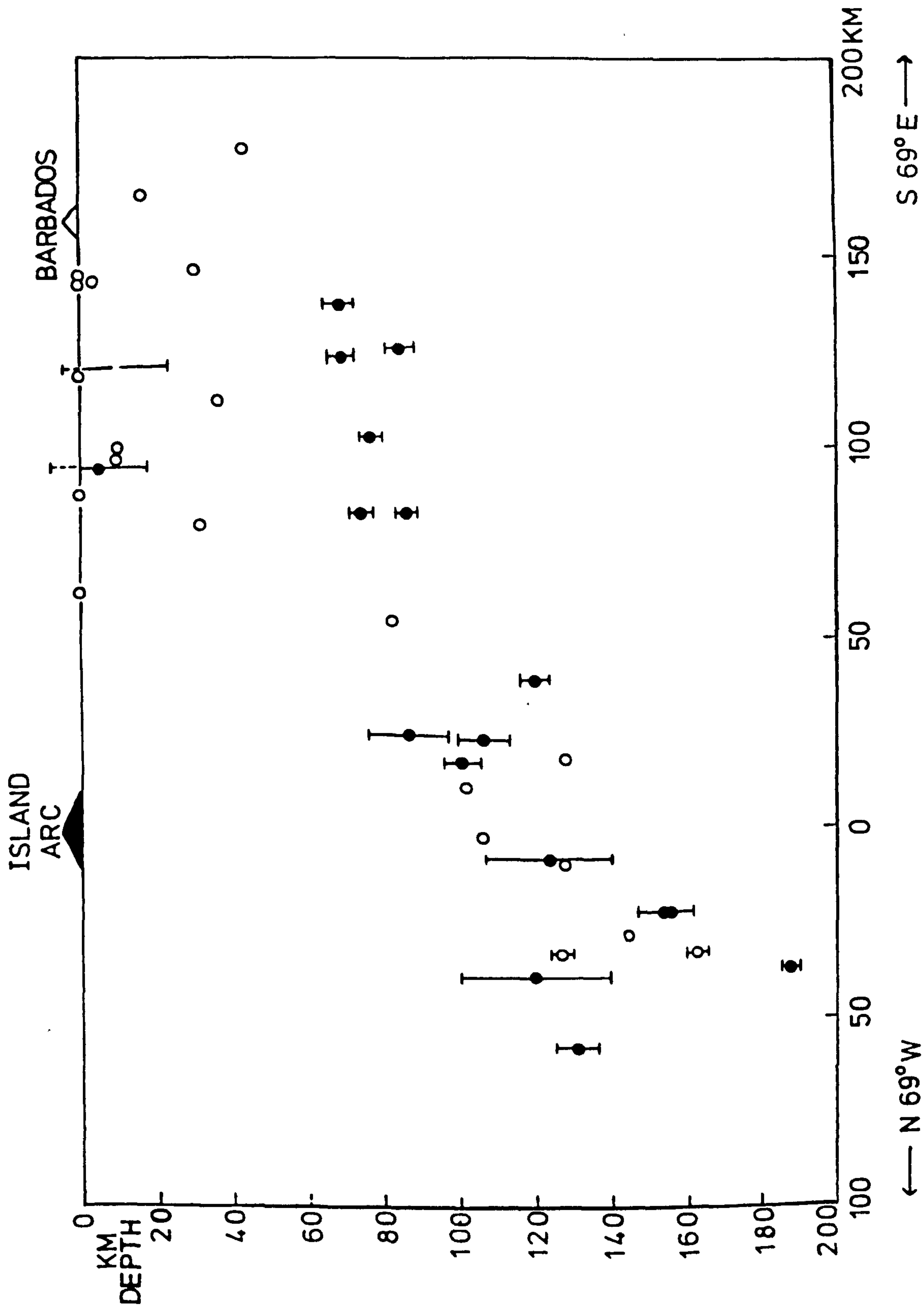
At present, the seismicity of the Lesser Antilles suggests that the depth to the Benioff zone centre is shallower at the southern end of the arc (115 km beneath Grenada) than further north (160 km beneath Dominica). In addition the dip of the Benioff zone is steeper ( $50^{\circ}$ ) in the north than in the south ( $30^{\circ}$ ). The configuration of the seismic zone beneath Grenada is shown in Fig. 6 . The relative velocity of collision of the Caribbean

Fig.6

Cross section perpendicular to the southern Lesser Antilles showing focii of larger earthquakes with epicentres between  $11^{\circ}$  and  $14^{\circ}$ N projected onto a single plane orientated  $N69^{\circ}W-S69^{\circ}E$ .  
(After Sigurdsson et al., 1973).

Solid circle events were located by ISC computations.  
Open circle events located by Seismic Research Unit, Trinidad.





and Americas Plates has been estimated as below  $2.0 \text{ cm yr}^{-1}$  (Molnar and Sykes, 1969).

Recent syntheses of the geological history of the Caribbean tend to be in agreement only over the complexities involved (e.g. Freeland and Dietz, 1971; Malfait and Dinkelman, 1972; Meyerhoff and Meyerhoff, 1972). It is apparent that the area has been tectonically active at least since the Jurassic but the Cretaceous ages determined in rock samples obtained from the Beata Ridge (Fox et al., 1970) and in sediments on the Caribbean floor (Purrett, 1971) suggest that the formation of the Caribbean Plate itself was a Cretaceous event, and lend support to the hypothesis of Edgar et al. (1971) that the area has been an isolated structural unit since then.

Refinements of the interpretation of the evolution of the Caribbean must result in future from the current volume of interest and research in the region.

## CHAPTER 3

### GRENADA - GENERAL BACKGROUND

The island of Grenada was discovered by Columbus in 1498. The name is probably derived from an anglicised corruption of the area in southern Spain. The climate is tropical and a comparatively dry season may occur between January and May. The average annual temperature is 27°C. Average annual rainfall in the mountainous interior is 150 inches per annum but diminishes towards the coasts and arid southwestern peninsula.

The original inhabitants were Carib Amerindians. Initial European colonisation was primarily by the French but alternated between British and French possession according to peace treaty settlements. After 1783 however, the British remained in control. In 1795, a year-long slave rebellion, led by one Julien Fedon took possession of practically the whole island but was finally defeated by an expeditionary force. The population has greatly expanded in recent years and is now approximately 100,000.

Slavery was abolished in 1838 and sugar was gradually replaced by cocoa and nutmegs. Subsequently, other spices such as cloves, bay and cinnamon were successfully introduced. In 1955, the nutmeg industry was devastated by Hurricane Janet and bananas were substituted as a cash crop. The return to full maturity of replanted nutmegs will prove invaluable during the present decline of the banana industry. Apart from agriculture, the other major source of income for the island is tourism.



## CHAPTER 4

GRENADA - GEOLOGICAL BACKGROUND4:1 Previous work

The island of Grenada has not been extensively studied previous to the present investigation. The earliest account was by Harrison (1896) who noted the dominantly volcanic nature, and listed the first chemical analyses of the silica-undersaturated basalts occurring on this island. Earle (1923) commented on the folded Lower Tertiary basement, noting the presence of gypsum in some horizons. The unusual hourglass-zoned, augite-phyric basalts and what would now be termed cumulus plutonic blocks were also recognised.

The Lower Tertiary basement was more extensively studied by Martin-Kaye (1956-61). In a series of reports, the stratigraphic relationships and age determinations by means of their contained fossil fauna are described. A brief account of the overlying volcanics is given by Robson and Tomblin (1966), where mention is made of the unusually basic nature of the volcanicity. A number of the explosion craters indicated on the geological map presented in this account (Robson and Tomblin, 1966 ) have been shown by the author's field-work to be misidentifications of other topographic features.

Grenada was also visited by Drs. J.G. Holland (Durham University) and J.F. Tomblin (U.W.I., Trinidad) in the course of a geochemical sampling project in the Lesser Antilles, supervised by Professor G.M. Brown (Durham). The author is grateful for access to this data during the present study.

#### 4:2 Volcanic Activity

There have been no erupted volcanics in historical time reported from the island of Grenada. Anderson and Flett (1903) dismiss the eruptions of sulphurous vapours within the harbour of St. George's the capital, in 1867 and 1902, as being over-dramatised phenomena associated with tidal waves generated by eruptions elsewhere in the Lesser Antilles. The only indications of volcanic activity are the presence of numerous hot springs, especially in the vicinity of Mt. St. Catherine.

Eight kilometres to the north of Grenada (Fig. 7 ) is one of the most frequently active volcanoes of the Lesser Antilles. It is submarine but named Kick-em-Jenny after the prominent, conical, andesite-dome rock, 5 km to the north-east. Robson and Tomblin ( 1966 ) report an eruption in 1939 when solid products were ejected above sea level, and seismic events centred on the volcano in 1943, 1953, 1965 and 1966. A similar event took place in 1972 (J. Shepherd, pers.comm.). A survey of this volcano, supervised by Drs. H. Sigurdsson and J. Shepherd (U.W.I.) aboard H.M.S. Hekla in 1972, revealed a submarine cone of diameter 100 m at a depth of 200 m below sea level.


#### 4:3 Physiography and bathymetry

The island of Grenada is roughly oval in shape, elongated in a northeast-southwest direction. It is approximately 33 km in length by 20 km in width, and 300 sq. km in area. The general topography is rugged, rising to a maximum height of 910 m at the summit of Mt. St. Catherine. A chain of mountains strikes nearly

Fig. 7

Bathymetric map of Kick-em-Jenny volcano.

(After Robson and Tomblin, 1966).

Probable location of cone is indicated by   
Submarine contour interval shown in fathoms.



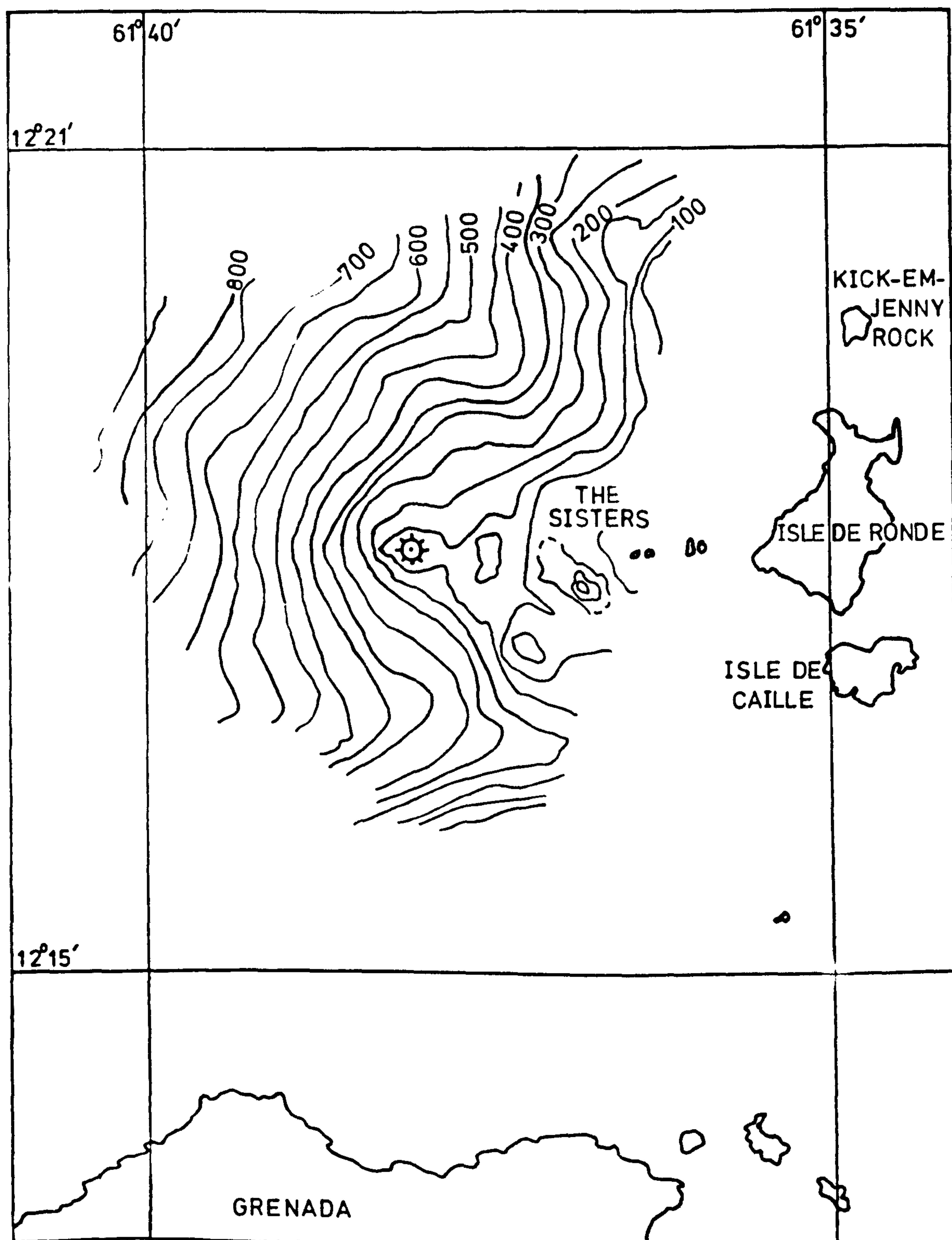
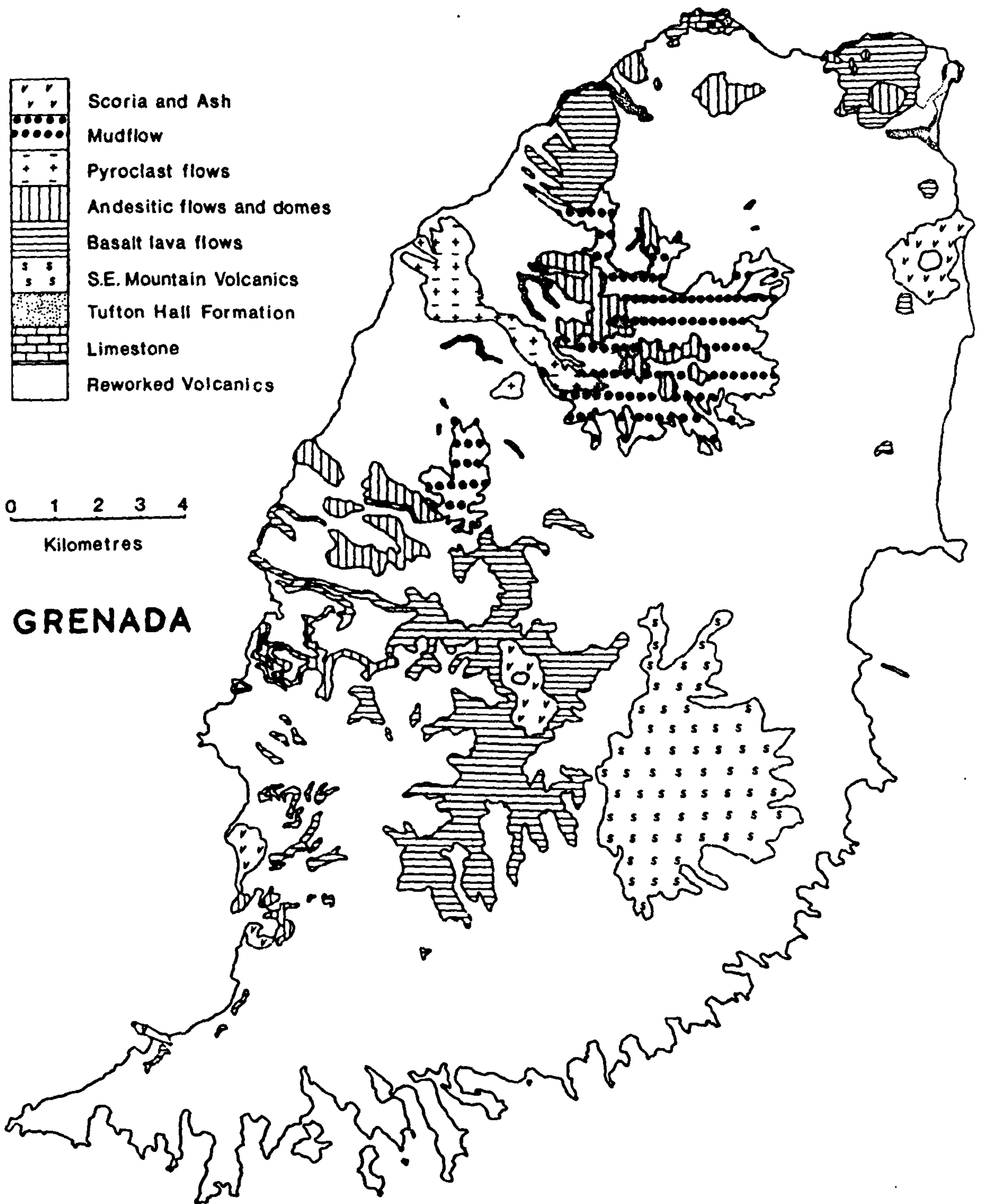


Fig.8

Surface Geology of Grenada.





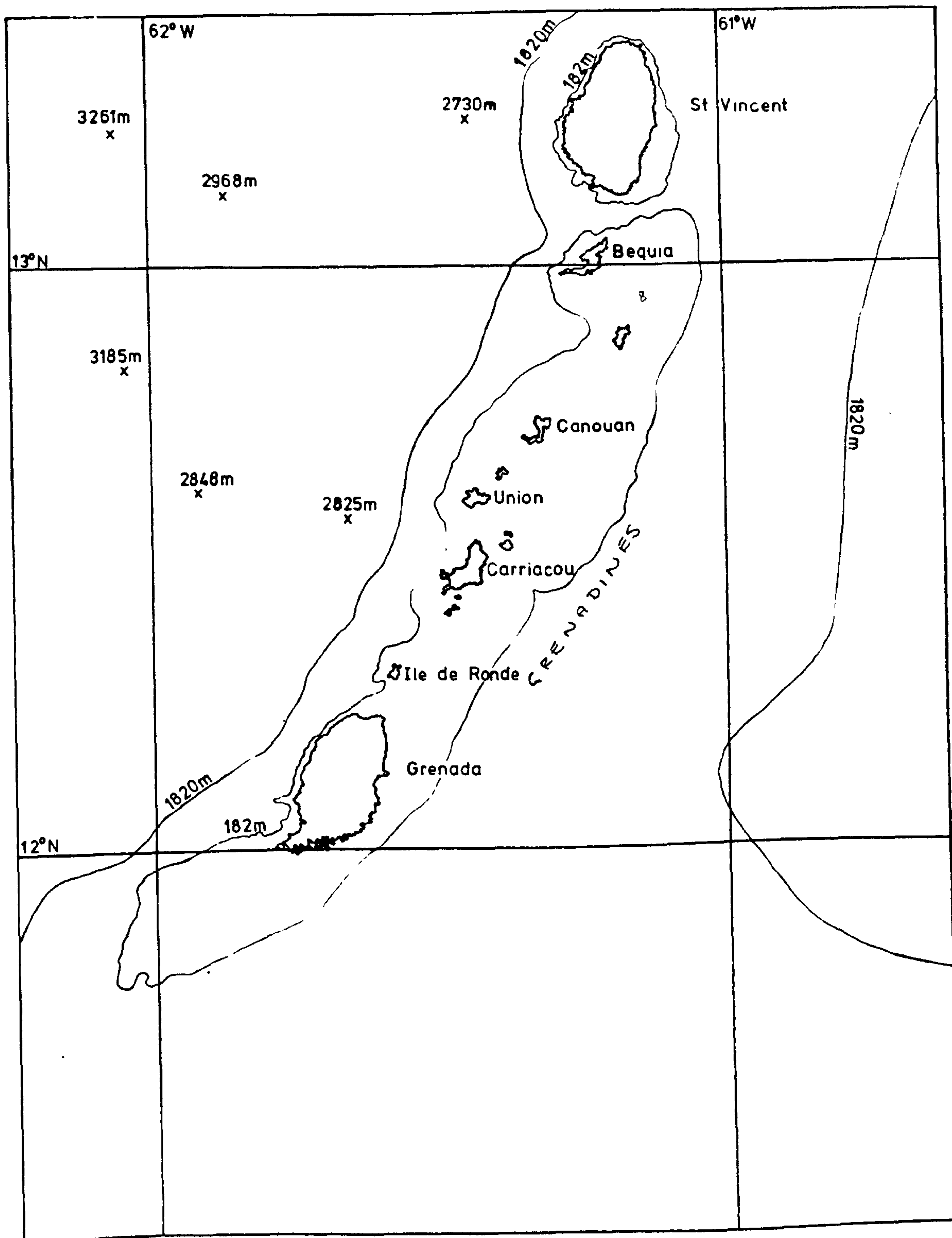
the length of the island but is offset towards the western coast. From north to south, this high ground is composed of the massifs of Mt. St. Catherine (910 m), Mt. Granby - Fedon's Camp (835 m) and South East Mountain - Sinai - Mt. Maitland (780 m) (Fig. 8 ).

The island is asymmetric in profile (east-west); the western side being considerably steeper and more indented by deep valleys than the eastern. Geological exposure is consequently better on the west. The submarine bathymetry shows that the contrast in slope is maintained offshore (Fig. 9 ). On the Caribbean side of the island (west), a depth of 2500 m is attained in the Grenada Trough within 40 km. An extensive area of shallow ( 40 m) submarine banks extends to the east for 10 km, the bottom profile steepens further east, and a depth of 2000 m is reached in the Tobago Trough. This asymmetric profile seems to be generally true of the other major volcanic islands in the Lesser Antilles as far north as Guadeloupe. It is significant that the older (pre-Miocene) and younger arcs diverge further north (Martin-Kaye, 1969). The post-Miocene volcanic islands of Montserrat, St. Kitts, St. Eustatius and Saba are more regular in profile both terrestrial and submarine. It is possible that the westward shift of the axis of volcanic activity in the southern part of the arc was not so pronounced, and the observed profiles are due to the structural influence of older volcanic products to the east (Fig. 5 ).

To the south and south-west of Grenada, there is another extensive area of shallow submarine banks extending for 20 km. The depth does increase further south but is not greater than 870 m between Grenada and Trinidad (Fig. 2 ). The indented

Fig.9

Submarine bathymetry of the southern Lesser Antilles; submarine contours and individual depths are indicated in metres. (Adapted from Admiralty charts). Note ridge extending off shore westwards from Moliniere Point in southern Grenada.





southern coastline of Grenada appears to represent the recent drowning of a ridge-valley topography. The ridges are flat-topped at only 10 m above sea-level and inland slope gently upwards on a graded profile. In addition, the inlets are shallow and sediment deposition is taking place forming areas of swamps. Thus the coastline form appears to be due to a recent, slight relative uplift of the land. This movement was probably differential, because other parts of the coastline of the island do not display these features. Macintyre (1972) has suggested that a complicated sequence of eustatic changes in sea-level during the Quaternary, have been a major factor in producing coral reefs in the Eastern Caribbean. In particular, it seems possible that the widespread shelf-reef colonies established on the marine bank to the east of Grenada and the Grenadines were initiated before the Holocene transgression of 8,000 years B.P. Thus it appears that the formation of the present coastline and submarine bathymetry of Grenada is the result of a combination of local tectonic, sedimentary and structural conditions together with more widespread changes in sea-level.

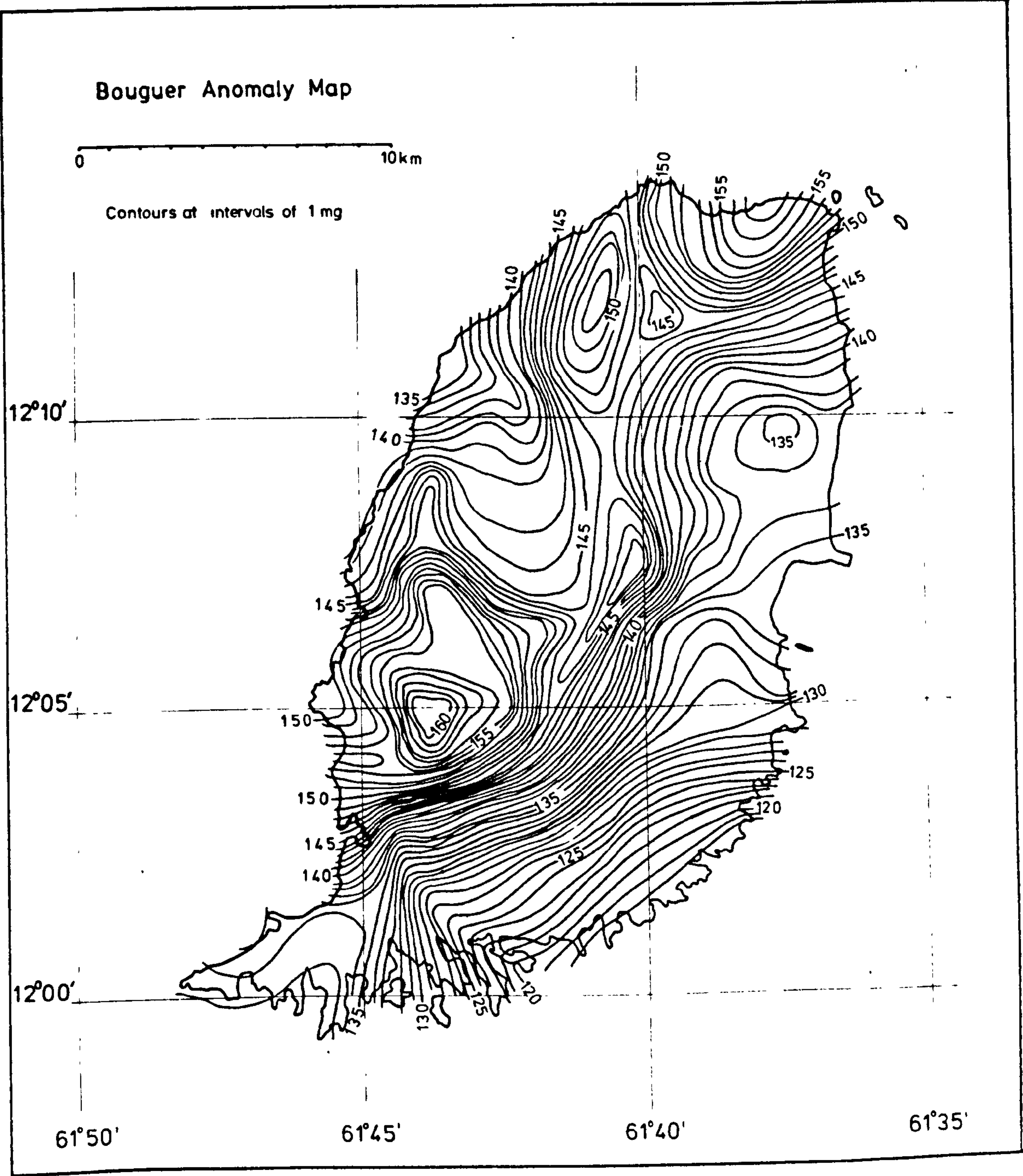
Apart from these general features of submarine bathymetry, only the existence of a ridge extending offshore from Moliniere Point on the west coast need be noted (Fig. 9 ). This probably represents the submarine continuation of lava flows that are associated with the Mt. Maitland - Mt. Moritz volcanic centre.

#### 4:4 Geophysical investigations

A gravity survey of the island has been completed by Andrew, Masson-Smith and Robson (1970). In preference to the

Fig.10

Bouguer Anomaly Map of Grenada.  
(After Andrew et al., 1970).





published isostatic anomaly map, a Bouguer anomaly map by the same authors is adapted here (Fig. 10). This represents more clearly the contrasts in crustal densities of the island. Notable features are the coincidence of the Mt. Maitland - Mt. Moritz centre, mentioned above, with one of the pronounced areas of high gravity anomaly. There is an extensive area of high, positive gravity anomaly extending northwards from this centre towards the Mt. Granby - Fedon's Camp and Mt. St. Catherine centres. A similar correspondence may be observed between the Northern Domes centre and another high. The Lake Antoine centre, largely constructed at surface of loosely consolidated pyroclastic deposits, corresponds with the gravity low in the north-east of the island.

## CHAPTER 5

THE GEOLOGICAL HISTORY OF GRENADA I5:1 Notes on Mapping and Nomenclature of Field Units

During field mapping, a study of the volcanic evolution of the morphologically best preserved centre, Mt. St. Catherine, was initially undertaken. However, extensive vegetation cover prevented the completion of a comprehensive synthesis of the eruptive history, and consequently the scope of the project was broadened to include the whole of Grenada. Reconnaissance-style mapping indicated several centres on the island, and by a comparative study of these it was hoped that a more general view of the nature of the vulcanicity of the island could be obtained. The relatively subdued topography and hence reduced rainfall of the nearby Grenadine islands combine to provide excellent geological exposures. Visits to these islands, apart from extending the range of samples collected were useful in clarifying some of the geological processes occurring on Grenada itself.

It became apparent during geochemical and petrographic investigations of the Grenada suite of volcanic rocks that an unusual variety of genetically related rock types were present. Further discussion is presented later, but in order to avoid an over-complicated nomenclature for describing field occurrences, a classification based primarily on arbitrary divisions according to silica weight percentage is used. Obvious mineralogical features in hand specimen, such as the abundance of olivine or clinopyroxene are then added as prefixes to the appropriate names. The divisions used are based on those recently proposed by

Middlemost (1973). These differ slightly from those used by Rea (1970) and previous workers in the Lesser Antilles based on the divisions proposed by Robson and Tomblin 1966. A comparison of the two schemes is given below (Fig. 11 ). The advantages of the new boundaries are the slight shift to lower weight percentages of silica. In view of the abundance of basalts and andesites on the island of Grenada, this is useful for descriptive purposes.

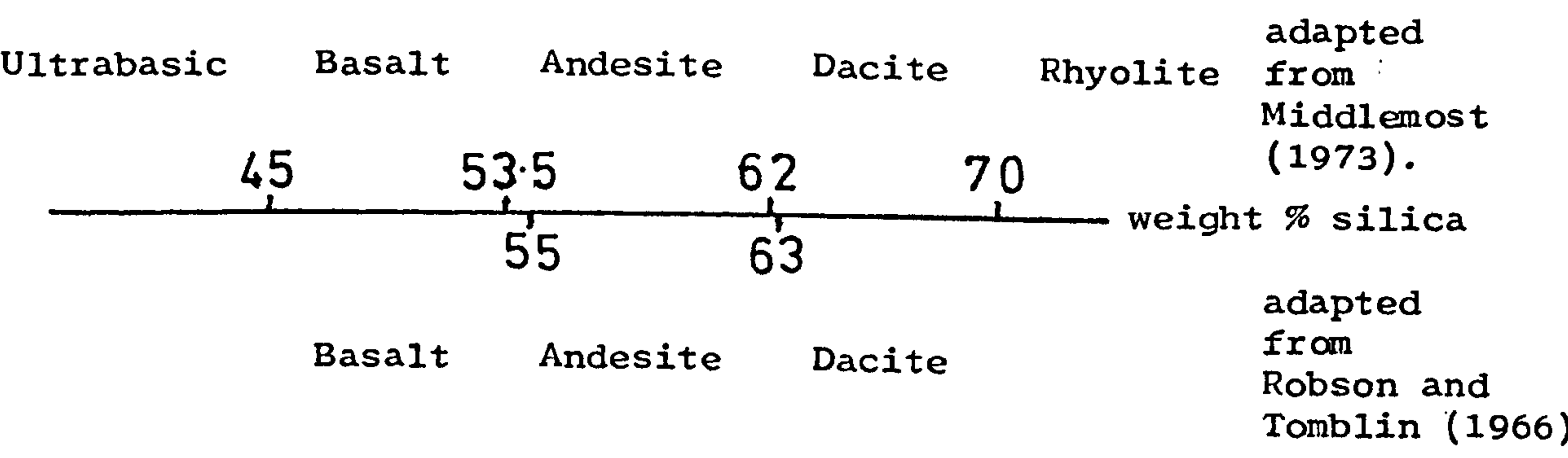


Figure 11. A comparison of class divisions used in the present study with those proposed by Robson and Tomblin (1966).

5:2 Primary Rock units

5: 2:1 Lava Flows and Domes

Most of the basalt lava flows on Grenada may be described by the terms aa or block flows (Macdonald, 1972). They consist usually of a platy or columnar jointed, massive interior underlain and usually overlain by angular blocks derived after cooling by mechanical grinding of the same flow. Total thicknesses of individual flows may range up to 20 m but are generally less than 5 m thick.

Numerous andesite lava flows exist on the island. These are



TABLE 1

## Classification of pyroclastic material

<u>Size of fragments</u> <u>average diameter</u>	<u>Condition on</u> <u>ejection</u>	<u>Name of</u> <u>fragments</u>
Greater than about 60 mm	plastic or solid	bomb
Between 3 and 60 mm	liquid or solid	scoria
Less than about 3 mm	liquid or solid	ash

difficult to characterise by any current, general descriptive term. As in aa and block flows, layers of autobrecciated material a few metres thick are present above and below massive interiors. However, maximum thicknesses of these interiors may be up to 100 m. Thus the ratios of thickness of rubble layer to massive interior is unlike that of typical aa or block flows. Some andesite flows are quite extensive up to 2 or 3 km in length. Most tend to be shorter and it is probable that there is a complete gradation between these flows and domes. Domes are formed by the extrusion of numerous short, thick viscous flows or solid and semi-solid material. The disintegration of the flanks of these domes produces scree mantling the solid rock. In some instances it may be difficult to determine whether a particular rock unit is a flow or dome.

#### 5: 2:2 Fragmental Deposits

Primary fragmental deposits in Grenada are either pyroclast fall or pyroclast flow material (Robson and Tomblin, 1966 ). Pyroclast fall deposits are formed by fragments settling more or less vertically from the air above, mantling the underlying topography. The deposits are often well sorted, vertically and laterally since larger fragments fall faster and nearer to vents. Repeated explosions may give rise to sequences containing many coarse to fine graded units, though variations in force of eruption may cause inversions of size grading. A classification of fall deposits based on arbitrary divisions of size of fragments has been followed (Table 1 ), (Fisher, 1961).

Pyroclast flows transport material laterally and downwards from the eruptive vent in a direction generally controlled by the pre-existing drainage pattern. Macdonald ( 1972 ) describes the resulting deposit as "a mixture of finely pulverised rock material (ash) with angular blocks of rock ranging up to several yards in diameter and often many fragments of pumice. The great turbulence in the avalanche prevents any great degree of sorting of the material".

### 5:3 Secondary Rock Units

Any mountainous topography in the tropics will generate considerable relief rainfall. A characteristic feature of Grenadian geology is the large surface area of the island occupied by secondary or reworked volcanic detritus (Fig. 8 ). The effect of the heavy rainfall on loosely consolidated mountain slopes composed of primary fragmental deposits is to initiate renewed movement. The eruption of the Soufriere volcano, St.Vincent in 1902 provided examples of the processes envisaged. Anderson and Flett (1903) observed that on the higher ground of the volcano, most of the ash fall had been washed away a few months after the eruption. This erosion was partly a result of the precipitation associated with the actual eruption but mainly due to subsequent rainfall. Anderson (1908) returned to St. Vincent to examine the changes that had occurred in the five-year period after the eruption. Stabilisation of slopes had only taken place by re-colonising vegetation where the 1902 ash had been removed. Pyroclast flows totally destroy plant life, and ash falls have only slightly less effect. The stabilisation of primary deposits



by revegetation is related to the type of devastation, altitude and proximity to sources of new plants (Howard, 1962). Apparently a complete vegetation cover may be decades in returning to a devastated area.

The pyroclast flows associated with the eruption of 1902 had followed the deep river valleys draining the slopes. Anderson (1908) found that these flows were being actively reworked by the rivers, with deposition of sands, gravels and conglomerates and transport of much of the material into the sea. The extent of this reworking varies according to the amounts of material and the distance it is transported by fluvial action. Heavy rain on unconsolidated slopes may initiate movement of vast amounts of material as mudflows. The ejection of the crater lake of the Soufriere in 1902 gave rise to a mudflow composed of older material on the mountain flanks. Macdonald ( 1972 ) cites the descent of pyroclast flows into streams as another possible initiative cause. The resulting deposits of reworking range from a chaotic mass of unsorted blocks to finely graded and indurated sands, silts and clays. Thus it may be difficult to distinguish particular exposures as primary or secondary fragmental deposits.

#### 5:4 Discussion of the geological map

The variety of volcanic and geomorphologic processes occurring on the island combine to create a complex outcrop distribution (Fig. 8 ). The main restriction on detailed mapping of this distribution is the vegetation cover. In some cliff exposures a relatively precise stratigraphy has been determined, but usually

Fig.12

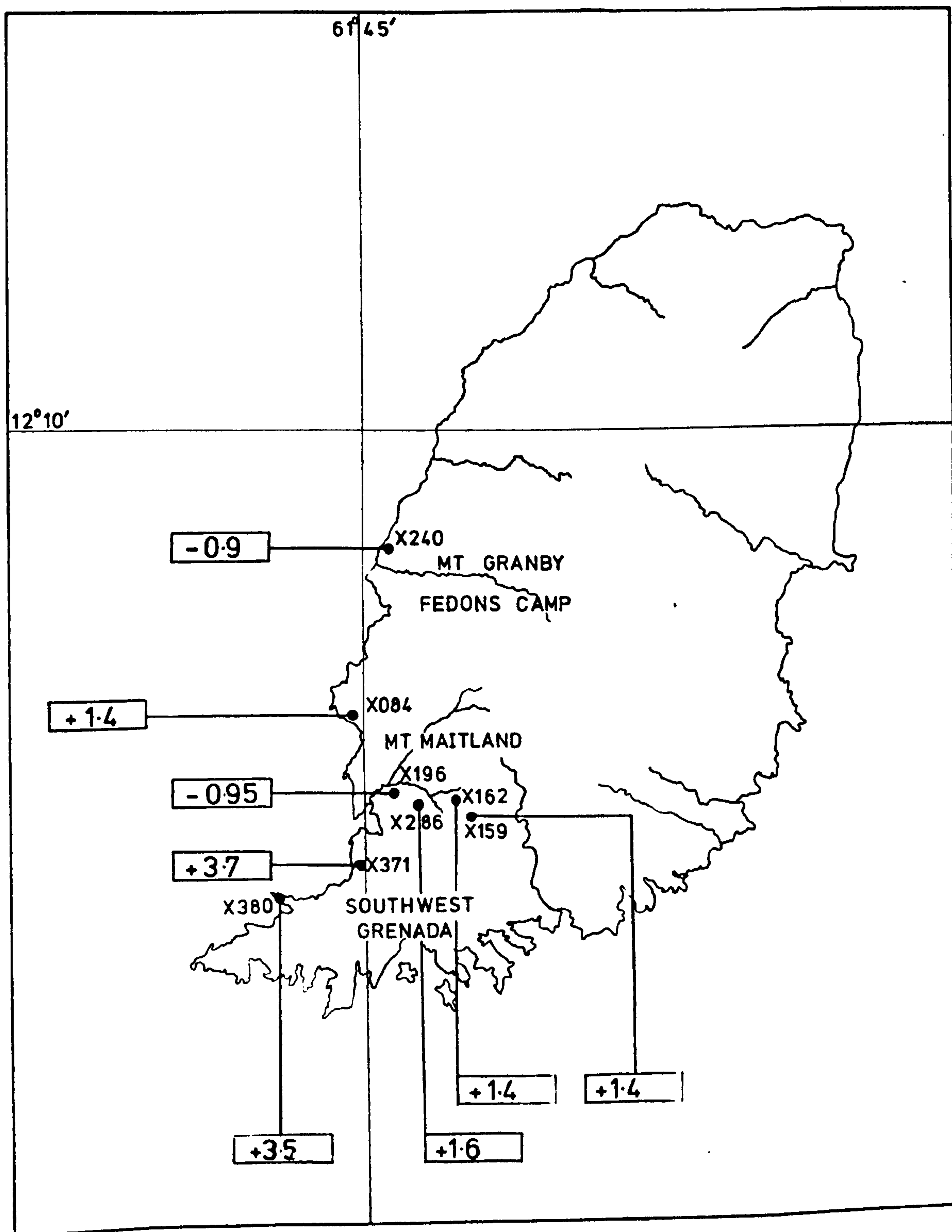
Locality map of age dated (K-Ar) Grenadan volcanic rocks. (Ages determined by Dr. J. Briden and Dr. D. Rex)

Numbers prefixed with x's refer to U.W.I. collection file.

Numbers in boxes are ages in millions of years.

+ = reversed polarity

- = normal polarity





this cannot be traced inland. Roadcuts may reveal thin airfall sequences, but differential weathering and absence of correlatable horizons prevents their attribution to a definite locus or period of activity. The isolation of exposures, and essentially linear nature of distribution of lava and pyroclast flows adds to the uncertainty in determining sequences of eruption at centres.

Most of the prominent ridges of the island owe their existence to the resistant nature of massive, capping flows. Often it is only possible to suggest the presence of a lava or pyroclast flow by the predominance of unusually massive and unweathered appearance of a particular type of block. The depth of weathering, which can be tens of metres, is then a problem on the higher ground both from a recognition and sampling point of view. An abundance of a wide variety of angular and rounded, heterogeneous fragments suggests the presence of mudflow or reworked volcanic deposit. In general, the identification of a deposit as primary or secondary depends on the degree and type of sorting displayed, homogeneity of constituents and where visible the lateral continuity of the unit.

A determination of centre of activity is usually based on the radial distribution of lava flows. Often the proximal ends of these have been eroded in the higher parts of the island, leaving butt-ending escarpments. This obscures the exact location of their original source, but a general estimate is possible. The degree of dissection of a centre is an approximate indicator of age, and combined with the K-Ar age dates (Fig. 12 ), the following table of the probable order of activity of the volcanic centres of Grenada has been constructed (Table 2 ).

TABLE 2

Probable order of activity of the  
volcanic centres of Grenada

<u>Centre</u>	<u>probable period of activity</u>
Explosion craters	10? - 1000 yrs?
Mt.St.Catherine	?50,000 yrs-20,000 yrs
Mt.Granby-Fedon's Camp	?1m35?50,000 yrs
Sinai-Mt.Maitland- Mt.Mortiz	2-1 myrs
South East Mountain	?2 myrs
Southwest Grenada	about 4 to 3 myrs
Northern Domes	? 4 myrs

Ages based on K-Ar age dates obtained by  
Dr. J. Briden and Dr. D. Rex (Leeds University)

## CHAPTER 6

THE GEOLOGICAL HISTORY OF GRENADA II6:1 Eocene to Miocene

The post-Miocene volcanics of Grenada are underlain by a tectonically disturbed series of volcano-sedimentary rock units ranging from Eocene to Miocene in age. No pre-Tertiary horizons have been discovered. Martin-Kaye ( 1969 ) has proposed that the well-bedded sequences of calcareous shales, siltstones and sandstones exposed in the northern half of the island, be called the Tufton Hall Formation after the type locality on the estate of that name (Fig. 13 ). The foraminiferal fauna contained within the shale horizons in particular, have been dated as Upper Eocene to Lower Oligocene in age. Tuffaceous horizons are present within the Formation and become more prominent in strata of Lower Oligocene age. Thin limestone lenses are also occasionally present. Limestone of a more massive character is exposed at Tempe Parnassus and Hope Vale in the south of the island. The contained fossils suggest ages of Oligocene and Miocene respectively. Fig.13 is a locality map of all recorded Lower and Middle Tertiary outcrops of the island.

Despite the wide age-range of these rock units, the lack of exposure has prevented the completion of a more exact stratigraphic description. Almost all of the outcrops are folded or faulted. The estimated thickness of the Tufton Hall Formation is at least 300 m (Martin-Kaye, 1969 ) but since neither base nor top of the strata is seen, the total thickness may well be in excess of 1000 m.



Fig.13

Lower and Middle Tertiary outcrops of Grenada. Outcrops in black shading. The Eocene-Oligocene volcano-sedimentary formation is named after the type locality on Tufton Hall Estate. Outcrops of Oligocene and Miocene limestone are labelled Lst.

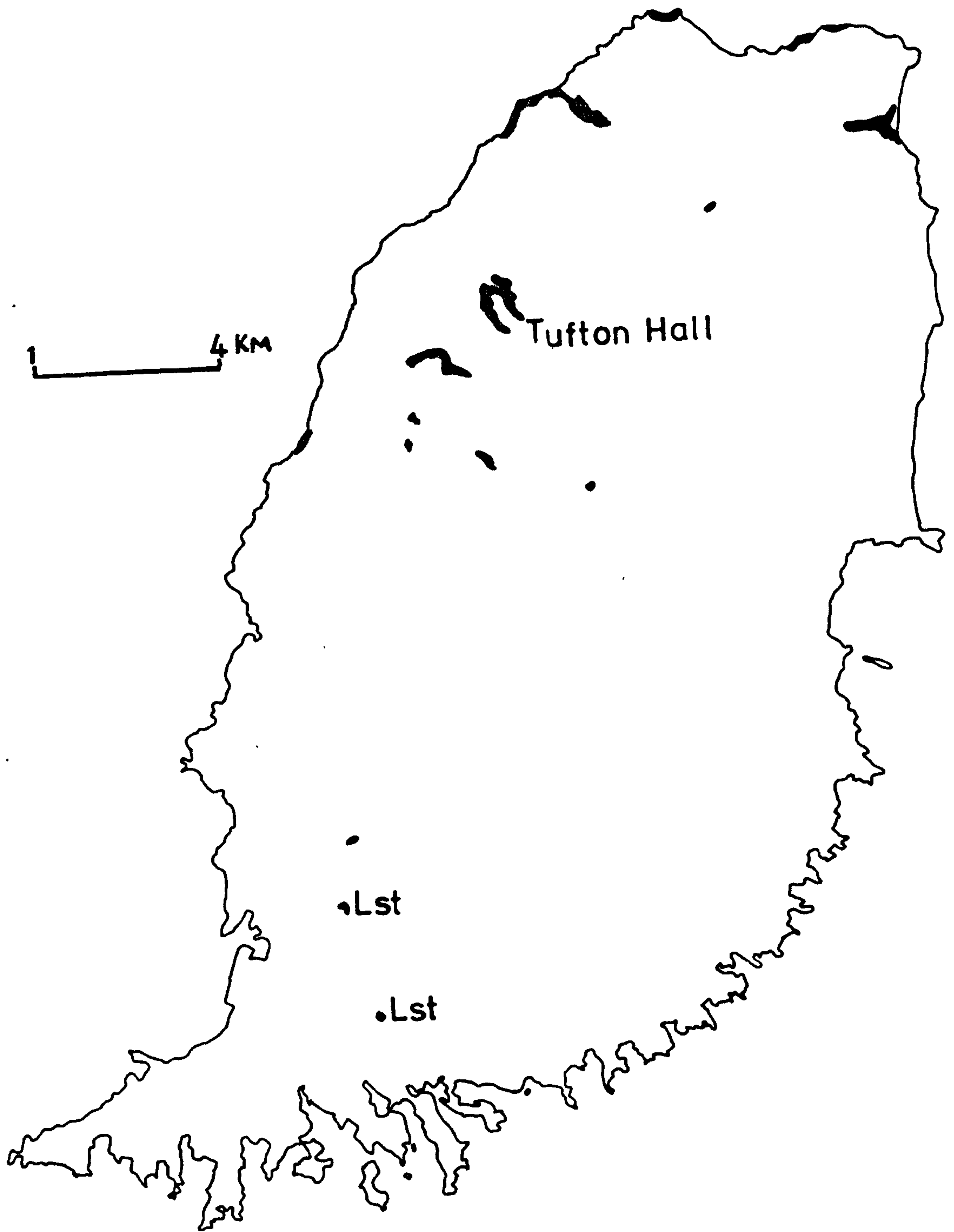


Plate 1

Folded and faulted Tufton Hall Formation near Palmiste.

Plate 2

Neptunian dyke of angular igneous rock fragments in the  
Tufton Hall Formation, Irvins Bay.







Plate 3

Folded dyke of clinopyroxene-phyric basalt in south-westerly dipping Tufton Hall Formation, Levera Bay.

Plate 4

Unfolded clinopyroxene-phyric basalt dyke cutting a south-westerly dipping sequence of Tufton Hall Formation shales and silts, Grenada Bay.







Thrust faulting and boudinage features are particularly well developed on the north coast of the island at Levera and Laurant Bays. In general the Tufton Hall Formation is gently folded about predominantly east-west striking fold axes. However the intensity of the folding varies considerably (Plate 1 ) and occasional north-south striking folds are also observed. In the Levera Bay area there are Neptunian dykes containing basaltic and andesitic rocks of a variety of shapes and compositions, together with fragments of locally derived Tufton Hall Formation in a fine-grained sandy matrix (Plate 2 ). Also cross-cutting the bedding of the sediments, but folded together with it are igneous dykes of pyroxene-phyric\* basalt (Plate 3 ). These dykes are unfortunately too weathered to permit petrological studies or age determinations to be made, but relict hourglass zoning can be distinguished in the pyroxenes.

In thin section, the prominent features of these sedimentary units are the abundance of detrital carbonate fragments, microfossils and the carbonate cement. Minerals of volcanic origin in varying stages of preservation of form and degree of alteration are also present. Characteristic of post-Miocene volcanic activity are lavas containing abundant oscillatory and hourglass-zoned clinopyroxenes. Chemical features will be described in more detail, but it is important to note similar pyroxenes are also present in the pre-Miocene Tufton Hall Formation. Oscillatory-zoned plagioclase feldspars and brown amphiboles (probably basaltic hornblendes) are also common.

\*calcic augites

It is apparent from the presence of allochthonous volcanic minerals and tuffaceous horizons that igneous activity was already taking place in the Eocene and probably continued into the Oligocene. Tuffaceous horizons of similar age have been reported from Carriacou, 40 km north of Grenada (Robinson and Jung, 1972). The evidence of the folded dyke and volcanic minerals within the Tufton Hall Formation shows that igneous activity preceded at least one period of deformation. An unfolded pyroxene-phyric basalt dyke however, is exposed at the south end of Grenada Bay (Fig. 14 ) cutting a southwesterly dipping sequence of the Tufton Hall Formation (Plate 4 ). Martin-Kaye ( 1969 ) has suggested at least two phases of deformation took place. The first occurred in the Oligocene and the second within the Miocene. It appears that volcanic activity of calc-alkaline affinities was occurring in the region throughout this period.

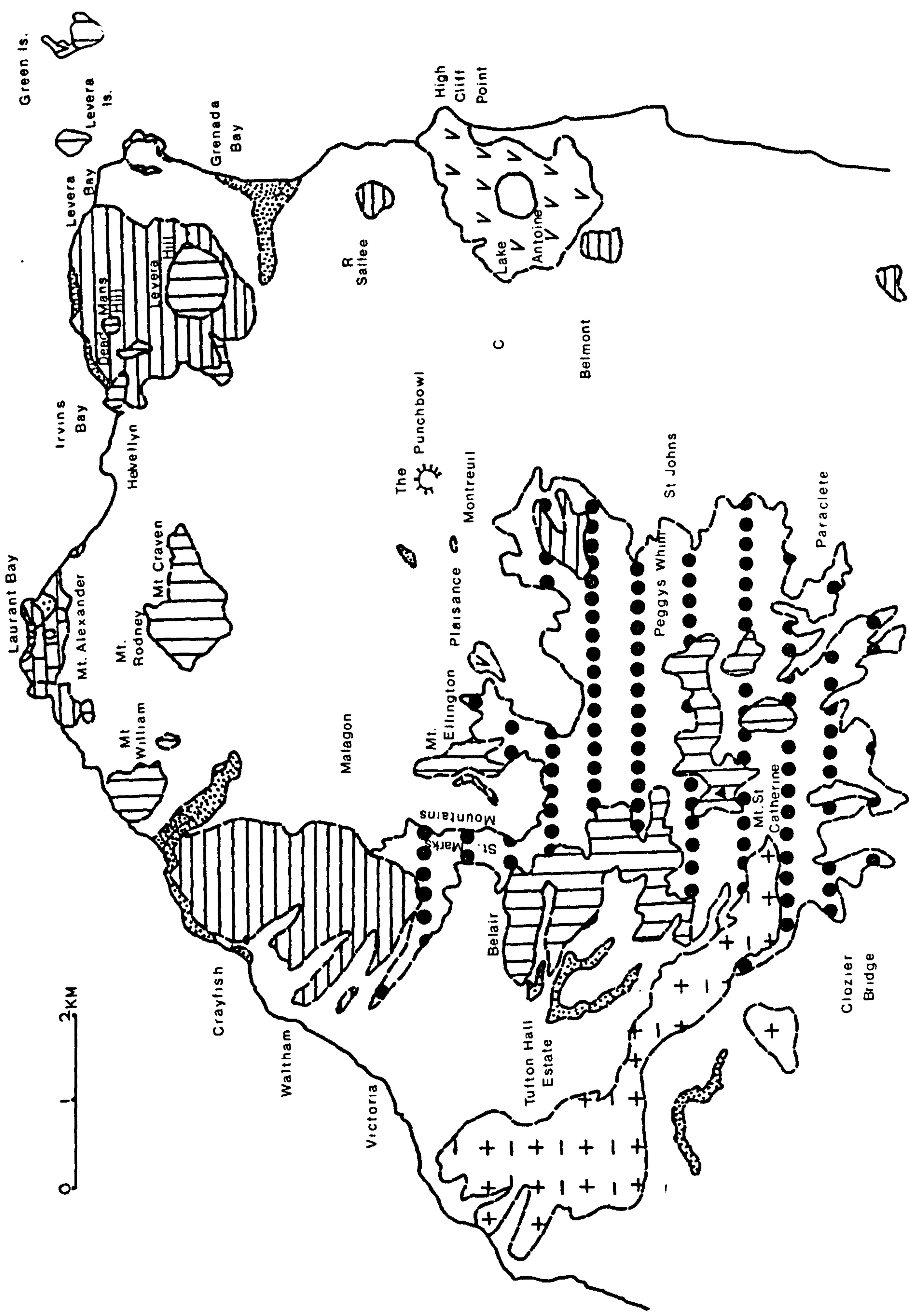
The term flysch has previously been used to describe the Tufton Hall Formation (Martin-Kaye, 1969 ). The Alpine connotation of this term with the creation and contemporaneous erosion of a nearby mountain belt may not be true in the local context. Unlike the Scotland Formation of Barbados, also of Eocene age, there does not appear to be a significant proportion of metamorphic minerals within the Grenada Formation. The derivation of these metamorphic minerals has been attributed to a source in South America. It seems possible that sedimentary deposits, similar in general nature to the Tufton Hall Formation, may be forming offshore of the volcanic arc at the present time.

Fig.14

Outcrop and locality map of northern Grenada.

Key as for Fig.8 page 18





The general east-west strike of the fold axes suggests a north-south oriented principal stress. This may be due however, to a local rather than regional stress field, since the intensity of deformation varies greatly and is completely absent in Carriacou (Robinson and Jung, 1972 ). A possible cause may be gravity sliding due to uplift on the flanks of a volcanic massif. A similar general origin for the deformation of the Barbados Scotland Formation has been proposed by Daviess (1972). The Neptunian dykes of north Grenada however, were probably created by post-Miocene fracturing of the Tufton Hall Formation allowing the inclusion of overlying volcanic rocks, rather than deformation occurring during the general folding.

The importance of the Lower and Middle Tertiary basement of Grenada is the evidence of early igneous activity in the arc. In addition, the post-Miocene volcanics are fully represented overlying this basement. Elsewhere in the active arc, such exposure is not generally available. The repetitions of the variable geochemistry occurring on Grenada since the Miocene are thus well exposed. A description of this activity follows, initially in terms of the field geology of the volcanic centres.

#### 6:2 The Northern Domes Centre

The Northern Domes centre lies at the northern end of Grenada (Fig. 8 ). Although the summits of the domes are prominent above the surrounding terrain, the maximum height is only 280 m. The area consists of two main areas of dome outcrop, approximately 4 sq. km in total extent. A crater is no longer present, although

the circular distribution of the andesite domes of Mt. William, Mt. Rodney and Mt. Alexander suggests the possible massive infilling of a pre-existing crater. Lava flows are observed on the coast dipping northwards as though derived from a source now occupied by these domes. Inter-layered flows with reworked and primary pyroclast fall are also exposed with a similar dip, north of Mt. William. The range of rock compositions present is from basalt to dacite. Most of the domes are weathered, but a recent fresh exposure at Little David has revealed a vertically lineated hornblende andesite. The amphiboles are apparently oriented in the direction of flow or extrusion of the dome. The history of the centre is much obscured by the mantle of derived reworked volcanic detritus. However, it appears that local eruptions of basalt and andesite lavas, interspersed with periods of explosive activity culminated with the intrusion of the now remnant domes. Probably much of the scree that mantled the massive rock of these domes has been removed by the subsequent erosion.

Separated geographically from this area of dome outcrop is the Levera Hill 'centre'. Compositional similarities and advanced state of weathering suggests the constituent volcanic units belong to the same general period of activity. Levera Hill itself is a hornblende andesite dome surrounded by the remnants of a pyroxenephritic basalt flow. On the northern flanks of this hill, two smaller domes are exposed at Helvellyn and Dead Man's Hill (Fig. 14). The Helvellyn dome has intruded the Tufton Hall Formation, which is generally exposed surrounding the Northern Domes centre. On the northwest margin of Helvellyn at sea-level,



brecciated Tufton Hall fragments are caught up in a matrix of the intruding andesite (Plate 5 ). Towards the core of the dome, the rock becomes more massive grading into a typical jointed hornblende andesite (Plate 6 ).

In Irvins Bay, north of Helvellyn and Dead Man's Hill, a breccia composed of angular basaltic and andesitic fragments, together with blocks of Tufton Hall Formation is exposed. A pyroxene-phyric basalt dyke has intruded the breccia, and also appears to be a prominent component of the breccia. On the southern slope of Levera Hill, a similar breccia is exposed, underlying the numerous blocks of pyroxene-phyric basalt strewn over the ground surface. No massive lava is present, so it is probable that the original flow was blocky in nature.

The local sequence of events appears to have been the initial extrusion of a variety of basalt and andesite lavas, subsequently intruded by the domes of Helvellyn and Dead Man's Hill causing local brecciation. Renewed activity with extrusion of the pyroxene-phyric basalt flows culminated in the extrusion of the Levera Hill Dome itself, causing brecciation around the flanks and intermixing of the previously erupted rock units.

Examination of the Bouguer gravity anomaly map (Fig. 10 ) reveals an area of high positive anomaly trending northeastwards away from the Northern Domes centre. Levera Island is another dome andesite situated 200 m offshore in this direction (Plate 7 ). It probably represents activity associated with this centre. The distribution of lava flows and domes around Levera Hill suggests

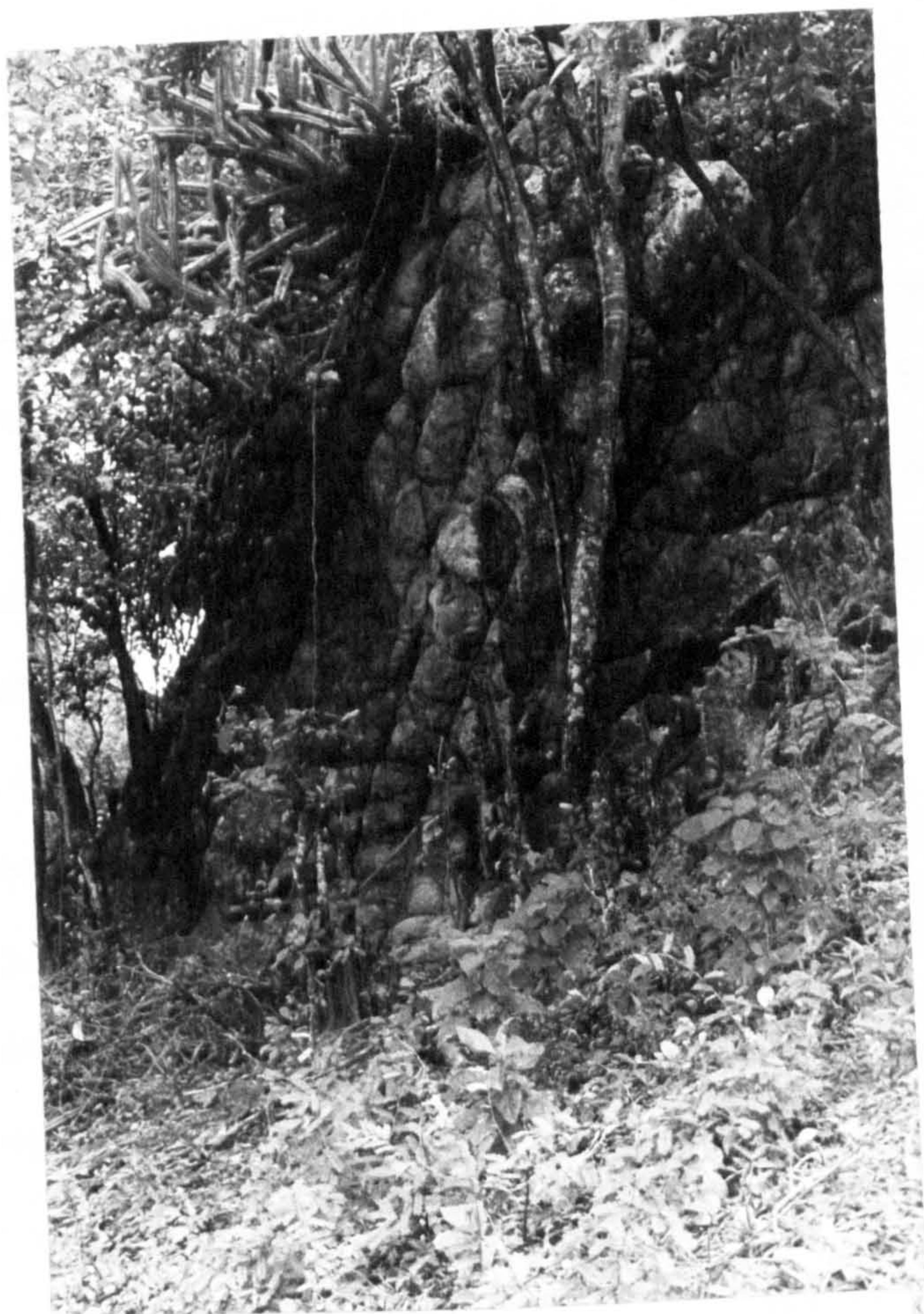
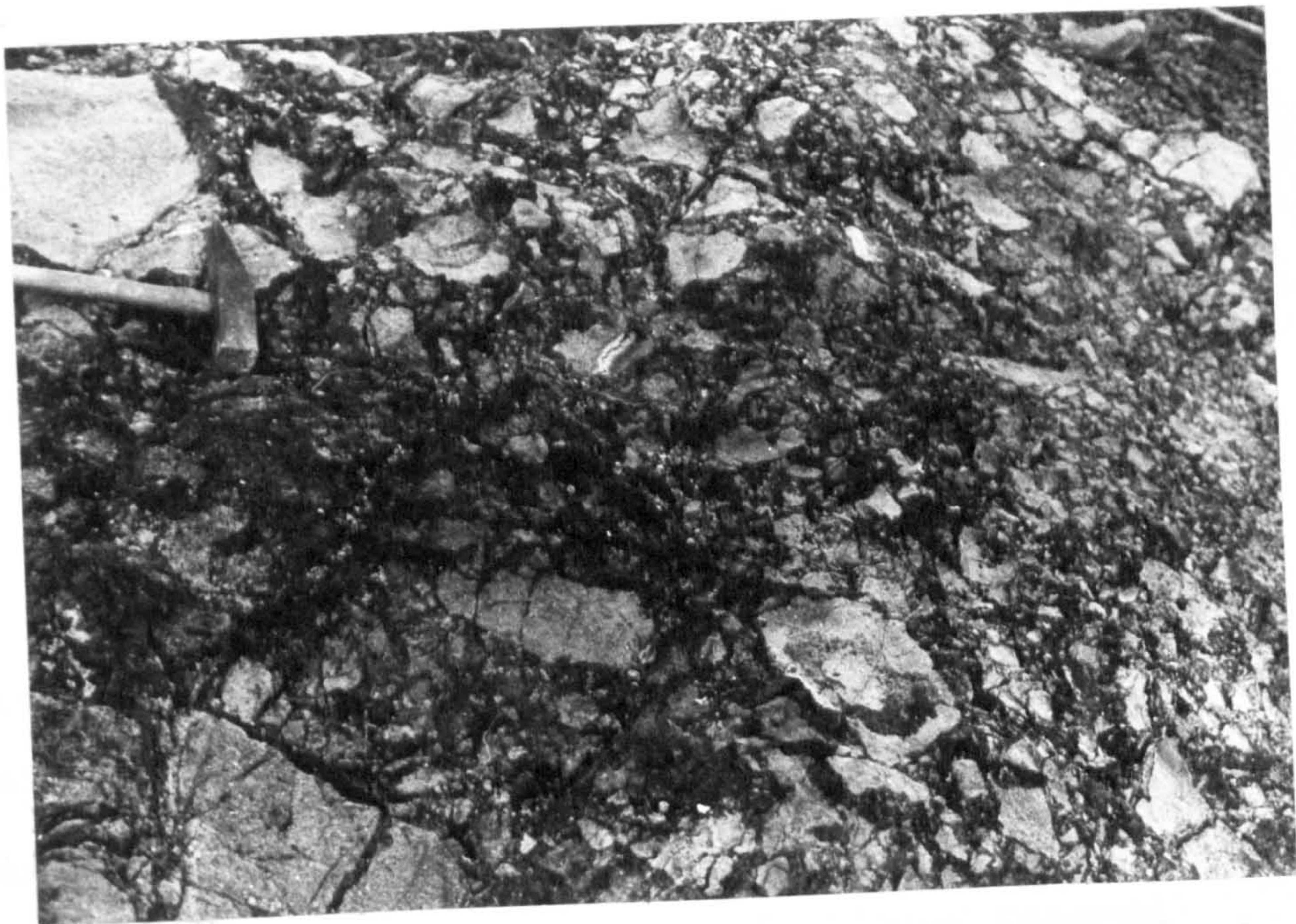
Plate 5

Breccia of andesite domes fragments and Tufton Hall  
Formation northwest of Helvellyn dome.

Plate 6

Massively jointed andesite forming the dome of Helvellyn.







the eruptive source was local. Compositional differences (discussed later) between the domes of Levera Island and Levera Hill suggest that the former is related to a different centre of activity. The positive anomaly may represent denser crustal rocks, connected with this concealed activity. The subdued topography south of the Northern Domes centre consists predominantly of reworked volcanics with occasional primary airfall horizons. The constituents of these beds are probably derived from centres both to the north and south. The area was sampled extensively but no consistent stratigraphy was discovered. Pleistocene limestones are exposed at an elevation of 100 m on Mt. Alexander. This uplift of the area has initiated renewed erosion both of the massive rock units and reworked horizons.

### 6:3 Southwest Grenada

The flat-lying terrain of southwest Grenada is composed of reworked volcanic detritus interlayered with basalt lava flows. The maximum height of the area is approximately 200 m, and the lack of dissection has probably concealed the existence of some lava flows (Fig. 15 for locality map). Despite the relative aridity of this part of the island, many of the flows are deeply weathered. Some were originally columnar jointed but have suffered spheroidal weathering (Plate 9 ). Fresh samples have been dated at 3.7 to 3.5 m.y. (J. Briden, pers. comm.) and so indicate volcanic activity in the area during the Pliocene. Unfortunately lava flows and reworked deposits derived from the younger (1.6 to 1.4 m.y.) Sinai-Mt.Maitland-Mt.Moritz centre overlie much of the area, particularly in the north. This has

Plate 7

Levera Island andesite dome.

Plate 8

Spheroidally weathered and columnar-jointed clinopyroxene-  
phyric lava flow, Grand Anse.







Fig. 15

Outcrop and locality map of southern Grenada.

Key as for Fig. 8 page 18

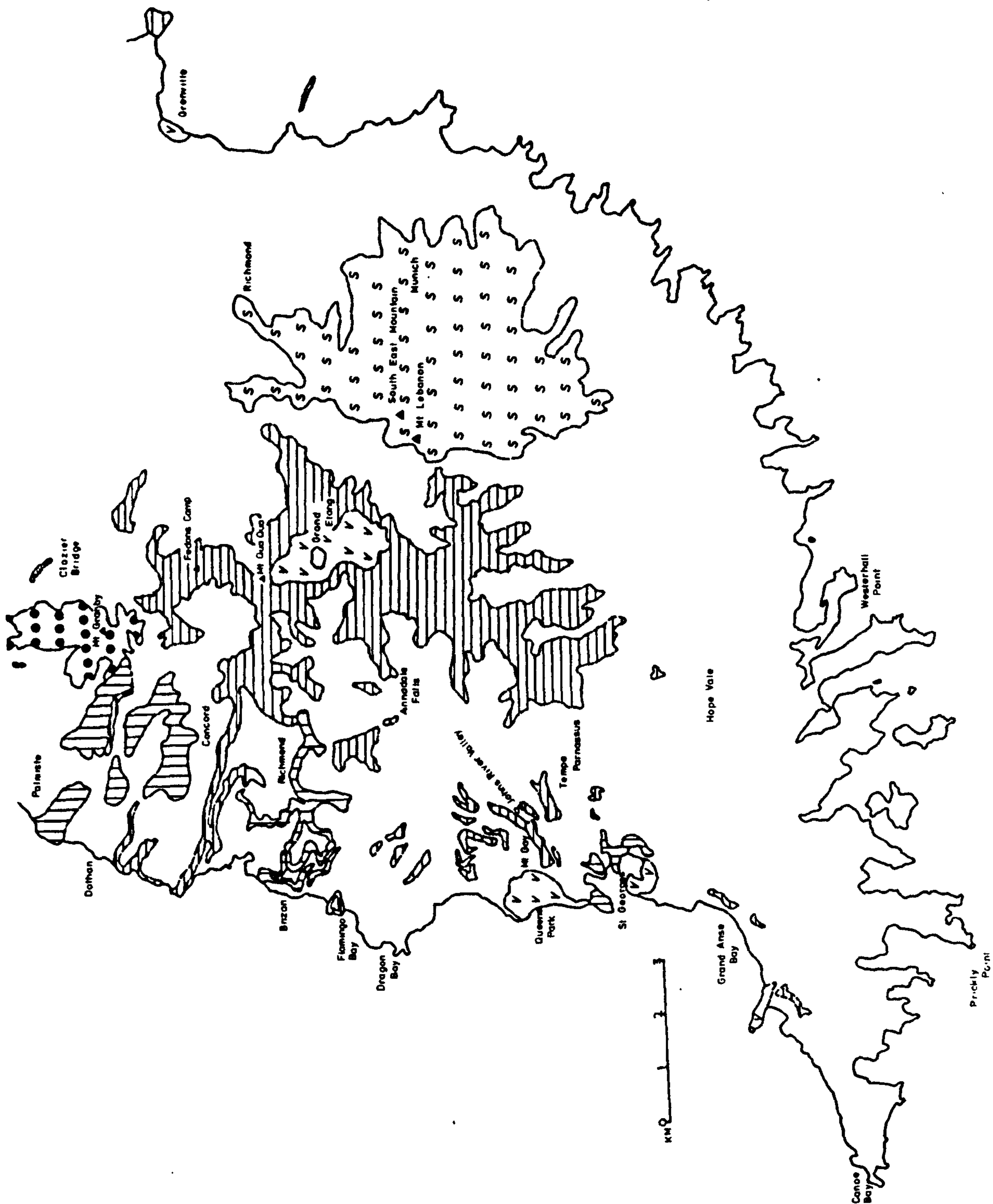




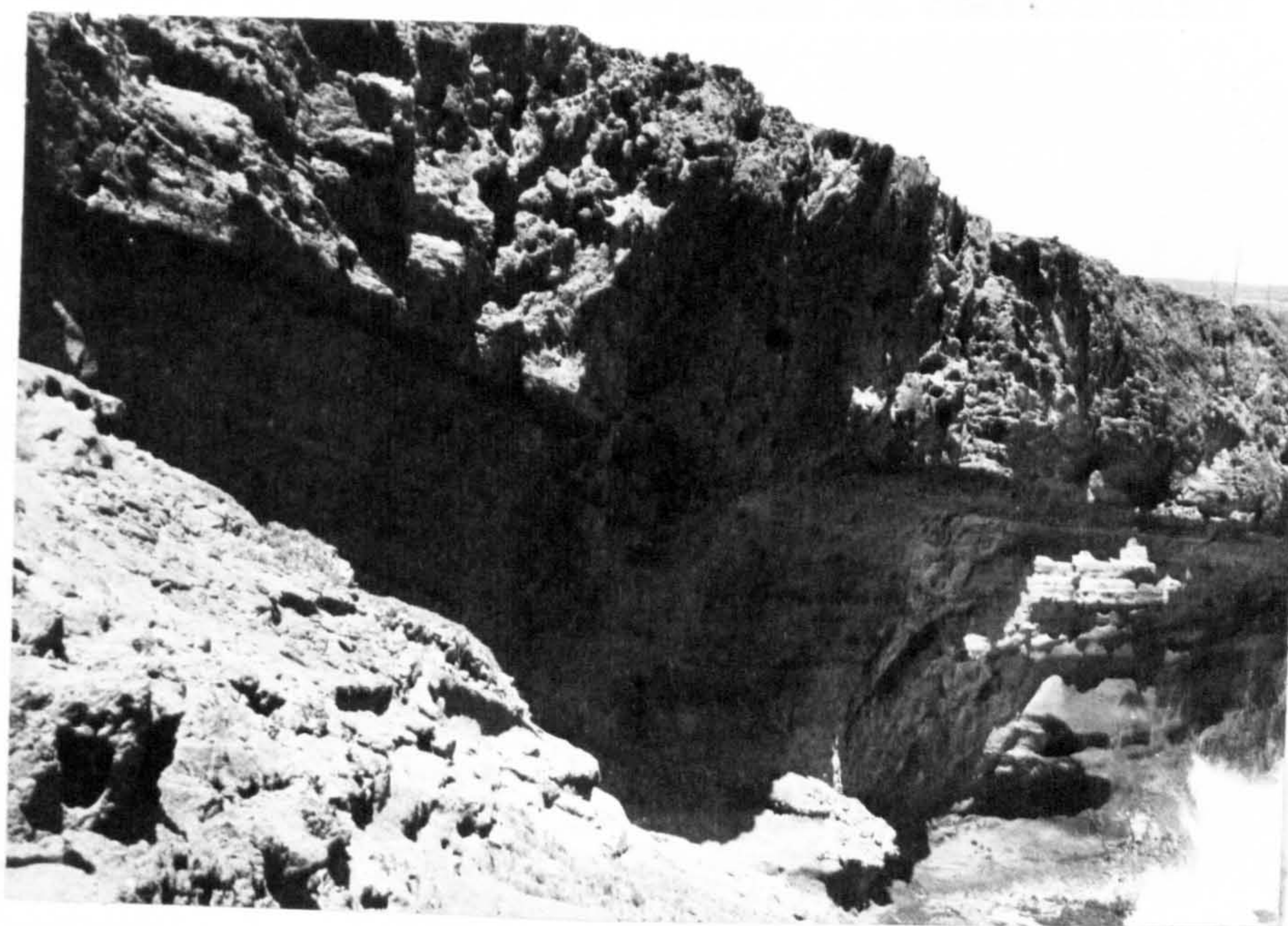
Plate 9

Prickly Point basalt plug overlain by secondary fragmental deposits.

Plate 10

Cumulus-block bearing conglomerates and gravels unconformably overlying finer reworked volcanics at Prickly Point.







probably obscured the source of the older deposits. It is thus difficult to determine with any confidence the local volcanic history.

At the southernmost tip of Grenada is Prickly Point. This headland has proved more resistant to erosion due to the presence of a basalt plug (Plate 9 ). The plug is mantled by a sequence of reworked volcanic detritus. This appears to represent two major periods of deposition. The older series is more fine-grained, of silt and clay grade, and contains fragments of andesitic pumice and occasional non-carbonised plant fragments. Following a period of erosion and channelling of the upper surface of this series, a more coarse grained volcanic conglomerate was deposited (Plate 10 ). A prominent component of this sequence is cumulus plutonic blocks composed of variable proportions of amphibole, clinopyroxene, spinel and plagioclase feldspar. Towards the east, this sequence is frequently displayed in coastal cliff sections, but the coarser horizon gradually obscures the underlying unit. Beyond Westerhall Point (Fig. 15 ), although reworked material is prominent in cliff sections and roadcuts, it is likely that most of the detritus has been derived from the South East Mountain centre to the north (Fig. 15 ).

The reworked units of southwest Grenada display the characteristic features of secondary fragmental deposits. On occasions current bedding and channelling is observed (Plate 11 ). The coarser beds are composed of a variety of rock fragments of basaltic, andesitic and dacitic composition. At Canoe Bay (Fig. 15 ) at the southwest tip of the island, fairly continuous lateral beds

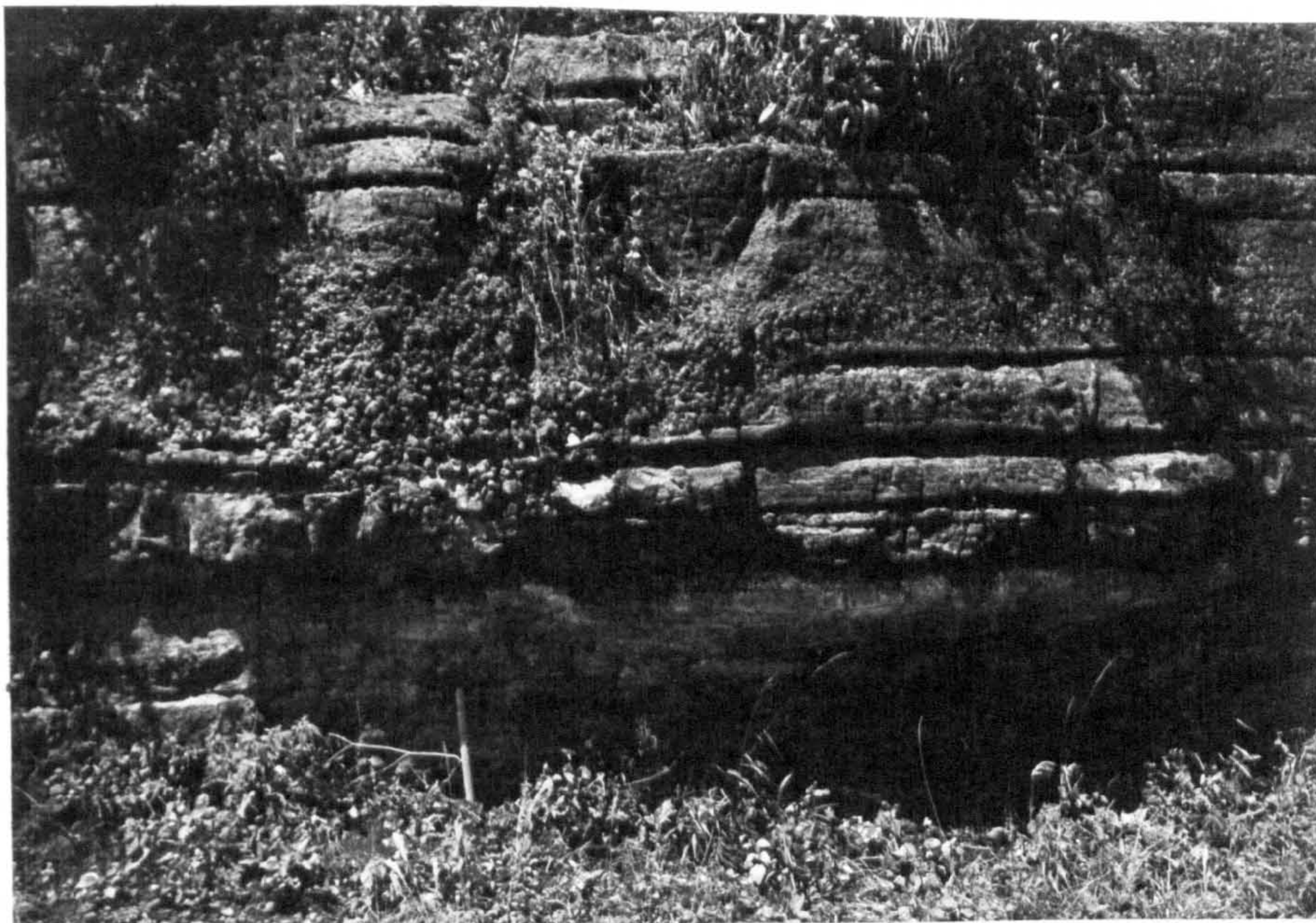
Plate 11

Channelling and current-bedding in reworked volcanics  
near Hope Vale, Southwest Grenada.

Plate 12

Large scale current-bedding in reworked volcanic deposits,  
Canoe Bay.







of reworked material are exposed (Plate 12). On some bedding surfaces, horizontal sheets of calcite are present. These are often traversed by ramifying worm casts and possibly represent periods of marine exposure. It is likely that the area has been submerged on occasions and that some marine deposition has taken place. Slight relative oscillations in sea level were inferred previously (see Section 4:3) from the indented nature of the coastline.

Although it has not proved possible to determine the source of the lava flows and reworked deposits, it is evident that the range of composition of included fragments is equivalent to the better exposed, younger centres of activity.

#### 6:4 The South East Mountain centre

The South East Mountain is probably another Pliocene centre of volcanic activity though no ages have so far been determined. This estimate of the age is based on the advanced state of erosion and weathering of the constituent volcanics. The topography is dominated by a ridge extending southwards from South East Mountain (780 m) towards Mt. Lebanon (700 m) (Fig. 15).

In general the area is composed of andesite and basalt flows that radiate from South East Mountain itself. The distal ends of these flows overlies and appear to pass into reworked volcanic detritus. This material forms a coastal sheet approximately 2 km wide that is continuous around the southern and eastern coasts of Grenada.



At individual contacts between lava flows and reworked volcanics, often the only indication that a solid flow was once present is the bright red lateritic soil. This contrasts markedly with the grey weathering appearance of the reworked volcanics. The lateritic soil seems to be the ultimate weathering product of the lava flows. All stages of disintegration can be traced from solid flow, through spheroidally weathered shells and relict decomposing boulders to thin soil.

It was apparent in the field that both basaltic and andesitic compositions were present as lava flows, but the complex intermixing and weathered state of many of the flows prevented meaningful differentiation on the map. Only the broad distribution of rock types could be determined. However, the range of compositions present is from basalt to dacite, although in this centre there appears to be a predominance of basalt compositions at surface.

The northern and northeastern ridges of South East Mountain are mostly capped by pyroxene-phyric basalt lava flows. Some of these extend for at least 2 km towards Richmond (Fig. 15 ). The summit of Mt. Lebanon and the surrounding slopes appear to be a weathered andesite dome. An andesite lava flow forms the southern ridge of Mt. Lebanon about 1 km in length. An extensive field of angular andesite boulders is present in the vicinity of Munich (Fig. 15 ) suggesting the former presence of another flow.

#### 6:5 Sinai - Mt. Maitland - Mt. Moritz centre

The topography of this centre is relatively subdued, though

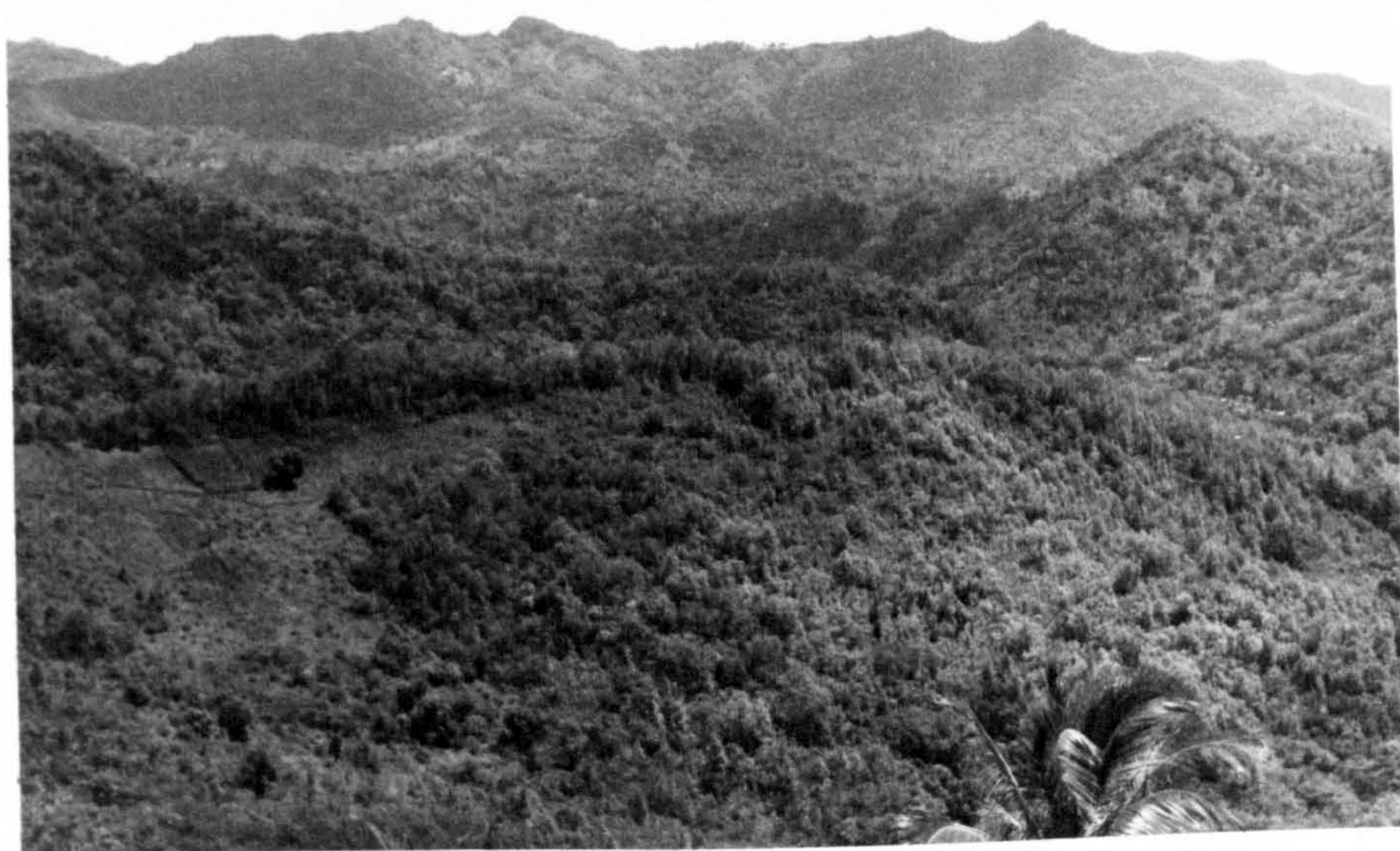
Plate 13

Columnar-jointed ultrabasic lava flow, Mt. Gay.

Plate 14

Northern scarp face of Sinai - Mt. Maitland from  
Richmond.







nevertheless many of the rock units are discontinuous. It is divided into two main areas by the St. Johns River which flows from northeast to southwest dividing Mt. Maitland from Mt. Moritz (Fig. 8 ). The highest ground is in the vicinity of Mt. Sinai (765 m) and decreases in elevation westwards. The dominant directions of lava flow are also westwards, since the mass of South East Mountain probably blocked alternative flow paths. Lava flows from Mt. Moritz and Mt. Maitland have been dated at 1.6 to 0.95 m.y. (J. Briden pers. comm.).

Most of the surface outcrop of this centre is dominated by lava flows of basaltic composition. No andesite flows or domes were discovered, although andesitic and dacitic fragments were collected from reworked volcanics interlayered with some of the flows. One of the few ultrabasic lava flows of the island is exposed at Mt. Gay, 1 km north of St. George's (Fig. 15 ). The flow has baked the underlying pyroclastic deposit, and both massive and fragmental material displays columnar jointing (Plate 13).

It is possible that the trend of the St. Johns river has been determined partly by faulting. The steep northern faces of Mt. Maitland and Sinai may represent eroded fault scarps (Plate 14 ). Martin-Kaye ( 1969 ) has suggested that the location of the explosion craters of St. George's, Grand Etang and Lake Antoine was controlled by northeast-southeast faulting (Fig. 17 ). The trend of this proposed disturbance is in the same orientation and in the same location as the faulting



Plate 15

The Southern Annandale Falls formed of southerly dipping Tufton Hall Formation.

Plate 16

Indurated reworked volcanics at Snug Corner, west of Annandale Falls.



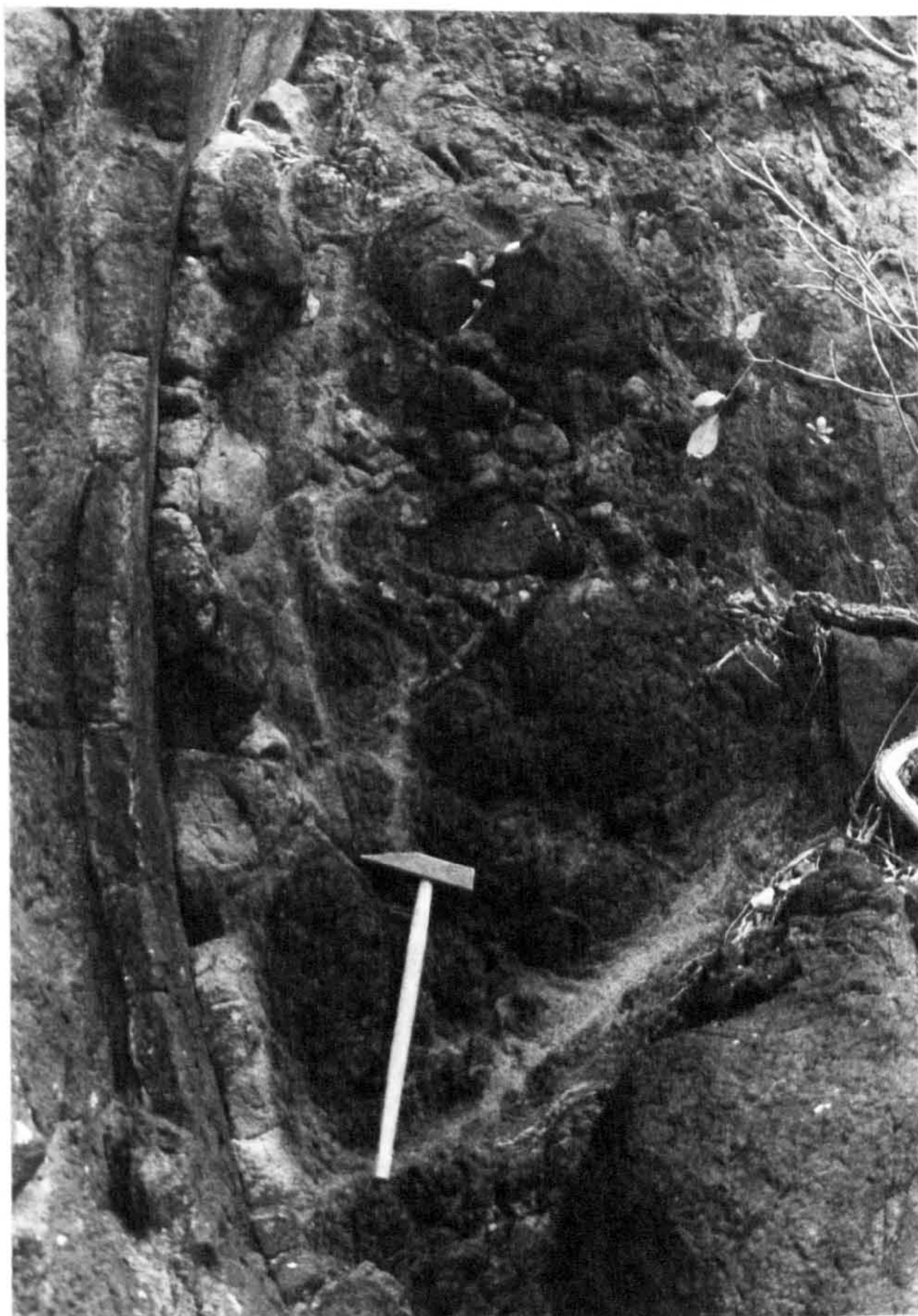




Plate 17

Sheared and jointed clinopyroxene-phyric lava flows,  
Flamingo Bay.







suggested here. Further support for the hypothesis of local faulting may be found in the exposure of Lower and Middle Tertiary basement rocks in the St. Johns valley.

The southern Annandale Falls, at an altitude of 200 m, 5 km northeast of St. George's (Fig. 15 ), are composed of southeasterly dipping shales and silts of the Tufton Hall Formation (Plate 15 ). Part of the outcrop is extensively sheared and brecciated. Large blocks of shales and siltstones are incorporated in a matrix of more calcareous lithology. At Tempe Parnassus, 1 km east of St. George's, blocks of Oligocene limestone are exposed at an altitude of 50 m. Apparently overlying this Lower and Middle Tertiary basement are indurated reworked volcanics. These are well exposed at Snug Corner, 1 km southwest of Annandale Falls (Plate 16 ). These volcanics are probably associated with the same general period of activity as Southwest Grenada.

Thus it appears that uplift of the basement has taken place in the St. Johns valley. This may be associated with faulting both before and after the activity of the Mt. Maitland centre, and is in detail unlikely to be simple movement along a single fault.

On the coast of Flamingo and Dragon Bays a series of basalt flows is exposed (Fig. 15 ). Most of these flows are massive, but one exposure reveals curious shear planes apparently representing continued movement after solidification of some of the lava (Plate 17 ). In this area there is a gradual transition in the basalt flows, approximately related to topographic height,

from undersaturated to saturated compositions. The transition appears to be the general case for this centre for the ultra-basic flow at Mt. Gay is succeeded at greater elevations on Mt. Maitland by pyroxene-phyric lava flows of greater silica content.

The centre of volcanic activity appears to have been located somewhere in the vicinity of Mt. Maitland and Sinai. A series of flows and pyroclastic deposits of predominantly basaltic composition were erupted in the Upper Pliocene to Lower Pleistocene from this centre.

#### 6:6 Mt. Granby - Fedon's Camp centre

##### 6:6:1 Introduction

The Mt. Granby-Fedon's Camp centre forms the high ground in the middle of the island of Grenada (Fig. 8). It is probably composed of the products of several eruptive vents that are no longer recognisable. However, lava flows radiate from Mt. Granby (720 m), Fedon's Camp (820 m) and Mt. Qua Qua (760 m), and are treated in this account as belonging to a single, if composite volcanic structure. Some flows have been dated at 0.9 m.y. (J. Briden pers. comm.). The dominant direction of flow of the lavas was westwards, where the sea cliffs and deep river valleys expose examples of the repeated eruption of basalt and andesite magma. The importance of this volcanic behaviour is the cyclical nature of the transition from undersaturated to oversaturated compositions. In general there appears to have been a shift southwards in source origin of the flows, probably reflecting the



Plate 18

Current-bedded reworked volcanics, Dothan.

Plate 19

Andesitic and basaltic air-fall material, Dothan.







migration of the main eruptive vents in time. In the following sections, the more interesting field details are described followed by a brief summary of the volcanic history of the centre. The variations of chemical composition of the centre will be discussed later (p. 130).

#### 6:6.2 Details of field exposures

Reworked pyroclastic deposits form an important component of the area. The deposits are widespread and appear to represent some of the earliest activity of the centre. At Dothan, 4 km west of Mt. Granby (Fig. 15 ), a sea cliff 70 m high is formed predominantly of these secondary fragmental deposits. There are examples of current bedding on a major scale between units (Plate 18 ) and on a fine scale within a thin layer. Graded and ungraded beds containing an assortment of different size fragments of a wide variety of composition are present. Grossly unsorted heterogeneous material probably represents mudflow-type deposition. Some thin horizons that display homogeneity of composition and lateral continuity appear to be primary airfall. Basaltic ash and andesitic pumice horizons are exposed (Plate 19). Cumulus plutonic blocks are also common in some beds. The range of mineralogical composition of these blocks is similar to those found in southwest Grenada. The Dothan cliff is probably the eroded remains of an east-west ridge of high ground that deflected the younger lavas to the north and south. The more resistant nature of these flows has caused an inversion of the topography since the Grand Roy river is now removing the deposits forming the Dothan cliff

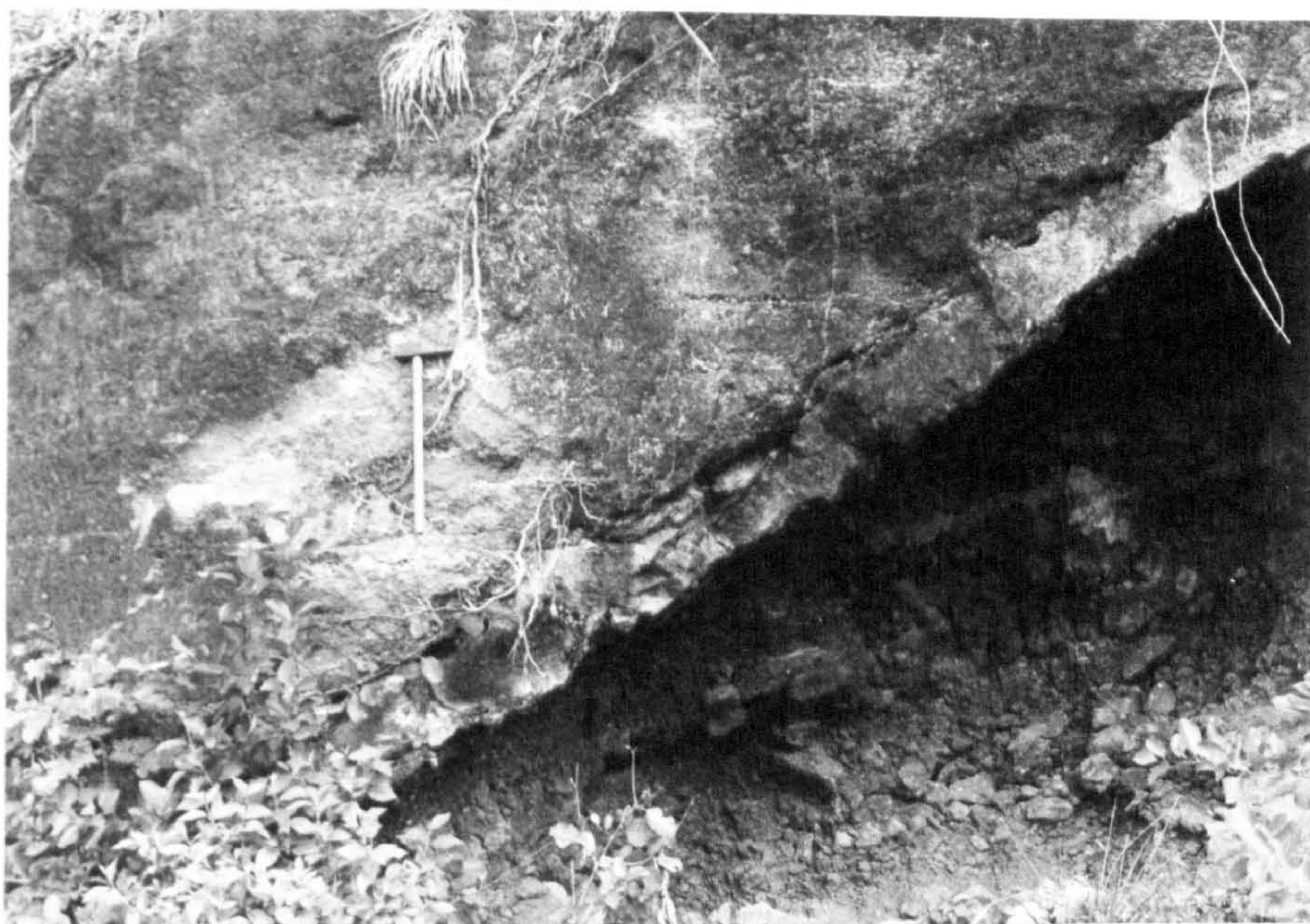
Plate 20

Steeply dipping clinopyroxene-phyric lava flows  
overlying autobrecciated material, Concord.

Plate 21

Massive andesite flow, 60 m thick, near Richmond.







The lava flows probably followed a valley floor. The present base of the flows defines the slope of that floor and since this is not graded relative to present sea level, there has possibly been a relative uplift of the area. Further evidence of uplift of the centre is the exposure at an altitude of 530 m,  $\frac{1}{2}$  km south of Mt. Granby, of indurated reworked volcanics. The degree of sorting and current bedding displayed suggests fluviatile deposition. It seems unlikely that this occurred at the present altitude. On the northern margin of the centre, the Tufton Hall Formation is exposed at a height of 350 m at Clozier Bridge, and 300 m on Dougaldston Estate (Fig. 15 ). Thus it is probable that this represents uplift of the area since the deposition of the early volcanics of the centre.

The basalt lava flows of the centre are often up to 5 km in length. Massive interiors are often columnar jointed. Inland this feature is not exposed but typical aa features are developed. Vesicular and platy flow units overlie and are covered by rubble horizons. Often quite steep ( $25^{\circ}$ ) dips are seen in the flow units which probably represent primary depositional gradients (Plate 20 ). Often interleaved between lavas are basaltic ashes, sometimes baked and reddened by overlying flows. The lengths of andesite flows of this centre are comparable with basalt flows but thicknesses of up to 70 m are present in the former (Plate 21 ).

### 6:6.3 Volcanic history

A brief description of the volcanic history follows :-



Plate 22

The Grand Roy valley. Massive andesite flows cap the ridges and overlie scarp-forming basalt lava flows.







(1) The earliest activity was in the north associated with a source near Mt. Granby. A series of basalt and andesite lavas were erupted together with fragmental pyroclastic material. Solid flows are preserved near Mt. Nesbit and Palmiste. However, much of the area now consists of reworked material. On high ground this is usually mudflow but the local basement volcanics are all fine-grained, fragmental deposits.

(2) The eruptive source moved southwards towards the vicinity of Fedon's Camp. A series of pyroxene-phyric basalt lavas flowed from this source, controlled in direction by the eroded topography of the older Mt. Granby volcanics. A sequence of these lavas, greater than 80 m in total thickness extended down the Grand Roy valley area. Intervening layers of basaltic ash show explosive activity was also associated with the eruptions.

(3) After a period of erosion, the character of the compositions erupted changed. Basalt flows followed by a series of massive andesite lavas were erupted, partially obscuring the older pyroxene-phyric basalt lavas. The eroded andesite lavas form the prominent scarp features of the Grand Roy valley (Plate 22 ).

(4) The locus of source activity moved southwards probably somewhere nearer Mt. Qua Qua. Renewed eruptions of pyroxene-phyric basalt lavas occurred gradually changing to lavas of andesitic composition. The sequence is exposed south of the Concorde valley and near Richmond and Brizan. Infilling of this



Plate 23

The andesite dome forming the summit of Fedon's  
Camp.





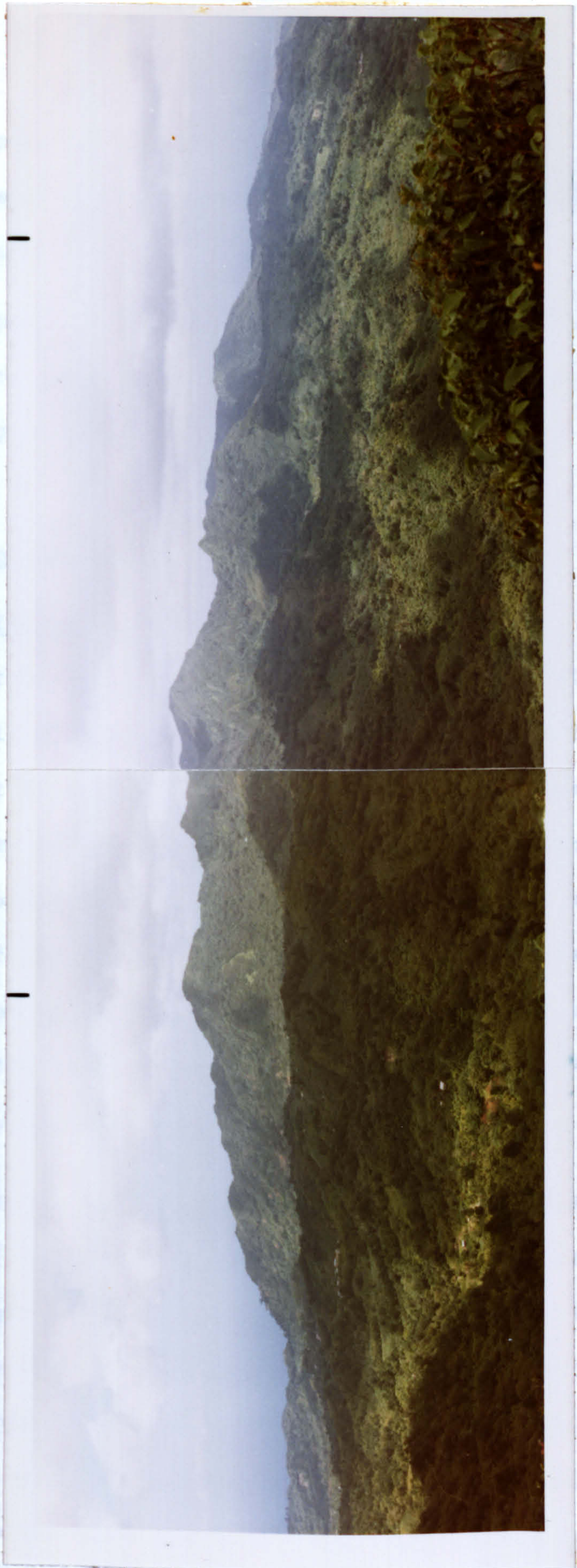


Plate 24

Panorama of Mt. St. Catherine from South East  
Mountain,









vent is probably represented by the andesitic and dacitic lava flows and domes forming the present summits of Fedon's Camp and Mt. Qua Qua (Plate 23).

(5) The final phase of activity before erosion modified the topography of the centre was an outpouring of basalt lava. This forms a capping on the western ridges of Mt. Qua Qua.

#### 6:7 Mt. St. Catherine centre

##### 6:7.1 General features of the centre

The Mt. St. Catherine centre is the youngest major volcanic structure on the island of Grenada. No age dates have so far been obtained but it is probably of Pleistocene to Holocene age. The centre forms a massif in the northern half of the island (Plate 24). The summit of Mt. St. Catherine at 910 m is also the highest point of the island. It is situated on the western rim of a crater, approximately  $1\frac{1}{2}$  km in diameter that has been breached to the southeast (Fig. 16). An andesite dome, mantled by a boulder scree occupies the centre of the crater.

Surrounding Mt. St. Catherine are a number of hot springs (Fig. 16). Most of these are sulphurous, but none are currently (1972) emitting water at temperatures greater than  $50^{\circ}\text{C}$ . Table 3 lists the temperatures of these springs in 1971-72 and recorded temperatures by previous workers. Since the first records were made, there appears to have been a general decrease in spring temperatures. It is possible that this represents a waning heat supply but may be due to unknown variables such as annual pre-



Fig. 16

Hot spring localities in northern Grenada.

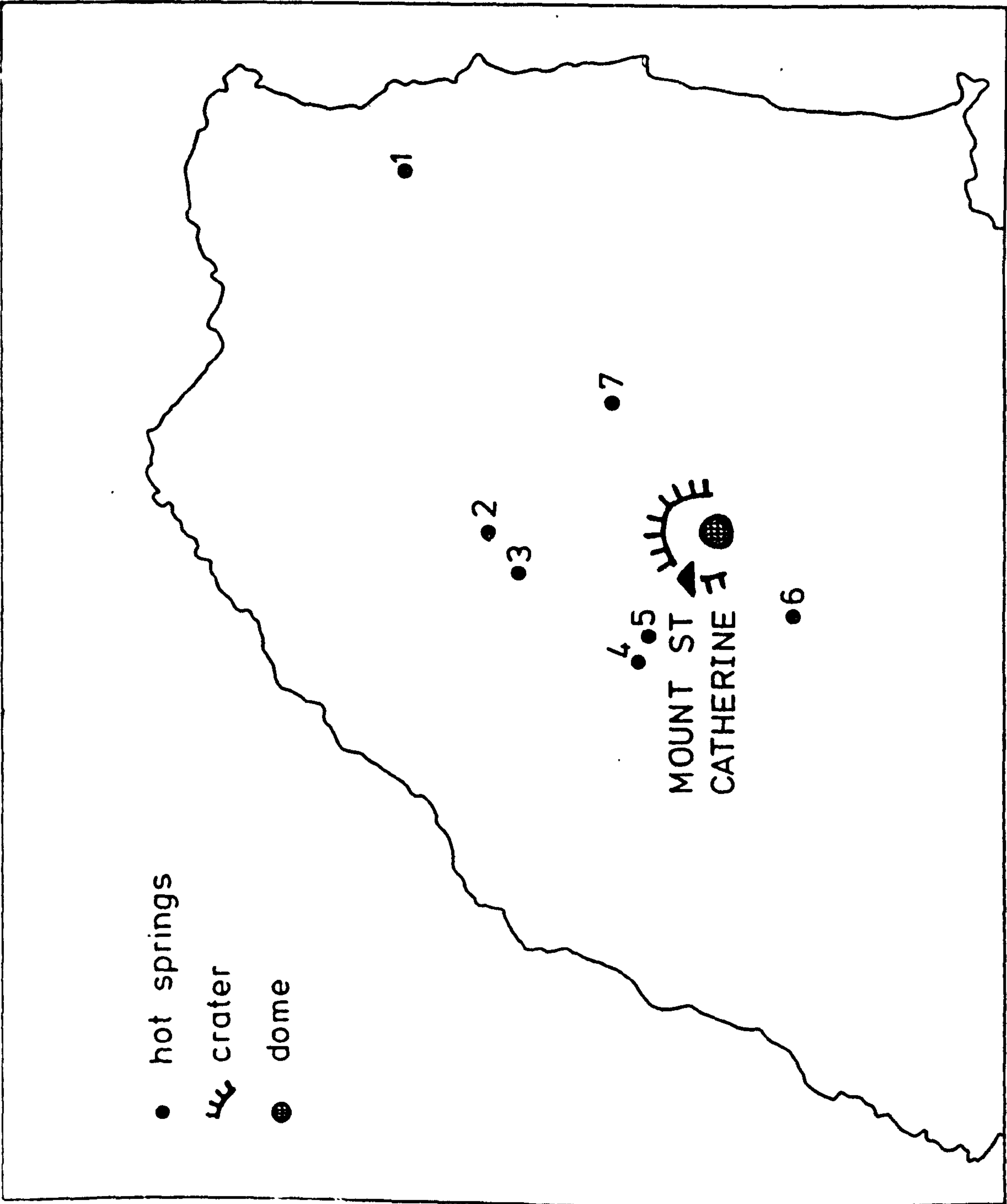




TABLE 3

Recorded temperatures of Hot Springs  
in Grenada.  
Numbers refer to localities in Fig. 16.

<u>Hot Spring</u>		<u>Temperature (°C)</u> <u>and date of measurement</u>				
<u>No.</u>	<u>Locality</u>	1896	1903	1965	1971	1972
1	Riviere Sallee			31.9	32.0	31.9
2	Bellevue Mt.				50.0	50.4
3	Mt. Ellington(2)				37.5 41.0	37.5 39.7
4	Tufton Hall (upper)		48.9	37.4	36.4	36.0
5	Tufton Hall (lower)				36.5	36.1
6	Lavez Chaud			34.7	35.5	35.6
7	Peggy's Whim	44.4		38.8	39.5	39.4

Dates from Harrison (1896), Sapper (1903) and  
Robson and Tomblin (1966).

cipitation and cyclical temperatures. Several of the springs issue from massively jointed igneous rock. However, a blanket of sulphurous tufa obscures the bedrock at Riviere Sallee and in Peggy's Whim the basement is indurated mudflow material.

The Tufton Hall Formation outcrops at scattered localities around the Mt. St. Catherine centre (Fig. 13 ). Elevation of this basement is believed to have occurred during the evolution of the Mt. Granby-Fedon's Camp centre, and may have been further uplifted during the activity of Mt. St. Catherine. The early distribution of lava flows associated with Mt. St. Catherine was predominantly eastwards. It appears that the Tufton Hall Formation formed an upstanding area in the west of the island that initially deflected the flows towards the east. As the volcanic structure increased in height, the Tufton Hall Formation was over-ridden by lava and pyroclast flows.

Unlike the southern centres of activity, there is a predominance of andesitic and dacitic compositions exposed at surface. In general there does not appear to have been as many repetitions of the sequence from undersaturated to oversaturated composition as in the Mt. Granby-Fedon's Camp centre. However, the range of compositions is similar and will be discussed later (p. 130).

The terrain below 350 m altitude on Mt. St. Catherine is generally covered by a mantle of secondary fragmental deposits. The thickness of this material varies greatly but cliffs 70 m



Plate 25

Slump features in clay-grade, plant-bearing, reworked volcanic deposits, Belmont.

Plate 26

Mudflow deposits on the western summit scarp of Mt. St. Catherine.







high are exposed at Waltham and Victoria on the Northeast coast (Fig. 14 ). Characteristics similar to the Dothan cliff are displayed. At Belmont, 5 km northeast of Mt. St. Catherine, 40 m of predominantly fine-grained, reworked ash and pumice is exposed. Many of the beds are of clay grade and display current bedding. Some contain non-carbonised plant remains and slump features (Plate 25 ). Andesitic pumice and basalt fragments collected from sequences like this correspond closely in composition with material occurring on the higher ground of Mt. St. Catherine.

On the dissected northern and eastern slopes of the centre, near Plaisance and Montreuil (Fig. 14 ), outcrops of primary airfall material, dominantly andesitic in composition are exposed. Usually this material has been removed from the higher parts of the island. These primary deposits are thinly-bedded and laterally continuous showing occasional bomb impact features. The source of this material may have been Mt. St. Catherine or the younger explosion craters. The activity of the latter was dominantly basaltic so it is more likely that the source of this ash was Mt. St. Catherine.

The summit region of Mt. St. Catherine appears to be formed of deeply weathered andesitic lava. However, a recent cliff fall to the west of the summit has exposed mudflow material (Plate 26 ). It is probable that the greater proportion of the highest ground of the centre is formed of these deposits since relatively fresh, massive rock is rarely exposed.



### 6:7:2 Volcanic history of the centre

A brief account of the evolution of the Mt. St. Catherine centre follows.

(1) The earliest activity was associated with the region in the vicinity of Plaisance and Malagon. Only scattered exposures of the early basalt flows are available, for example at Riviere Sallee and Mt. Ellington. The extent of these flows was probably originally more widespread. More acidic lava flows ranging from andesite to dacite in composition were deposited on top of these early flows. As the volcanic pile grew in height, a return to undersaturated compositions occurred. Basalt flows including a series of pyroxene-phyric lavas were erupted, forming the Crayfish area and flows also to the east around Peggy's Whim.

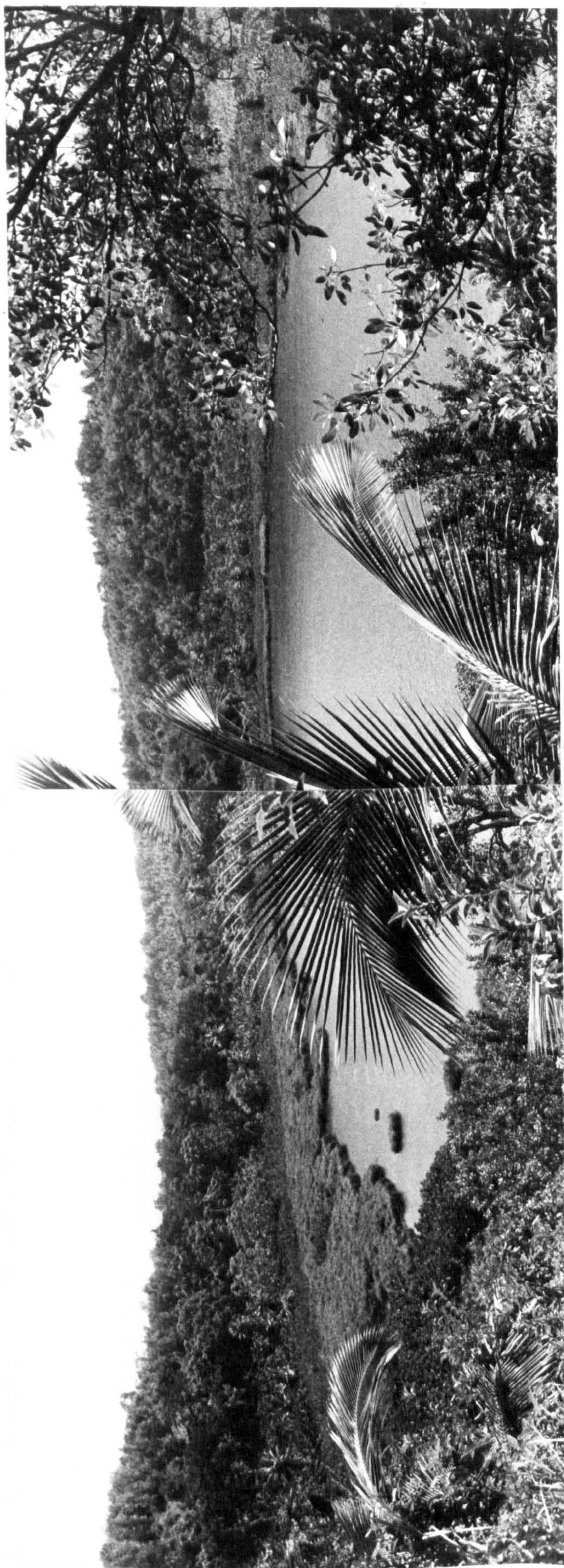
(2) The centre of activity moved southwards, probably near to the present crater of Mt. St. Catherine. The area to the northwest of this centre is dominated by a thick sequence of andesitic and dacitic lavas and pyroclast flows, forming the St. Marks Mountain and local bedrock of the rivers. Dacitic flows are inferred to overlies the Tufton Hall Formation in the area around Tufton Hall and Belair estates. The Pyroclast flows forming the western ridge of Mt. St. Catherine reach the sea north of Gouyave. These represent the best preserved, and probably most voluminous outpourings of this type of activity on Grenada. Contemporary andesitic and dacitic flows formed



Plate 27

Interior of Lake Antoine explosion crater.







the eastern ridges of the centre above St. Johns and Paraclete. The climax of activity was probably the partial infilling of the crater by the dome andesite. Explosive activity and resulting fragmental deposits probably constituted a major proportion of the erupted products, but erosion and lack of exposure has prevented the correlation of this activity with the solid flows.

#### 6:8 Explosion Craters

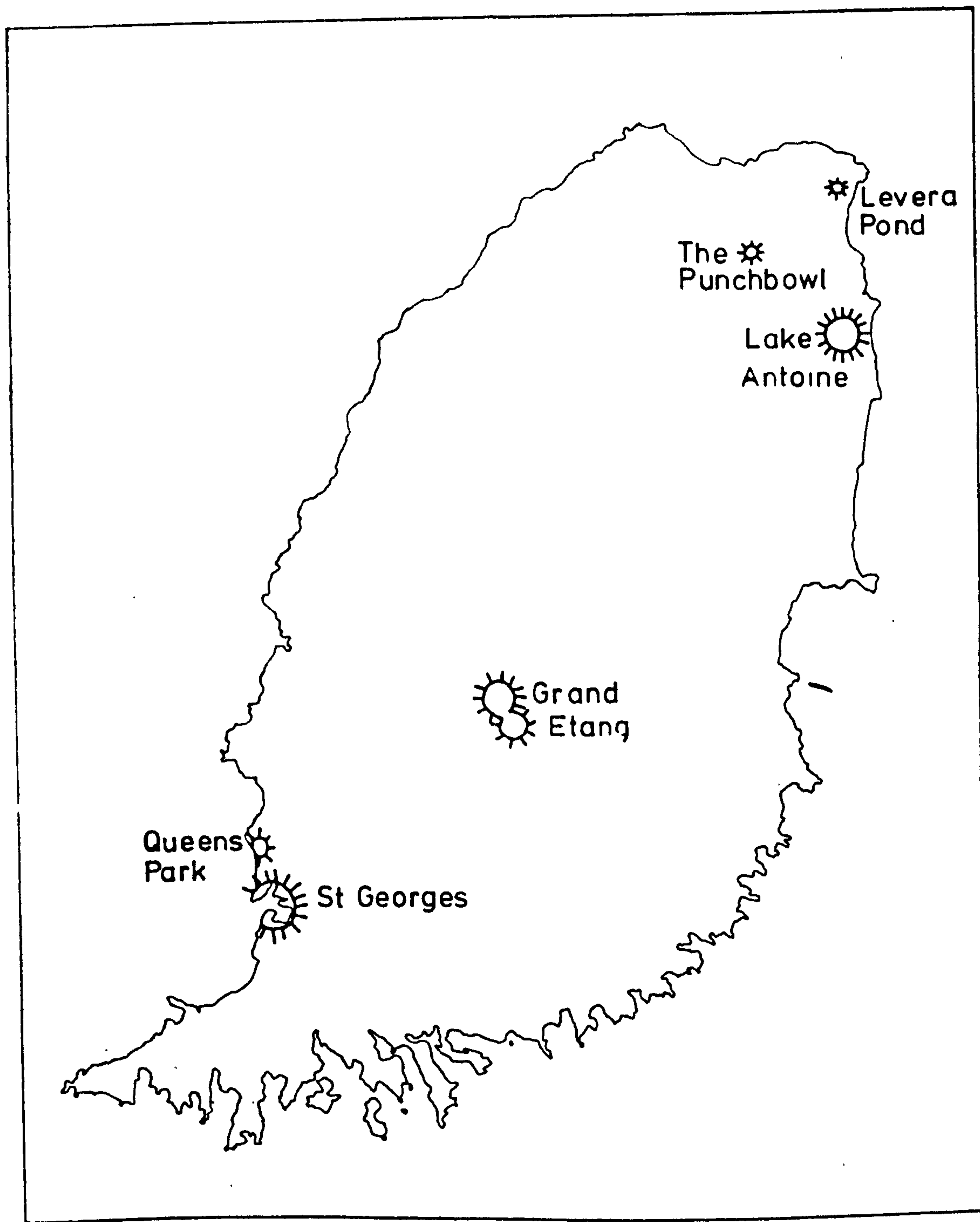
The most recent activity on the island has been explosive with the development of several small ( $< \frac{1}{2}$  km diameter) craters. The distribution of these craters is illustrated in Fig. 17. Some are better preserved morphologically than others, but most appear to have erupted silica-undersaturated alkali basalt scoria and ash together with a variety of basement and wall-rock fragments. A crater associated with aa lava flows occurs on the island of Ile de Caille, 7 km north of Grenada. In general however, lava flows are not associated with the recent explosion craters.

The best preserved of these craters is Lake Antoine in the northeast of the island (Plate 27). A lake 500 m in diameter occupies the floor of the crater surrounded by a low rim 60 m high of ejected blocks, scoria and ash. The overall morphology is similar to Maars (Ollier, 1967) and usually associated with the explosive activity of hydrous magma or contact between magma and local groundwater. The nature of the explosive activity of Lake Antoine crater is well exposed in cliff exposures to the east. These exposures are discussed in some detail after a brief summary

Fig.17

Locality map of explosion craters.





of the other craters of Grenada.

The Punchbowl crater, 3 km northwest of Lake Antoine is of small diameter (100 m) and remarkably steep-sided. The walls of the crater are up to 30 m high sloping at angles of up to 60°. The majority of the ejected material forming these walls appears to be allocthonous wall-rock fragments but weathered basaltic ash is also present in places. The twin craters of the Grand Etang and its dry neighbour are situated between the volcanic massifs of Mt. Qua Qua and Sinai at an altitude of 500 m. Most of the ash associated with these craters has been deeply weathered to form a lateritic soil. Green Island, one of the trio of small islands off the northeast coast of Grenada is unusual in that the volcanic activity has been entirely andesitic in composition. A sequence of andesitic ash and scoria representing several periods of explosive activity has been uplifted and intruded by an andesitic dome. The dome appears to occupy the site of a crater which, prior to its infilling by the dome, erupted several andesite lava flows towards the east. Green Island may be a more recent example of the type of activity that formed the crater of St. Georges. The capital of Grenada occupies the northern rim of a series of coalescing explosion craters. The weathered appearance of the andesite domes forming the hill of Fort St. George and Fire Station Point, and the weathered fragmental deposits surrounding these domes suggests the activity preceded the formation of the craters described above. A better morphologically preserved crater that erupted alkali basalt scoria and ash is located at Queens Park to the north of St. Georges (Plate 28). The ejecta is being quarried for a construction aggregate and is present in scattered



exposures as far north as Mt. Moritz.

Apart from the preserved craters, there are localised deposits of coarse scoria and ash of fresh appearance that are not associated with any recognisable crater form. The alkali basalt composition and unweathered aspect of these deposits suggests however, that they are associated with the same type and period of activity as the craters already described. Scattered exposures of basalt scoria and ash occur at the south end of Grand Anse Bay, Plaisance Estate and Grenville (see Fig. 15 ). The deposits at Grenville include small rounded cumulate blocks formed of olivine, clinopyroxene and feldspar. Finally, it is possible that Levera Pond in the north-east of the island occupies the floor of another explosion crater.

The nature of these primary fragmental deposits are best exposed on the north-east coast of Grenada. In general the fall sequence thickens southwards from Grenada Bay approaching the assumed source in the Lake Antoine crater. In addition, the maximum size of ejected blocks also increases up to 50 cm in diameter. The sequence contains examples of several pulses of explosive activity represented by numerous repetitions of size-graded layers of ash, interspersed with layers of larger scoria and bombs. At the southern end of the High Cliff Point exposure, the earliest horizons are predominantly of alkali basalt scoria and ash, but rock fragments of andesitic composition and blocks of pre-consolidated (older ash) are also present. Some of the layers have suffered bomb

Plate 28

The Queens Park explosion crater.

Plate 29

Alkali basalt bomb, High Cliff Point.



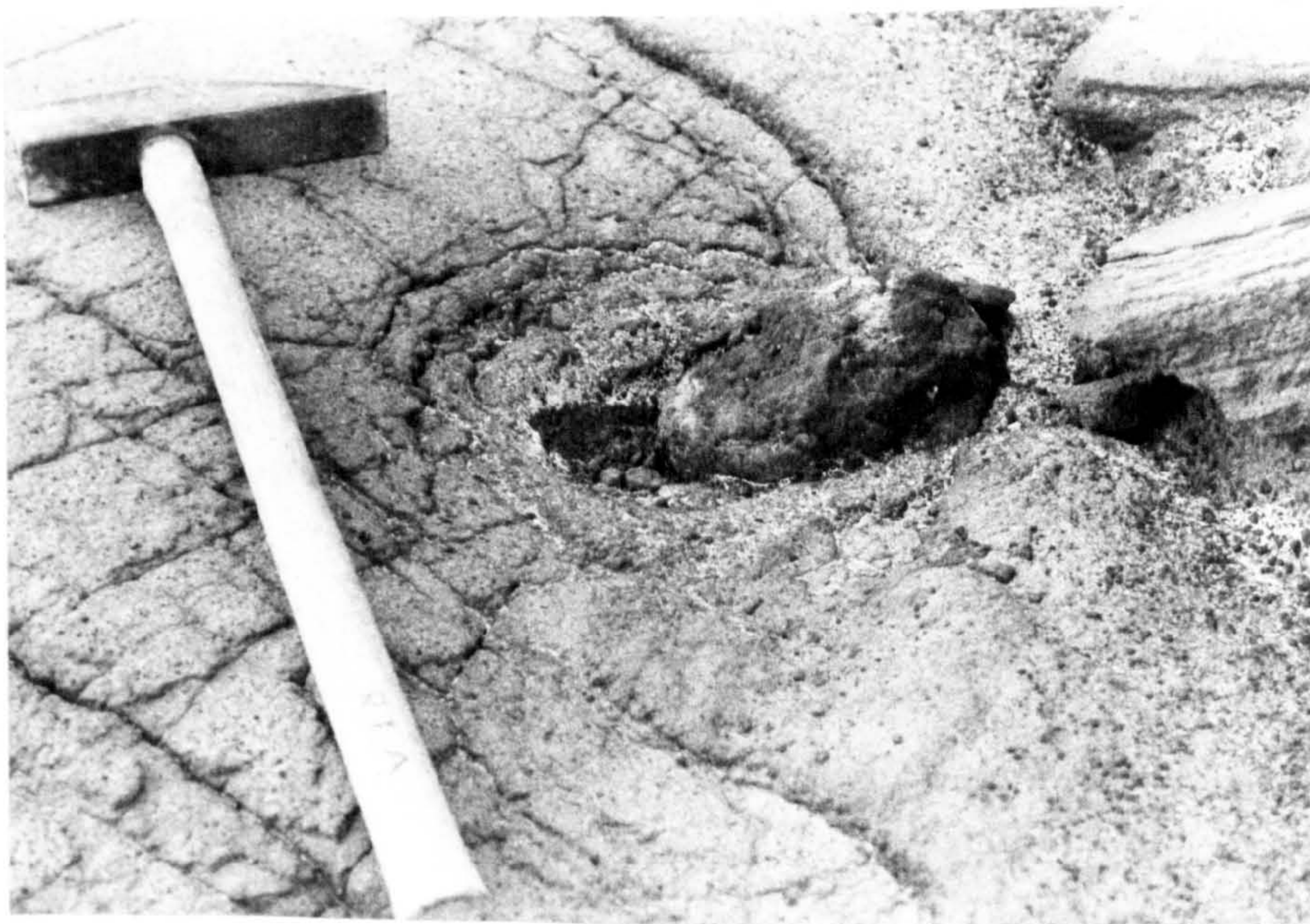




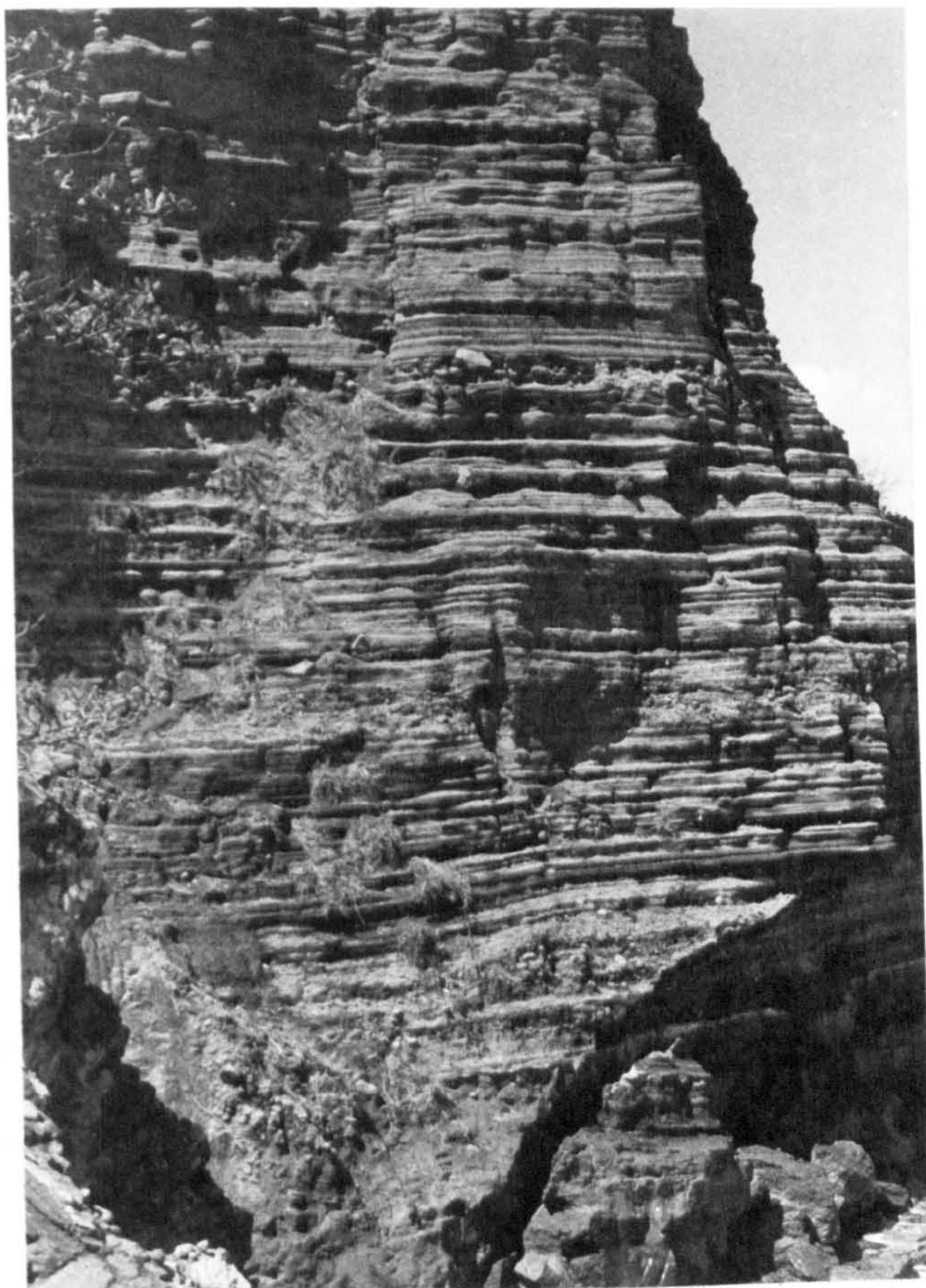
Plate 30

Ash & scoria, High Cliff Point.

Plate 31

Contorted ash beds, High Cliff Point.







impacts with resulting distortion of the bedding (Plate 29).

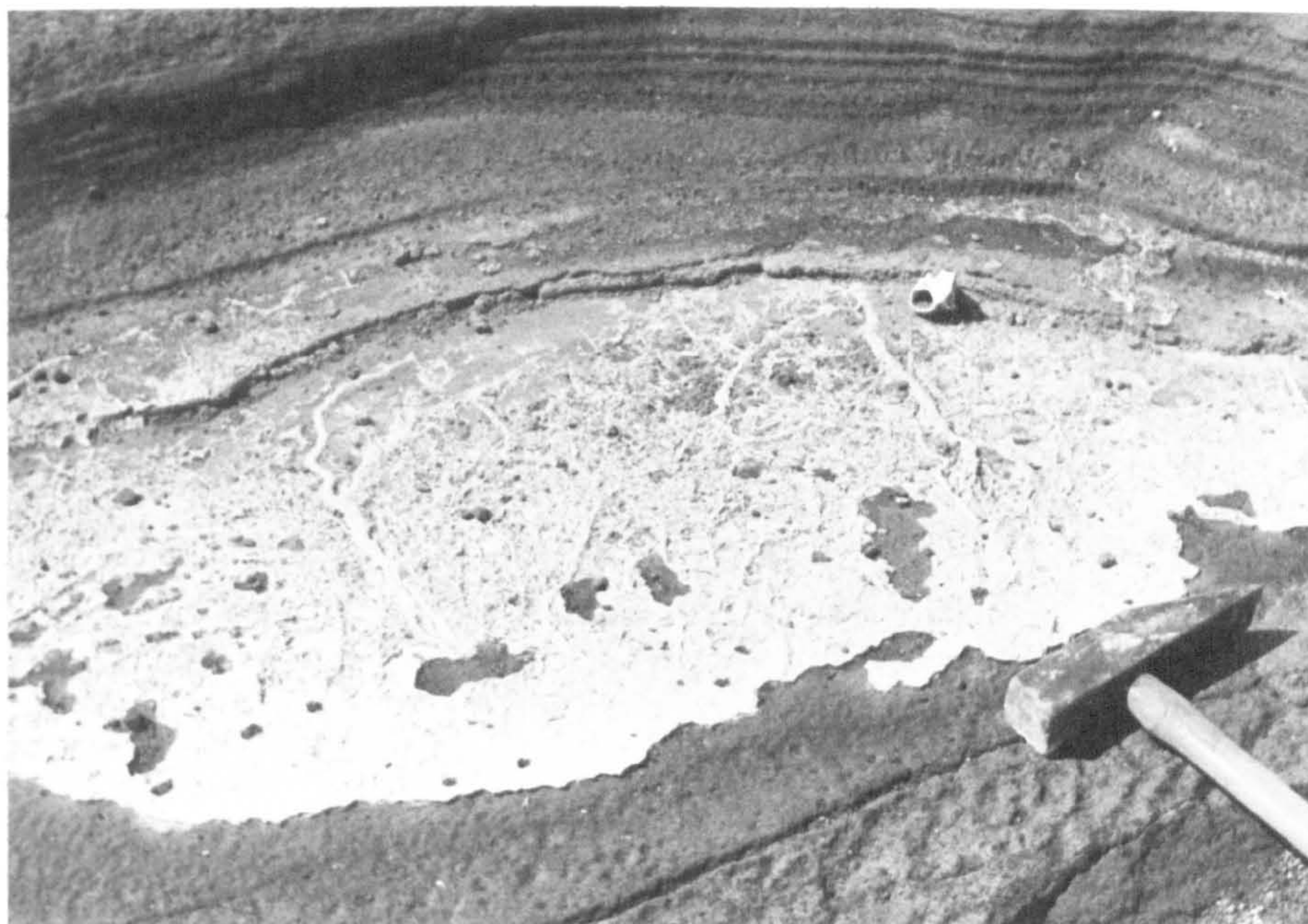
The finely size-graded layers of this sequence grade upwards into a much more heterogeneous bed that is faulted and slumped. Fragments of a wide range of rock types are present, both rounded and angular, often current and chaotically bedded. This horizon grades upwards into a thin (50cm) airfall horizon of alkali basalt scoria and ash succeeded by a weathered pumiceous andesite horizon. The whole of this sequence is at least 8 m thick and the base is not seen. It is also much cut by faults and small graben-like features are developed. The andesite pumice horizon represents a cessation of explosive activity for it was colonised by trees and plants whose roots seam the reddened and weathered pumice. Some of the trees are preserved as hollow, silicified trunks up to 5 m in height and 50 cm in diameter. The trees are buried by the overlying ash and scoria layers forming High Cliff Point itself (Plate 30 ). Some trees collapsed and were buried by the initial coarse agglomerate and scoria in a horizontal position, whilst others have remained vertical. In this airfall sequence (40 m thick) there are at least four major horizons containing large ( < 50 cms) basaltic and andesitic bombs, indicating periods of more intensive explosions. The scoria and ash layers are probably primary airfall for the most part since the thin laminations ( < 2 cm) are laterally continuous and good size grading is exhibited. However, some units have undoubtedly suffered reworking since sole marking, fossil mudcracking, current and contorted bedding is present (Plate 31 ). Sheets of carbonate are also widespread between some of the ash horizons. These contain what appear to be 'worm' casts, suggesting exposure to



Plate 32

Horizontal calcite sheets containing worm casts  
interleaved with volcanic ash and scoria, High Cliff  
Point.







marine conditions (Plate 32 ). However, some carbonate is present as vertical, ramifying sheets probably of fumarolic nature due to post-depositional migration of groundwater through the ash and scoria.

Northwards of High Cliff Point the sequence is the same but the conglomeratic horizon near the base of the High Cliff Point exposure varies considerably in thickness. This apparently reflects infilling of a pre-existing undulating topography, primarily by fluviatile deposition. Some of the graded and cross-bedding of these deposits may be due to base surge phenomena (Moore, 1967). Crowe and Fisher (1973) have described current bedding due to deposition from horizontally ejected pyroclastic material. However, many of the depositional features displayed at High Cliff Point can be attributed to fluviatile conditions.

It is apparent that the unconsolidated (nature of the) fragmental deposits associated with these explosion craters are readily erodable. It is unlikely that crater morphologies are preserved for any great length of time. Thus it is quite possible that explosion craters and explosive basaltic activity have been a characteristic feature of Grenada vulcanicity and are not solely a recent phenomena.

#### 6:9 Summary of Grenada Vulcanicity

The repeated eruptions of silica-undersaturated basalt magma is the most important feature of the vulcanicity of Grenada. In addition there is an intimate field relationship with silica-saturated calc-alkaline andesites and dacites. The geochemical



association of basaltic and calc-alkaline compositions is discussed in the following chapters. The most recent activity has been the explosive eruption of alkali basalt magma. This confirms that the geochemical evolution of the island has not been a single one-way process in time from undersaturated to oversaturated compositions but has been repeated many times in the various volcanic centres.

The total volume of erupted volcanic products appears to be considerably less than the other major islands of the Lesser Antilles island arc. The undisturbed volcanics overlying the Lower and Middle Tertiary basement of Grenada are nowhere greater than 900 m in thickness. In comparison the undisturbed Upper Tertiary and Quaternary volcanics of Dominica are at least 1500 m in thickness (K. Wills, pers.comm., 1973). This may be directly relevant not only to the problem of volumetric proportions of individual members of the calc-alkaline rock suite but also to the unusual composition of the Grenada basaltic magmas. These aspects are examined in more detail in Chapter 11.

The presence of some andesitic and dacitic pyroclast flows, domes and lava flows although smaller in total volume on Grenada than elsewhere in the arc are similar to the erupted products of other islands in the Lesser Antilles, and typical of island arcs in general. However, the presence of the undersaturated basalt lava flows seem to be a unique feature of the island of Grenada and the nearby Grenadines.

Appendix III contains a brief analysis of the likelihood



of future eruptions occurring on the island and possible danger zones for populated areas.

## CHAPTER 7

### GEOCHEMISTRY I

#### Classification of Volcanic Rock Series and the Picrites and Basalts of Grenada

##### 7:1 Classification of calc-alkaline rock series

The original use of the term 'calc-alkaline rock series' (Holmes, 1920; Peacock, 1931) was to distinguish those rocks characterised by silica enrichment relative to alkalis. In other words the gabbros, diorites, granodiorites and their volcanic equivalents typical of active continental margins and island arcs could be distinguished from feldspathoidal alkaline rocks. Subsequently, with the identification of the 'tholeiitic trend' towards iron-enrichment of magmas (Wager and Deer, 1939), the calc-alkaline rock series has been distinguished by the lack of this magmatic trend.

The nature of the parental magma compositions of the calc-alkaline rock series has to be studied initially in the context of basalt magma classification. Kennedy (1930) and Tilley (1950) identified two 'primary' types of basalt magma called alkali olivine and tholeiitic respectively. In general, the calc-alkaline rock suite was regarded as being derived by fractional crystallisation of tholeiitic basalt magma. The tholeiitic and calc-alkaline trends of differentiation may be distinguished by means of an AFM diagram (a triangular oxide plot of total alkalis vs total iron vs magnesium). Fenner (1926) regarded the tholeiitic trend as the normal fractionation sequence of tholeiitic basalt magma, whilst Bowen (1928) maintained the calc-alkaline trend was more usual.



Kuno (1950) proposed a third 'primary' magma called 'high-alumina basalt', which he regarded as the parental magma of the calc-alkaline rock series. However, Kuno (1968) has also suggested that the calc-alkaline trend could be established during fractional crystallisation of tholeiitic magma under conditions of early precipitation of magnetite, or by sialic contamination of alkali olivine basalt magma. The zonation of magma types across the Japanese volcanic belt is from tholeiitic through high-alumina to alkali olivine basalt with increasing distance from the trench. The most voluminous andesites and dacites occur associated with high-alumina basalt. Wilkinson (1968) also suggested that the parental basalt magma of the calc-alkaline rock suite typical of island arcs and active continental margins is high-alumina basalt. However, Jakes and Gill (1970) have restated the evidence for the development of a calc-alkaline trend by fractional crystallisation of tholeiitic basalt in island arcs. The voluminous eruptions occurring at early stages in the evolution of the volcanic arcs of the south-west Pacific are characterised by tholeiitic basalt magma and calc-alkaline derivatives. Similarities exist between the composition of these tholeiitic basalts and 'oceanic tholeiite' (see p. 249 ). Jakes and Gill (1970) propose the term 'island-arc tholeiitic series' to distinguish the type occurrence of the former basalt magma.

After an extensive review of the geochemical data, Irvine and Baragar (1971) have suggested a classification of the volcanic rocks that adequately separates rock associations typical of most tectonic environments. Irvine and Baragar specifically state that

the scheme is not designed as a genetic classification, but serves to identify the common rock associations. However, in the following discussion the discriminant features proposed in this classification are used to illustrate the gradational nature of the basaltic compositions of the Grenada calc-alkaline rock series.

There is a considerable variation in degree of crystallinity of the basalt compositions of Grenada ranging from microphyric to highly porphyritic. A consistent modal classification is accordingly difficult to apply. Evidence is presented later (p.107 ) to show that the porphyritic rocks are representative of liquid compositions and not enriched in particular phases by cumulus processes. Thus, a generalised normative classification is proposed in order to group the compositions for descriptive purposes, and for comparison with other volcanic suites.

The analyses of the rocks were completed by X-ray fluorescence, by which method total iron only is determined. Details of the methods of geochemical analysis are contained in Appendix I . During calculation of the normative compositions, a fixed oxidation ratio of 1:3 ( $\text{Fe}_2\text{O}_3:\text{FeO}$ ) has been assumed. The least oxidised rocks of Grenada have a similar ratio (Sigurdsson et al., 1973), and it is suggested that only oxidation processes have been effective near, or at the surface environment. Coombs (1963) employed a similar oxidation ratio in a normative classification of volcanic rocks. Reduction of reported oxidation states by Coombs of  $\text{Fe}_2\text{O}_3:\text{FeO}$  to 1:3 produced a much tighter distribution of analyses in the normative projections employed, suggesting oxidation of the rocks was responsible for the original scatter. The effect of



TABLE 4

Chemical compositions of 'primary' magma  
types in Japan, after Kuno (1968)

	<u>BASALT</u>		
	<u>3. Tholeiite</u>	<u>2. High-Alumina</u>	<u>1. Alkali Olivine</u>
SiO <sub>2</sub>	48.73	48.10	47.95
Al <sub>2</sub> O <sub>3</sub>	16.53	16.68	16.46
Fe <sub>2</sub> O <sub>3</sub>	3.37	3.88	4.40
FeO	8.44	7.75	5.86
MgO	8.24	8.89	8.99
CaO	12.25	10.48	10.46
Na <sub>2</sub> O	1.21	2.51	2.72
K <sub>2</sub> O	0.23	0.46	1.09
TiO <sub>2</sub>	0.63	0.73	1.09
P <sub>2</sub> O <sub>5</sub>	0.10	0.15	0.41
MnO	0.29	0.54	0.21
Total	100.02	100.17	99.64

higher oxidation states is to move the calculated normative mineralogy towards more saturated compositions. Fig.I.1 , (Appendix I ) is a graph illustrating the effect of increasing oxidation ratio on the amount of normative nepheline in the Grenada basalts. Even at high oxidation ratios of  $\text{Fe}_2\text{O}_3:\text{FeO}$  of 3:1, nepheline is still present in the norm of the most undersaturated compositions. Powder diffraction analysis and reconnaissance studies of these compositions with the electron microprobe, have shown nepheline to be present in the groundmass (see Appendix for methods used). Therefore there is also modal justification for classifying some of the Grenada basalts as critically undersaturated, but it is possible that the arbitrary oxidation ratio employed does not accurately reproduce the precise oxidation state of the basalt magmas existing during fractional crystallisation and evolution of the calc-alkaline suite.

## 7:2 Classification of the Grenada Rock Series; General Aspects

### 7:2:1 Calc-Alkaline vs Tholeiitic suites

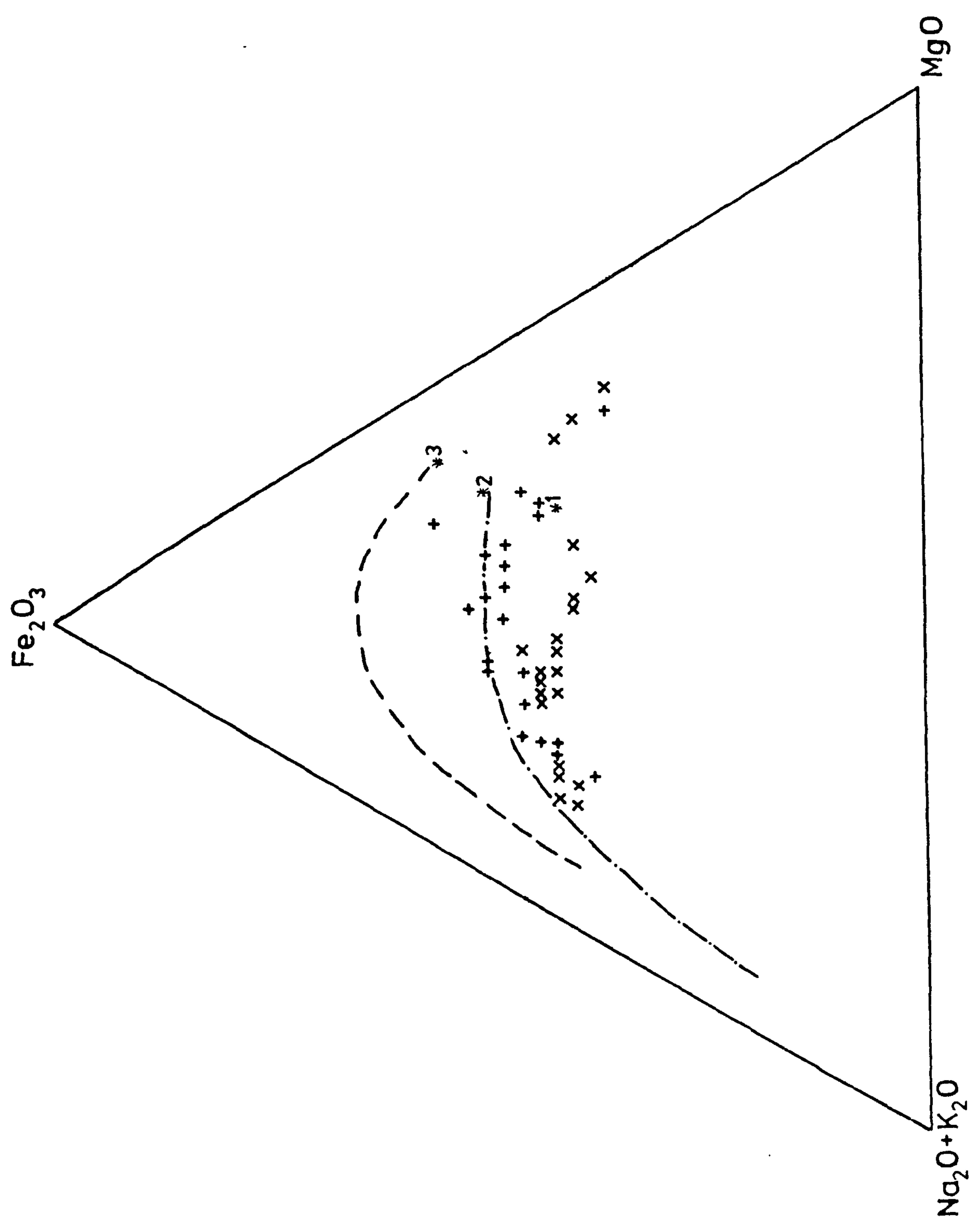
Fig. 18 is an AFM diagram showing the compositions from a single volcanic centre of Grenada (Mt.Granby-Fedon's Camp centre). A single centre has been selected for clarity. The overlap with the hypersthenic trend (calc-alkaline s.s. of Kuno, 1950) is indicated, suggesting that the lack of iron enrichment in the Grenada suite is typically calc-alkaline. The composition of magmas identified by Kuno (1968) as the primary tholeiitic, high-alumina and alkali olivine basalts in Japan are also indicated on this AFM diagram and their compositions given in full in Table 4 .



Fig.18

A-F-M diagram for the Mt. Granby - Fedon's Camp  
volcanic suite.

- x = low Sr series
  - + = high Sr series
  - .- = hypersthenic rock series of Izu-Hakone
  - = pigeonitic rock series of Izu-Hakone
- (after Kuno 1950).
- \* = 'primary' magma compositions of Kuno (1968)  
numbers refer to column headings of Table 4





### 7:2:2 Alkaline vs Tholeiitic basalt

It has been customary to distinguish tholeiitic and alkali olivine basalts on the basis of total alkali contents at equivalent silica weight-percentages. The Grenada basaltic compositions ( $< 48 \text{ wt.} \% \text{ SiO}_2$ ) are plotted in Fig. 19, where the complete overlap of the dividing line used by Macdonald (1968) to distinguish Hawaiian tholeiitic and alkali olivine basalt series may be seen. Some of the Grenada compositions are undoubtedly alkaline on the basis of modal nepheline and the presence of highly aluminous and titaniferous clinopyroxenes (p. 157), together with olivine, both as a phenocryst and groundmass phase. However, the lack of any defined trend towards increasing silica-undersaturation, the appearance of orthopyroxene and the disappearance of olivine as a groundmass phase distinguish the Grenada suite from the normal alkali olivine basalt series.

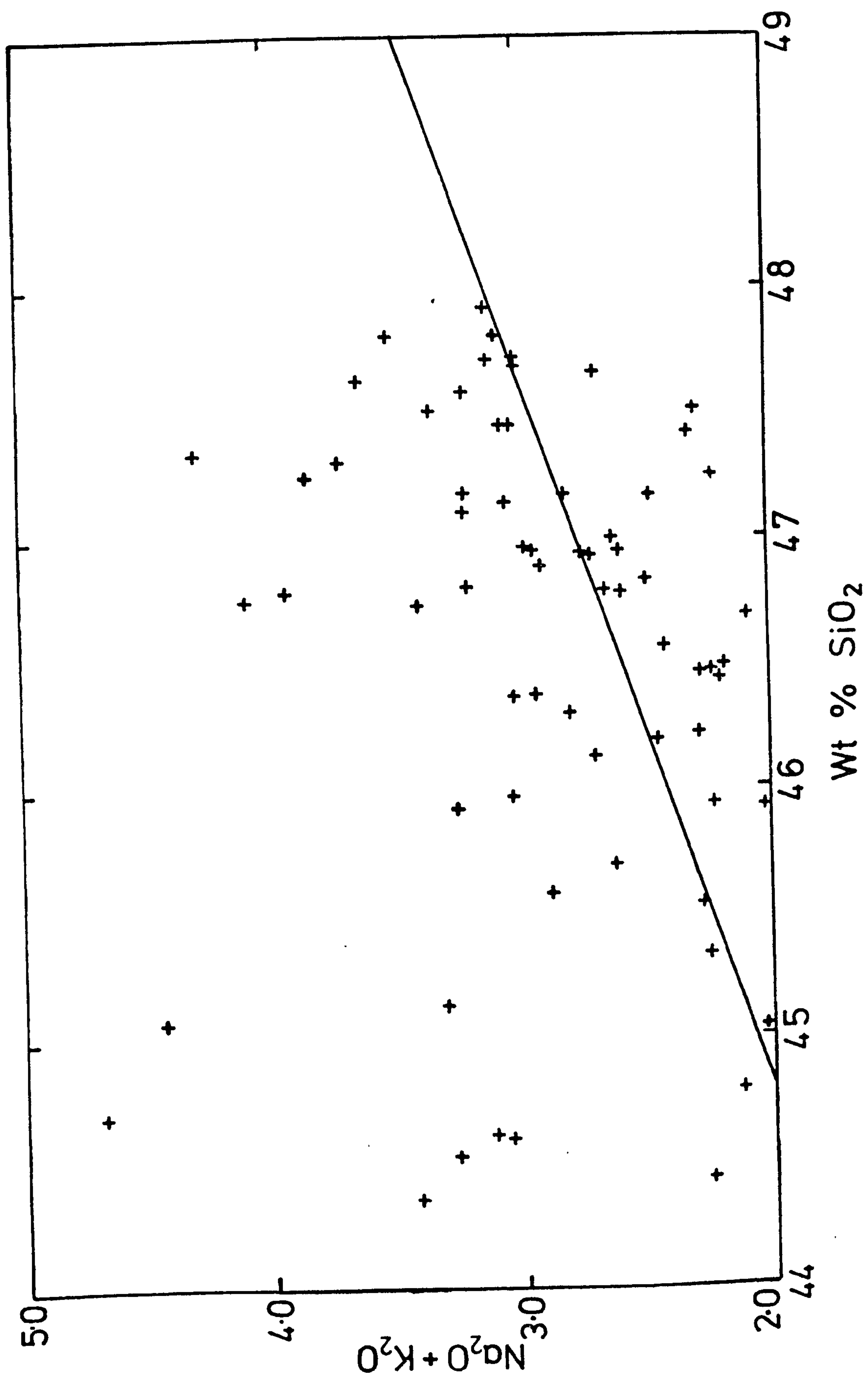
### 7:2:3 High-Alumina vs Tholeiitic basalt

The distinction between high-alumina and tholeiitic basalt has proved controversial in the past. This is due to the possibility that the highly plagioclase-phyric basalts typical of island arcs represent cumulus-enriched, and accordingly high-alumina compositions. However, the primary high-alumina basalt of Kuno (1968) Table 4, is aphyric, and represents a genuine liquid composition. Middlemost (1973) has suggested that the distinction between 'subalkaline' basalts may be made when, at a given weight-percentage total alkalis, the alumina content exceeds 16 wt.%. In this case the basalt may be termed high alumina. Irvine and

Fig.19

Alkalies-silica plot of Grenada picrites and basalts.  
The solid line is MacDonald's (1968) dividing line  
for Hawaiian tholeiitic and alkaline rocks.





Baragar (1971) propose that in a plot of wt.%  $\text{Al}_2\text{O}_3$  versus normative plagioclase feldspar ( $100 \frac{x}{k} \text{An} / \% (\text{An} + \text{Ab} + 5/3 \text{Ne})$ ), the high-alumina and tholeiitic basalts are generally clearly separated. In Fig. 20 selected analyses of Grenada basalts are presented. The complete overlap between the fields of high alumina and tholeiitic basalt magma may be observed. In general there is a tendency amongst the Grenada basalt compositions for increasing wt.%  $\text{Al}_2\text{O}_3$  with increasing  $\text{SiO}_2$  content (Fig. 27). However, even some of the most basic compositions contain more than 16 wt.%  $\text{Al}_2\text{O}_3$ . In Fig. 20 selected analyses from the islands of St. Kitts, Montserrat and St. Vincent are also plotted. These compositions project into the high-alumina basalt field. Lewis (1971) has shown that the majority of the basalts of the Lesser Antilles are of high-alumina character.

The gradational nature of the Grenada basalt compositions and the possible links between basalt magma types are discussed in Chapter 10. In order to emphasise further the manner in which the spread of these compositions transgress previous classificatory divisions, selected analyses are presented in a series of normative projections in Fig. 21. Coombs (1963) divided areas of these projections into named fields and these are included for comparison. In addition the discriminant lines proposed by Chayes (1966) to separate 'alkaline' and 'subalkaline' basalts in the Di-Ol-Hy projection are drawn. The spread of the Grenada basalt compositions across all of these classificatory boundaries may be observed.



Fig. 20

Plot of weight %  $\text{Al}_2\text{O}_3$  v normative plagioclase content of selected picrite<sup>2,3</sup> and basalt compositions.

Tholeiitic and calc-alkaline fields from Irvine and Baragar (1971). Basalt composition of 1 (Montserrat), 2 (St. Kitts) and 3 (St. Vincent) from Rea (1970), Baker (1968) and Lewis (1971) respectively.

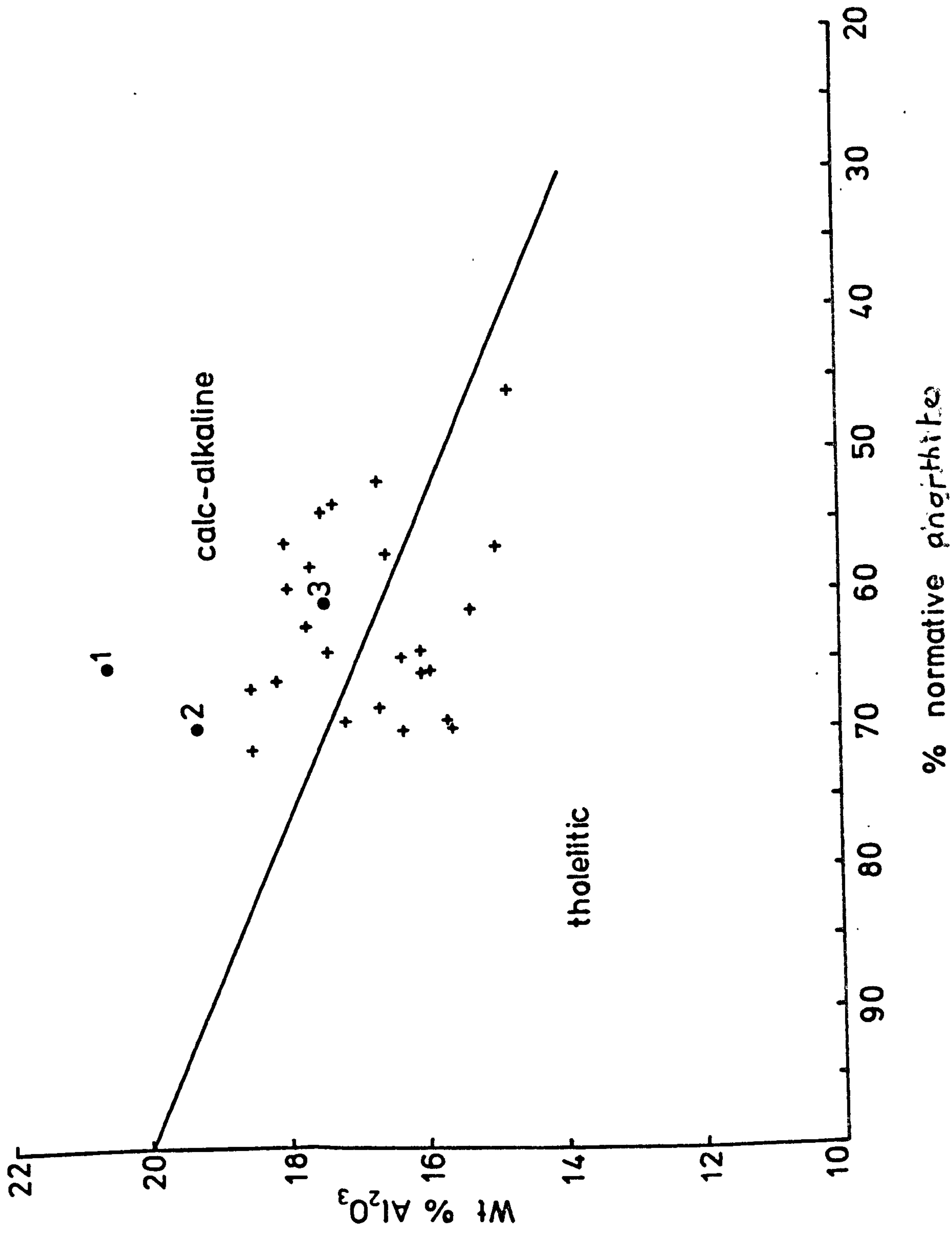




Fig.21

Normative compositions of selected picrites and basalts projected in Ni-Di-Hy-Ol and Ne-Ol-Hy-Ab diagrams.

Ne = Nepheline    Di = Diopside    Hy = Hypersthene  
Ol = Olivine      Ab = Albite

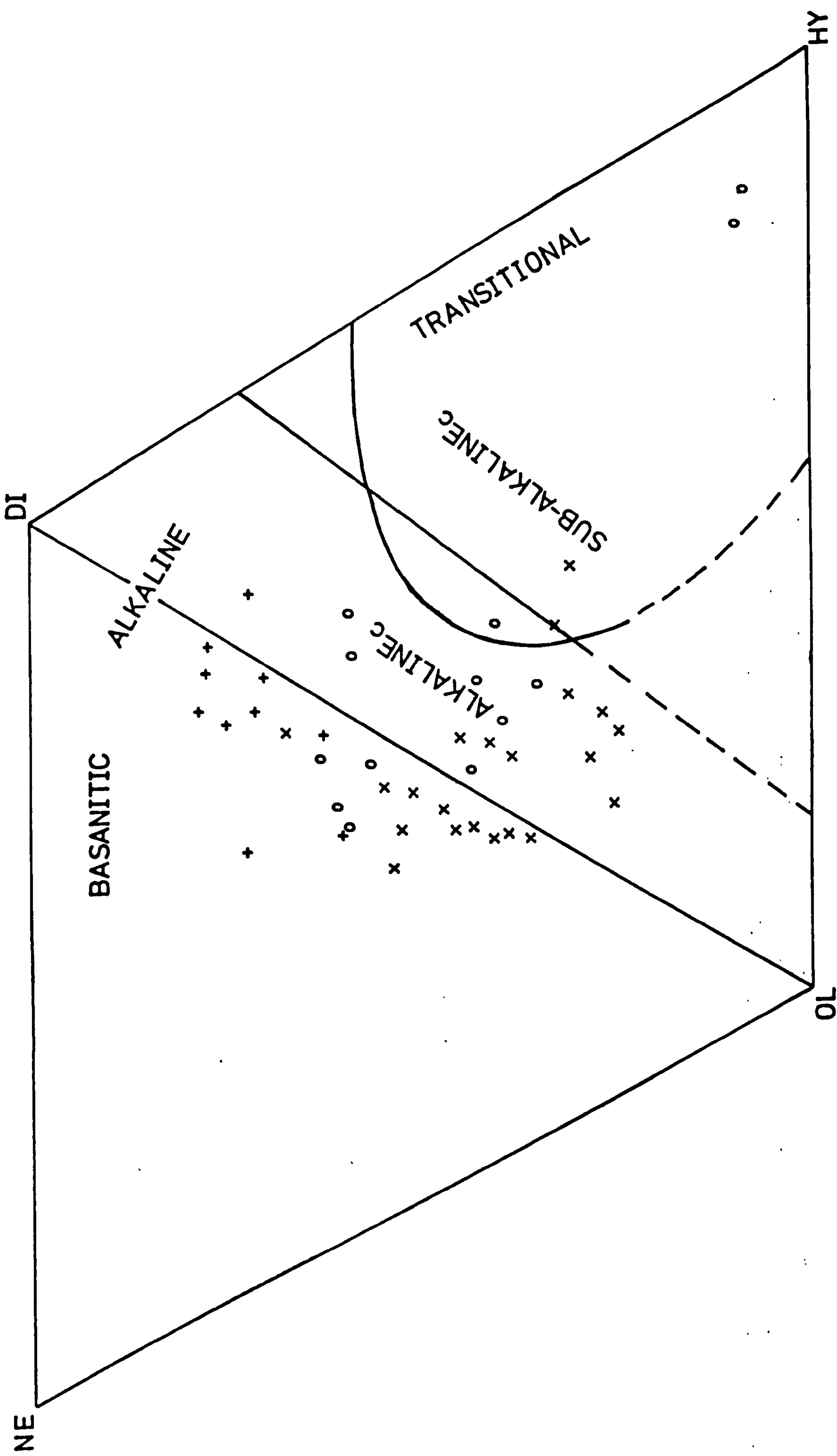
Symbols refer to relative degree of incompatible trace element enrichment.

+ = highly enriched

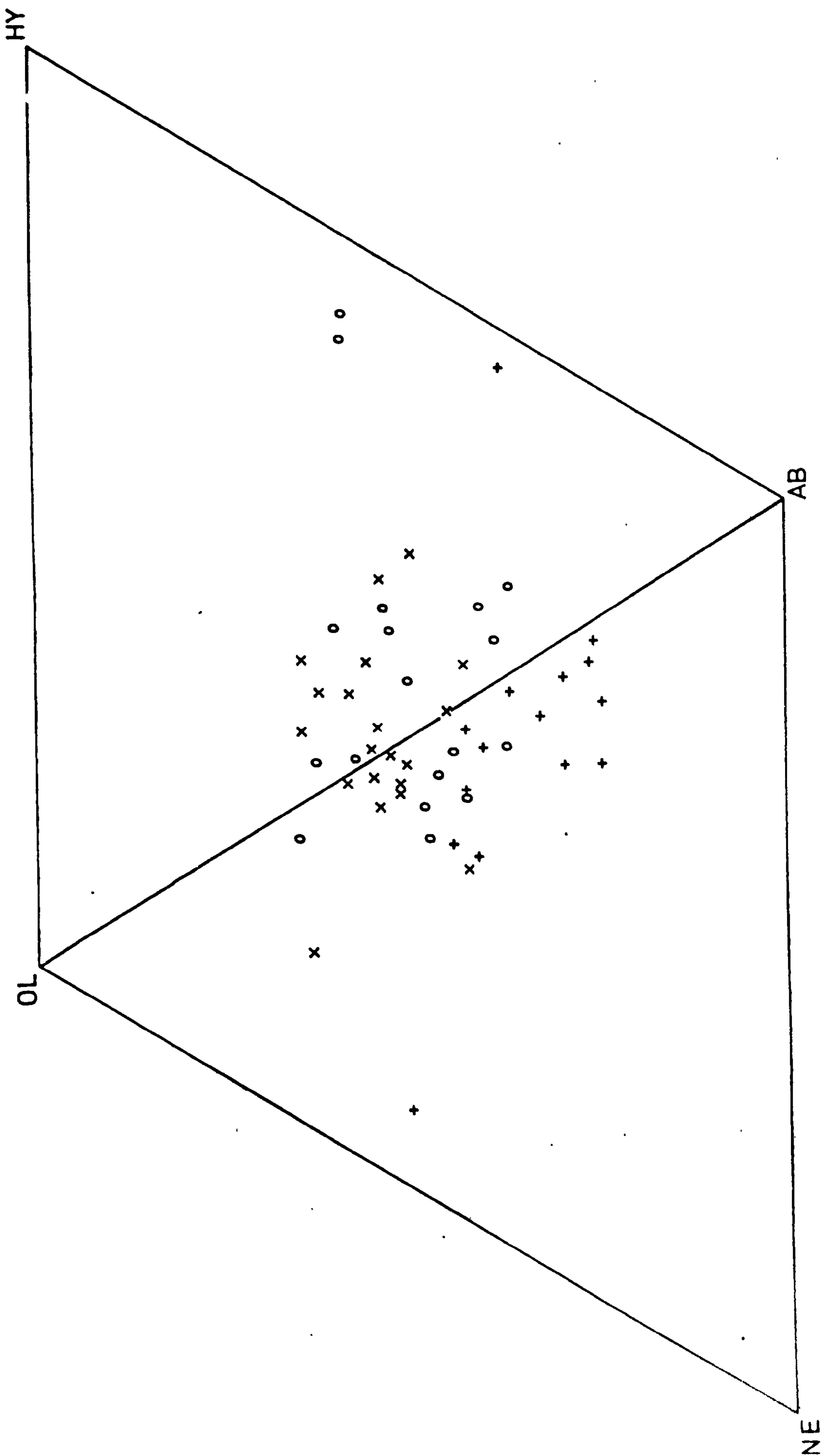
0 = average

x = depleted

Named fields are after Coombs (1963). The dashed and complete lines are the discriminant functions proposed by Chayes (1966) to distinguish alkaline and subalkaline basalt compositions (subscripted c).







### 7:3 Classification of the Grenada calc-alkaline series

It is necessary for the following discussion to classify the Grenada volcanic suite so that important features are stressed, whilst recognising the gradational nature of the compositions. The following classification is proposed:

picrite: - contains  $> 25\%$  normative olivine  
or  $< 45 \text{ wt.}\% \text{ SiO}_2$

alkali basalt: - contains normative nepheline

transitional basalt:- contains normative olivine,  
hypersthene and diopside or  
normative hypersthene, diopside  
and quartz where  $\text{SiO}_2 < 53.5 \text{ wt.}\%$

andesite: - contains 53.5 - 62 wt.% SiO<sub>2</sub>

dacite: - contains  $> 62$  wt.%  $\text{SiO}_2$

During the investigation of a suite of volcanic rocks, it is often customary to describe the petrography of the rocks first, followed by the geochemistry. This is a logical approach where the geochemical evolution of the suite has been fairly uniform in time, and consists of a typical association of rock types suitably described by terms already in the literature. However, the Grenada calc-alkaline rock suite is unusual in the transition displayed from undersaturated to silica-oversaturated compositions. In addition there is a considerable diversity of composition within the basaltic and picritic members of the suite. This diversity of composition occurs not only between dissimilar petrographic types, but also between rock types of strikingly similar petrography. Thus the diversity of chemical composition is discussed first, since it is essential to the understanding of the



TABLE 5

Major and trace element analyses of selected Grenadan picrites and basalts

<u>Specimen</u> <u>No.</u>	61	82	483	286	373	262	314	375	475	470	202	124	33
SiO <sub>2</sub>	44.63	46.63	44.70	46.82	46.78	46.79	46.22	46.57	47.01	47.67	47.11	47.46	47.34
Al <sub>2</sub> O <sub>3</sub>	15.30	17.38	14.76	17.62	18.21	16.01	15.65	17.11	16.17	18.12	16.53	18.10	16.66
Fe <sub>2</sub> O <sub>3</sub>	10.10	10.44	10.36	9.52	9.07	0.65	0.69	9.80	9.94	9.46	9.22	8.93	9.28
MgO	14.27	11.62	11.81	9.59	9.11	13.99	13.14	11.44	12.50	10.33	12.06	10.11	10.17
CaO	11.36	9.63	11.99	11.86	11.49	9.81	11.63	11.44	10.59	10.54	10.72	11.01	10.79
Na <sub>2</sub> O	2.46	2.37	3.40	2.50	2.85	2.07	1.80	1.99	2.26	2.33	2.85	2.24	3.10
K <sub>2</sub> O	0.65	0.39	1.27	0.71	1.08	0.52	0.48	0.43	0.37	0.37	0.37	0.79	1.19
TiO <sub>2</sub>	0.32	0.89	1.16	0.89	0.86	0.80	0.93	0.89	0.84	0.84	0.79	0.84	1.01
MnO	0.22	0.21	0.24	0.22	0.21	0.22	0.22	0.21	0.21	0.21	0.21	0.21	0.21
S	0.00	0.00	0.00	0.00	0.00	0.00	0.00	0.00	0.00	0.00	0.00	0.00	0.00
P <sub>2</sub> O <sub>5</sub>	0.18	0.11	0.32	0.27	0.34	0.15	0.25	0.13	0.11	0.14	0.15	0.31	0.25

TABLE 5 (continued)

<u>Specimen</u> <u>No.</u>	61	82	483	286	373	262	314	375	475	470	202	124	33
Ba	170	120	640	474	538	146	454	109	108	109	125	50	509
Nb	9	8	25	14	13	6	12	9	8	6	7	16	19
Zr	75	52	176	102	170	69	109	63	61	69	65	144	138
Y	17	13	20	16	21	18	20	16	17	19	20	18	16
Sr	617	300	973	829	749	382	692	380	326	313	402	730	786
Rb	17	12	40	27	29	10	11	12	12	6	7	12	38
Zn	73	81	81	87	75	81	75	70	78	79	74	75	76
Cu	86	60	128	65	119	105	124	99	82	66	96	87	86
Ni	434	565	292	260	267	472	271	306	464	368	371	320	263
Ce	25	11	46	52	62	12	38	14	13	12	16	44	48
Fe <sub>2</sub> O <sub>3</sub> /MgO	0.71	0.90	0.88	1.03	1.02	0.69	0.74	0.86	0.80	0.92	0.76	0.88	0.91
Ce/Y	1.47	0.85	2.3	3.25	2.95	0.67	1.90	0.88	0.76	0.63	0.80	2.45	2.35
K/Rb	317	270	264	218	309	431	362	297	256	512	439	546	260
Plot Symbol	O	X	+	+	+	X	+	X	X	X	X	+	+



geochemistry of the more evolved members of the volcanic association.

In a previous account (Sigurdsson et al., 1973) a more exact normative classification based on the work of Green (1969) was used. However, it was discovered that grouping of the compositions on the basis of major element chemistry was not so successful with regard to separation on the basis of trace element abundances. The classification proposed in this account is designed to permit a more critical review of this diversity of composition.

#### 7:4 The Geochemistry of the Grenada Picrites and Basalts

In Table 5 selected analyses of picrites, alkali and transitional basalts of the Grenada suite are presented. The normative projections of these analyses are given in Fig. 21. The analyses have been selected from several volcanic centres and localities are listed in Appendix I. The most important feature to note of these compositions, apart from the under-saturated nature of many, is that within a restricted range of major element composition (eg. within a  $\text{SiO}_2$  range of 3 wt.% in the Table), there is a considerable range of trace element abundances. In the case of Sr and Ce for example, the range varies up to a factor of 3 or more. The notable feature of the abundances of the trace elements is the general inverse correlation between the levels of 'incompatible' and compatible trace elements. The incompatible trace elements are those not incorporated in large quantities in the early forming mafic

silicates and oxides of basic magmas and include barium, rubidium, strontium and the Rare Earth elements. These are mainly large lithophile cations. Fig. 22 illustrates by means of binary plots the inverse relationship between these incompatible trace elements and the compatible element nickel (in olivine) within a restricted silica wt.% range. Appendix I contains the complete analyses of all the basalts used in the construction of these plots. There are several possible explanations for the range of trace element abundances observed:

- 1) crystal fractionation processes of one or more mineral phases
- 2) wall-rock reaction with the magma en route from site of melting to the surface
- 3) cumulus enrichment of mineral phases
- 4) varying degrees of partial melting of source material

In the following discussion, the basalts and picrites are assumed to have been generated by partial melting of an upper mantle peridotite. The reasons for preferring this source have been stated (Sigurdsson et al., 1973; Arculus and Curran, 1972) and are examined further in Chapter 10. The site of melting is estimated at a depth of approximately 100 km or 30 kb pressure.

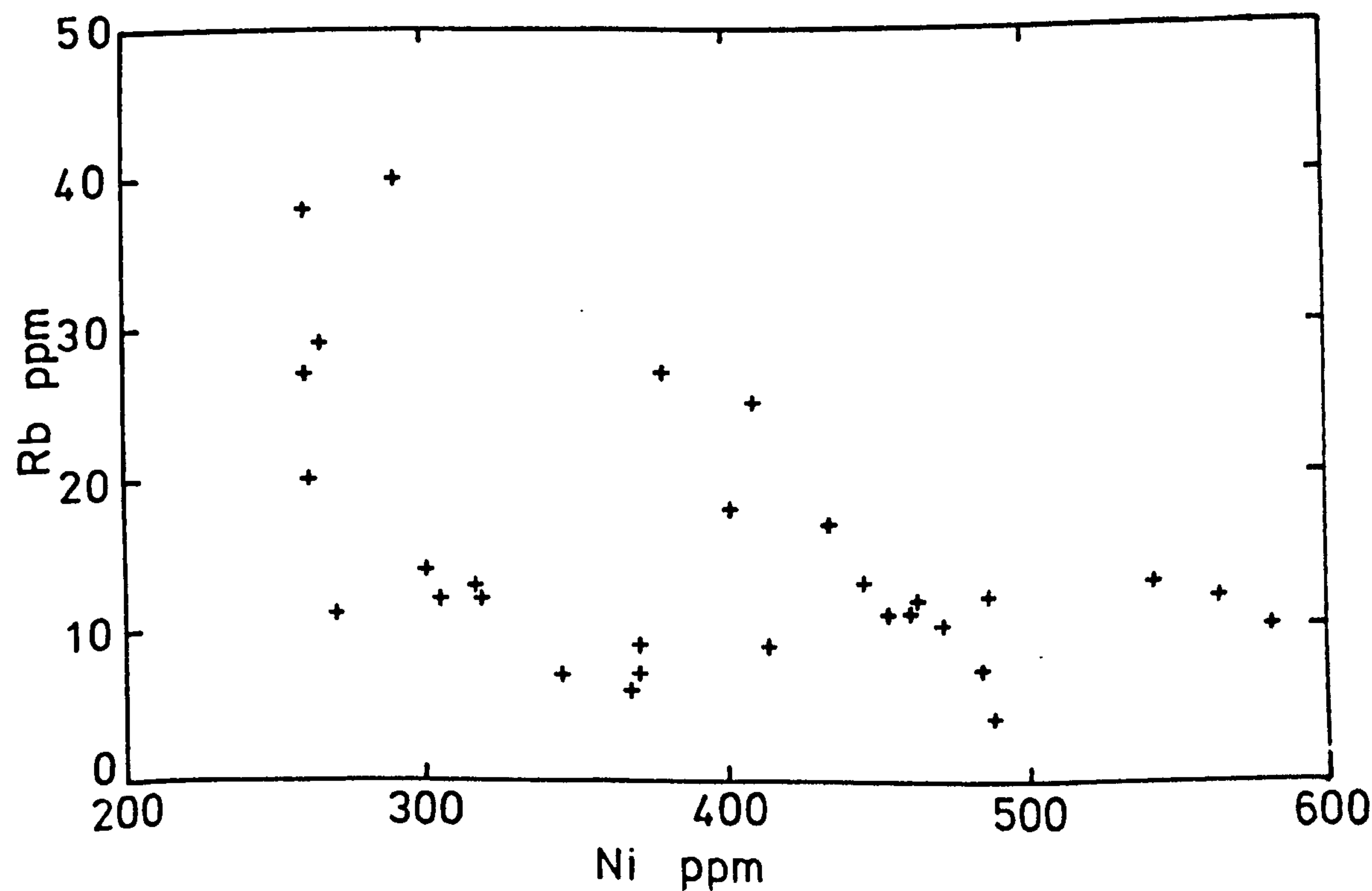
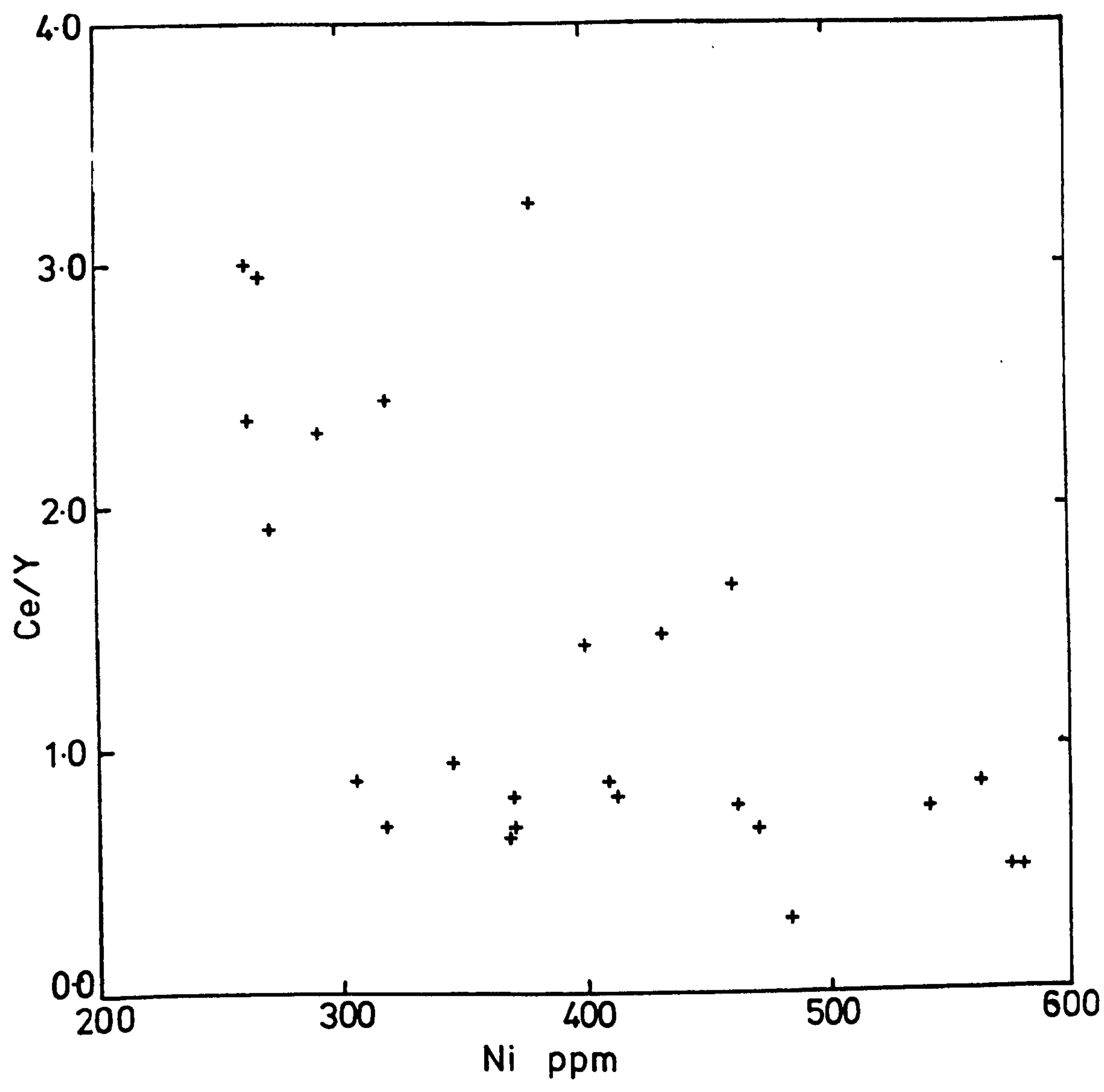
#### 7:4:1 Crystal fractionation

The important mineral phases that may have been fractionated from the Grenada magmas are orthopyroxene, clinopyroxene, olivine, spinel, amphibole and plagioclase. At high pressures (c.25 kb)



Fig.22

Plot of Ce/Y and Rb v Ni of some Grenadan basalts  
containing less than 48 weight %  $\text{SiO}_2$ .





with high  $P_{H_2O}$ , plagioclase is unlikely to be a stable phase (Yoder and Tilley, 1962).

Green (1970) has suggested that orthopyroxene fractionation is the main control during the evolution of nephelinitic rocks. Sigurdsson et al. (1973) examined the possibility that orthopyroxene fractionation at high pressure (25 kb) was responsible for a trend towards increasing silica-undersaturation of the Grenada magmas. Orthopyroxene crystallising at pressures of 25 kb within the Upper Mantle is likely to be enriched in MgO and  $SiO_2$  relative to the undersaturated melts under discussion. The solubility of  $Al_2O_3$  in orthopyroxene at this pressure however, is unlikely to exceed 5 wt.% (O'Hara, 1968). In addition other major components of the magma including CaO,  $Na_2O$  and  $K_2O$  are unlikely to have any great solubility in orthopyroxene, and during fractionation of this phase would be preferentially enriched in the melt. It is possible to select undersaturated compositions of the Grenada suite of basaltic rocks that apparently reflect an appropriate decrease of MgO and  $SiO_2$ , and increase in CaO and alkalis with increasing silica-undersaturation (Sigurdsson et al., 1973, Table 1). However, the alumina content decreases in the direction of postulated fractionation. This means that orthopyroxene would have to contain more than 15.8 wt.%  $Al_2O_3$  in order for the melt to be depleted during fractionation. A similar restriction would apply in the case of clinopyroxene if this phase was also precipitating. O'Hara (1968) has, however, indicated a limited solubility of  $Al_2O_3$  in clinopyroxenes ( $< 5$  wt.%) at pressures of 25 kb. It seems most unlikely that the solubility of  $Al_2O_3$



in pyroxenes during high pressure fractionation of the Grenada undersaturated magmas was sufficient to produce the observed variation. However, the range of trace element abundances of these picritic and basaltic compositions is a far more important restriction on the possible amounts of crystal fractionation.

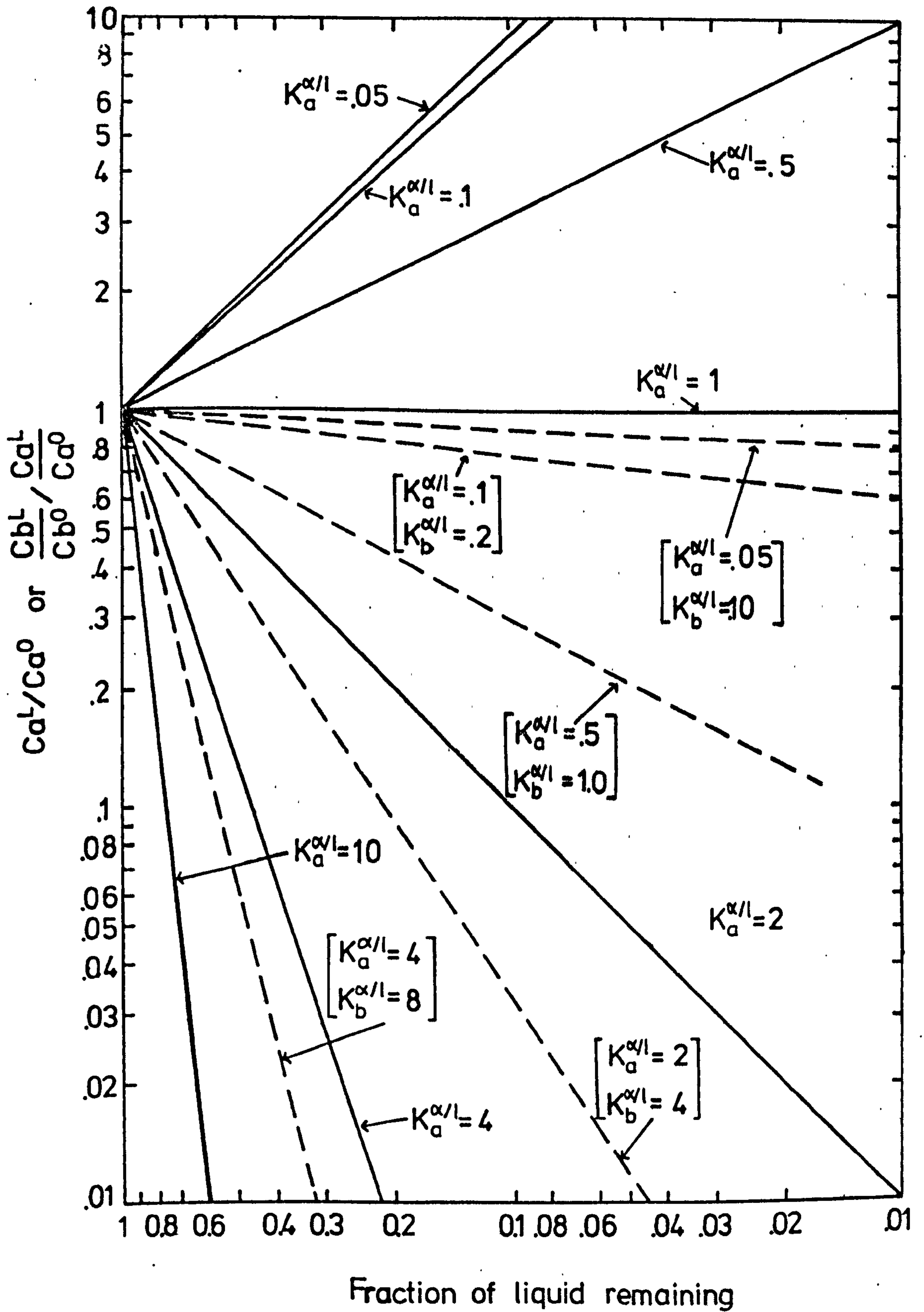
Gast (1968) has shown that "a given degree of magnitude of fractionation between liquid and solid produces much greater changes in the residual liquid where concentration is into the crystals". Fig. 23 illustrates the changes in concentration of a given element in a residual liquid for crystallisation with a constant partition coefficient (Rayleigh distillation model). Since we are dealing with a fractional crystallisation situation, it is permissible to apply calculated partition coefficients to the surface-equilibrium conditions prevailing between crystal and melt. In fact, since the crystals are likely to be zoned, and partition coefficients are determined between whole crystals and host matrix (eg. Schnetzler and Philpotts, 1970) the calculated partition coefficients are likely to be smaller than the actual value in the case where an element is preferentially enriched in the melt. In addition, Albarede and Bottinga (1972) have examined kinetic disequilibrium effects in trace element partitioning between phenocrysts and host magma, and conclude that partition coefficients less than unity (concentration in solid less than concentration in liquid) determined by assuming Rayleigh distillation, are generally smaller than the actual partition coefficients.



Fig. 23

Logarithmic plot of Rayleigh curves for fractional crystallization. Solid lines show change in concentration of a given element in a residual liquid for crystallization with a constant distribution coefficient. Dashed lines show changes in relative abundance of two elements as crystallization proceeds.

(After Gast, 1968)





Schnetzer and Philpotts (1970) calculated the partition coefficient of Ce between orthopyroxene and liquid as 0.04. In order to change the abundance of Ce by a factor of 5 (the observed range of the Grenada picrites and basalts) it can be seen from Fig. 22 that only 20% of the original melt would remain. Fractionation of this amount of orthopyroxene would completely alter the major element chemistry of the residual liquid. In view of the previous statements concerning the value of the partition coefficient, it is likely that the actual partition coefficient of Ce between orthopyroxene and melt is slightly larger. This would place even greater restriction on the amount of orthopyroxene fractionation required in order to achieve the range of Ce abundance observed in the Grenada compositions.

Ce is more effectively partitioned with residual melts by olivine fractionation (Schnetzer and Philpotts, 1970), but subtraction of forsteritic olivine would alter the composition of the residual melt in a very different sense from orthopyroxene fractionation. Fractionation of olivine from a basaltic melt causes a decline in the concentration of Ni in the residual melt (eg. Hakli and Wright, 1967). As Gast (1968) has stated, great changes in the melt are possible with concentration into the crystals. It is possible that part of the diversity in abundance of Ni in the Grenada picrites and basalts is caused by olivine fractionation. It seems most probable that the variation in Ni and MgO for suites from single volcanic centres are indeed explicable by olivine fractionation (p. 279 ). However, Table 5 shows that some basalts with higher silica contents and lower

incompatible trace element abundances, contain higher Ni contents than compositions of more silica-undersaturated nature. If the former compositions were consistently related to the most undersaturated compositions by olivine fractionation alone, then the compositions should reflect olivine removal by lower Ni and higher incompatible trace element levels.

Cawthorn et al. (1973) suggested on the basis of experiments conducted at 5 kb ( $P_{H_2O} = P_{tot}$ ) on natural Grenada compositions that fractional crystallisation of undersaturated amphibole was primarily responsible for the development of a trend towards silica-saturation in the Grenada suite. However, Kesson and Price (1972) have reported consistently high K/Rb ratios (1200 to 4300) for kaersutites from basic alkaline rocks. Fractional crystallisation of amphibole would rapidly reduce the K/Rb ratio of the residual melt. The study by Sigurdsson et al. (1973) showed that K/Rb ratios in general increase from the most undersaturated compositions to more silica-rich basalts. This feature is also displayed in the K/Rb ratios of the picrites and basalts listed in Table 5. In addition Schnetzler and Philpotts (1970) have shown that fractionation of amphibole should result in an increase of Ce and marked increase of Ce/Y ratios in residual melts. The abundance of Ce and variation in Ce/Y ratios of the Grenada compositions do not consistently display the expected trends.

A further control on the absolute amount of amphibole fractionation possible is the concentration of  $Na_2O$  in amphibole relative to the melt. In Chapter 9 the compositions of coexisting



amphibole and host rock are examined. It is found that amphibole frequently contains high contents of  $\text{Na}_2\text{O}$  relative to the host rock. Lewis (1973) has described the relationship between cumulus amphibole and residual melt from St. Vincent compositions and has reported a similar feature. The experimental results quoted by Cawthorn et al. (1973) and Holloway and Burnham (1972) show a tendency for  $\text{Na}_2\text{O}$  to be greater in amphiboles than the host rock composition. In some instances it may be possible to ascribe a reduction in the  $\text{Na}_2\text{O}$  content between selected basalt compositions of Grenada as being the result of amphibole fractionation. The geochemical parameters described above do not permit this possibility. Nevertheless, it is apparent that amphibole is a major crystallising phase in the Grenada calc-alkaline suite. The presence of amphibole in some basaltic compositions, and crystallisation with olivine and clinopyroxene suggest that it has been significant in the evolution of the series. Amphibole is also a common phase in the cumulus plutonic blocks and analysis of individual volcanic centres show the geochemical trends expected of amphibole fractionation. However, the aim of the present discussion is to illustrate that amphibole is unlikely to have played a major role in producing the major and trace element variation within the picritic and basaltic compositions.

Thus the general point is made that the range of major and trace element abundances in the Grenada compositions is such, that the removal of one or more mafic phases is insufficient to explain consistently the observed variation. However, the variation of major and trace elements within suites belonging to separate rock series of single volcanic centres is more readily explained by crystal fractionation. This topic is examined later but alternative

possibilities for producing the element variation of the entire basaltic suite are discussed first.

#### 7:4:2 Wall-Rock reaction

It is possible that the variation in trace element compositions represents selective wall-rock contamination. This process has been suggested by Green (1970) for example, in order to explain the abundance of incompatible elements in alkali basalt magmas. The exact medium of exchange of elements between wall-rock and magma is uncertain, but would presumably involve a fluid or melt medium that selectively leached elements from the walls of the magma channelways. A certain amount of heat would be required to melt the wall-rock causing crystallisation of one or more mineral phases in the magma. A finite length of time would be required in order to generate an element exchange, during which it is likely crystal fractionation would occur. On both counts a more evolved magma in terms of major element chemistry and higher incompatible trace element contents would result. However, the preceding discussion has shown that the chemistry of the Grenada basalts and picrites does not consistently reflect a trend towards more silica-saturated (or undersaturated) compositions with higher incompatible trace element abundances. Thus, although wall-rock contamination may be partly responsible for the variation in trace elements of erupted basalts, the contamination has not been consistent, and is therefore not easily discernible.

#### 7:4:3 Cumulus enrichment of mineral phases

The Grenada basalts containing high ( > 20%) proportions of



modal olivine usually have high Ni contents as well. However, some compositions whilst containing high modal olivine, are characterised by relatively low Ni contents and high incompatible trace element abundances. There is a good correlation between porphyritic basalts containing abundant modal plagioclase and clinopyroxene, and high Sr contents. In both cases, the level of trace elements is related to the initial concentrations in the basaltic liquid and not directly attributable to the presence of cumulus phases. In the case of high-Sr levels, analysis of single volcanic centres indicates that this feature may be explained by crystal fractionation of liquids of originally high Sr contents (p. 300). The smooth trends of variation of Sr with  $\text{SiO}_2$  content of volcanic suites of Grenada suggest liquid lines of descent. There are no discontinuities in these trends suggestive of cumulus enrichment. In addition, the clinopyroxene and plagioclase phenocrysts are strongly zoned, often in an oscillatory fashion which is unlike normal cumulus mineral phases (Wager and Brown, 1968). In addition, experimental evidence is presented in Fig. 24, based on the results of Cawthorn et al. (1973). At 5 kb ( $P_{\text{H}_2\text{O}} = P_{\text{tot}}$ ), the order of appearance on the liquidus of some examples of Grenada basalts and picrites (compositions given in Table 6), is olivine followed by clinopyroxene. The appearance of these phases is within a few degrees at a temperature of  $1130^\circ\text{C}$ . The petrographic description of the samples investigated is given below Table 6. The feature to note is that the order of appearance on the liquidus of olivine and clinopyroxene in composition 158 occurs at a temperature  $80^\circ$  below that of the more basic compositions, despite the predominance of clinopyroxene and

TABLE 6

Major and trace element analyses of a picrite and basalts used in the experimental study by Cawthorn et al. (1973) together with a petrographic summary.

<u>Sample</u> <u>No.</u>	<u>483</u>	<u>476</u>	<u>286</u>	<u>158</u>	<u>342</u>
SiO <sub>2</sub>	44.70	45.33	46.82	51.98	52.59
Al <sub>2</sub> O <sub>3</sub>	14.76	15.22	17.62	19.10	18.73
Fe <sub>2</sub> O <sub>3</sub>	10.36	10.04	9.52	8.11	8.10
MgO	11.81	14.66	9.59	5.64	3.93
CaO	11.99	11.17	11.86	10.09	10.43
Na <sub>2</sub> O	3.40	1.72	2.50	3.00	3.54
K <sub>2</sub> O	1.27	0.53	0.71	0.76	1.43
TiO <sub>2</sub>	1.16	0.93	0.89	0.91	0.87
MnO	0.24	0.22	0.22	0.17	0.18
S	0.00	0.00	0.00	0.00	0.00
P <sub>2</sub> O <sub>5</sub>	0.32	0.18	0.27	0.23	0.21
Ba	640	193	474	214	536
Nb	25	25	14	16	9
Zr	176	88	102	94	130
Y	20	18	16	19	22
Sr	973	555	829	594	1199
Rb	40	11	27	18	44
Zn	81	80	87	74	51
Cu	128	61	65	140	24
Ni	292	461	260	186	35
Ce	46	35	52	n.a.	45

Ol = olivine cpx = clinopyroxene sp = spinel pl = plagioclase

483 picrite microphenocrysts of ol, cpx, sp, in a glassy groundmass with microlites of the same minerals plus pl.

476 alkali basalt microphenocrysts of ol, cpx and sp in a glassy groundmass with microlites of the same minerals together with pl.

286 alkali basalt phenocrysts of zoned ol and cpx in a vesicular glassy groundmass with microphenocrysts of ol, cpx, pl and sp.

158 transitional basalt zoned cpx and marginally iddingsitised ol phenocrysts in a groundmass dominantly composed of pl laths with minor cpx and magnetite.

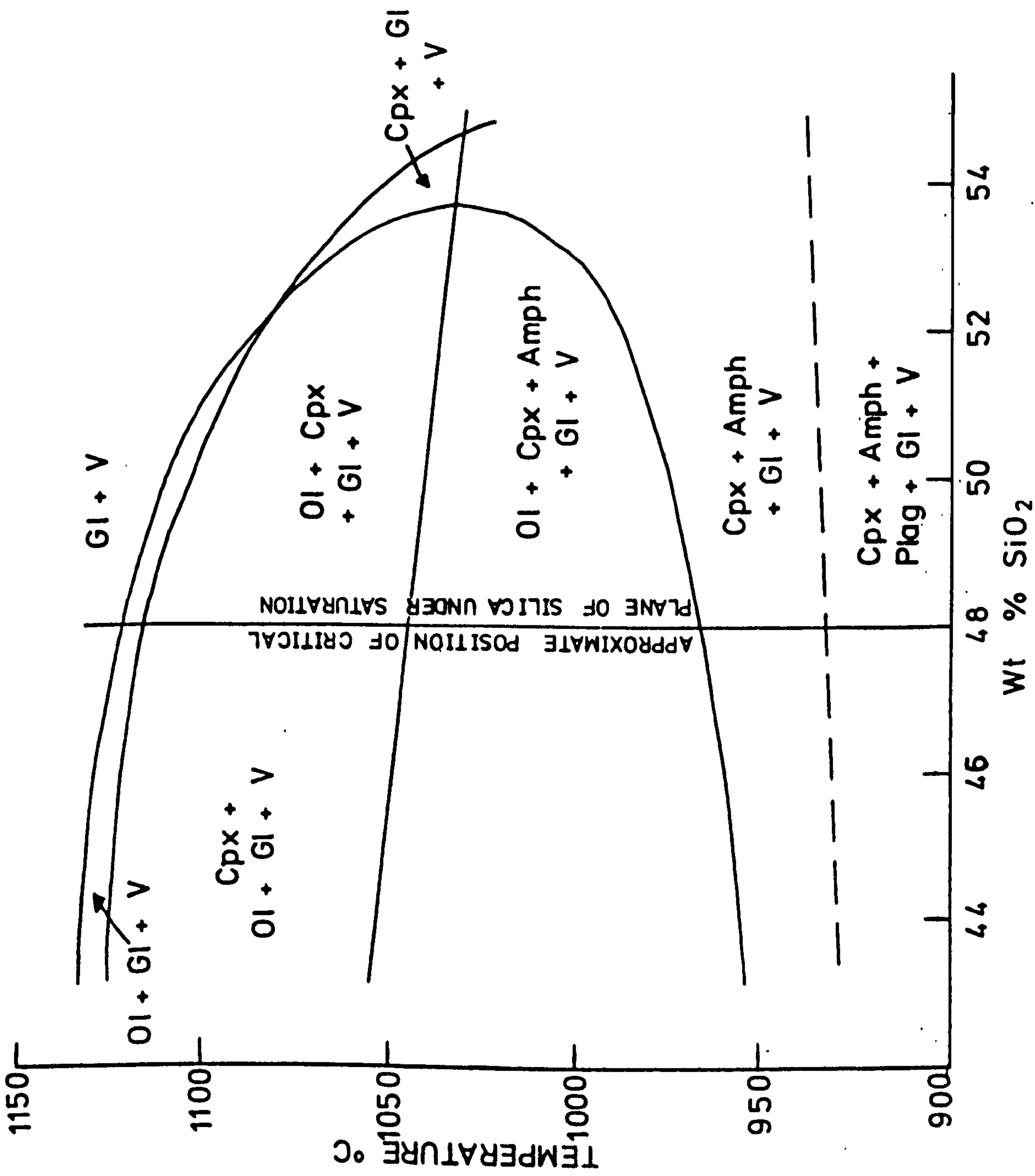
342 transitional basalt cpx and pl phenocrysts and minor iddingsitised phenocrysts in a vesicular groundmass containing pl, cpx, magnetite and interstitial biotite.



Fig.24

Correlation diagram of silicate phase relationships with increasing silica-content of the Grenada suite. Adapted from Cawthorn et al. (1973). Experiments completed under 5 kb-pressure with excess water and Ni-NiO buffer.

Ol = Olivine	Cpx = Clinopyroxene
Amph = Amphibole	Plag = plagioclase
Gl = glass	V = Vapour





plagioclase phenocrysts of this rock. The contrasting physical properties of olivine and clinopyroxene make it unlikely that they should have been preserved in exactly the correct proportions, so that their order of appearance on the liquidus is the same as the more basic compositions, lacking the same abundant phenocrystic clinopyroxene and plagioclase. The transitional basalt 342 is dominated by large oscillatory zoned clinopyroxene and plagioclase phenocrysts. Olivine is not observed as a liquidus phase in the experimental runs, and the liquidus temperature of appearance of clinopyroxene is 1050°C. If this composition represents cumulus enrichment of clinopyroxene, the liquidus temperature of appearance of this phase should be higher than in compositions truly representative of magmatic liquids. Thus it seems from different lines of evidence that the geochemical variation of the Grenada basalts and picrites is not explicable by cumulus enrichment of phases.

#### 7:4:4: Varying Degrees of partial melting

The wide range of trace element abundances of the Grenada basalt compositions, may be due to differing initial quantities of partial melt of the Upper Mantle source material. O'Hara (1968) has shown that variations in the percentage of early partial melting of a peridotite source may produce a variation in incompatible trace element abundances of a factor of 3 within 3% total volume of melt. Fig.25 illustrates the enrichment factors resulting from melting of a peridotite source.

Whilst recognising that some of the trace element abundances of the Grenada basalts may have been affected by crystallisation en route from source to surface, it has already been qualitatively

Fig. 25

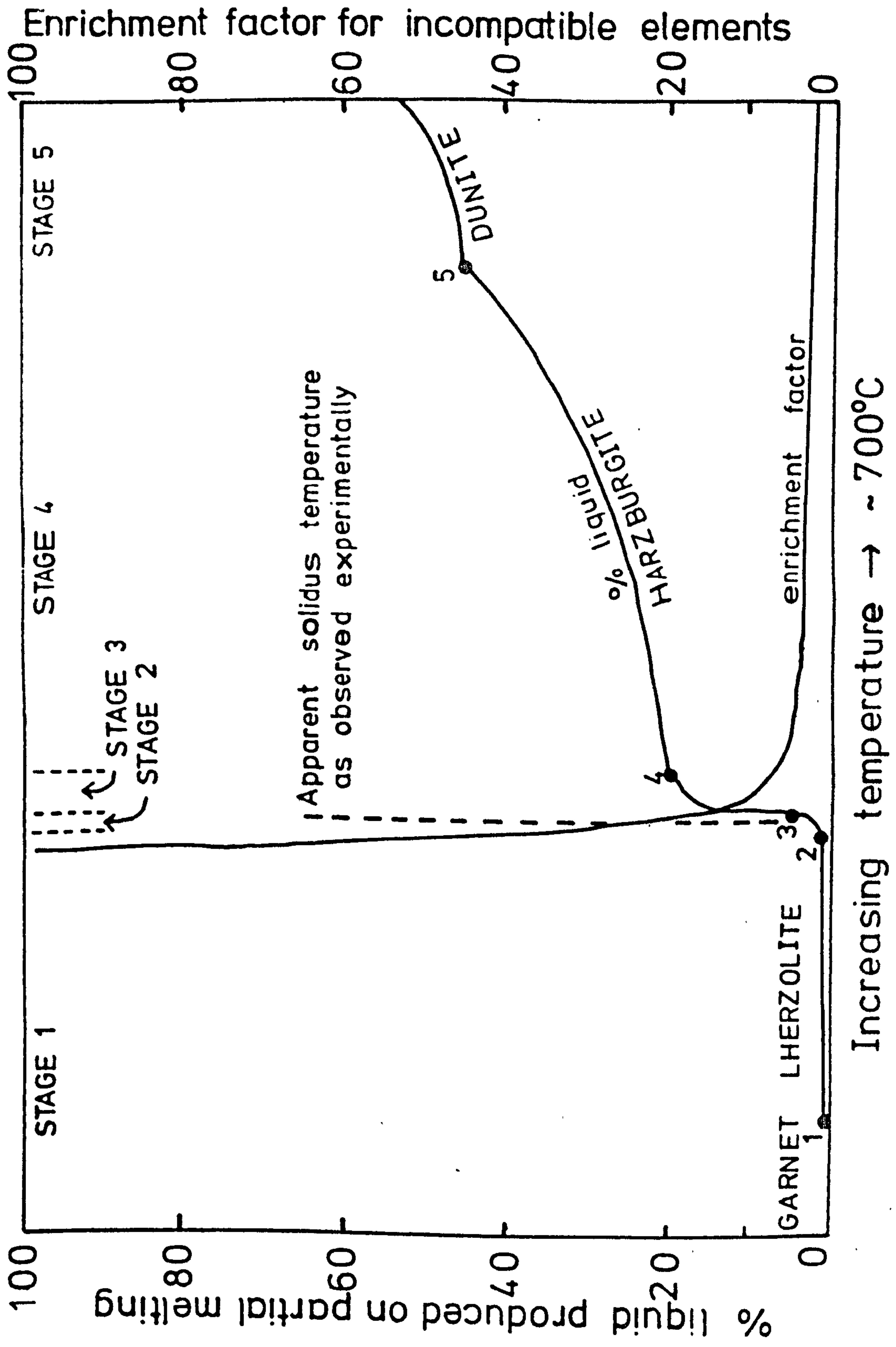
Variations in partial melt composition and enrichment factors of incompatible elements as the result of melting of a garnet.

Iherzolite. (After O'Hara, 1968).

Five main stages are recognized:

- 1) Small amount ( $\sim 1\%$ ) of partial melting between temperatures 1 and 2 with extreme enrichment of the melt in incompatible trace elements.
- 2) Between temperatures 2 and 3, increase in volume of melt to  $\sim 5\%$ . Major element concentration strongly controlled by major solid phases present and considerable variation in Fe/Mg/Ni, Ca/Na, Al/Cr ratios are predicted within a small temperature interval ( $\sim 10^\circ\text{C}$ ). A marked dilution of incompatible trace element concentration takes place so that absolute concentrations and ratios to major oxides vary rapidly but ratios to each other vary only slightly.
- 3) Increase in volume of liquid between temperatures 3 and 4 to approximately 15%. One of the major crystalline phases (clinopyroxene or garnet) disappears. Marked dilution up to a factor of 4 of the incompatible trace elements.
- 4) Gradual increase in volume of liquid with gradual dilution of incompatible trace elements. Concentration of  $\text{MgO}$ ,  $\text{FeO}$  and  $\text{SiO}_2$  will increase with dilution of  $\text{CaO}$ ,  $\text{Al}_2\text{O}_3$  and  $\text{Na}_2\text{O}$  leaving residual harzburgite mineralogy.
- 5) Continuing increase in volume of liquid and dilution of trace elements leaving residual dunite mineralogy.





shown that the total variation of these trace elements is inexplicable by fractionation of mafic phases. Thus it is possible to a first approximation, to regard the trace element abundances as reflecting genuine initial variation in melt composition.

The Mg-rich end members of the mineral solid-solution series forming the peridotite Upper Mantle, melt at higher temperatures than the Fe-rich end members. Consequently the initial melting (low temperature) product will be enriched in Fe relative to Mg. In general, the Grenada basaltic compositions containing higher incompatible trace element abundances are also characterised by higher Fe/Mg ratios (Table 5). This feature is observed when considering compositions within a restricted silica weight-percentage range. Fractionation of mafic phases early in the evolution of these magmas will cause a rapid increase in the Fe/Mg ratio of the residual melts. Consequently comparison of Fe/Mg ratios is only attempted between broadly similar major element compositions.

During increased partial melting of the same source material at the same pressure, the Fe/Mg ratios and concentrations of incompatible trace elements are reduced in the melt, and abundance of Ni increased. The range of element abundances of the Grenada basalts and picrites generally display the variation predicted by a model of variable degrees of partial melting.

Partial melting at varying depths (pressures) in the Upper Mantle must be regarded as a refinement of the model proposed.



In the case of silica-undersaturated compositions at pressures of approximately 25 kb, O'Hara (1968) and Green (1970) have shown that a greater volume of melt is required at higher pressures in order to generate a similar composition. Consequently the greater volume of melt should be less enriched in incompatible trace elements. Similar volumes of partial melt generated at differing depths results in a melt of greater silica-undersaturation at the higher pressure, but should possess similar trace element abundances. In Chapter 10, the petrogenesis of the Grenada magmas is discussed and derivation by partial melting of the Upper Mantle peridotite overlying a subducted lithospheric plate proposed. It is most probable that melting takes place within a range, rather than at a unique pressure. Although the Grenada picrites and basalts vary widely in major and trace element composition, this variation is not easily reconciled with consistent derivation at clearly defined and differing pressures.

In order that the model of variable partial melting be tested further, a study of the Rare Earth elements of the Grenada suite was undertaken (O'Nions et al., in MS). The ionic radius of the Rare Earth elements decreases with increasing atomic number, and the light Rare Earths are in general too large to be easily incorporated into mineral phases fractionating from basaltic liquids. Consequently the distribution patterns of the Rare Earth elements are useful petrogenetic indicators of fractionation and melting processes. Compositions ranging from basalt to dacite were selected for determination of complete Rare Earth element distribution patterns (O'Nions et al., in MS). In addition, Ce

TABLE 7

Major and trace analyses of alkali basalts  
476 and 239

\*Ce analyses by O'Nions et al. (in MS)

<u>Sample No.</u>	<u>476</u>	<u>239</u>
SiO <sub>2</sub>	45.33	49.65
Al <sub>2</sub> O <sub>3</sub>	15.22	17.74
Fe <sub>2</sub> O <sub>3</sub>	10.04	9.14
MgO	14.66	5.47
CaO	11.17	12.41
Na <sub>2</sub> O	1.72	3.10
K <sub>2</sub> O	0.53	1.22
TiO <sub>2</sub>	0.93	0.89
MnO	0.22	0.20
S	0.18	0.19
P <sub>2</sub> O <sub>5</sub>	0.18	0.19
Ba	193	471
Nb	25	8
Zr	88	95
Y	18	20
Sr	555	1305
Rb	11	17
Zn	80	62
Cu	61	149
Ni	461	40
Ce*	39.6	33.9

Petrographic summary and estimated  
mode (% in brackets)

- 476 Microphenocrysts of olivine (20, clinopyroxene (5) and spinel (chrome sp. and magnetite)(2) in a glassy groundmass with abundant plagioclase microlites and minute grains of olivine, clinopyroxene and magnetite.
- 239 Phenocrysts of clinopyroxene (30) and plagioclase (35) up to 2 mm in length together with olivine (5) and magnetite (5) in a groundmass composed of plagioclase feldspar, clinopyroxene and magnetite microlites.



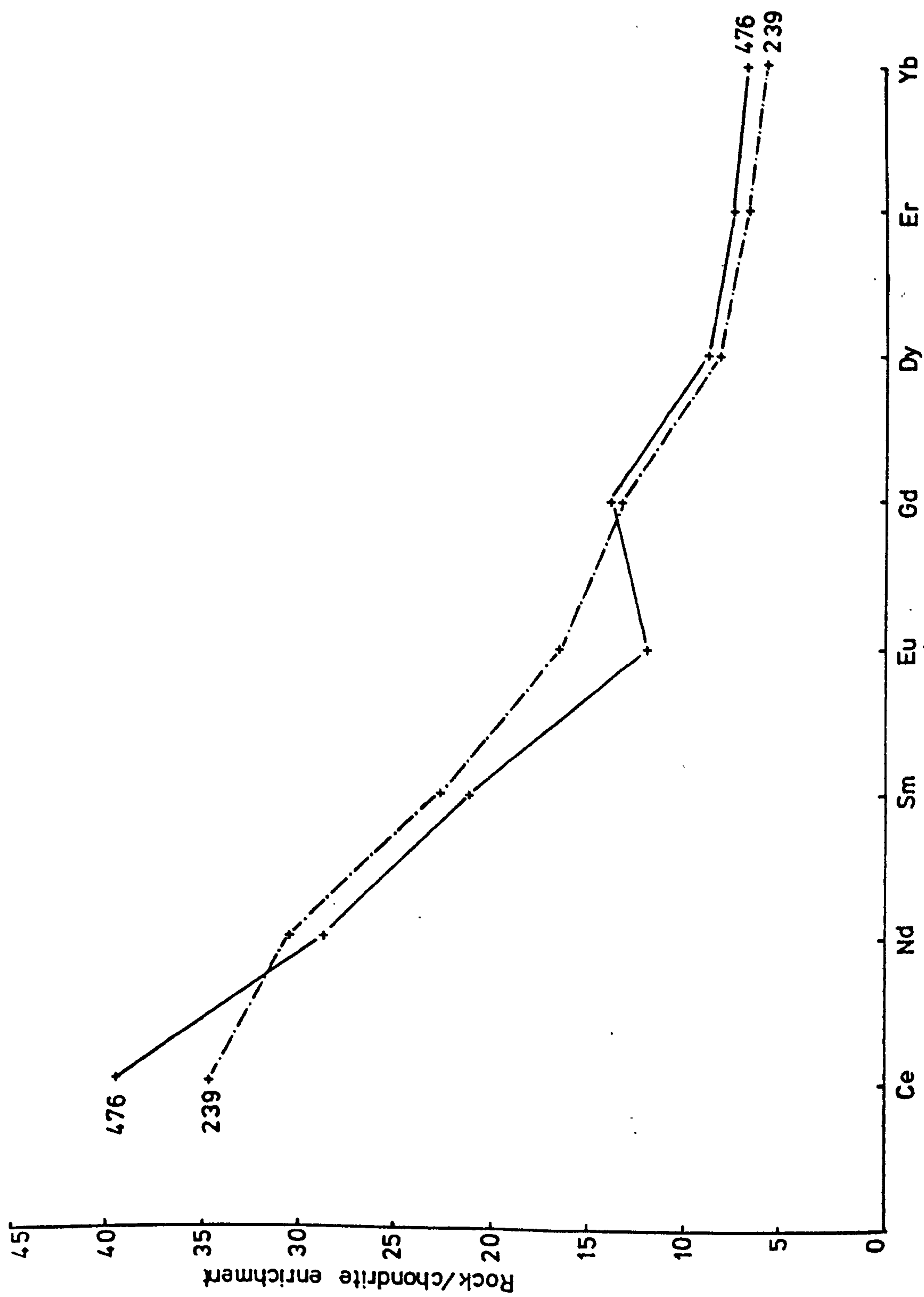
and Y were determined by X-ray fluorescence. The geochemical behaviour of Y is similar to the heavy Rare Earths (Goldschmidt, 1954), and the Ce/Y ratio is consequently a good indicator of the degree of light Rare Earth enrichment.

The enrichment of the Rare Earth elements relative to the Leedy chondrite (Masuda et al., 1973) of two basalt compositions is given in Fig. 26. The compositions of these two basalts are listed in Table 7. The light Rare Earth element enrichment relative to chondrite displayed by these basalts is similar to alkali basalts from other volcanic provinces (Gast, 1968). In general, there is a greater degree of light Rare Earth enrichment in the alkali basalt (239) containing the higher incompatible trace element abundances. However, the petrography (given in Table 7) and composition of the alkali basalt 239, indicate that it represents a derivative melt from a more basic composition. Consequently, the greater degree of light Rare Earth enrichment relative to the alkali basalt 476 may be due to a higher degree of fractionation. In this case, the degree of enrichment may not be directly related to a smaller initial volume of partial melt of the Upper Mantle. However, the Ce/Y ratios of the basalts and picrites listed in Table 5 indicate that in similar major element compositions, a wide range of light Rare Earth enrichment exists. In general the high Ce/Y ratios of the picrites and basalts correlate with high incompatible trace element abundances. This feature is in accord with a model of variable initial quantities of partial melt of the Upper Mantle. The Rare Earth element distribution patterns and Ce/Y ratios of selected andesites and dacites from the Grenada suite have also been determined. The

Fig.26

Rare Earth element distribution in basalts  
239 and 476.





details are discussed later (p. 148), but in general it is possible to detect degrees of enrichment in these silica-saturated compositions that reflect the nature of the parental basic magmas. In other words high incompatible trace element abundances and light Rare Earth enrichment are associated with basaltic compositions of similar nature. This general feature is in accordance with the predictions of Gast (1968) and Fig. 22, where it is shown that the differences in incompatible trace element abundances cannot be readily altered by fractionation of mafic phases alone from basaltic liquids, without greatly altering the character of the residual melts. Accordingly the trace element distribution of the Grenada calc-alkaline suite appears to be related to the differences in trace element abundance generated at the source of melting in the Upper Mantle.

#### 7:5 $\text{Sr}^{87}/^{86}$ ratios of the Grenada Calc-Alkaline Suite

The  $\text{Sr}^{87}/^{86}$  ratios of selected Grenada compositions were determined by O'Nions et al. (in MS). In Table 8, the  $\text{Sr}^{87}/^{86}$  ratios of alkali basalts 360 and 239, and transitional basalts 474, 479 and 342 are given, together with their chemical composition. The use of the terms alkali and transitional basalt does not imply necessarily that the latter are derived from the former by fractional crystallisation. The terms are discussed later (p.125) but it is stressed that the alkali basalts are not exclusively those with high incompatible trace element contents.

It can be seen that there are significant differences between the extremes of the  $\text{Sr}^{87}/^{86}$  ratios of the basalts in Table 8. The range is from 0.7043 to 0.7050. The Rb/Sr ratios, errors in deter-



TABLE 8

Strontium isotope results for basalts, andesites and a dacite of the Grenada calc-alkaline rock suite together with major and trace element analyses of the basalts.

<u>Sample No.</u>	<u>Rock Type</u>	<u>Rb/Sr</u>	<u>Sr<sup>87</sup>/86</u>	<u>Max.Age Corrections</u>
474	Transitional basalt	0.021	0.70501 <sup>+12</sup> <sub>-12</sub>	-2
360	Alkali basalt	0.022	0.70430 <sup>+11</sup> <sub>-11</sub>	-2
239	Alkali basalt	0.013	0.70449 <sup>+7</sup> <sub>-7</sub>	-1
479	Transitional basalt	0.098	0.70466 <sup>+8</sup> <sub>-8</sub>	-8
342	Transitional basalt	0.037	0.70481 <sup>+10</sup> <sub>-10</sub>	-3
67	Andesite	0.077	0.70497 <sup>+8</sup> <sub>-8</sub>	-6
381	Andesite	0.058	0.70461 <sup>+5</sup> <sub>-5</sub>	-4
214	Dacite	0.039	0.70543 <sup>+12</sup> <sub>-12</sub>	-3

TABLE 8 (continued)

<u>Sample No.</u>	<u>474</u>	<u>360</u>	<u>239</u>	<u>479</u>	<u>342</u>
SiO <sub>2</sub>	46.50	47.72	49.65	50.69	52.59
Al <sub>2</sub> O <sub>3</sub>	16.31	15.96	17.74	18.50	18.73
Fe <sub>2</sub> O <sub>3</sub>	10.31	10.56	9.14	9.17	8.10
MgO	13.00	8.01	5.47	4.06	3.93
CaO	10.50	13.27	12.41	11.74	10.43
Na <sub>2</sub> O	1.85	1.96	3.10	2.60	3.54
K <sub>2</sub> O	0.33	1.16	1.22	1.23	1.43
TiO <sub>2</sub>	0.88	0.94	0.89	0.94	0.87
MnO	0.22	0.22	0.20	0.23	0.18
S	0.00	0.00	0.00	0.00	0.00
P <sub>2</sub> O <sub>5</sub>	0.09	0.21	0.19	0.25	0.21
Ba	108	216	471	439	526
Nb	7	10	8	7	9
Zr	62	105	95	97	130
Y	17	18	20	22	22
Sr	327	1434	1305	1606	1199
Rb	7	31	17	10	44
Zn	81	65	62	61	51
Cu	62	137	149	166	24
Ni	485	70	40	23	35
Ce	5	35	33.9*	n.a.	45
Ce/Y	0.34	1.94	1.69		2.05

\*analysis by O'Nions et al. (in MS)      n.a.=not analysed.



minations and the maximum age corrections are also given in Table 8 . The Rb/Sr ratios are not correlated with the  $\text{Sr}^{87}/86$  ratios and the errors are within the observed range of  $\text{Sr}^{87}/86$  ratios. There are three main alternative explanations for the differences between the  $\text{Sr}^{87}/86$  ratios of these basalts.

- 1) isotope equilibration with wall-rock
- 2) differences imposed by melting of different parental material
- 3) differences imposed at source of melting of similar parental material

#### 7:5:1 Isotope equilibration

It is possible that the higher  $\text{Sr}^{87}/86$  ratios of some of the basalt compositions are due to isotope equilibration or contamination with radiogenic strontium. However the strontium content of basalt 474 (327 ppm) is lower than basalts of lower  $\text{Sr}^{87}/86$  ratio. In addition the major element geochemistry and petrography of basalt 474 are not suggestive of significant sialic contamination. The rock is microphyric containing abundant (20%) modal olivine with small euhedral clinopyroxene phenocrysts, opaque oxide granules and plagioclase laths in a glassy groundmass. Pankhurst (1969) has described differences in  $\text{Sr}^{87}/86$  ratios of differentiated basalt magmas and attributed these to isotope equilibration with the country rock. If isotope equilibration has occurred in the Grenada basalt compositions, it has not been a consistent process. The geochemistry and  $\text{Sr}^{87}/86$  ratios of the basalts are not correlated with higher degrees of fractionation suggesting longer periods of repose and equilibration with wall-rock.

TABLE 9

Strontium isotope data for a basanite of  
southeastern California and individual  
minerals of a lherzolite inclusion  
(Peterman et al., 1970)

	<u>Material</u>	<u>Rb/Sr</u>	<u>Sr<sup>87</sup>/86</u>
host	basanite	0.066	0.7031
	olivine	0.14	0.7087
inclusion	chrome diopside	0.014	0.7016
	orthopyroxene	0.5	0.708



### 7:5:2 Melts of different Parental Material

Although there is considerable variability in the major and trace element chemistry of the Grenada basalts, the overall similarity (Table 5) and gradational nature of these compositions does not suggest that different parental source material has been partially melted. In order that similar compositions be produced by partial melting at similar depths and temperatures within the Upper Mantle, the nature of the parental material must be relatively homogeneous in terms of chemical composition and mineralogy. This does not preclude however, the existence of small chemical and isotopic inhomogeneities.

### 7:5:3 Differences imposed at Melting Source

There is evidence from the investigations of Mantle-derived ultrabasic nodules that isotopic disequilibrium between nodules and host magma, and between the component mineral phases of the nodules exists. Peterman et al. (1970) examined the  $\text{Sr}^{87}/86$  ratios of the minerals forming a lherzolite xenolith and host basanite. The results are given in Table 9. It is apparent that there is isotopic disequilibrium between the xenolith and host basanite and within the xenolith itself. Peterman et al. suggest that if this disequilibrium can exist at magma temperatures, and perhaps even in the zone of Upper Mantle partial melting, differences in  $\text{Sr}^{87}/86$  ratios displayed by basalts on a world-wide scale could be a primary feature determined by original melting conditions. Leggo and Hutchinson (1968) determined the  $\text{Sr}^{87}/86$  ratios for a variety of ultrabasic xenoliths and host rocks from Cenozoic volcanics of the Massif Central, France. The results obtained again indicate

not only isotopic disequilibrium between host rocks and xenoliths, but also a range of  $\text{Sr}^{87}/86$  ratios within the xenoliths of 0.703 to 0.710.

Leeman and Manton (1971) reported consistently high  $\text{Sr}^{87}/86$  ratios for the Pliocene-Holocene Snake River tholeiites of southern Idaho. The average of these ratios is 0.7070. However, the late Cenozoic alkali olivine basalts of the Basin and Range Province (U.S.A.) have lower  $\text{Sr}^{87}/86$  ratios of 0.704 (Leeman and Rogers, 1970). The results of ocean floor sampling projects have shown that in basalts of similar composition (oceanic tholeiite) the  $\text{Sr}^{87}/86$  ratios differ on a global scale (eg. Subbarao, 1973; Hart, 1971).  $\text{Sr}^{87}/86$  isotopic differences within magmas of similar major element chemistry and restricted geographic distribution are not so common.

O'Hara (1968) has shown that during the partial melting of Upper Mantle lherzolite, clinopyroxene or garnet/spinel (depending on the depth of melting, p. 266 ) is the first phase to disappear. Further heating dissolves greater proportions of olivine into the melt but olivine is always the residual phase. Given that isotopic equilibrium is ever locally established in the Upper Mantle, a small amount of partial melting, as may occur in the Low Velocity Zone (see Chapter 10), would be dominated by the chemistry of clinopyroxene. In time, isotopic disequilibrium may become established between increments of melt that are removed or re-crystallised, and residual olivine. In other words, the  $\text{Sr}^{87}/86$  ratio of clinopyroxene may be altered by the removal of trace quantities of radiogenic  $\text{Rb}^{87}$ , producing in time, a lower  $\text{Sr}^{87}/86$  ratio.



The composition of the Grenada basalt 474 with a high  $\text{Sr}^{87}/^{86}$  ratio of 0.7050 apparently reflects a greater degree of partial melting of the Upper Mantle source. The lower Ce/Y ratio, higher Ni content and lower abundance of incompatible trace elements contrast markedly with the basalts (239 and 360) of low  $\text{Sr}^{87}/^{86}$  ratio. If the major and trace element composition reflects higher degrees of partial melting involving a greater proportion of olivine, the generation of higher  $\text{Sr}^{87}/^{86}$  ratios may result from the melting of an Upper Mantle source characterised by isotopic disequilibrium between mineral phases.

In a model of variable degrees of partial melting of an Upper Mantle source in isotopic disequilibrium, a gradation between high and low  $\text{Sr}^{87}/^{86}$  ratios may be predicted. Table 8 shows that such a gradation does exist between the basalt compositions within the total range of errors of the determinations. The  $\text{Sr}^{87}/^{86}$  ratios of two andesites and a dacite of the Grenada suite were also determined by O'Nions et al. (in MS), and given in Table 8. Evidence for the evolution of these compositions from trace element 'enriched' and 'depleted' basalt magma is presented later (p. 130). The significant point at this stage is the span of  $\text{Sr}^{87}/^{86}$  ratios of Grenada magmas probably varies from 0.7043 to 0.7055 taking into account the ratios determined for silica-saturated compositions. Thus the variability of  $\text{Sr}^{87}/^{86}$  ratio in the Grenada rock-suite is in accord with a variable partial melting model provided that isotopic disequilibrium prevails between constituent phases of the source material. A comparison between the observed variation of  $\text{Sr}^{87}/^{86}$  ratios of Grenada and the other islands of the Lesser Antilles is presented in Chapter 11.

### 7:6 Notes on the presentation of the Grenada Geochemical Data

The variety of major and trace element composition of the Grenada calc-alkaline rock suite creates difficulties in presentation of the data. In Fig. 21 the normative projections of Grenada picritic and basaltic compositions are plotted. Relating trace element abundances and element ratios produces a complete gradation between those compositions enriched and those depleted in incompatible trace elements. There is a tendency for those basalts associated with higher degrees of partial melting to contain higher normative olivine and lower normative diopside, albite and nepheline. A simple symbolic notation has been used in Fig. 21 to indicate the gradation of trace element chemistry and normative mineralogy. The symbols used refer to relative degrees of enrichment of incompatible trace elements within picrites and basalts and are given below Fig. 21. In addition the symbols used for plotting individual compositions are given in Table 5. The simple notation proved useful in distinguishing rock suites of individual volcanic centres. The geochemical trends are examined in more detail in the following section. However, it is possible to distinguish trace element abundances that reflect the initial concentrations within more basic magmas. The relative abundance of Sr provides one of the most distinctive trace element distribution patterns in the evolved compositions. The terms 'high-Sr' and 'low-Sr' are used in a descriptive sense to identify series within centres of contrasting degrees of trace element enrichment. The absolute degree of enrichment varies from centre to centre, and the terms only relate series within



centres.

Fig. 21 shows that the degree of trace element enrichment is not directly related to the classification proposed earlier (p. 96 ). The term 'alkali basalt' for example covers a range of major and trace element contents, related only by the fact that all have nepheline in the norm. In the following section and chapters, the evolution of the Grenada calc-alkaline rock suite is described. In brief, the lengthy volcanic history of the island (Chapter 6) has involved a series of separate partial melting episodes that have, on occasions, given rise to silica-saturated calc-alkaline derivatives. Although some of the basalts are related by crystal fractionation processes, the range of chemical compositions reflects the individual characteristics of a melting episode. Consequently the use of the term 'parental magma' is not applicable to a unique chemistry. Individual rock series within volcanic centres have apparently been derived by crystal fractionation of picritic, alkali and transitional basalt parent magmas. The major and trace element variation of these rock series is described in the next section.

## CHAPTER 8

### GEOCHEMISTRY II

#### The Basalt-Andesite-Dacite association of Grenada

In this chapter, the geochemical gradation between basalt, andesite and dacite compositions of the Grenada calc-alkaline suite is discussed. The trend towards increasing silica-saturation from the silica-undersaturated basalts is examined, and related to the variable partial melt compositions described in Chapter 7.

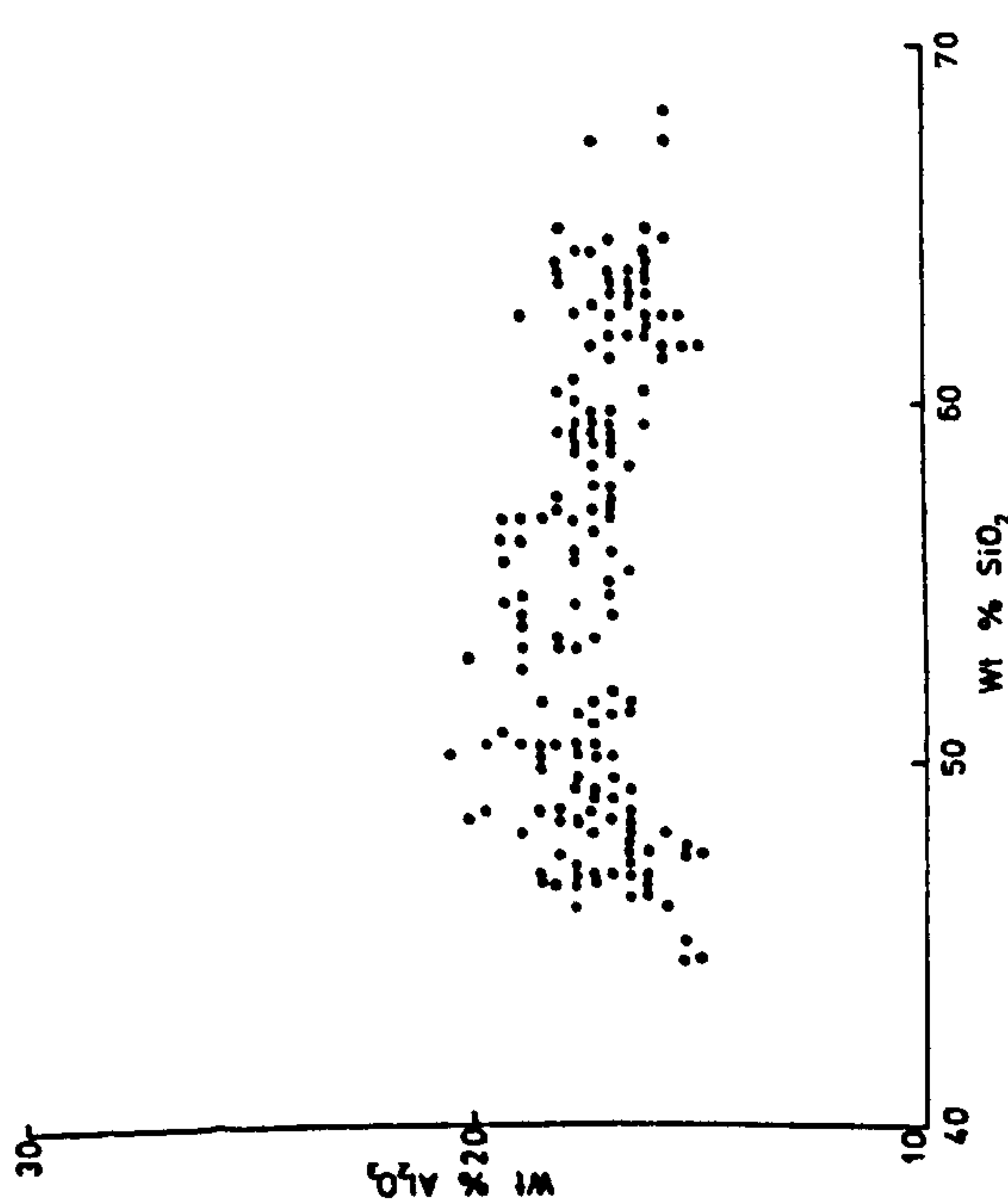
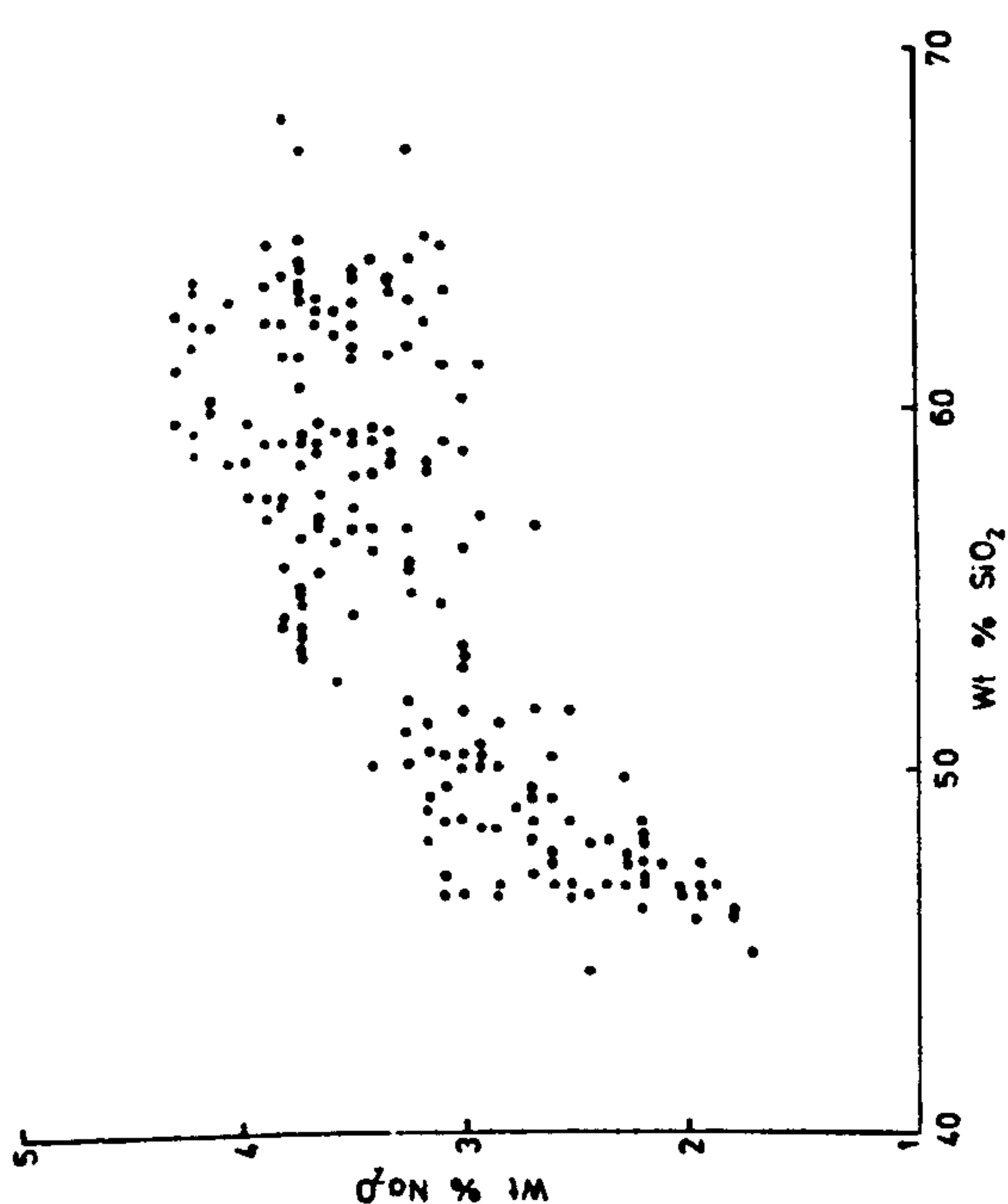
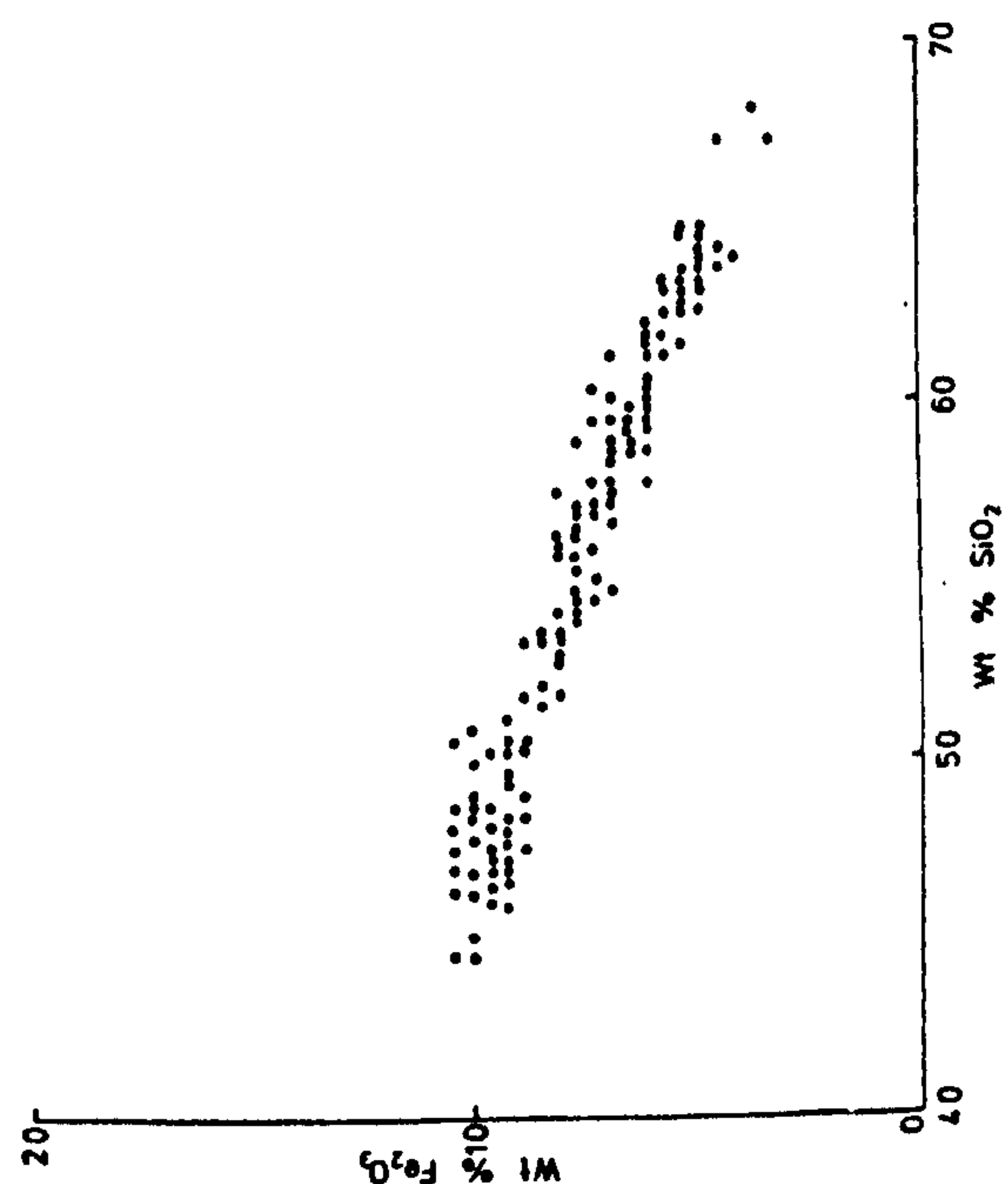
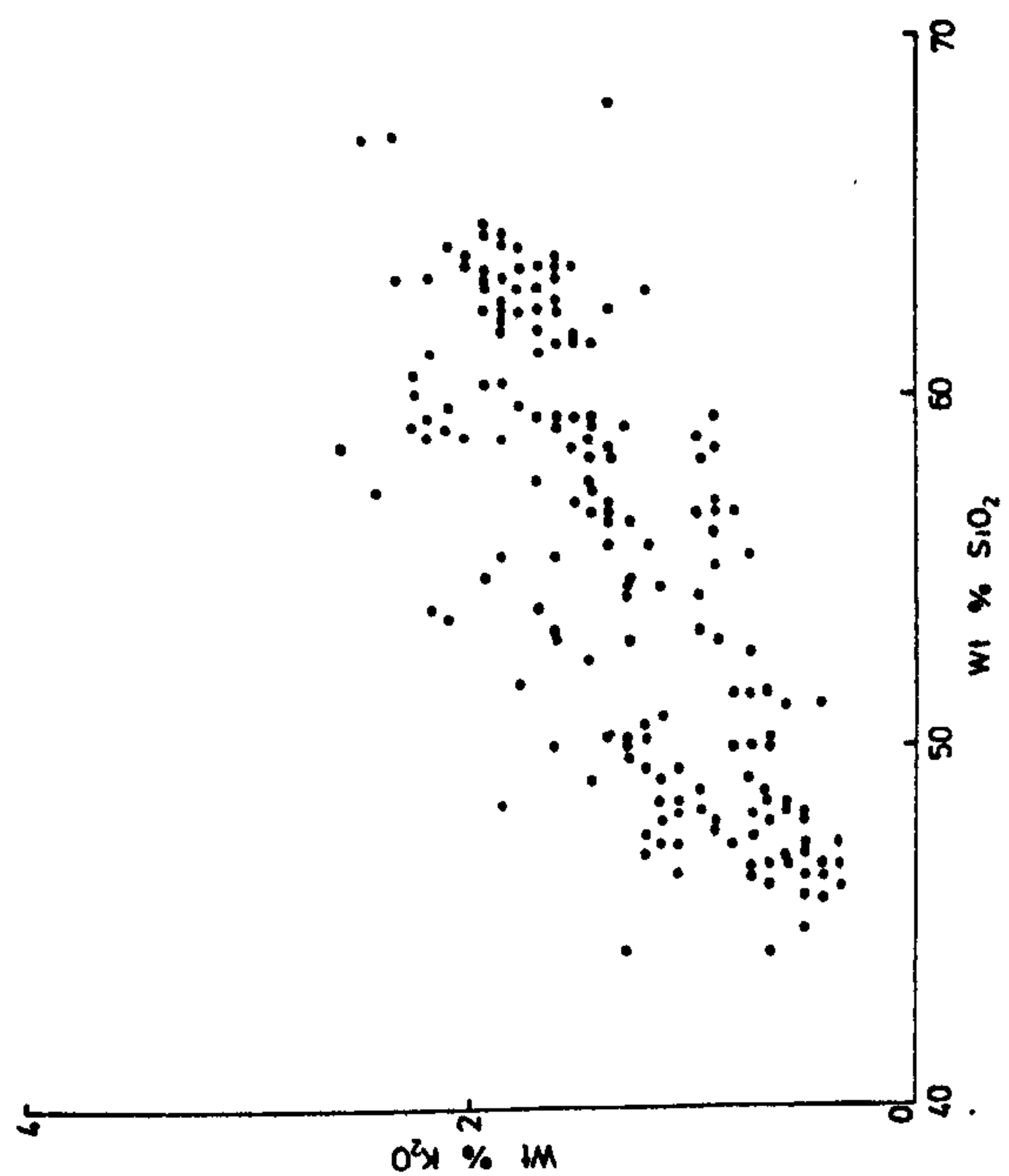
#### 8:1 Major oxide variation

The major oxide variation with increasing silica content of the Grenada volcanic suite is presented in the form of a series of Harker diagrams in Fig. 27. Analyses of samples from all types of volcanic units and centres are included in these diagrams. Apart from the presence of very basic compositions, the general trend of oxide variation is similar to previously described calc-alkaline suites of the Lesser Antilles (Baker, 1968; Rea, 1970). The derivation of these calc-alkaline suites by fractional crystallisation of high-alumina basalt magma has been suggested by Baker (1968), Rea (1970) and Lewis (1971). The oxide variation diagrams of Fig. 27 however, reveal in total a considerable distribution of concentrations at a given SiO wt.%. These concentrations are more variable than in the Lesser Antilles calc-alkaline suites mentioned above. In Chapter 7, the range of basaltic and picritic compositions was related to a variable partial melting model of an Upper Mantle peridotite source. The

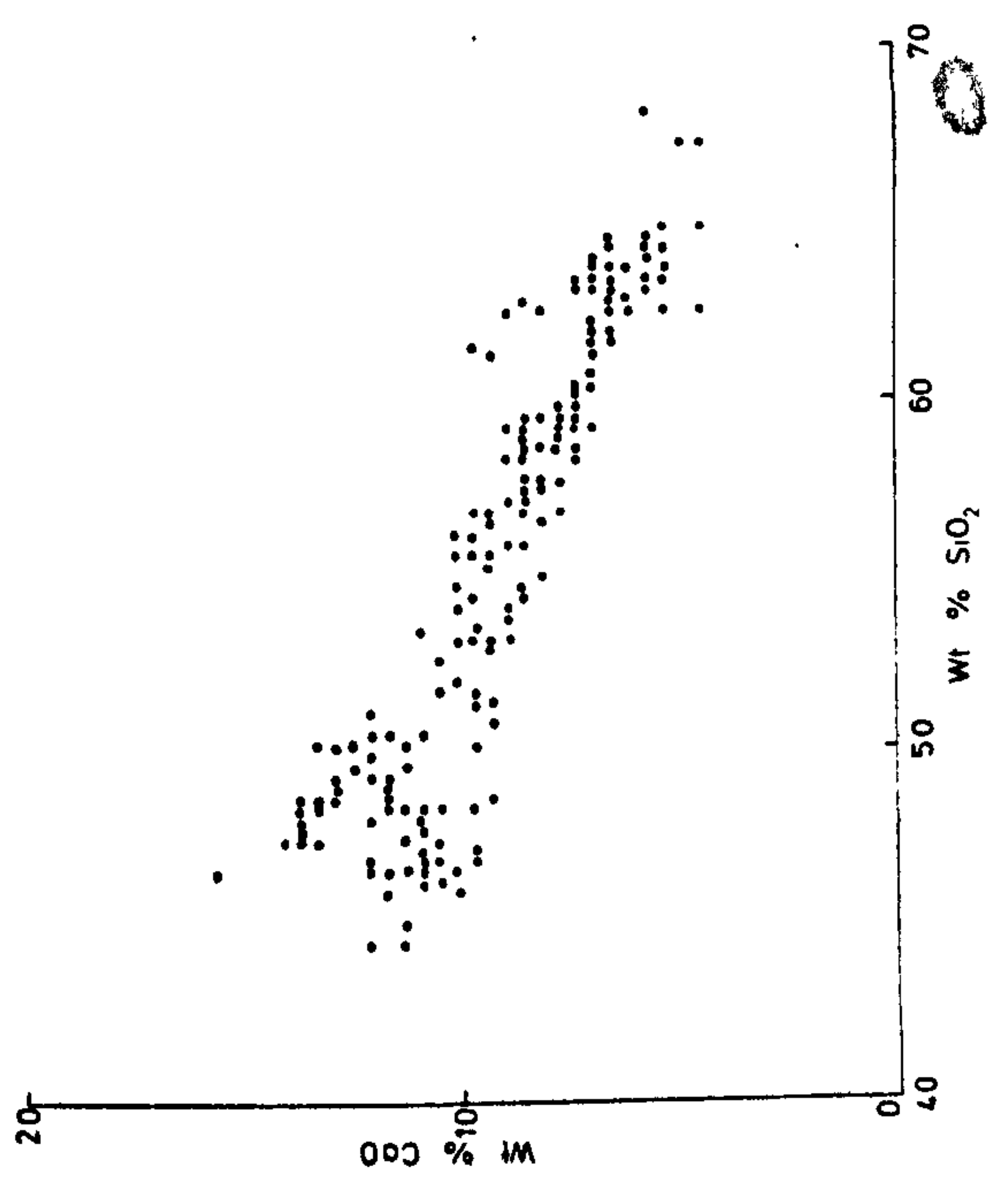
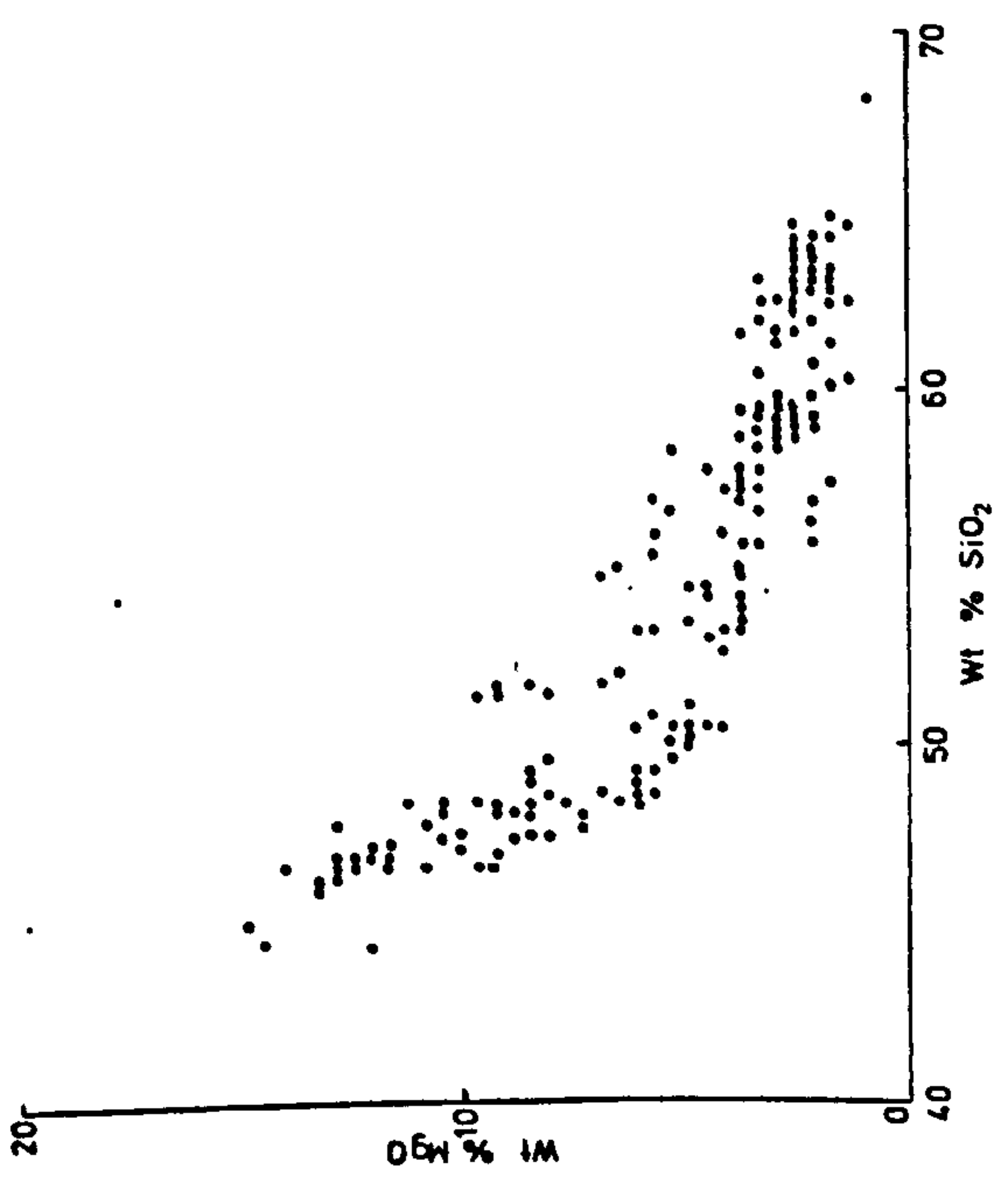
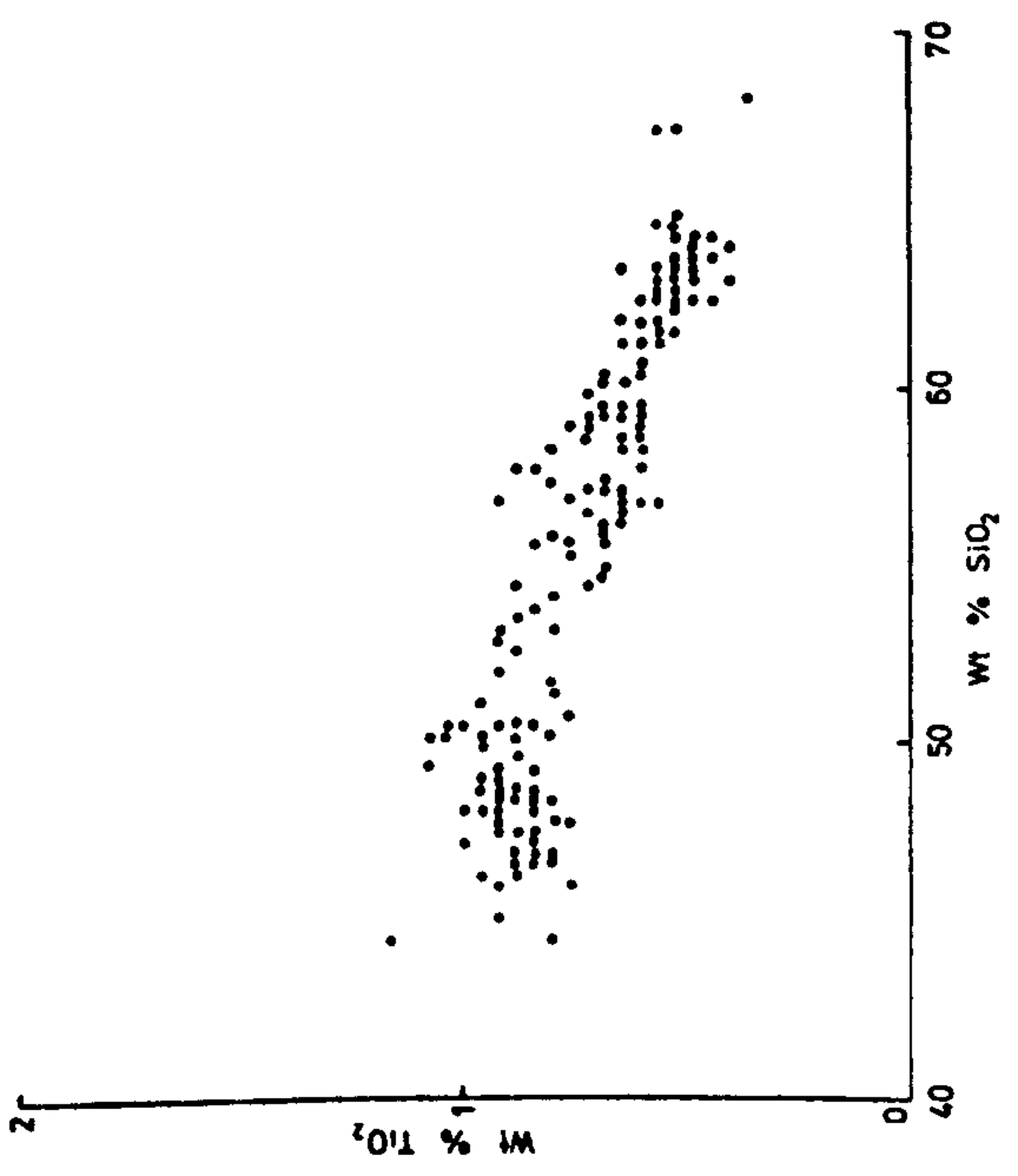


Fig. 27

Major oxide variation of the Grenadan rock suite.







andesites and dacites of Grenada are believed to be derived from these basic melts by fractional crystallisation processes. The evidence for these processes is presented in the following pages and chapters, but may be summarised by:

- 1) The smooth trend of major element variation within volcanic series from individual centres of activity.
- 2) The petrographic gradation between picrites, basalts, andesites and dacites.
- 3) The presence of cumulus plutonic blocks containing mafic and feldspathic minerals, suggesting crystallisation and settling of these minerals has occurred.

#### 8:2 Fractional crystallisation and trace element variation

Fractional crystallisation of similar mineral phases in precisely the same proportions from basaltic melts of different major and trace element composition, would result in the preservation of these differences. In Chapter 9, the mineralogy of the Grenada calc-alkaline rock suite is examined and the similarity between component minerals of volcanic series of contrasting composition discussed. The modal abundance of these minerals however, is different and may explain the patterns of major and trace element variation observed (Chapter 10).

The interpretation of the geochemical data is simplified by examination of rock suites from individual volcanic centres. Presentation of the complete data for the whole island in this manner would be unwieldy. Accordingly, the volcanic centres of Mt. Granby - Fedon's Camp and Mt. St. Catherine have been selected in order to illustrate the geochemical features observed. The variation of major and trace elements with increasing  $\text{SiO}_2$  wt. %



of the volcanic suites of these centres is given in Fig. 28 . Only analyses of samples from lava flows and primary fragmental deposits were used in the construction of these diagrams. Samples from secondary fragmental deposits were also used where the centre of derivation of the deposit is unambiguous. The derived nature of secondary fragmental deposits means that in some cases the true affinity with a volcanic centre is uncertain. The chemical analyses of the samples used are given in Appendix I .

The features to note in particular of Fig. 28 are the variation of Sr, Ni and MgO with increasing  $\text{SiO}_2$  wt.%. In general, it is apparent that there are at least two rock series present within the centres of Mt. Granby - Fedon's Camp and Mt. St. Catherine characterised by different patterns of chemical variation. In order to distinguish these series, the terms 'high-Sr' and 'low-Sr' are applied since the behaviour of the trace element Sr is particularly striking. For example, the high-Sr series of the Mt. Granby - Fedon's Camp centre is associated with a rapid increase in the abundance of Sr from approximately 600 ppm in alkali basalts to 1500 ppm in transitional basalts and andesites followed by a steady decline to dacites. In the same sense of increasing  $\text{SiO}_2$  wt.%, there is a rapid decline in the abundance of Ni from 300 ppm in alkali basalts to 30 ppm in transitional basalts and andesites. In contrast, there is a steady increase in the abundance of Sr in the low-Sr series of this centre from 300 ppm in alkali basalts to 900 ppm in the andesites and dacites. The abundance of Ni is generally higher in the low-Sr series than the high-Sr series. Thus the Sr/Ni ratio is a particularly useful parameter for

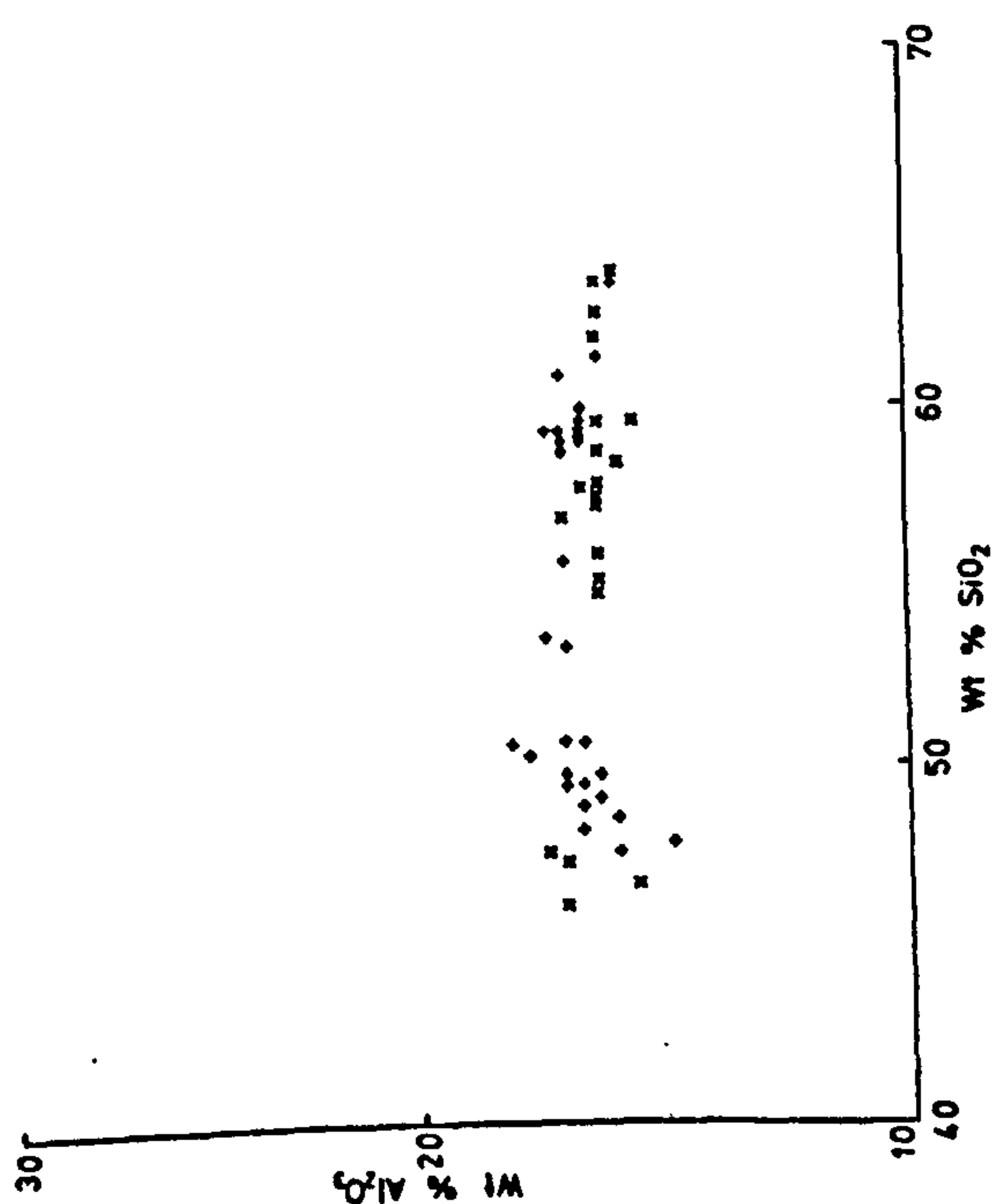
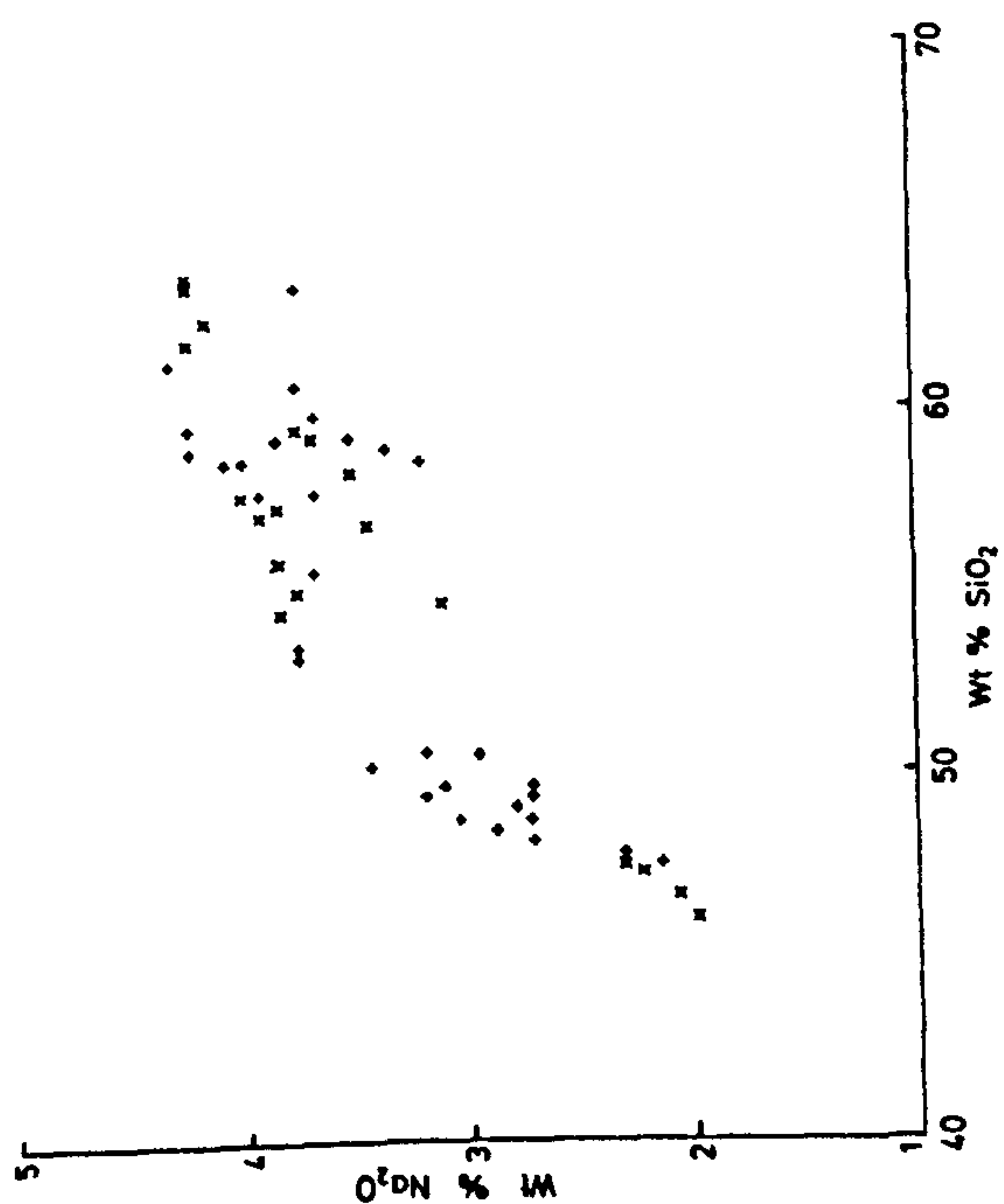
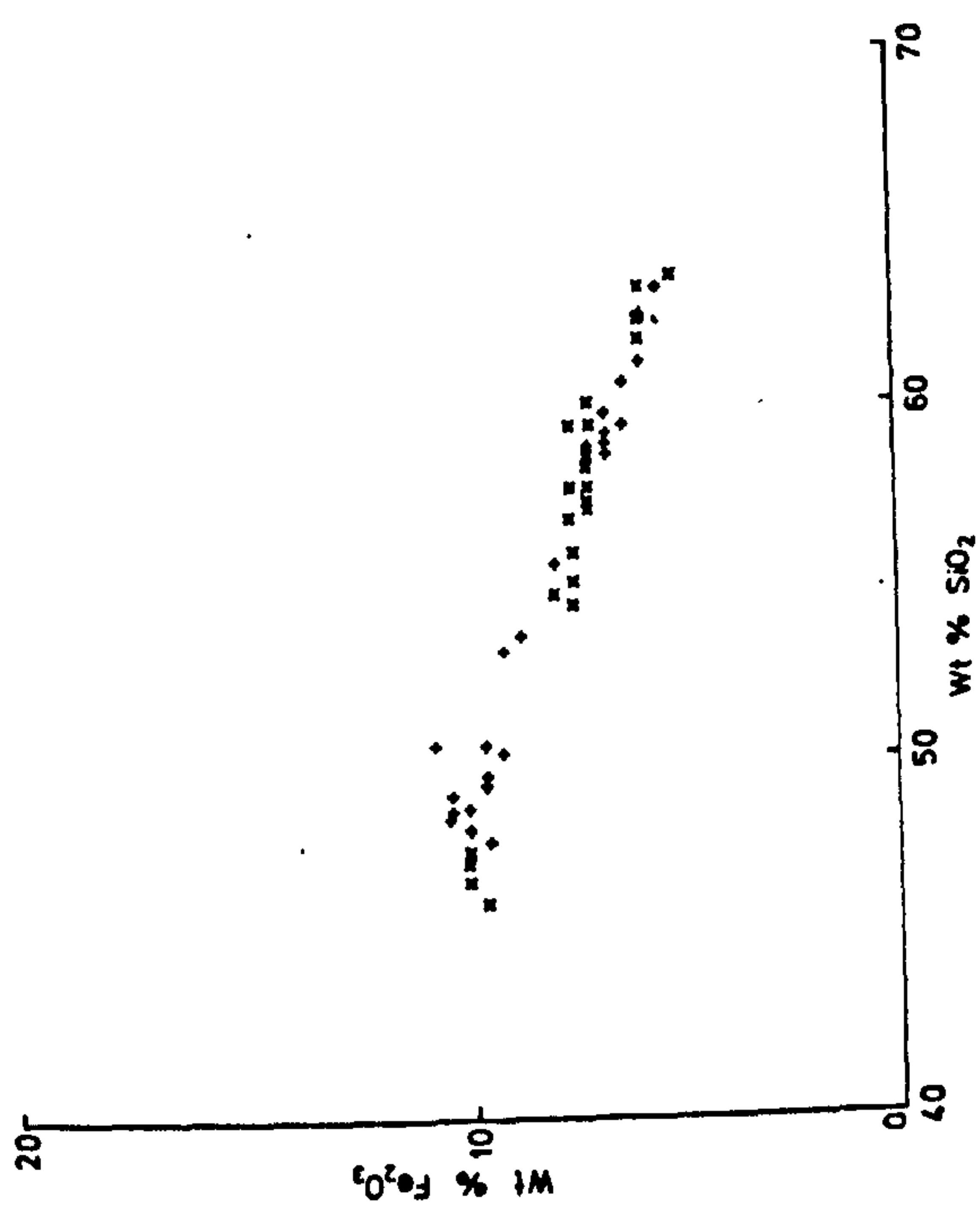
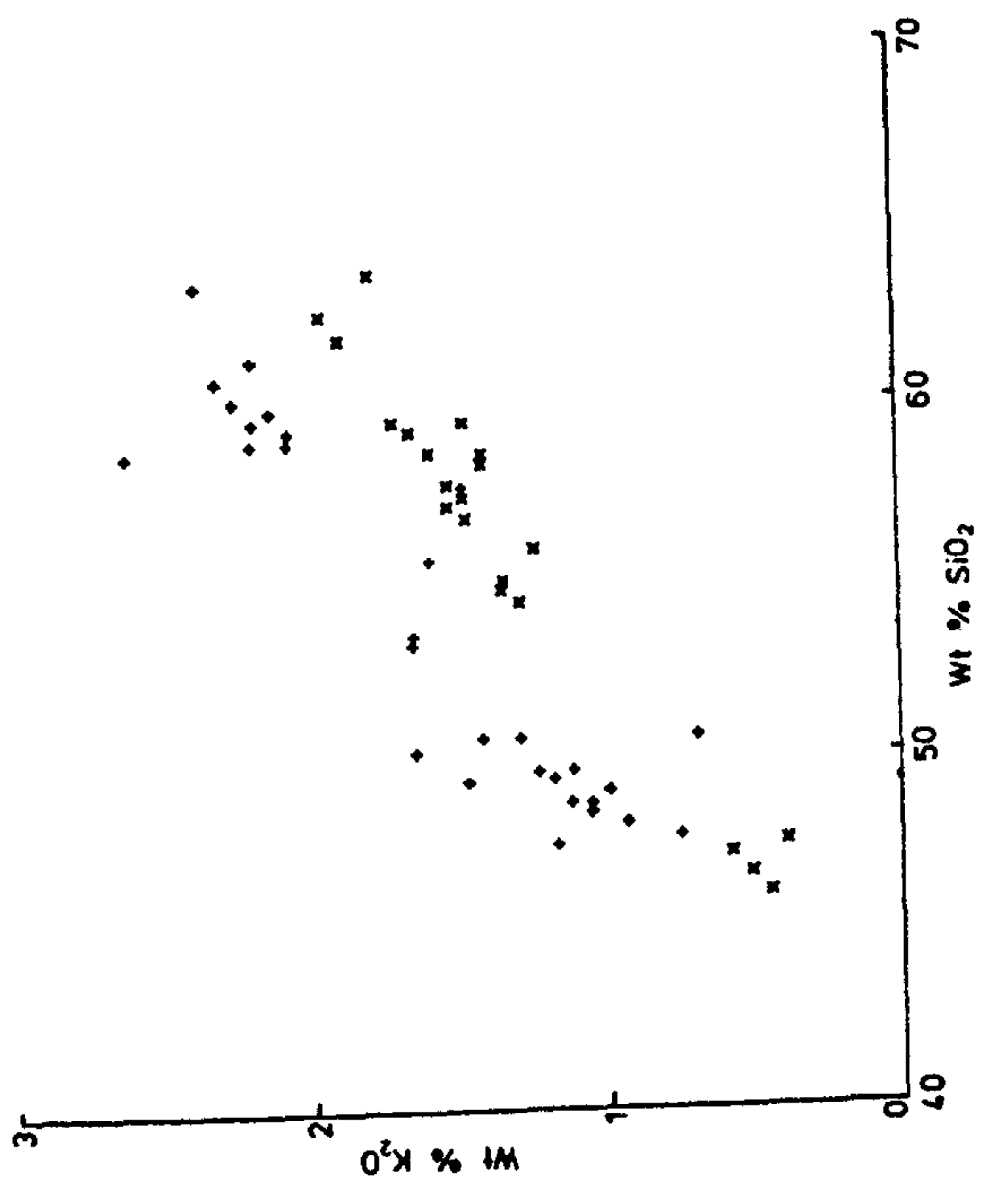
Fig.28a

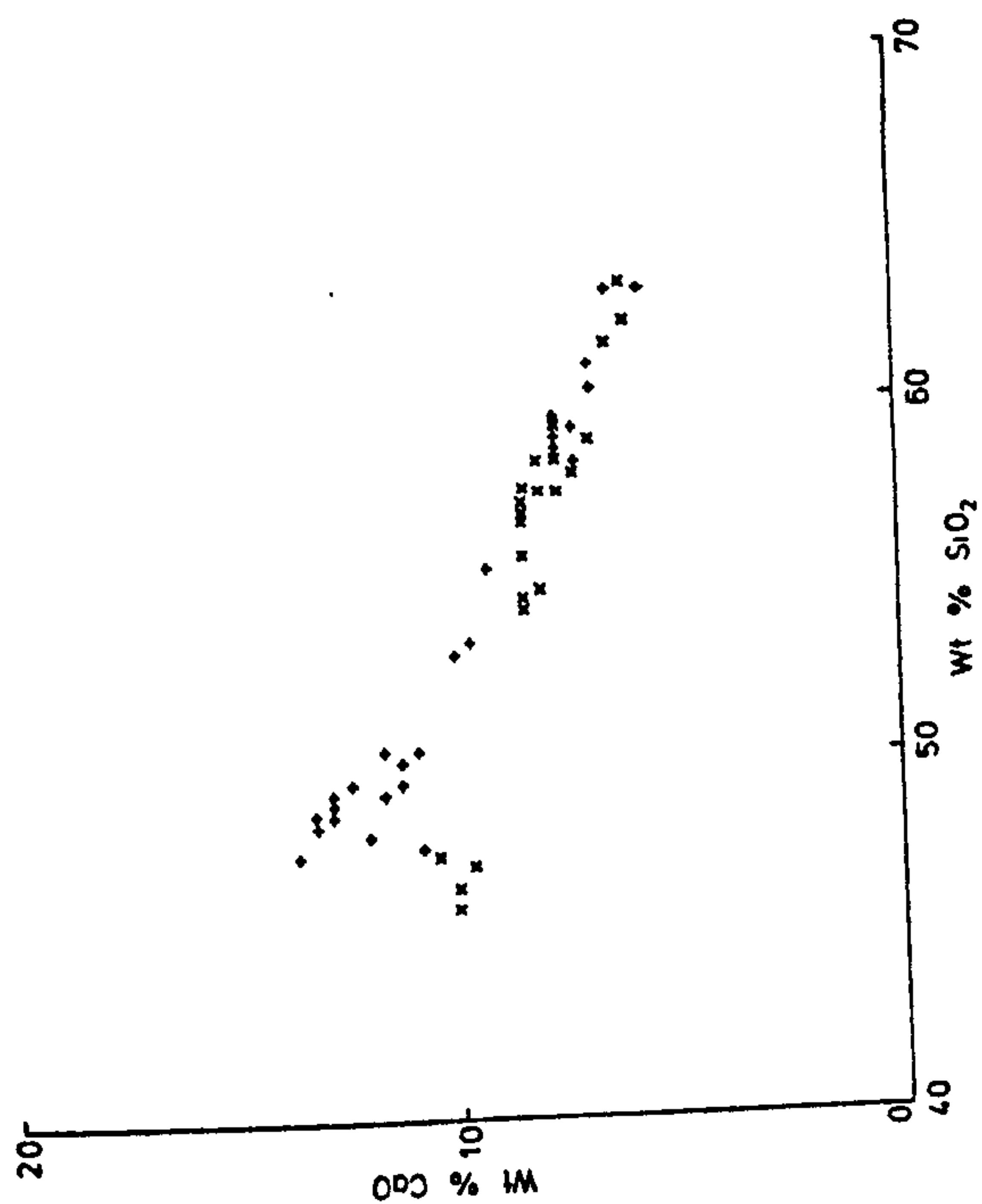
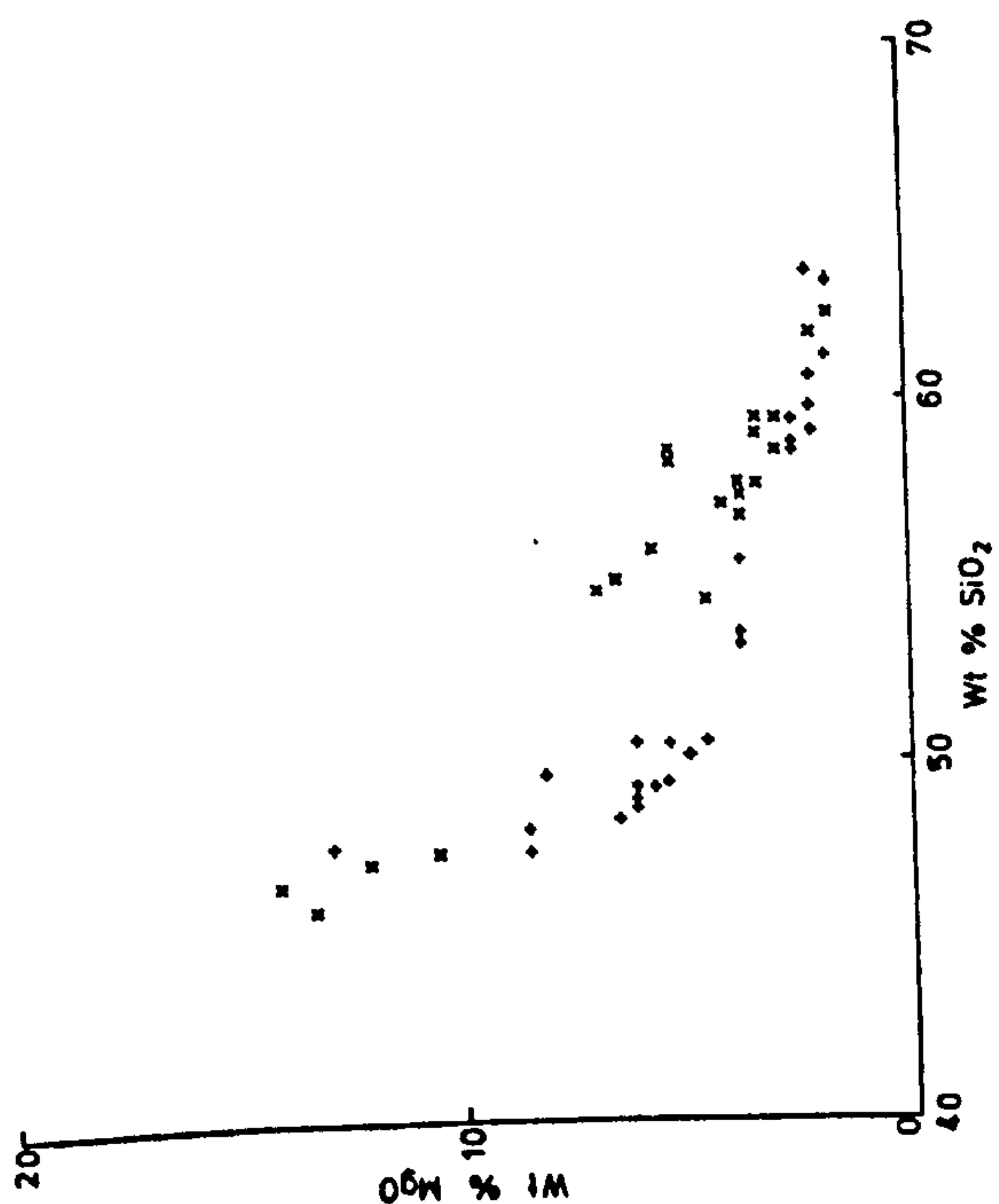
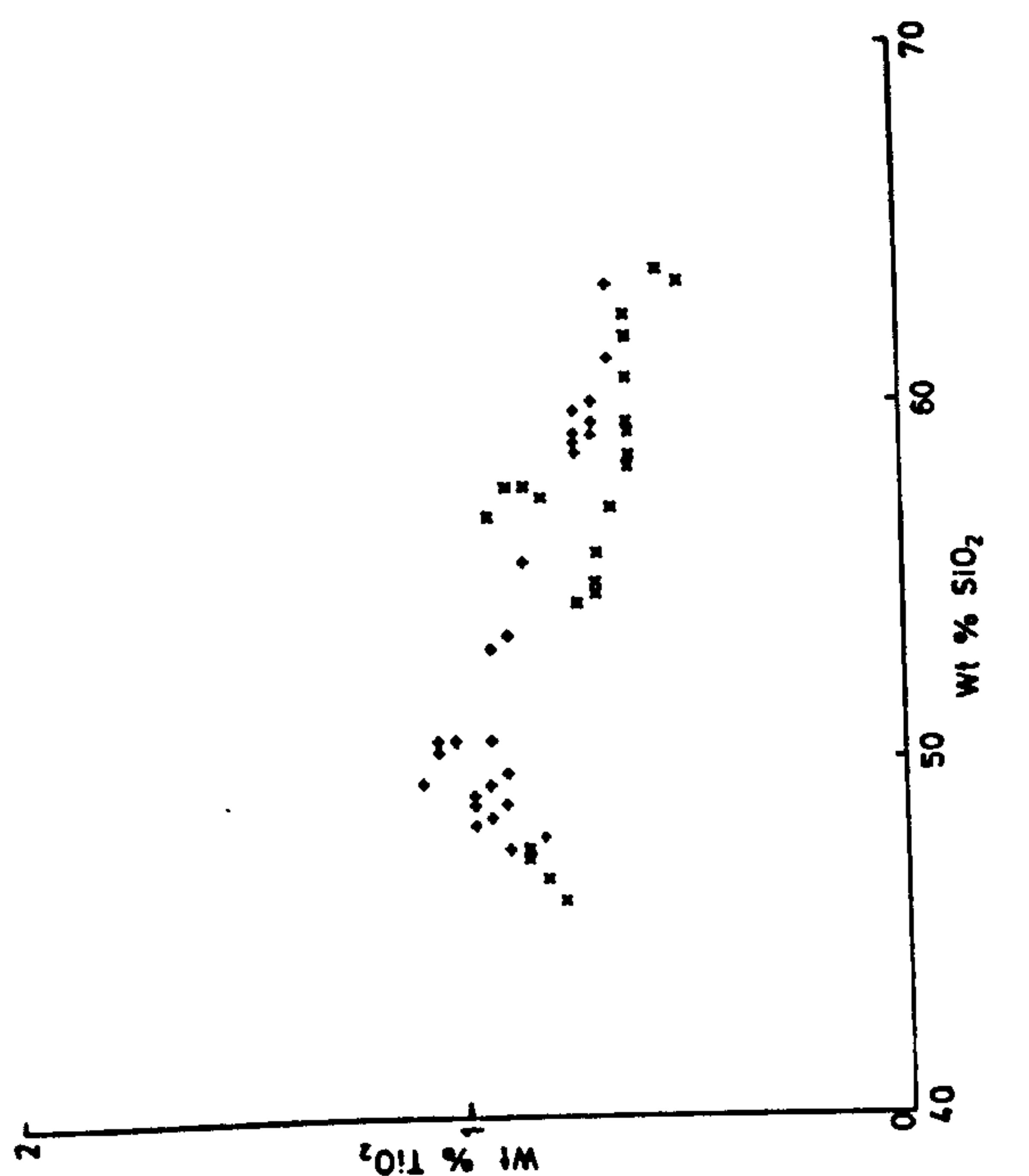
Major and trace element variation in the Mt. Granby -  
Fedon's Camp volcanic centre.

X = low-Sr series

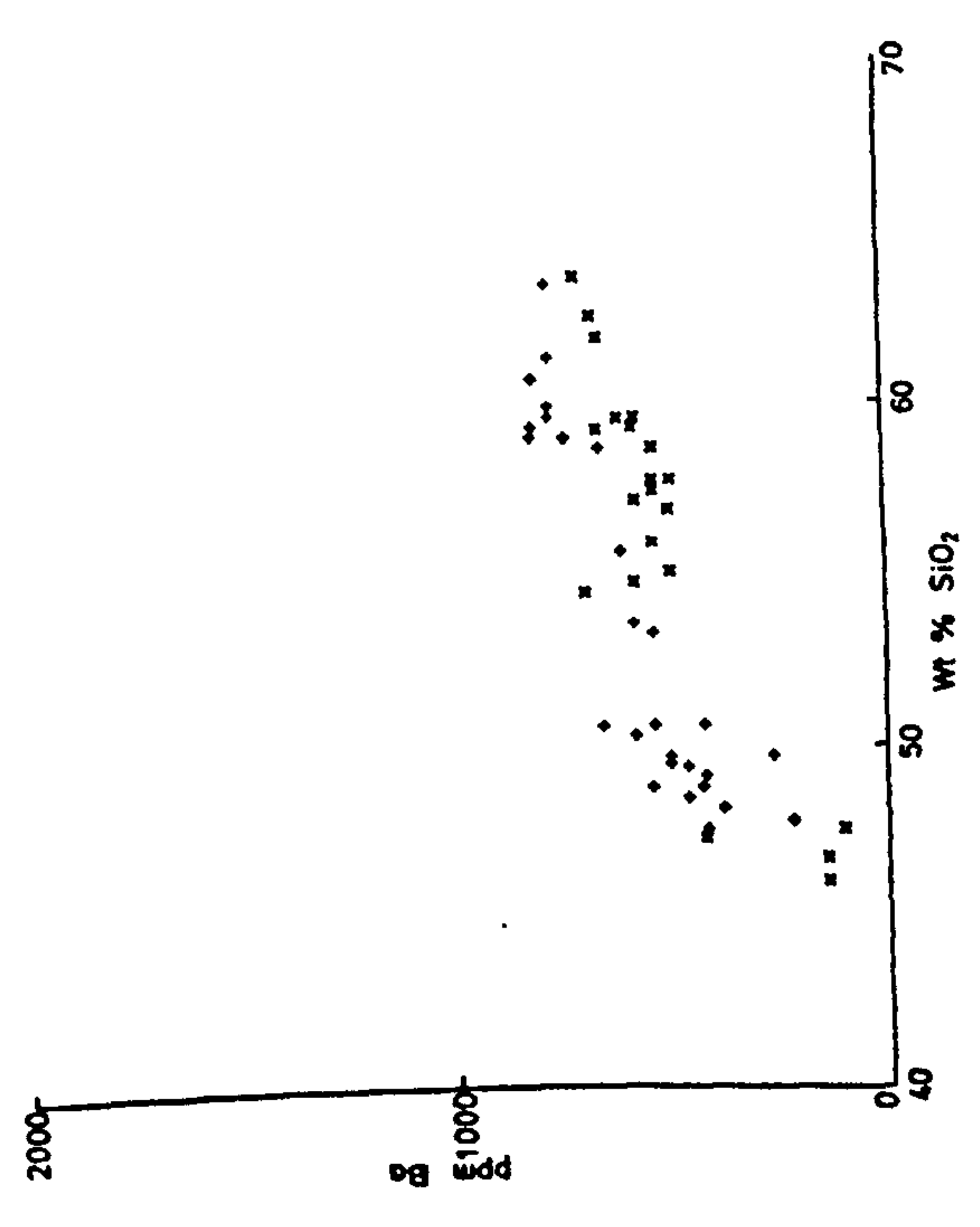
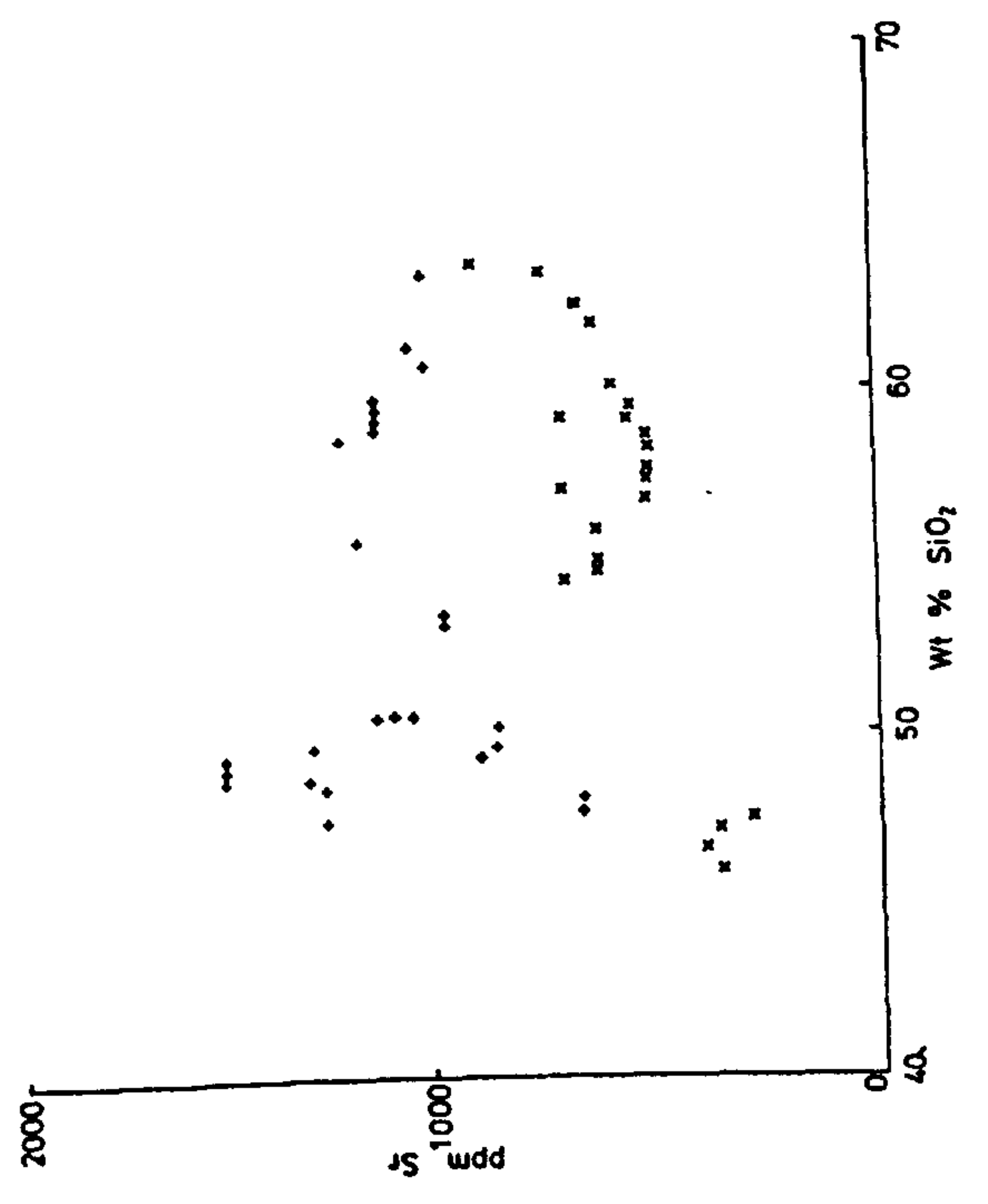
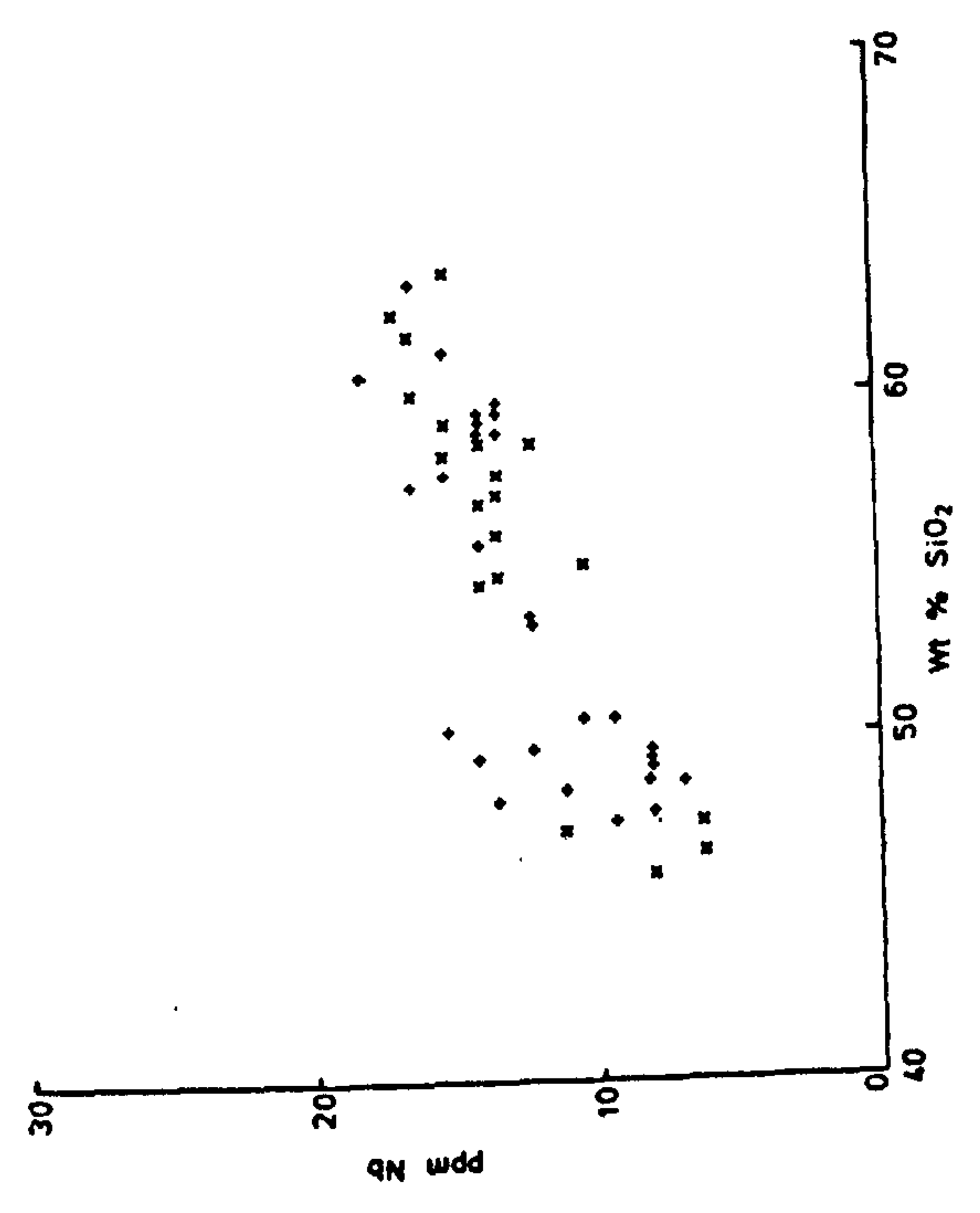
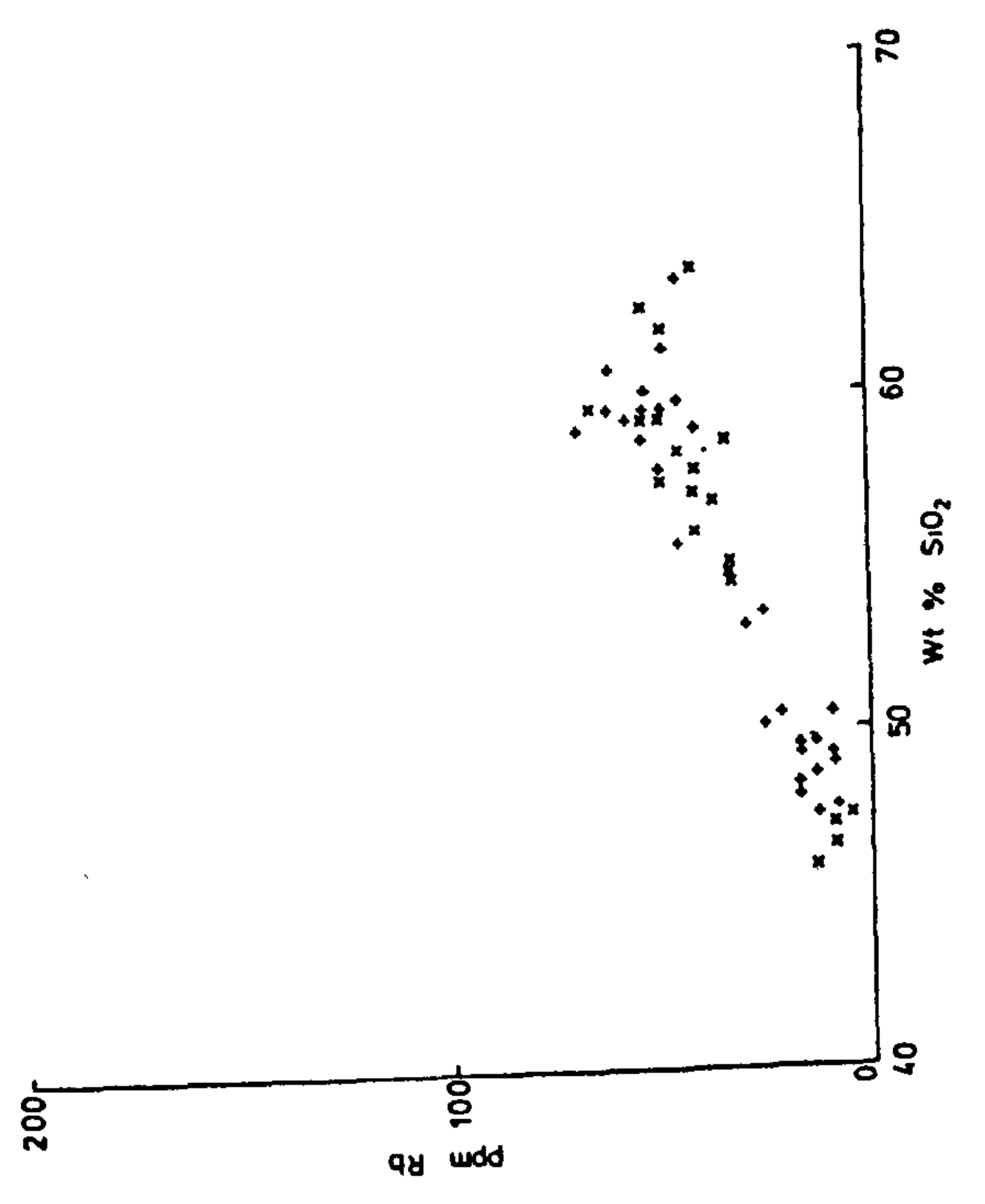
+ = high-Sr series











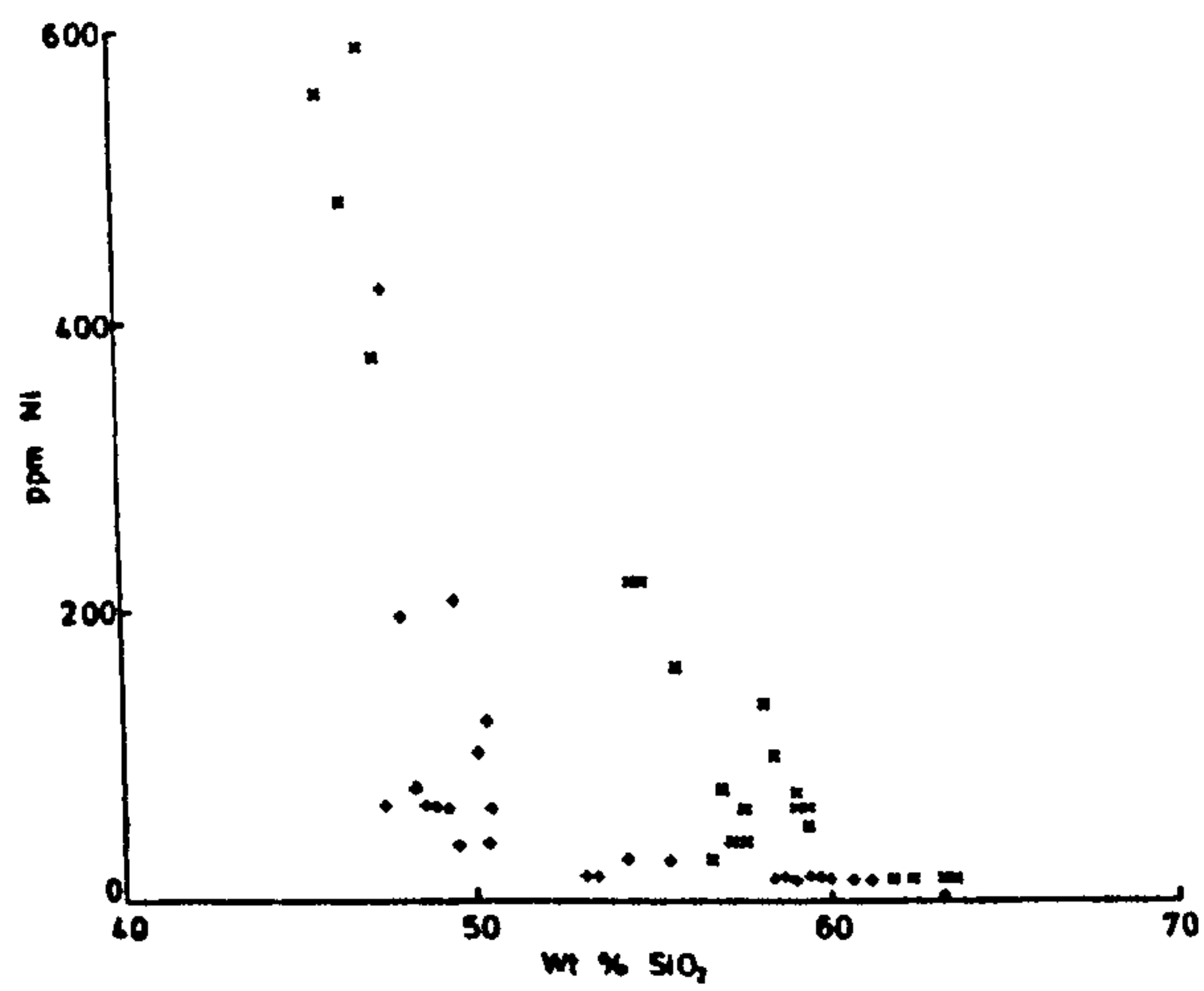
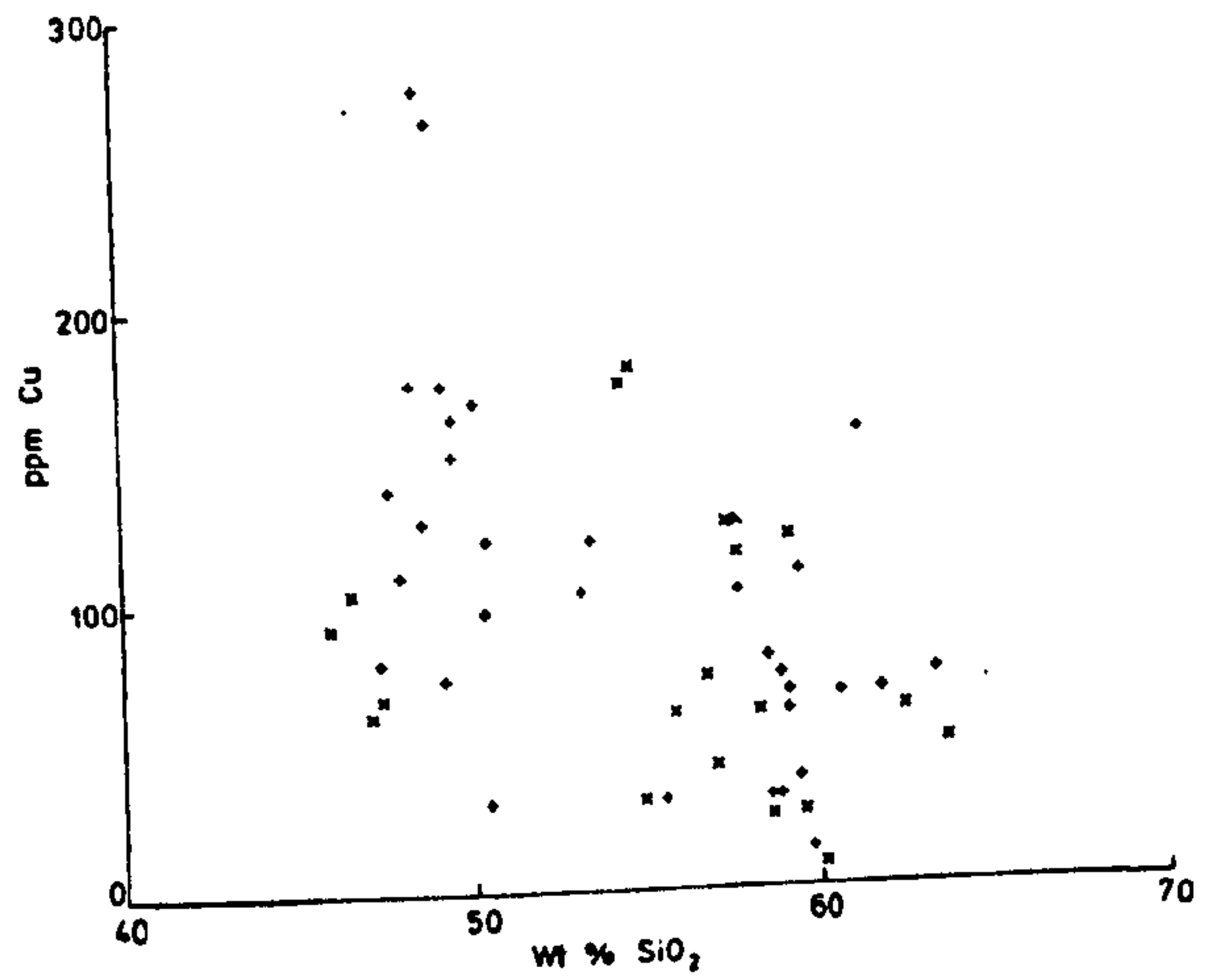
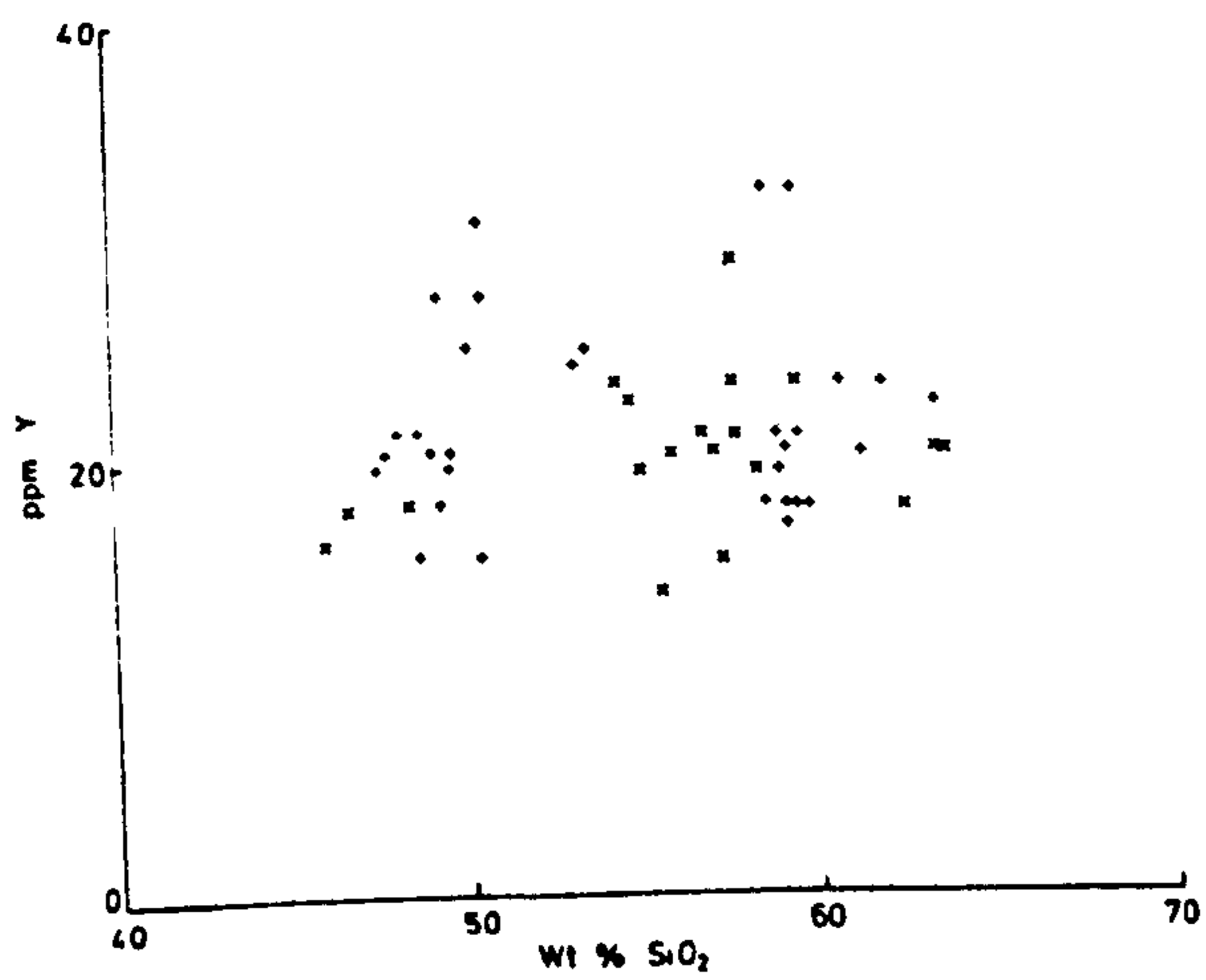
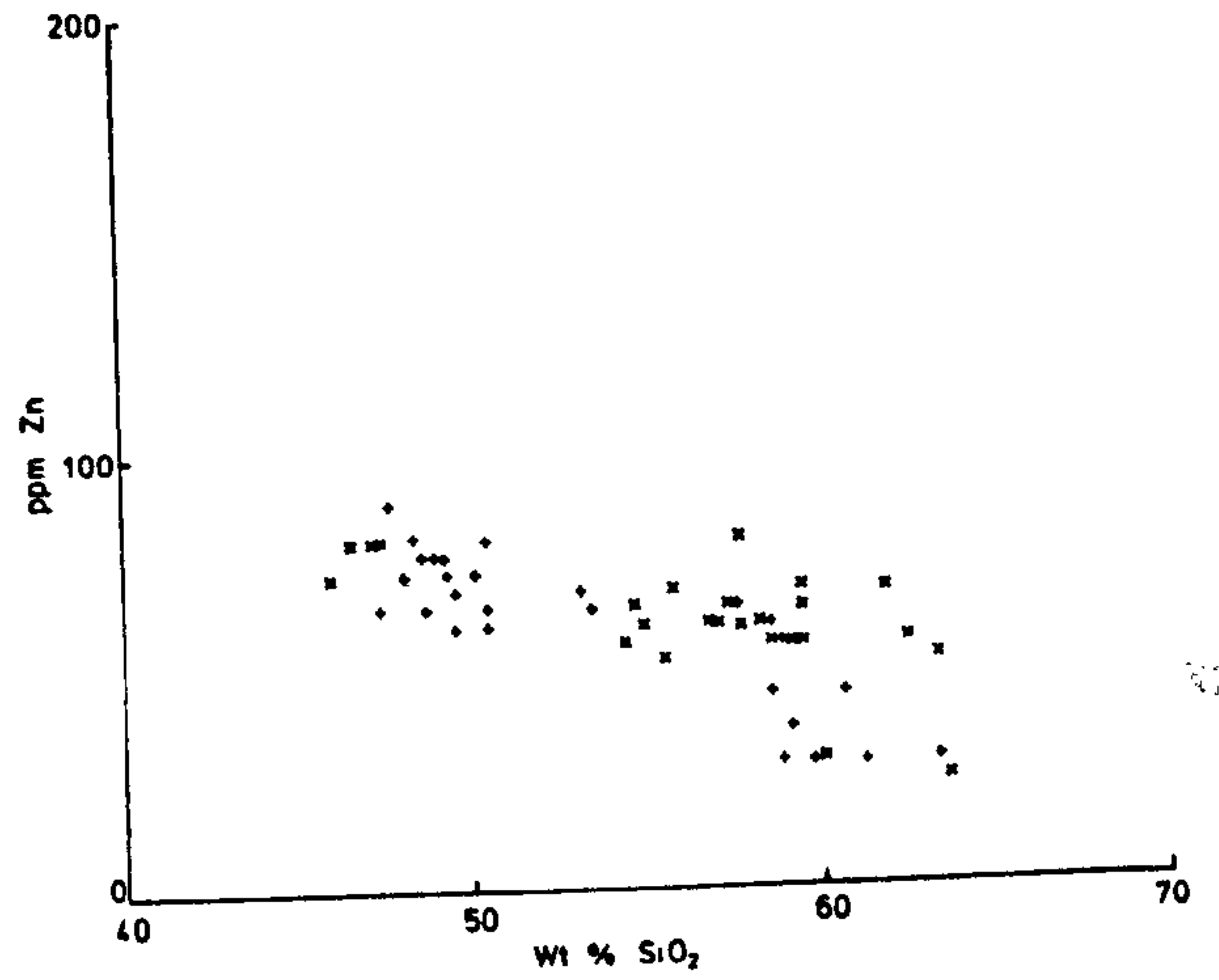
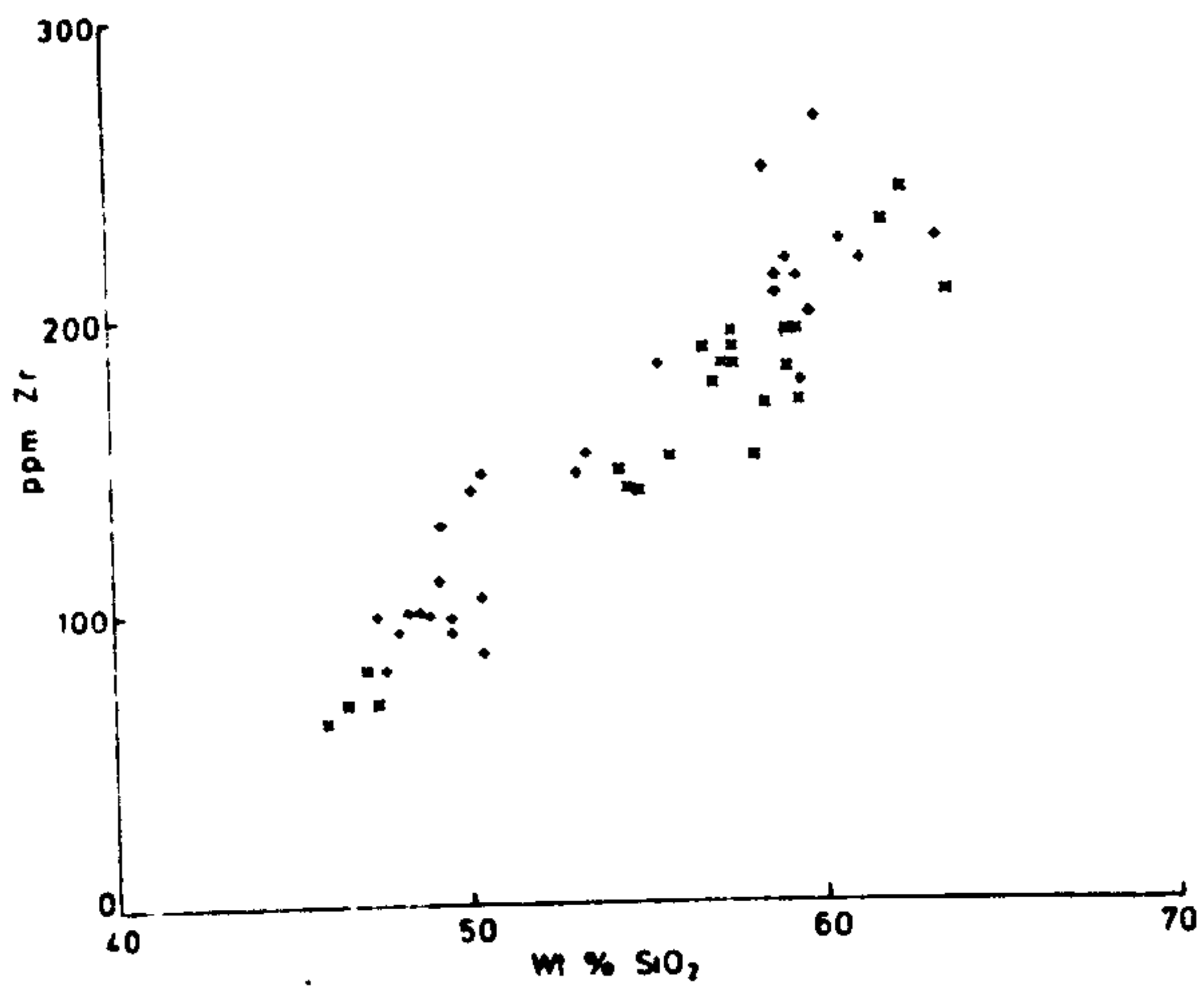


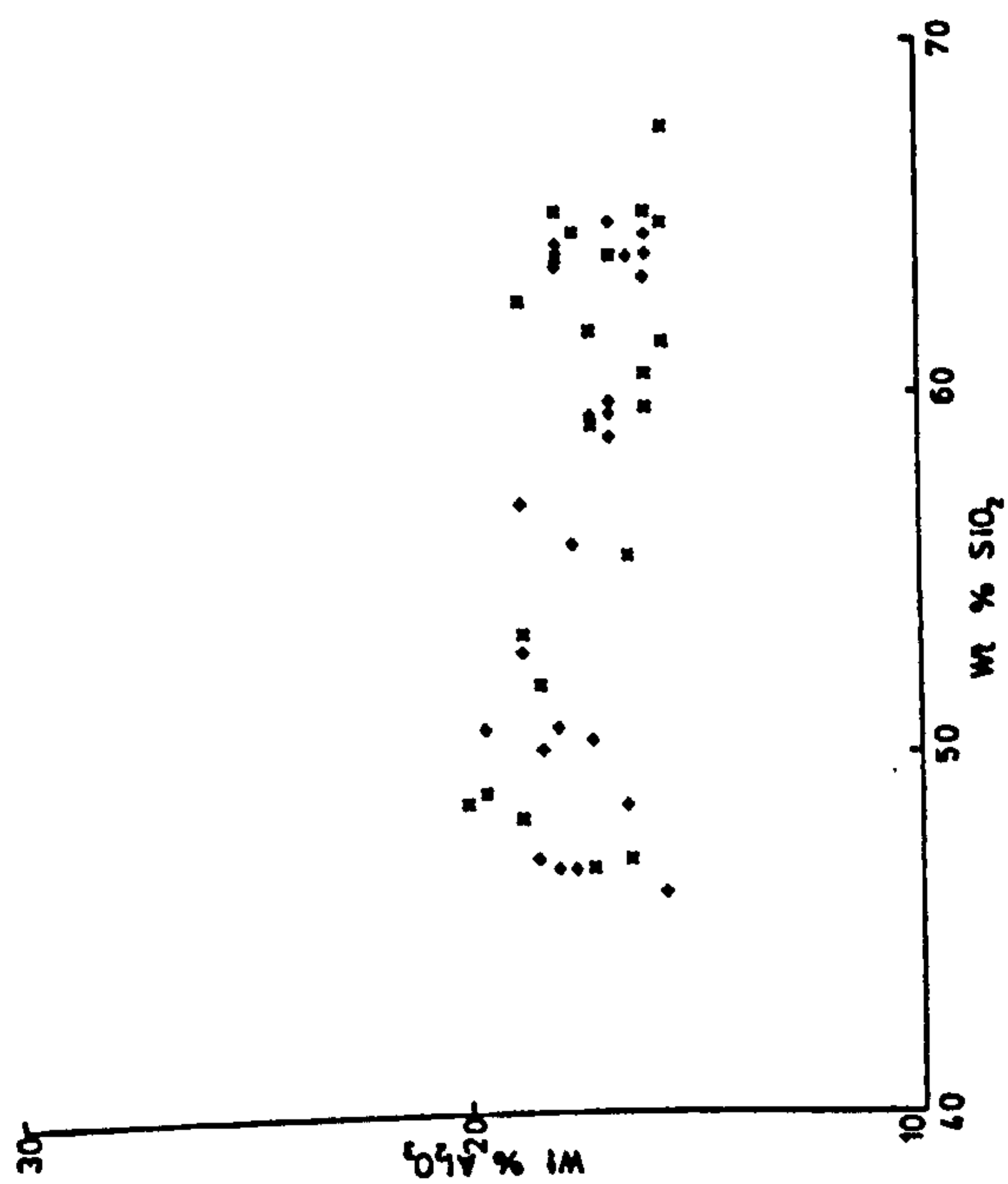
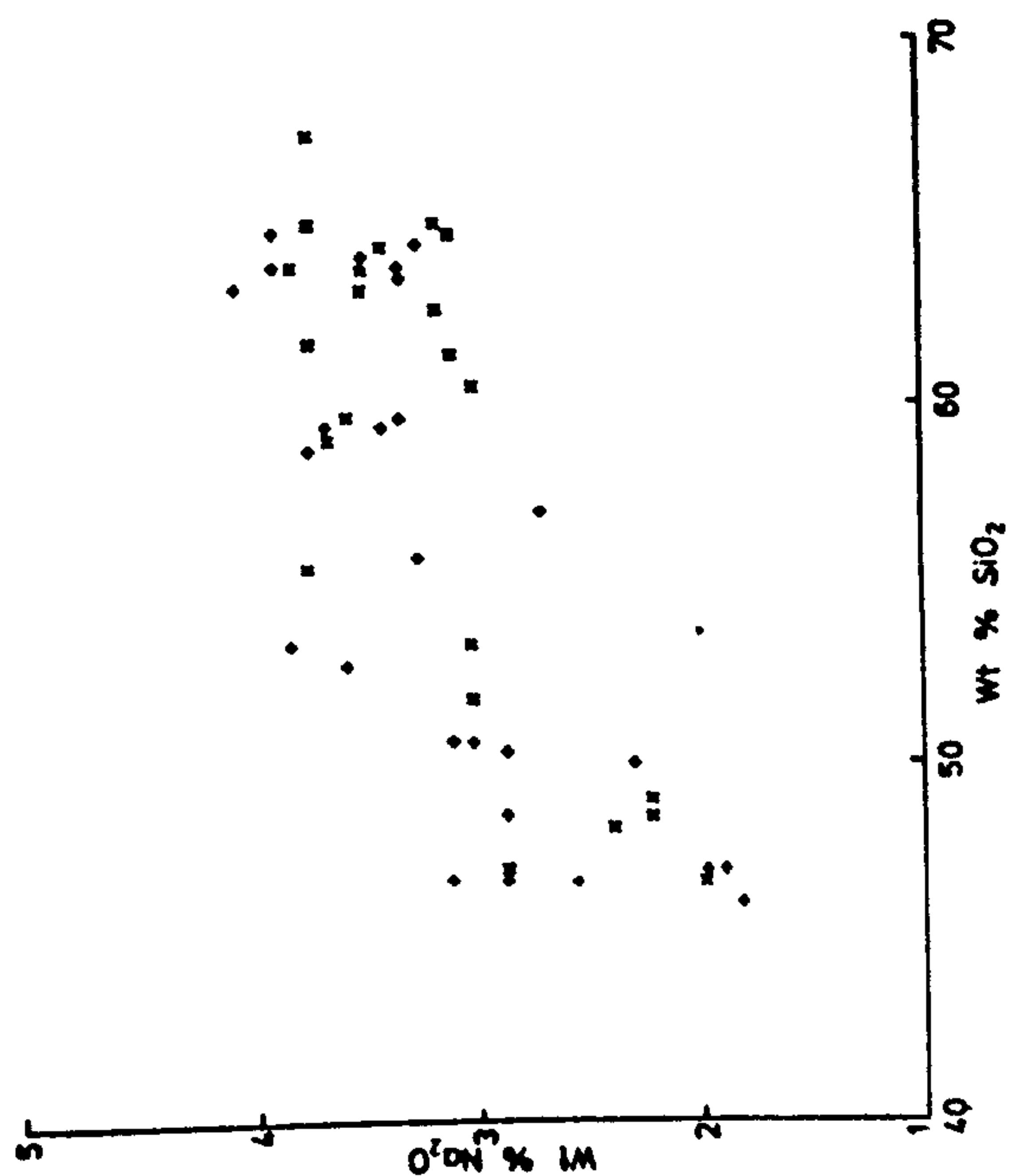
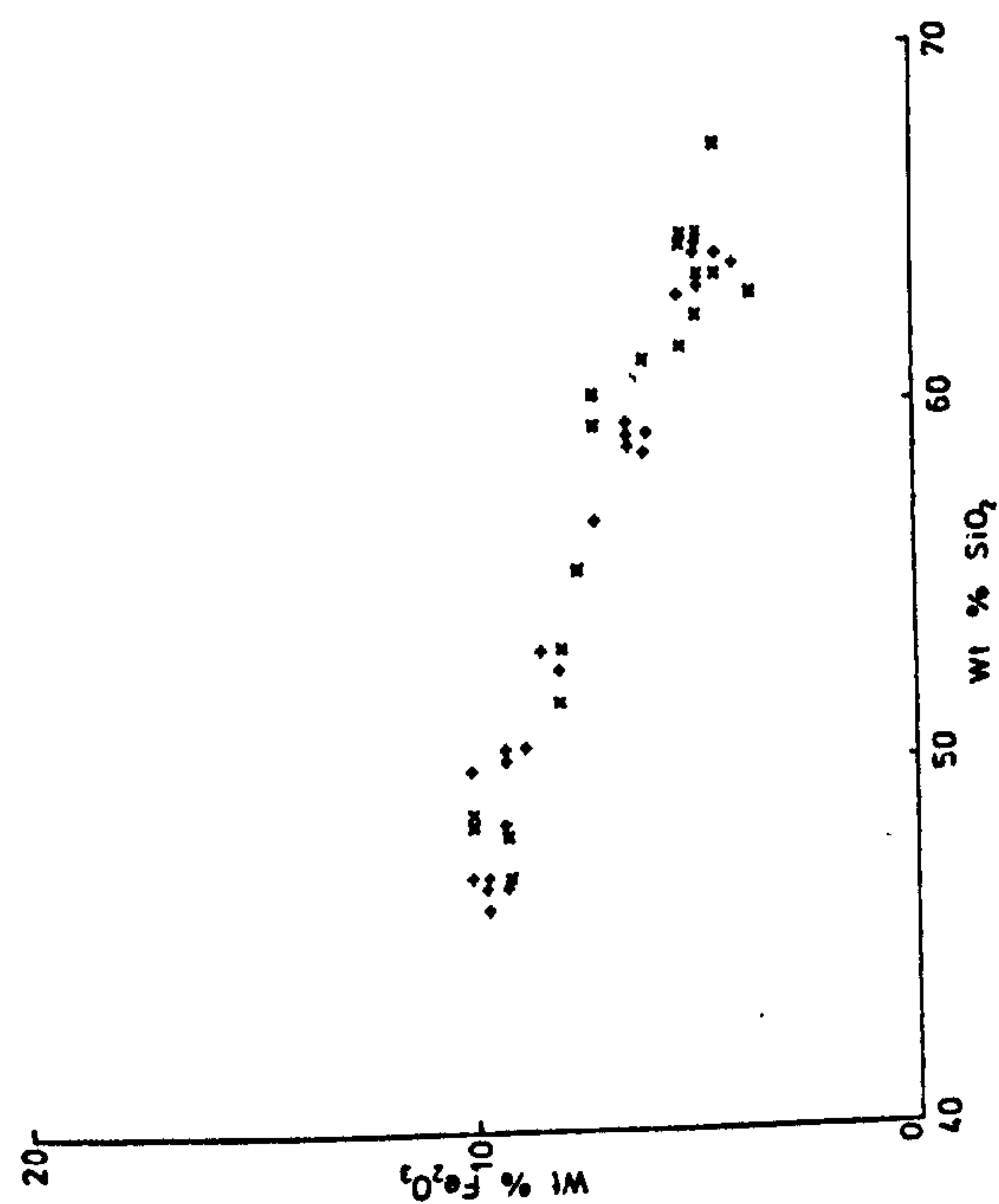
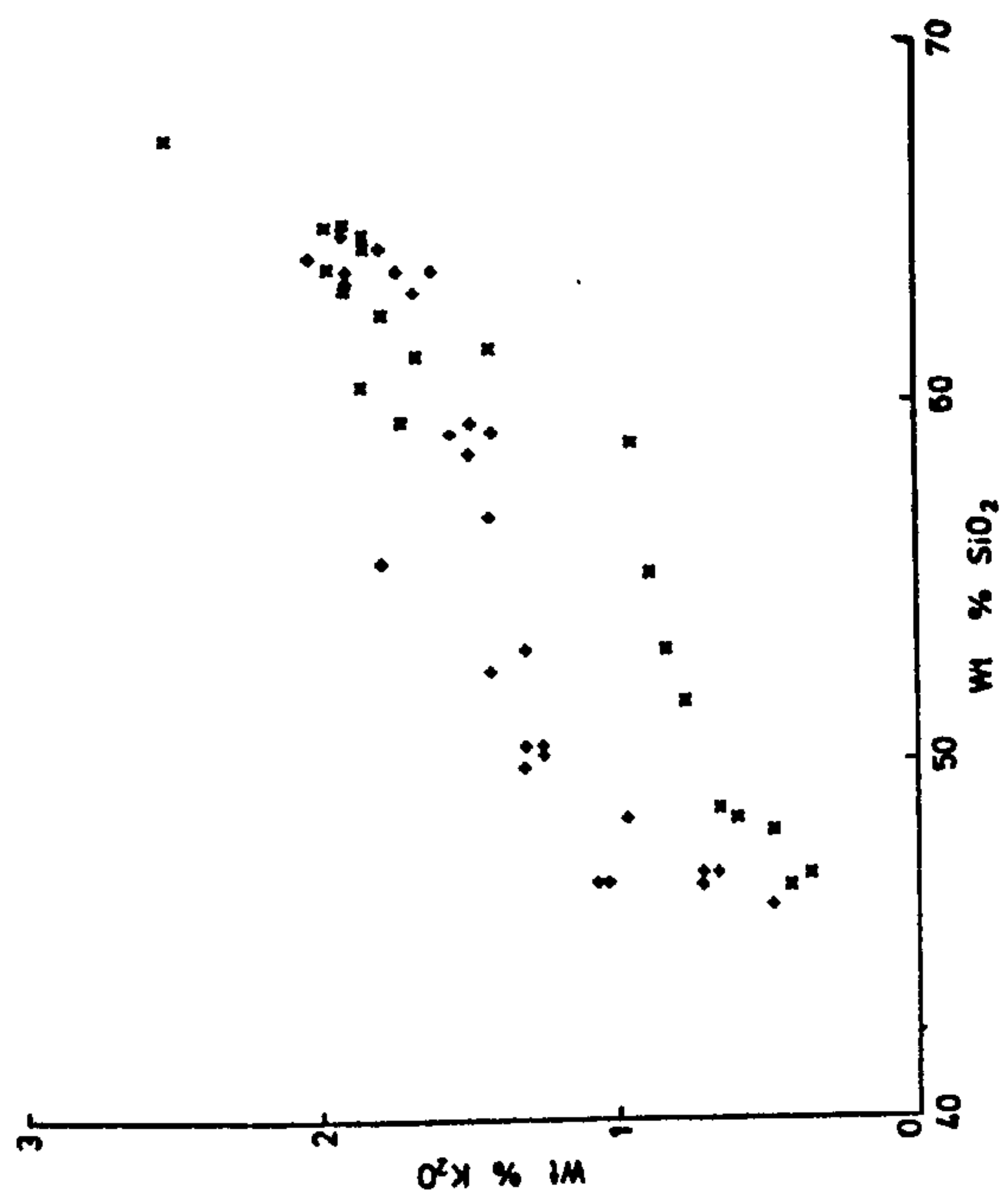


Fig. 28b

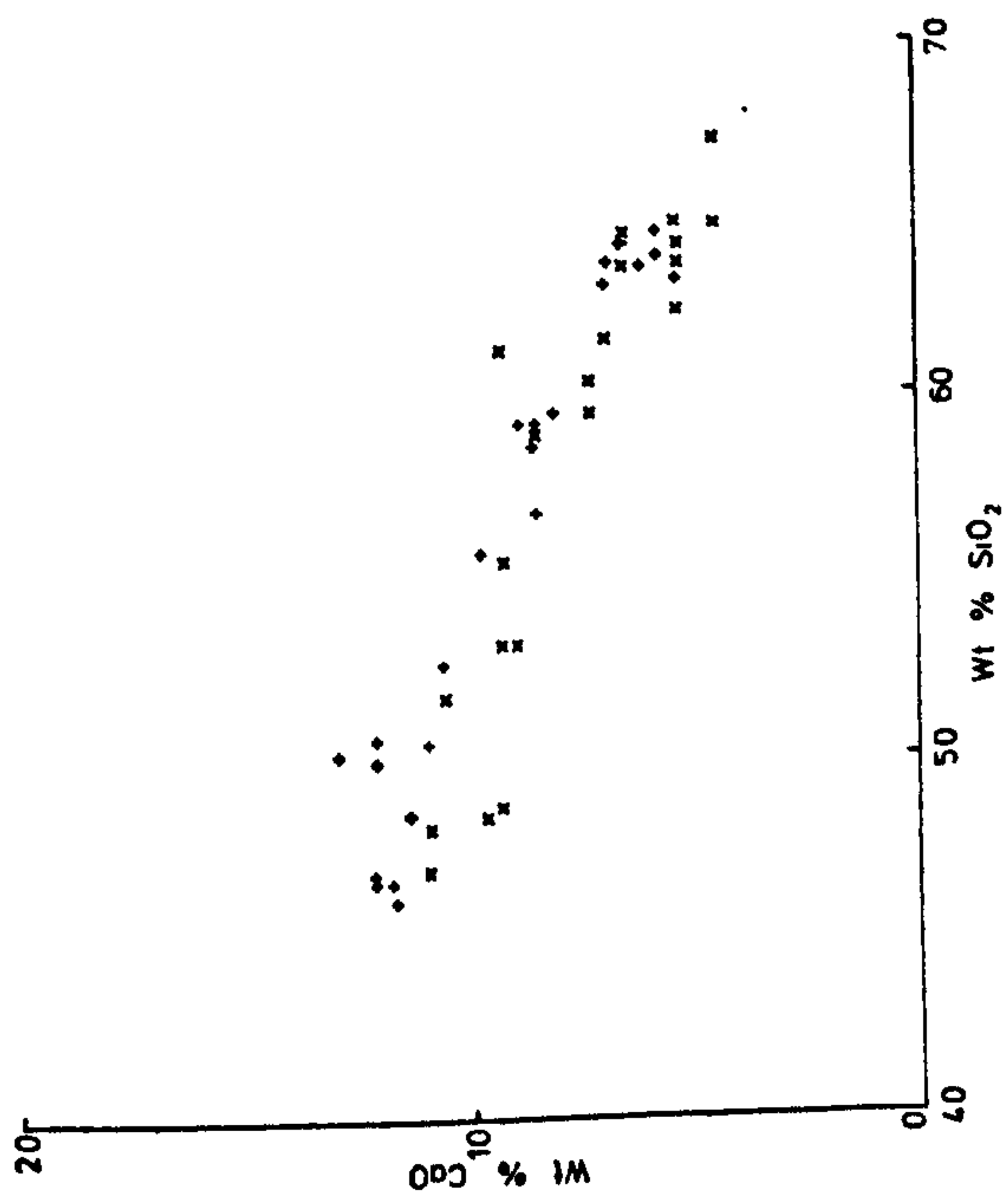
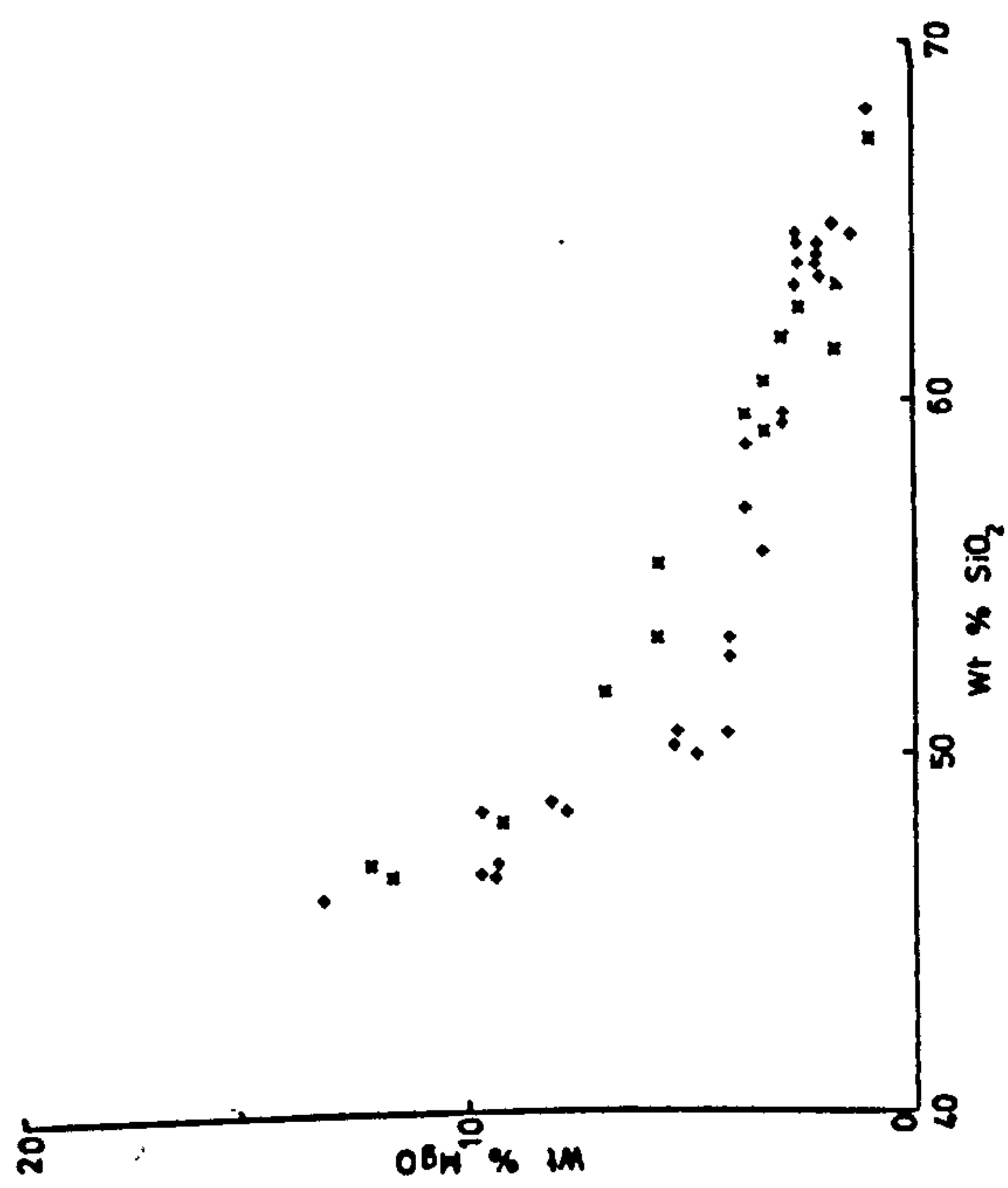
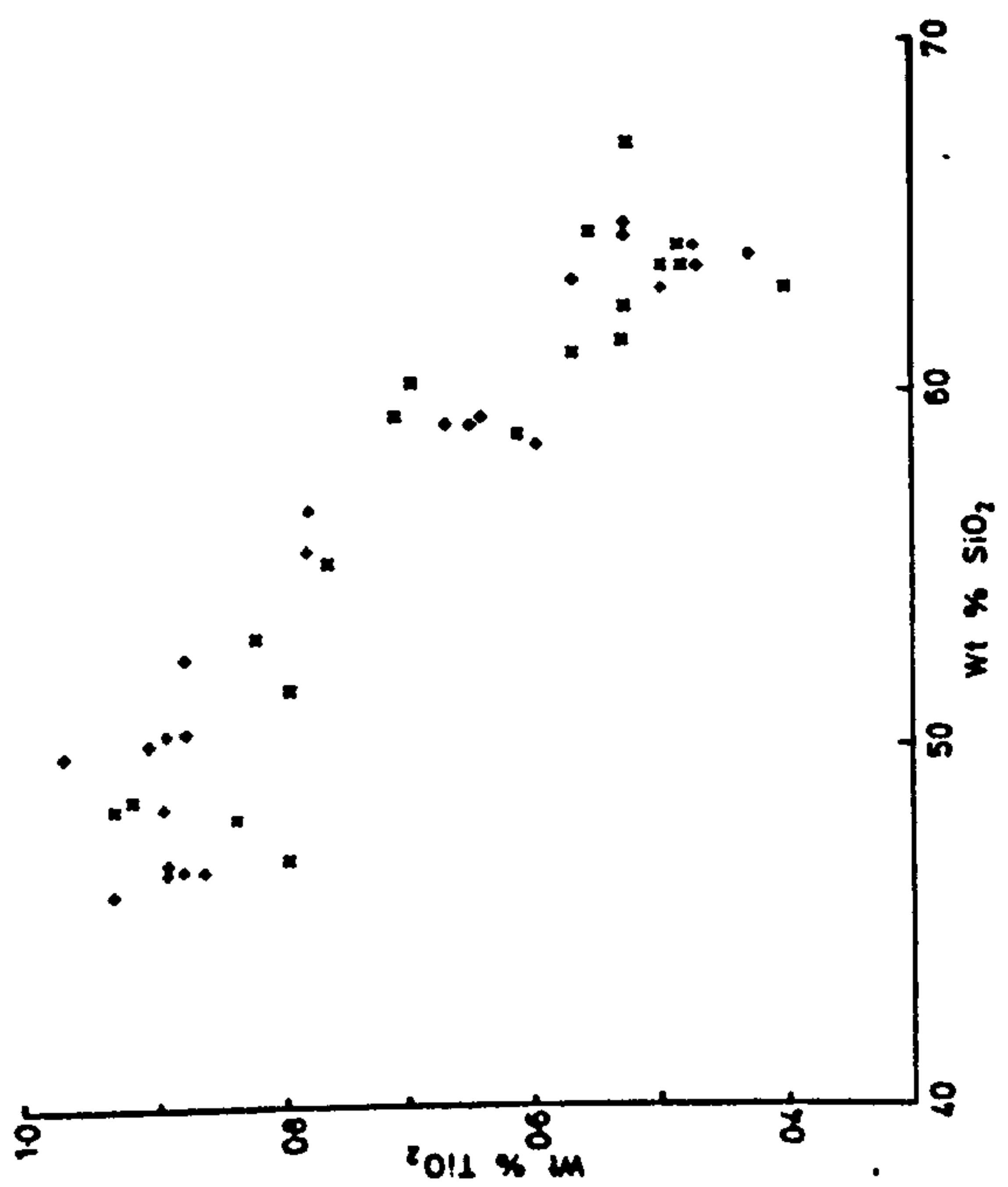
Major and trace element variation in the Mt. St.  
Catherine volcanic centre.

x = low-Sr series

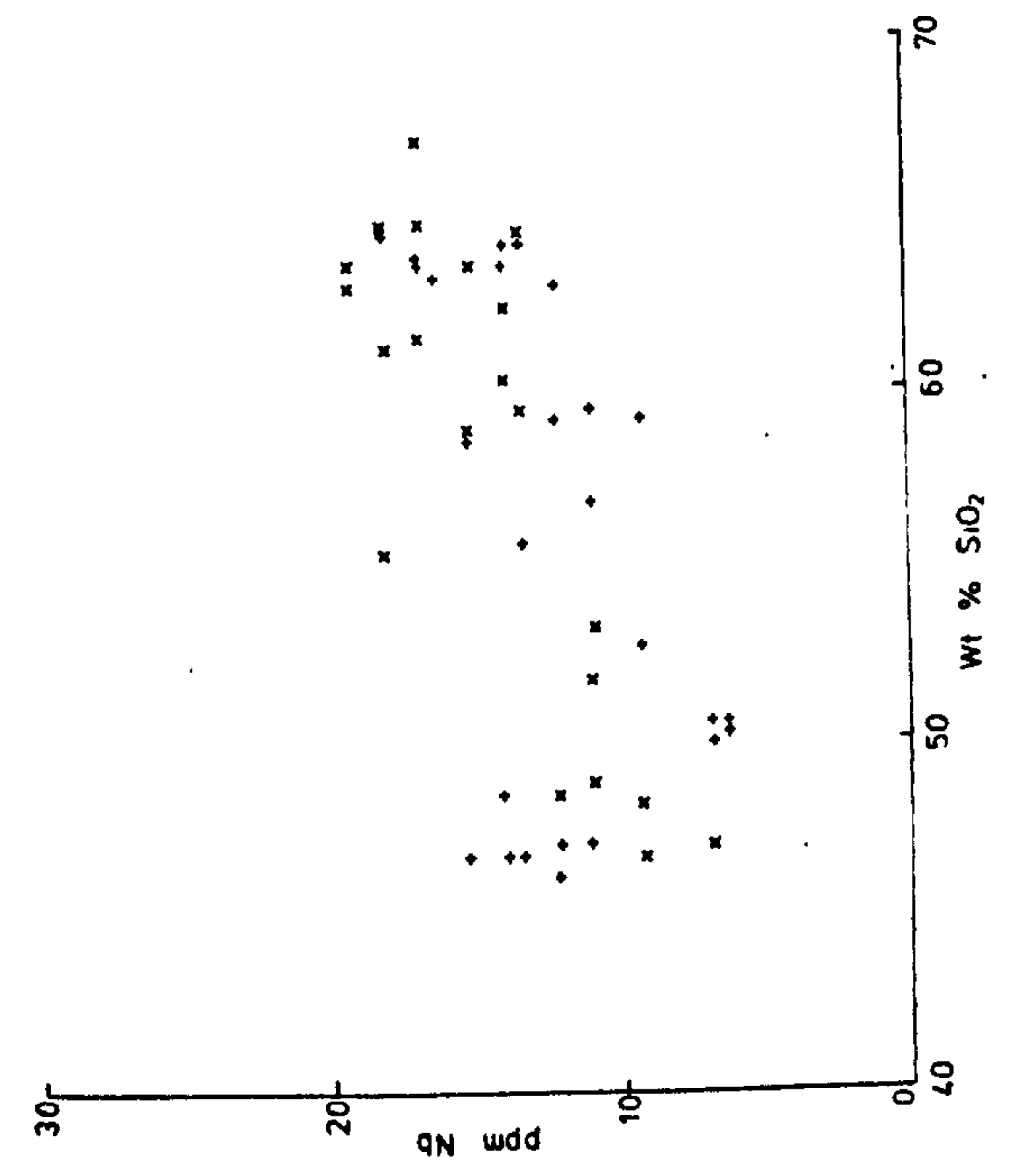
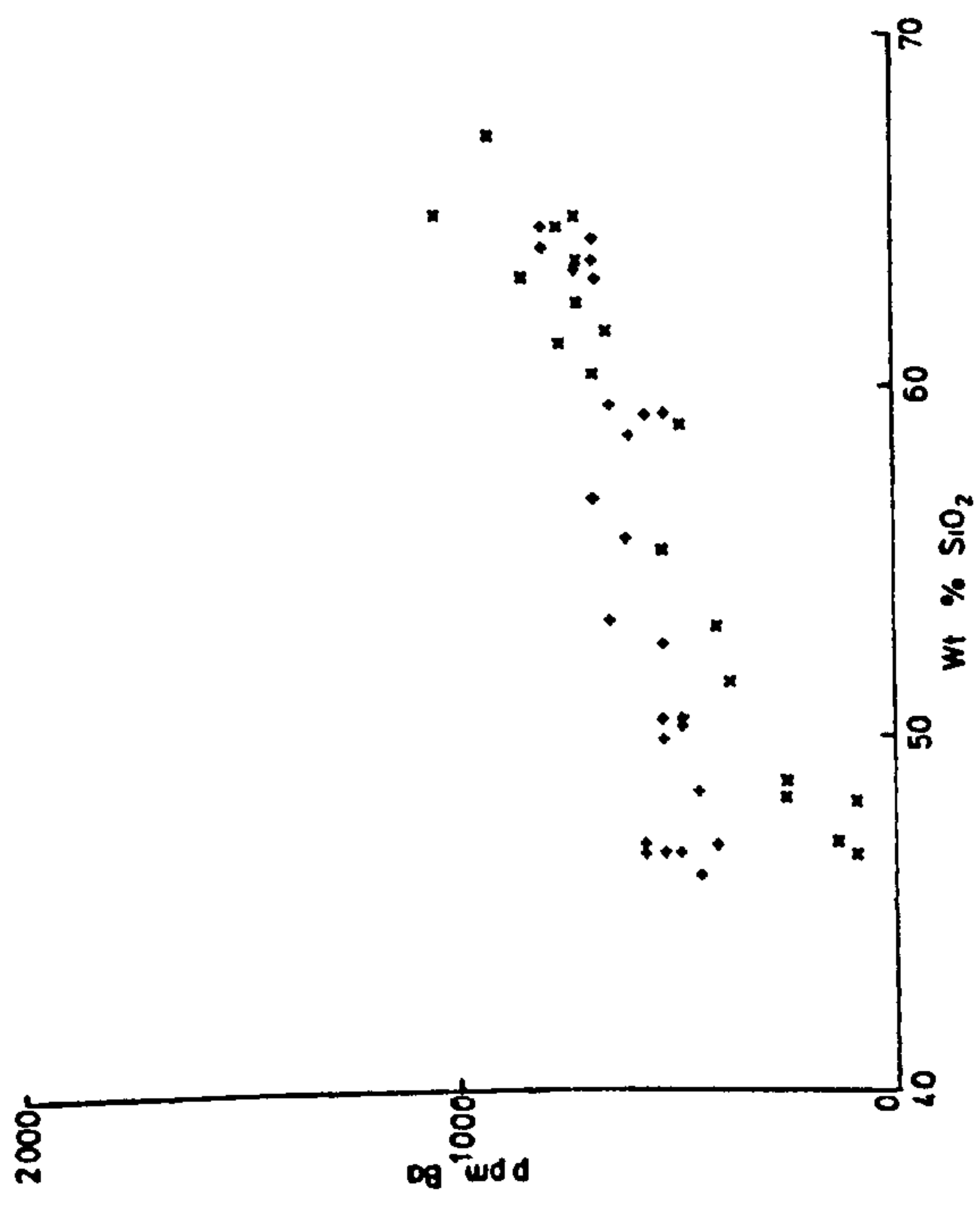
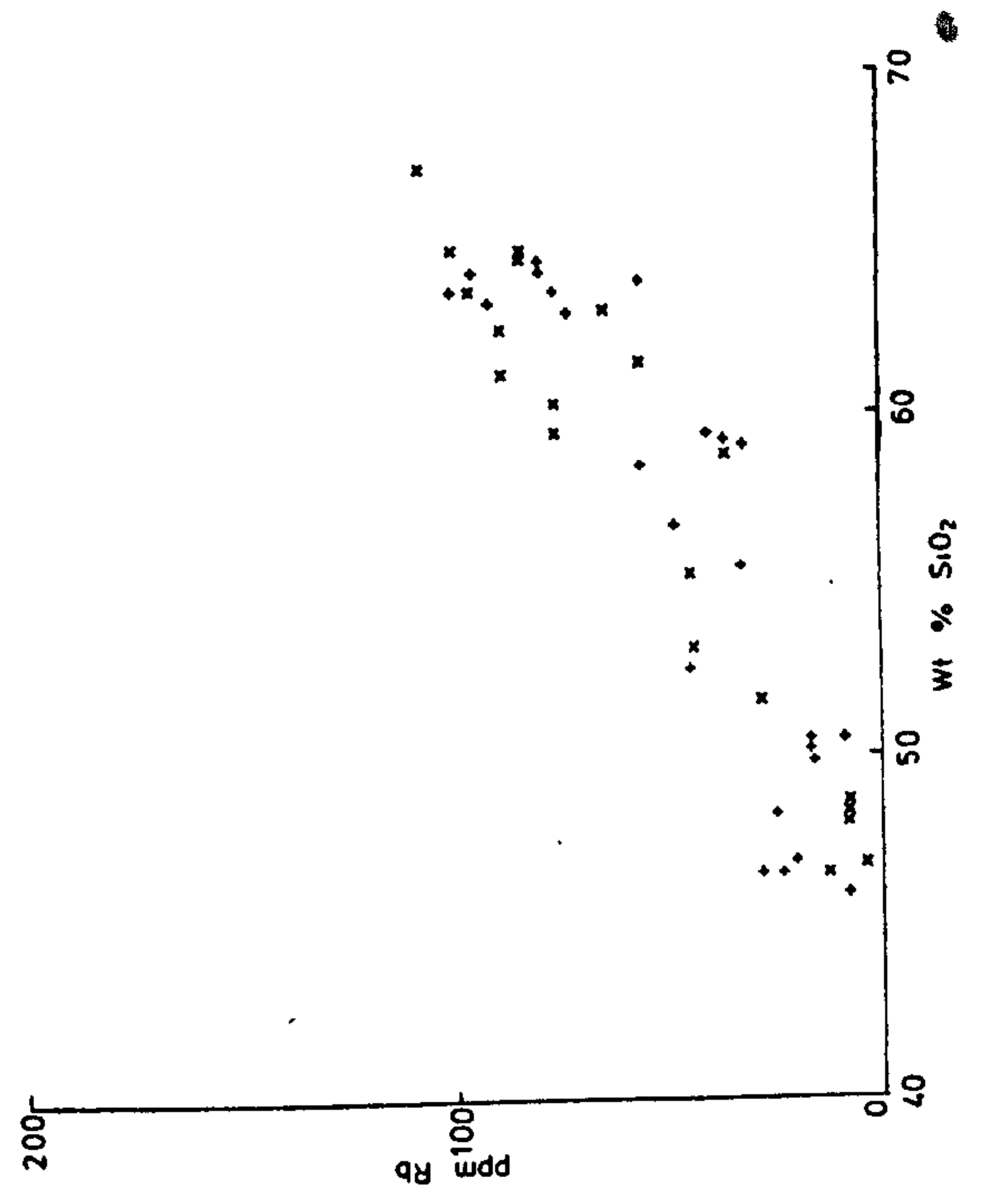
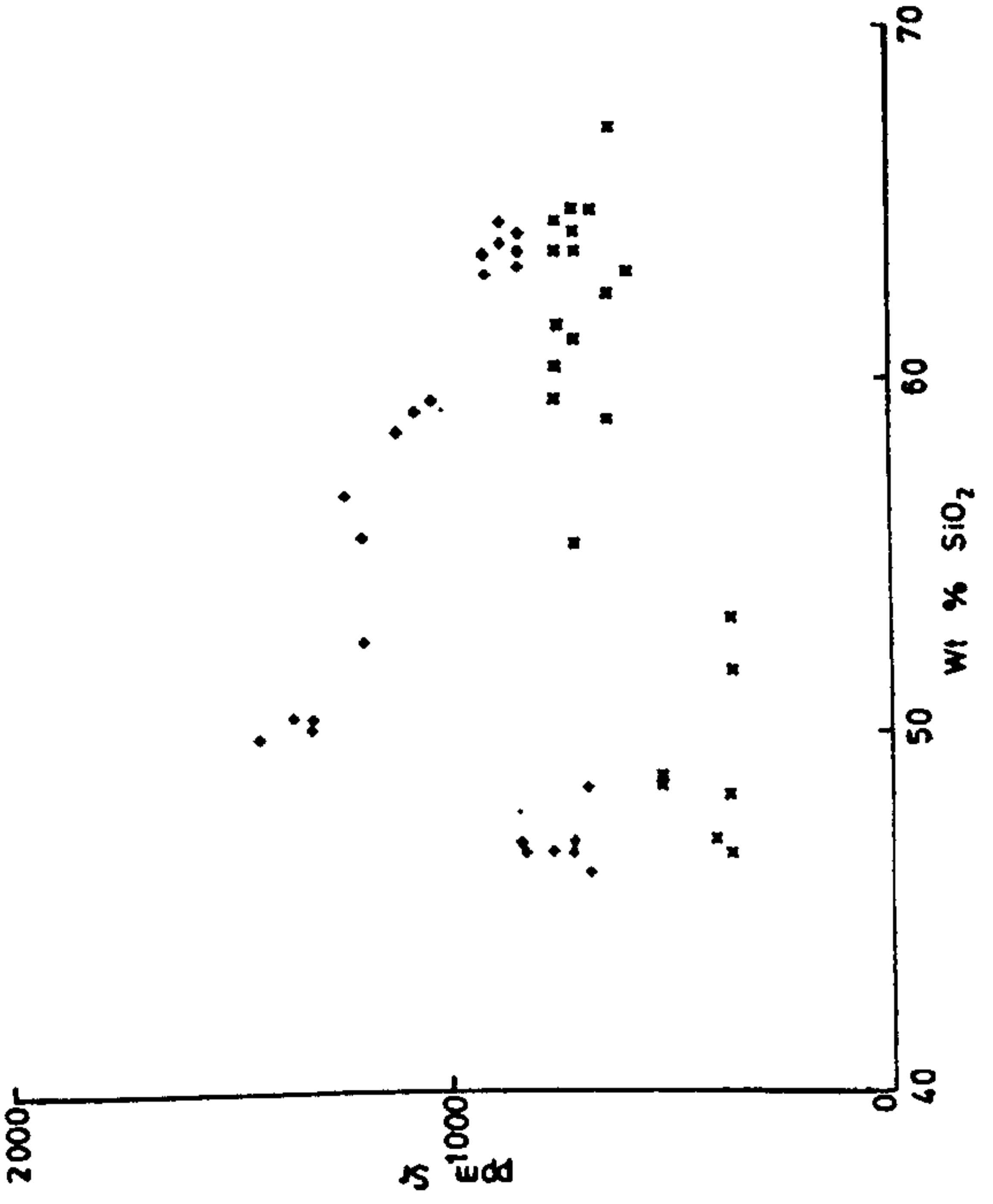
+ = high-Sr series



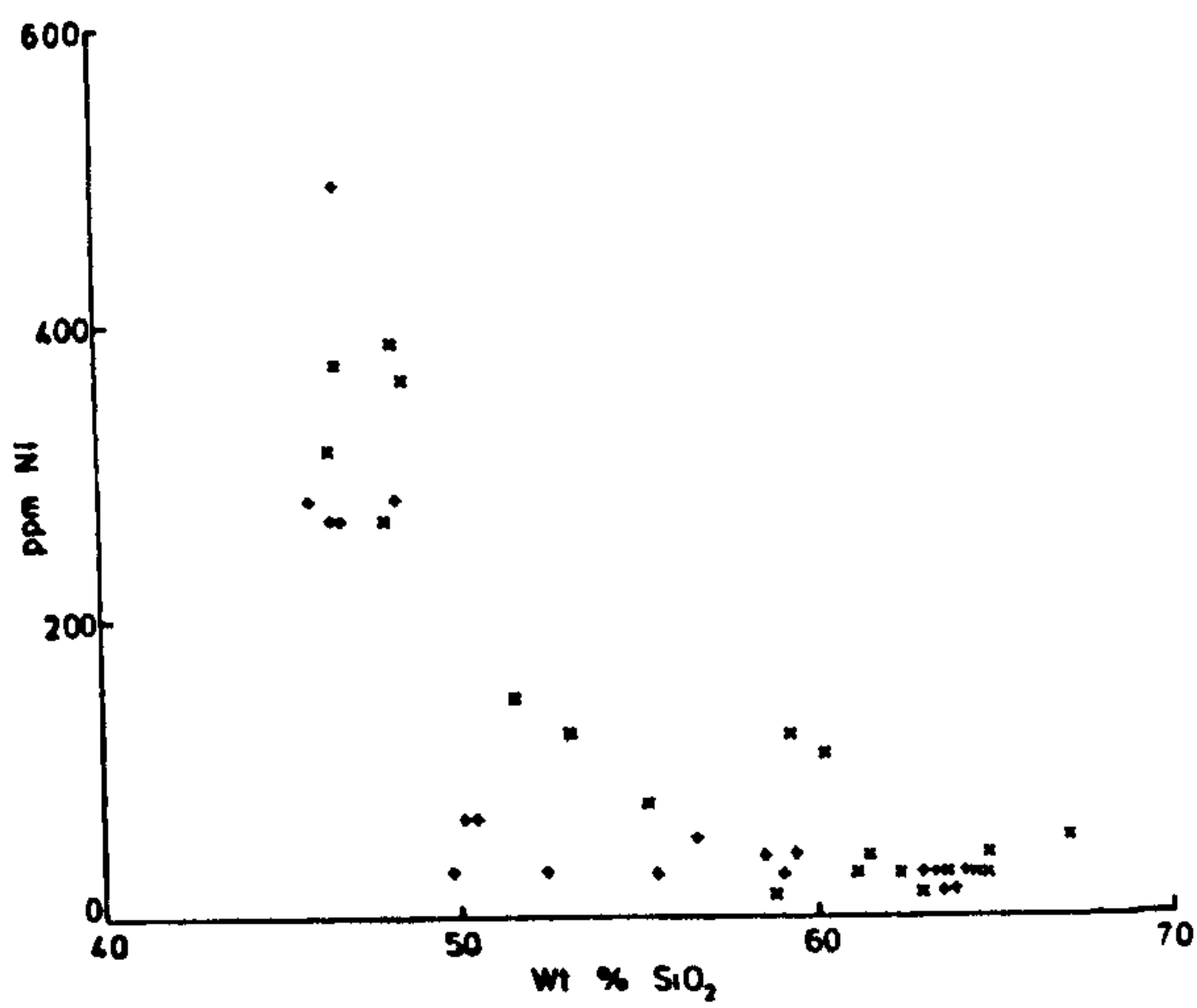
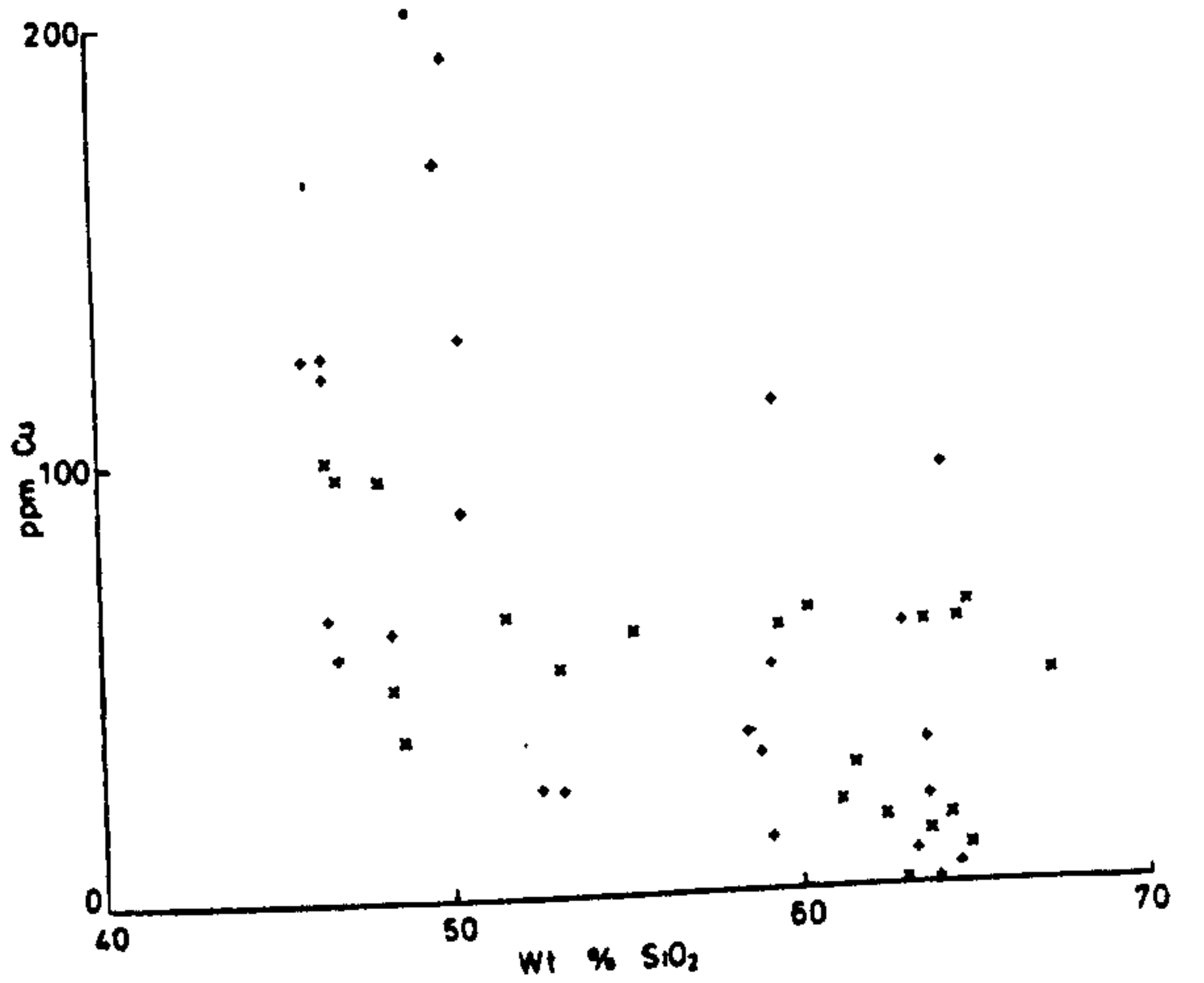
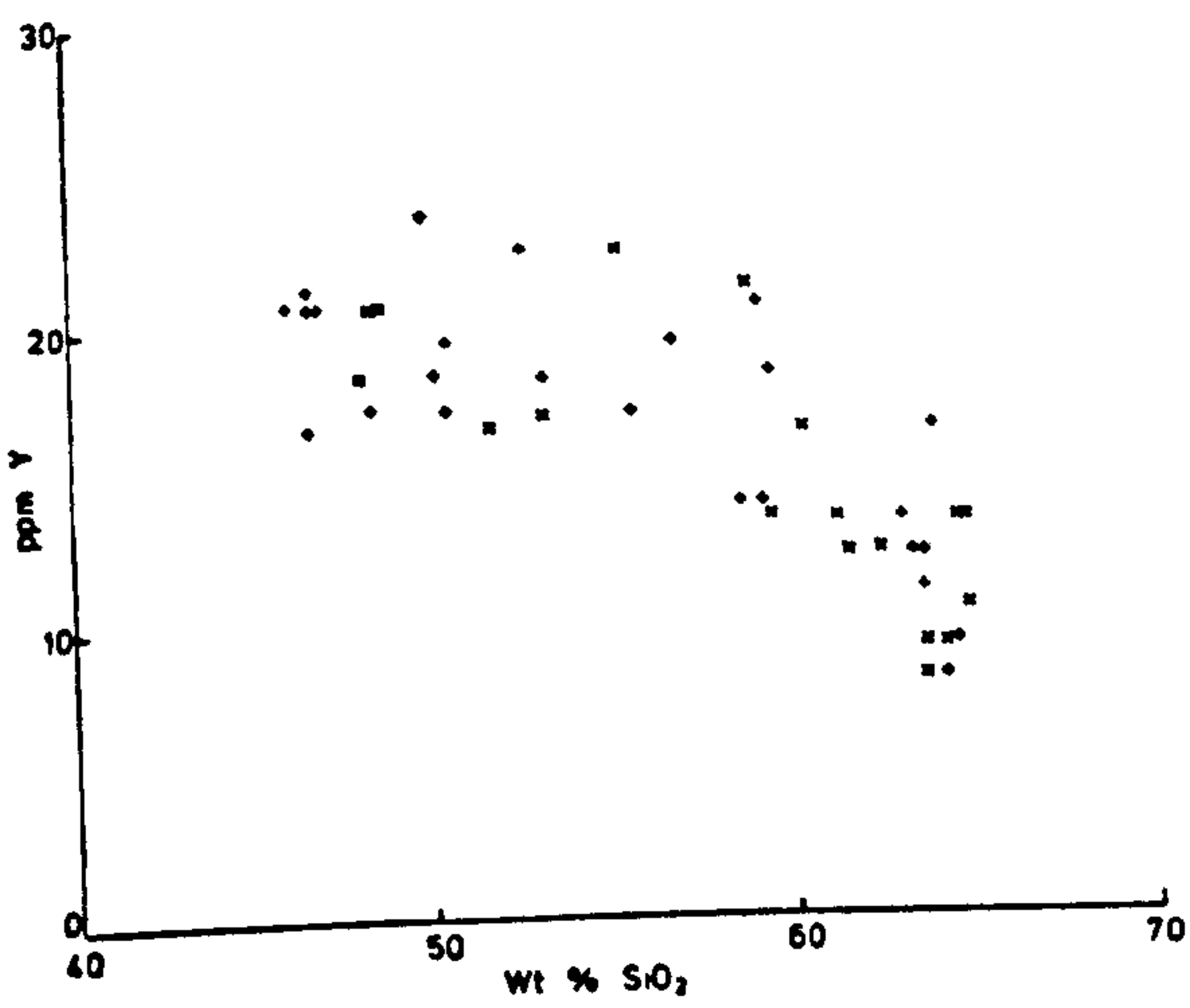
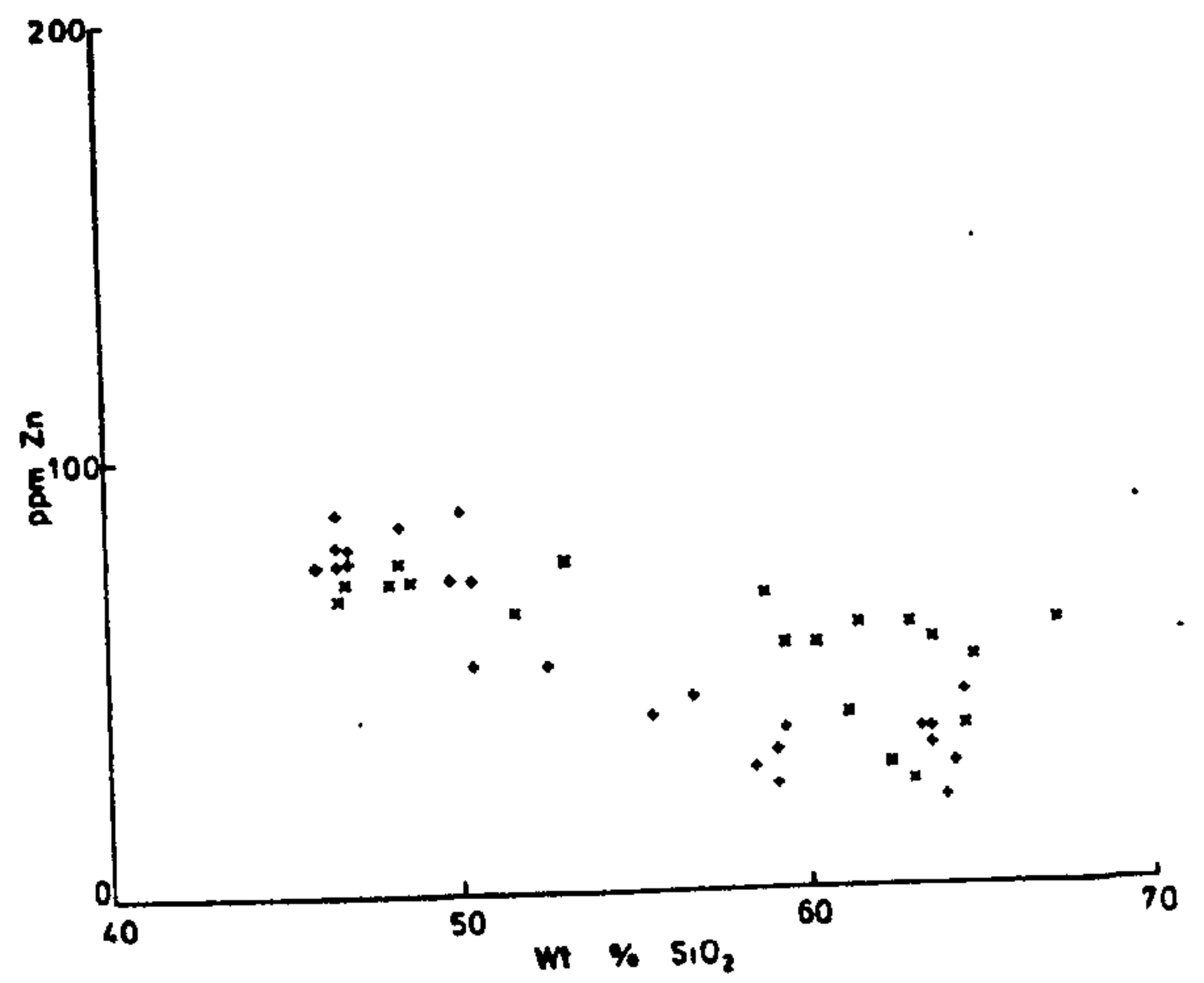
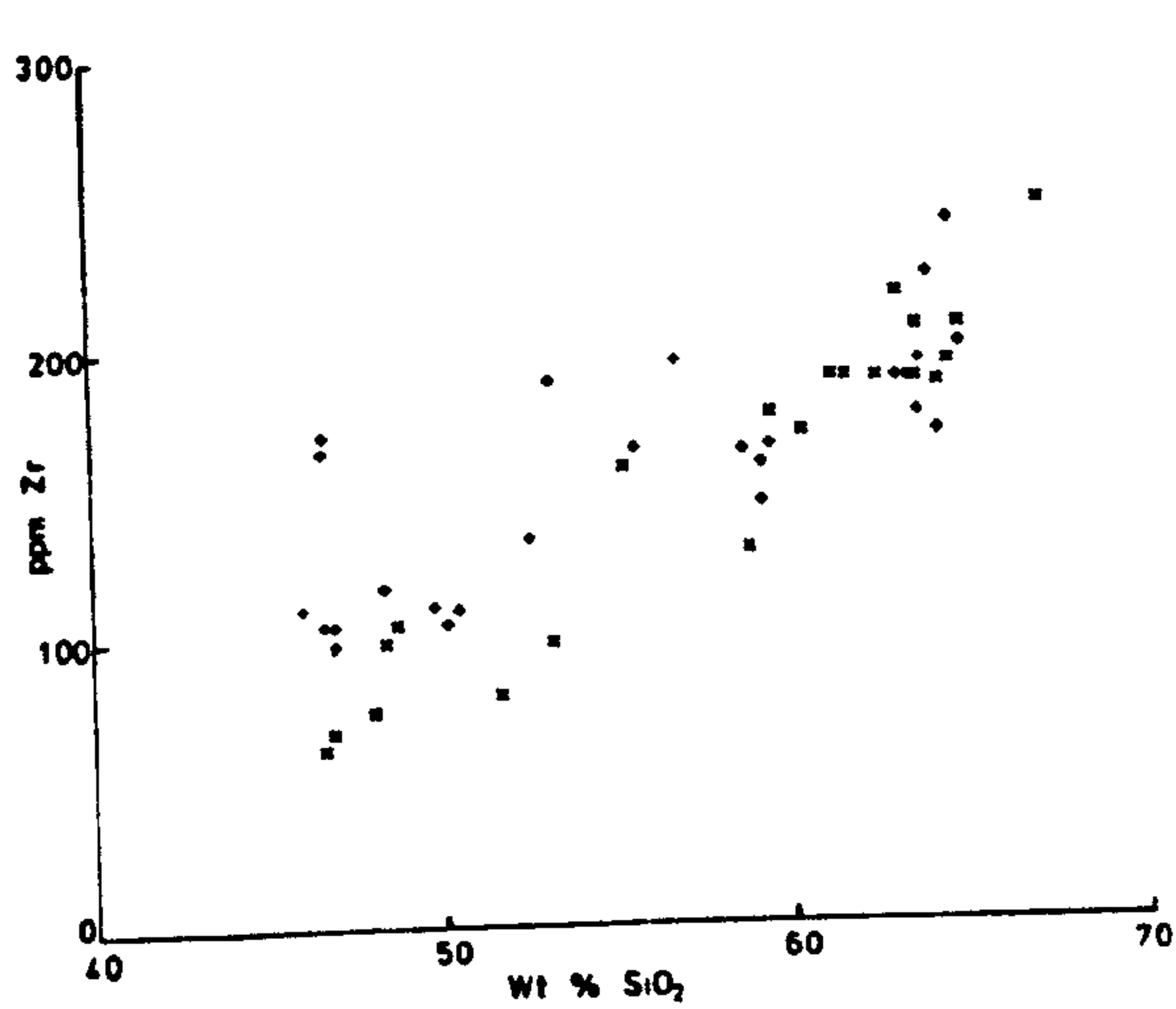




2







distinguishing the chemical affinities of a particular composition. In Fig. 29 the Sr/Ni ratios of the volcanics of the Mt. Granby - Fedon's Camp centre are plotted against  $\text{SiO}_2$  wt.%, where the clear separation between the high and low-Sr series may be seen.

The degree of Fe enrichment in the two series of Mt. Granby - Fedon's Camp is shown in Fig. 18 (Chapter 7). The high-Sr series is characterised by a greater degree of relative Fe enrichment. The same feature is shown in a different manner in Fig. 27 where the rate of depletion of MgO with increasing  $\text{SiO}_2$  wt.% is shown to be lower in the low-Sr series. The differences in major element composition of the two series are displayed by the projections of normative mineralogy in Fig. 30. The higher normative diopside and albite and lower normative olivine contents of the high-Sr series may be observed.

General features of the volcanicity of the centres and geo-chemical aspects of the series are discussed later but alternative explanations for the chemical variation observed must be examined. The high-Sr series are characterised by high modal abundances (up to 35%) of calcic augite and plagioclase feldspar, and low modal olivine (less than 10%). At similar  $\text{SiO}_2$  wt.%, the low-Sr series generally contain a greater proportion (up to 25%) of modal olivine in the alkali and transitional basalts and more basic andesites. Sr is preferentially enriched in plagioclase feldspar relative to the melt during crystallisation (Brooks, 1968; Philpotts and Schnetzler, 1970). Thus there is a possibility that the abundance of Sr in the high-Sr series is the result of cumulus enrichment of plagioclase feldspar. However, the complex



Fig. 29

Plot of Sr/Ni v weight % SiO<sub>2</sub>

- x = low-Sr series of Mt. Granby-Fedon's Camp centre
- + = high-Sr series of Mt. Granby-Fedon's Camp centre
- = selected Northern Domes.

Subscript L refers to two analyses of the Levera Island Dome.

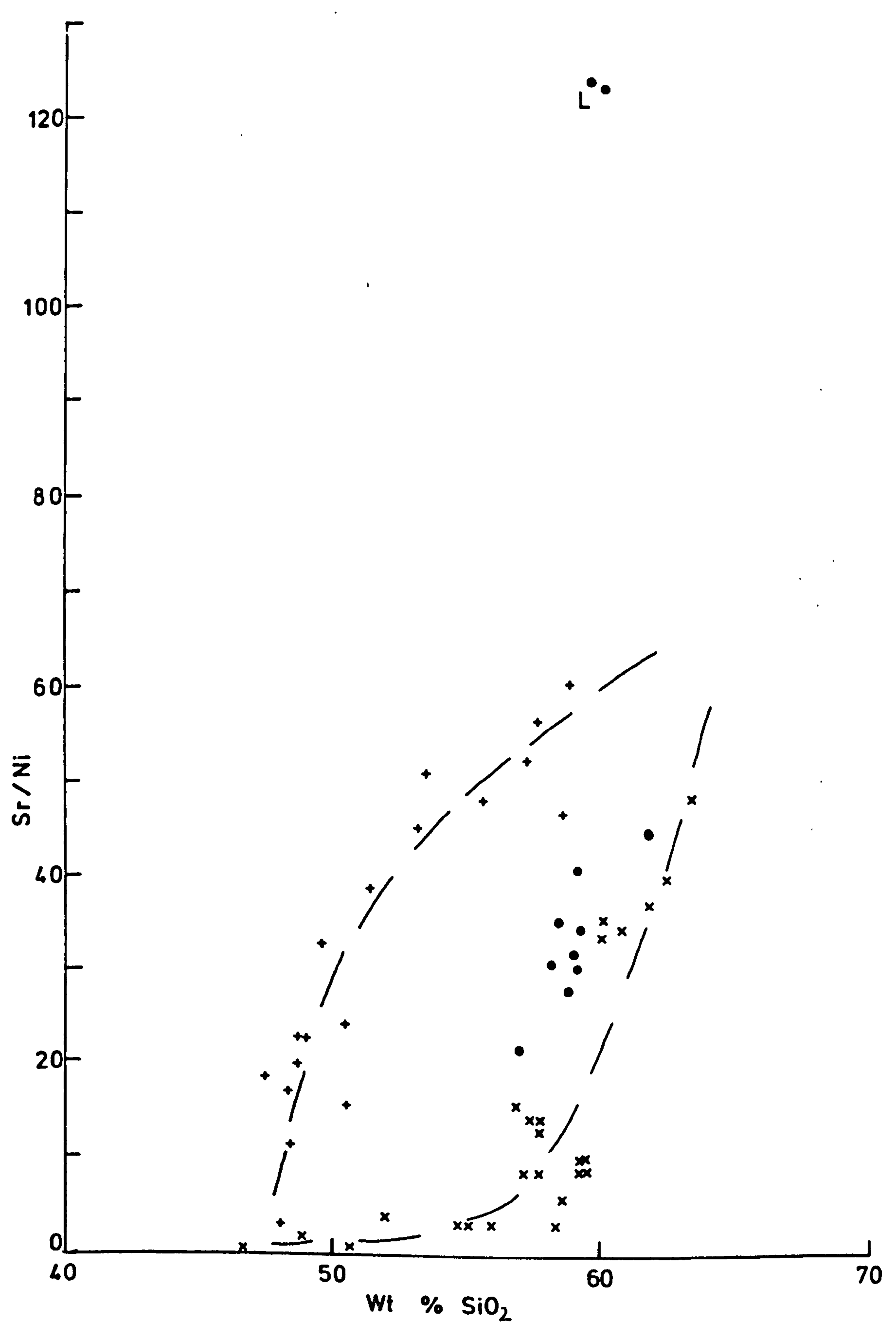




Fig. 30a

Normative compositions of the Mt. Granby - Fedon's Camp  
centre projected in a Ne-Ol-Hy-Qtz-Ab diagram.

Qtz = quartz. Other abbreviations as in Fig. 21.

x = low-Sr series

+ = high-Sr series

● = silica-rich compositions of both high- and  
low-Sr series.

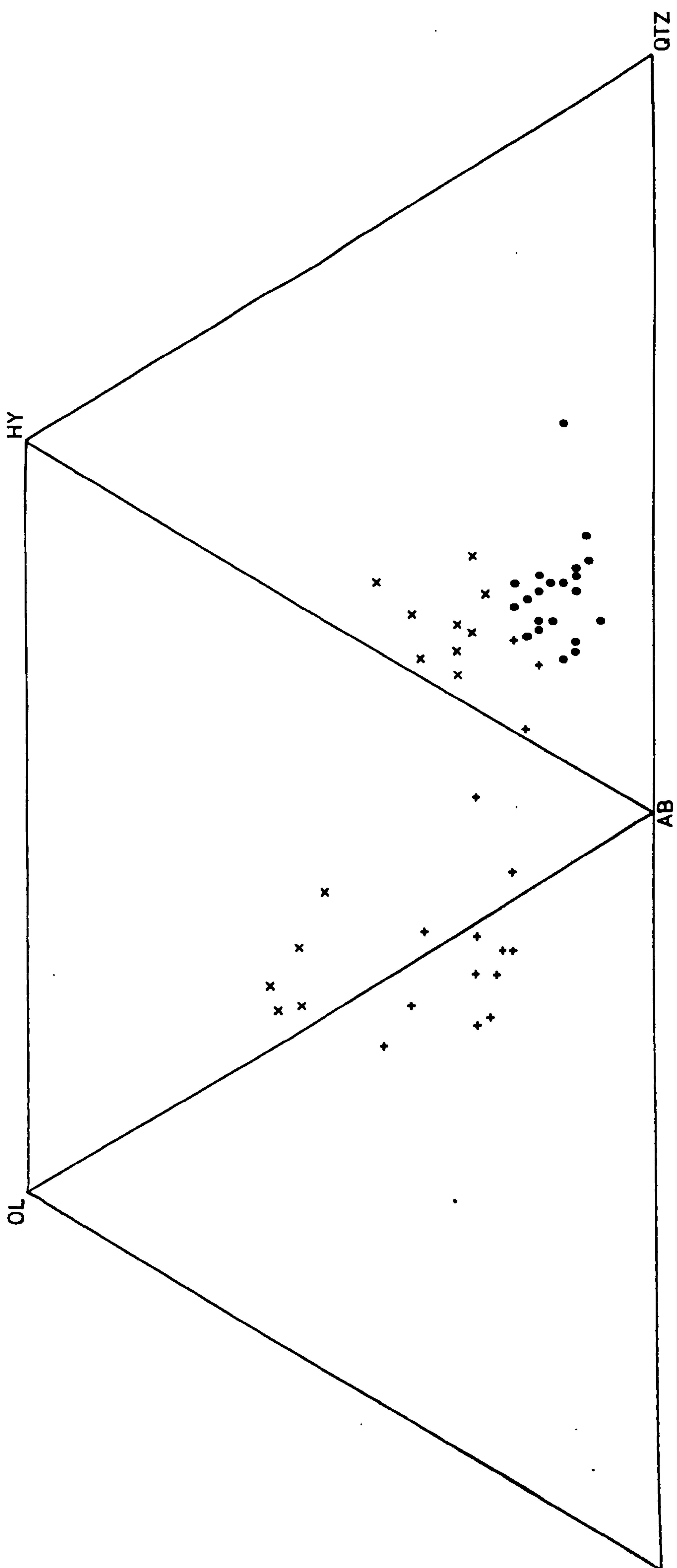




Fig. 30b .

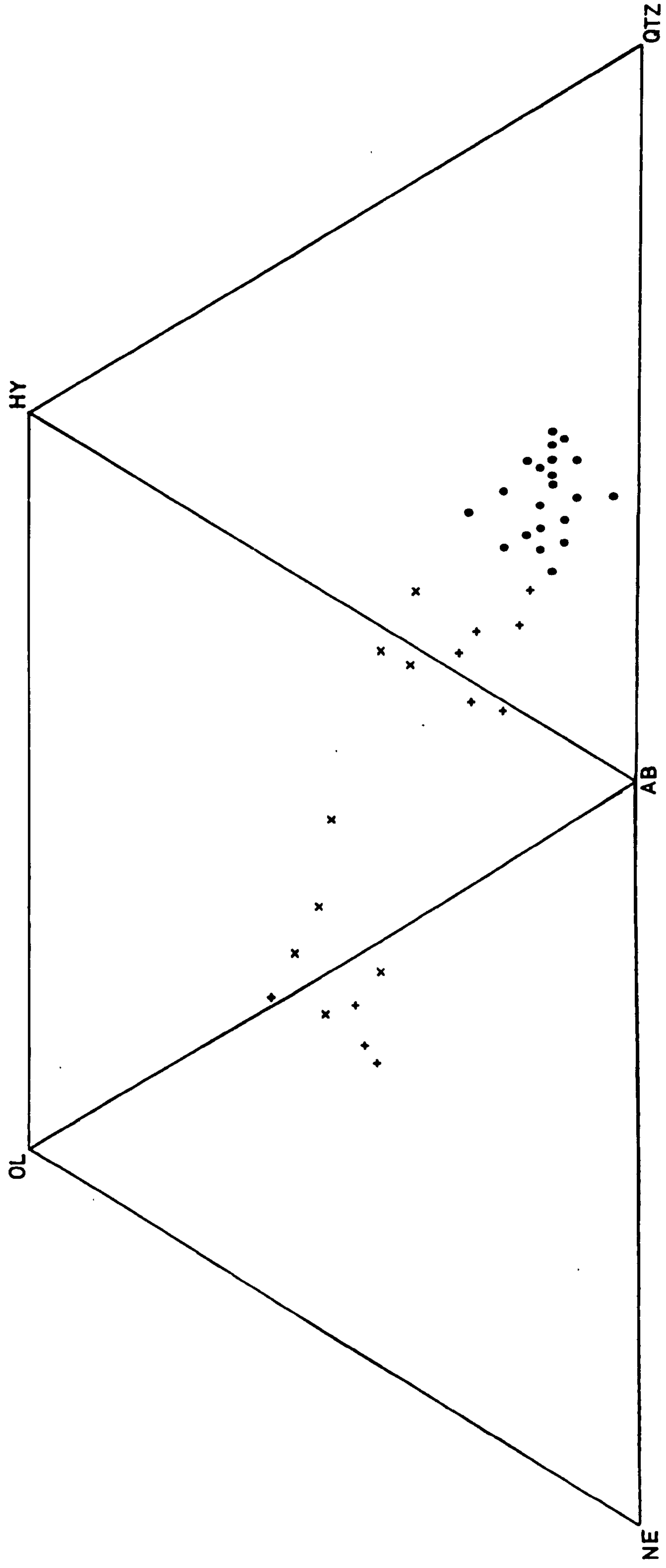
Normative compositions of the Mt. St. Catherine  
centre projected in a Ne-Ol-Hy-Qtz-Ab diagram.

Qtz = Quartz. Other abbreviations as in Fig. 21.

x = low-Sr series

+ = high-Sr series

● = silica rich compositions of both high- and  
low-Sr series.





oscillatory zoning of the feldspars and crystallisation concurrently with oscillatory and sector-zoned clinopyroxenes of contrasted physical properties are features unlike those previously described in cumulus minerals (Wager and Brown, 1968) and those actually observed in the cumulus blocks of Grenada (Chapter 9). In addition, it is unlikely that the proportions of clinopyroxene and plagioclase feldspar should have been preserved in such a way as to generate the smoothly varying curves of major oxides and trace elements observed in Fig. 28. A more random scatter of compositions dependent on varying proportions of these two phases would be expected.

Individual compositions of the postulated high and low-Sr series may be related by fractional crystallisation of one or more mineral phases. In Chapter 7, the degree of incompatible trace element enrichment possible as a result of fractional crystallisation of mafic mineral phases from basaltic magma was discussed. For example the possible enrichment of Ce between melts of generally similar major element composition by orthopyroxene fractionation was shown to be severely limited. In Chapter 10, simple and compound partition coefficients are discussed in relation to the petrogenesis of the Grenada calc-alkaline suite. At this stage, however, it is sufficient to suggest that the enrichment of Sr by factors up to 3 in compositions belonging to the high-Sr series relative to the low-Sr series, at similar  $\text{SiO}_2$  wt.%, is impossible by fractional crystallisation of one or more mineral phases. The chemical and petrographic gradations observed between individual compositions within the series is

more readily explained by fractional crystallisation of basaltic precursors, characterised themselves by contrasted geochemistry. However, the variation in proportions and onset of crystallisation of fractionating minerals are additional factors controlling the major and trace element variation of the volcanic series. The mineralogy and petrogenesis of the Grenada calc-alkaline suite is discussed in Chapters 9 and 10.

In the case of the Mt. Granby - Fedon's Camp centre it is relatively easy to distinguish high and low-Sr series. However, this is a simplification of the situation within the centre and the island as a whole. In fact the Mt. Granby - Fedon's Camp centre is constructed of two major cycles of activity involving high and low-Sr series of erupted volcanics. Lava and pyroclast flows belonging to individual series are often closely related in the field. The two major cycles of activity also appear to be associated with broadly similar high and low-Sr series of compositions. It must be stressed that there is no rigid division between these series denoting uniquely separate patterns of fractional crystallisation or geochemical behaviour of the evolving calc-alkaline magmas. The data from the centres displayed in Fig. 28 was selected in order to illustrate the range of element variation occurring in the silica-undersaturated to oversaturated sequence of compositions. The terms high and low-Sr are strictly only applicable for descriptive purposes within a centre. The degree of separation discernable between the series of the Mt. St. Catherine Centre for example, is much less than those of Mt. Granby - Fedon's Camp. It seems most probable that



the Mt. St. Catherine centre is constructed of more than two volcanic series of compositions. The distinction in the field of related flows in this centre proved more difficult than in the Mt. Granby - Fedon's Camp centre. Although the data from older volcanic centres on the island are not presented here, the range of compositions in the basalts and picrites described in Chapter 7, and for the entire suite of Grenada volcanic rocks displayed in Fig. 27, may be interpreted as forming a spectrum of major and trace element variation spanning the differences observed between high and low-Sr series of individual centres. In other words, it appears that fractional crystallisation processes occurring within variable initial partial melts have generated a range of isotopic, major and trace element compositions within the entire Grenada calc-alkaline rock suite.

Not all of the volcanic centres of Grenada are characterised by a complete range of compositions identifiable as belonging to series such as those described for Mt. Granby - Fedon's Camp. For instance, the Northern Domes centre is predominantly composed of andesitic and dacitic domes. By analogy with volcanic series containing a more extensive range of  $\text{SiO}_2$  wt.% however, it is possible to suggest that the domes were formed originally by fractional crystallisation of basalt magmas of contrasted chemical composition. Complete analyses of the Northern Domes are contained in Appendix I. In order to illustrate the geochemical differences, of the domes the Sr/Ni ratios are compared with the Sr/Ni ratios of the high and low-Sr series of the Mt. Granby - Fedon's Camp centre in Fig. 29. It can be seen that the andesite dome of Levera

TABLE 10

Major and trace element analyses of andesites 67 and 381 and dacite 214.

<u>Sample No.</u>	<u>67</u>	<u>381</u>	<u>214</u>
SiO <sub>2</sub>	56.76	59.71	62.92
Al <sub>2</sub> O <sub>3</sub>	19.07	17.15	15.91
Fe <sub>2</sub> O <sub>3</sub>	7.23	6.48	5.23
MgO	2.31	2.25	2.68
CaO	9.38	7.62	6.77
Na <sub>2</sub> O	3.22	3.65	4.03
K <sub>2</sub> O	0.96	2.09	1.66
TiO <sub>2</sub>	0.55	0.71	0.50
MnO	0.25	0.14	0.15
S	0.00	0.00	0.00
P <sub>2</sub> O <sub>5</sub>	0.27	0.20	0.16
Ba	236	754	683
Nb	10	13	12
Zr	119	198	184
Y	24	18	13
Sr	531	1167	934
Rb	31	46	72
Zn	93	28	59
Cu	1	14	60
Ni	1	18	29
Ce	*26.1	*52.4	*47.3

\* analysis by O'Nions et al. (in MS)



Island is distinctly different ('high-Sr') from the andesite domes and lavas of the Mt. Rodney and Levera Hill areas (see Chapter 6).

### 8:3 Rare Earth Element Distribution and $\text{Sr}^{87}/86$ Ratios

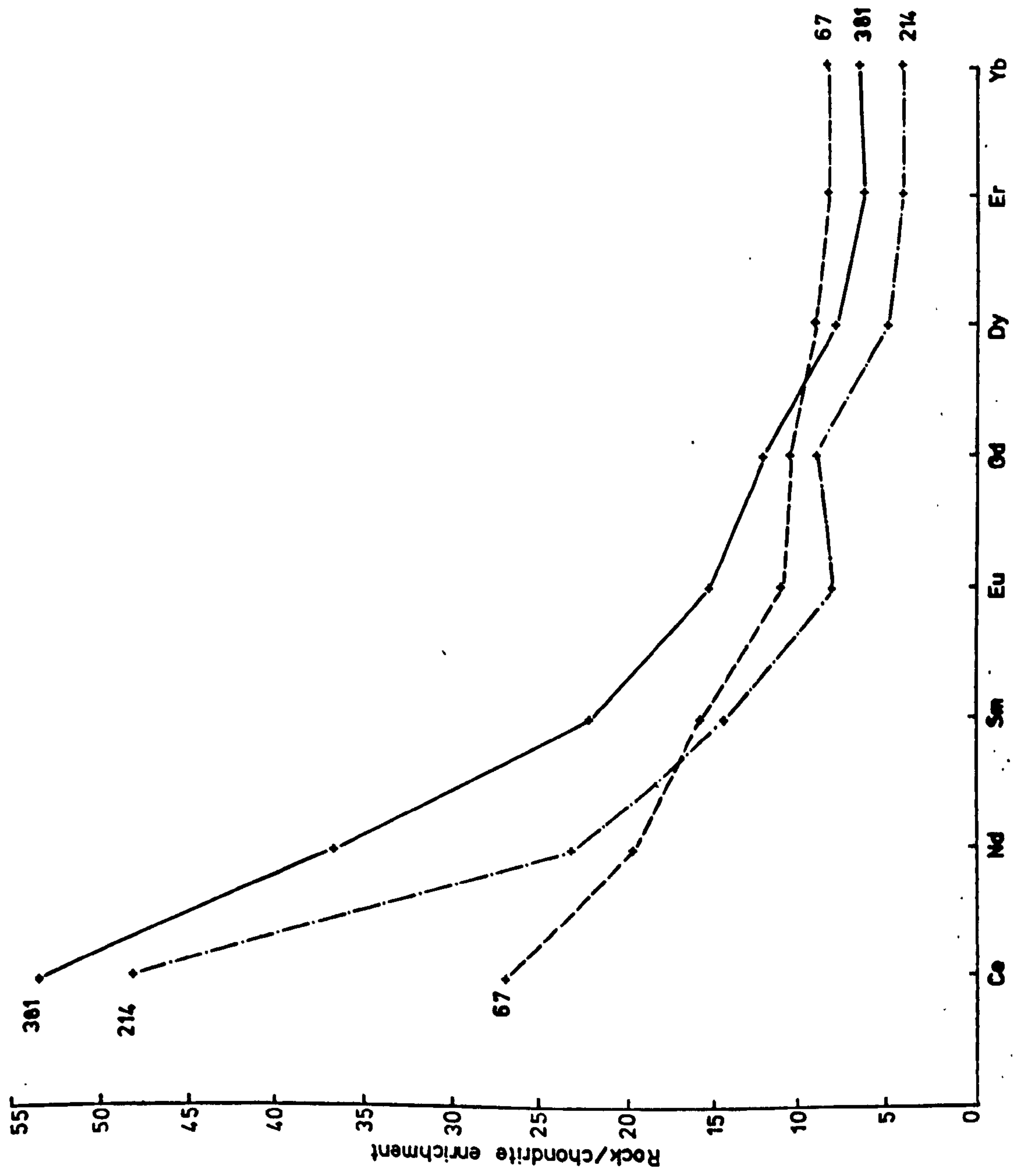
The study of the Rare Earth element distribution and  $\text{Sr}^{87}/86$  ratios of the Grenada calc-alkaline rock suite by O'Nions et al. (in MS), has proved useful in the interpretation of the geochemical affinities of the volcanic series and individual compositions. In Chapter 7, the REE distribution within the Grenada basalts and picrites was discussed, and related to varying degrees of partial melting of similar parental source material. The REE distribution of two andesites and a dacite were also determined by O'Nions et al., and is presented in Fig. 31 . The REE distribution of the Grenada calc-alkaline suite relative to island arcs of the Pacific is discussed in Chapter 11. The major and trace element geochemistry of the andesites and dacite of Grenada are given in Table 10 .

The dacite 214 is from a pyroclast flow belonging to the low-Sr series of Mt. St.Catherine whilst andesite 381 is from a lava flow of the high-Sr series of the Mt.Granby - Fedon's Camp centre. The degree of REE enrichment relative to chondrites is much higher in the andesite than dacite. If these compositions were directly related by fractional crystallisation of similar parental material, the REE distribution is the reverse of the predicted pattern. The Ce/Y ratios of selected compositions from the Mt. Granby - Fedon's Camp centre are plotted against  $\text{SiO}_2$  wt.% in Fig. 32 . The Ce/Y ratio is a good indicator of degree of relative light Rare Earth enrichment (p.116 ). It can

Fig. 31

Rare Earth element distribution in andesites 67  
and 381, and dacite 214.





Rare Earth elements

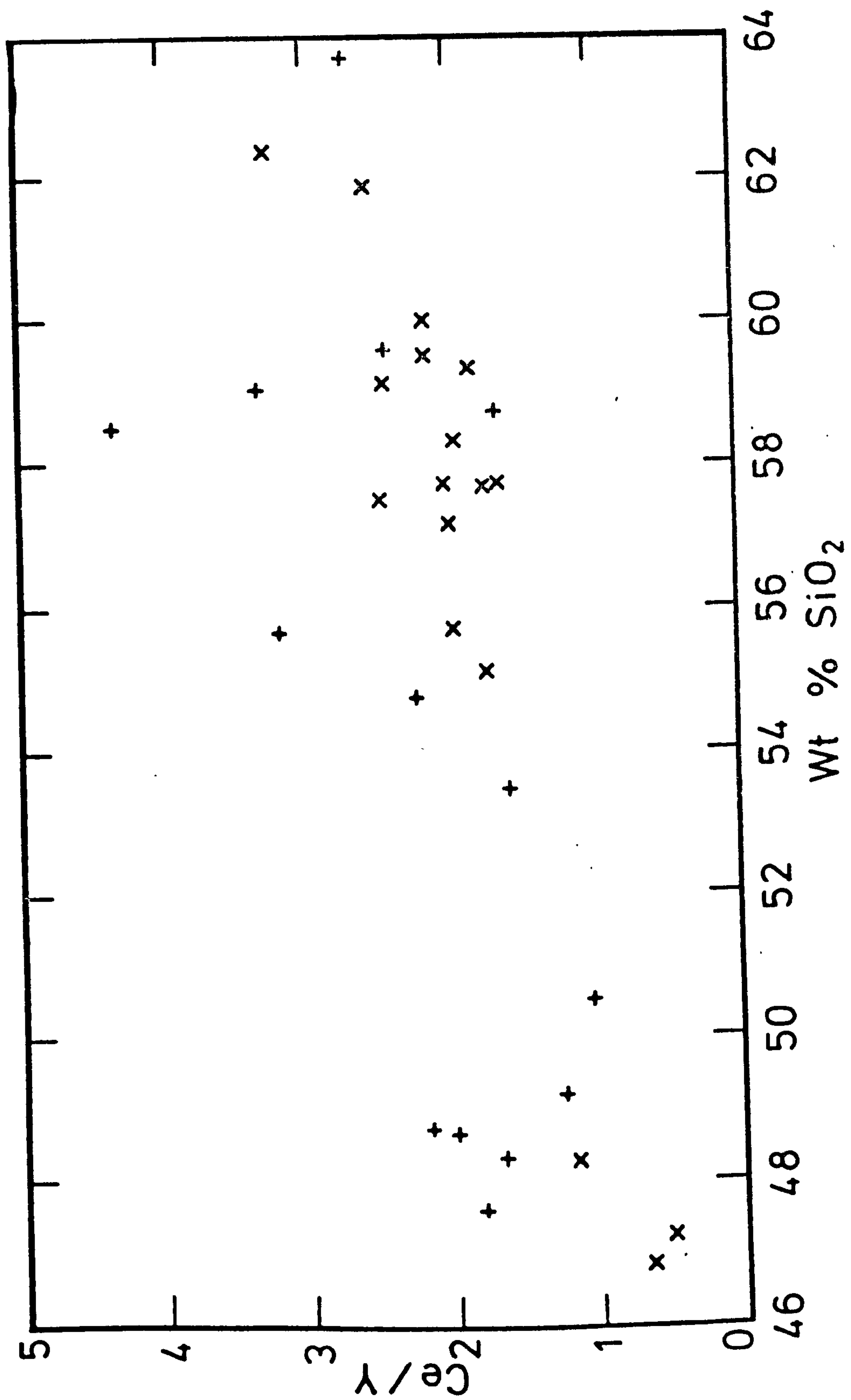
Fig. 32

Plot of Ce/Y v weight % SiO<sub>2</sub> for the Mt. Granby -  
Fedon's Camp centre.

X = low-Sr series

+ = high-Sr series





be seen that the greater degree of light REE enrichment of the high-Sr series relative to the low-Sr series is established in the most basic members of the series. The chemical characteristics imposed in the basaltic melts during the initial partial melting of the Upper Mantle are apparently maintained during subsequent fractional crystallisation processes.

Similar inherited geochemical features may be observed in the  $\text{Sr}^{87}/86$  ratios of the silica-saturated compositions. The  $\text{Sr}^{87}/86$  ratio of andesite 381 and dacite 214 were given in Table 8 (Chapter 7). The higher  $\text{Sr}^{87}/86$  ratio of dacite 214 ( $0.70497 \pm 8$ ) compared with andesite 381 ( $0.70461 \pm 5$ ) is noticeable. The overall geochemistry of dacite 214 suggests the composition has been derived by fractional crystallisation of basaltic magma generally less enriched in incompatible trace elements than the basaltic precursor of andesite 381. This may be related to the variable Upper Mantle partial melting model proposed in Chapter 7, where differences in  $\text{Sr}^{87}/86$  ratios of the basalts were attributed to isotopic inhomogeneity of the source composition.

The andesite 67 (Table 10) is from a flow on Green Island 1 km northeast of Grenada where there is a lack of exposed basaltic compositions. The major and trace element geochemistry however, by analogy with series from other volcanic centres suggest a 'low-Sr' basaltic precursor even less enriched in incompatible trace elements than the low-Sr series of Mt. St. Catherine. The degree of light REE enrichment of andesite 67 is much lower than dacite 214 and andesite 381 (Fig. 32). The  $\text{Sr}^{87}/86$  ratio is much higher however



( $0.70543 \pm 12$ ), in accord with the evolutionary model proposed.

The general point is that critical geochemical parameters observed in the basalts and picrites are maintained in the silica-saturated andesites and dacites of Grenada. Thus the range of major and trace element compositions of the Grenada calc-alkaline suite are explicable by fractional crystallisation processes occurring within a variety of parental basalt melts, generated in separate episodes during the evolution of the island.

#### 8:4 General geochemical features of the Grenada calc-alkaline rock suite

An important feature of the geochemical variability of the Grenada calc-alkaline suite is the evidence that the transition from silica-undersaturated to silica-oversaturated compositions, although an oft-repeated process, has not been consistent in time. The initial period of activity in the north of the Mt. Granby - Fedon's Camp centre (Chapter 6) consisted of a low-Sr followed by a high-Sr series of volcanics. The southwards shift in the centre of activity was marked by another high-Sr series followed after an interval represented by a period of erosion, by a low-Sr series. The lava flows forming this sequence are the clinopyroxene-phyric basalt flows of Grand Roy which are overlain by the massive andesite flows of the Upper Grand Roy valley. The sequence of high-Sr series of lavas followed by a low-Sr series was repeated again after a further southwards shift in activity. The Mt. St. Catherine centre does not display the same sequence of eruptions, but sampling difficulties prevent the determination

of precise volcanic histories in this and older centres. In general, however, there does not appear to be a uniform pattern of eruptions prevailing in the volcanic centres of Grenada.

The model of variable partial melting proposed in Chapter 7 suggests that the basaltic and picritic melts enriched in incompatible trace elements are of smaller volume than those relatively depleted in these elements. The total volume of andesites and dacites that it is possible to produce by fractional crystallisation of the trace element-enriched series should therefore be smaller than those of trace element depleted series. It has been shown however, that a considerable variation in degree of trace element enrichment may occur within differences of a few percent total volume of melt (p.111 ). In Chapter 10, the petrogenesis of the Grenada basalts and picrites is discussed and related to a small volume of partial melting of an Upper Mantle peridotite source. Thus a dramatic contrast between relative volumes of derivative andesites and dacites is not expected.

Any estimate of the abundance of derivative compositions is beset with sampling difficulties. Judging simply by the numbers of analyses there does not appear to be a preponderance of volcanic series characterised by relatively depleted incompatible trace element abundances. Andesite flows of comparable thickness (approximately 30 m) belonging to the high and low-Sr series of the Mt. Granby - Fedon's Camp centre are present at Grand Roy and Brizan (Chapter 6). However, the voluminous andesite and dacite flows of Mt. St. Catherine belong predominantly to the low-Sr



series of the centre. The high-Sr series of Grenada contain rock types of unusual petrographic and mineralogic composition. Oscillatory and sector-zoned calcic augites are remarkably abundant (up to 45% modally). Although similar phenocryst and groundmass clinopyroxenes are also present in the low-Sr series, they are never so prominent. Similar calcic augites have been reported from alkali basalt associations elsewhere (eg. Scott, 1972; Thompson, 1972) but are unusual in island-arc situations. The striking appearance in hand specimen of the lava flows containing these phenocryst clinopyroxenes, and the resistant nature of the flows probably introduces a major sampling bias towards collection and analysis of these compositions. A large part of the island of Grenada is covered at surface by andesites and dacites with relatively depleted incompatible trace element abundances. In general therefore, it seems probable that the volumes of compositions relatively depleted in incompatible trace elements exceeds the enriched compositions.

The volcanic series relatively depleted in incompatible trace elements on Grenada are in themselves enriched in these elements in comparison with the calc-alkaline suites of St. Kitts (Baker, 1968), Montserrat (Rea, 1970) and Dominica (K.Wills, pers. comm., 1973). In some cases the enrichment is by a factor of 2 or more at similar  $\text{SiO}_2$  wt.%. The significance of differences between calc-alkaline suites within and between island arcs is discussed in Chapter 11.

### 8:5 Discussion

In summary, the variable major and trace element geochemistry displayed in the basalt-andesite-dacite association of Grenada is probably the result of fractional crystallisation processes occurring within a variety of parental magma compositions. Features such as  $\text{Sr}^{87}/86$  ratios and degree of relative light Rare Earth enrichment, established during the generation of the basaltic and picritic melts are apparently preserved during the evolution of the melts towards increasing silica-saturation.



## CHAPTER 9

THE PETROGRAPHY AND MINERALOGY OF THE GRENADA ROCK SUITE9:1 Introduction

The petrography and mineralogy of the Grenada volcanic series is similar in many respects to previously described calc-alkaline suites in the Lesser Antilles island arc (Lewis, 1964; Baker, 1968; Rea, 1970). Some unusual features are also observed however, mainly due to the presence of silica-undersaturated, alkali basalt compositions. The following discussion concentrates initially on these picrites and basalts. Subsequently the andesites, dacites and cumulus plutonic blocks are described with a summary of the important petrographic and mineralogic features of the entire Grenada suite.

9:2 The Picrites and Basalts

The picrites and basalts are dominantly composed of olivine, clinopyroxene, spinel and plagioclase feldspar. In some basalts, amphibole is observed usually poikilitically enclosing the other ferromagnesian minerals and feldspars. Textures vary from microphyric to coarsely porphyritic with phenocrysts up to 5-10 mm in length. Dunite and pyroxenite inclusions are occasionally present. The larger phenocrysts are usually plagioclase feldspar and clinopyroxene. The striking appearance of the clinopyroxene-phyric basalts is one of the most characteristic features of Grenada geology. The picrite and basalt compositions are present as massive and disintegrated flows, and as isolated blocks in the reworked material. Microphyric textures are usually found in the highly vesicular scoria and ash associated with some of the

recent explosion craters.

The gradational nature of the compositional variation of these picrites and basalts is reflected to some extent in the petrography and mineralogy. Contrasted degrees of incompatible trace element enrichment are found in samples of similar petrographic appearance, but in general, the coarsely porphyritic compositions are associated with higher abundances of these elements.

An example of a microphyric picrite is shown in Plate 33. This rock is dominated by abundant modal olivine (25%), present as microphenocrysts up to 0.5 mm in length. Calcic augite, chrome spinel and magnetite are also present as microphenocrysts in this picrite 483. Some olivines poikilitically enclose oxide minerals (Plate 33b). The groundmass is composed of microlites of olivine, clinopyroxene, plagioclase and granules of chrome spinel and magnetite. Nepheline has been discovered in the groundmass of this particular picrite by a reconnaissance study with the electron microprobe (see Appendix II for method). The bulk composition of the rock, estimated mode and selected analyses of the constituent minerals are presented in Table 11. The olivines are zoned from  $Fo_{89}$  to  $Fo_{85}$  similar to olivines in ultrabasic lavas from other volcanic provinces (cf. Brown, 1968; Arculus and Curran, 1972).

However, the compositional variation of the clinopyroxenes are an unusual feature of the Grenada picrites and basalts, and the microphenocrysts of picrite 483 are an extreme example of



Plate 33

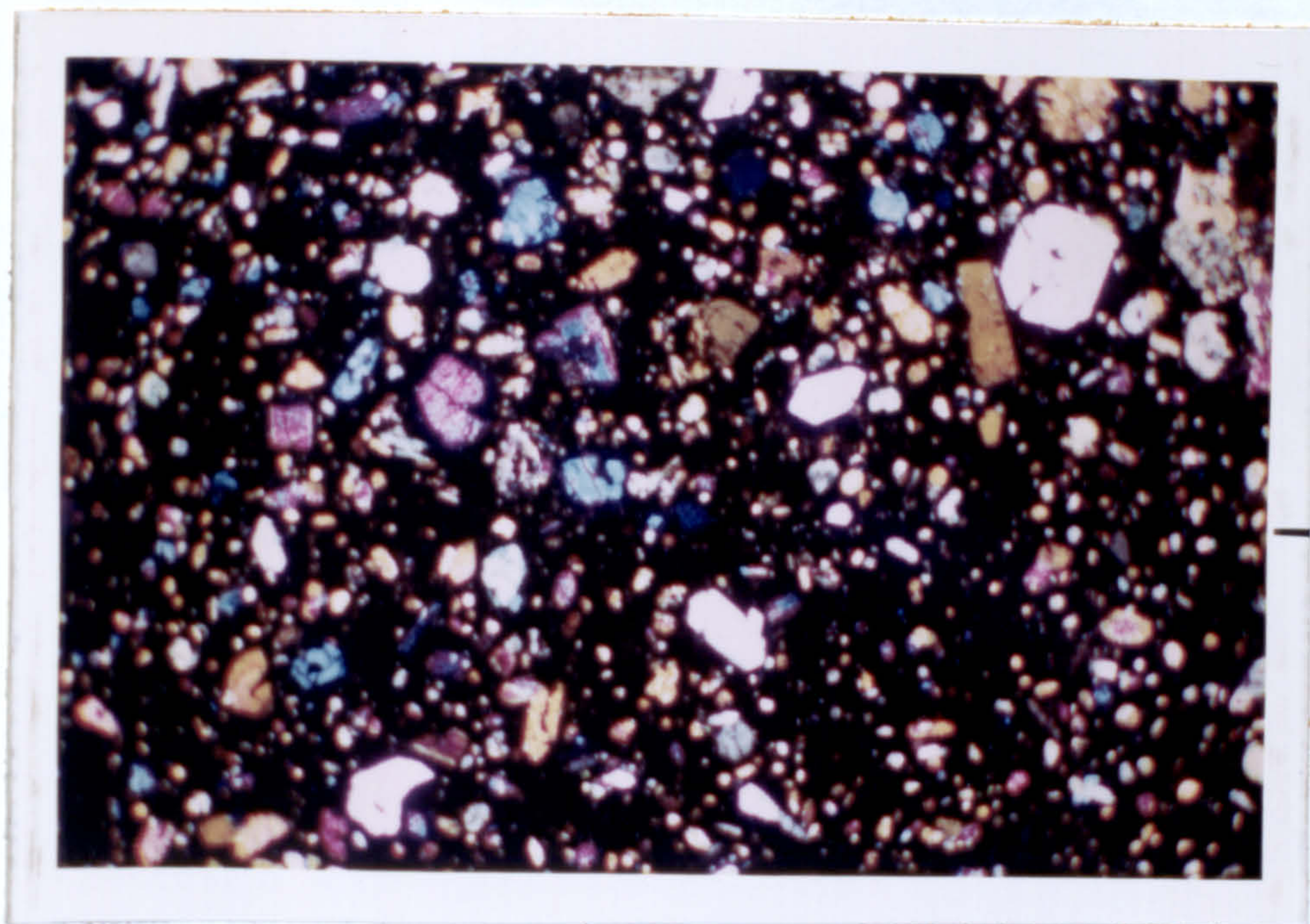
a) Photomicrograph of picrite 483, a loose block in the upper Concord Valley. Microphenocrysts of olivine and pyroxene are visible in a dark microcrystalline to glassy groundglass.

(Crossed polars magnification x5)

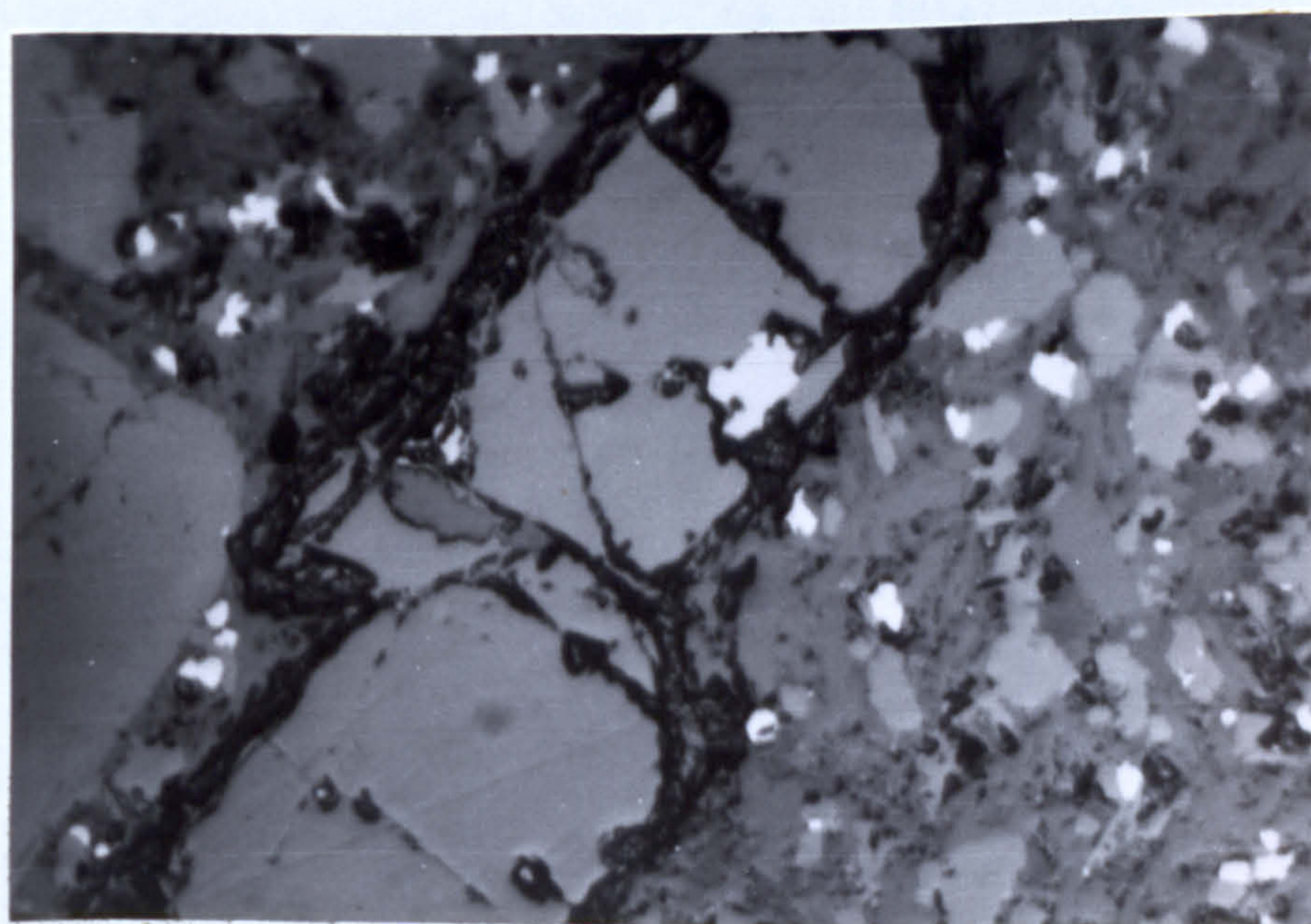
B) Photomicrograph of olivine microphenocryst containing chrome spinel crystals in picrite 483

( Reflected light magnification x20)





A



B



TABLE 11

Major and trace element analysis  
and estimated modal mineralogy  
of picrite 483

<u>Sample No.</u>	<u>483</u>
SiO <sub>2</sub>	44.70
Al <sub>2</sub> O <sub>3</sub>	14.76
Fe <sub>2</sub> O <sub>3</sub>	10.36
MgO	11.81
CaO	11.99
Na <sub>2</sub> O	3.40
K <sub>2</sub> O	1.27
TiO <sub>2</sub>	1.16
MnO	0.24
S	0.00
P <sub>2</sub> O <sub>5</sub>	0.32
Ba	640
Nb	25
Zr	176
Y	20
Sr	973
Rb	40
Zn	81
Cu	128
Ni	292
Ce	46

Estimated mode %

Olivine	25
Clinopyroxene	10
Spinel	2

Groundmas (63) microlites of  
olivine, clinopyroxene, plagio-  
clase, spinel in a dark glassy  
matrix.

TABLE 11 (continued)

Partial analyses of microphenocryst minerals in picrite 483  
 cpx=clinopyroxene ol=olivine sp=chrome spinel  
 subscript c=core subscript r=rim

	cpx <sub>c</sub>	cpx <sub>r</sub>	cpx <sub>c</sub>	cpx <sub>r</sub>	ol <sub>c</sub>	ol <sub>r</sub>		sp
SiO <sub>2</sub>	49.03	42.05	51.73	42.77	40.89	40.57	SiO <sub>2</sub>	0.31
TiO <sub>2</sub>	0.95	3.18	0.49	2.56	-	-	TiO <sub>2</sub>	3.86
Al <sub>2</sub> O <sub>3</sub>	4.49	12.25	2.43	10.74	-	-	Al <sub>2</sub> O <sub>3</sub>	14.91
FeO	5.53	9.83	5.49	8.38	10.50	13.21	V <sub>2</sub> O <sub>5</sub>	0.36
MgO	14.80	9.55	16.43	11.01	47.68	45.16	Cr <sub>2</sub> O <sub>3</sub>	31.56
CaO	23.67	23.37	22.65	23.38	0.21	0.30	FeO	29.48
Na <sub>2</sub> O	0.29	0.44	0.34	0.42	-		MnO	0.01
							MgO	14.62
Total	100.76	100.67	99.56	99.26	99.28	99.24	CaO	0.27
							Total	<u>97.39</u>

Atomic proportions on the basis of 4 (olivine)  
 and 6 (pyroxene) oxygens

Si	1.841	1.592	1.913	1.631	1.010	1.015
Ti	0.027	0.091	0.014	0.073	-	-
Al	0.199	0.547	0.106	0.483	-	-
Fe	0.174	0.311	0.170	0.267	0.217	0.276
Mg	0.828	0.539	0.906	0.626	1.756	1.684
Cu	0.952	0.948	0.898	0.956	0.006	0.008
Na	0.021	0.032	0.024	0.031	-	-



this variation. The clinopyroxene microphenocrysts are characterised in many cases by pale green cores irregularly surrounded by a dark green mantle. The cores sometimes appear corroded or discontinuous but there is usually a sharp boundary between core and mantle with no obvious sign of reaction. There is a remarkable variation between the composition of the differently coloured portions of the crystals. In the analyses presented in Table 11 the range of  $\text{Al}_2\text{O}_3$  is from 2.5 to 12.25 wt.% and  $\text{TiO}_2$  ranges from 0.5 to 3.2 wt.%. Variation in Al and Ti in clinopyroxenes in relation to sector and oscillatory zoning has been examined in several recent studies (eg. Hargraves et al., 1970; Thompson, 1972; Wass, 1973). These types of zoning are not prominent in the microphenocrysts of the picrite 483 but the variation in Ti and Al between differently coloured portions of the crystals is similar in some respects to the variation observed in sector and oscillatory zoning.

The dark green mantles are enriched in Ti and Al relative to the pale green cores. The sector-zoned titanaugites described by Wass (1973) contain both an overall higher concentration and greater variation of Ti between sectors, but the variation of Al in the Grenada clinopyroxenes is apparently more extensive than in any type of zoning previously reported. Al can exist in both tetrahedral and octahedral sites of the pyroxene structure and is probably involved in several coupled substitutions, with Na, Ti and  $\text{Fe}^{3+}$  for example (Kushiro, 1962). The variation in composition of the clinopyroxenes in relation to changing physical and chemical conditions of the host magma is discussed later.

It is useful however, to demonstrate graphically the variation of Al with Si and Ti in the clinopyroxenes under discussion in Fig. 33. Kushiro et al. (1970) described a linear variation of Ti with Al in lunar clinopyroxenes of 0.5 and Ross et al. (1970) explained this variation in terms of a simple coupled substitution:



In the case of the clinopyroxenes of picrite 483, the variation of Ti with Al is approximately  $Ti/Al = 0.17$  and the sum of Al + Si cations on the basis of 6 oxygens is not equal to 2.0. This suggests a more complex substitution than is indicated by the formula above is present (see p. 229 ).

The pale green core and dark green mantle relationship is observed in clinopyroxenes of other picrites, alkali and transitional basalts but the variation in composition is never as extreme as in the picrite 483.

There is a complete gradation between compositions dominated by abundant modal olivine and alkali and transitional basalts of coarsely porphyritic appearance. In the projections of normative mineralogy of the picrites and basalts (Fig. 21, Chapter 7) the higher contents of normative diopside and albite were generally associated with a greater degree of incompatible trace element enrichment. The modal composition of many of these trace-element-enriched basalts is similar to the predicted normative mineralogy being dominated by large ( < 5 mm) phenocrysts of clinopyroxene and plagioclase feldspar. However, there are many petrographic and mineralogical similarities between picrites and basalts with



Fig. 33a

Al/Si relationships in picrite clinopyroxene microphenocrysts. Each symbol represents an individual crystal.

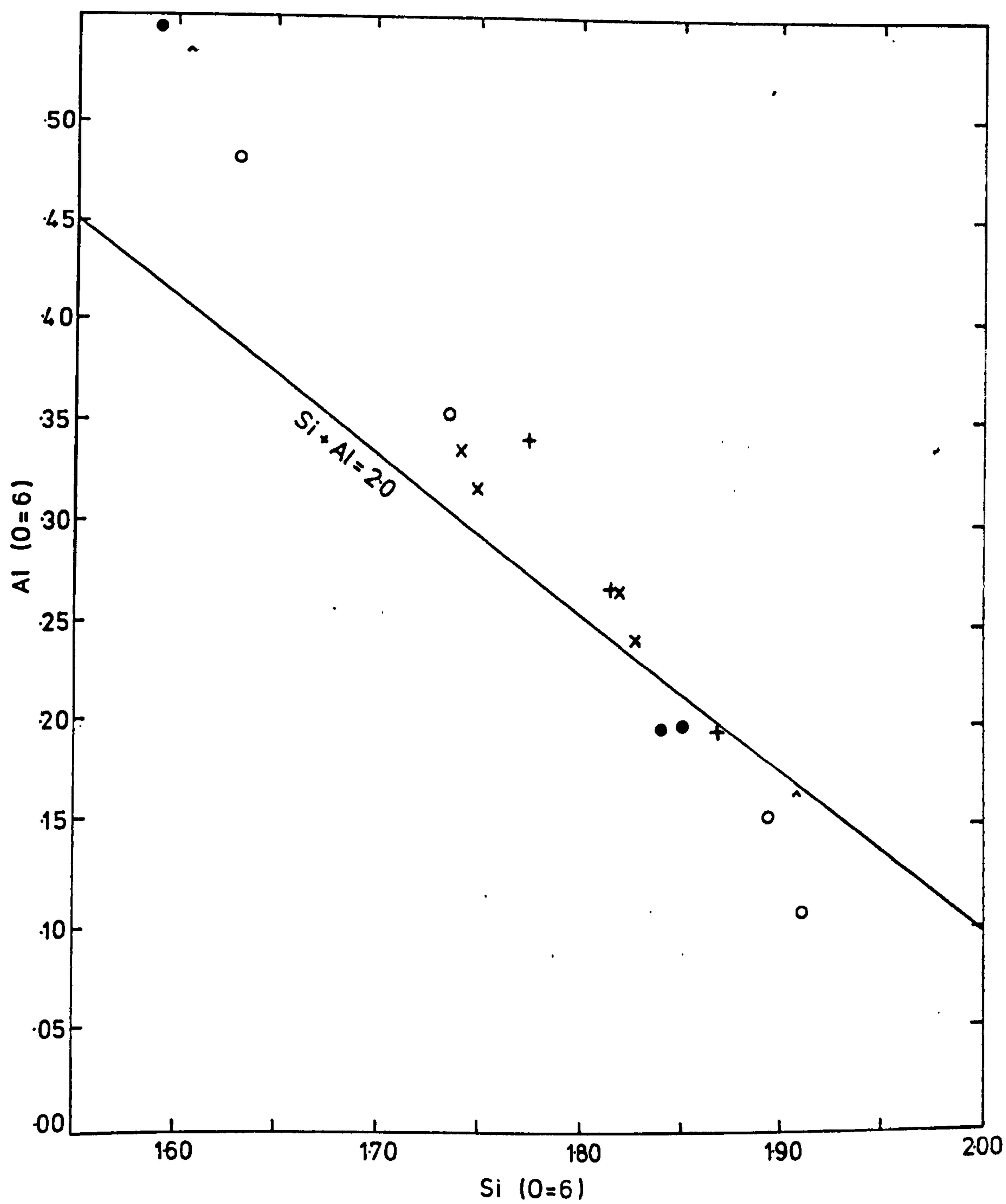




Fig. 33b.

Al/Ti relationships in picrite clinopyroxene microphenocrysts. Each symbol represents an individual crystal.

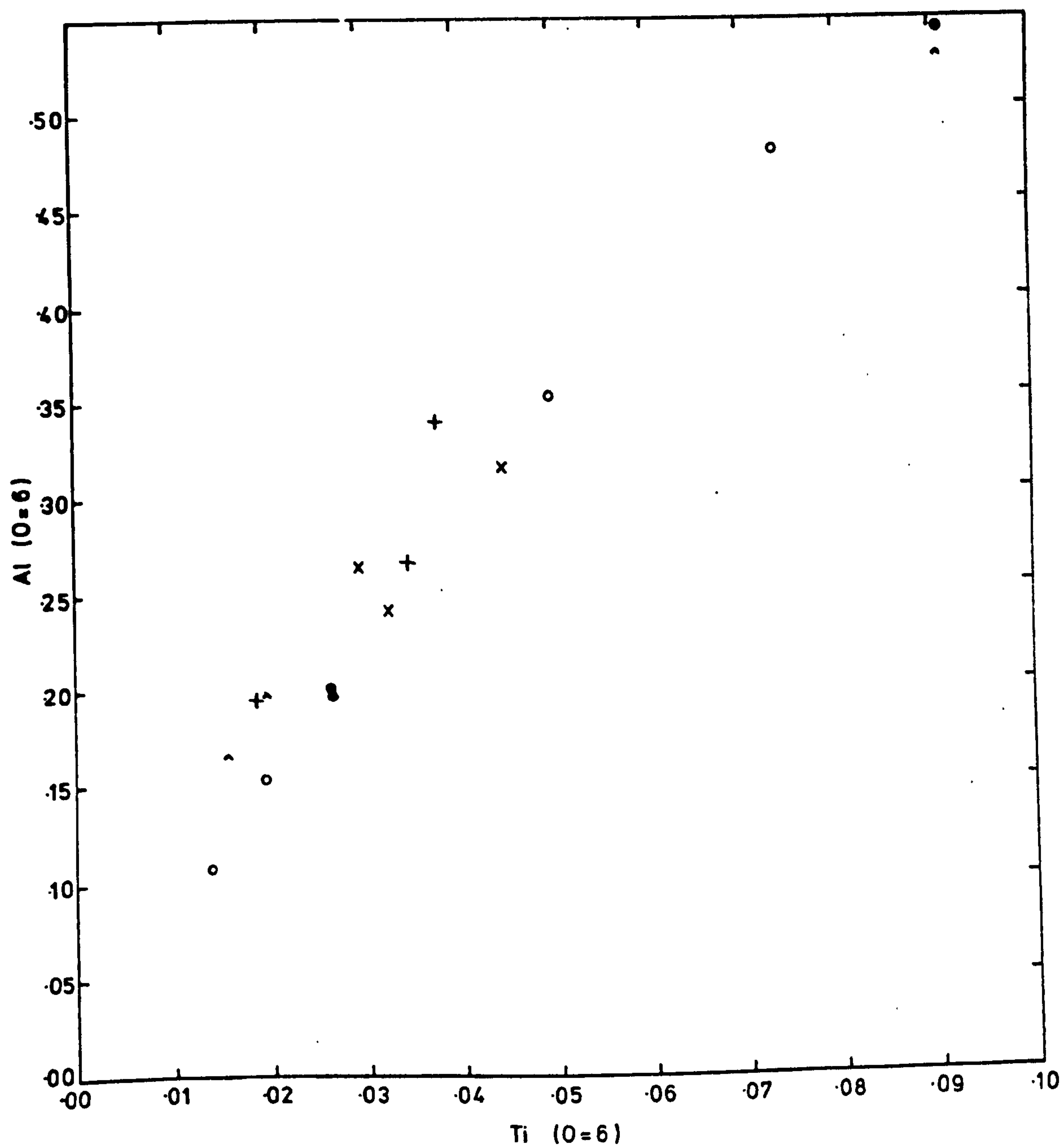




Plate 34

Photomicrograph of transitional basalts 375 and 468.

Microphenocrysts of olivine and clinopyroxene are present; in basalt 468 glomeroporphyritic clusters of olivine microphenocrysts are also visible.

(Crossed polars magnification x5)



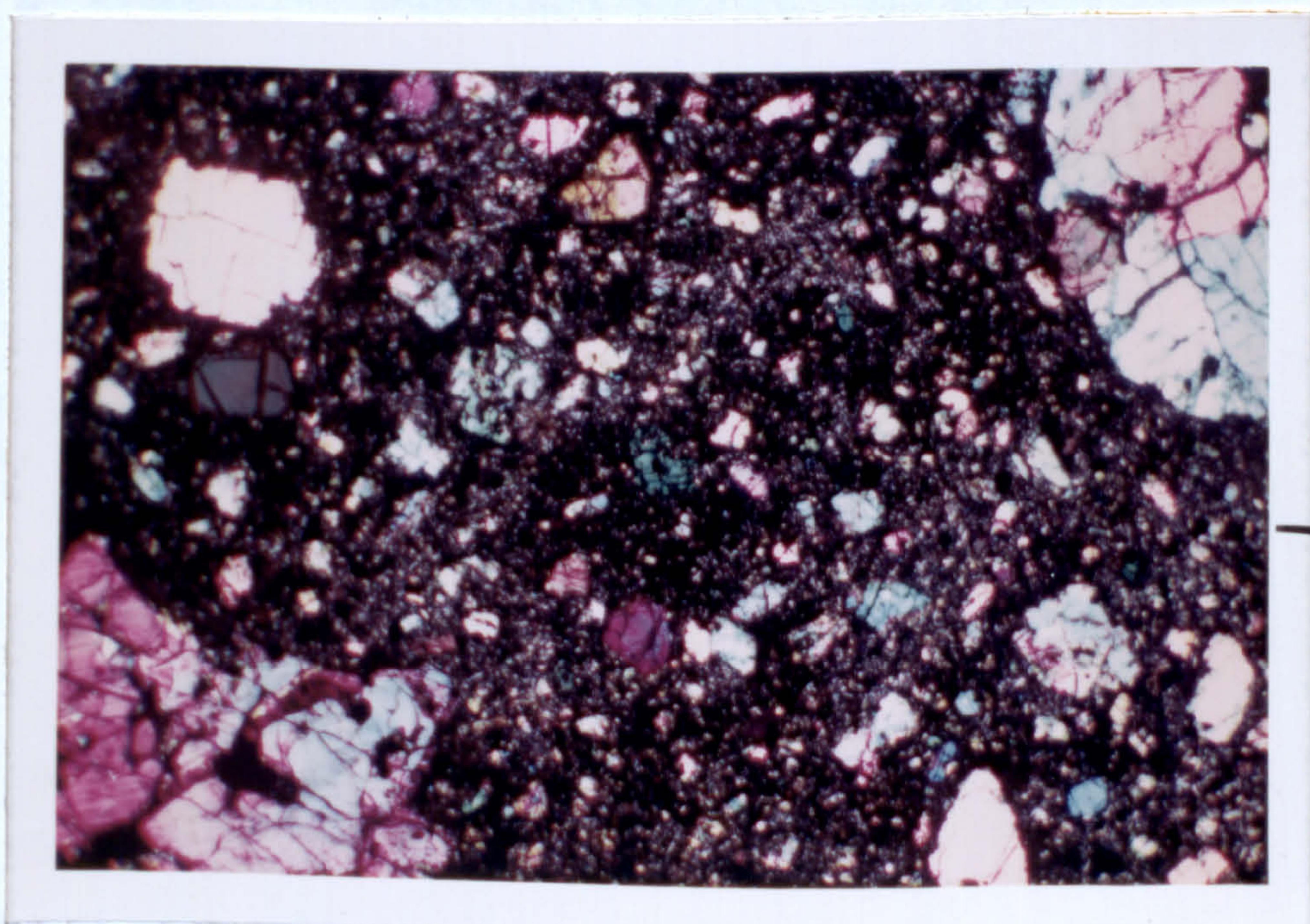
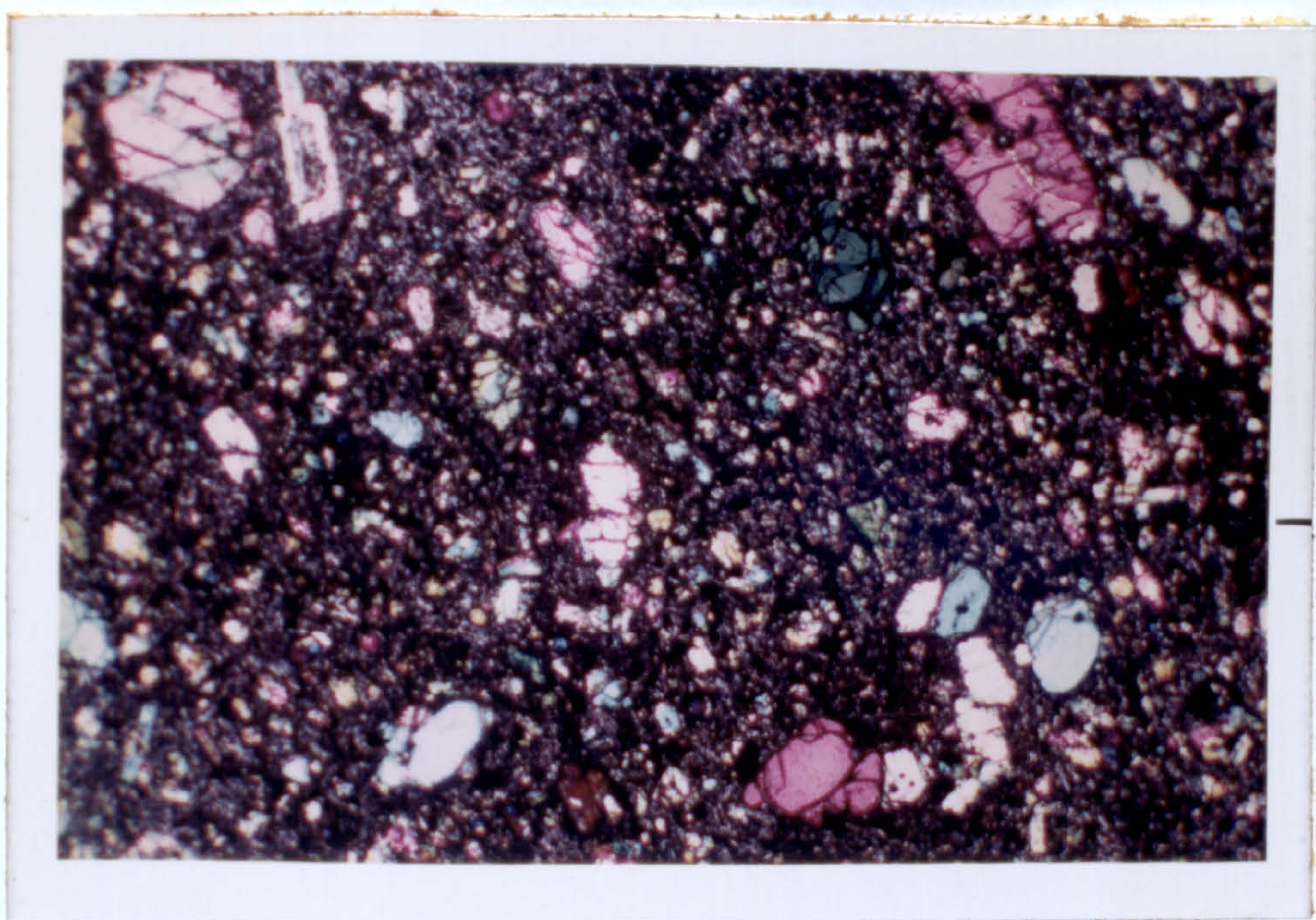




TABLE 12

Major and trace element analyses of transitional basalts 375 and 468 with estimated modal mineralogy.

Sample No.	<u>375</u>	<u>468</u>
SiO <sub>2</sub>	46.57	46.20
Al <sub>2</sub> O <sub>3</sub>	17.11	17.71
Fe <sub>2</sub> O <sub>3</sub>	9.80	9.22
MgO	11.44	13.15
CaO	11.44	10.17
Na <sub>2</sub> O	1.99	2.01
K <sub>2</sub> O	0.43	0.44
TiO <sub>2</sub>	0.89	0.77
MnO	0.21	0.20
S	0.00	0.00
P <sub>2</sub> O <sub>5</sub>	0.13	0.14
Ba	109	143
Nb	9	8
Zr	63	64
Y	16	16
Sr	380	354
Rb	12	13
Zn	70	72
Cu	99	91
Ni	306	543
Ce	14	12
Estimated mode %		
Olivine	25	25
Clinopyroxene	15	15
Plagioclase	5	5
Magnetite	2	2
Groundmass	50	50

Groundmass of both basalts composed of glass with dominant plagioclase microlites, clinopyroxene, olivine and oxide granules.

TABLE 13

Partial analyses of olivine, clinopyroxene  
and a magnetite phenocryst in transitional basalts 375  
and 468

	+=375		x=468				
	ol=olivine		cpx=clinopyroxene		mag=magnetite		
	ol <sup>+</sup>	ol <sup>+</sup>	cpx <sup>+</sup>	cpx <sup>x</sup>	ol <sup>x</sup>	ol <sup>x</sup>	mag <sup>x</sup>
SiO <sub>2</sub>	40.54	39.47	48.77	51.75	41.68	40.30	0.06
TiO <sub>2</sub>	-	-	1.37	0.60	-	-	10.84
Al <sub>2</sub> O <sub>3</sub>	-	-	5.75	3.92	-	-	4.03
FeO	20.74	18.93	8.45	5.10	10.56	16.67	78.25
MgO	36.94	40.91	13.62	14.95	47.73	42.00	0.75
CaO	0.34	0.27	21.95	22.68	0.04	0.07	0.42
Na <sub>2</sub> O	-	-	0.65	0.45			0.03
Total	99.11	99.58	100.56	99.45	100.01	99.04	94.38
Si	1.051	1.012	1.814	1.909	1.020	1.025	
Ti	-	-	0.038	0.017	-	-	
Al	-	-	0.252	0.170	-	-	
Fe	0.450	0.406	0.263	0.157	0.216	0.355	
Mg	1.427	1.563	0.755	0.822	1.741	1.592	
Ca	0.009	0.007	0.875	0.897	0.001	0.002	
Na	-	-	0.047	0.032	-	-	
			Ca 46.22	47.81			
Mg	75.55	74.38	Mg 39.88	43.82	Mg 88.95	81.78	
Fe	24.45	20.62	Fe 13.89	8.37	Fe 11.05	18.22	
			100 Mg/Mg+Fe ratios				
	76.0	79.4	74.8	84.0	89.0	81.8	



Plate 35

Photomicrograph of transitional basalt 454. Prominent oscillatory and sector-zoned calcic augite phenocrysts, oscillatory zoned plagioclase feldspar and a few olivine phenocrysts. (Crossed polars magnification x5).



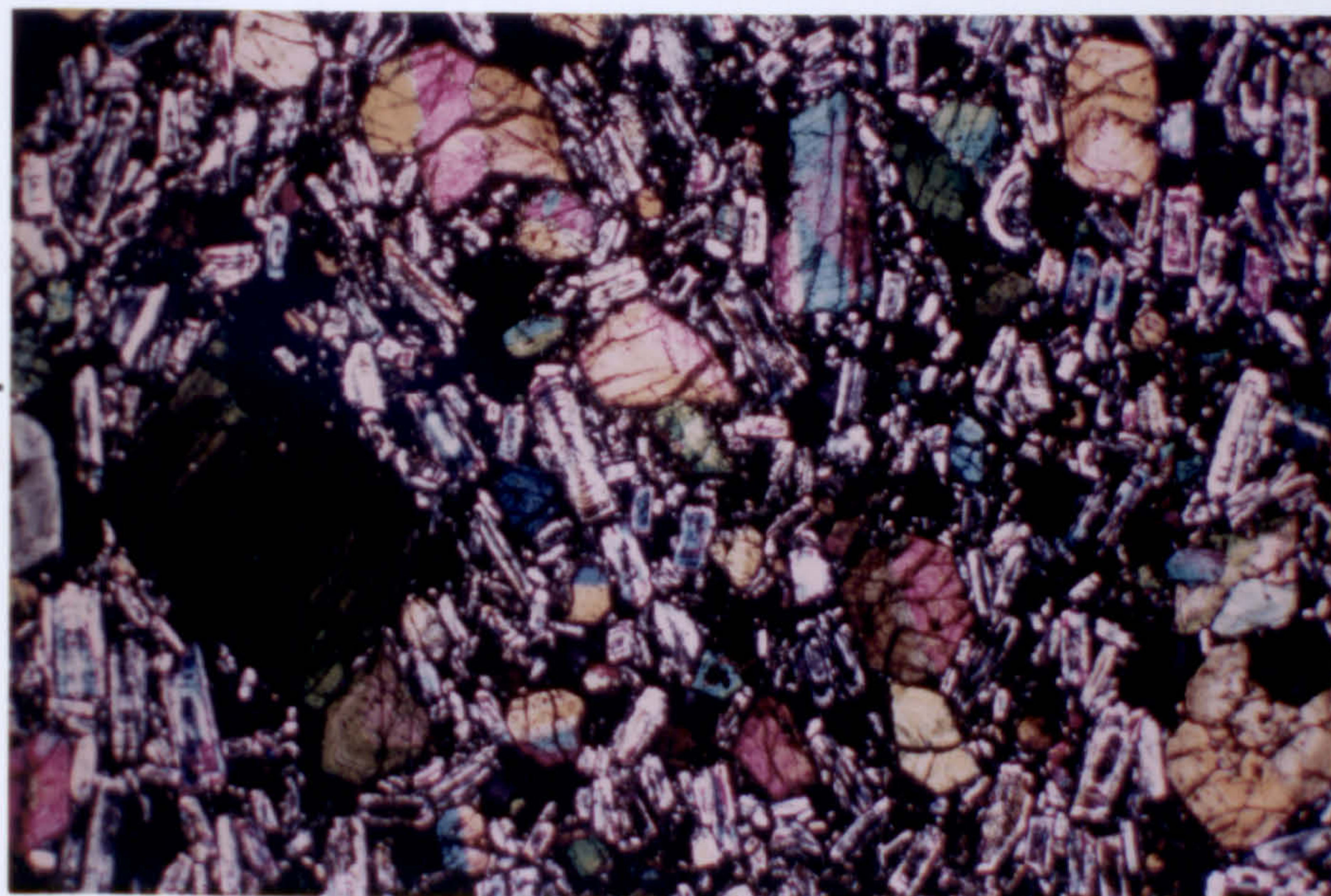
TABLE 14

Major and trace element analysis of  
 transitional basalt 414 together with  
 estimated modal mineralogy.

Sample  
 No.

SiO<sub>2</sub>

Al<sub>2</sub>O<sub>3</sub>



Sr

Rb

Zn

Ca

Mg

Ce

La

Pr

Nd

Sm

Eu

Gd

Tb

Dy

Ho

Er

Tm

Yb



TABLE 14

Major and trace element analysis of  
transitional basalt 454 together with  
estimated modal mineralogy.

Sample No.	<u>454</u>
SiO <sub>2</sub>	48.28
Al <sub>2</sub> O <sub>3</sub>	16.38
Fe <sub>2</sub> O <sub>3</sub>	10.32
MgO	7.27
CaO	13.56
Na <sub>2</sub> O	2.21
K <sub>2</sub> O	0.69
TiO <sub>2</sub>	0.91
MnO	0.22
S	0.00
P <sub>2</sub> O <sub>5</sub>	0.16
Ba	208
Nb	5
Zr	69
Y	17
Sr	1161
Rb	8
Zn	62
Cu	208
Ni	58
Ce	16
Estimated mode %	
Olivine	5
Clinopyroxene	20
Plagioclase	40
Magnetite	5
Groundmass	(30)

Groundmass coarsely crystalline with plagioclase,  
clinopyroxene, minor olivine and magnetite in a  
small amount of brown glass.

different trace element abundances.

The appearance of microphyric transitional basalts 375 and 468 is shown in Plate 35. The major and trace element compositions and estimated modes of these basalts are given in Table 12. In comparison with picrite 483, it can be seen that these basalts are considerably less enriched in the incompatible trace elements. Nevertheless, the mineralogy is very similar to the picrite excepting that groundmass nepheline has not been discovered. The composition of olivine, clinopyroxene and magnetite in these basalts is presented in Table 13. Chrome spinel is also present but was not analysed in this instance. The range of zoning in the olivines is from  $Fo_{89}$  to  $Fo_{75}$  which includes the range of zoning present in the olivines of the picrite. The clinopyroxene microphenocrysts contain pale green cores surrounded by oscillatory and sector-zoned darker green mantles. The groundmass is composed of microlites of the same ferromagnesian minerals, plagioclase feldspar laths and brown glass.

Thus the petrography and mineralogy of the microphyric basalts and picrites, despite major differences in trace element compositions are very similar in many instances.

The appearance of a porphyritic basalt is shown in Plate 35. The composition of this transitional basalt 454 and estimated mode is given in Table 14. Sector and oscillatory zoned clinopyroxene, oscillatory zoned plagioclase feldspar and olivine ( $Fo_{79-72}$ ) are the prominent phenocryst minerals up to 2-3 mm in length. Magnetite with exsolved ilmenite is also present sometimes poikilitically enclosed by olivine and clinopyroxene. The groundmass is composed



TABLE 15

Analyses of phenocryst minerals in transitional basalt 454

	ol=olivine		cpx=clinopyroxene		mag=magnetite
	ol	ol	cpx	cpx	mag
SiO <sub>2</sub>	39.08	40.01	48.54	47.13	0.46
TiO <sub>2</sub>	0.04	0.04	0.93	1.35	11.84
Al <sub>2</sub> O <sub>3</sub>	0.02	0.17	4.03	6.88	0.02
FeO	18.50	23.42	8.10	9.21	76.26
MnO	0.47	0.40	0.74	0.24	0.70
MgO	41.16	35.32	12.88	12.04	4.39
CaO	0.03	0.03	21.92	21.95	0.06
K <sub>2</sub> O	-	-	0.01	0.01	-
Na <sub>2</sub> O	0.02	0.02	1.73	0.36	0.02
Cr <sub>2</sub> O <sub>3</sub>	-	-	0.06	0.03	-
Total	99.33	99.48	98.94	99.20	93.75

Atomic proportions on the basis of  
4 (olivine) and 6 (pyroxene) oxygens

Si	1.005	1.045	1.849	1.787
Ti	0.001	0.001	0.027	0.038
Al	0.001	0.005	0.181	0.308
Fe	0.398	0.512	0.258	0.292
Mn	0.010	0.009	0.024	0.008
Mg	1.577	1.375	0.731	0.680
Ca	0.001	0.001	0.895	0.892
K	-	-	0.000	0.000
Na	0.001	0.001	0.128	0.026
Cr	-	-	0.002	0.001

End-member compositions

Ca	-	-	46.90	47.64
Mg	79.44	72.54	38.32	36.34
Fe	20.56	27.46	14.78	16.01

100 Mg/Mg+Fe ratios

79.9	72.9	73.8	70.0
------	------	------	------

of microlites of the phenocryst minerals but is relatively coarse (microlites 0.1 - 0.3 mm in length) with only a small amount of interstitial glass. A surprising feature of these porphyritic basalts is that despite the coarse-grained nature of the groundmass and the paucity of interstitial glass, there is very little fracturing of the phenocryst or groundmass microphenocrysts visible. It is apparent that during flow emplacement of the lavas, sufficient melt was present to prevent any damage to the crystals.

The range of mineral compositions in transitional basalt 454 are given in Table 15. The Mg/Mg+Fe ratios of the ferromagnesian minerals are similar to the microphyric basalts described previously. In general there are no detectable gaps in ranges of mineral composition in the Grenada picrites and basalts. The examples that have been described here have been selected in order to illustrate some of the range in petrographic appearance and modal abundance of phenocryst minerals. The gradational nature of the petrology and mineralogy is stressed since it is relevant to the petrogenesis of the Grenada calc-alkaline suite that a rigid separation of the basic magmas on the basis of chemical and petrographic criteria is not possible.

The nature of the sector and oscillatory zoned clinopyroxenes is discussed in the following section but additional features of the picrites and basalts are described first.

#### 9:2:1 Inclusions in the Basalts

Dunitic 'inclusions' are common in many of the basalts. For



Plate 36

Strained forsteritic olivine phenocryst in transitional  
basalt 468. (Crossed polars magnification x5).



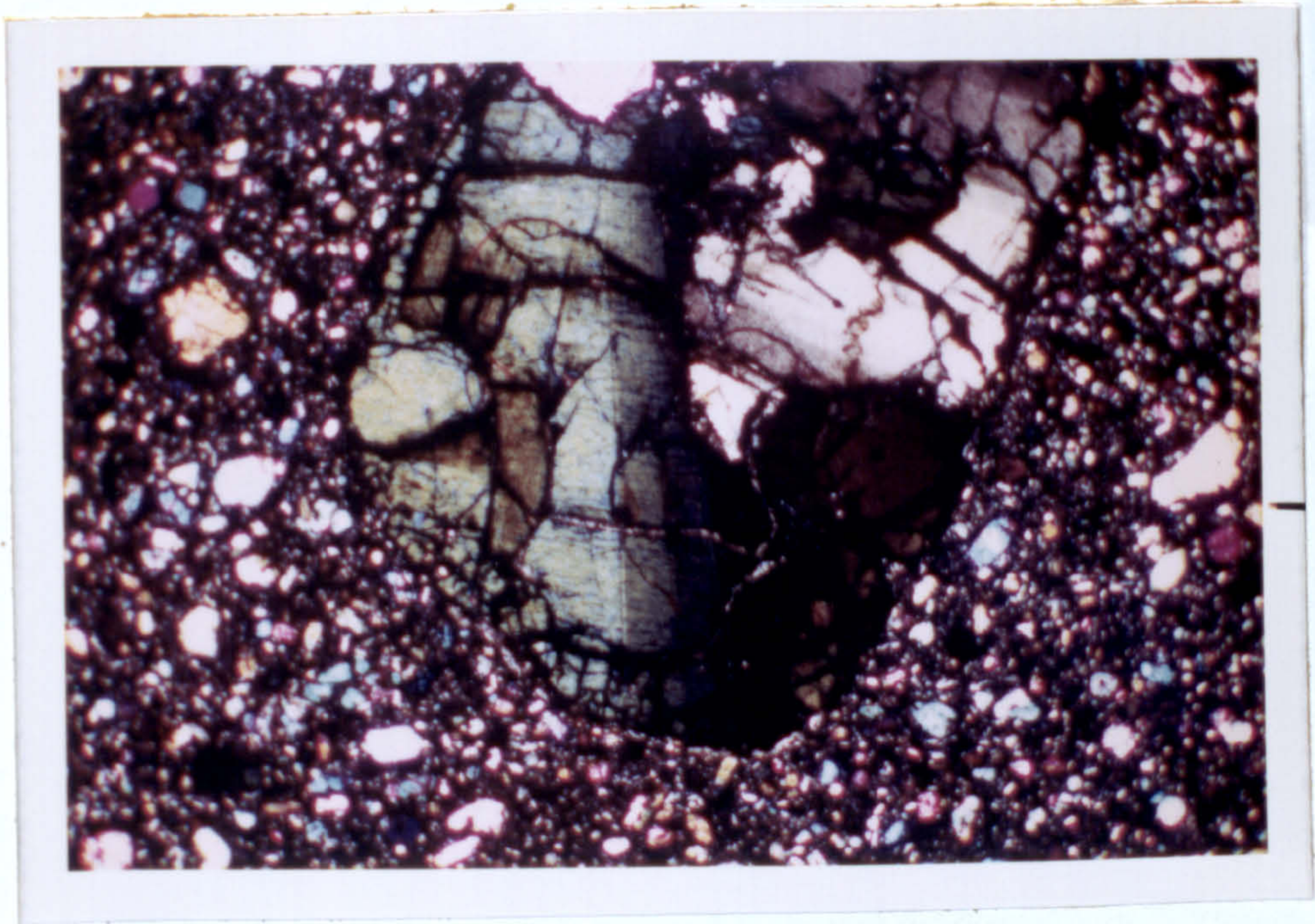
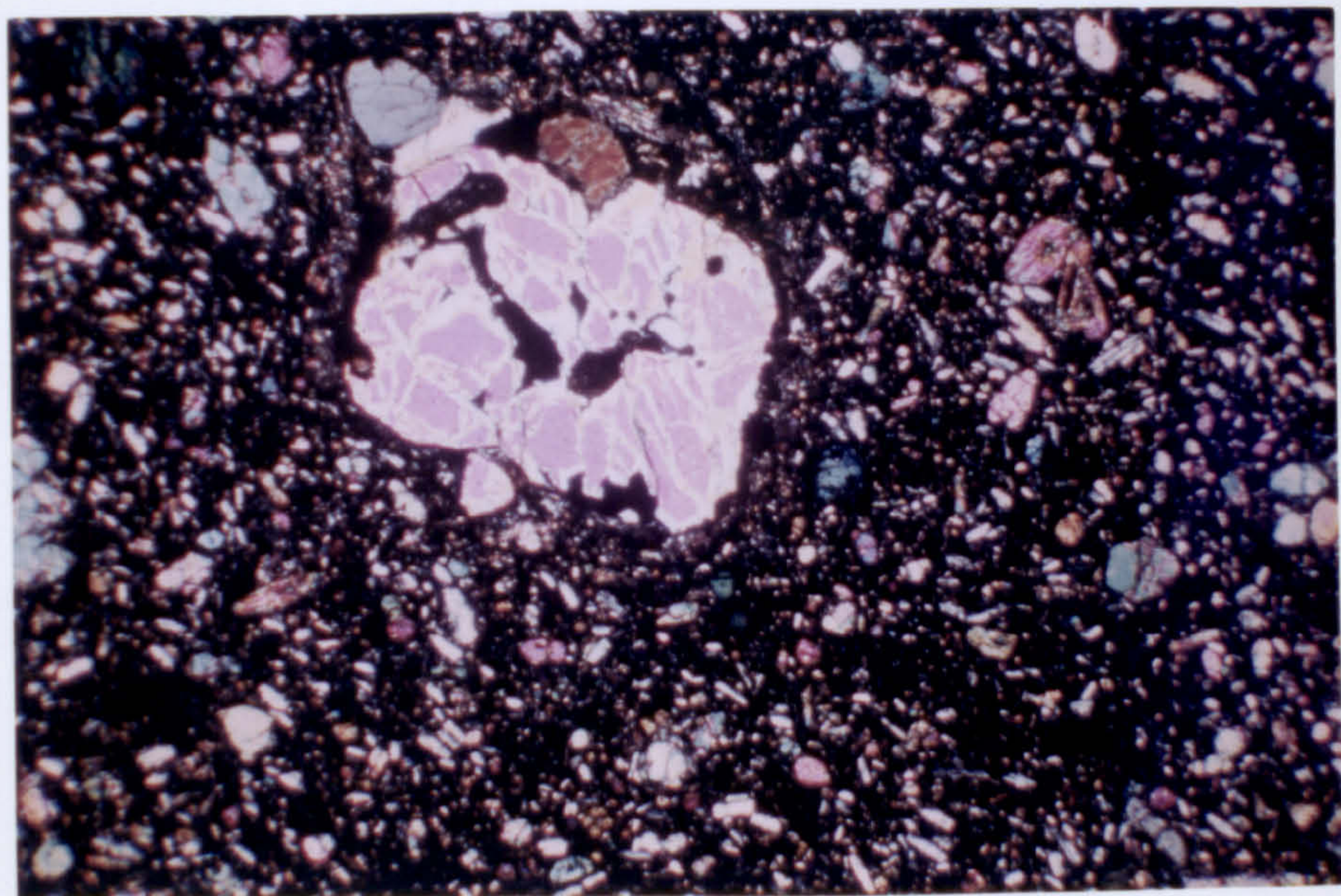




Plate 37

Quartz xenocryst in alkali basalt 33. Xenocryst, 3mm in length, is surrounded by clinopyroxene microlites. (Crossed polars magnification x10).





olivine and pyroxene clusters of olivine and pyroxene are frequently present in the coarsely crystalline basalt. The compositions of the minerals within these clusters are similar to the separate phenocrysts in the groundmass of the basalt and so probably represent cognate crystallization. No identifiable ultrabasic xenoliths of possible origin have been discovered.

### QUARTZ PHENOCRYSTS

Quartz phenocrysts have been reported from many basaltic andesites and basalts (e.g. Nicholls *et al.*, 1971). A few of the groundmasses contain phenocrysts of quartz up to 2-3 mm in diameter surrounded by a corona of minute clinopyroxene laths. Plate 17 shows the appearance of one of these phenocrysts in alkali basalt 31. The quartz crystals appear to contain minute



example in the transitional basalt 468 described above, an elongate cluster of olivine microphenocrysts 1 cm in length is present. The olivines are zoned from the core to the margin of the inclusion ( $\text{Fo}_{90-81}$ ) which is similar to the range of zoning in separate microphenocrysts in the groundmass. Chrome spinel and magnetite are the only other minerals present in the inclusion. In this example, the cluster of olivines is apparently of glomeroporphyritic origin representing cognate accumulation of the crystals. Sometimes elongate olivines show signs of plastic deformation reflecting distortion after crystallisation. In addition, some olivines show strained extinction features probably due to the same cause (Plate 36).

Glomeroporphyritic clusters of clinopyroxene, olivine and plagioclase feldspar are frequently present in the coarsely porphyritic basalts. The compositions of the minerals within these clusters are similar to the separate phenocrysts in the groundmass of the basalts and so probably represent cognate inclusions. No identifiable ultrabasic xenoliths of possible Upper Mantle origin have been discovered.

#### 9:2:2 Quartz xenocrysts

Quartz xenocrysts have been reported from many basaltic andesites and basalts (eg. Nicholls et al., 1971). A few of the Grenada basalts contain xenocrysts of quartz up to 2-3 mm in diameter surrounded by a corona of minute clinopyroxene laths. Plate 37 shows the appearance of one of these xenocrysts in alkali basalt 33. The quartz crystals appear to contain minute

TABLE 16

Analyses of selected quartz-bearing, alkali and transitional basalts, illustrating range of trace element abundances.

Sample No.	<u>* 33</u>	<u>+ 82</u>	<u>* 139</u>	<u>+ 311</u>
SiO <sub>2</sub>	47.34	46.95	47.46	51.79
Al <sub>2</sub> O <sub>3</sub>	16.66	17.38	14.97	18.33
Fe <sub>2</sub> O <sub>3</sub>	9.28	10.44	10.31	7.90
MgO	10.17	11.62	9.90	6.84
CaO	10.79	9.63	13.00	10.20
Na <sub>2</sub> O	3.10	2.37	2.57	3.03
K <sub>2</sub> O	1.19	0.39	0.50	0.82
TiO <sub>2</sub>	1.01	0.89	0.88	0.79
MnO	0.21	0.21	0.23	0.18
S	0.00	0.00	0.00	0.00
P <sub>2</sub> O <sub>5</sub>	0.25	0.11	0.16	0.11
Ba	509	120	143	198
Nb	19	8	6	11
Zr	138	52	72	80
Y	16	13	21	16
Sr	786	300	449	371
Rb	38	12	13	31
Zn	76	81	68	65
Cu	86	60	106	64
Ni	263	565	318	146
Ce	48	11	14	20

\* alkali

+ transitional



needles of rutile or apatite. The lack of co-existing iron-titanium oxides in the basalts makes an estimate of  $f_{O_2}$  and  $T$  after the method of Buddington and Lindsley (1964) difficult. Assuming the liquidus temperatures determined by Cawthorne et al. (1973) at 5 kb ( $P_{H_2O} = P_{tot}$ ) to represent the approximate temperature ( $1100^{\circ}C$ ) of Grenada basalt crystallisation then by analogy with the results of Nicholls et al. (1971), it is possible that quartz was stable in the basalt compositions at pressures of approximately 25 kb or more. In this sense perhaps the quartz crystals should not be regarded as xenocrysts but they are demonstrably unstable at the pressures and temperatures prevailing during the eruption of the basalts. It is a notable feature that quartz xenocrysts are present within basalt compositions of differing degrees of incompatible trace element enrichment. The major and trace element compositions of selected basalts containing xenocrysts are presented in Table 16.

### 9:2:3 Olivine alteration

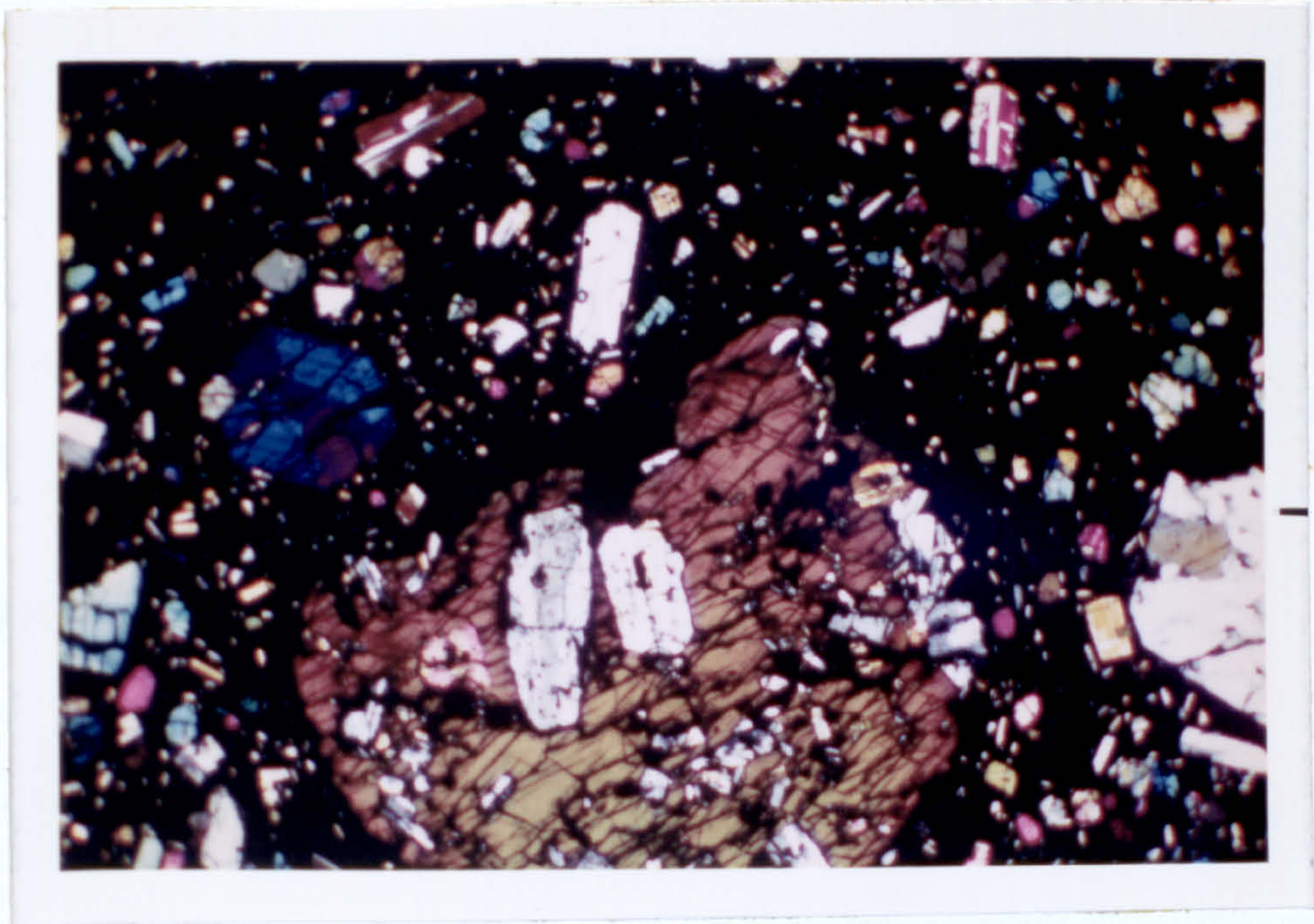
A characteristic of many of the olivine phenocrysts within transitional basalts in particular, is extensive 'iddingsitisation'. In some cases, a thin marginal rim of brown oxidation product is present around the crystals, but on occasions the intensity of alteration is such that only relict brown phenocrysts remain. In the samples examined in reflected light the coexisting oxide minerals frequently display coarse exsolution textures and the alteration of the olivines may reflect sub-solidus oxidation. However, the olivines are also iddingsitised in some of the plutonic blocks where the oxide mineral is a fresh magnetite.

Plate 38

Photomicrograph of alkali basalt scoria, Kick-em-Jenny Volcano.

Note pargasite phenocryst poikilitically enclosing olivine, clinopyroxene, plagioclase and spinel.  
(Crossed polars magnification x5).







In one basalt a zone of brown alteration product has been observed surrounding an unaltered olivine core and is itself mantled by fresh olivine. It appears that the alteration of olivine reflects the changing physical and chemical environment of crystallisation but the precise relationship remains obscure. Serpentinisation of olivine phenocrysts has also been observed, again indicative of subsolidus alteration.

#### 9:2:4 Amphibole phenocrysts in the Basalts

In a few of the Grenada basalts amphibole phenocrysts up to 6 mm in length are present. Cawthorn et al. (1973) have proposed that fractional crystallisation of silica-undersaturated amphibole is the main chemical control generating the trend towards increasing silica-saturation in the Grenada calc-alkaline suite. In addition, a reaction relationship was predicted in the fractional crystallisation situation between amphibole and the previously crystallising olivine and clinopyroxene. The suppression of the appearance of plagioclase on the liquidus at 5 kb ( $P_{H_2O} = P_{tot}$ ) was interpreted as meaning this mineral phase is not involved in the evolution from silica-undersaturated to oversaturated compositions.

In Chapter 7 the evidence for the lack of any amphibole control in the generation of the diversity of picritic and basaltic compositions was presented. The petrographic and mineralogical relationships of naturally occurring amphiboles in the Grenada basalts are examined at this stage. This evidence in combination with the geochemical variation from basalt to andesite and dacite is used to revise the petrogenetic model proposed by Cawthorn et al. (1973)



TABLE 17

Major and trace element analysis of Kickem-Jenny alkali basalt (KJ017) together with estimated modal mineralogy.

<u>Sample No.</u>	<u>KJ017</u>
SiO <sub>2</sub>	45.93
Al <sub>2</sub> O <sub>3</sub>	16.88
Fe <sub>2</sub> O <sub>3</sub>	10.05
MgO	11.18
CaO	12.24
Na <sub>2</sub> O	1.83
K <sub>2</sub> O	0.55
TiO <sub>2</sub>	1.06
MnO	0.17
P <sub>2</sub> O <sub>5</sub>	0.11
Ba	117
Nb	5
Zr	62
Y	19
Sr	300
Rb	19
Zn	72
Cu	88
Ni	235
Ce	5
<u>Estimated mode %</u>	
Olivine 15	Groundmass (60) predominantly grey glass with microlites of plagioclase clinopyroxene and oxide granules.
Clinopyroxene 10	
Plagioclase 10	
Amphibole 5	
Oxides 2	

TABLE 18

Partial analyses of phenocryst minerals in Kick-em-Jenny alkali basalt (KJ017)  
 amph=amphibole ol=olivine cpx=clinopyroxene fel=feldspar sp=spinel

	1	2	3	4	5	6	7	8	9	10	11
	amph	amph	amph	ol	ol	ol	ol	cpx	cpx	cpx	cpx
SiO <sub>2</sub>	42.05	42.65	42.22	41.02	40.93	39.04	39.29	51.75	51.23	48.12	48.94
TiO <sub>2</sub>	2.46	2.35	3.05	-	-	-	-	0.76	0.56	1.12	1.12
Al <sub>2</sub> O <sub>3</sub>	14.27	12.38	12.55	-	-	-	-	3.15	4.22	7.89	6.48
FeO	9.25	13.32	11.73	11.80	15.59	23.22	19.76	7.32	5.20	6.01	6.49
MnO	0.26	-	-	-	-	-	-	-	-	-	-
MgO	14.52	13.64	14.13	46.04	44.83	38.41	39.44	15.66	16.21	14.10	13.68
CaO	11.98	11.25	11.48	0.02	0.26	0.03	0.22	21.88	23.19	23.20	23.04
K <sub>2</sub> O	0.53	-	-	-	-	-	-	-	-	-	-
Na <sub>2</sub> O	2.45	2.56	2.65	-	-	-	-	0.32	0.26	0.34	0.34
Total	97.79	98.15	97.81	99.07	99.61	100.70	98.71	100.84	100.87	100.84	

Atomic proportions on the basis of 4 (olivines), 6 (pyroxene) and 23 (amphibole) oxygens											
Si	6.112	6.257	6.185	1.020	1.093	1.009	1.019	1.899	1.870	1.770	1.814
Ti	0.269	0.259	0.336	-	-	-	-	0.021	0.015	0.031	0.031
Al	2.446	2.142	2.168	-	-	-	-	0.136	0.182	0.342	0.283
Fe	1.125	1.635	1.437	0.246	0.284	0.502	0.429	0.225	0.159	0.185	0.201
Mn	0.032	-	-	-	-	-	-	-	-	-	-
Mg	3.145	2.983	3.085	1.707	1.666	1.479	1.525	0.857	0.882	0.773	0.756
Ca	1.866	1.769	1.802	0.006	0.007	0.001	0.006	0.861	0.907	0.914	0.915
K	0.098	-	-	-	-	-	-	-	-	-	-
Na	0.691	0.729	0.753	-	-	-	-	0.023	0.018	0.024	0.024



TABLE 18 (continued)

	12 fel	13 fel	14 sp	15 sp	Locations of analyses in the table.
SiO <sub>2</sub>	45.57	46.29	0.07	0.04	1) Small amphibole phenocryst core
TiO <sub>2</sub>	0.02	0.02	10.44	0.59	2) Rim of large ophitic amphibole phenocryst
Al <sub>2</sub> O <sub>3</sub>	33.91	33.61	5.13	17.36	3) Core of same ophitic amphibole
FeO	0.41	0.41	73.55	22.50	4) Core of separate olivine phenocryst
MnO	-	-	0.72	0.66	5) Rim of same olivine phenocryst
MgO	0.11	0.25	3.86	11.61	6) Olivine within amphibole (3)
CaO	18.51	18.15	0.01	0.01	7) Olivine in glomerophyritic cluster with clinopyroxene (11) and plagioclase feldspar (13)
K <sub>2</sub> O	0.01	0.01	0.04	0.01	8) Clinopyroxene within amphibole (3)
Na <sub>2</sub> O	1.07	1.45	0.02	0.06	9) Pale green core of separate clinopyroxene phenocryst
Total	99.61	100.19	94.23Cr <sub>2</sub> O <sub>3</sub>	48.67	
Atomic proportions on the basis of Total 101.51 8 oxygens					
Si	2.113	2.133			10) Dark green mantle of same clinopyroxene
Ti	0.001	0.001			12) Plagioclase feldspar within amphibole (3)
Al	1.854	1.826			14) Magnetite within amphibole (3)
Fe	0.016	0.016			15) Chrome spinel within amphibole (3)
Mg	0.008	0.017			
Ca	0.920	0.896			
K	0.001	0.001			
Na	0.096	0.130			

TABLE 18 (continued)

End-member compositions

	4	5	6	7	8	9	10	11	12	13
Ca	-	-	-	-	44.32	46.57	48.84	48.89	Ab	0.096
Mg	87.42	85.46	74.67	78.05	44.11	45.27	41.28	40.37	An	90.47
Fe	12.58	14.54	25.33	21.95	11.57	8.5	9.88	10.75	Or	0.06

100 Mg/Mg+Fe ratios

1	2	3	4	5	6	7	8	9	10	11
73.7	64.6	68.2	87.4	85.4	74.7	78.1	79.2	84.7	80.7	79.0



Plate 38 is a photomicrograph of a basalt fragment dredged from the submarine volcano Kick-em-Jenny (see Chapter 6). The rock is composed of fresh euhedral olivine, clinopyroxene, plagioclase feldspar, chrome spinel, titaniferous magnetite and pargasite. The groundmass is composed of brown glass together with microlites of all the phenocryst minerals apart from amphibole and obvious chrome spinel. The bulk composition of this basalt, trace element abundances and estimated mode are given in Table 17. Selected analyses of the constituent minerals are given in Table 18. The Kick-em-Jenny alkali basalt examined here may be classed as comparatively depleted in incompatible trace elements in the Grenada suite of picritic and basaltic compositions.

The important feature of this basalt is the presence of pargasite poikilitically enclosing olivine, clinopyroxene, plagioclase feldspar and spinel. The composition of these enclosed minerals is similar to the phenocrysts not enclosed by amphibole (see Table 18). It is apparent from the petrographic evidence that amphibole was the last major phase to crystallise in this composition. However, the rims of the ophitic amphiboles in contact with the groundmass of the basalt are apparently breaking down to form a dusty oxide margin. It seems that the physical and chemical conditions within the magma changed to a point where the previously crystallised amphibole was no longer stable.

The large ophitic pargasite in Plate 38 is zoned in Fe, Mg, Ti, Na and Si. In general there is an increase in Si, Fe/Mg ratio

and decrease in Ti and Na from core to rim (see Table 18 ). Some of the microphenocryst clinopyroxenes exhibit pale green cores surrounded by a darker green mantle. Analyses of the two zones show a higher content of Ti and Al in the darker green mantle relative to the core (Columns 9,10, Table 18 ). In addition some of the larger clinopyroxene phenocrysts display sector and oscillatory zoning surrounding a pale green core. The olivines are zoned from  $\text{Fo}_{90}$  to  $\text{Fo}_{72}$  and plagioclase feldspar zoned from  $\text{An}_{90}$  to  $\text{An}_{85}$ .

The marginal amphibole breakdown in the Kick-em-Jenny basalt is also seen in amphibole phenocrysts in other basalt compositions, andesites and dacites. A common occurrence is a euhedral intergrowth of plagioclase feldspar, clinopyroxene and magnetite within the relict outline of an amphibole crystal. Similar breakdown of amphibole has been observed in calc-alkaline suites of other islands in the Lesser Antilles (eg. Rea, 1970), and appears to be a ubiquitous feature of many of the amphibole phenocrysts. Various stages of breakdown may be observed from thin marginal opacitised rims, as in the Kick-em-Jenny basalt, to complete alteration. The breakdown appears to be similar to the dehydration reaction, suggested as a possible cause of instability of amphibole in calc-alkaline melts by Eggler (1972).

An analysis of a pargasite phenocryst within a transitional basalt of the Grenada suite was compared by Cawthorn et al. (1973) with the amphiboles produced in experiments conducted at 5 kb ( $P_{\text{H}_2\text{O}} = P_{\text{tot}}$ ) on natural Grenada compositions. The composition of the naturally occurring pargasite of transitional basalt 40



TABLE 19

Partial analyses of naturally occurring pargasite in Grenada transitional basalt 40, and amphiboles produced in experiments with natural Grenada compositions ( $P_{H_2O} = P_{tot} = 5 \text{ kb}$ ).

	40=natural pargasite		1 and 2 in basalt 286 3 in basalt 342		
	40	40	1	2	3
SiO <sub>2</sub>	42.13	40.97	43.3	43.7	43.7
Al <sub>2</sub> O <sub>3</sub>	13.74	14.21	13.4	13.5	15.9
TiO <sub>2</sub>	1.76	1.98	1.2	1.1	0.9
FeO	9.24	9.62	8.7	9.1	10.3
MgO	16.42	15.73	12.5	12.2	9.8
CaO	11.20	11.45	13.5	13.7	12.2
Na <sub>2</sub> O	2.59	2.65	2.3	2.1	2.2
K <sub>2</sub> O	0.35	0.45	0.7	0.6	0.9
Total					

Structural formulae on the basis of 23 oxygens  
( $Fe^{3+} = 0.0$ )

Si	6.119	6.005	6.42	6.45	6.45
Al(IV)	1.881	1.995	1.58	1.55	1.55
Al(VI)	0.472	0.461	0.76	0.80	1.22
Ti	0.192	0.218	0.13	0.12	0.10
Fe	1.122	1.179	1.08	1.12	1.27
Mg	3.554	3.436	2.76	2.68	2.16
Ca	1.743	1.798	2.14	2.17	1.93
Na	0.730	0.753	0.66	0.60	0.63
K	0.065	0.084	0.13	0.11	0.17

100 Mg/Mg + Fe ratios

76.2	74.5	71.9	70.5	50.0
------	------	------	------	------

TABLE 20

Analyses of coexisting ferromagnesian minerals in Grenada transitional basalt 40 together with whole rock analysis.

	amph	cpx	cpx	ol	ol		40
SiO <sub>2</sub>	42.17	49.83	50.69	41.77	41.06	SiO <sub>2</sub>	51.88
TiO <sub>2</sub>	2.17	0.73	0.34	0.03	0.07	TiO <sub>2</sub>	0.79
Al <sub>2</sub> O <sub>3</sub>	13.71	5.07	4.98	0.03	0.06	Al <sub>2</sub> O <sub>3</sub>	16.39
FeO <sup>+</sup>	9.19	4.82	4.53	17.13	9.08	Fe <sub>2</sub> O <sub>3</sub>	8.65
MnO	0.14	0.14	0.19	0.24	0.23	MnO	0.20
MgO	16.19	14.99	15.24	41.33	48.43	MgO	9.23
CaO	11.53	22.83	22.61	0.37	0.39	CaO	9.45
K <sub>2</sub> O	0.40	0.06	0.07	n.d.	n.d.	K <sub>2</sub> O	0.76
Na <sub>2</sub> O	2.81	0.34	0.29	0.03	0.03	Na <sub>2</sub> O	2.53
Cr <sub>2</sub> O <sub>3</sub>	0.19	0.79	0.08	n.d.	n.d.	S	0.00
Total	98.50	99.60	99.09	100.93	99.35	P <sub>2</sub> O <sub>5</sub>	0.11

Atomic proportions on the basis of 4 (olivine)  
6 (pyroxene) and 23 (amphibole) oxygens

						Ba	206
						Nb	11
Si	6.086	1.845	1.876	1.043	1.009	Zr	99
Ti	0.236	0.020	0.009	6.001	0.001	Y	17
Al	2.333	0.221	0.217	0.001	0.001	Sr	401
Fe	1.109	0.149	0.140	0.358	0.187	Rb	43
Mn	0.017	0.004	0.006	0.005	0.005	Zn	72
Mg	3.482	0.827	0.841	1.537	1.773	Cu	47
Ca	1.783	0.906	0.897	0.010	0.010	Ni	304
K	0.074	0.003	0.003	-	-		
Na	0.787	0.024	0.026	0.001	0.001		
Cr	0.022	0.023	0.002	-	-		

100 Mg/Mg + Fe ratios of ferromagnesian minerals

75.9      84.7      85.7      81.1      90.4

Note the concentration of Na<sub>2</sub>O in the amphibole phenocryst relative to the host basalt.<sup>2</sup>



is given in Table 19 together with selected analyses of the experimentally produced amphiboles. The natural pargasite contains higher Ti, Na and Mg relative to the experimental compositions. The chemical differences in amphibole compositions are discussed later but the significant petrographic evidence of the natural pargasite of basalt 40 is the relationship with olivine and plagioclase feldspar in the rock. The amphibole poikilitically encloses these two mineral phases indicating late crystallisation. Selected analyses of coexisting amphibole, clinopyroxene and olivine in basalt 40, together with the major and trace element composition of the basalt are given in Table 20 .

In summary, the petrographic relationships of the amphibole phenocrysts within the basalts suggest crystallisation of amphibole after spinel, olivine, clinopyroxene and plagioclase feldspar. A similar sequence of crystallisation is inferred in the cumulus plutonic blocks (see p.204 ). The observed sequence of crystallisation and subsequent breakdown of amphibole is discussed further in Chapter 10 in relation to the petrogenesis of the Grenada calc-alkaline suite. It is important however, to emphasise that the dominant modal mineralogy of the picrites and basalts is olivine, clinopyroxene, spinel and plagioclase feldspar. Thus the variation in chemical composition of the basalts belonging to individual volcanic centres is likely to be related to fractional crystallisation of these anhydrous mineral phases.

### 9:3 The Andesites and Dacites

The andesites and dacites of Grenada are comparable in

Plate 39

Photomicrograph of twin-textured dacite 462.  
(Plane polarized light magnification x4).





TABLE 21

Major and trace element analysis of dacite 462 together with selected partial analyses of constituent minerals of separate zones. The bulk analysis is of the porphyritic zone only.

<u>Sample No.</u>	<u>462</u>
SiO <sub>2</sub>	62.38
Al <sub>2</sub> O <sub>3</sub>	15.59
Fe <sub>2</sub> O <sub>3</sub>	5.18
MgO	1.91
CaO	8.65
Na <sub>2</sub> O	3.50
K <sub>2</sub> O	1.74
TiO <sub>2</sub>	0.55
MnO	0.30
S	0.00
P <sub>2</sub> O <sub>5</sub>	0.20
Ba	719
Nb	16
Zr	185
Y	11
Sr	838
Rb	97
Zn	772
Cu	6
Ni	14



TABLE 21 (continued)

	amph=amphibole		fel=feldspar			
	(1)	(2)	(3)	(4)	(5)	(6)
	amph	amph	fel	fel	fel	fel
SiO <sub>2</sub>	46.18	41.12	52.55	57.88	52.46	56.01
TiO <sub>2</sub>	1.08	1.76	0.02	0.02	0.02	0.02
Al <sub>2</sub> O <sub>3</sub>	10.98	14.39	29.71	26.90	29.51	27.92
FeO	13.01	9.33	0.26	0.21	1.20	0.41
MnO	0.02	0.02	0.02	0.02	0.02	0.02
MgO	14.18	15.00	0.10	0.03	0.60	0.05
CaO	10.51	12.28	11.53	8.20	12.09	10.20
K <sub>2</sub> O	-	-	0.02	0.03	0.01	0.02
Na <sub>2</sub> O	1.18	2.24	4.72	6.31	3.10	4.28
Total	97.17	96.17	98.93	99.60	99.01	98.93

Atomic proportions on the basis of 8 (feldspar)  
and 23 (amphibole) oxygens

Si	6.727	6.066	2.402	2.593	2.398	2.532
Ti	0.118	0.195	0.001	0.001	0.001	0.001
Al	1.886	2.503	1.601	1.421	1.590	1.488
Fe	1.585	1.151	0.010	0.008	0.046	0.016
Mn	0.002	0.002	0.001	0.001	0.001	0.001
Mg	3.078	3.298	0.007	0.002	0.041	0.003
Cu	1.641	1.942	0.565	0.394	0.592	0.494
K	-	-	0.001	0.002	0.001	0.001
Na	0.333	0.641	0.419	0.548	0.275	0.375

Feldspar end-member compositions

Ab	42.51	58.10	31.68	43.11
An	57.37	41.71	68.25	56.76
Or	0.12	0.18	0.07	0.13

amphibole (1) and feldspars (3) and (4) in porphyritic zone; amphibole (2) and feldspars (5) and (6) in even-textured/granular zone.

general petrographic appearance with similar compositions elsewhere in the Lesser Antilles island-arc (cf. Baker, 1963; Rea, 1970; Tomblin, 1964). The dominant phenocryst minerals are plagioclase feldspar, clino- and orthopyroxene, amphibole and magnetite. Apatite is frequently present and quartz phenocrysts are occasionally found in some dacites. Characteristically the andesites and dacites are extremely porphyritic with abundant oscillatory-zoned plagioclase feldspar. Groundmass textures vary from coarsely crystalline to glassy. The typical textures are illustrated in the accompanying plates.

#### 9:3:1 Variations in texture

A common occurrence in many of the silica-saturated compositions of the Grenada calc-alkaline suite is the presence of zones of variable texture within individual rock units. There is often a marked contrast between a zone of finely interlocking plagioclase laths, mostly less than 0.25 mm in length, enclosed by a zone dominated by large (2-3 mm) oscillatory-zoned plagioclase phenocrysts in a glassy groundmass. Additional phenocryst minerals present within both zones may be pyroxene (both Ca-rich and Ca-poor), amphibole, apatite and spinel.

A typical example of contrasted textural zones is shown in Plate 39 . The dacite 462 illustrated shows no apparent reaction margin between the two zones. The bulk major and trace element composition of the dacite and selected analyses of minerals within the two zones are presented in Table 21 . The dacite is composed predominantly of plagioclase feldspar and amphibole

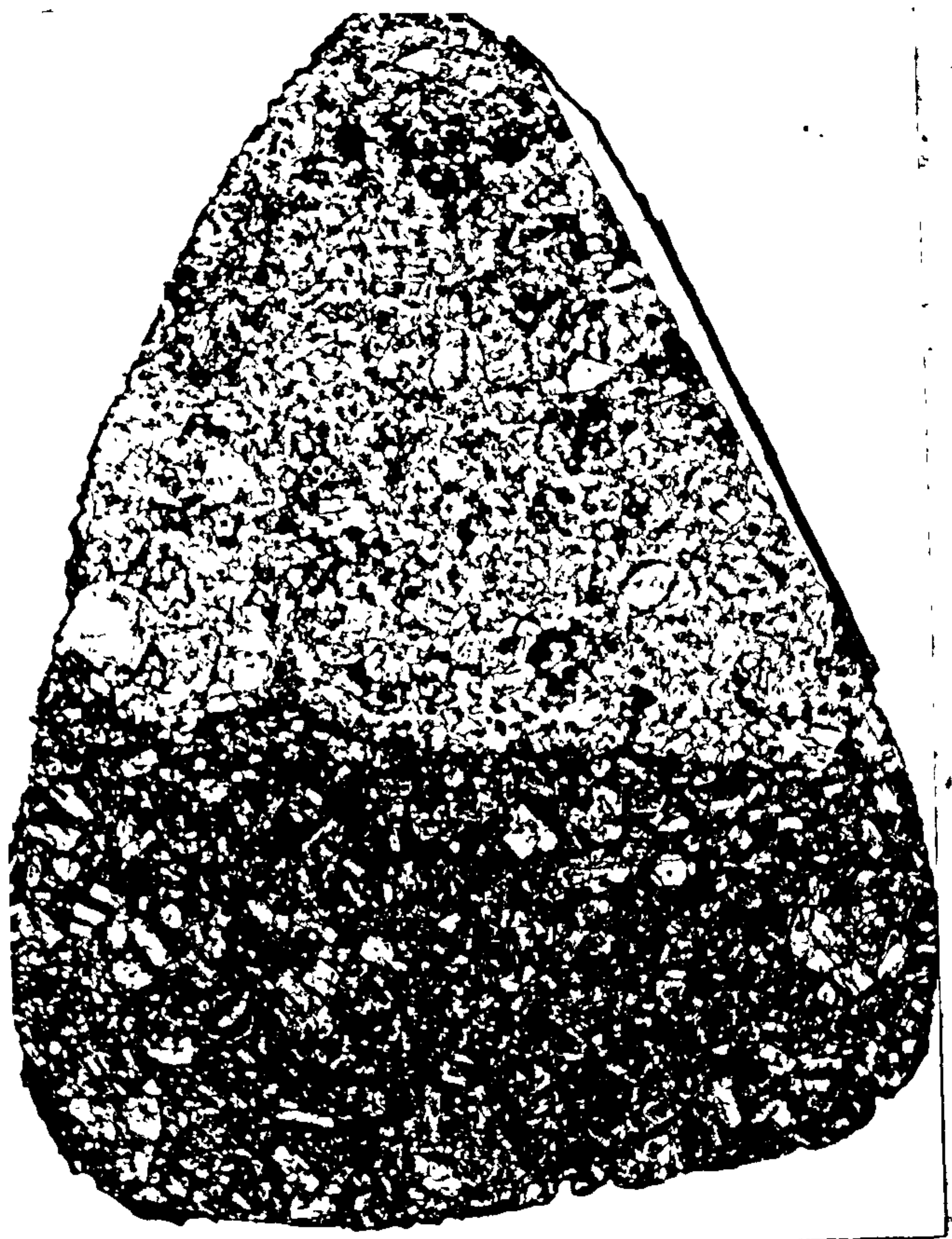


Plate 40

Photomicrograph of andesite 212.

This shows an olivine-anorthite-clinopyroxene-magnetite cumulus fragment enclosed by the andesite.

(Plane polarized light magnification x4).





phenocrysts. The differences in composition between the constituent minerals of different zones is quite striking in regard to the amphiboles. The porphyritic zone is characterised by a tschermakitic amphibole of higher  $\text{SiO}_2$  wt.% (46.2) than the pargasite (41.1 wt.%  $\text{SiO}_2$ ) of the even textured zone. In addition the composition (and the range of zoning) of the plagioclase feldspars is different. In the porphyritic zone, the plagioclases are zoned from  $\text{An}_{57-42}$ , whereas in the even-textured zone the plagioclases are more calcic and the range of zoning more restricted ( $\text{An}_{68-57}$ ). The margin between the zones shows no sign of instability of the constituent minerals. It appears that the more calcic plagioclases of the even textured zone have not equilibrated with the groundmass glass of the porphyritic zone.

The contrasted amphibole compositions and differences in An content of the plagioclase feldspars may indicate a completely accidental relationship between the two zones in a type of host-inclusion relationship. In other words, the even-textured zone may be an accidental xenolith incorporated by the dacite during eruption. Other types of inclusion are also present within the andesites and dacites and are more readily recognisable as xenoliths. Plate 40 shows a plutonic cumulus fragment composed of forsteritic olivine, calcic augite, spinel and plagioclase feldspar enclosed by an andesitic composition (andesite 212). In this instance, where the calcic plagioclase ( $\text{An}_{90}$ ) of the inclusion is in contact with the host andesite, the crystals are ragged showing signs of resorption. Fragments of basaltic

Major and trace element analyses of separated zones of contrasted texture in Grenada andesites and dacites. In the same rock sample: C=porphyritic texture F=microphyric or even-granular texture.

	<u>436C</u>	<u>436F</u>	<u>255C</u>	<u>255F</u>	<u>224C</u>	<u>224F</u>	<u>312C</u>	<u>312F</u>	<u>465C</u>	<u>465F</u>
SiO <sub>2</sub>	61.42	59.02	62.76	57.22	57.98	56.56	58.47	63.56	62.25	52.36
Al <sub>2</sub> O <sub>3</sub>	15.60	17.10	16.96	17.39	17.91	17.51	17.60	16.60	15.22	11.64
Fe <sub>2</sub> O <sub>3</sub>	6.71	7.31	5.26	7.87	6.34	7.03	6.25	4.62	5.21	9.15
MgO	3.57	2.83	2.35	4.00	3.11	3.99	3.19	2.27	2.83	6.69
CaO	6.49	7.04	6.39	7.95	8.67	9.18	7.96	6.20	8.46	15.93
Na <sub>2</sub> O	3.70	4.19	3.85	3.10	3.84	3.41	4.13	4.27	3.47	1.65
K <sub>2</sub> O	1.54	1.56	1.59	1.30	1.19	1.24	1.40	1.67	1.65	1.22
TiO <sub>2</sub>	0.59	0.57	0.55	0.80	0.61	0.74	0.65	0.48	0.53	0.80
MnO	0.17	0.17	0.09	0.16	0.12	0.12	0.15	0.12	0.15	0.31
S	0.00	0.00	0.00	0.00	0.00	0.00	0.00	0.00	0.00	0.00
P <sub>2</sub> O <sub>5</sub>	0.19	0.32	0.23	0.25	0.24	0.19	0.27	0.23	0.26	0.27
Ba	533	492	584	470	487	419	504	581	676	384
Nb	8	8	11	7	7	7	12	13	15	7
Zr	196	197	189	155	177	191	174	203	194	114
Y	22	34	12	14	16	19	14	12	14	15
Sr	560	697	838	816	1107	978	732	739	701	565
Rb	45	53	55	42	35	54	76	98	92	55
Zn	60	70	28	42	30	50	69	48	38	77
Cu	62	64	18	31	58	80	66	56	7	15
Ni	45	21	22	39	39	44	30	23	45	165
Ce	52	59	44	45	57	51	51	60	71	35

TABLE 22



composition have also been observed in andesite hosts but in these examples it is comparatively easy to determine the xenolithic or accidental nature of the inclusions. It seems probable that during the eruption of lavas and pyroclasts, fragments of previously consolidated wall-rock are likely to be incorporated. In the case of similar chemical compositions in host and inclusion however, it is more difficult to ascertain the precise nature of the relationship. The absence of reaction between the feldspar and groundmass of dacite 462 may be explained by the short period of time available for equilibration in the near-surface eruptive environment between plagioclase compositions differing only by 15 mol.% An. There is an alternative possibility that the variable textures in some andesites and dacites have a cognate rather than xenolithic relationship. In order to examine more closely the contrast in chemical composition between zones, separated portions of andesites and dacites were analysed. The major and trace element compositions of the separated zones of individual andesites and dacites are presented in Table 22.

In the preceeding chapters, evidence for the repeated eruptions of magmas of contrasted chemical composition has been presented. In some cases, eruptions within a restricted locality were characterised by widely different trace element abundances. If the inclusions in the andesites and dacites are completely accidental, in origin, one would expect to find major differences in degree of incompatible trace element enrichment between host and inclusion. The analyses presented in Table 22 do not show in general a marked divergence in trace element abundance. In

Plate 41

Photomicrograph of twin-textured andesite 218.  
Plagioclase feldspar phenocrysts are the dominant  
modal minerals.  
(Plane polarised light magnification x4).





TABLE 23

Major and trace element analysis of andesite 218 (porphyritic zone only) together with selected partial analyses of constituent minerals of separate zones in the andesite.

<u>Sample No.</u>	<u>218</u>
SiO <sub>2</sub>	58.95
Al <sub>2</sub> O <sub>3</sub>	17.25
Fe <sub>2</sub> O <sub>3</sub>	6.44
MgO	3.83
CaO	7.79
Na <sub>2</sub> O	3.26
K <sub>2</sub> O	1.48
TiO <sub>2</sub>	0.65
MnO	0.10
P <sub>2</sub> O <sub>5</sub>	0.24
Ba	517
Nb	6
Zr	180
Y	16
Sr	1000
Rb	44
Zn	72
Cu	28
Ni	23



TABLE 23 (continued)

	opx=orthopyroxene		cpx=clinopyroxene		fel=feldspar			
	x=porphyritic zone		+=even textured/granular zone					
	opx <sup>x</sup>	opx <sup>+</sup>	cpx <sup>x</sup>	cpx <sup>+</sup>	fel <sup>x</sup>	fel <sup>+</sup>	fel <sup>x</sup>	fel <sup>+</sup>
SiO <sub>2</sub>	52.21	51.36	52.54	52.29	54.50	54.16	54.54	65.61
TiO <sub>2</sub>	0.18	0.23	0.33	0.28	0.02	0.02	0.02	0.02
Al <sub>2</sub> O <sub>3</sub>	1.06	0.87	1.35	1.28	29.64	29.96	29.15	27.12
FeO	27.15	26.69	10.95	12.44	0.30	0.38	0.41	0.37
MgO	17.84	18.31	12.99	12.22	0.02	0.02	0.02	0.02
CaO	1.01	1.12	21.95	20.44	10.76	10.41	10.11	10.28
K <sub>2</sub> O	0.06	0.28	0.03	0.06	0.02	0.02	0.02	0.02
Na <sub>2</sub> O	0.07	0.26	0.29	0.32	4.68	4.37	4.97	4.79
Total	99.58	99.12	100.43	99.33	99.94	99.34	99.24	

Atomic proportions on the basis of 6 (pyroxene)  
and 8 (feldspar) oxygens

Si	1.994	1.977	1.966	1.984	2.452	2.446	2.469	2.555
Ti	0.005	0.007	0.009	0.008	0.001	0.001	0.001	0.001
Al	0.048	0.039	0.060	0.057	1.572	1.596	1.556	1.443
Fe	0.867	0.859	0.343	0.395	0.011	0.014	0.016	0.014
Mg	1.015	1.050	0.724	0.641	0.001	0.001	0.001	0.001
Ca	0.041	0.046	0.880	0.831	0.519	0.504	0.490	0.497
K	0.003	0.014	0.001	0.003	0.001	0.001	0.001	0.001
Na	0.005	0.019	0.021	0.024	0.408	0.383	0.436	0.419

## End-member compositions

Ca	2.15	2.36	45.20	43.36	Ab <sup>44.00</sup>	43.12	47.03	45.70
Mg	52.78	53.70	37.20	36.05	An <sup>55.88</sup>	56.75	52.85	54.18
Fe	45.08	43.93	17.60	20.60	Or <sup>0.12</sup>	0.13	0.12	0.13

## Pyroxene 100 Mg/Mg+Fe ratios

53.9    55.0    67.9    63.6

many cases, individual compositions are classified as belonging to particular volcanic series of a single centre (see Chapter 8). It is possible that the majority of inclusions likely to be incorporated into a magma are those already crystallised on the walls of the eruptive channelways. Geochemical affinity would then be predicted due to a co-magmatic origin. Thus, there may be a gradation in the nature of host-inclusion relationships from completely accidental to cognate.

The dacite 462 contains zones composed of contrasted mineral compositions. In some examples however, there is a close similarity in the constituent minerals. A twin-textured andesite (218) is illustrated in Plate 41. The bulk composition of this andesite and analyses of constituent minerals in the separate zones are given in Table 23. The mineralogy of both zones consists of plagioclase feldspar, ortho- and clinopyroxene, magnetite and pargasite. There is a greater modal abundance of plagioclase feldspar in one zone though the size of the crystals (1-2 mm) is similar in both zones. The plagioclase feldspar forms an even, granular texture in one portion of the rock compared with a porphyritic texture in the other, with microlites of pyroxene and feldspar in groundmass glass. The composition of the feldspars and pyroxenes in the different zones are very similar (see Table 23). The range of zoning of the plagioclases is  $An_{56-53}$  in both textures and the  $Mg/Mg+Fe$  ratios of the pyroxenes do not suggest crystallisation from contrasted magma compositions. In this instance it appears that the even textured zone of andesite 218 is of a type of glomeroporphyritic origin since the phenocrysts



Plate 42

Photomicrographs of andesites 337 and 410. Prominent phenocrysts of oscillatory-zoned plagioclase feldspar, clino- and orthopyroxene and occasional pargasite phenocrysts. (Crossed polars magnification x5).



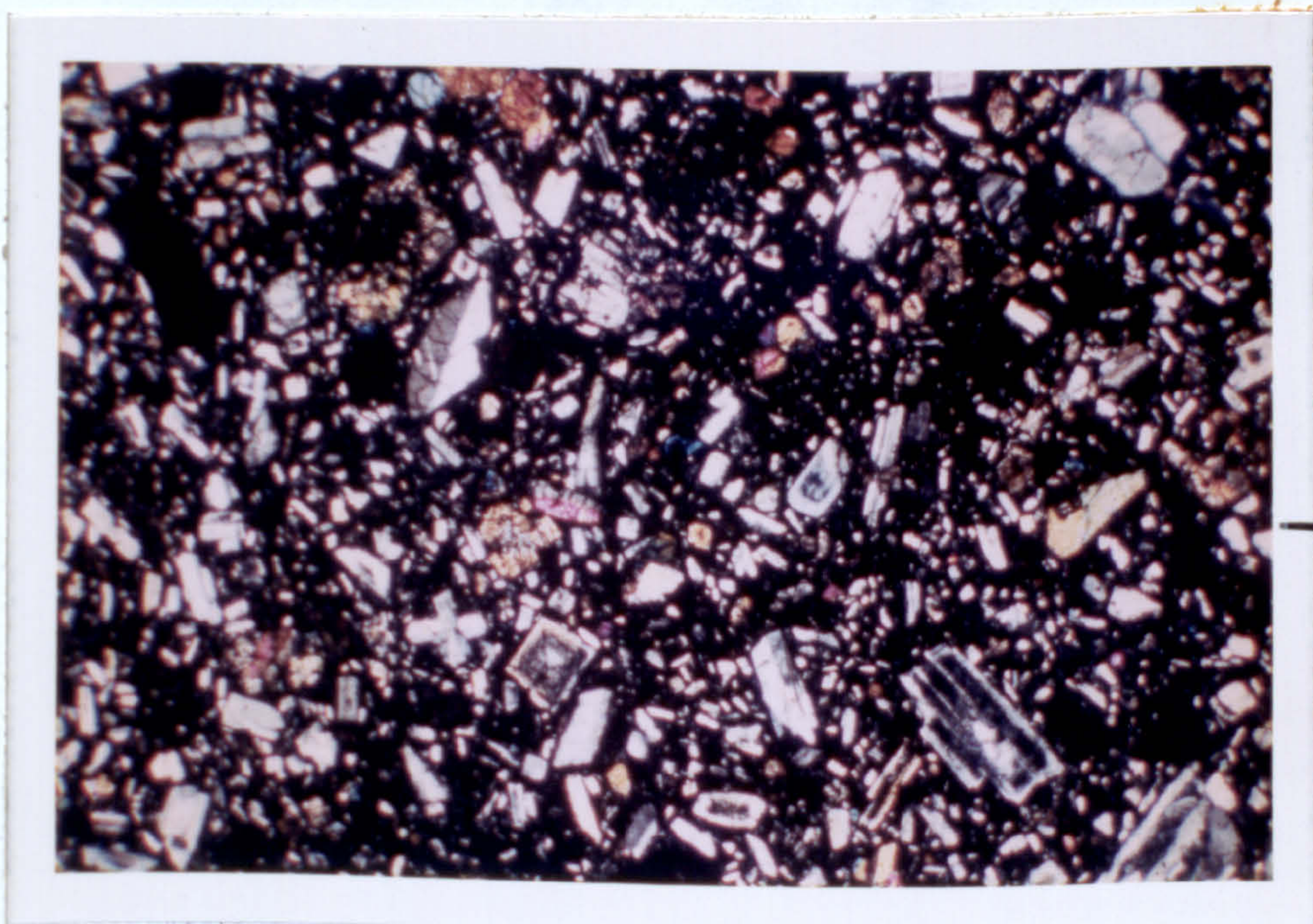
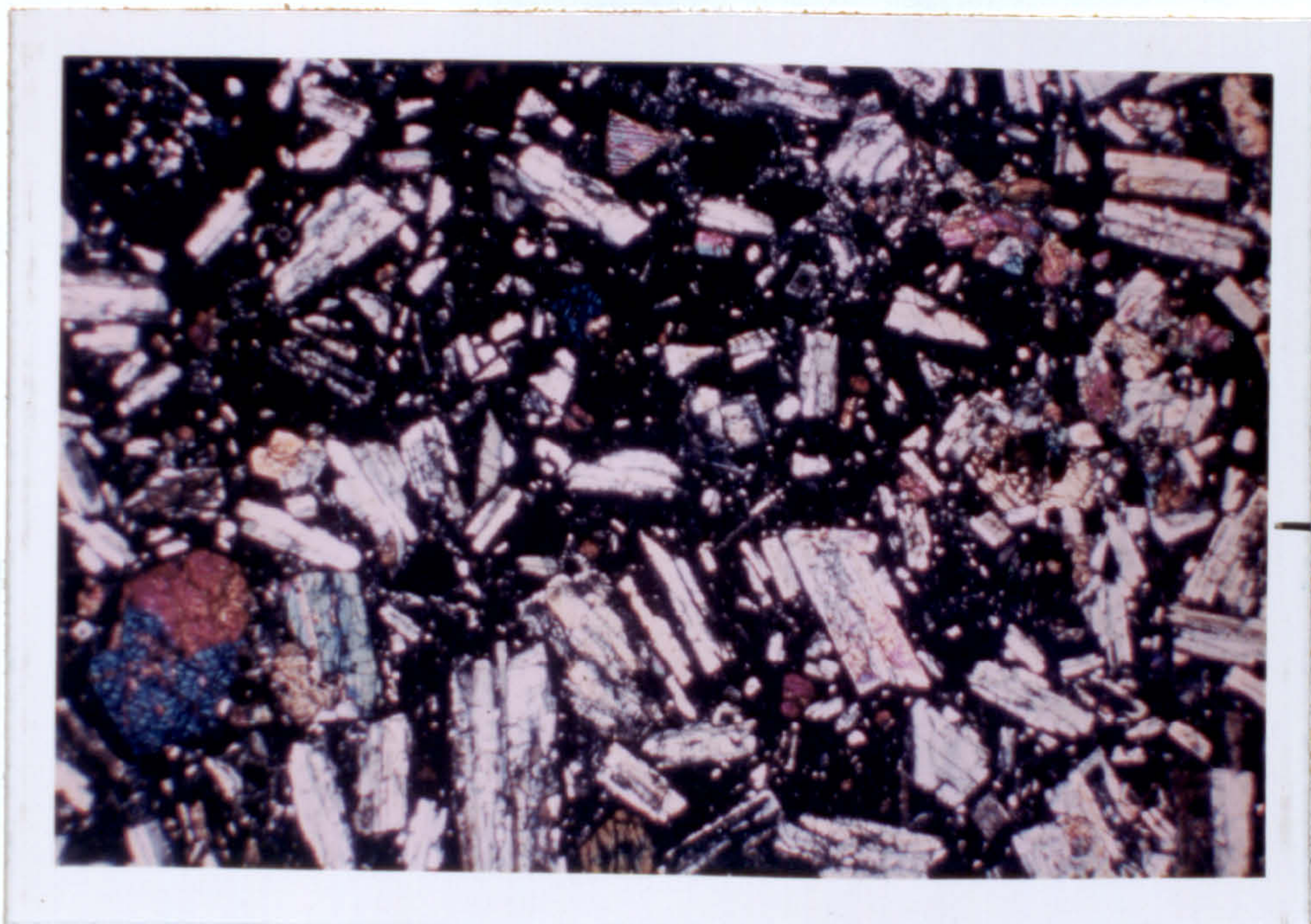




TABLE 24

Major and trace element analyses of andesites 337 and 410 together with estimated modal mineralogy.

Sample No.	<u>337</u>	<u>410</u>
SiO <sub>2</sub>	55.73	57.52
Al <sub>2</sub> O <sub>3</sub>	17.54	17.03
Fe <sub>2</sub> O <sub>3</sub>	7.52	6.81
MgO	3.29	3.83
CaO	9.68	8.36
Na <sub>2</sub> O	3.25	3.82
K <sub>2</sub> O	1.81	1.44
TiO <sub>2</sub>	0.78	0.82
MnO	0.19	0.19
S	0.00	0.00
P <sub>2</sub> O <sub>5</sub>	0.21	0.17
Ba	591	529
Nb	13	16
Zr	164	178
Y	17	15
Sr	1188	538
Rb	33	50
Zn	40	65
Cu	198	126
Ni	26	36
Ce	52	37

Estimated mode %

Orthopyroxene	2	2
Clinopyroxene	10	5
Plagioclase	40	30
Amphibole	3	2
Magnetite	2	1
Groundmass	40	60

In both andesites groundmass dominantly dark-grey glass with abundant plagioclase microlites, minor pyroxene and numerous oxide granules.

appear to be in equilibrium with the host composition.

In summary, the origin of the variable textures in the andesites and dacites may be due to a variety of causes involving both cognate and accidental relationships. In regard to geochemical sampling procedures, it is obvious that chemical heterogeneity is present on a local scale within samples. Care must therefore be exercised in the interpretation of the analyses of these variable-textured rocks of contrasted chemical composition.

#### 9:3:2 Mineralogical Distinction between Volcanic Series

In Chapter 8 a distinction between volcanic series associated with contrasted degrees of trace element abundance was proposed. In addition, the tendency for convergence of major and trace element compositions in the silica-saturated andesites and dacites of the different series was indicated. Andesite samples from the 'high-Sr' series of Mt. St. Catherine and 'low-Sr' series of Mt. Granby - Fedon's Camp centre were selected for analysis of the constituent minerals by electron microprobe. In Plate #2 the appearance of the andesites in thin section is shown. Major and trace element compositions and estimated modes are presented in Table 24. The enrichment of the incompatible trace elements such as Ce and Rb in andesite 337 (high-Sr series) compared with 410 (low-Sr) can be seen. Both andesites are porphyritic in texture with dominant plagioclase feldspar ( $An_{70-35}$ ) phenocrysts up to 2 mm in length. The other phenocryst minerals present are pargasite, clino- and orthopyroxene and magnetite in a glassy



TABLE 25

Analyses of phenocryst ferromagnesian minerals in andesites  
337 and 410

opx=orthopyroxene

cpx=clinopyroxene

amph=amphibole.

	337=*				410=+			
	opx*	opx*	cpx*	amph*	amph*	opx <sup>+</sup>	cpx <sup>+</sup>	amph <sup>+</sup>
SiO <sub>2</sub>	54.13	54.19	50.65	40.59	40.18	53.31	51.27	42.96
TiO <sub>2</sub>	0.31	0.22	0.69	2.56	2.30	0.24	0.67	1.98
Al <sub>2</sub> O <sub>3</sub>	1.46	1.36	3.40	14.50	13.85	1.20	3.19	11.88
FeO*	15.42	15.49	8.03	10.45	10.47	16.82	8.46	11.52
MgO	25.78	26.27	15.64	13.78	14.53	26.44	15.27	14.81
CaO	1.95	1.52	21.03	12.13	11.88	1.46	21.25	11.70
Na <sub>2</sub> O	0.07	0.02	0.44	2.57	2.35	0.04	0.34	2.43
K <sub>2</sub> O	0.04	0.04	0.03	0.93	0.87	0.03	0.24	0.37
Total	99.16	99.11	99.91	97.51	96.43	99.54	100.69	97.65

Atomic proportions on the basis of 6 oxygens (pyroxenes) and 23  
oxygens (amphiboles)

Si	1.970	1.971	1.883	5.982	5.989	1.947	1.895	6.303
Ti	0.008	0.006	0.019	0.284	0.258	0.007	0.019	0.218
Al	0.063	0.058	0.149	2.520	2.434	0.052	0.139	2.055
Fe	0.469	0.471	0.250	1.288	1.305	0.514	0.262	1.414
Mg	1.398	1.424	0.867	3.027	3.228	1.439	0.841	3.238
Ca	0.076	0.059	0.838	1.916	1.818	0.057	0.842	1.839
Na	0.005	0.001	0.032	0.735	0.679	0.003	0.024	0.692
K	0.002	0.002	0.001	0.175	0.165	0.001	0.011	0.069

100Mg/Mg+Fe ratio

74.9	75.1	77.6	70.2	71.2	73.7	76.3	69.4
------	------	------	------	------	------	------	------

Pyroxene end-member compositions

Ca	3.91	3.03	42.88	2.84	42.29
Mg	71.94	72.86	44.35	71.60	43.26
Fe	24.15	24.11	12.78	25.56	13.45

Plate 43

Photomicrograph of andesite 307. Phenocrysts of oscillatory zoned plagioclase together with glomeroporphyrific clusters of orth- and clinopyroxene and minor pargasite phenocrysts. A few olivines have altered margins (Plate polarized light magnification x5).





TABLE 26

Major and trace element analysis of andesite 307 with estimated modal mineralogy.

Sample No.	<u>307</u>
SiO <sub>2</sub>	59.42
Al <sub>2</sub> O <sub>3</sub>	17.11
Fe <sub>2</sub> O <sub>3</sub>	6.70
MgO	2.97
CaO	7.29
Na <sub>2</sub> O	3.72
K <sub>2</sub> O	1.70
TiO <sub>2</sub>	6.69
MnO	0.20
S	0.00
P <sub>2</sub> O <sub>5</sub>	0.19
Ba	580
Nb	14
Zr	193
Y	23
Sr	560
Rb	52
Zn	65
Cu	41
Ni	52
Ce	50

Estimated mode %

Olivine	3
Orthopyroxene	3
Clinopyroxene	5
Plagioclase	30
Amphibole	2
Magnetite	2
Apatite	1

Groundmass (55%) predominant microlites of plagioclase, pyroxene and oxide granules in grey glass.



groundmass containing microlites of the same minerals except for amphibole. Analyses of the ferromagnesian minerals are presented in Table 25. There is a slight difference in the composition of amphiboles in the two andesites but the composition of the pyroxenes and optically estimated plagioclase compositions are very similar. The amphibole in andesite 337 is richer in Ti, Al and Na than the amphibole in andesite 410, but the oscillatory zoning of these elements in individual amphibole crystals (see p. 238) is as great as the differences observed here. In general, therefore, no distinction between the volcanic series on the basis of mineralogical composition seems possible.

In some andesites of the low-Sr series of volcanic centres however, olivine phenocrysts are present as well as amphibole and Ca-rich and Ca-poor pyroxenes. The generally higher modal abundance of phenocryst olivine in basalts comparatively depleted in the incompatible trace elements has been described previously. The andesites containing phenocryst olivine appear to be geochemically and petrographically related to these basalts. In Plate 43 the appearance of andesite 307 of the low-Sr series of the Mt. Granby - Fedon's Camp centre is shown. Major and trace element composition and estimated mode of this andesite are given in Table 26. Analyses of constituent minerals are presented in Table 27. The olivines in this andesite are marginally altered and appear unstable.

The absence of olivine as a phenocryst mineral in many andesitic compositions, the corroded and altered margins of the phenocrysts where present and the absence of this phase from the

TABLE 27

Partial analyses of phenocryst ferromagnesian minerals in andesite 307.

ol = olivine opx = orthopyroxene cpx = clinopyroxene amph = amphibole.

	ol	opx	cpx	amph
SiO <sub>2</sub>	34.61	53.77	47.34	39.47
TiO <sub>2</sub>	0.04	0.22	1.08	1.95
Al <sub>2</sub> O <sub>3</sub>	0.10	1.23	6.65	14.30
FeO*	12.02	16.05	5.71	12.60
MnO	0.20	1.01	0.13	0.09
MgO	47.96	27.19	15.15	13.67
CaO	0.01	1.48	22.59	12.25
K <sub>2</sub> O	n.d.	0.02	0.08	0.58
Na <sub>2</sub> O	0.01	0.02	0.55	2.62
Cr <sub>2</sub> O <sub>3</sub>	n.d.	0.09	0.58	0.09
Total	99.95	101.08	99.86	97.62

Atomic proportions on the basis of 4 (olivine), 6 (pyroxene) and 23 (amphibole) oxygens.

Si	0.983	1.936	1.764	5.883
Ti	0.001	0.006	0.030	0.219
Al	0.003	0.052	0.292	2.513
Fe	0.249	0.483	0.178	1.571
Mn	0.004	0.031	0.004	0.011
Mg	1.773	1.459	0.841	3.036
Ca	0.000	0.057	0.902	1.957
K	0.000	0.001	0.004	0.110
Na	0.000	0.001	0.040	0.757
Cr	0.000	0.003	0.017	0.011

Olivine and pyroxene end-member compositions

Mg<sub>815</sub>Fe<sub>12.5</sub> Ca<sub>2.8</sub>Mg<sub>719</sub>Fe<sub>25.3</sub> Ca<sub>464</sub>Mg<sub>416</sub>Fe<sub>12.0</sub>

100 Mg/Mg + Fe ratios

87.7      75.2      82.6      66



groundmass of the andesites indicate that olivine is no longer stable in the bulk composition of the andesitic melts in the low-pressure eruptive environment. The petrogenetic significance of the differences in modal composition of the basalts and andesites of the Grenada volcanic series is discussed in Chapter 10.

Olivine phenocrysts have been reported in basic andesites in St. Kitts (Baker, 1968) and Montserrat (Rea, 1970) but are rare in compositions as silica-rich as some of the olivine-bearing andesites of Grenada. This feature, combined with the oscillatory and sector-zoned clinopyroxenes and trace element geochemistry, are the only indication that the andesites and dacites of Grenada are unusual in comparison with the calc-alkaline suites of islands further north in the Lesser Antilles island arc.

#### 9:4 The Cumulus Plutonic Blocks of Grenada

Plutonic blocks composed of variable proportions of plagioclase feldspar, amphibole, olivine, clinopyroxene and magnetite are found in several localities in Grenada (see Chapter 6). The appearance of one of these blocks in thin section is shown in Plate 44. Generally an equigranular mosaic texture is evident with interlocking feldspar, clinopyroxene and amphibole crystals. In some blocks, however, large (up to 3 cm or more) ophitic amphiboles are present. The general sequence of crystallisation inferred in these blocks is olivine followed by clinopyroxene and plagioclase together, followed by amphibole. Spinel apparently crystallises throughout,

Plate 44

Photomicrograph of clinopyroxene-plagioclase-magnetite-amphibole cumulus block 521. Slight layering features are present with varying proportions of feldspar and ferromagnesian minerals.  
(Plane polarized light magnification x4).





but apart from post-crystallisation alteration of olivine, all the mineral phases appear to be stable together. A similar feature has been reported in the St. Vincent cumulate blocks by Lewis (1973). Orthopyroxene has only been observed poikilitically enclosing olivine and spinel in a single inclusion within a basalt. Orthopyroxene has not yet been found in any of the plutonic blocks so far examined.

The occasional layering observed in the blocks, together with the relatively unzoned nature and high-temperature paragenesis suggested by the constituent minerals suggests an origin by cumulus processes (Wager and Brown, 1968). Cumulus plutonic blocks have been reported from many of the islands in the Lesser Antilles. Lewis (1964) examined the petrology and mineralogy of the St. Vincent blocks and an inter-island comparison is in progress by K.J.A. Wills (Ph.D. thesis, Durham, in prep'n). In Table 28, estimated modal compositions of some of the Grenada blocks are presented. In comparison with the blocks from other islands the abundance of amphibole and the absence of orthopyroxene are unusual features (K.J.A.Wills, 1973, pers. comm.). Olivines frequently show signs of iddingsitisation varying from marginal alteration to complete replacement. Magnetite is apparently homogeneous without any exsolution features. Frequently there is a lack of any ground-mass and in hand specimen many samples crumble rapidly reflecting the lack of cement. In some examples, a brown glass containing microlites of feldspar, pyroxene and magnetite is present interstitially.



TABLE 28

Major and trace element analyses of Grenada cumulus blocks together with estimated modal mineralogy. X refers to U.W.I. collection. X245 analyst Dr. J.G. Holland. X254,403,407 K.J.A. Wills. n.a. = not analysed.

	X245	X254	X403	X407
SiO <sub>2</sub>	40.80	42.73	43.62	44.87
Al <sub>2</sub> O <sub>3</sub>	10.12	13.22	22.37	9.01
Fe <sub>2</sub> O <sub>3</sub>	11.32	12.16	8.72	10.64
MgO	22.75	13.59	6.25	14.40
CaO	11.71	15.25	17.57	19.02
Na <sub>2</sub> O	1.75	0.98	0.37	0.07
K <sub>2</sub> O	0.34	0.36	0.17	0.26
TiO <sub>2</sub>	0.96	1.43	0.72	1.39
MnO	0.17	0.16	0.09	0.15
S	0.04	n.a.	n.a.	n.a.
P <sub>2</sub> O <sub>5</sub>	0.06	0.13	0.11	0.19
Ba	180	86	63	36
Nb	1	1	1	4
Zr	35	41	41	60
Y	18	20	9	16
Sr	283	408	925	215
Rb	1	1	1	1
Zn	64	54	51	64
Cu	12	2	1	2
Ni	591	204	50	64
Cr	1467	n.a.	n.a.	n.a.
V	244	n.a.	n.a.	n.a.
Estimated mode %				
Olivine	50	5	-	-
Clino- pyroxene	20	20	5	70
Amphibole	25	55	30	20
Magnetite	5	5	2	-
Plagioclase	-	15	65	10

Analyses of individual minerals from an olivine-clinopyroxene-amphibole-magnetite cumulus block are presented in Table 29 . The layered nature of many of the blocks and coarse grain size creates difficulty in assessing the validity of bulk chemical analyses as being representative of genuine subtractive compositions. Nevertheless, the blocks analysed so far are all ultrabasic in bulk composition (Table 28 ) and significantly different from the composition of erupted lavas and pyroclasts of Grenada. In comparison with the phenocrysts in the lavas and pyroclasts only limited zoning is observed in the cumulus minerals. In a few samples however, faint oscillatory zoning has been observed in clinopyroxene and amphibole crystals. The high Mg/Fe+Mg ratios of the ferromagnesian minerals of the cumulus blocks are notable features, but are not as high as some of the phenocrysts of the picrites and basalts. In Fig. 34 the composition of the Grenada and St. Vincent cumulus ferromagnesian minerals are compared and are seen to be similar. Lewis (1973) has suggested that the assemblage is in equilibrium with a subalkaline basalt magma. It is apparent therefore, that although the cumulus assemblages are important evidence for fractional crystallisation processes they do not in themselves represent the earliest phases to have crystallised from the parental basalt magmas of the island of Grenada.

#### 9:5 Mineralogical variation in the Grenada Rock Suite

In the following discussion the variation in mineralogical composition of the Grenada suite of volcanic rocks is examined with particular reference to the zoning features observed. The



TABLE 29

## Partial analyses of cumulus minerals in block X245

	ol	ol	cpx	amph	mag
SiO <sub>2</sub>	40.25	40.47	50.27	42.78	0.05
TiO <sub>2</sub>	-	-	0.48	1.44	8.94
Al <sub>2</sub> O <sub>3</sub>	-	-	4.54	13.00	7.12
FeO	16.40	17.04	5.24	7.63	75.32
MgO	43.54	42.98	15.10	16.24	3.50
CaO	0.09	0.09	23.25	12.33	0.21
K <sub>2</sub> O	-	-	0.02	0.56	-
Na <sub>2</sub> O	-	-	0.27	2.43	0.02
Total	100.28	100.58	99.17	96.41	95.16

Atomic proportions on the basis of 4 (olivine),  
6 (pyroxene) and 23 (amphibole) oxygens

Si	1.011	1.016	1.869	6.257
Ti	-	-	0.013	0.158
Al	-	-	0.199	2.242
Fe	0.345	0.358	0.163	0.933
Mg	1.630	1.607	0.837	3.540
Ca	0.002	0.002	0.926	1.933
K	-	-	0.001	0.105
Na	-	-	0.019	0.689

## End-member compositions

Ca	-	-	48.10
Mg	82.55	81.80	43.44
Fe	17.45	18.20	8.46

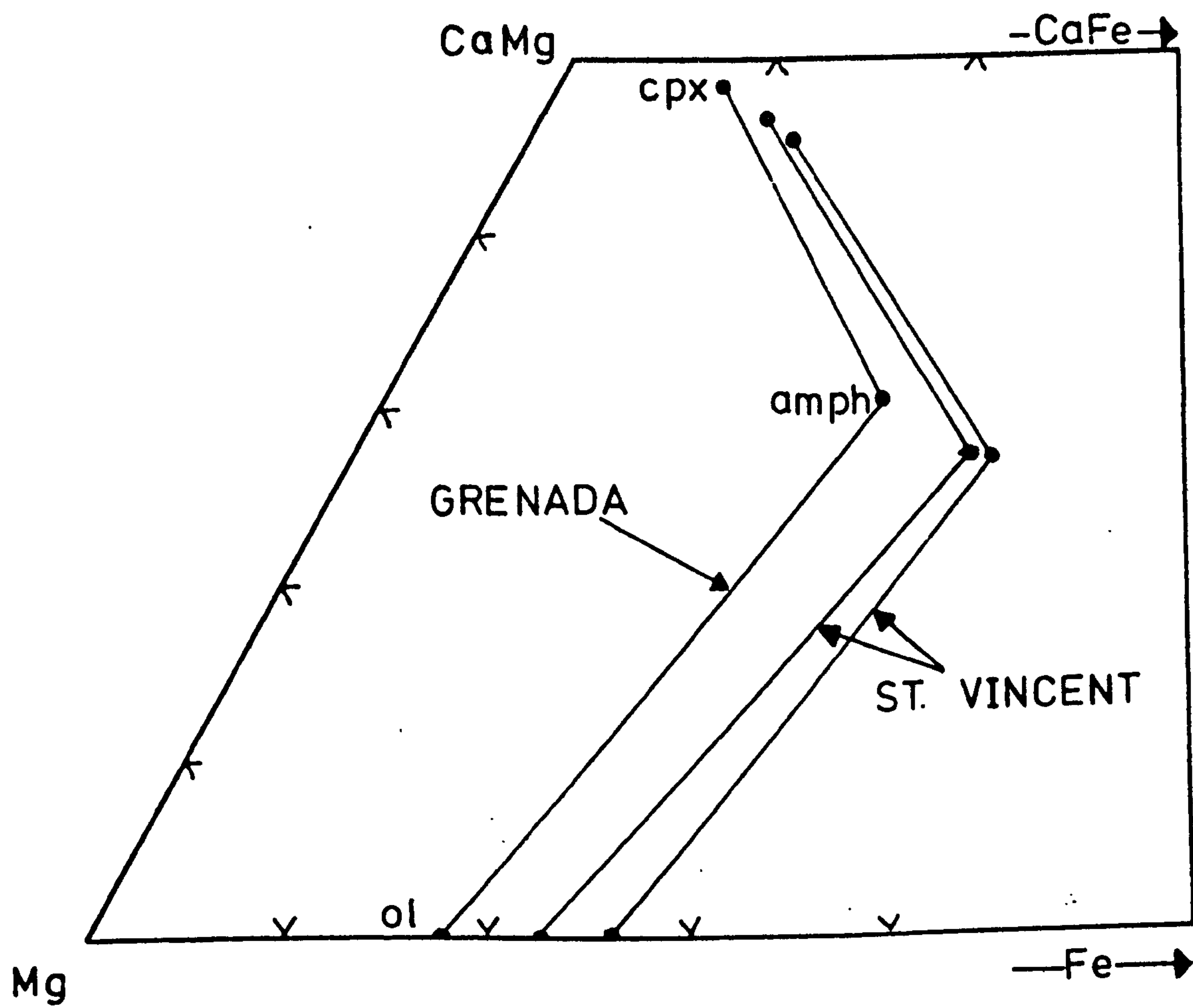
## 100 Mg/Mg+Fe ratios

82.5	81.8	83.7	79.1
------	------	------	------

Fig. 34

Comparison of Grenada and St. Vincent cumulus ferro-magnesian minerals. Grenadan cumulus minerals from block x245 (U.W.I. collection). St. Vincent data from Lewis (1973).





important phenocryst minerals are treated separately. In Fig. 35 the variation in minerals of the Grenada volcanic series is summarised.

#### 9:5:1 Olivine

Olivine varies continuously in composition from  $\text{Fo}_{91}$  in the picrites and basalts to  $\text{Fo}_{70}$  in some of the andesites. Individual phenocrysts from a variety of compositions display a considerable part of this zoning. There is no compositional break and reappearance of more fayalitic olivine as in some fractionated tholeiitic magmas (Wager and Brown, 1968).

In individual phenocrysts there is a tendency for a small increase in CaO with increasing fayalite content (Arculus and Curran, 1972). However, the data for the entire suite shows a considerable variation in CaO content for a given Mg/Mg+Fe ratio in the olivines. Arculus and Curran (1972) also showed a gradual increase in MnO content from 0.2 to 0.7 wt.% with decreasing Mg in the olivine ( $\text{Fo}_{90-80}$ ), and decreasing NiO from 0.24 to 0.21 wt.% ( $\text{Fo}_{90-80}$ ).

The trend of olivine variation in the Grenada suite is similar to previously described calc-alkaline assemblages and unlike typical alkaline and tholeiitic associations.

#### 9:5:2 Pyroxenes

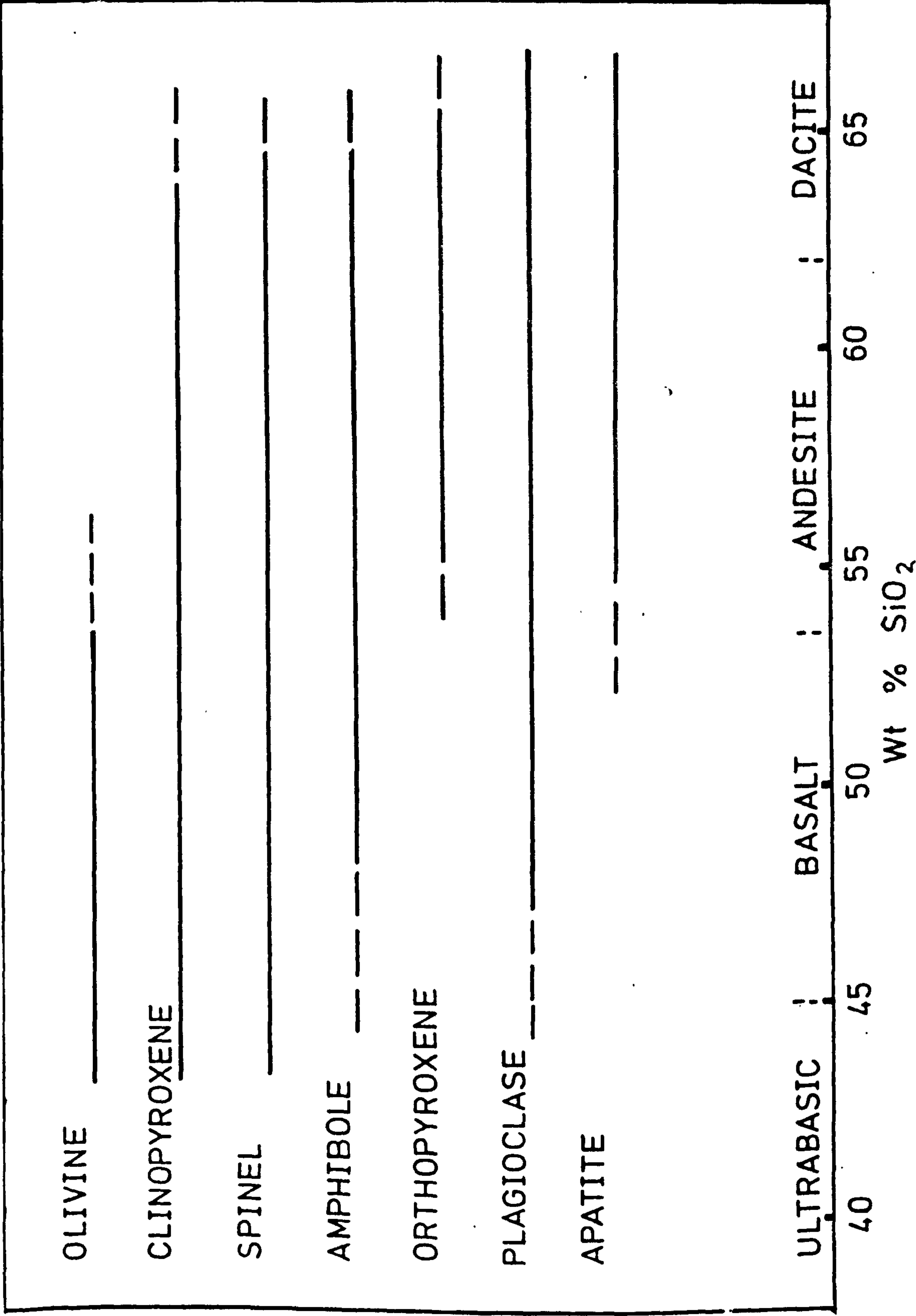
The nature of the pyroxene assemblage in rocks of basaltic composition, and the subsequent changes in composition of the



Fig.35

Mineral variation in the Grenada calc-alkaline rock suite.

Dashed lines indicate occasional appearance of minerals but minerals are only stable at indicated weight %  $\text{SiO}_2$  under certain P, T, and  $P_{\text{H}_2\text{O}}$  conditions outlined in the text.





pyroxenes during the evolution of associated volcanic suites are regarded as important criteria in distinguishing the affinity of the suites. The Skaergaard intrusion is regarded as the type example of equilibrium crystallisation of tholeiitic magma (Wager and Brown, 1968). A Ca-rich and Ca-poor pyroxene crystallise together throughout much of this intrusion. With increasing Fe-enrichment however, crystallisation of Ca-poor pyroxene ceases and only a Ca-rich composition is present. In contrast, alkali basalt magmas are generally characterised by the presence of a single Ca-rich pyroxene in both initial and derivative bulk compositions. In strongly silica-undersaturated alkaline magmas, the trend of pyroxene variation is towards Na and Fe enrichment, and only minor variation is observed when these compositions are projected into the system:



Fig. 36 illustrates the compositional variation described.

Barberi et al. (1971) and Gibb (1973) have reported transitional types of compositional variation intermediate between the tholeiitic and alkaline trends. It is apparent therefore that the pyroxene compositional relationships with changing physico-chemical conditions in differentiating magmas remains of fundamental research interest in igneous petrogenesis.

The Grenada volcanic suite is characterised by the early crystallisation of a single Ca-rich composition, calcic augite, in picritic and basaltic compositions. Superimposed on the variations in Ti and Al already described in some clinopyroxenes,

Fig. 36

Trends of pyroxene crystallisation in the system  
 $\text{CaMgSi}_2\text{O}_6(\text{Di}) - \text{CaFeSi}_2\text{O}_6(\text{Hed}) - \text{MgSiO}_3(\text{En}) -$   
 $\text{FeSiO}_3(\text{Fs})$  showing contrasted evolution within  
tholeiitic and alkali basalt compositions.

I. Differentiated teschenite sill, Gunnedah,  
New South Wales.

II. Garbh Eilean Sill, Shiant Isles.

III. British and Icelandic Tertiary acid glasses.

IV. Skaergaard intrusion.

Line A-B crystallisation trend of primary  
orthopyroxenes

Line C-D crystallisation trend of inverted pigeonites.

Tie lines are for coexisting Ca-rich and Ca-poor  
pyroxenes in the Skaergaard intrusion. After Deer,  
Howie and Zussman (1966).





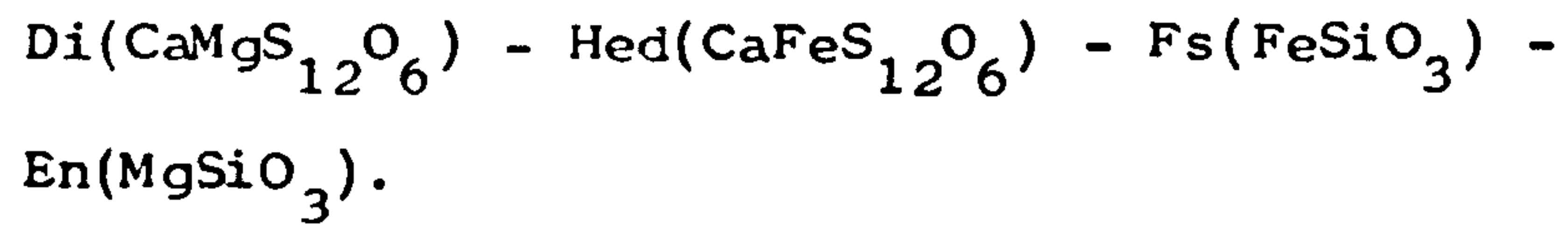
is a gradual change towards enrichment in Fe and Mg with increasing silica content of the host rock. A Ca-poor pyroxene begins to crystallise jointly with a Ca-rich pyroxene (augite in the terminology of Brown, 1968) in the andesites when the concentration of  $\text{SiO}_2$  in the rock is approximately 55 wt.%. The Ca-poor pyroxene is always orthohombic bronzite or hypersthene. The crystallisation of augite and hypersthene together continues into silica-rich andesites and dacites. Ca-poor clinopyroxene has not been observed during the present investigation as a phenocryst or groundmass phase in the Grenada suite. The appearance of pigeonite at compositions near  $\text{En}_{70-65}$  as a primary-crystallising Ca-poor phase in tholeiitic assemblages is reported in some calc-alkaline suites of tholeiitic affinities (eg. "the pigeonitic series" of Kuno, 1950). In the Grenada pyroxenes there is no evidence that the hypersthene has inverted from a monoclinic structure and no exsolution lamellae of a Ca-poor pyroxene have been observed in the hypersthene. The appearance of orthohombic pyroxene as the primary crystallising phase is similar to other calc-alkaline suites (eg. Wilkinson, 1971; Fodor, 1971).

In Fig. 37 the restricted enrichment of Fe in coexisting clino- and orthopyroxenes with increasing silica-saturation of the host rock is shown. The most Fe-rich orthopyroxene observed in the present study are  $\text{Fs}_{50}$ . Fodor (1971) has suggested that calc-alkaline trend of reduced iron enrichment relative to the tholeiitic trend controls the Fe content of the pyroxenes. In other words, the bulk composition of the host magma is the important factor in determining the degree of Fe-enrichment in

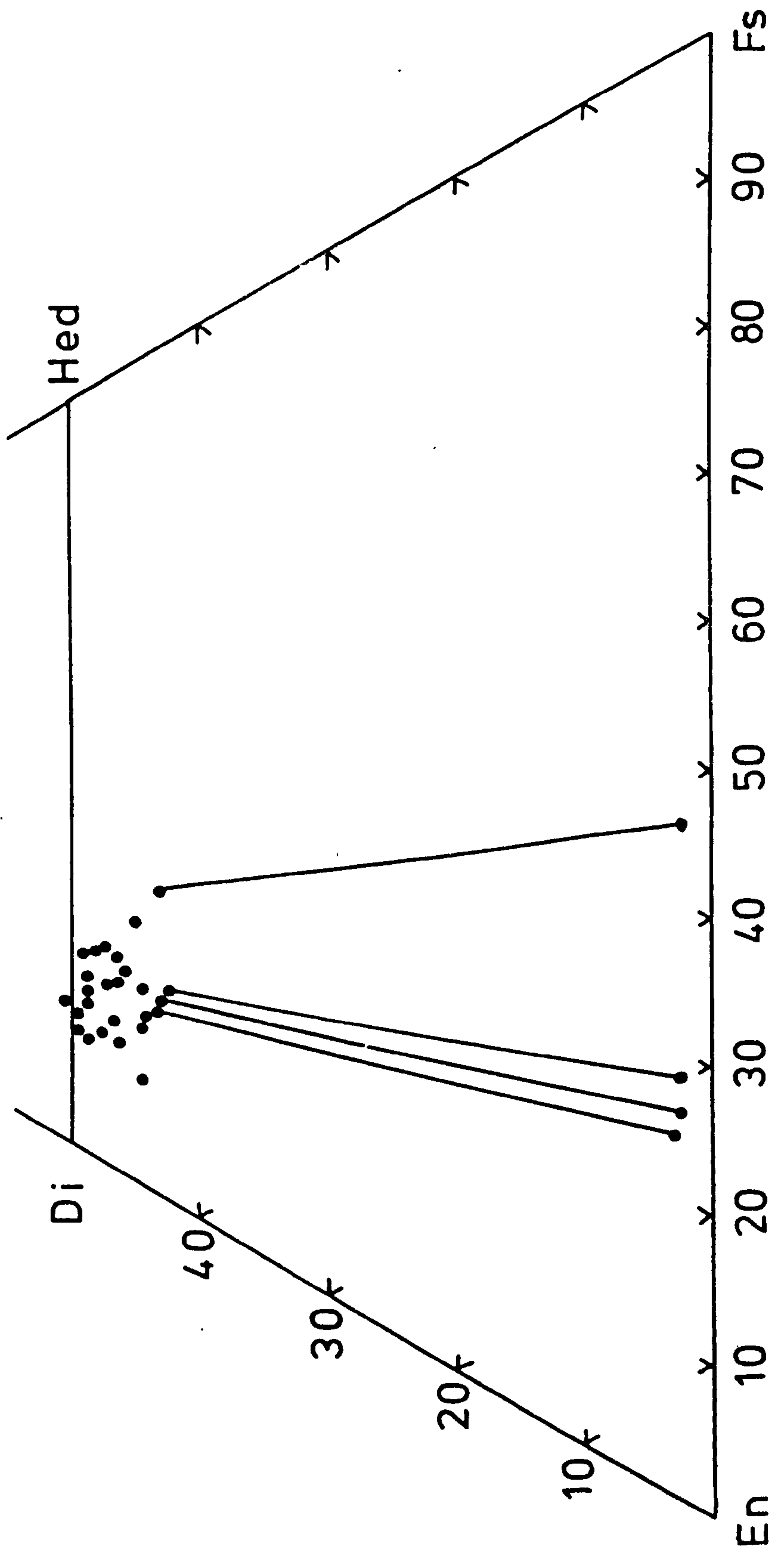


Fig.37

Pyroxene compositional variation in the Grenada calc-alkaline suite projected into the system:



Tie lines are for coexisting Ca-rich and Ca-poor pyroxenes.





the pyroxenes. The miscibility gap between coexisting Ca-rich and Ca-poor pyroxenes in the Grenada suite is similar to the gap in tholeiitic compositions (cf. Atkins, 1969).

Le Bas (1962) suggested that the magmatic affinities of a clinopyroxene could be determined on the basis of Ti and Al contents. However the variation of  $\text{Al}_2\text{O}_3$  with  $\text{SiO}_2$  of the Grenada clinopyroxenes spans the non-alkaline, alkaline and peralkaline groups of Le Bas. Arculus and Curran (1972) showed this variation occurred in individual clinopyroxene crystals and the data obtained from a more extensive study of the clinopyroxenes is presented here (Fig. 38 ). Gibb (1973) has shown that the variation in composition of the clinopyroxenes within the Shiant Sill also spans the groups of Le Bas (1962). It is apparent therefore, that the content of Ti and Al alone does not necessarily confirm the magmatic affinities of a particular pyroxene.

The content of Al in pyroxenes probably varies according to pressure, temperature and the bulk composition of the magma (Brown, 1968). Entry of Al into the octahedral sites of the clinopyroxene structure is favoured by high pressure but the activity of silica in the magma is also an important factor (Brown, 1968). Lower silica activity promotes the entry of increasing amounts of Ca-tschermak's molecule ( $\text{CaAl}_2\text{SiO}_6$ ) into the pyroxenes. However, the variation of Ti with Al in the clinopyroxenes (Fig. 39 ) suggests a more complex substitution. Ross et al. (1970) suggested on the basis of a linear relationship between Ti and Al that a coupled substitution of the form:

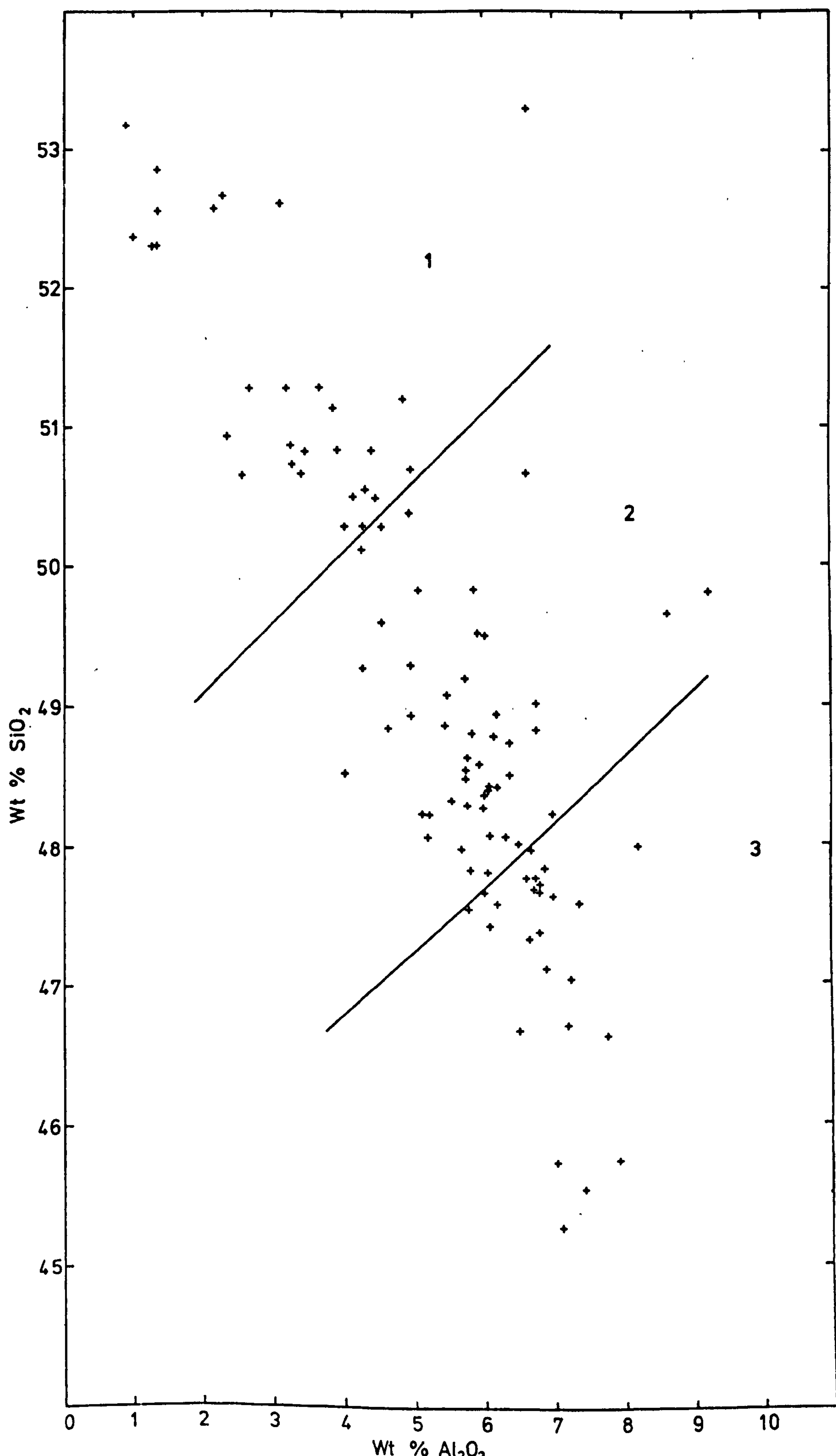
Fig. 38

$\text{SiO}_2$  v  $\text{Al}_2\text{O}_3$  plot of the Grenadan clinopyroxenes.

Numbers refer to fields of Le Bas (1962)

- 1 subalkaline
- 2 alkaline
- 3 peralkaline







was present where the ratio of Ti/Al equals 0.5. The ratio of Ti/Al in the Grenada clinopyroxenes is extremely variable within rocks of different composition (compare Fig.39 with Fig.33 ). Thus a simple coupled substitution of the form suggested by Ross et al. is inadequate to describe the variation in composition observed. This is probably related to the presence of  $Fe^{3+}$  in the Grenada clinopyroxenes and difficulties are experienced in determining the  $Fe_2O_3/FeO$  ratios from electron microprobe analyses. Further discussion of this aspect of the pyroxene chemistry follows the description of the sector and oscillatory zoning features (p.229 ).

Gibb (1973) has suggested that the initial increase in Ti and Al of the clinopyroxenes of the Shiant Sill is controlled by increasing Ti activity in the magma due to the lack of early Fe-Ti oxide precipitation. The presence of titaniferous magnetite as an early crystallising phase in the picrites and basalts suggests that although the activity of Ti in the magma must be important, it is only one of several factors determining the clinopyroxene composition.

It is interesting to note that the change in composition of the clinopyroxene microphenocrysts of picrite 483 (p.160 ) is towards increasing Ti and Al content. Nicholls et al. (1971) have shown that activity of silica increases in a given basaltic composition with increasing pressure. The growth of Ti- and Al-enriched mantles around the clinopyroxene microphenocrysts may



Fig. 39a

Al/Ti relationships in an oscillatory zoned clinopyroxene phenocryst in transitional basalt 479.

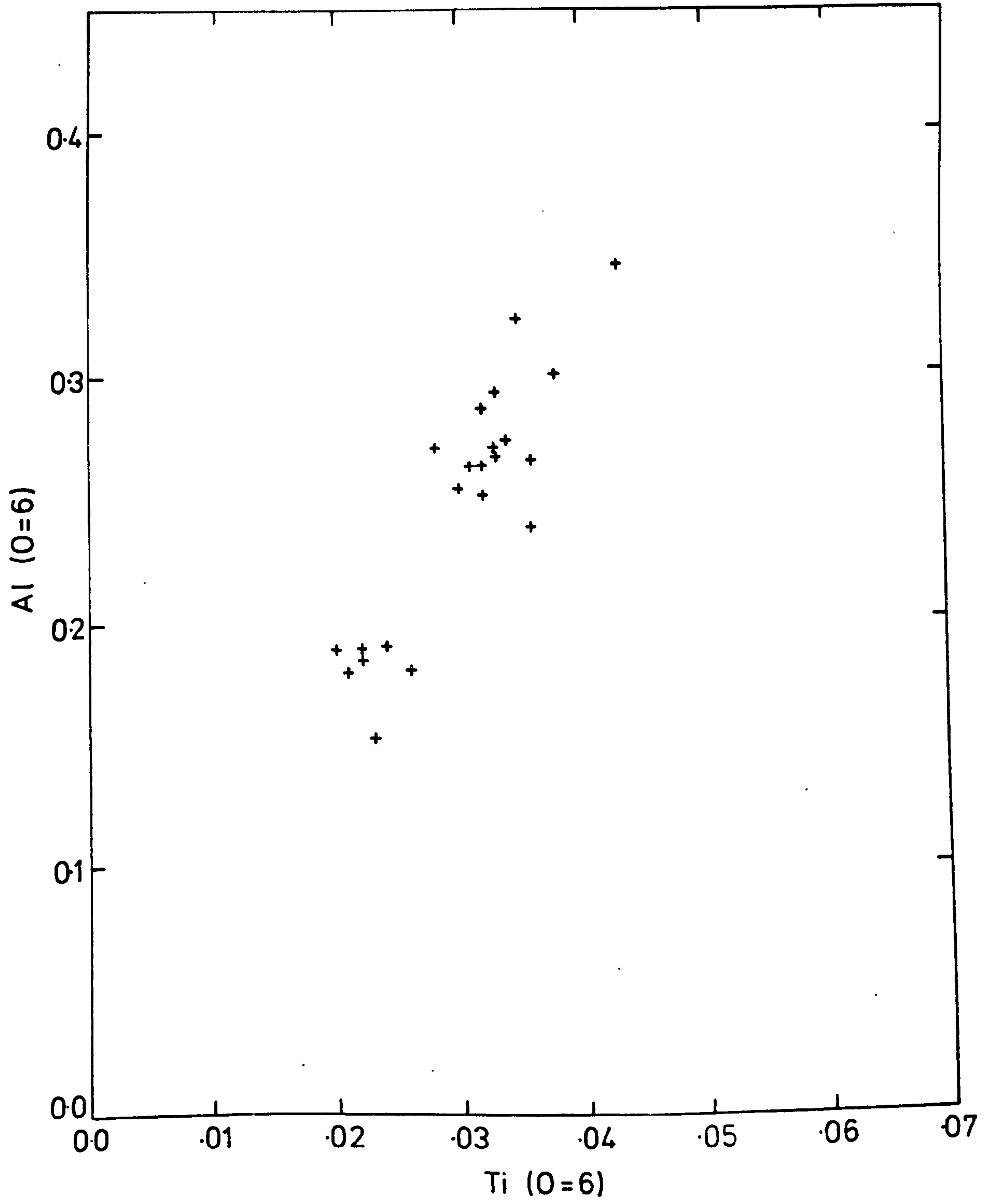




Fig. 39b

Al/Si relationships in an oscillatory zoned clinopyroxene phenocryst in transitional basalt 479.

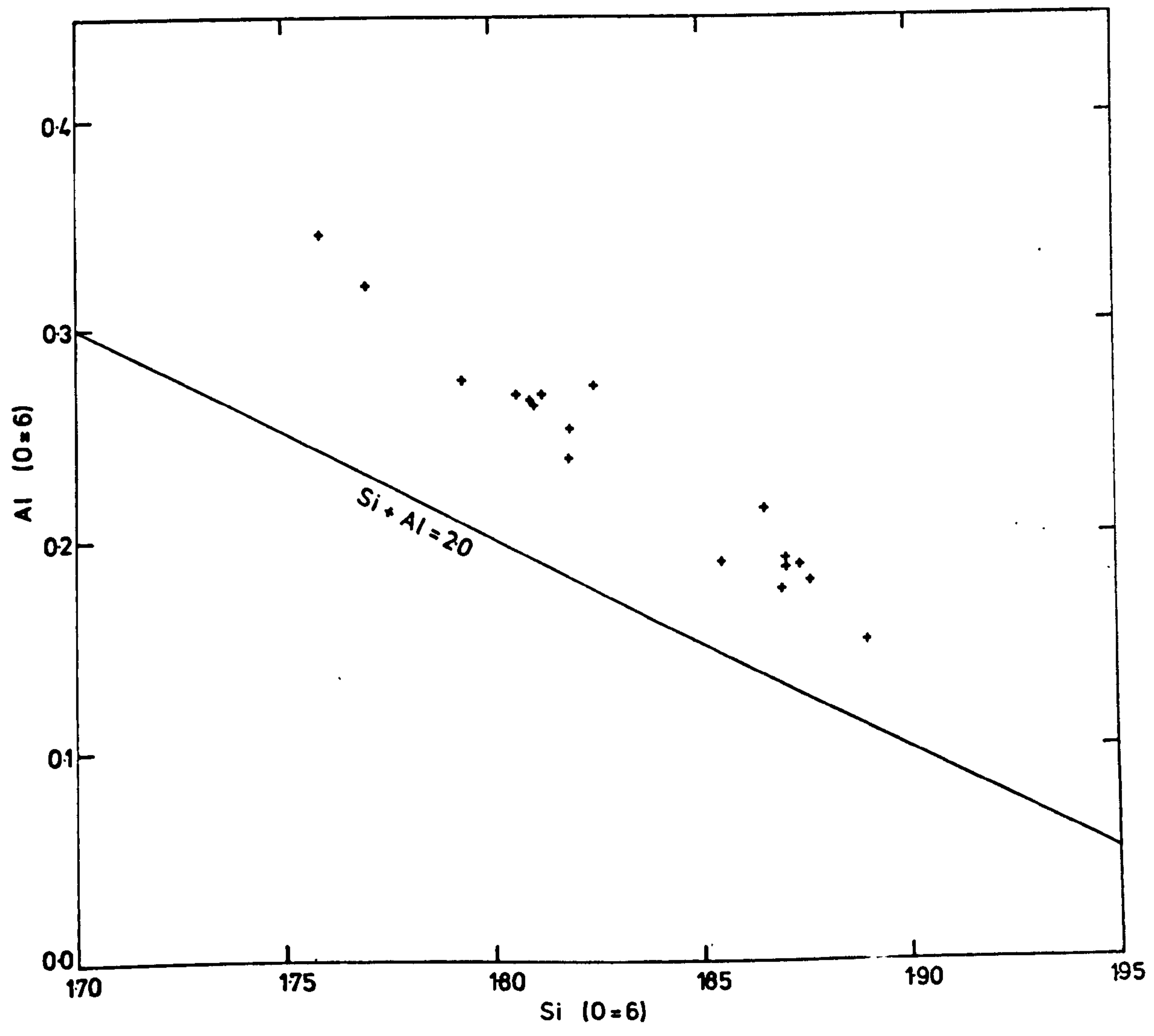




Plate 45

Photomicrograph of transitional basalt 479. Oscillatory and sector-zoned clinopyroxene phenocrysts together with olivine and oscillatory-zoned plagioclase feldspars can be seen. (Plane polarised light magnification x4).





be due to the reduced Si-activity in the magma during a rise to a lower pressure environment. Major changes in the pressure of the magma may generate changes in composition, but oscillation in element concentration also occurs on a much finer and often repeated scale.

### 9:5:3 The Sector and Oscillatory zoned Clinopyroxenes

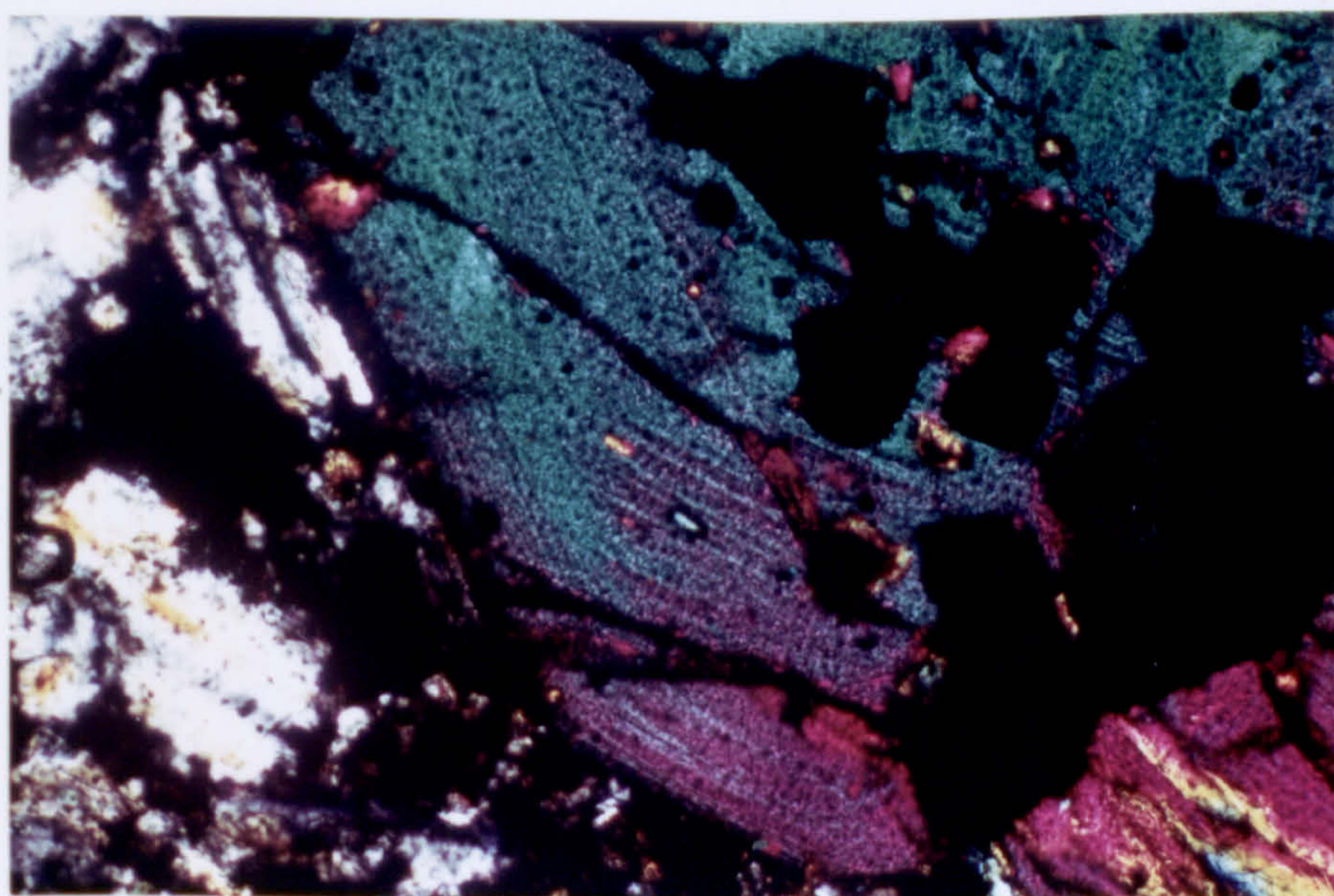
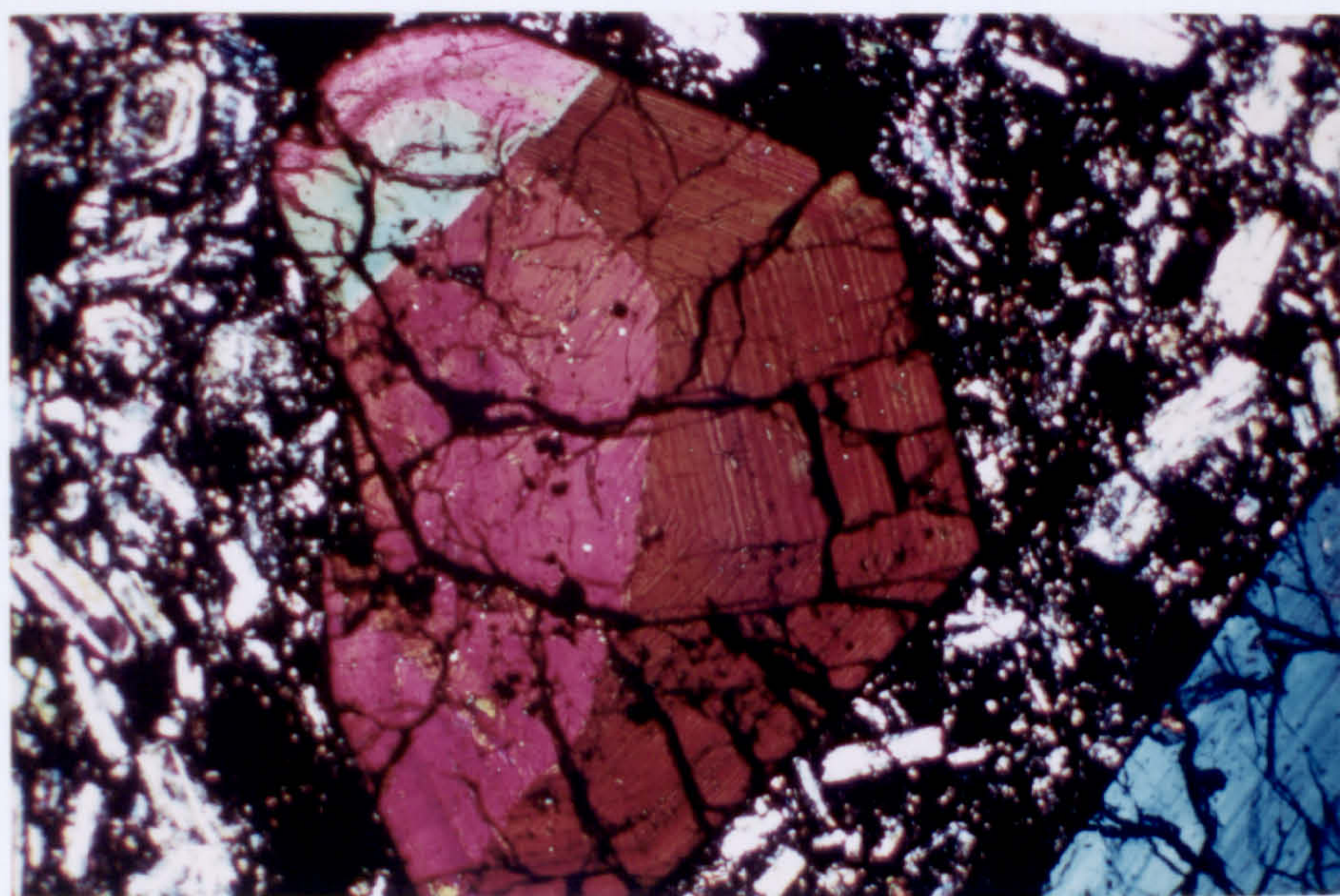
Sector and oscillatory zoned clinopyroxenes have been reported in many terrestrial and lunar environments (eg. Hargraves et al., 1970; Thompson, 1972; Wass, 1973). In most cases extremely fluid, volatile-rich or alkaline magmas appear to have formed the host composition. The occurrence of these types of zoning in clinopyroxenes is unusual in island-arc magmas. However in a study of Etna pillow lavas (Sicily), similar features were observed in alkali basalt compositions (Arculus, 1973). Weakly oscillatory zoned clinopyroxenes have also been observed in basalt samples from the South Sandwich and Tonga island arcs (in samples donated to the author by Dr. P.E. Baker, Leeds). If Mt. Etna is regarded as part of the Calabrian island arc (Ninkovich and Hays, 1972) sector and oscillatory zoning of clinopyroxenes may be a relatively common feature of basalts of calc-alkaline as well as alkaline associations.

The appearance of a typical clinopyroxene-phyric transitional basalt is shown in Plate 45 . The majority of the clinopyroxenes in this section have been sectioned oblique to the c-axis. Oscillatory zoning of individual phenocrysts is shown in Plates 46 .

Plate 46

Photomicrographs of oscillatory and sector-zoned clinopyroxene phenocrysts in transitional basalt 479.  
(Crossed polars magnification x10).







The sector-zoning may be observed in the (010) sections shown in Plate 35 of alkali basalt 454. Individual crystals may not have been sectioned through the core and frequently exhibit continuous oscillatory zoning. In many cases however, an unzoned pale green core is visible even in (010) sections. In plane polarised light, the oscillatory zones appear as different shades of green. The darker green is associated with a higher content of Ti and Al. The nature of the oscillatory zones is a gradual change from pale to dark green within a distance of 10-50  $\mu\text{m}$  followed by a sharp reversal to pale green again. Minute oscillations up to 2-4  $\mu\text{m}$  in width are superimposed on the broader divisions of contrasting composition. The relationship of individual oscillations within sector zoning of a (010) section are shown in Fig. 40. It can be seen that individual zones are continuous around the crystal and across sector boundaries but the thickness of the zone varies. The sector boundary is thus by no means a plane surface, and the configuration of the oscillatory zones and this boundary does not support the suggestion of Strong (1969) that hourglass growth followed by later pyramidal infilling of contrasted composition forms the sector zoning.

Orientation of individual crystals was achieved on the universal stage and the greatest enrichment of Ti and Al observed, was usually in the (100) sector (terminology of Hollister, 1970). However, many instances of oscillation in composition between zones of individual sectors equivalent to differences between sectors were observed. In Fig. 40 the relationship between oscillatory zones of a (100) and (110) sector are sketched from Plate 46.



Fig.40

Oscillatory and sector zoned clinopyroxenes.

- (A) Configuration of sector (hour-glass) zoning in 010 section, stipple denotes higher relative concentration of Ti and Al.
- (B) Configuration of sector and oscillatory zone boundaries in analysed clinopyroxene, in oblique (001) section. Numbers refer to analyses in Table 29.

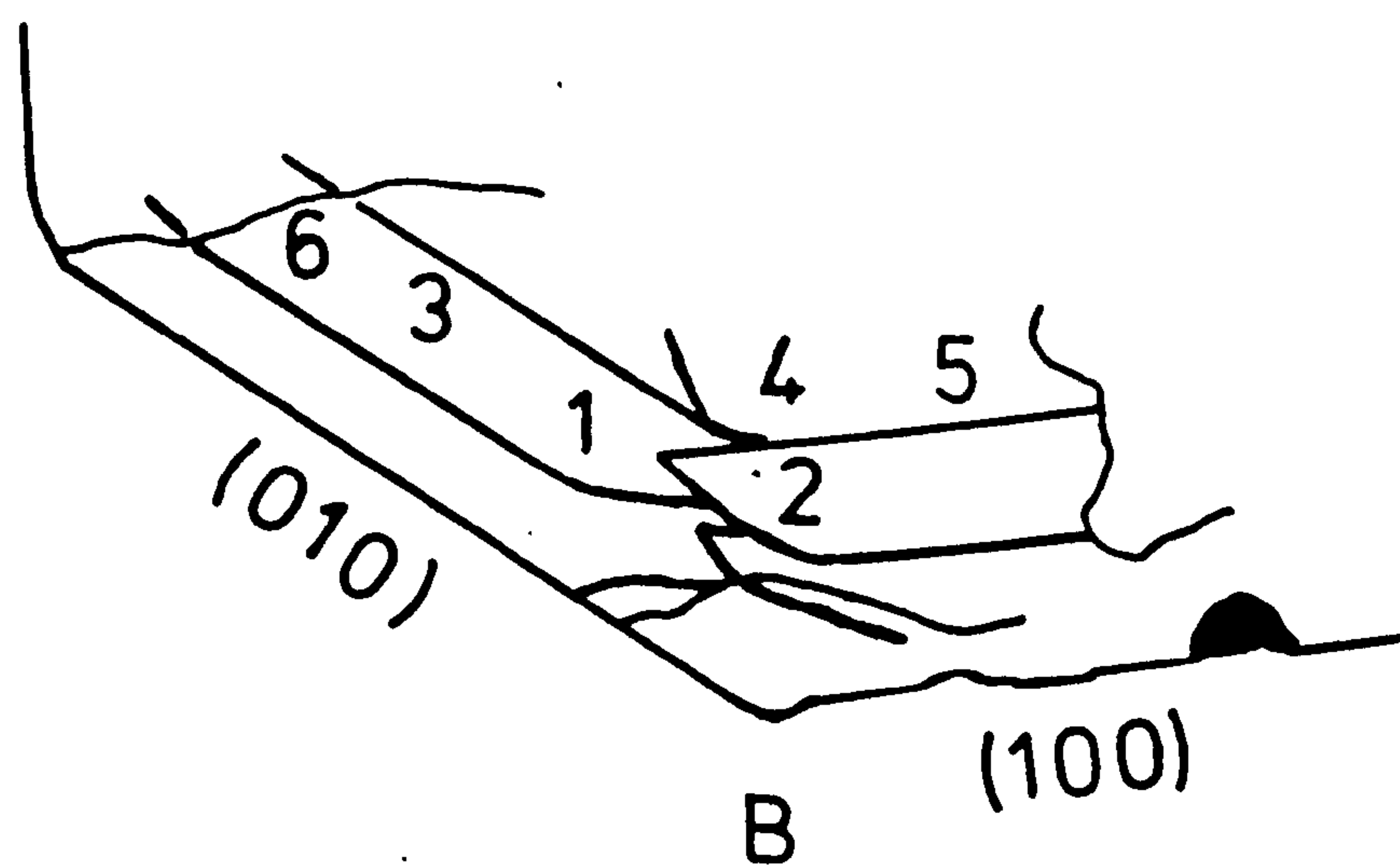
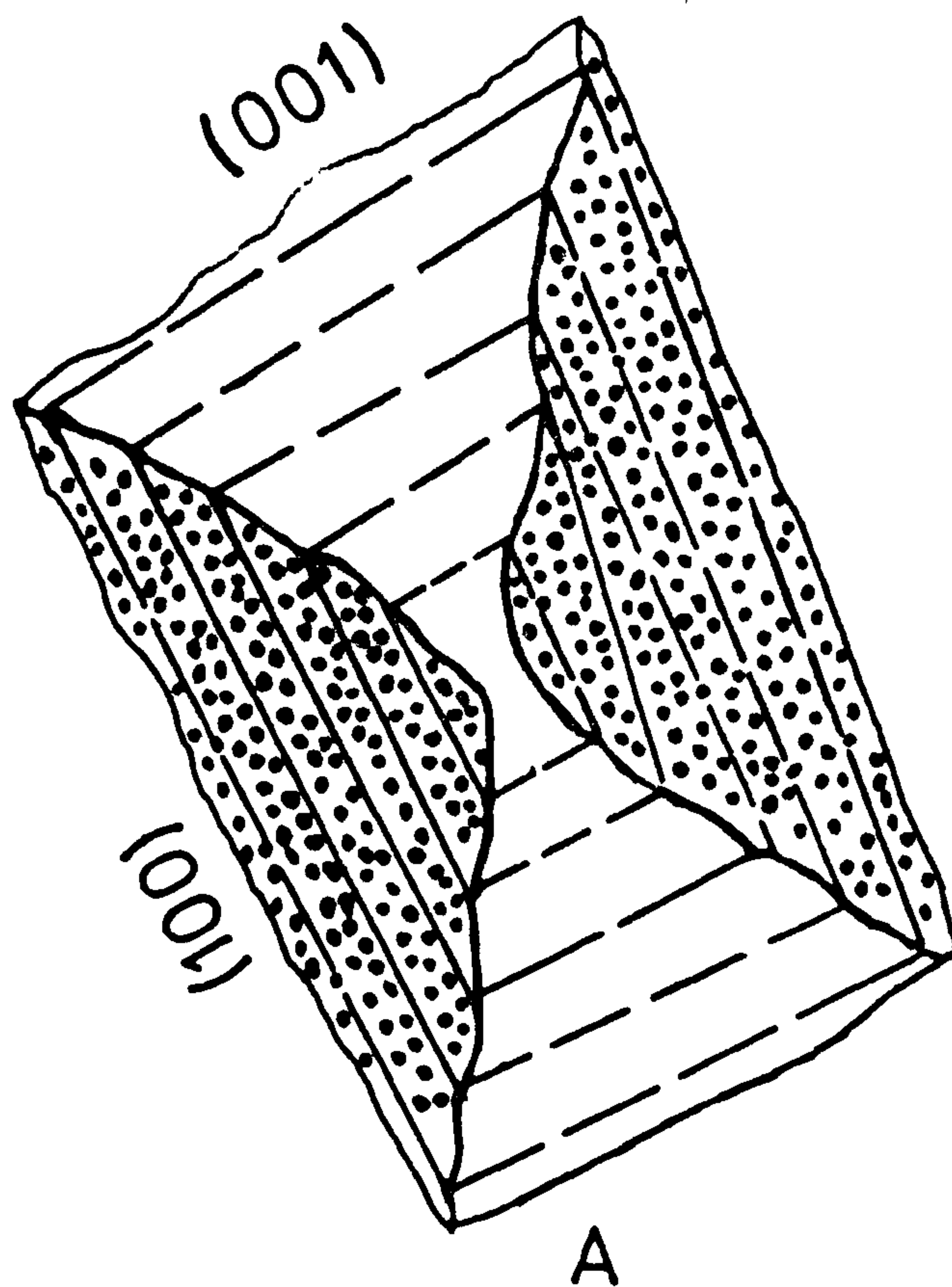




TABLE 30

Partial analyses of several zones of an oscillatory-zoned clinopyroxene in transitional basalt 479. Numbers refer to points analysed (locations in Fig.40).

	6	3	1	2	4	5
SiO <sub>2</sub>	47.60	47.83	48.44	48.81	48.03	47.67
TiO <sub>2</sub>	1.21	1.15	1.04	1.07	1.14	1.16
Al <sub>2</sub> O <sub>3</sub>	6.19	6.05	6.17	5.83	6.50	6.65
FeO	7.88	8.03	8.13	7.86	8.02	8.15
MgO	13.02	13.20	12.75	13.63	13.14	12.82
CaO	22.95	22.27	22.11	22.60	22.28	22.22
Na <sub>2</sub> O	0.49	0.51	0.47	0.50	0.52	0.59
K <sub>2</sub> O	0.32	0.04	0.03	0.03	0.04	0.06
Total	99.37	99.67	99.15	100.33	99.67	99.33

Atomic proportions on the basis of 6 oxygens

Si	1.793	1.806	1.824	1.817	1.801	1.796
Ti	0.034	0.033	0.029	0.030	0.032	0.033
Al	0.275	0.269	0.274	0.256	0.287	0.295
Fe	0.248	0.254	0.256	0.245	0.252	0.257
Mg	0.731	0.743	0.715	0.756	0.734	0.720
Ca	0.927	0.901	0.892	0.902	0.895	0.897
Na	0.036	0.037	0.034	0.036	0.038	0.043
K	0.015	0.002	0.001	0.001	0.002	0.003

End-member compositions

Ca	48.62	47.49	47.87	47.39	47.59	47.88
Mg	38.36	39.15	38.39	39.75	39.04	38.42
Fe	13.03	13.36	13.74	12.86	13.37	13.71

The configuration of the boundaries between the sectors suggest that the surface of the section is somewhat oblique to the c-axis of the crystal. In Table 30, analyses of individual points within these oscillatory zones is presented. An attempt was made during the analysis of these zones to determine the variation within a single oscillation in composition away from a sector boundary. Unfortunately it is impossible to be certain that equivalent growth stages were analysed. Nevertheless, the analyses reveal that the variation in chemical composition within a sector may be equivalent to the differences between a sector.

Analyses of the St. Vincent cumulus clinopyroxenes (Lewis, 1963) and sector zoned augites from Vesuvius (Bell et al., 1972) suggest the presence of  $\text{Fe}^{3+}$  in the tetrahedral sites of the pyroxene structure. The proportion of  $\text{Fe}^{3+}$  in the Grenada crystals cannot be determined directly by electron microprobe analysis. Assuming stoichiometry and accurate analysis of cations other than  $\text{Fe}^{2+}$ , it is possible to estimate  $\text{Fe}^{3+}$  by a normative-type procedure such as that devised by Kushiro (1962). However, Finger (1962) has shown the low accuracy likely to be achieved by this procedure with electron microprobe analyses, particularly when small variations in total Fe are being considered.

The oscillatory and sector zoning of the Grenada clinopyroxenes probably involves a complex substitution of several cations. Thompson (1972) has summarised the possible coupled substitutions in an oscillatory and sector zoned augite, and suggested that these may indicate the range of complex element



variation possible. These are:

- 1)  $\text{Ti}_2\text{Al} \quad \text{Mg}_2\text{Si}$  leads to theoretical end-member  $\text{R}^{2+}\text{TiAl}_2\text{O}_6$  (Yagi and Onuma, 1967).
- 2)  $2\text{Al} \quad \text{MgSi}$  leads to  $\text{R}^{2+}\text{Al AlSiO}_6$  (Thompson, 1972).
- 3)  $2\text{Fe}^{3+} \quad \text{MgSi}$  leads to  $\text{R}^{2+}\text{Fe FeSiO}_6$  (Huckenholz et al., 1969).
- 4)  $\text{NaFe}^{3+} \quad \text{CaMg}$  leads to  $\text{NaFeSi}_2\text{O}_6$  (Nolan and Edgar, 1963).
- 5)  $\text{NaAl} \quad \text{CaMg}$  leads to  $\text{NaAlSi}_2\text{O}_6$  (Thompson, 1972).
- 6)  $\text{Fe}^{3+}\text{Al} \quad \text{MgSi}$  leads to  $\text{R}^{2+}\text{FeAlSiO}_6$  (Thompson, 1972).

Further consideration of the element variation in the Grenada clinopyroxenes must await accurate  $\text{Fe}^{3+}$  determinations. The formation of sector zoning has been discussed by Hollister and Gancz (1971). They considered four main factors were involved:

- "1) the size and composition of ionic complexes added to the crystal as it grows
- 2) the rate of addition of material
- 3) the rate of equilibrium of the new material with the matrix at the surface of growth steps
- 4) the rate of re-equilibration with the matrix by exchange of ions perpendicular to the crystal faces."

Hargraves et al. (1970) suggested that simultaneous exposure of the tetrahedral and octahedral sites on growing (010) and (001) faces would facilitate the type of coupled substitutions listed above. Alternate exposure of these sites by growth parallel to (110), (100) and (101) faces does not permit simultaneous coupled sub-

stitutions and may involve alternate charge compensations. The complication of the superimposed oscillatory zoning must also be considered. Bottinga et al. (1966) after Harloff (1927) proposed a disequilibrium crystallisation model for the formation of oscillatory zoning in plagioclase feldspars. Element concentration gradients measured in glasses adjacent to crystal faces suggest that the interplay between rate of ionic diffusion in the melt and the growing crystal surface control the reversals of composition observed. Bottinga et al. also suggested a mechanism for the sudden reversal in composition at the start of a new zone. During the slower stages of crystallisation near the completion of a zone, it is assumed that the crystal surface becomes relatively perfect with few energetically favourable sites of nucleation. Crystallisation almost ceases as the concentration of the higher-temperature end-member composition (An) builds up again to slight supersaturation, followed by rapid nucleation on the crystal face and depletion of the adjacent melt once more.

In the case of plagioclase feldspars, oscillatory zones are sometimes reduced in number or absent in one crystallographic plane. The reduction in width of some of the oscillatory zones of particular growth surfaces in clinopyroxenes has already been suggested. It is a consequence of this disequilibrium-crystallisation model that the existence of structurally favourable nucleation sites will control the relative amounts of oscillatory zoning. The formation of the oscillatory zones in the clinopyroxenes appears analogous to the origin of the oscillatory zones of the plagioclase feldspars. The formation of sector and oscillatory zoning appears to be related not only to the bulk composition of the melt and



the kinetics of diffusion and growth, but also to the strong influence of crystallographic orientation. It is interesting to note that the cumulus clinopyroxenes of the plutonic blocks are generally unzoned. It seems possible that the settling of the crystals in the host magma may produce equilibrium growth as the crystal faces are continuously in contact with undepleted melt. Further nucleation may take place under equilibrium conditions by the process of adcumulus growth suggested by Wager and Brown (1968). Oscillatory zoning in plagioclase may be generated by fluctuations in  $P_{H_2O}$  of the magma (Yoder, 1969) and it is apparent that major physical changes in pressure and temperature of the magma must also control the composition of the nucleating phenocrysts.

In summary, the sector and oscillatory zoned clinopyroxenes are probably formed under disequilibrium conditions prevailing in the magma prior to eruption. It seems unlikely that the unzoned cumulus pyroxenes are formed at the same time as the strongly zoned crystals, and may relate to periods of quiescence and equilibrium growth. The occasional large (4-5 mm) unzoned calcic augites observed in the basalts and picrites are probably cumulus xenocrysts incorporated in the magma during ascent.

### Discussion

The important feature of the Grenada pyroxenes is the trend from compositions previously recognised as typically alkaline to calc-alkaline assemblages. This trend constitutes a type of pyroxene compositional variation additional to those described in differentiated alkaline and tholeiitic magmas.

### 9:5:4 Feldspars

Plagioclase feldspars are the dominant phenocryst minerals of many of the basalts, andesites and dacites of the Grenada calc-alkaline suite. Alkali feldspar is suspected in the groundmass of some microphyric picrites and basalts but is never present as an obvious phenocryst or groundmass phase. The high An content of plagioclase feldspars in the Grenada suite is typical of calc-alkaline associations. It is apparent that highly calcic plagioclase can be precipitated from basaltic magma, possibly under conditions of elevated  $P_{H_2O}$  (Yoder, 1969). The total range in composition observed is from  $An_{90-15}$ , and individual phenocrysts are often prominently zoned. In general there is a gradual decrease in An content with increasing silica-saturation of the bulk composition but bytownite cores are often present in the phenocrysts of andesitic compositions. The content of  $K_2O$  is uniformly low in the plagioclase feldspars ranging from 0.01 wt.% ( $An_{90}$ ) to 0.04 wt.% ( $An_{40}$ ).

The disequilibrium growth mechanism described previously appears to be the most satisfactory explanation for the origin of the oscillatory zoning in the plagioclase phenocrysts. It is possible that additional zoning is present due to fluctuations in  $P_{H_2O}$  during crystallisation (Tuttle and Bowen, 1958). Individual zones may be of the order of  $2\ \mu m$  in width and some larger phenocrysts may contain 100 or more of these zones. An example of the range of variation between zones of a phenocryst in dacite 462 is given in Table 31. The oscillations in composition are superimposed on a normal zoning trend towards more sodic



TABLE 31

Analyses of several zones of an oscillatory-zoned plagioclase feldspar phenocryst in dacite 462. Oscillatory zones in order 1 to 7 approaching margin of crystal.

	1	2	3	4	5	6	7
SiO <sub>2</sub>	54.87	55.91	57.88	56.72	56.71	56.40	57.64
TiO <sub>2</sub>	0.02	0.02	0.02	0.02	0.02	0.02	0.02
Al <sub>2</sub> O <sub>3</sub>	28.49	29.56	26.90	27.76	27.38	28.45	26.84
FeO	0.24	0.26	0.21	0.18	0.17	0.30	0.18
MnO	0.02	0.02	0.02	0.02	0.02	0.02	0.02
MgO	0.05	0.05	0.03	0.02	0.02	0.08	0.07
CaO	9.92	9.96	8.20	9.33	8.59	8.97	9.26
K <sub>2</sub> O	0.02	0.02	0.03	0.02	0.03	0.03	0.02
Na <sub>2</sub> O	5.71	4.61	6.31	5.42	5.95	5.12	6.24
Total	99.34	100.41	99.60	99.49	98.89	99.39	100.29

Atomic proportions on the basis of 8 oxygens

Si	2.485	2.490	2.593	2.549	2.562	2.533	2.575
Ti	0.001	0.001	0.001	0.001	0.001	0.001	0.001
Al	1.521	1.552	1.421	1.471	1.458	1.506	1.414
Fe	0.009	0.010	0.008	0.007	0.006	0.011	0.007
Mn	0.001	0.001	0.001	0.001	0.001	0.001	0.001
Mg	0.003	0.003	0.002	0.001	0.001	0.005	0.005
Ca	0.481	0.475	0.394	0.449	0.416	0.432	0.443
K	0.001	0.001	0.002	0.001	0.002	0.002	0.001
Na	0.502	0.398	0.548	0.472	0.521	0.446	0.541

End-member compositions

Ab	50.97	45.53	58.10	51.19	55.53	50.72	54.89
An	48.92	54.34	41.71	48.68	44.29	49.09	45.00
Or	0.12	0.13	0.18	0.12	0.18	0.20	0.12

compositions from core to rim. In many phenocrysts, zones densely populated by minute oxide grains or glassy blebs are present. These zones may occupy the cores, or occur at any stage during the growth of the crystal.

Bottinga et al. (1966) suggested that the presence of oxide inclusions is the result of the same disequilibrium growth that may initiate oscillatory zoning. The saturation in ferromagnesian constituents in the melt adjacent to a growing plagioclase crystal may initiate nucleation of ferromagnesian silicates or oxides. On the other hand, the rarer occurrence of oxide and silicate inclusions within the feldspar compared with the frequency of oscillatory zoning may be the result of fluctuations in  $P$ ,  $T$  and  $P_{H_2O}$  of the magma. In this case resorption of previously crystallised compositions or alternatively nucleation of different phases may take place.

#### 9:5:5 Amphiboles

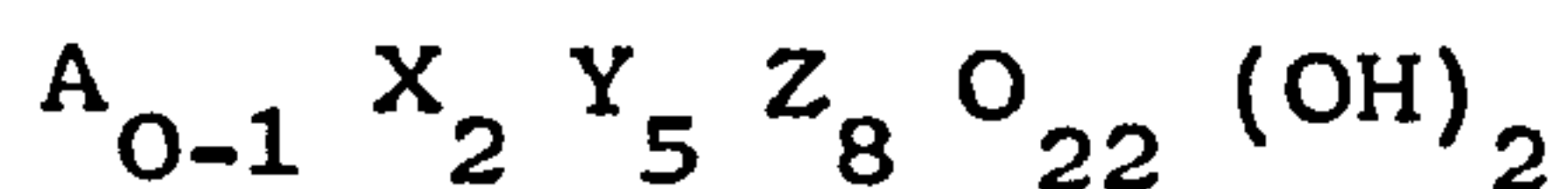
The amphiboles of the Grenada basalts, andesites and dacites are of pargasite-tschermakite composition in the classification of Phillips (1966). Selected analyses have been presented previously in this Chapter. The complex substitutions possible in amphiboles and the variation in composition with changing  $P$ ,  $T$ ,  $f_{O_2}$  and bulk composition are of considerable interest in the interpretation of the evolutionary trends of hydrous magmas. The appearance of amphibole phenocrysts in Grenada basalts and cumulus plutonic blocks is important with regard to the petrogenesis of the calc-alkaline suite. The most important features of these amphiboles is the silica-undersaturated composition and the order



of crystallisation after spinel, olivine, clinopyroxene and plagioclase.

An attempt was made to allocate  $\text{Fe}^{3+}$  and  $\text{Fe}^{2+}$  in the amphiboles from total Fe in the analyses determined with the electron microprobe. Uncertainty in the determination of other elements besides Fe and the possible presence of  $\text{O}^-$  as well as  $\text{OH}^-$  anions in the structure render this procedure even less likely to succeed than in the case of clinopyroxenes. Amphiboles analysed by wet chemical methods (Lewis, 1964; Rea, 1970) in the Lesser Antilles reveal high average  $\text{Fe}_2\text{O}_3/\text{FeO}$  ratios ( 0.68 ). Structural formulae in this account have been based on  $\text{Fe}_2\text{O}_3 = 0.0$  following the method of Ross et al. (1969). This involves the least adjustment of the actual data and allows comparisons to be made directly but it is recognised that the Grenada amphiboles probably also contain high  $\text{Fe}_2\text{O}_3/\text{FeO}$  ratios.

The amphibole structural formula is:



Ross et al. (1969) suggest that any excess in the Y site above 5.00 may be considered as Fe in the  $\text{M}_4$  site (X). The content of the A site is then given by:

$$\text{Ca} + \text{Na} + \text{K} + \text{Fe} (\text{M}_4) - 2.00$$

In a study of the variation of amphibole composition in experiments conducted under hydrous conditions ( $\text{P}_{\text{H}_2\text{O}} = \text{P}_{\text{tot}} = 5 \text{ kb}$ ) in natural basalt compositions, Helz (1973) has shown that there is a correlation between increasing Al(IV), Ti and A site occupancy

Plate 47

Photomicrograph of andesite 355. Oscillatory zoned amphiboles are the prominent phenocryst minerals. (Crossed polars, magnification x5).



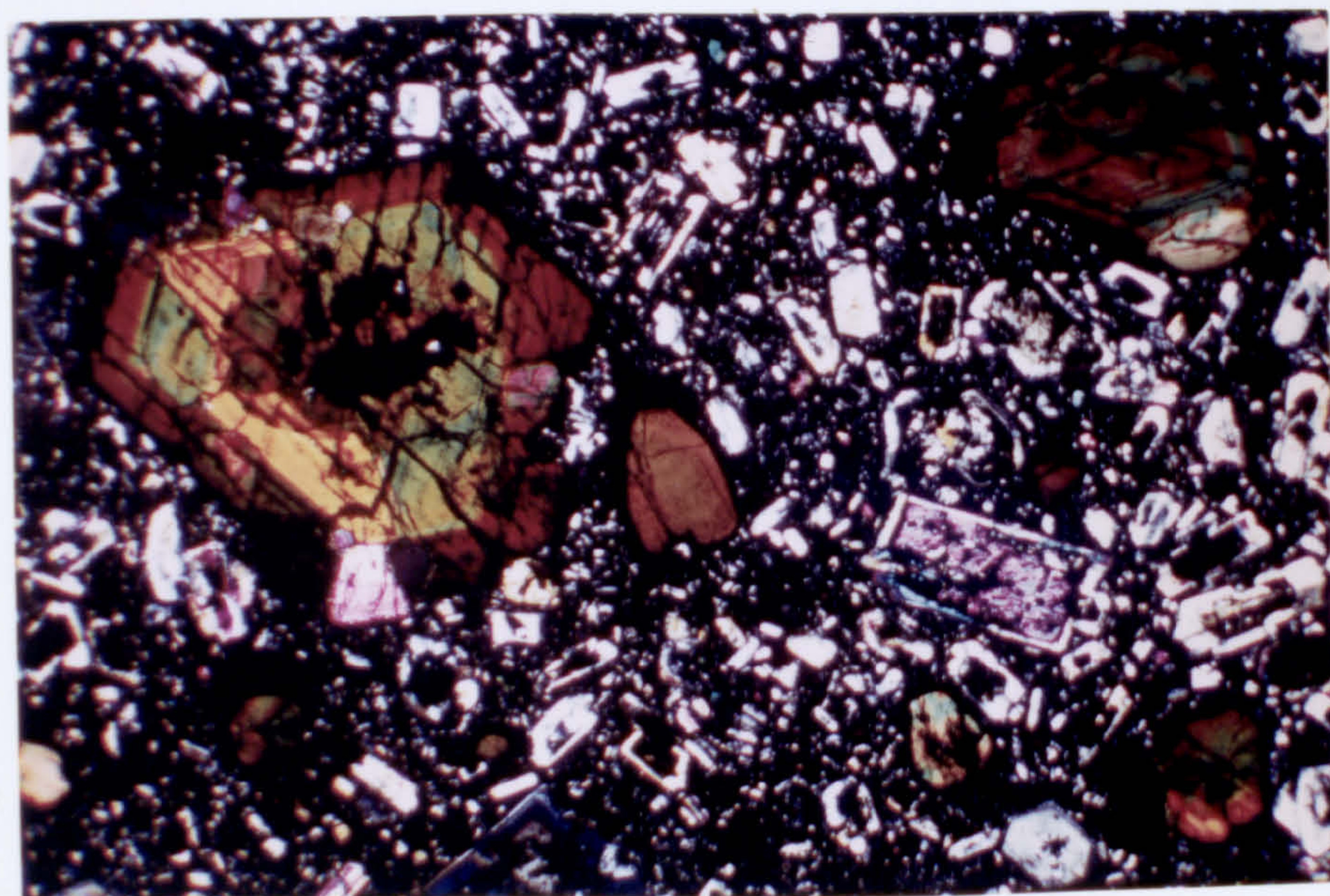




TABLE 32

Partial analyses of oscillatory zoned pargasite phenocryst in andesite 355. Points analysed on single traverse perpendicular to prismatic face. Core to rim in order 1-7.

	1	2	3	4	5	6	7
SiO <sub>2</sub>	41.82	42.22	41.61	40.67	41.03	41.90	42.06
Al <sub>2</sub> O <sub>3</sub>	15.51	14.25	14.62	15.72	15.70	14.93	14.80
TiO <sub>2</sub>	1.95	1.70	1.74	1.83	1.86	1.69	1.60
FeO*	9.40	10.84	11.60	11.70	11.64	10.68	13.11
MgO	14.15	13.91	13.42	12.72	11.75	14.20	12.86
CaO	12.30	12.01	12.12	11.99	12.33	11.93	11.57
Na <sub>2</sub> O	2.48	2.48	2.38	2.45	2.44	2.62	2.44
Total	97.61	97.41	97.49	97.08	96.73	97.95	98.44

Structural formulae on the basis of 23 oxygens (Fe<sup>3+</sup> = 0.0)

Si	6.066	6.173	6.107	6.001	6.071	6.092	6.137
Al(IV)	1.934	1.827	1.893	1.999	1.929	1.908	1.863
Al(VI)	0.719	0.630	0.637	0.736	0.810	0.651	0.683
Ti	0.213	0.187	0.192	0.203	0.207	0.185	0.176
Fe	1.140	1.326	1.424	1.444	1.441	1.299	1.600
Mg	3.059	3.031	2.935	2.797	2.587	3.077	2.797
Ca	1.912	1.882	1.906	1.896	1.955	1.859	1.809
Na	0.698	0.703	0.678	0.701	0.700	0.739	0.691

Atoms in A site (Ca+Na+Fe(M<sub>4</sub>) - 2.00)

0.741	0.759	0.772	0.777	0.690	0.810	0.756
-------	-------	-------	-------	-------	-------	-------

100/Mg/Mg+Fe ratio

72.9	69.6	67.3	66.0	64.2	70.3	63.6
------	------	------	------	------	------	------



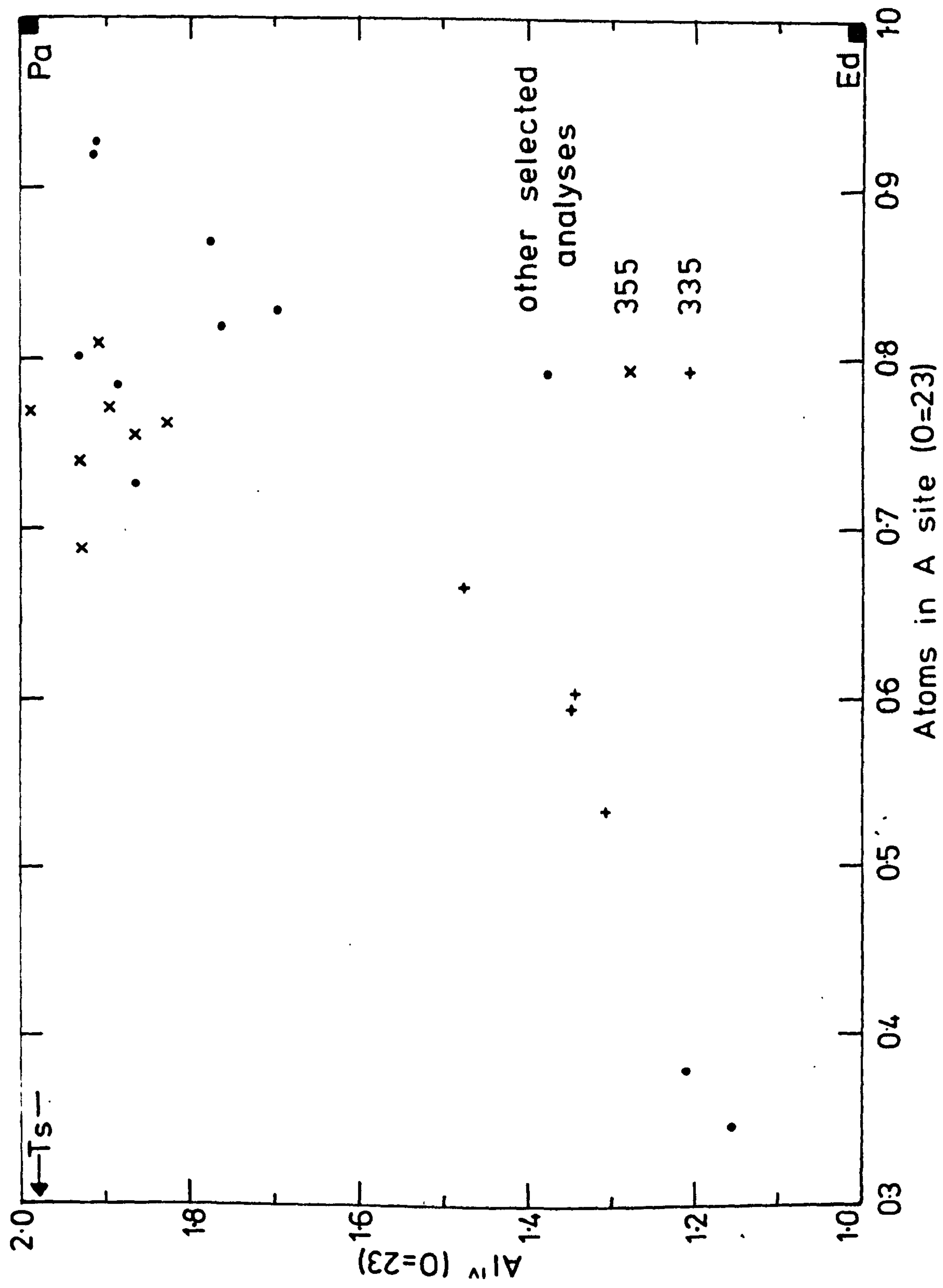
with increasing temperature. However, increasing  $f_{O_2}$  at a given temperature produces the reverse effect due to the increasing stability of the Fe-Ti oxides. In Fig. 41, the variation in Al(IV) and A site occupancy of the Grenada amphiboles is illustrated. In general, increasing silica-saturation of the bulk composition correlates with decreasing Al(IV) and A site occupancy but the control of bulk compositional differences between basalt and dacite is probably a much more important factor than declining liquidus temperatures. The effect of increasing  $Fe_2O_3/FeO$  ratio in these amphiboles is to shift the plotted compositions towards the Ts corner of Fig. 41 (Helz, 1973).

Oscillatory zoned amphiboles are frequently present in the Grenada andesites and dacites. The appearance of these amphiboles in andesite 355 is shown in Plate 47. The crystals have been sectioned perpendicular to the prismatic faces. The other phenocryst minerals are plagioclase feldspar ( $An_{70-62}$ ), calcic augite and magnetite. Partial analyses at points on a single traverse from the core towards the opacitised margin of the larger pargasite phenocryst seen in Plate 47 were completed with the electron microprobe. The analyses are presented in Table 32. In general the  $FeO/MgO$  ratio gradually increases from core to margin reflecting the normal magmatic zoning trend. However, several fluctuations are superimposed upon this variation including a major reversal of composition near the margin of the crystal to a more Mg-rich composition. In addition there is a variation in Ti and Al from zone to zone. Another traverse was made parallel to the prismatic faces of an oscillatory zoned

Fig. 41

Al(iv) v A-site occupancy in amphiboles. The position of the hornblende end-members; edenite, Ed; pargasite, Pa; and tschermakite, TS.





pargasite in dacite 335. The other phenocryst minerals in this dacite are plagioclase feldspar ( $An_{50-42}$ ), calcic augite, apatite and magnetite. The variation in composition of this pargasite are presented in Table 33. The range of composition includes the pargasite composition of andesite 355, but in general the dacite amphibole is richer in Si, lower in Ti and Al and the variation in composition is not as great. In Fig. 41 the Al(IV) and A site occupancy of these oscillatory zoned amphiboles is plotted. There is no definite correlation suggesting that bulk composition and disequilibrium-growth are probably the most important factors influencing the formation of the oscillatory zoning.

The Al(IV) vs A site plot has been used to illustrate the compositional variation observed in the Grenada amphiboles. It is not believed that there is a simple correlation between amphibole composition with  $P$ ,  $T$ ,  $f_{O_2}$  and bulk composition of the host magma and the inter-relationship of these factors remains an intriguing field of research. The results of experimental investigations into the stability of amphibole in basaltic and andesitic melts at various  $P$ ,  $T$  and  $P_{H_2O}$  conditions, and the petrogenetic significance of these results is discussed in Chapter 10.

#### 9:5:6 Oxide minerals

Chrome spinel and magnetite are the common oxide minerals of the Grenada volcanic suite. Chrome spinel is observed in picrites, alkali and transitional basalts often poikilitically enclosed by olivine and clinopyroxene. Magnetite containing appreciable quantities (up to 15 wt.%)  $TiO_2$  is observed in



TABLE 33

Partial analyses of oscillatory-zoned pargasite phenocryst in dacite 335. Points analysed on a single traverse parallel to the prismatic faces. Core to rim in order 1-4.

	1	2	3	4
SiO <sub>2</sub>	43.76	44.88	44.66	45.08
Al <sub>2</sub> O <sub>3</sub>	10.41	9.65	9.50	9.68
TiO <sub>2</sub>	1.88	1.77	1.82	1.59
FeO*	12.46	11.96	13.16	12.99
MgO	13.90	14.40	13.90	13.72
CaO	11.41	11.25	11.05	11.25
Na <sub>2</sub> O	2.21	2.12	2.01	1.82
Total	96.03	96.03	96.10	96.13

Structural formulae on the basis of 23 oxygens  
(Fe<sup>3+</sup> = 0.0)

Si	6.523	6.656	6.653	6.696
Al(IV)	1.477	1.344	1.347	1.304
Al(VI)	0.353	0.343	0.321	0.391
Ti	0.211	0.197	0.204	0.178
Fe	1.554	1.484	1.640	1.614
Mg	3.088	3.183	3.086	3.037
Ca	1.823	1.788	1.764	1.791
Na	0.639	0.610	0.581	0.524

Atoms in A site (Ca+Na+Fe (M<sub>4</sub>) - 2.00)

0.668	0.605	0.596	0.535
-------	-------	-------	-------

100Mg/Mg+Fe ratios

66.6	68.2	65.3	65.3
------	------	------	------

compositions ranging from picrites and basalts to andesites and dacites. Magnetite is also present as a cumulus phase in the plutonic blocks. Textural relations suggest crystallisation throughout the entire suite. Exsolution features are common ranging from fine lamellae to coarse intergrowths. In some unexsolved magnetite phenocrysts there appears to be a zonation in Ti content from core to rim, decreasing in concentration towards the margin. The absence of a separately crystallising rhombohedral phase is a feature in common with the calc-alkaline suites of St. Kitts (Baker, 1968) and Montserrat (Rea, 1970).

#### 9:5:7 Minor Constituents

Quartz is present as a minor constituent in some basaltic compositions, probably as a relict phase stable at high pressure. Occasional corroded and embayed quartz grains are observed in some dacites. It is possible that reduction in load pressure (Green and Ringwood, 1968) or reduction in  $P_{H_2O}$  (Tuttle and Bowen, 1958) may cause resorption of previously crystallised quartz phenocrysts in the dacitic magmas.

Apatite is a common phenocryst mineral present in small amounts ( $< 5\%$  modally) in andesites and dacites. Reconnaissance analysis for F with the electron microprobe did not reveal detectable quantities of this element. Frequently the apatite phenocrysts appear to be full of minute iron-oxide inclusions.

Biotite is occasionally present in vesicles or as a minor, interstitial groundmass phase in alkali and transitional basalts.



It is more common in the coarsely porphyritic compositions perhaps reflecting the late-stage build up of volatiles.

#### 9:5:8 Summary

In summary the mineralogy and petrography of the Grenada volcanic suite provides important information concerning the nature of the parental compositions, evolutionary trends and the behaviour of the differentiating magmas. The gradation from typically alkaline ultrabasic to calc-alkaline mineralogical assemblages is unusual in an island-arc environment and complicated by the variable chemical composition of the magmas. However, the continuous variation in mineral composition and abundance provides support for the hypothesis that the silica-saturated andesites and dacites are derived by fractional crystallisation of basaltic magma.

## CHAPTER 10

PETROGENETIC RELATIONSHIPS AMONGST GRENADA MAGMAS

This chapter is concerned with several aspects of the petrogenesis of volcanic rocks. Following an introduction to general problems associated with the Grenada volcanic suite, a discussion of the relevant features of island arcs and the global theory of plate tectonics is developed. Subsequently evidence from Grenada is used to explore concepts of magma generation in the Upper Mantle and the evolution of these magmas during movement towards the surface of the earth.

10:1 Introduction

The problem of generation of magmas in the Upper Mantle has been studied by experimental petrologists for several decades, but there is still a lack of agreement on this subject. Points of dispute include:

- 1) the exact chemical and mineralogical composition of the Upper Mantle.
- 2) the nature of liquids produced during partial melting under different P, T and volatile-present conditions.
- 3) the role of various fractionating crystalline phases during the subsequent evolution of the partial melts.

O'Hara (1968) concluded that even the most primitive basalt compositions at surface have suffered crystal fractionation to some degree. During the study of a differentiated volcanic suite, it is often possible to infer the composition of the most primitive liquids of the suite. Since these have probably also



suffered crystal fractionation processes, deductions can only be made concerning source conditions and evolutionary paths of the liquids. However, these data still provide invaluable constraints on hypotheses of the nature and origin of liquids generated in the Upper Mantle.

Particularly important in this field of enquiry are suites of rocks that represent compositional links between magmas that occur elsewhere in isolation, or are associated with other types of volcanic rock. The presence of strongly undersaturated basaltic magmas in the island-arc situation of Grenada, constitutes one of these unusual occurrences (Sigurdsson et al., 1973). The more usual appearance of undersaturated alkali basalt magma is in mid-oceanic islands or in continental rift volcanoes. The normal evolutionary trend of magmas in these situations is towards increasing degrees of undersaturation (Kuno, 1968). Thus the Grenada suite is unusual in two respects. Firstly, the occurrence in the island arc situation of strongly undersaturated magmas. Secondly, the subsequent evolution of these magmas towards more silicic compositions reflects the local tectonic environment and is unlike the behaviour of similar compositions found in other environments.

The study of the alkali basalt association of Grenada is further concerned with three fundamental topics of igneous petrology:

- 1) The chemical and physical nature of the Upper Mantle beneath island arcs.
- 2) The processes of magma generation in island arcs and

the evolution of this system with time.

- 3) The comparison of petrogenetic processes in island arcs with the petrogenesis of volcanic suites in other tectonic situations.

### 10:2 Island arc tectonics

It is appropriate to explore aspects of the global theory of plate tectonics relevant to island arcs. The term "plate" denotes the rigid lithosphere formed of crust plus rigid portion of the underlying Upper Mantle. This plate is decoupled from the rest of the mantle by the non-rigid asthenosphere (Fig. 42 ). The theory of plate tectonics (Isacks et al., 1968) identifies segments of the lithosphere (plates) of the Earth that are in motion relative to one another. The three main types of boundary that can exist between these plates and the topographic features associated with them are:

<u>Type of boundary</u>	<u>Topographic feature</u>
1) spreading boundary	mid-ocean ridge or continental rift
2) collision boundary	island arc or mountain belt
3) shear boundary	transform fault

The calc-alkaline rock suite is typical of collision boundaries. The bulk composition of andesite, the predominant individual member of this suite, is equivalent to the average composition of continental crust (Taylor and White, 1965). It is probable that the calc-alkaline rock suite is a major component of the continental crust. The lower density of this crust relative to the mantle makes its subduction into the mantle along a collision



boundary unlikely. Thus the nature of the differentiation of the crust from the mantle may be a one-way process in time. In addition the range and abundance of compositions of the crust may result from the mode of differentiation of the calc-alkaline rock suite.

The relative densities of lithospheric plates determine whether subduction of one beneath another is possible. It appears that only lithosphere created at spreading boundaries forming oceanic crust is normally dense enough to be subducted. Since island arcs are related to zones of subduction, a major role for the downgoing plate in this situation has been advocated for the origin and development of island arc magmas. Partial melting of the plate itself has been suggested as a possible magma source (Fitton, 1971). However, it is possible that the subducted plate merely acts as a physical trigger for the initiation of melting in the Upper Mantle, or that selective release of volatiles from the plate initiates the same process.

The explosive nature of the eruptions of island arc volcanoes, and the frequent occurrence of hydrous minerals within the rocks, suggest that volatiles such as water are important components of the magmas. Possible sources of volatiles may be:

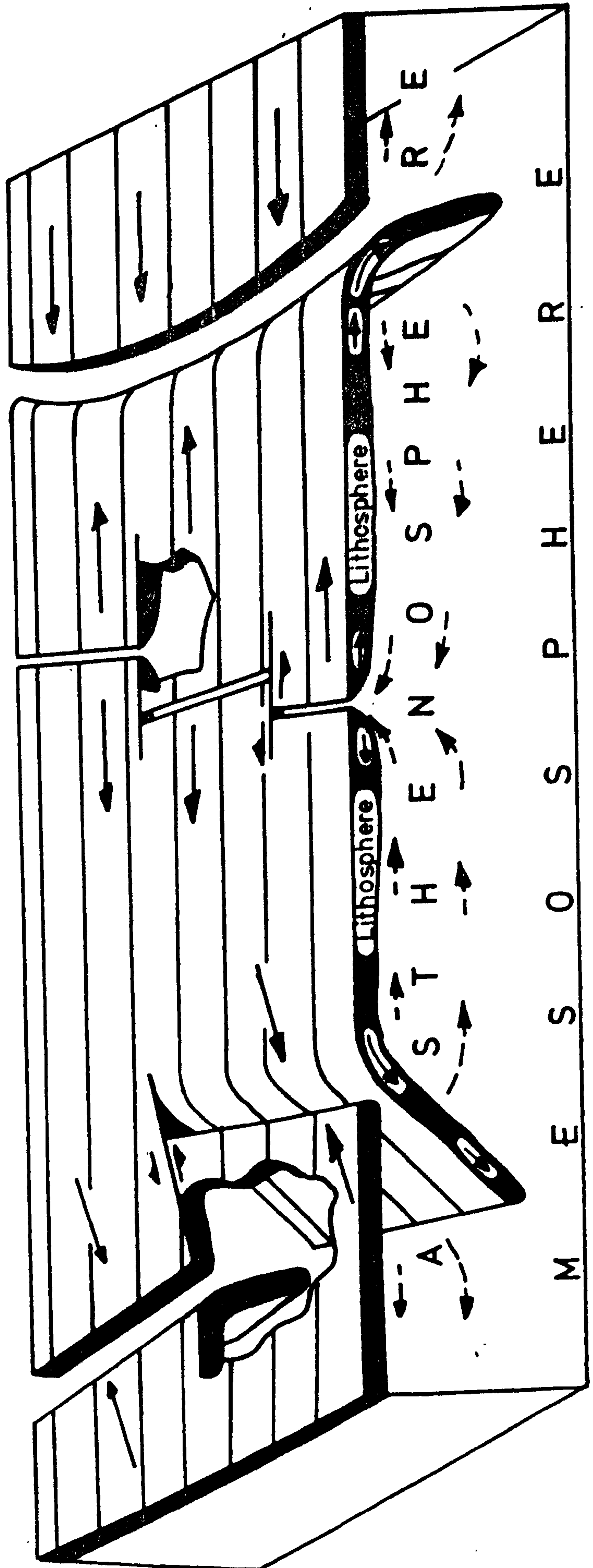
- 1) the hydrated surface layers of the subducted oceanic plate
- 2) juvenile water within the Upper Mantle
- 3) water contained within the crust through which the magmas are erupted

It is important to assess the possible role played by each of these sources in the development of the calc-alkaline rock suite.

Fig.42

Model of upper 700 km of the Earth showing possible relative motions of lithosphere. (After Isacks et al., 1968)  
The model consists of relatively cold lithosphere (30-100 km thick) underlain by the asthenosphere, a layer of low, long term strength. Dashed arrows indicate possible return flow in the Upper Mantle.





Current information and hypotheses concerning these topics will be explored in the following sections.

#### 10:2:1 Dehydration of the subducted plate

The oceanic crust has been extensively explored by geophysical and geochemical methods, particularly in the last decade. The results of numerous magnetic and seismic surveys have not only provided support for the theory of plate tectonics, but also revealed the strikingly uniform, layered nature of the oceanic crust Table 34. Direct sampling, by the Deep Sea Drilling Project research vessel, has shown that the uniform nature of the (basaltic) layer 2 of the oceanic crust and the measured ages of this material are also in accordance with the predictions of plate tectonics. A model for the formation of the lithosphere formed at oceanic ridges by the upwelling and differentiation of basalt magma has been proposed by Cann (1970) and is illustrated in Fig. 43 . This magma is produced by partial melting of the asthenosphere of the Upper Mantle. The exact mechanism of movement of the lithosphere away from the ridge is unknown. It is believed to be related to a complex convective motion within the Upper Mantle (e.g. Elsasser, 1971). The partial melting giving rise to the basalts extruded at the ridges is probably related to decreased pressure and thermal upwelling associated with this convective motion.

The composition of the upper surface of layer 2 of the oceanic crust has been found to be distinct and remarkably uniform in all oceans so far sampled (Engel, Engel and Havens, 1965). It has been given the term 'oceanic tholeiite' and since



Fig.43

Model of the structure of oceanic crust generated  
at mid-ocean ridges.

(After Cann, 1970).

The lower part of layer 3 is believed to contain  
a considerable proportion of cumulus rock compositions.

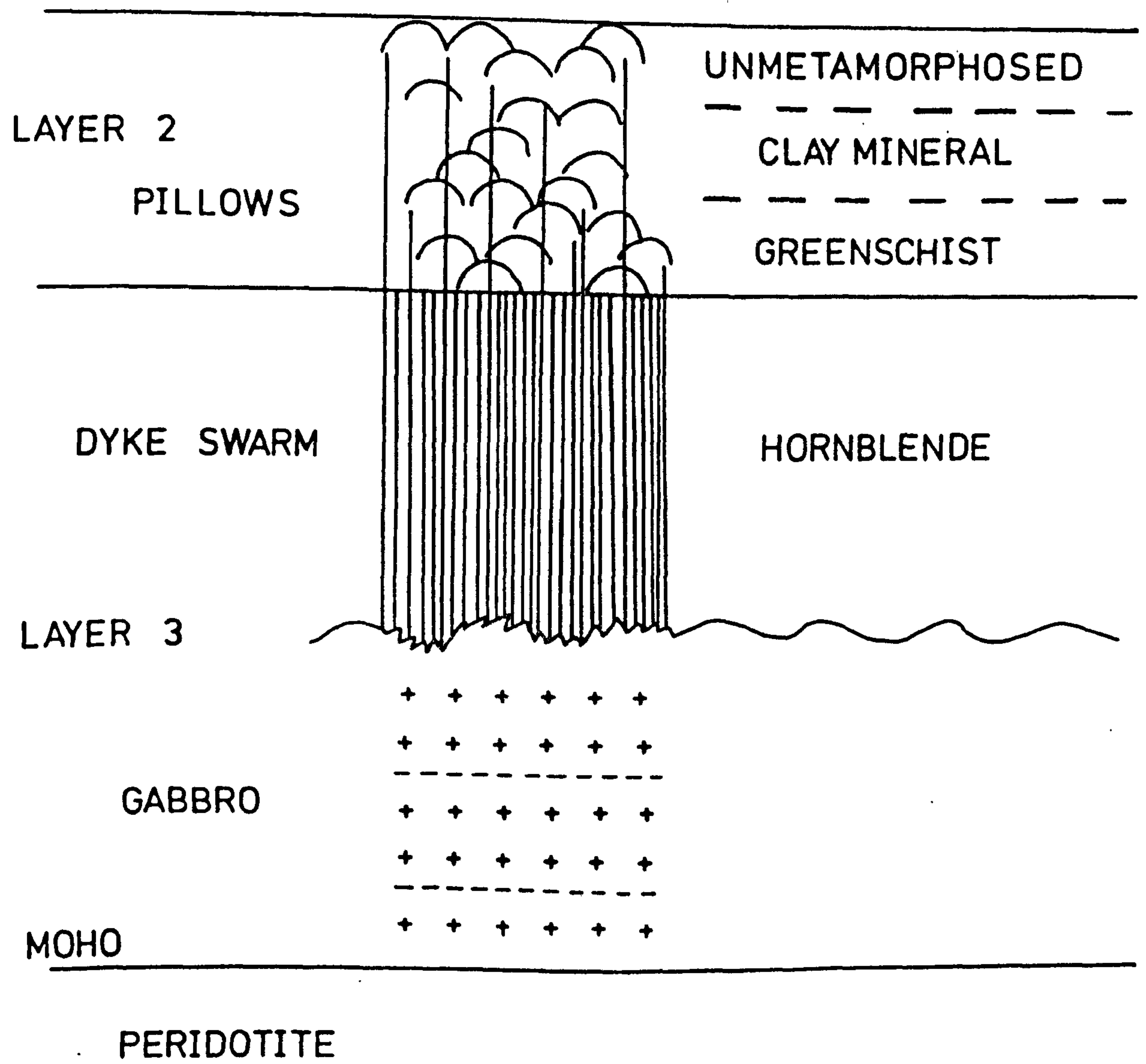




TABLE 34

Velocity structure of the oceanic crust

	<u>P velocity</u> (km/sec)	<u>Average</u> <u>thickness</u> (km)
Layer 1	1.6-2.5	0.4
Layer 2	4.0-6.0	1.5
Layer 3	6.4-7.0	5.0
- - - - - MOHO - - - - -		
Upper Mantle	7.4-8.6	

TABLE 35

Comparison of oceanic tholeiite and oceanic alkali  
basalts with a Grenadan picrite and alkali basalt

	1	2	3	4	5	6
	OT	OT	AB	AB	61	476
SiO <sub>2</sub>	49.94	49.48	48.00	44.90	44.63	45.33
Al <sub>2</sub> O <sub>3</sub>	16.69	16.72	17.42	22.80	15.30	15.22
Fe <sub>2</sub> O <sub>3</sub>	9.01	8.62	10.19	6.41	10.10	10.04
MgO	7.28	8.20	4.55	5.09	14.27	14.66
CaO	11.86	11.14	9.60	9.16	11.36	11.17
Na <sub>2</sub> O	2.76	2.66	4.00	4.00	2.46	1.72
K <sub>2</sub> O	0.16	0.24	1.30	1.76	0.65	0.53
TiO <sub>2</sub>	1.51	1.39	3.20	2.85	0.82	0.93
MnO	0.18	0.19	0.13	0.12	0.22	0.22
P <sub>2</sub> O <sub>5</sub>	0.16	0.12	0.54	1.26	0.18	0.18
Ba	14	19	340	740	170	193
Nb	30	30	64	82	9	25
Zr	95	88	300	340	75	88
Y	43	44	46	52	17	18
Sr	130	160	510	740	617	555
Rb	10	10	26	44	17	11
Cu	77	86	58	34	86	61
Ni	97	140	28	63	434	461

1-4 from Engel et al. (1965)

5 and 6 are from this study.



the composition is important in future discussion, representative analyses are given in Table 35. The low abundance of alkalis and incompatible trace elements are particularly noticeable features. Many samples recovered from the oceanic crust, however, have been metamorphosed and hydrated since their formation. Chemical changes related to the extent of marine exposure have been discovered (Hart, 1973). These may result in an increase of Mg and Fe relative to oceanic tholeiite, and depletion of Si, Ca and alkali elements. The composition of the altered basalt is still probably nearer basaltic than ultrabasic in nature, and the effect is probably limited to the near surface layers. As the cooling lithosphere moves away from the ridge, it gradually becomes covered with a layer of sediment (Layer 1), and may be transported to a zone of subduction. It is possible that varying proportions of sediment cover may be either subducted into the Upper Mantle or scraped off and left at the crustal surface.

The plate is initially cold relative to the mantle at the site of subduction, and this may be a factor contributing to its descent (Ringwood, 1972). However, a combination of processes will raise the temperature of the plate. Toksöz et al. (1971) have proposed a temperature configuration, primarily due to shear strain heating along the subduction zone, which is here represented in Fig. 44. During this heating process, the hydrated sedimentary and amphibolitic upper layers of the oceanic crust will decompose, releasing water and other volatiles. It is at this stage of the subduction process that the role of water from the subducted slab

Fig.44a

Thermal model for the mantle in a subduction region.

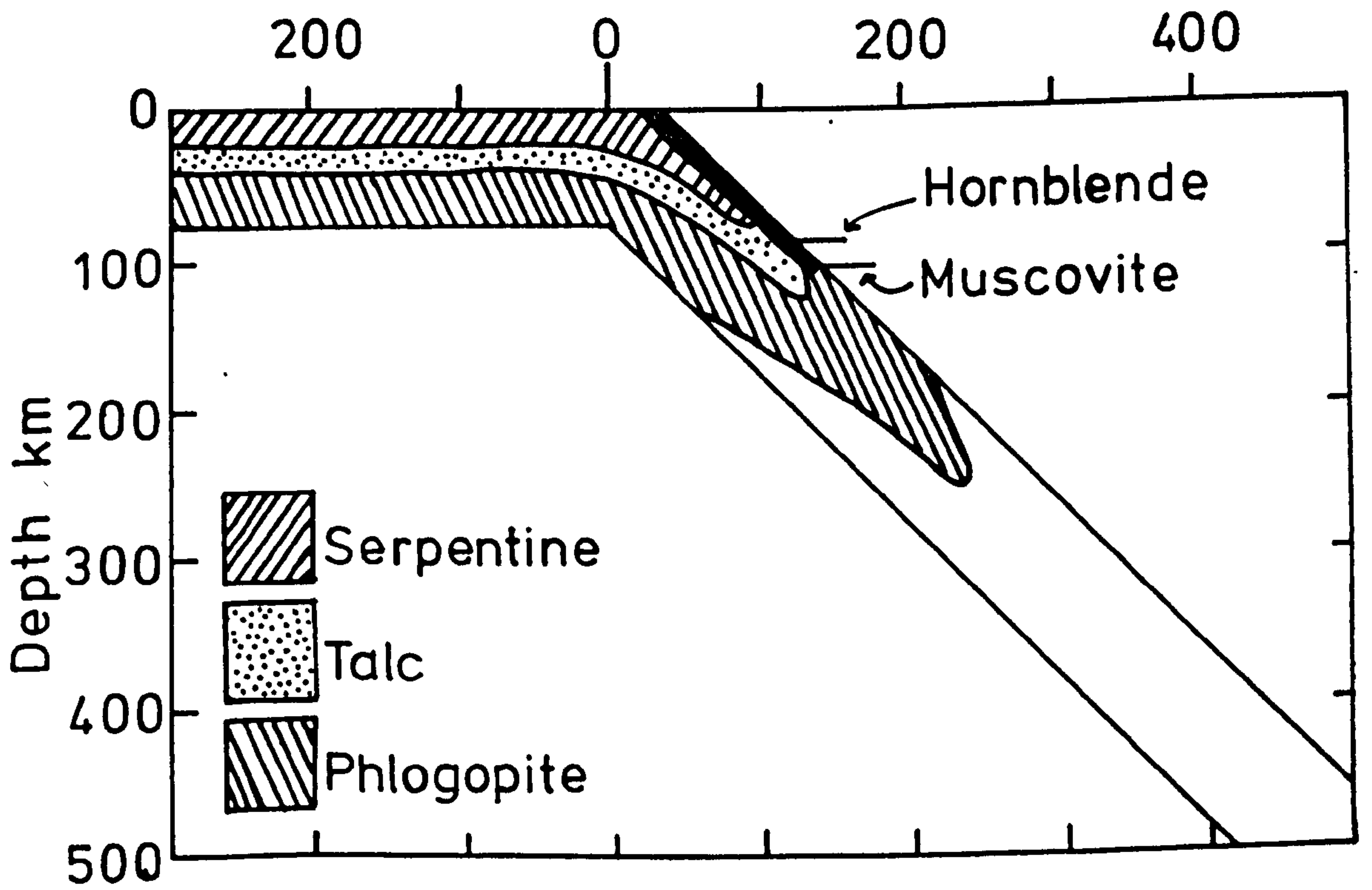
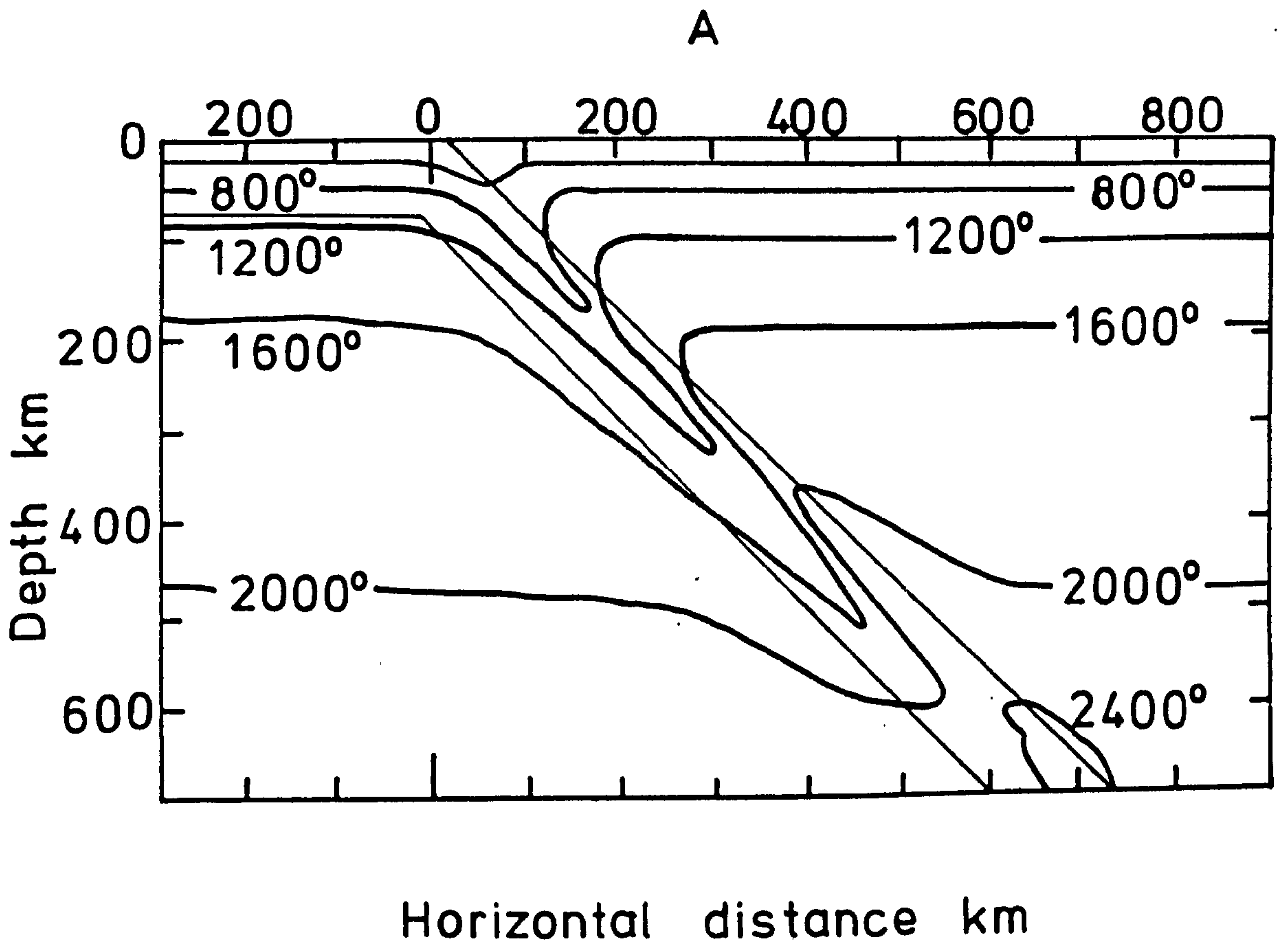
(After Toksöz et al., 1971)

Fig.44b

Schematic cross section through subducted slab showing oceanic crust (in black) and maximum depths to which hydrous minerals can be carried according to the temperature distribution in the upper diagram.

(After Wyllie, 1973).





may become crucial in the development of island arc magmas.

Fitton (1971) suggested that the breakdown of amphibole leads to the generation of magmas of the island arc tholeiite series (Jakes and Gill, 1970). Partial melting of eclogite during further subduction of the dehydrated slab would lead directly to the development of andesitic magmas (Green and Ringwood, 1968). The stability fields and dehydration temperatures of the appropriate minerals have been reviewed by Wyllie (1973), and the temperature profile data of Toksöz <sup>"</sup>et al. (1971) may be used to predict the depths at which the dehydration reactions will occur (Fig.44).

The important point about the temperature distribution in a subduction regime, according to Wyllie (1973), is that "the hydrous minerals likely to be reasonably abundant in oceanic crust and sediments become dehydrated before they reach a depth of 100 km". In most island arcs, this depth is reached before the 'volcanic front' of Sugimura (1967). Fig. 45 illustrates the spatial relations of subducted plate, depth to which hydrous minerals are stable and the locus of volcanic activity in Japan. In this situation it seems most likely that volatiles derived from the subducted plate are not involved in generation of the island arc magmas.

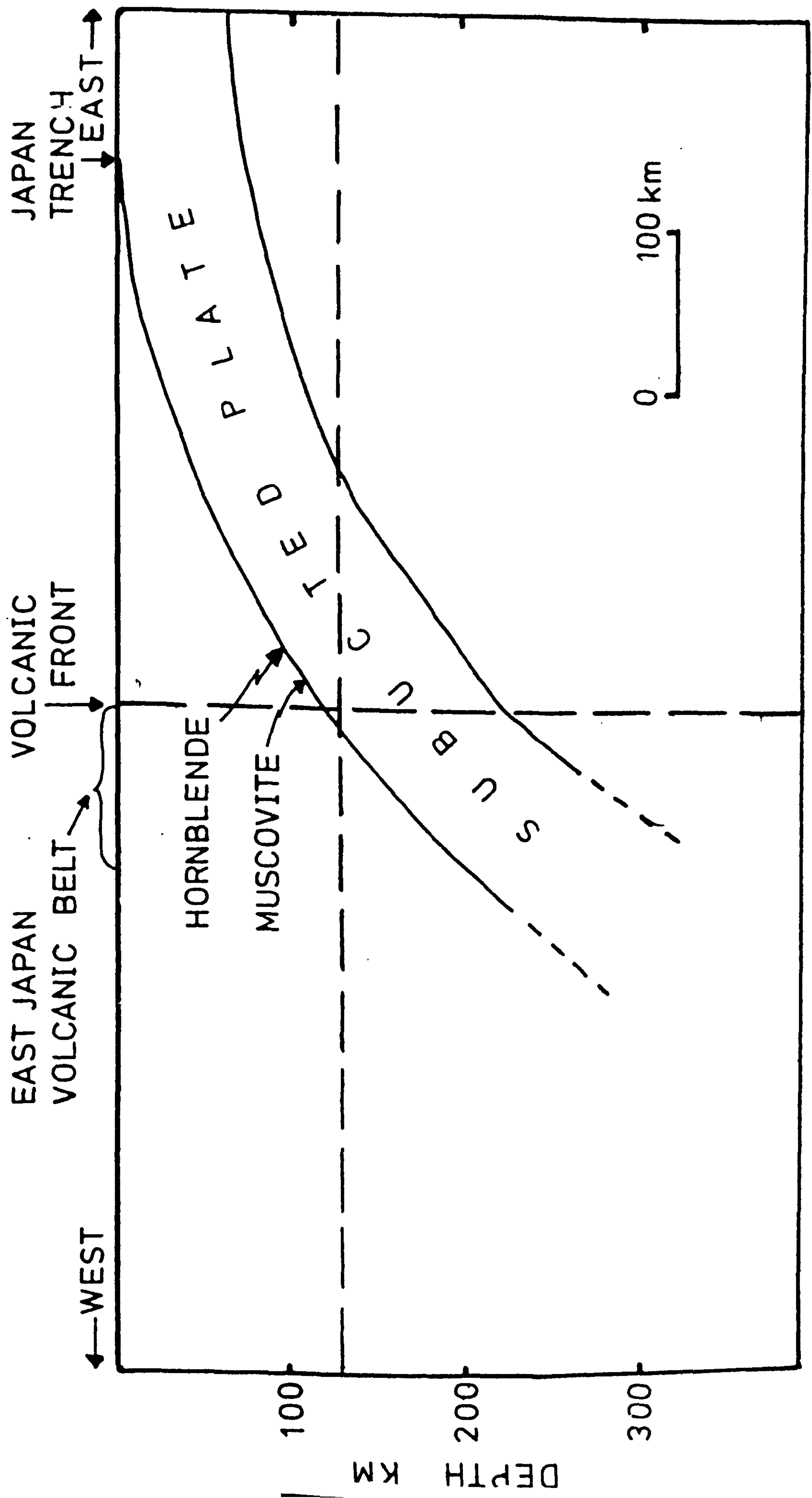
The location of the subducted plate beneath an island arc is generally assumed to be coincident with the locus of earthquakes or Benioff zone. The results of recent island arc earthquake studies have been summarised by Sykes (1972), and the inaccuracy



Fig.45

Relationship of volcanic front, subducted plate and predicted stability limits of hydrous minerals in an island arc environment.

The figure is adapted from Sugimura (1967) who suggested that the intersection of the dashed lines at 130 km depth beneath the volcanic front in East Japan locates the replacement of frequent earthquakes as an energy release mechanism by magma generation in the Upper Mantle. Note that the active volcanism occurs beyond the depth/distance stability limits of hydrous minerals in the subducted plate (Wyllie, 1973).





associated with the identification of the Benioff zone as the locus of plate-mantle contact . described. The configuration of the Benioff zone beneath the Lesser Antilles island arc was described in Chapter 2 . It is present at a depth of approximately 115 km beneath Grenada and reaches a maximum depth beneath the arc of 160 km further north. Allowing for inaccuracies in location of the upper surface of the subducted plate beneath Grenada, it is possible that dehydration reactions within the plate may be associated with the volcanicity of Grenada. It seems unlikely that plate-derived volatiles are involved in the arc further to the north. Chemical considerations of the possible role of this effect will be pursued further (p.311 ), and magma zonation in island arcs generally will be discussed in Chapter 11 . However, alternative sources of volatiles that may be associated with island arc volcanicity will now be discussed.

#### 10:2:2 Juvenile water within the Upper Mantle

Analysis of the travel times of earthquake-induced shock waves have revealed a widespread zone of reduced seismic velocities within the Upper Mantle (Dorman et al., 1968). This occurs between 60 km and 160 km depth beneath oceanic crust and between 120 km and 220 km beneath continents. The theory of plate tectonics equates this 'Low Velocity Zone' with the asthenosphere. Lambert and Wyllie (1970) have suggested that the physical characteristics of the Low Velocity Zone are the result of a hydrous, interstitial melt produced at pressures greater than the stability limit of amphibole. The presence of CO<sub>2</sub> in mantle-derived magmas has been

inferred by Roedder (1965) and the characteristics of the Low Velocity Zone specifically attributed to the presence of this phase by Green (1972).

The production of the atmosphere and hydrosphere by degassing of the Earth's mantle is unlikely to have been completed (e.g. Roedder, 1965). Thus it is probable that volatiles such as  $H_2O$  and  $CO_2$  are still present in the mantle. Hill and Boettcher (1970) have shown that if  $P_{H_2O}$  approaches  $P_{tot}$  at mantle pressures, considerable quantities of silicate melt would be produced. The geophysical data do not permit this possibility on a widespread scale. The lowering of  $P_{H_2O}$  by the presence of  $CO_2$  has been shown to have a slight effect on the solidus at mantle temperatures and pressures (Fig.46) (Hill & Boettcher, 1970). It is thus unlikely that the content of water stored in hydrous mineral phases, or dissolved in interstitial silicate melts where these phases are unstable, exceeds 1% by weight. However, it is most probable that the Low Velocity Zone does contain a small proportion of hydrous interstitial melt, and this must be taken into account as a source of volatiles in island arc magmas.

#### 10:2:3 Water in the crust

The hypothesis that the calc-alkaline trend is determined by the dissociation of water added to a differentiating basalt magma leading to constant or increased oxygen fugacities, was proposed by Osborn (1969). The suggested source of this element exchange was in the crustal sediments surrounding the magma chamber. Arguments will be developed in this account which suggest



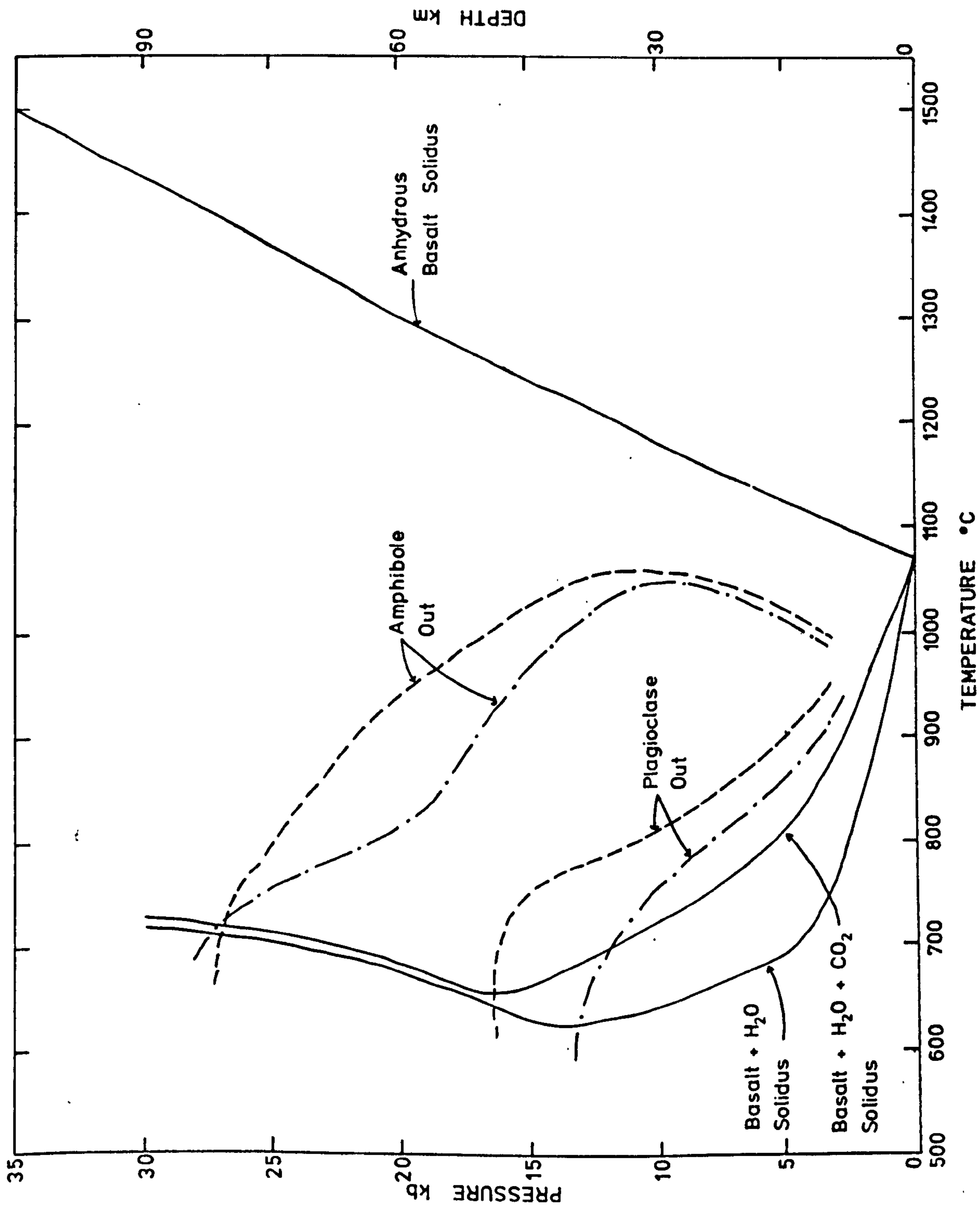
Fig.46

Pressure-temperature projection of curves representing the beginning of melting of vapour saturated basalt-water and basalt-water-carbon dioxide ( $P_{H_2O} = 0.5 P_{tot}$ ) compositions.

The dashed curves for the upper stability of plagioclase and amphibole represent the basalt-water-carbon dioxide compositions.

The dash-dot curves refer to the basalt-water compositions.

(After Hill and Boettcher, 1970).





that the evolution of the Grenada calc-alkaline suite was initially determined at greater depths than the crust. However, the importance of  $P_{O_2}$  in determining the evolution of a differentiating magma has been summarised by Hamilton and Anderson (1967). This subject will be discussed further in relation to the role of volatiles within magmas (p.286).

### 10:3 The origin of the undersaturated magmas of Grenada

It is now possible to examine critically the occurrence of undersaturated magmas in Grenada, and to consider alternative models for their generation. From the preceding account it is apparent that two main parental composition must be considered as a possible source of island arc magmas. The first consists of the basaltic Layer 2 of the subducted oceanic plate plus possible sedimentary contaminants. The complete melting and removal of Layer 2 of the plate is required in order to involve the more basic to ultrabasic compositions of the plate in magma generation. This is considered unlikely. The alternative source is in the ultrabasic, Upper Mantle wedge overlying the subducted plate. Combinations of varying proportions of melt from both sources may be possible.

#### 10:3:1 Partial melting of the subducted lithospheric plate

In all experiments, whether under dry or hydrous conditions of varying pressure, the partial melts produced from basaltic compositions are consistently more siliceous than the parental material (Green and Ringwood, 1967). Complete equilibrium melting

will of course produce a melt identical in composition to the parent rock. Many of the Grenada basalts are considerably less siliceous than the average composition of oceanic tholeiite. Table 34 shows representative analyses of these basalts in comparison with oceanic tholeiite. Included in this table are some silica-undersaturated basalts dredged from oceanic ridges (Engel et al., 1965). Subduction of similar compositions may possibly have occurred at some stage in the evolution of the Lesser Antilles island arc. However, even complete equilibrium melting of these latter compositions would still produce liquids unlike those of the Grenada suite. This is particularly noticeable in regard to the trace element contents.

The possibility that the Grenada compositions represent erupted cumulate rocks was examined in Chapter 7, and shown to be unlikely. Arculus and Curran (1972) examined a multi-stage process involving intermediate episodes of crystal accumulation and complete remelting of the products of a plate-derived magma, and showed that the resulting compositions would still be unlike those observed. Arculus and Curran (1972) also showed that the erupted Grenada compositions are most similar to ultrabasic and basic lavas in tectonic situations remote from any collision margin and possible subduction regimes. The source region of these magmas is most probably the Upper Mantle. The origin of the Grenada suite is therefore believed to have been in the ultrabasic Upper Mantle wedge overlying the subducted plate at a depth less than 115 km. Thus it is necessary to examine the nature of the Upper Mantle and possible melting processes within



the postulated source region.

#### 10:4 Composition of the Upper Mantle

Knowledge of the composition of the Upper Mantle is derived from a combination of geophysical and geochemical techniques. Our chemical knowledge of the Upper Mantle is based to a large extent on the analysis of ultrabasic nodules transported to the Earth's surface within basalts and kimberlites. The nature of these compositions has been the subject of much research (see Wyllie (editor), 1967, for a recent review). In general, it is now believed that the Upper Mantle is composed mainly of a peridotite formed of olivine, orthopyroxene and clinopyroxene. A more aluminous phase such as plagioclase feldspar, spinel or garnet may also be present, depending upon pressure and temperature. Earthquake shock-wave data suggest a considerable proportion of eclogite (garnet plus aluminous clinopyroxene) must also be present. According to Press (1968), up to 50% eclogite may be present in localised pockets beneath oceanic crust. It is unlikely that all basalt melts generated in the Upper Mantle are erupted. Crystallisation of these melts at Upper Mantle temperatures and pressures would form eclogite (Green and Ringwood, 1967). In addition to these compositions, residual peridotite depleted by magma extraction, together with dunites and peridotites precipitated from basaltic magmas during crystal fractionation, may also be present (Harris et al., 1967). One of the consequences of incomplete melting of a subducted lithospheric plate could be the local preservation of eclogite within the Upper Mantle (Arculus and Curran, 1972). Partial

melting of these refractory compositions is unlikely by itself to give rise to the observed range of major and trace element chemistry of erupted magma. However, the inhomogeneity of the Upper Mantle must be considered as a complicating factor during investigation of partial melting processes. The consequences with regard to island arc magmas are discussed in Chapter 11. Experimental petrologists have followed two main lines of investigation of possible melts from ultrabasic compositions. The first approach is the examination of selected synthetic systems designed to model Upper Mantle compositions (e.g. Kushiro, 1972). The alternative method makes use of natural compositions in two ways. Firstly, the crystallisation of basalt melts at Upper Mantle temperatures and pressures should reveal the mineral phases in equilibrium with the melt under these conditions (Green and Ringwood, 1967). If the melt really was derived from the mantle unchanged, the crystallising phases should be those stable in the mantle at the same temperatures and pressures. Secondly, a variety of ultrabasic nodules have been selected as representative of primary, undepleted Upper Mantle peridotite and their melting behaviour studied (e.g. Ito and Kennedy, 1967).

It was mainly to avoid the difficulties associated with selection of truly representative natural peridotites that Green and Ringwood (1963) proposed the term 'pyrolite' to cover the parental material. A specific composition was calculated by combining an average basalt composition (Nockolds, 1954) with very refractory dunite in the proportions 1:3. A more refined model using an olivine tholeiite from Hawaii and harzburgite



residua (olivine plus orthopyroxene), again in the proportions 1:3, was later proposed by Ringwood (1966). The predicted mineralogical stability fields of pyrolite are shown in Fig. 47 . At the solidus temperatures, there is a considerable zone (10-30 kb) where a separate aluminous phase is absent and the mineralogical assemblage is olivine + aluminous pyroxenes.

O'Hara (1968) has criticised this scheme on several counts. Firstly he suggests the results of Ito and Kennedy (1967) show that a natural garnet peridotite, with lower  $Al_2O_3$  content than pyrolite, has spinel or garnet at the solidus up to 40 kb. The coexisting pyroxenes also show appreciably less solution of  $Al_2O_3$  than predicted by the pyrolite model. The proposal of Clark and Ringwood (1964) that the existence of the Low Velocity Zone depends on the presence of such aluminous pyroxenes has been superceded by the suggestion of the presence of interstitial melt (Lambert and Wyllie, 1970). O'Hara (1967) has also shown that solubility of  $Al_2O_3$  in coexisting pyroxenes from a wide variety of mantle-derived ultrabasic nodules are consistently lower (less than 5% in both pyroxenes) than the predicted solubility in pyroxenes of the model pyrolite. The zonation of mantle mineralogy according to O'Hara (1965) is given in Fig. 47 . The differences between the schemes of O'Hara and of Green and Ringwood are important during discussion of both melting and subsequent crystallisation of basalt magmas. The model according to O'Hara (1965) is preferred here for the consistency displayed between experimental and naturally occurring phase relationships.

Fig.47

Upper Mantle mineralogical stability fields.

Upper diagram according to O'Hara (1967). Lower diagram according to Green and Ringwood (1967).

Note the broad field of stability (10-30 kb) of olivine plus aluminous pyroxenes, and absence of a separate aluminous phase on the solidus in the Green and Ringwood model.

Ol = olivine

Opx= orthopyroxene

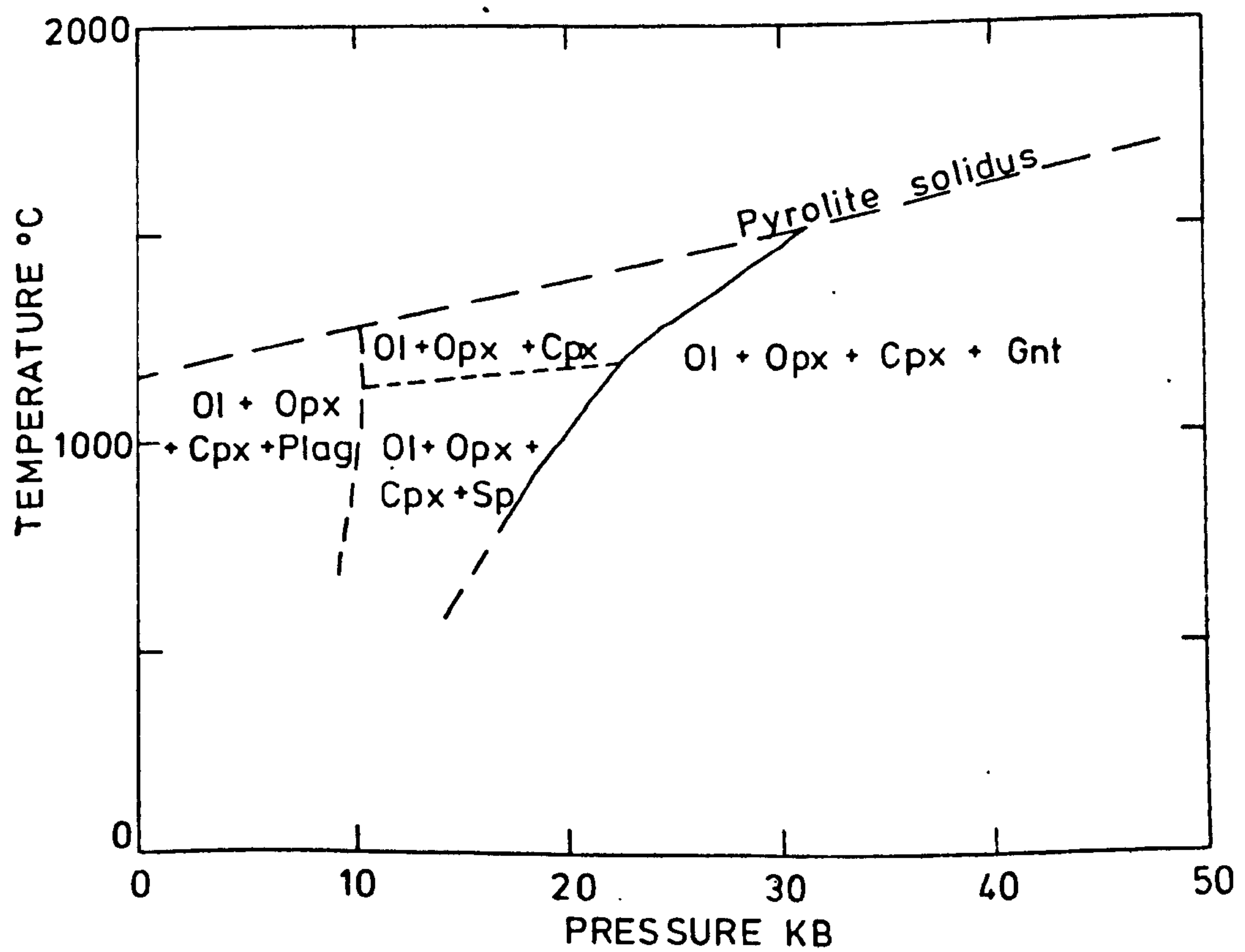
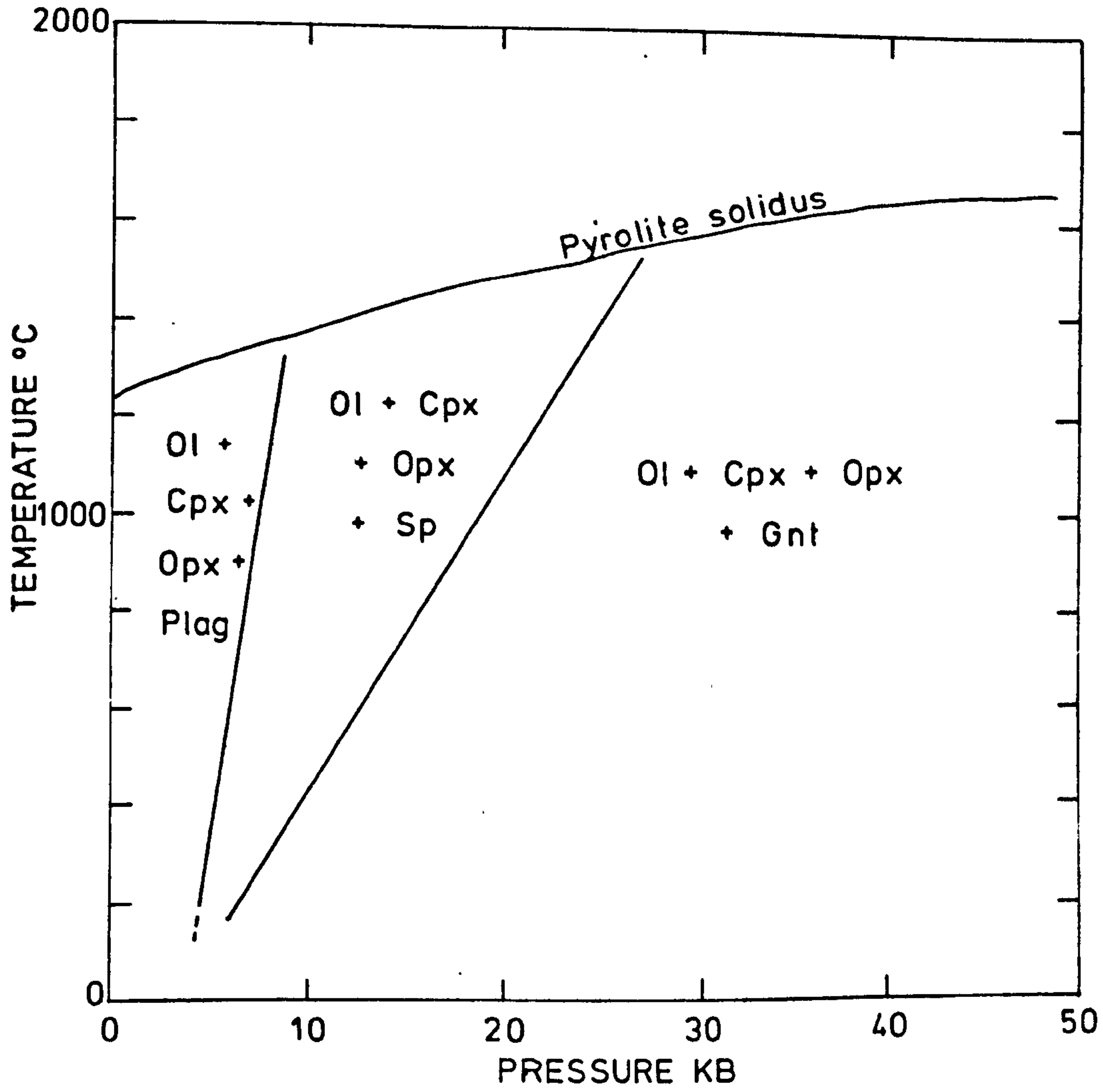
Cpx= clinopyroxene

Pl = plagioclase

Sp = spinel

Gnt= garnet





### 10:5 Partial melting of the Upper Mantle

The results of several experiments relating to dry and wet melting of the Upper Mantle have been reported in recent years (Wyllie, 1971, for a review). The results of these are summarised in the following sections, but it is recognised from the preceding discussion that the situation beneath island arcs is probably one where  $P_{H_2O} = P_{tot}$ . In view of the continued experimental difficulties encountered during investigations of Fe-bearing systems (Merrill and Wyllie, 1973) the results of such experiments must always be reconciled with natural evidence.

The nature of basalt magmas generated by partial melting of the Upper Mantle are determined by:

- 1) the depth at which melting occurs
- 2) the mineralogical and chemical composition  
at the depth of melting
- 3) the temperature interval in excess of solidus  
temperature
- 4) the amount of water present and its physical state.

#### 10:5:1 Dry partial melting

The most comprehensive schemes of dry partial melting have been proposed by O'Hara (1968) and Green and Ringwood (1967). Although points of conflict exist between these schemes, particularly with regard to the nature of the parent material and the role of orthopyroxene fractionation, there is broad agreement concerning the nature of the melts produced at increasing



depths under dry conditions. The two schemes are shown in Fig. 48 . In general, for a given percentage of partial melt, these melts become progressively less siliceous with depth. O'Hara (1968) has pointed out that under dry conditions with predicted mantle geotherms, partial melting of peridotite (ol + cpx + opx + aluminous phase) is impossible. Uprise of mantle diapirs intersecting the peridotite solidus was suggested as a possible mechanism for initiating dry melting by Green and Ringwood (1967).

#### 10:5:2 Wet partial melting

Although controversy exists regarding dry melting of the Upper Mantle, the situation where water is present is much more complicated.

Kushiro (1972) has summarised the results of a series of investigations of synthetic ultrabasic systems under conditions where  $P_{H_2O} = P_{tot}$ . In all cases, the initial melt produced is oversaturated with silica. Only with a large volume of equilibrium partial melting does the liquid become undersaturated. Fig. 49 illustrates the relationships discovered. Kushiro suggests that quartz tholeiite and andesitic magmas may be produced from the Upper Mantle by partial melting under conditions where  $P_{H_2O} = P_{tot}$  and the volume of partial melt is generally less than 30%. Similar results have been reported by Kushiro (1972) by experiments carried out under the same conditions ( $P_{H_2O} = P_{total}$ ) with a naturally occurring spinel peridotite. The production of silica-saturated melts from Upper Mantle compositions depends upon the presence of the reaction relationship.

Fig.48a

Summary diagram of basalt fractionation relationships according to O'Hara (1965).

Vertical sequences are dominated by olivine fractionation. Mineral phases fractionating during arrested ascent and isobaric crystallisation indicated by right hand column.



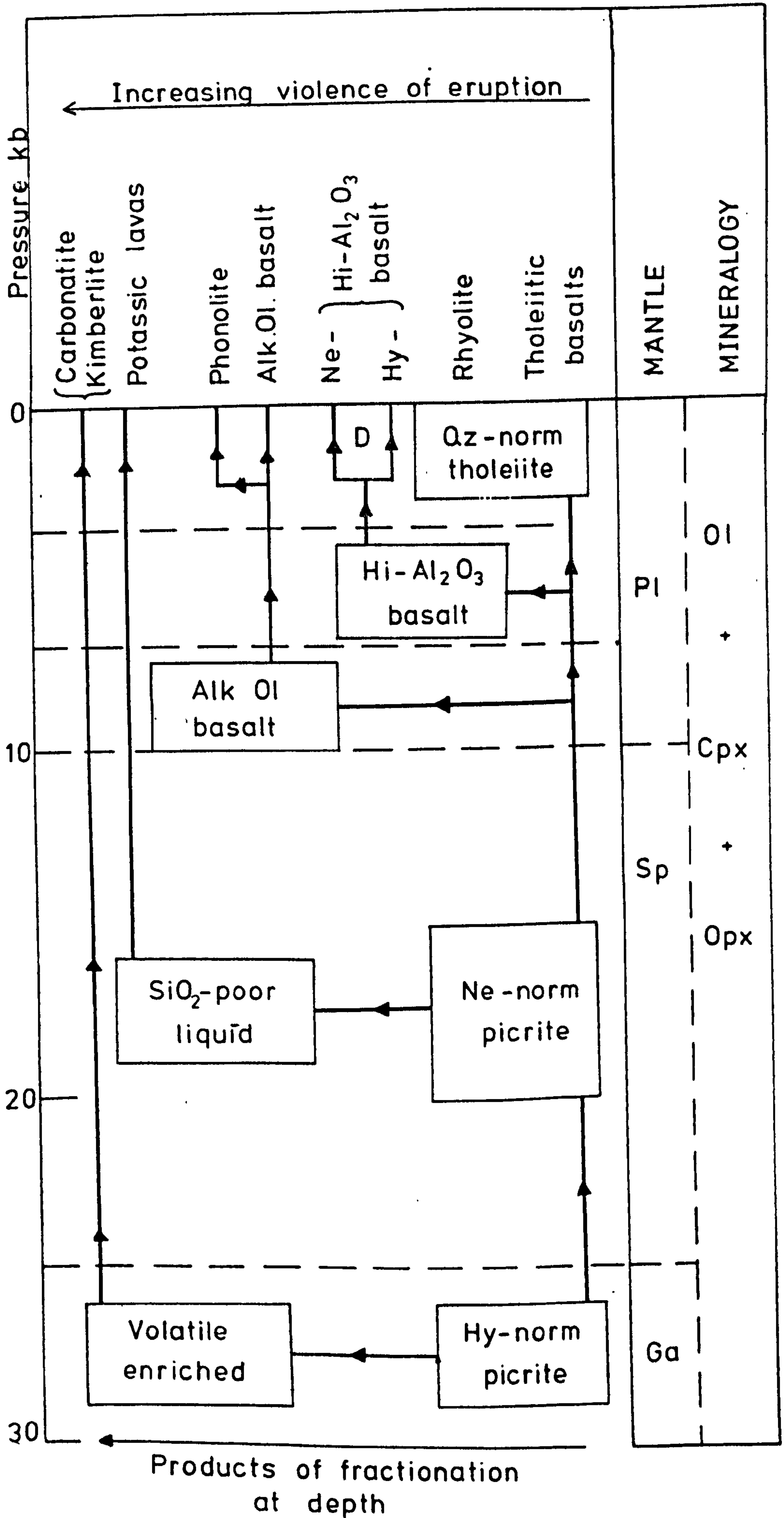
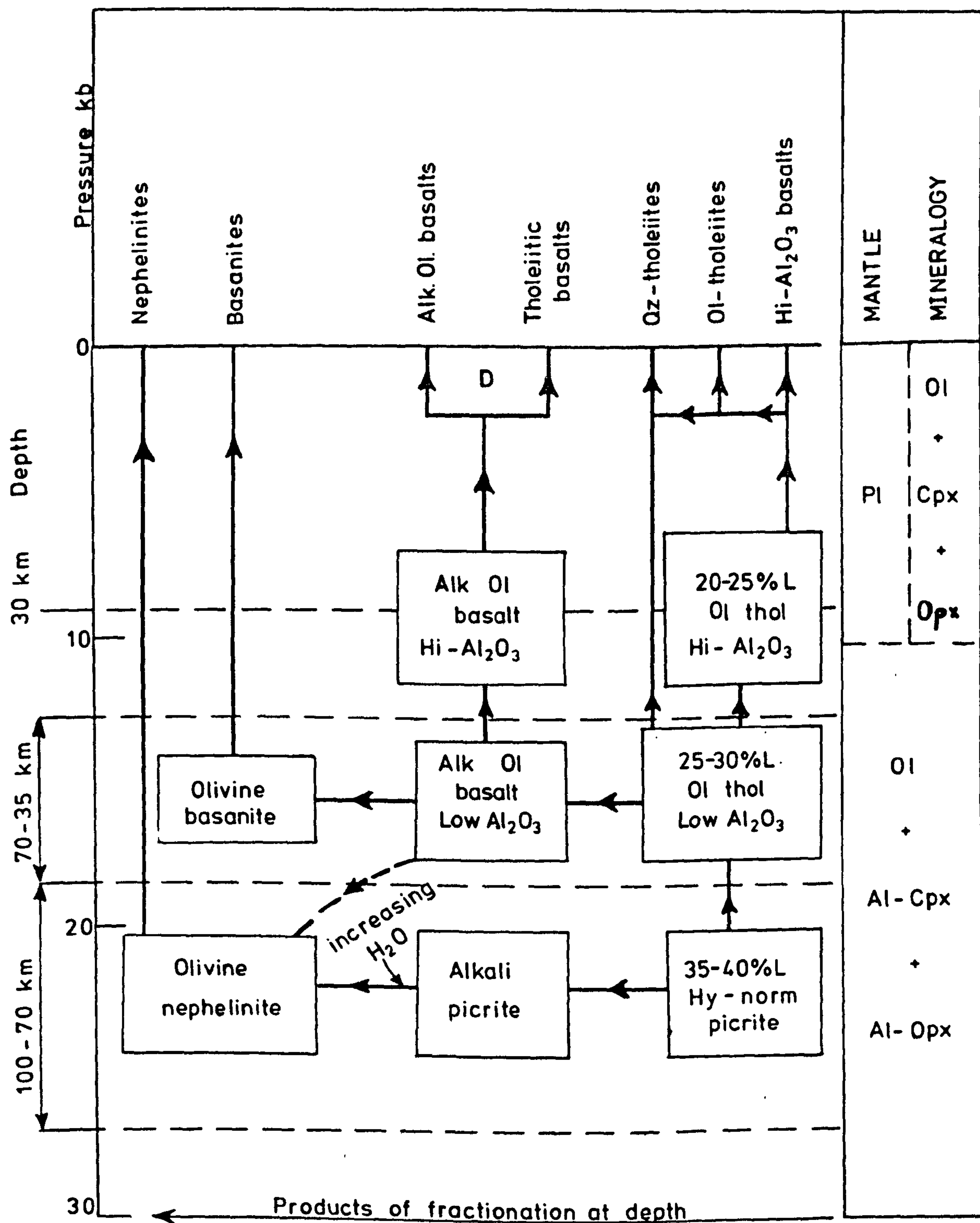


Fig.48b

Summary diagram of basalt fractionation relationships according to Green and Ringwood (1967) and Green (1970). Vertical sequences are dominated by olivine plus aluminous pyroxenes fractionation. Pyroxenes become progressively less aluminous with decreasing pressure. Aluminous pyroxenes are the dominant crystallising phases during isobaric fractional crystallisation. Stable mantle mineralogy indicated in right hand column.





Mg-olivine + Qtz-normative liquid      Mg-orthopyroxene.

The incongruent melting of enstatite (Mg-orthopyroxene) is suppressed in the dry system at pressures greater than 5 kb (Boyd et al., 1964), but persists under conditions where  $P_{H_2O} = P_{tot}$  at least to 30 kb (Kushiro et al., 1968).

In direct opposition to the above hypothesis, Bultitude and Green (1968) reported a major liquidus role for orthopyroxene at 20-30 kb in nephelinitic magmas for conditions reported to be  $P_{H_2O} = P_{total}$ . As a result of criticism of the experimental method by Kushiro (1969), Green (1969) confirmed the original results with 2%  $H_2O$  at 27 kb. Green (1970) suggests that a major fractionation role for orthopyroxene under hydrous conditions may produce the range of strongly undersaturated nephelinitic magmas at pressures greater than 18 kb.

The conflict about the nature of the wet partial melting products of the Upper Mantle may be resolved when experiments at controlled  $P_{H_2O}$  are completed. Unfortunately the high reaction rates of buffers currently employed would make such an investigation difficult at the appropriate temperatures and pressures (Holloway, Burnham and Millhollen, 1968). However, in view of the evidence from Grenada it is possible to discuss further the predictions of these experimental results.

O'Hara (1968) has shown that the enrichment of incompatible elements in the melt is not a linear relationship with percentage of partial melt produced. Fig. 25 (Chapter 7) shows that the greater enrichment occurs during the early stages of partial



Fig. 49

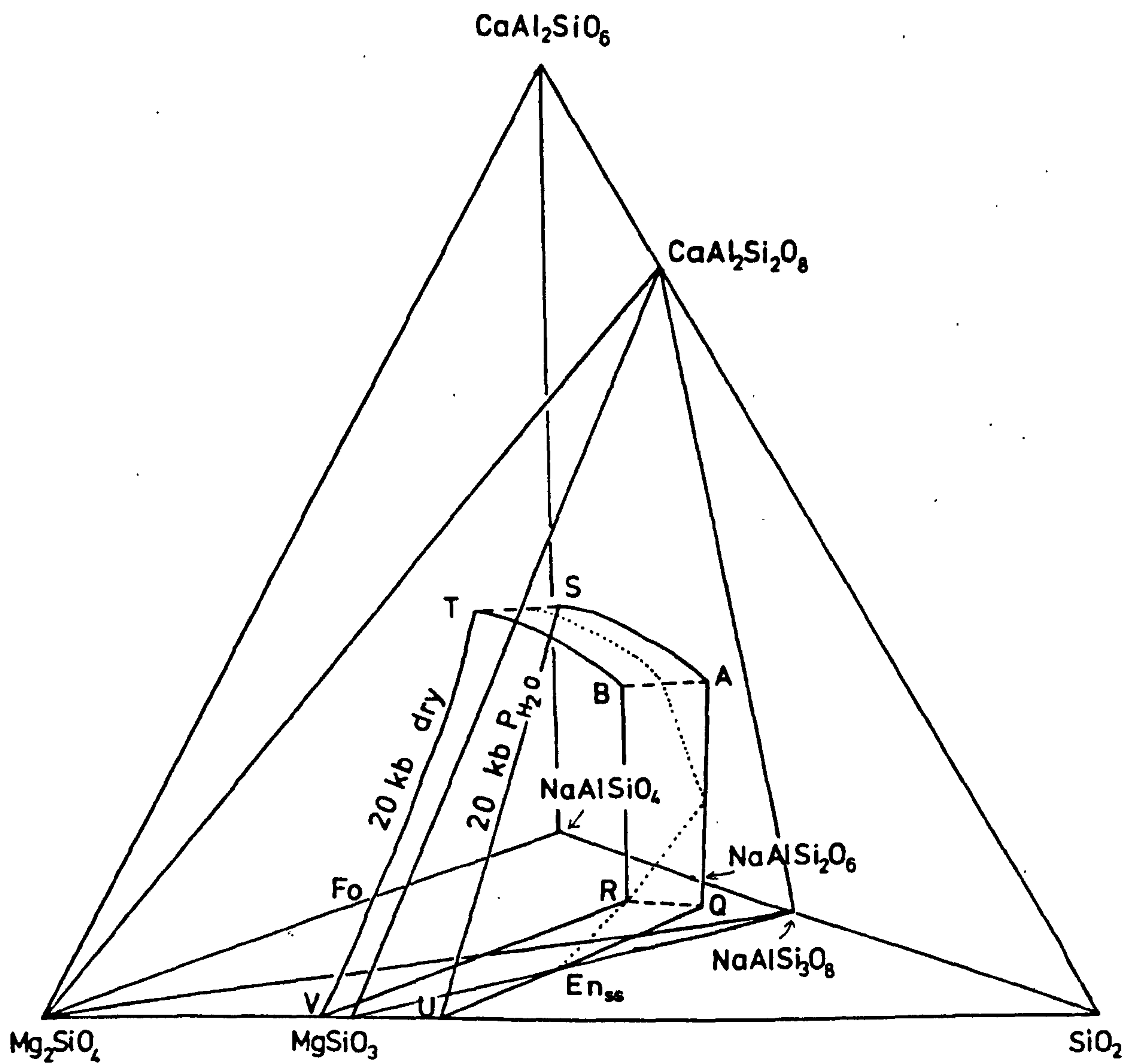
The forsterite-orthopyroxene liquidus boundaries in the system forsterite-nepheline- $\text{CaAl}_2\text{SiO}_6$ -silica- $\text{H}_2\text{O}$  at 20 kb under water saturated and dry conditions.<sup>2</sup>

The dotted line indicates the intersection of the plane  $\text{MgSiO}_3$ - $\text{CaAl}_2\text{SiO}_8$ - $\text{NaAlSi}_3\text{O}_8$  with the volume AQUSTVRB.

Point B gives the composition of the first liquid formed by partial fusion of an assemblage including Fo, Opx, Cpx and an aluminous phase under anhydrous conditions. It is probably in the Ne-normative region of the tetrahedron at 20 kb.

Point A is the first liquid formed by partial fusion of Fo, Opx, Cpx and Ga (a synthetic garnet peridotite) in the presence of excess water. The liquid is silica-saturated at 20 kb.

For water deficient conditions the vapour dissolves in the liquid and with increasing temperature the liquid composition follows a path from A towards B close to the line AB becoming Ol and Hy normative but still tholeiitic in nature when it crosses the plane En-An-Ab. If it crosses the plane Fo-An-Ab it becomes Ne-normative.





melting, and may vary by two orders of magnitude within a 3% difference in amount of partial melt. In Chapter 7 it was shown that a considerable variation of incompatible element abundances occur in the undersaturated magmas of Grenada. This range is attributed to fluctuations in the initial percentage of partial melt produced in separate melting episodes, during the evolution of the volcanic suite. If the undersaturated magmas were generated by prolonged equilibrium hydrous partial melting, as envisaged by Kushiro (1972), one would not expect the range of abundances of incompatible elements that is observed. Since quartz tholeiites and andesites are predicted by Kushiro to be the initial products of melting, where enrichment variation should be greater, the trace element abundances of these compositions should reflect this variability. Comparison of the Grenada suite with other islands of the Lesser Antilles (Chapter 8 ) has shown that this is not the case. The range of incompatible elements in the Grenada suite is considerably larger than in the saturated rocks of the northern part of the arc. Unless a different, more highly enriched source region is postulated for the Grenada magmas, this is the reverse of the situation predicted by Kushiro.

It appears that the initial melting products of the Upper Mantle beneath Grenada were usually undersaturated in composition. This is similar to the results obtained by O'Hara (1968) in investigations of dry systems where the initial melt at 20-25 kb pressure is predicted to be a nepheline-normative picrite in composition. It is also in accord with the observations of Green (1970) under conditions where  $P_{H_2O} \approx P_{tot}$ . Thus the natural

evidence from Grenada would appear to suggest that under the melting conditions that existed in the Upper Mantle, the melting relationship:



was not present. This conclusion is important in discussing the evolution of the primary melts.

#### 10:6 Evolution of primary melts

Factors influencing the evolutionary path of a magma en route from mantle source to the surface of the Earth include:

- 1) the rate of movement of the magma
- 2) the extent of crystal-liquid fractionation during uprise
- 3) the amount of isobaric fractionation during pauses in the ascent
- 4) changes in  $P_{H_2O}$  and  $PO_2$  during uprise
- 5) wall-rock reaction with the magma.

Green (1970) has proposed that orthopyroxene is the major liquidus phase during fractionation of hydrous undersaturated melts at pressures greater than 18 kb. The character of the evolving melt would trend towards increasing undersaturation. O'Hara (1968) has previously shown that unless the reaction relationship of



can be shown to have existed, a melt in equilibrium with the Upper Mantle must have olivine on the liquidus. As a result of the expansion of the primary crystallisation field of olivine at lower



pressures, olivine-normative liquids produced at high pressures must retain olivine as a liquidus phase during uprise. It is for this reason that O'Hara rejects the concept of primary magmas from the mantle (see Introduction, this Chapter). The data of Green (1970) specifically exclude a reaction relationship of olivine with the liquid. Fractionation of magnesian orthopyroxene at high pressures should deplete the melt in  $\text{SiO}_2$  and  $\text{MgO}$  and enrich the melt in  $\text{CaO}$ ,  $\text{K}_2\text{O}$  and  $\text{Na}_2\text{O}$ . In addition, the limited natural solubility of  $\text{Al}_2\text{O}_3$  in orthopyroxene at pressures greater than 18 kb should result in the relative enrichment in the melt of this component as well (O'Hara, 1968). The measured partition coefficients of Rare Earth elements between orthopyroxene and alkali olivine basalt indicate that these elements would also be enriched in the melt though Opx fractionation (Onuma et al., 1968). In a previous discussion of the undersaturated compositions of Grenada (Sigurdsson et al., 1973), it was tentatively suggested that in accordance with the petrogenetic scheme of Green (1971), orthopyroxene fractionation may have produced a trend towards undersaturation. In this account (Chapter 7 ) the diversity of major and trace element compositions is attributed to variations in amount of partial melt. In particular there is no evidence of Rare Earth enrichment consistent with orthopyroxene fractionation. Accordingly the role of orthopyroxene fractionation in the undersaturated magmas of Grenada is believed to have been minor relative to other phases.

In Chapter 9 it was suggested that the dominant fractionating phases were olivine, clinopyroxene and spinel. However, since the

initial melt was probably hydrous, it is necessary to discuss the role of  $P_{H_2O}$  and  $P_{O_2}$  in controlling the stability of hydrous phases. The most important hydrous phase likely to be precipitated from an undersaturated melt is amphibole. Since the pioneering study of Yoder and Tilley (1962) the stability field of this mineral in basaltic and ultrabasic melts has been explored by several workers (e.g. Holloway and Burnham, 1972; Cawthorn et al., 1973). Fig. 46 & 50 show the stability field of amphibole in basaltic compositions (Hill and Boettcher, 1970) and ultrabasic compositions (Kushiro, 1968). These experiments have been completed under conditions where  $P_{H_2O} = P_{tot}$ . Experiments at 10 kb with  $P_{H_2O} = P_{tot}$  have shown that the stability of amphibole in basaltic melts is increased (Holloway and Burnham, 1972). However, experiments carried out at pressures greater than 18 kb with  $P_{H_2O} = P_{tot}$  have not shown amphibole to be present on the liquidus (Green, 1971). There is a lack of data on the stability of amphibole at pressures greater than 10 kb with  $P_{H_2O} = P_{tot}$  due to experimental difficulties previously described. In contrast to a previous account (Cawthorn et al., 1973) it was shown in Chapter 7 that amphibole was unlikely to have been a major fractionating phase during the early evolution of the Grenada suite. Rare Earth element distribution patterns K/Rb ratios and alkali element contents of the Grenada suite do not reveal the trends expected to result from any extensive fractionation of amphibole. It seems more likely that the stable fractionating phases were anhydrous during the initial evolution of the melts.

Fig. 51 is based on the projections of phases stable at various



Fig. 50

Pressure-temperature diagram for a lherzolite nodule from the Salt Lake tuff (Hawaii) in the presence of excess water after Kushiro (1968)

Note the broad stability field of amphibole in this ultrabasic composition up to temperatures of 1000°C at 20 kb pressure when  $P_{H_2O} = P_{tot}$ .

V = vapour   Amph = amphibole   Gnt = garnet  
Ol = olivine   Cpx = clinopyroxene.

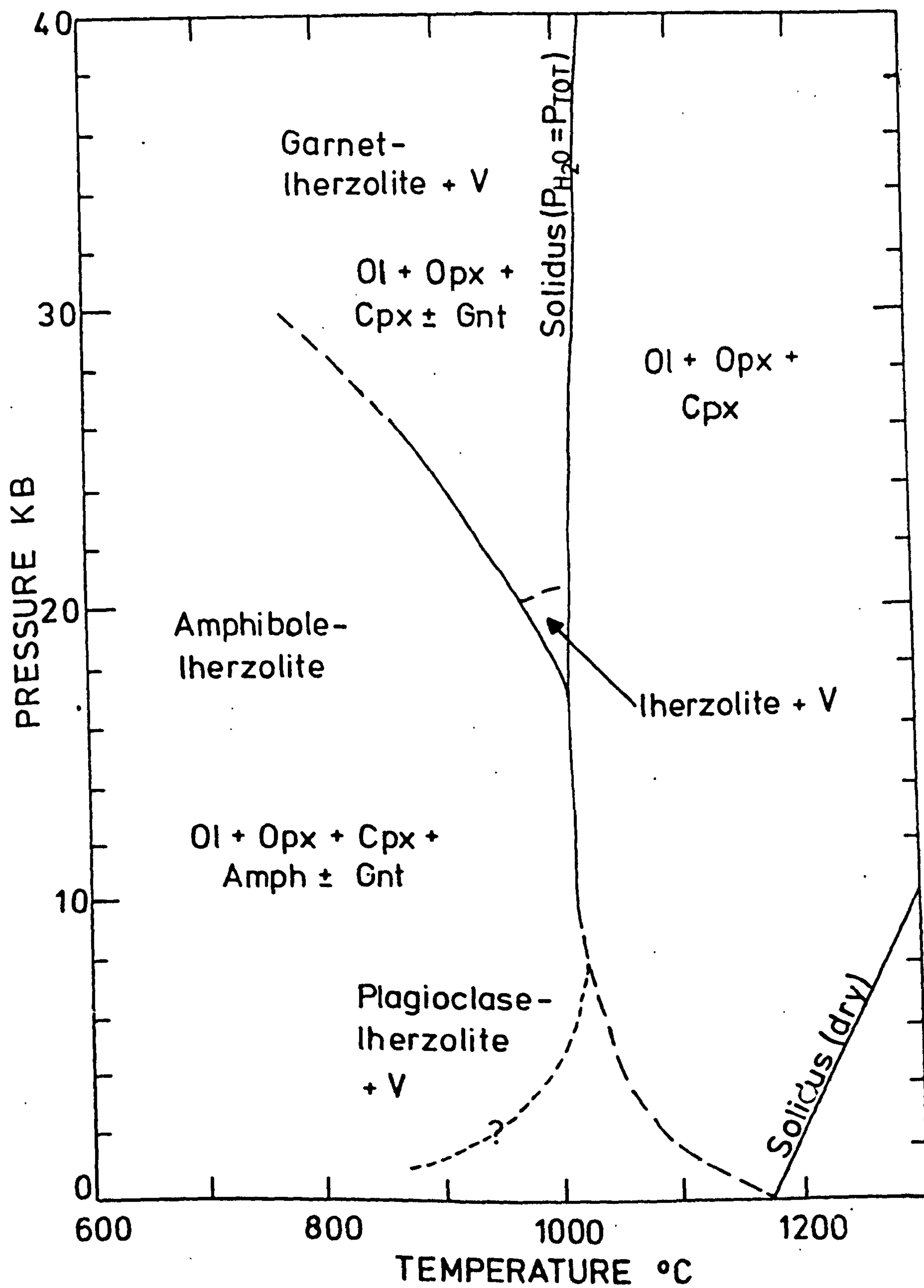




Fig. 51

Phase boundary shifts with pressure variation in the C.M.A.S. system after O'Hara (1968).



Upper diagram is a sub-projection from orthopyroxene (MS) into the plane  $M_2S$  (olivine)- $C_2S_3$ - $A_2S_3$  which includes the olivine - diopside ( $CM_2S_3$ ) - pyrope ( $M_3AS_3$ ) plane.

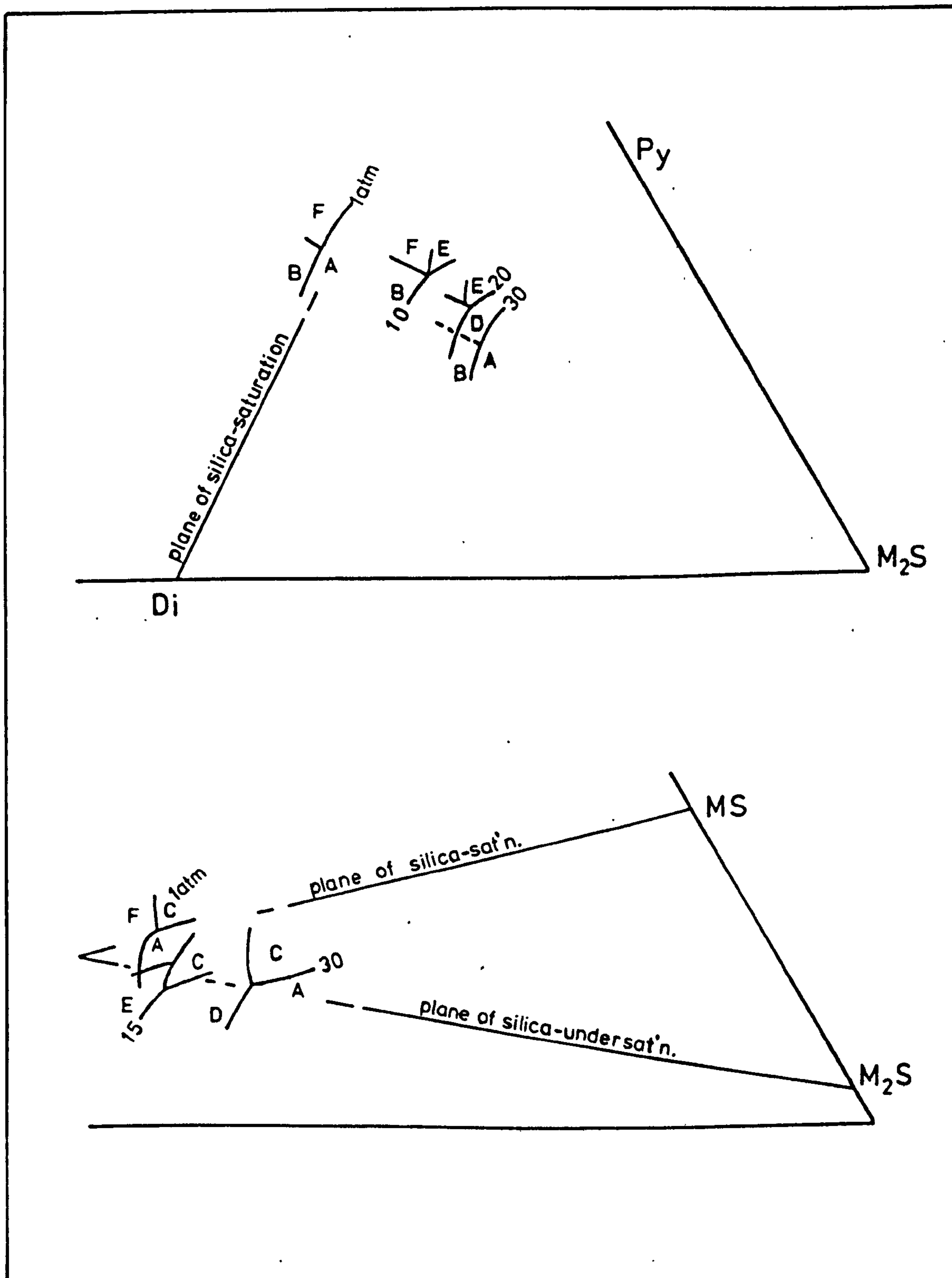
Lower diagram is a sub-projection from diopside into part of the plane  $C_3A$ - $M$ - $S$  which includes the orthopyroxene (MS) - grossular ( $C_3AS_3$ ) join.

The letters indicate compositional stability fields as follows:

A = olivine    B = clinopyroxene    c = orthopyroxene  
D = garnet    E = spinel                      F = plagioclase.

Numbers indicate pressure of equilibrium phase boundaries.

Note the expansion of the olivine stability field with reduced pressure and the expansion of the clinopyroxene stability field between 30 and 10 kb; both primarily at the expense of orthopyroxene.





mantle pressures in the  $\text{CaO-MgO-Al}_2\text{O}_3\text{-SiO}_2$  system (O'Hara, 1968). Thompson (1972) has shown that difficulties arise in using projections into this system for relatively iron-rich natural basalts at low pressures. The order of crystallisation of the phases predicted in the synthetic system, where Fe is grouped with Mg, are not observed in the natural rocks. However, the following discussion is designed to show in a qualitative manner the possible shifts in phase boundaries at high pressures that may be applicable to the Mg-rich, undersaturated liquids of the Grenada suite. O'Hara (1968) has stressed the possibility of prolonged crystallisation of a single phase during polybaric fractionation. The features to note of Fig. 51 are the expansion of the primary crystallisation field of olivine as the pressure is lowered. In addition, a similar expansion of the primary crystallisation field of clinopyroxene occurs at pressures below 30 kb and above 10 kb. Both olivine and clinopyroxene stability fields expand primarily at the expense of orthopyroxene.

If the movement of the magma towards the surface is sufficiently rapid, the reduction in pressure causes the primary phase volume of olivine to overrun the liquid composition continuously and only olivine may crystallise from the melt. In addition it is possible to predict during the evolution of the suite, that the presence of the reaction relationship:



at reduced pressures, or when  $P_{\text{H}_2\text{O}}$  is sufficiently high relative to  $P_{\text{tot}}$ , would serve to further prolong the crystallisation of olivine from silica-saturated liquids. In detail, the fractionation

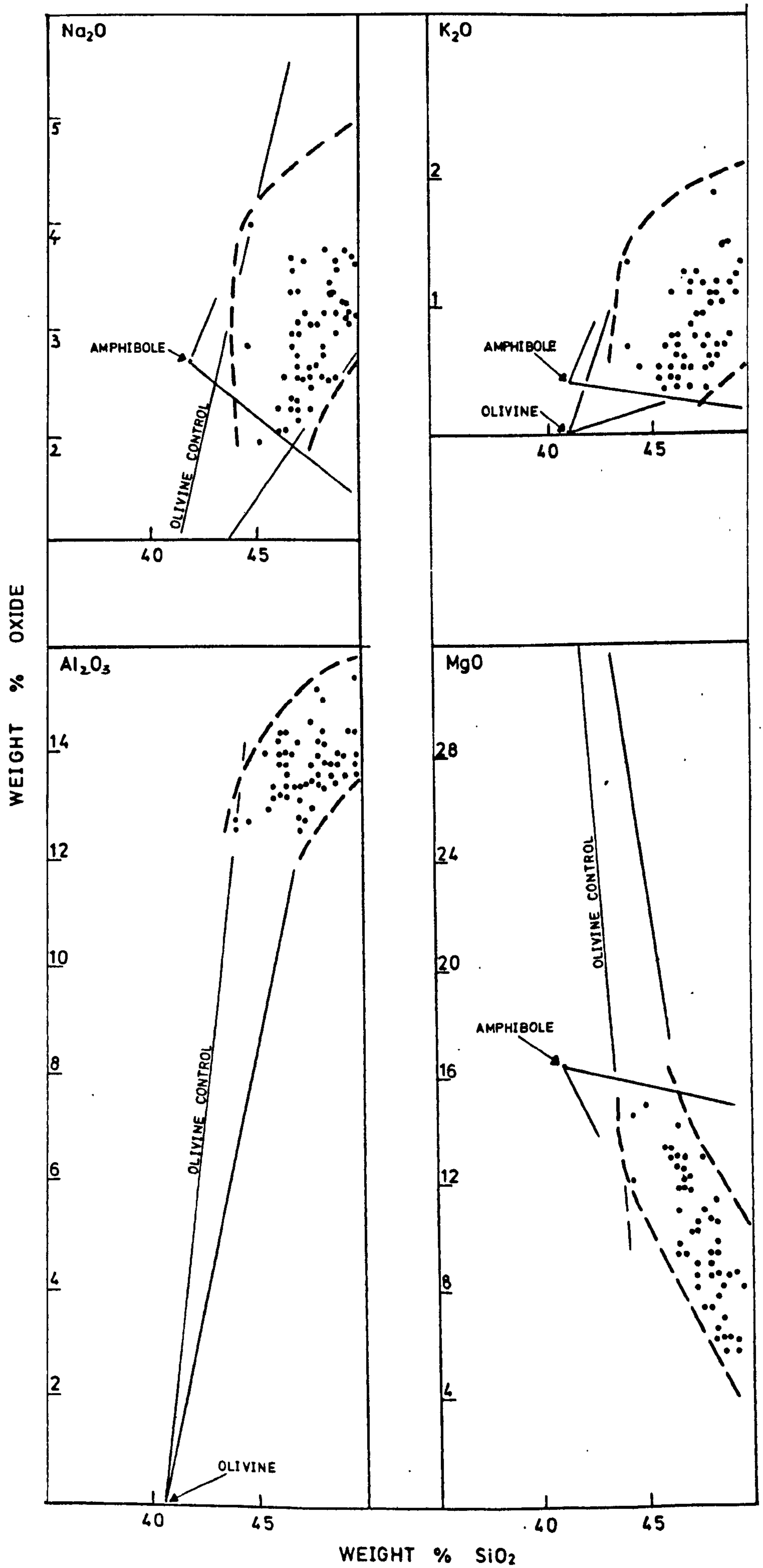
may be complex but it is possible that a liquid may fractionate only olivine during rapid uprise to the surface.

Arculus and Curran (1972) suggested that the early stages of fractionation of the Grenada suite were dominated by the separation of olivine, clinopyroxene and spinel. It was suggested previously that the source region of the Grenada magmas was at a depth of less than 115 km (35 kb). The stable aluminous phase is likely to be a spinel. It is appropriate at this point to recall the analysed microphenocryst assemblages of the picrites and basalts (Chapter 9). These consist of forsteritic olivine, calcic augite and spinel and depending upon the exact proportions of these phases subtracted from the melt, the observed variation from silica-undersaturated towards silica-saturated compositions may be accounted for. The modal variation of phenocryst olivine and clinopyroxene is considerable within the Grenada picrites and basalts, and it is useful to plot the analysed bulk compositions in mineral-control type diagrams (Powers, 1955). In Fig.52 the variation of  $\text{MgO}$ ,  $\text{Al}_2\text{O}_3$  and alkalis are plotted against  $\text{SiO}_2$ . Analysed phenocryst olivines of the picrites and basalts are used to determine the likely compositional control in these figures. In addition, a naturally occurring amphibole phenocryst is plotted and in contrast to a previous account (Cawthorn et al., 1973) the absence of any simple amphibole control in determining the major element variation within these basic compositions may be observed. On the basis of the rapid depletion of  $\text{MgO}$  and  $\text{Ni}$  with increasing content of  $\text{SiO}_2$  in the Grenada suite, it is likely that olivine is the dominant crystallising phase during the early evolution of the melts with lesser proportions of clinopyroxene and spinel crystallising.



Fig. 52

Mineral compositional control during the early evolution of the Grenada suite. The variation of  $\text{MgO}$ ,  $\text{Al}_2\text{O}_3$ ,  $\text{Na}_2\text{O}$  and  $\text{K}_2\text{O}$  within the picrites and basalts<sup>213</sup> is probably partly the result of variable melting within the Upper Mantle. However the diagrams illustrate that the pargasite composition (in transitional basalt 40) does not lie on the back-projection of the broad compositional variation trend within these basics compositions. Dashed lines are inferred from the more extensive oxide variation diagrams of Fig. 27.





Changes in the relative proportions subtracted of these phases may partly account for the variation in compositions observed at the surface, but it is also apparent that the subsequent crystallisation of plagioclase and amphibole are important factors in determining the range of major and trace element abundances. It is suggested in this account that fractional crystallisation of magmas ranging from critically silica-undersaturated to silica-saturated has generated a trend towards andesitic and dacitic compositions. The variable geochemistry, petrography and mineralogy of these basic magmas has been described in the preceeding chapters. Initial differences in parental magma compositions are reflected in the major and trace element geochemistry of the andesites and dacites. However, the relative timing of the first appearance of crystallising mineral phases within the Grenada magmas is probably an important factor in determining the range of chemical variation observed within the silica-saturated compositions. The differences in variation of Sr and Ni in particular may be related to the relative proportions of plagioclase feldspar and olivine subtracted from the melt.

The crucial question in this instance is concerned with the nature of the factors that determine the trend towards silica saturation in the Grenada situation. The more usual evolutionary trend of critically undersaturated magmas is towards increasing silica-undersaturation. The proposed liquid evolutionary path breaches the low pressure thermal divide of olivine-clinopyroxene-plagioclase (Yoder and Tilley, 1962). In addition, the direction of liquid migration is the reverse of that predicted by any high pressure ( > 20 kb) crystallisation mechanism (O'Hara, 1968).

The role of the alkali elements is particularly striking in this respect. In many classifications of basaltic rocks (e.g. Yoder and Tilley, 1962; Coombs, 1963; Green, 1969) the relative concentration of silica and alkalis is one of the most important variables considered. In addition volcanic associations tend to be grouped according to the degree of silica-saturation displayed. The appearance either in the mode or the norm of feldspathoidal minerals is indicative of alkaline compositions. The alkali elements do not show extensive solubility in the Grenada clinopyroxenes ( $\text{Na}_2\text{O} < 1.73\%$ ;  $\text{K}_2\text{O} < 0.09\%$ ) and have negligible solubility in olivine and spinel. Therefore an increase in concentration of the alkali elements is predicted in the residual melt as the result of fractional crystallisation of these mineral phases, since the concentration of Na and K in the magmas is higher than in the ferromagnesian minerals. The rapid increase of the alkali elements with increasing  $\text{SiO}_2$  content of the Grenada magmas is illustrated in Fig. 27 (Chapter 8). However, the dominance of olivine control outlined above suggests that the resulting increase in silica content of the melt is sufficient to prevent the appearance of feldspathoidal minerals and a trend towards silica-undersaturation relative to alkalis. This feature is illustrated in the normative projections of compositions belonging to individual volcanic series (Fig. 30 Chapter 8). The compositional trend is initially towards the albite corner in these projections reflecting the increase in concentration of silica relative to alkalis. Before further discussion of the low pressure ( $< 15$  kb) evolution of the Grenada suite, it is necessary to examine in more detail the experimental data concerning the stability relationships of olivine, clinopyroxene, spinel, plagioclase



and amphibole in basaltic melts.

#### 10:7 Mineral Stability Relations in Basaltic Melts

The study by Yoder and Tilley (1962) was the first comprehensive approach to the problem of phase relationships in natural basalt compositions under various  $P$ ,  $T$  and  $P_{H_2O}$  conditions. There is general agreement that  $H_2O$  is a component of basalt magmas but some dispute concerning the relative importance of  $H_2O$  during differentiation (see Hamilton and Anderson, 1968, for a recent review). Consequently the anhydrous and water-saturated melting relationships of basalt compositions will be summarised first as examples of the extreme cases likely to occur in the natural situation.

In Fig. 53 the melting relationships of an olivine tholeiite composition, studied by Yoder and Tilley, is given for conditions where  $P_{H_2O} = P_{tot}$ . In Fig. 54 the anhydrous melting relationships of a tholeiite studied by Cohen et al. (1967) is given. This anhydrous tholeiitic composition is similar to the oceanic tholeiite described by Engel and Engel (1964). O'Hara (1970) has suggested that the absence of olivine as a liquidus phase above 10 kb in this composition precludes a direct derivation of this melt from the Upper Mantle. For the purposes of this study however, the anhydrous and  $P_{H_2O} = P_{tot}$  melting relationships may be taken as a starting point for the investigation of mineral stability fields in basaltic magmas at pressures below 10 kb.

The important features to note of Figs. 53, and 54 are the reduction in temperature of crystallisation of plagioclase and the appearance of amphibole as a stable phase in the hydrous state in comparison with the anhydrous situation. Where  $P_{H_2O} = P_{tot}$ ,

Fig. 53

H<sub>2</sub>O-saturated melting relations in an olivine tholeiite (After Yoder and Tilley, 1962). Names alongside lines indicate phase stability limits. Dash-dot lines, 1 and 2, indicate possible crystallization paths producing the crystallization sequence observed in natural Grenadan compositions.



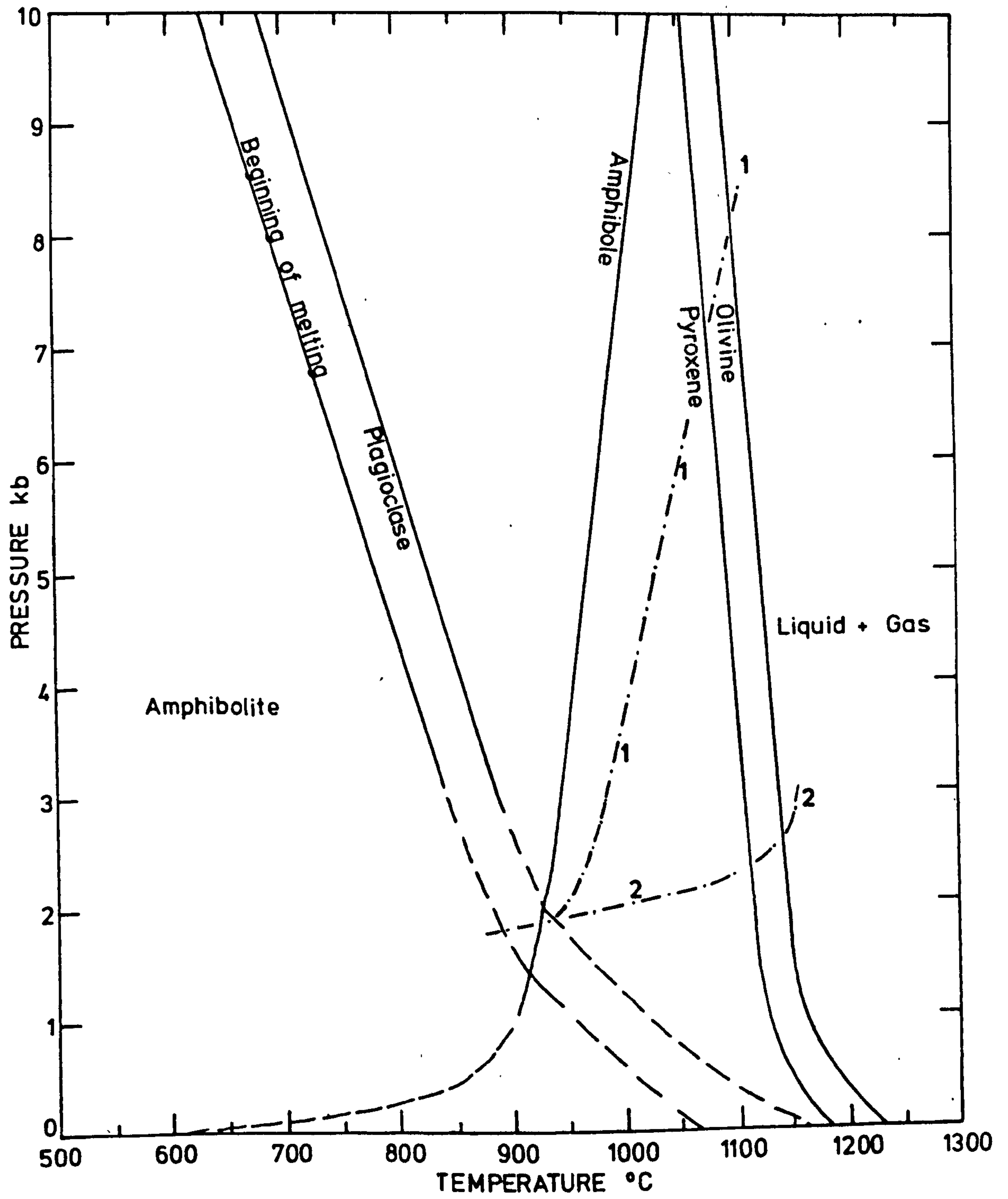


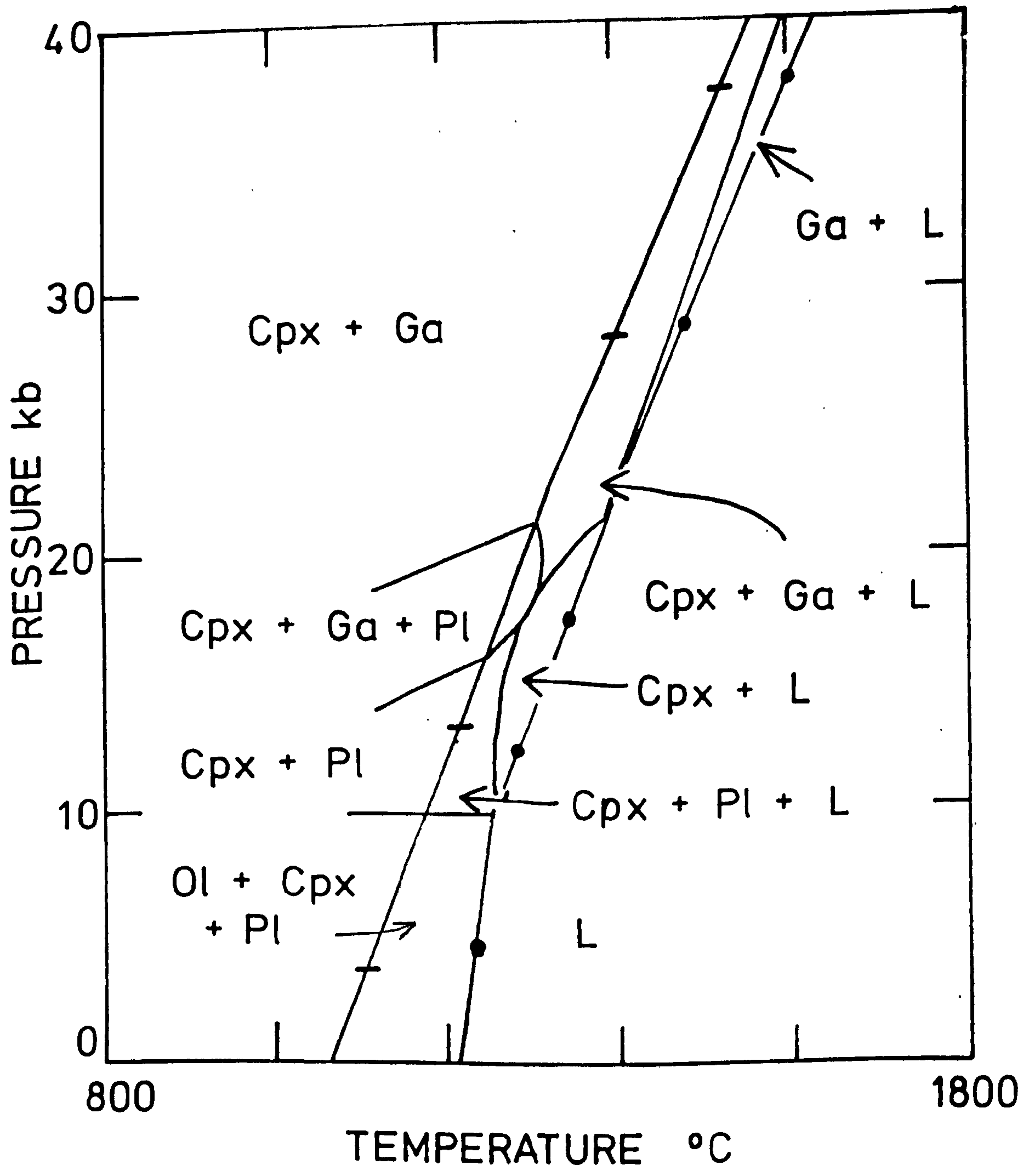
Fig. 54

Pressure-temperature projection of phase stability  
limits for an anhydrous tholeiitic composition.

(After Cohen et al., 1967).

Ol = olivine  
Cpx = clinopyroxene  
Ga = garnet  
Pl = plagioclase  
L = liquid.





crystallisation of olivine and clinopyroxene occurs at a higher temperature than amphibole but both react with amphibole once this phase is stable (Yoder and Tilley, 1962, p.449). In Fig. 46 the maximum temperature of stability of amphibole is seen to increase to 1050°C at pressures up to 10 kb but the slope of the boundary curve becomes negative at higher pressures. Also in Fig. 46 the increased stability of amphibole when  $P_{H_2O}$  is reduced relative to  $P_{tot}$  is illustrated. However, the significance of the melting curves as applied to the natural situation is the indication that only at pressures below 2 kb is plagioclase stable at higher temperatures than amphibole. In experiments under controlled  $P_{H_2O}$  and  $PO_2$  conditions, Nesbitt and Hamilton (1970) found that plagioclase crystallised 110°C below the temperature of appearance of amphibole in alkali olivine basalt composition at 2 kb.

The available data suggests that  $H_2O$  is the most abundant and  $CO_2$  the second most abundant component of the fluid phase in the magma (Heald et al., 1963). Fig. 46 shows that at high pressures ( $> 15$  kb) the effect of  $P_{CO_2}$  on  $P_{H_2O}$  in the melt is negligible but becomes increasingly important at lower pressures effectively reducing  $P_{H_2O}$  relative to  $P_{tot}$ . The great reduction in basalt solidus temperatures by the addition of  $H_2O$ , and the large volumes of melt likely to be present in the Upper Mantle if  $P_{H_2O}$  is high relative to  $P_{tot}$ , suggest that in fact  $P_{H_2O}$  is considerably less than  $P_{tot}$  at the site of melting. There are a variety of factors other than  $P_{CO_2}$  that may affect the  $P_{H_2O}$  of the melt. The solubility of  $H_2O$  in the melt decreases as pressure is reduced (Fig. 55) and consequently  $P_{H_2O}$  will tend to increase as the magma rises to the



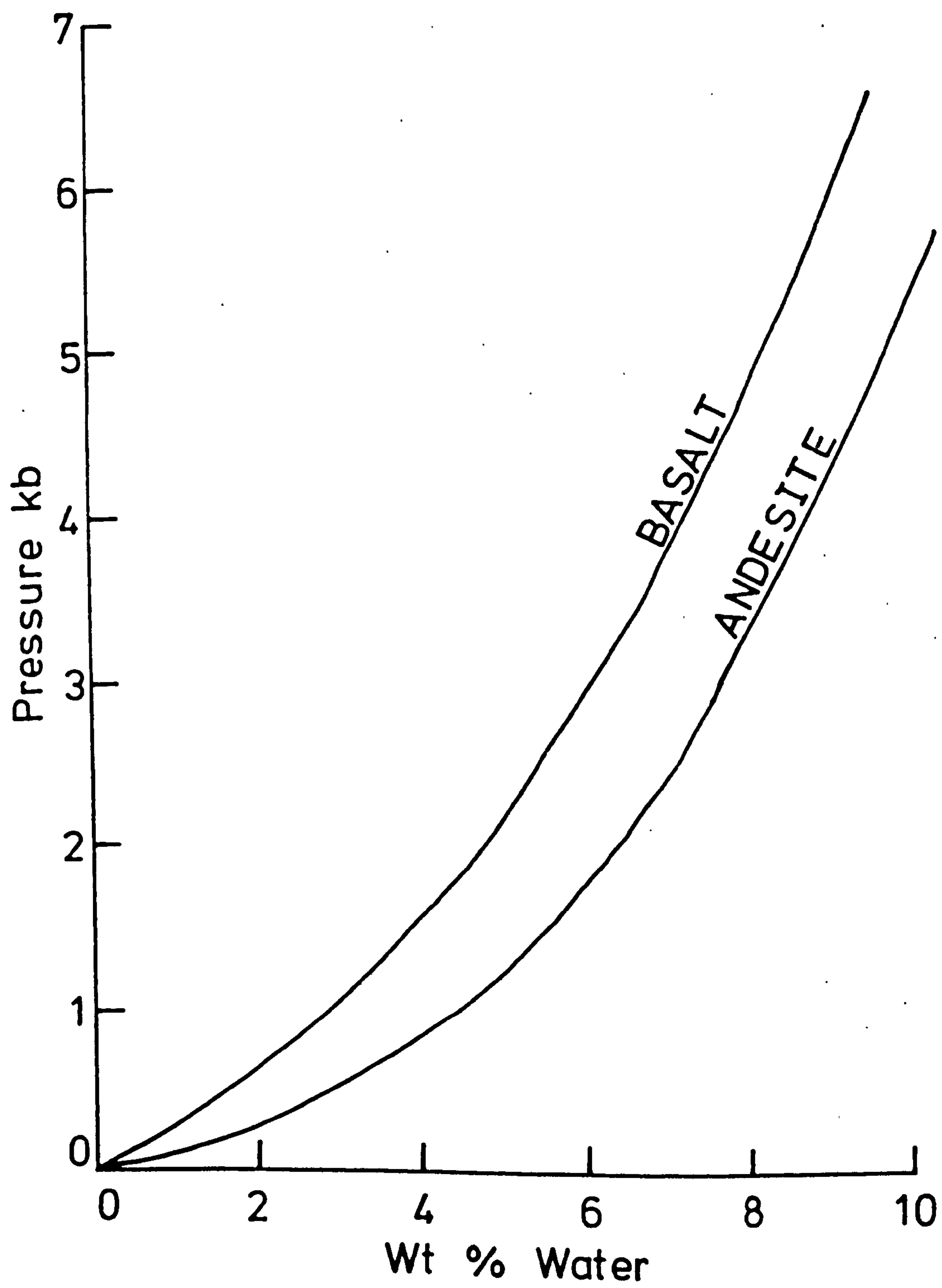
Fig. 55

Solubility of water as a function of  $P_{H_2O}$  in basalt and andesite melts at 1100°C.

(After Hamilton and Anderson, 1968).

Basalt = a Columbia River basalt

Andesite = a Mt. Hood andesite





surface. In addition the crystallisation of anhydrous mineral phases will tend to reduce the residual volume of available melt and so raise the  $P_{H_2O}$  of the melt. Nevertheless, it is unlikely that the  $P_{H_2O}$  of the magma is ever equal to  $P_{tot}$  due to the effect of the other dissolved volatiles.

Holloway and Burnham (1972) have examined the melting relationship in an olivine tholeiite composition (similar to one of the compositions used by Yoder and Tilley (1962) and illustrated in Fig. 53) under conditions where  $P_{H_2O} = 0.6 P_{tot}$  using a  $H_2O - CO_2$  buffer. The results are presented in Fig. 56. In comparison with the situation where  $P_{H_2O} = P_{tot}$  (Fig. 53) the increase in solidus temperature ( $50^\circ C$ ) and thermal stability of amphibole ( $60^\circ C$ ) should be noted. Amphibole is again stable at higher temperatures than plagioclase feldspar at pressures above 2.25 kb, and once present in the melt, a reaction relationship between amphibole and previously crystallised olivine and clinopyroxene is suggested by Holloway and Burnham (1972, Fig. 6). Holloway (1973) has examined the stability of pargasite alone under a variety of  $P_{H_2O}$  and  $P_{tot}$  conditions using a  $H_2O - CO_2$  buffer. Some of the results of this investigation are presented in Fig. 57. It can be seen that as  $P_{H_2O}$  decreases relative to  $P_{tot}$ , the stability of amphibole in general increases to an isobaric temperature maximum but with further reduction in  $P_{H_2O}$  the stability decreases. The temperature maximum of stability shifts to a lower  $P_{H_2O}$  with increasing  $P_{tot}$ . Eggler (1972) has shown similar stability relationships in natural melts of andesitic composition.

In summary, the experimental results suggest that olivine and

Fig. 56

Pressure-temperature projection of phase stability limits for olivine tholeiite under conditions of  $P_{H_2O} = 0.6 P_{tot}$ .

The minerals are stable on the side of the curves along which the name is printed except for olivine (Ol) and clinopyroxene (cpx) whose stability limits were not determined.

Dashed lines are uncertain.

lqd = liquid.

(After Holloway and Burnham, 1972).



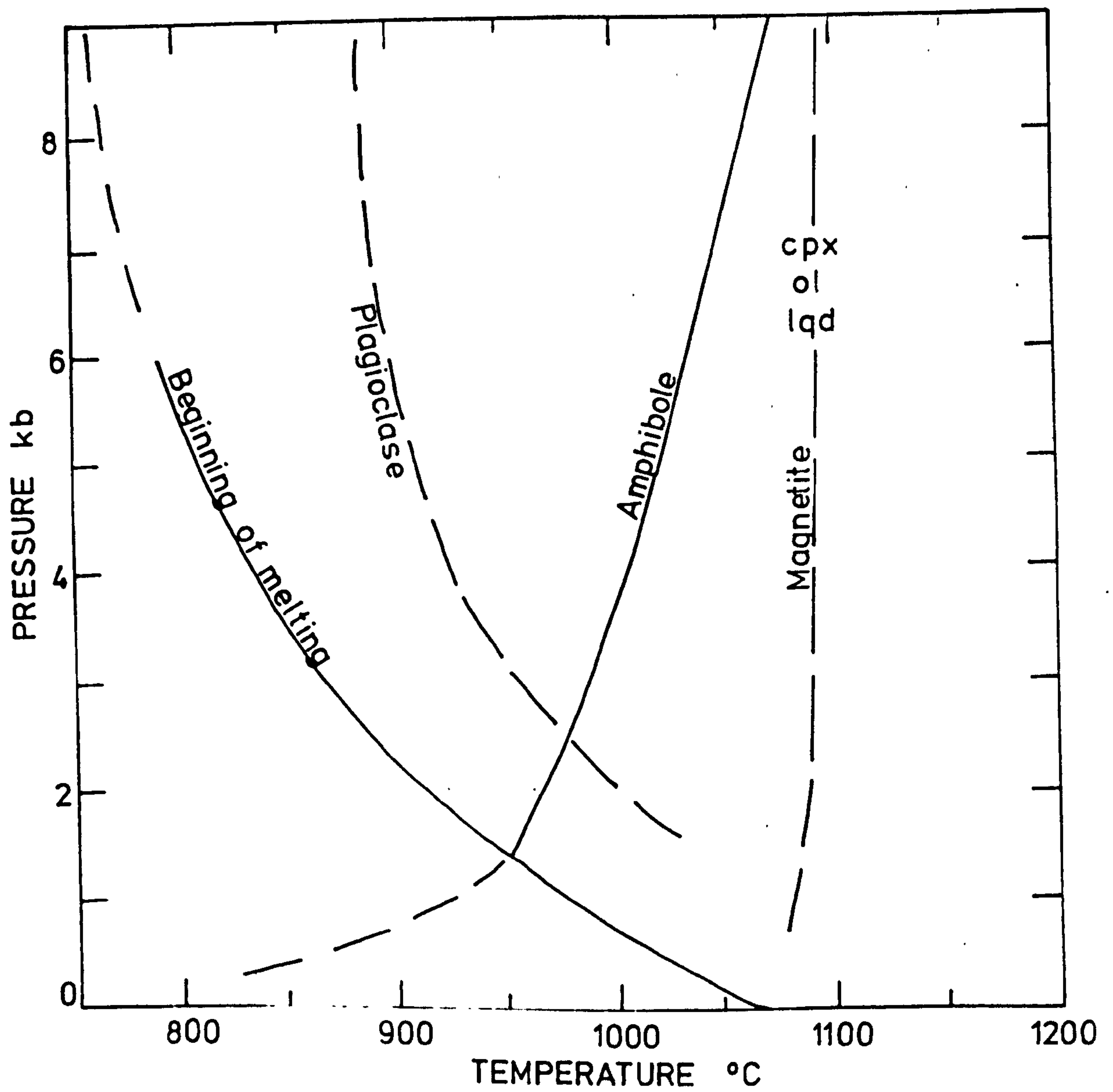


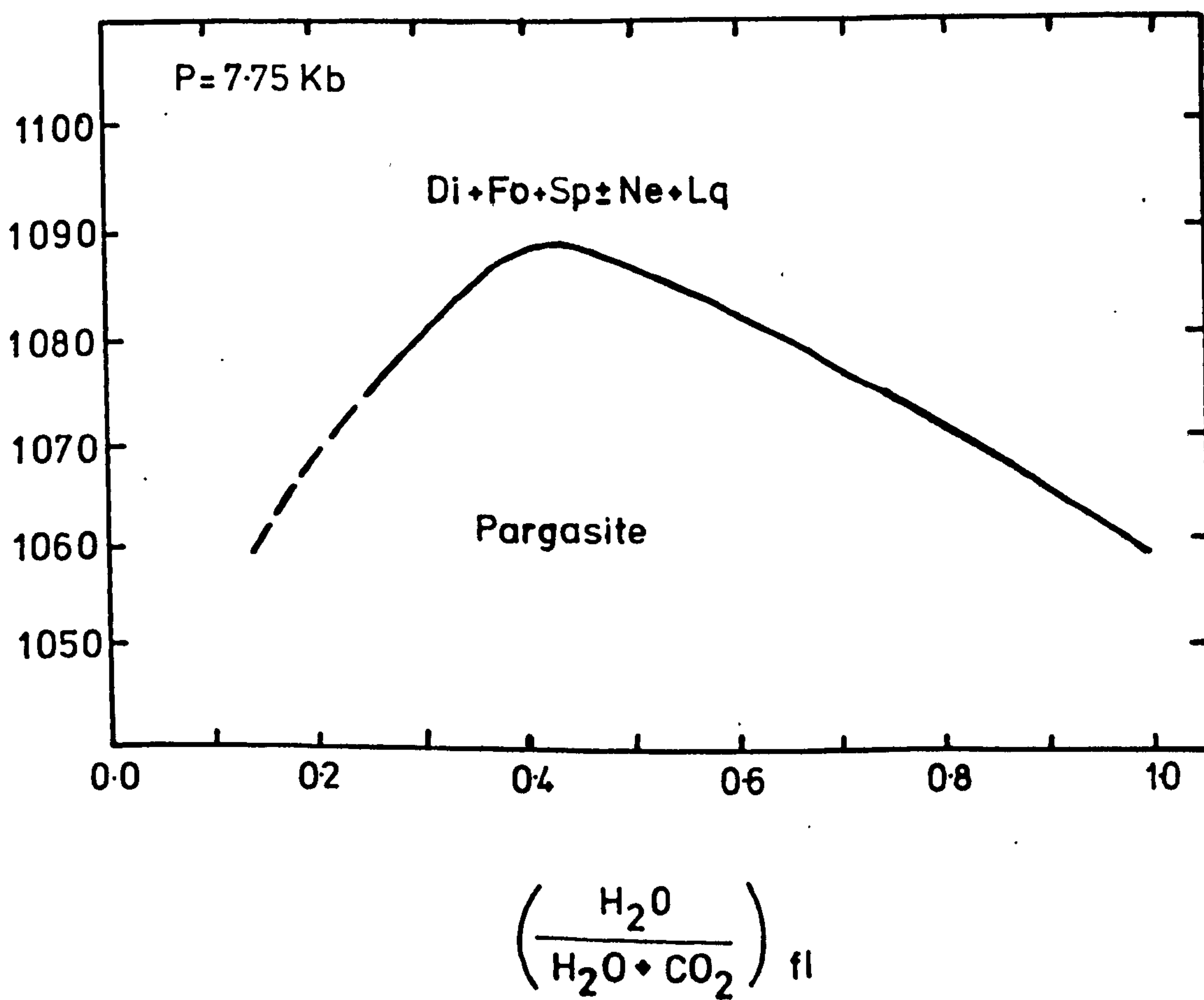
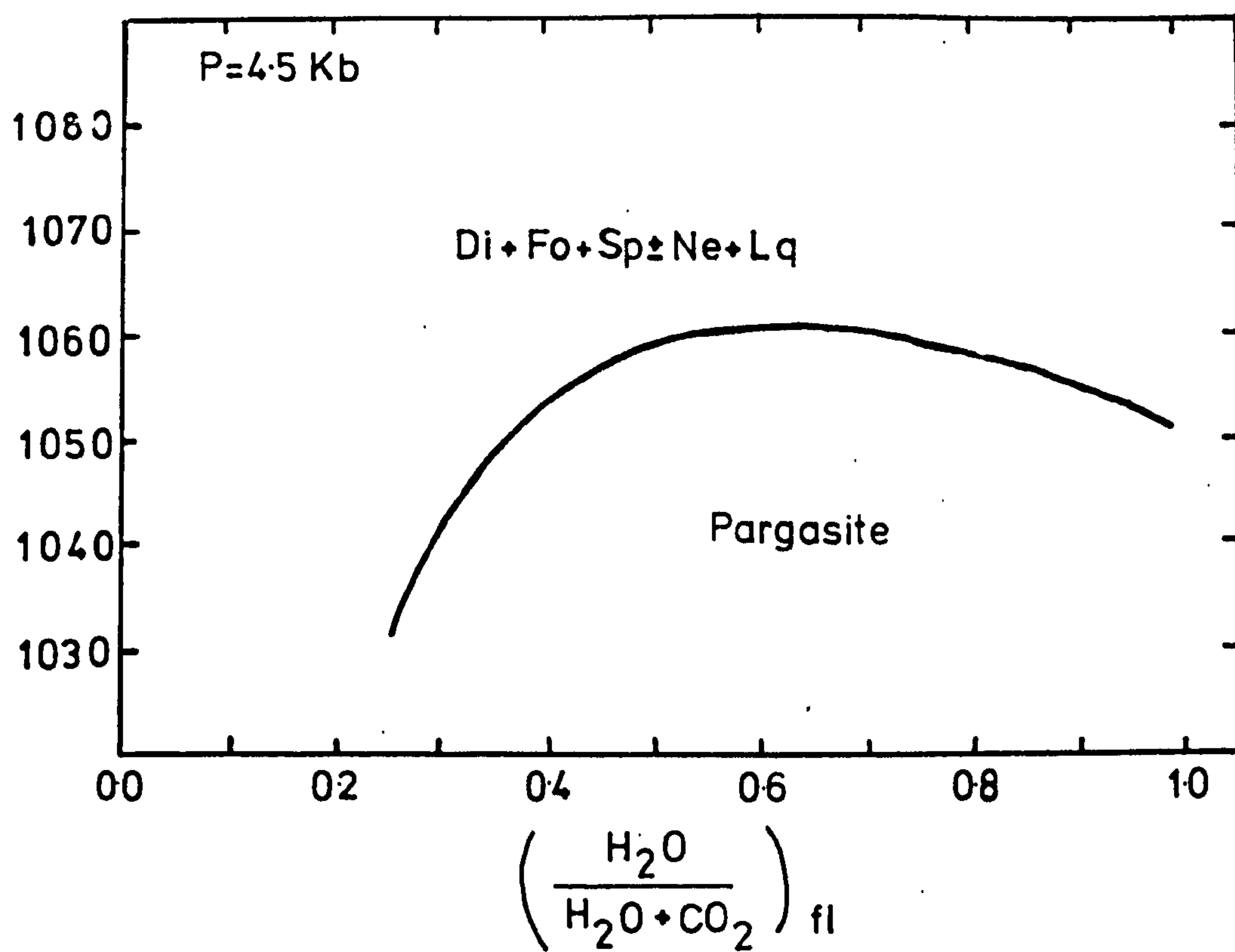
Fig. 57

$T - x_{H_2O}^{fl}$  isobaric projections for pargasite melting relationships:

where  $x_{H_2O}^{fl}$  is the mole fraction of  $H_2O$  in the fluid phase and at these temperatures and pressures under consideration, is approximately equal to  $P_{H_2O}$  in the system.

(After Holloway, 1973).





clinopyroxene are the highest temperature melting phases in basaltic compositions under a range of  $P_{H_2O}$  and  $P_{tot}$  conditions. In addition amphibole is stable at higher temperatures than plagioclase feldspar in basaltic melts at pressures above 2 to 2.25 kb at least where  $P_{H_2O} = 0.6 P_{total}$  to  $P_{total}$ . A reaction relationship between amphibole and previously crystallised olivines and clinopyroxene is predicted. However, the petrographic evidence of the basalts and cumulus plutonic blocks of Grenada suggests that amphibole crystallises after plagioclase. A similar feature has been reported in the plutonic blocks of St. Vincent (Lewis, 1963) and attributed to crystallisation at pressures below 2 kb.

It is difficult to reconcile the experimental results with the natural evidence on the basis of the crystallisation of the assemblage ol-cpx-plag-magnetite-amph at high  $P_{H_2O}$ , (at a depth less than 8 km) Lewis (1964) suggests that the natural assemblages represent a higher temperature paragenesis than in the experimental conditions, and attributes the absence of any reaction relationship and continued crystallisation of olivine and clinopyroxene with amphibole to this feature. This implies either:

1) The experimentally determined stability limit for plagioclase and amphibole is too low and should be placed at higher temperatures,

or 2) the composition of olivine and clinopyroxene coexisting with amphibole in the magma, whatever P/T gradient has been followed en route to the surface (see paths 1 and 2, Fig.53 ) should reflect a drop in liquidus temperatures of approximately 70 to 100°C.

It is possible that reduction of  $P_{H_2O}$  relative to  $P_{tot}$  below



0.6  $P_{\text{tot}}$  would increase the thermal stability of plagioclase and amphibole further relative to the  $P_{\text{H}_2\text{O}} = P_{\text{tot}}$  situation. However, a prerequisite for the crystallisation of amphibole after plagioclase in the Grenada compositions on the basis of the experimental data outlined above seems to be a combination of rapid decline in liquidus temperatures and arrest of the ascent of the magmas to occur at pressures below 2 kb. The continued crystallisation of olivine and clinopyroxene with amphibole (Lewis, 1964) remains unexplained on the basis of the experimentally predicted stability relationships, and the stability of the assemblage ol-cpx-plag-amph-magnetite is predicted to be of extremely limited extent. The crystallisation of clinopyroxene together with amphibole in andesitic compositions is also unlike the predicted stability relationships in basalts.

The high Mg/Fe+Mg ratios of the coexisting amphibole, olivine and clinopyroxene together with the high An content of the plagioclase feldspars in the Kick-em-Jenny alkali basalt (Table 17, Chapter 9) suggest an even higher temperature paragenesis than in the St. Vincent, plutonic blocks. It is interesting that amphibole is always observed to crystallise after plagioclase in the basalts whereas a slight deviation in P/T gradient followed by the magma or a different depth at which arrested ascent might occur would produce the reverse order of crystallisation. It is possible that an alternative explanation for the observed mineral paragenesis and crystallisation sequence is available in the relationship of  $P_{\text{H}_2\text{O}}$  and  $P_{\text{tot}}$  in the magma.

As  $P_{\text{H}_2\text{O}}$  is reduced still further below 0.6  $P_{\text{tot}}$ , the thermal stability of plagioclase feldspar must eventually become greater

than amphibole over a considerable pressure range with the ultimate disappearance of amphibole as a liquidus phase. In this case the thermal stability of plagioclase must increase more rapidly than the increase in thermal stability of amphibole with reduced  $P_{H_2O}$  as illustrated in Fig. 57. Some experimental evidence for the appearance of plagioclase before amphibole in a synthetic andesitic composition under conditions of  $P_{H_2O} < P_{tot}$  (10 kb) has been presented by Green and Ringwood (1968). However, addition of similar quantities (unspecified) of water to a synthetic basaltic andesite at the same pressure produced amphibole at a higher temperature (960°C) of crystallisation than plagioclase (900°C). It is possible that the reduced solubility of  $H_2O$  in the more basic melt (cf. Fig. 55) produced a higher  $P_{H_2O}$  with resulting increase in stability of amphibole relative to plagioclase. At present melting relationships in basaltic magmas at low  $P_{H_2O}$ 's ( $P_{H_2O} < 0.3 P_{tot}$ ) remains a possible future line of investigation though problems with homogenisation of the melt may be encountered.

The influence of variables other than  $P_{H_2O}$  in relation to the differentiation of basalt magma have been studied. Osborn and his co-workers have shown the important effect of variation in  $P_{O_2}$  on the course of fractional crystallisation (e.g. Roeder and Osborn, 1966). Osborn (1959) has considered two general cases which are probably limits of the natural situation. These are respectively fractional crystallisation under

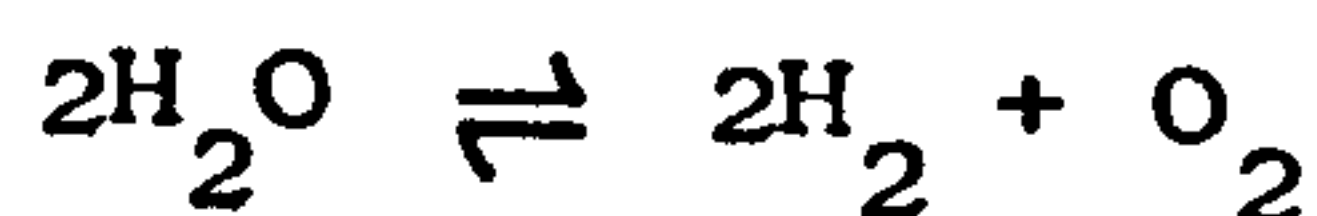
- 1) constant total composition
- 2) constant  $P_{O_2}$

The crystallisation paths of liquids within increasingly



complex and thus more realistic synthetic systems have been analysed under these conditions. In the first case, the resulting trends are towards increasing iron-enrichment in the residual melt with a small amount of liquid of extreme composition produced. Alternatively with constant  $P_{O_2}$  (non-constant total composition) early precipitation of Fe-Ti oxides occurs and a trend towards increasing silica-enrichment results with considerable quantities of silica-rich melt being produced. Osborn envisaged constant  $P_{O_2}$  conditions being maintained in a differentiating magma by dissociation of water in the surrounding rocks and diffusion of  $O_2$  inwards to the magma. Gradations between these end-member models were postulated as the likely natural course of events (Osborn, 1959). However, in some calc-alkaline suites magnetite is not a phenocryst phase (e.g. Eggler, 1972), and difficulties are experienced in reconciling the trace element abundances in andesites with extensive magnetite precipitation from basaltic parent magma (Taylor et al., 1969).

Hamilton and Anderson (1968) have suggested that in general the quantity of water present in basalt melts is sufficient for the  $P_{O_2}$  of the magma to be buffered by the dissociation reaction:



The equilibrium constant for this reaction may be written

$$K_w = \frac{(f_{H_2})^2 \times f_{O_2}^*}{(f_{H_2O})^2}$$

Providing there is a significant quantity of water in the region of 1% (Hamilton and Anderson, 1968, p.478) in the basaltic

\*At high T and P, fugacity is approximately equal to partial pressure.

melt, the oxidation state of precipitated minerals during fractional crystallisation will be controlled by the natural buffer provided by the dissociation of  $\text{H}_2\text{O}$ . Hamilton and Anderson point out however, that even with  $\text{H}_2\text{O}$  present in the magma, a decline of several orders of magnitude in  $P_{\text{O}_2}$  is likely to occur during cooling of the melt. This is due to the rapid decline in the value of  $K_w$  with decreasing temperature. Nevertheless the  $P_{\text{O}_2}$  of a crystallising hydrous basalt does not fall as quickly or rapidly as it would in a dry melt.

Calculated  $T$  and  $P_{\text{O}_2}$  in differentiated calc-alkaline suites from the coexisting Fe-Ti oxides after the method of Buddington and Lindsley (1964) show in general a similar initial level of  $P_{\text{O}_2}$  in the parental melts as in tholeiitic magmas. However, the rate of fall of  $P_{\text{O}_2}$  with decreasing temperature is not as great in calc-alkaline as in tholeiitic suites and is similar to the model predicted by Hamilton and Anderson (1968), for magmas with small quantities ( $\sim 1\%$ ) of dissolved  $\text{H}_2\text{O}$ . Fig.58 illustrates calculated  $P_{\text{O}_2}$  and  $T$  variation in differentiated calc-alkaline and tholeiitic suites. It seems therefore that a possible explanation for the differences between calc-alkaline and tholeiitic differentiation trends is dissolved water content. However, Hamilton and Anderson (1968) point out that with declining  $P_{\text{O}_2}$  either iron- or silica-enrichment is possible in the residual melts. Barberi et al. (1971) have suggested a trend towards iron-enrichment may have occurred in alkali and transitional basalt suites due to high  $P_{\text{O}_2}$ . Recently volcanic series with marked calc-alkaline affinities have been described which show iron-enrichment in the course of fractionation (Lowder, 1970). In general, although  $P_{\text{O}_2}$  is an important factor particularly with



Fig. 58

Log  $f_{O_2}$  - T diagram after Carmichael (1967).

QFM = quartz-fayalite-magnetite buffer

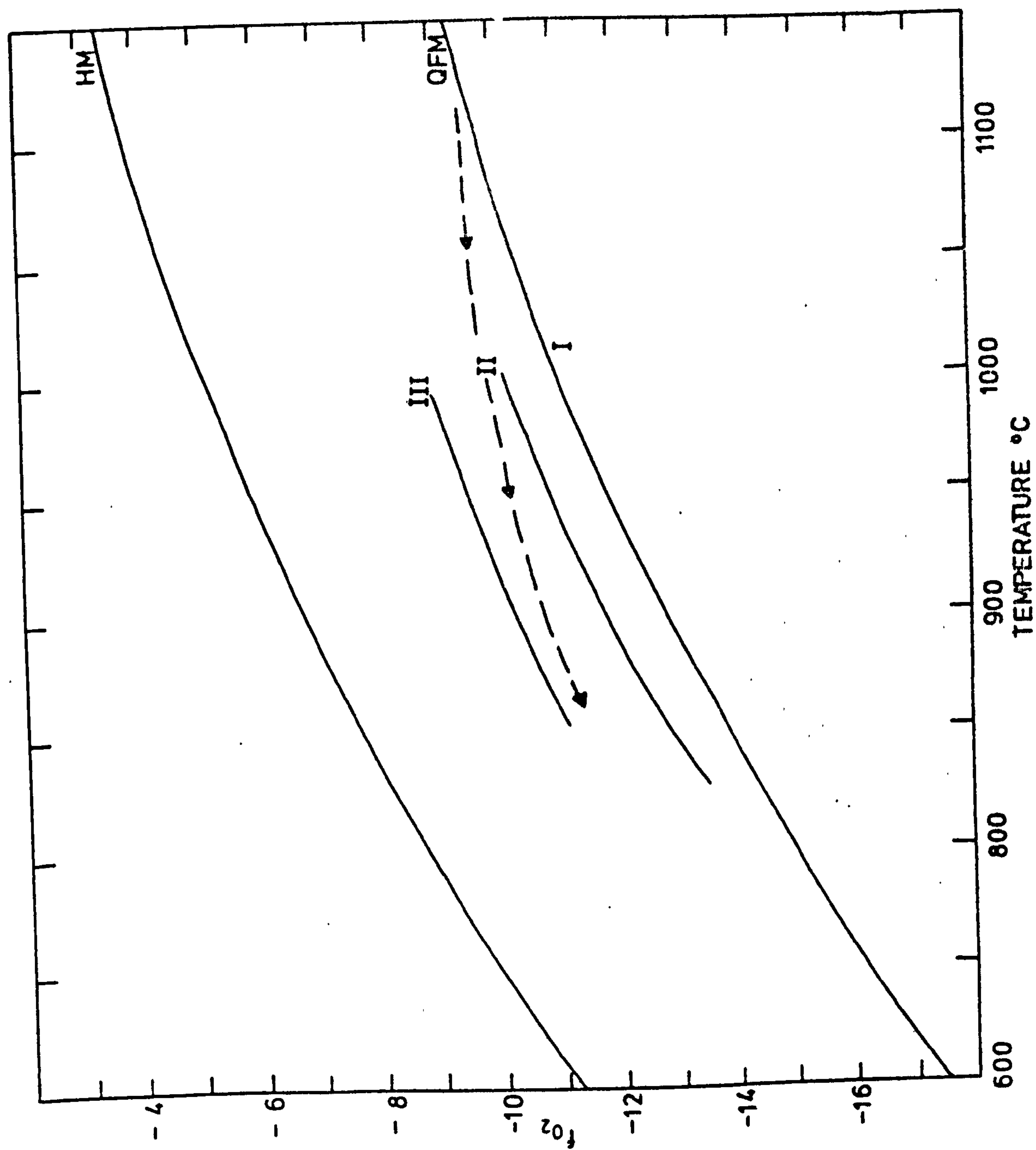
HM = hematite-magnetite buffer

Curve I indicates coexistence of Fe-Ti oxides with olivine (e.g. Thingmuli tholeiitic suite)

Curve II coexistence of Fe-Ti oxides with orthopyroxene (approximately defining the Ni-NiO buffer).

Curve III coexistence of Fe-Ti oxides with amphibole and biotite (e.g. Lassen dacites).

Dashed line indicates the changing  $f_{O_2}$  - T relationships in the Talasea calc-alkaline suite after Lowder (1970).





respect to the stability of the Fe-Ti oxides, it is not an independent variable in hydrous magmas and is related to the same factors that determine  $P_{H_2O}$  described previously.

In the Grenada calc-alkaline suite, magnetite is a phenocryst phase within basalt compositions and a trend towards increasing silica rather than iron-enrichment may have been predicted on this basis. There is a lack of a coexisting rhombohedral phase in the Grenada suite but some generalisations are possible with rocks of similar mineralogy. Carmichael (1967) found that for lavas in which the iron-titanium oxides coexist with olivine, the indicated  $f_{O_2}$  and T fell along the fayalite-magnetite quartz buffer (Fig. 58 ). This suggests an approximate temperature of crystallisation in the region of 1100°C at  $f_{O_2}$  of  $10^{-10}$  bars. However the absence of phenocryst plagioclase feldspar in many of the Grenada picrites and alkali-basalts suggests that the suppression of the liquidus temperature of appearance of this phase by small quantities of water, predicted to be present in the melt, may be a factor of equal importance in producing the trend towards silica- as opposed to iron-enrichment.

Roeder and Emslie (1970) have suggested that iron-enrichment in the melt may only take place when extensive early precipitation of plagioclase feldspar occurs. Olivine is preferentially enriched in Fe relative to the melt except at unnaturally high  $P_{O_2}$ 's ( $< 10^{-7}$  bar). Thus it is possible that extensive fractional crystallisation of olivine before the appearance of plagioclase feldspar as a liquidus phase in differentiating calc-alkaline suites may be an additional factor in determining the trend towards increasing silica-enrichment

relative to the tholeiitic trend of magmatic differentiation.

In summary therefore, it appears from the evidence of compositional and mineralogical relationships in the Grenada suite of basaltic compositions that the fractional crystallisation trend displayed is primarily due to the presence of water in the magma. In comparison with a tholeiitic trend of differentiation, the  $P_{H_2O}$  and  $P_{O_2}$  was probably sufficiently high to initiate the early precipitation of magnetite and also to retard the appearance of plagioclase and amphibole. In addition the eventual crystallisation of plagioclase feldspar before amphibole and the high-temperature paragenesis of the coexisting minerals once plagioclase and amphibole are stable, suggests that  $P_{H_2O}$  was initially considerably lower than  $P_{tot}$ . The abundance of amphibole in the cumulus plutonic blocks of Grenada suggests however, that crystallisation of this phase is important in the development of the trend from basaltic to an andesitic composition and may explain the absence of a trend towards increasing alkalinity in the compositions with  $SiO_2$  content greater than 50 to 52 wt.%  $SiO_2$  (see Fig.27 , Chapter 7).

The high An content of the plagioclase feldspars are an additional feature of calc-alkaline suites likely to generate a trend towards silica-enrichment by fractional crystallisation (Brown and Schairer, 1971). The inflexion of the curve of variation of  $Al_2O_3$  with  $SiO_2$  occurs at 48-50 wt.%  $SiO_2$  (Fig.27 , Chapter 7) suggesting that subtraction of calcic plagioclase begins to occur at this stage in the evolution of the Grenada series. Thus the breach of the low-pressure thermal divide apparently occurs mainly by fractional crystallisation of olivine, clinopyroxene and spinel, but the accentuation of



the trend towards silica-enrichment is accomplished by subtraction of nepheline-normative amphibole and calcic plagioclase feldspar. In comparison with the tholeiitic and alkaline trends of magmatic evolution the influence of  $H_2O$  in the melt is the most important factor determining the differences displayed by the Grenada calc-alkaline trend. The early crystallisation of magnetite, delayed precipitation of plagioclase feldspar, but eventual crystallisation of highly calcic plagioclase compositions are a direct result of the presence of  $H_2O$  in the melt.

#### 10:8 Compositional variation in the Basalt-Andesite-Dacite

##### Sequence

It was suggested earlier in this account of the evolution of the Grenada suite that differences in proportions of subtracted mineral phases may be partly responsible for the variation in major and trace element geochemistry observed in the sequence basalt-andesite-dacite. The enrichment of Sr in plagioclase feldspar relative to the melt (Brooks, 1968; Philpotts and Schnetzler, 1970), suggests an explanation for the observed variation in Sr of the volcanic series of Grenada. It was suggested in Chapter 8 that the high-Sr volcanic series are associated with basalt compositions initially comparatively enriched in Sr and other incompatible (in the ferromagnesian phases) trace elements. However, the rapid increase in abundance of Sr from 600 ppm to 1500 ppm in the alkali and transitional basalts of the high-Sr series is greater than in basalts of the low-Sr series over a similar  $SiO_2$  wt.% range. It is possible that some of the highly porphyritic basalts represent cumulus

compositions and part of the variability in the geochemical data may be due to this factor. However, the strong oscillatory zoning displayed by the phenocrysts of plagioclase and clinopyroxene suggests prolonged crystallisation within a magma and the major and trace element variation with  $\text{SiO}_2$  suggest that many of the bulk compositions are truly representative of magmatic liquids. Apart from the increase in Sr, the high-Sr series are also associated with a more rapid decline in the abundance of Ni and MgO relative to the low-Sr series. A possible explanation is that more extensive olivine fractionation has occurred in the high-Sr series prior to the precipitation of plagioclase feldspar. Direct evidence for the general enrichment of Sr in plagioclase feldspar in the Grenada situation is available in the analyses of the cumulus plutonic blocks presented in Table 28, (Chapter 9). The high Sr content ( $\sim 925$  ppm) of the block (x407) dominated by modal anorthite is noticeable in comparison with the other blocks where the content of plagioclase feldspar is much smaller.

The peak in the Sr vs  $\text{SiO}_2$  variation curve of the high-Sr series in the transitional basalts ( $\sim 49\text{-}51$  wt.%  $\text{SiO}_2$ ) suggests that fractional crystallisation of plagioclase feldspar becomes important at this stage. The absence of any similar peak and gradual increase in Sr-abundance in the low-Sr series is more typical of differentiated volcanic suites (Brooks, 1968). Sr is preferentially partitioned into the melt by olivine and clinopyroxene (Philpotts and Schnetzler, 1970). The level of Sr abundance is therefore determined by the relative proportions of the fractionating minerals subtracted from the melt, and generally the ferromagnesian minerals predominate in the Grenada basaltic compositions. It is possible that the greater



TABLE 36

Average simple and compound phenocryst/  
matrix partition coefficients for Sr, K,  
Rb and Ba from Philpotts and Schnetzler  
(1970).

	$D^{\text{Sr}}$	$D^{\text{K}}$	$D^{\text{Ba}}$	$D^{\text{Rb}}$	$D^{\text{K/Rb}}$	$D^{\text{Rb/Sr}}$
Olivine	0.01	0.007	0.01	0.01	0.07	0.7
Clino- pyroxene	0.1	0.04	0.03	0.03	1.5	0.3
Plagio- clase	1.7	0.2	0.25	0.05	3.0	0.04
Horn- blende	0.5	0.8	0.3	0.3	5.0	0.5

increase in Sr of the high-Sr series is due to the delayed fractionation of plagioclase feldspar relative to the low-Sr series. This may be a reflection of the level of  $P_{H_2O}$  in the melt, determined originally at the site of melting but also affected by rates of ascent of individual magma batches and variations in rate of increase of  $P_{H_2O}$  relative to  $P_{tot}$ .

It is possible to examine more critically at this stage some of the element variation in the sequence basalt-andesite-dacite. In particular the simple and compound partition coefficients calculated for the important phenocryst minerals of volcanic rocks can be used to assess the relative importance of the fractionating phases. The partition coefficients for Rb, Sr, Ba and K calculated by Philpotts and Schnetzler (1970) are summarised in Table 36. In Fig. 59 the variation of K/Rb and Rb/Sr with increasing  $K_2O$  and  $SiO_2$  content respectively in the Grenada suite are presented.

The basalts associated with the high K/Rb ratios are those compositions enriched in Sr of the high-Sr series. In general, however, the K/Rb ratios decline slightly from basalt to dacite and decrease markedly in the high-Sr series from the peak in the basalt compositions. With reference to Fig. 23 (Chapter 7), it is reemphasised that for a given degree of fractionation between phenocryst and residual melt, much greater changes occur in the abundance of an element or variation in element ratios when concentration is into the crystal. The high compound partition coefficient of K/Rb ( $\sim 5.0$ ) between hornblende and matrix indicates that a rapid depletion in the K/Rb ratios would be expected as the result of extensive fractional crystallisation of this phase. The peak in the K/Rb ratios

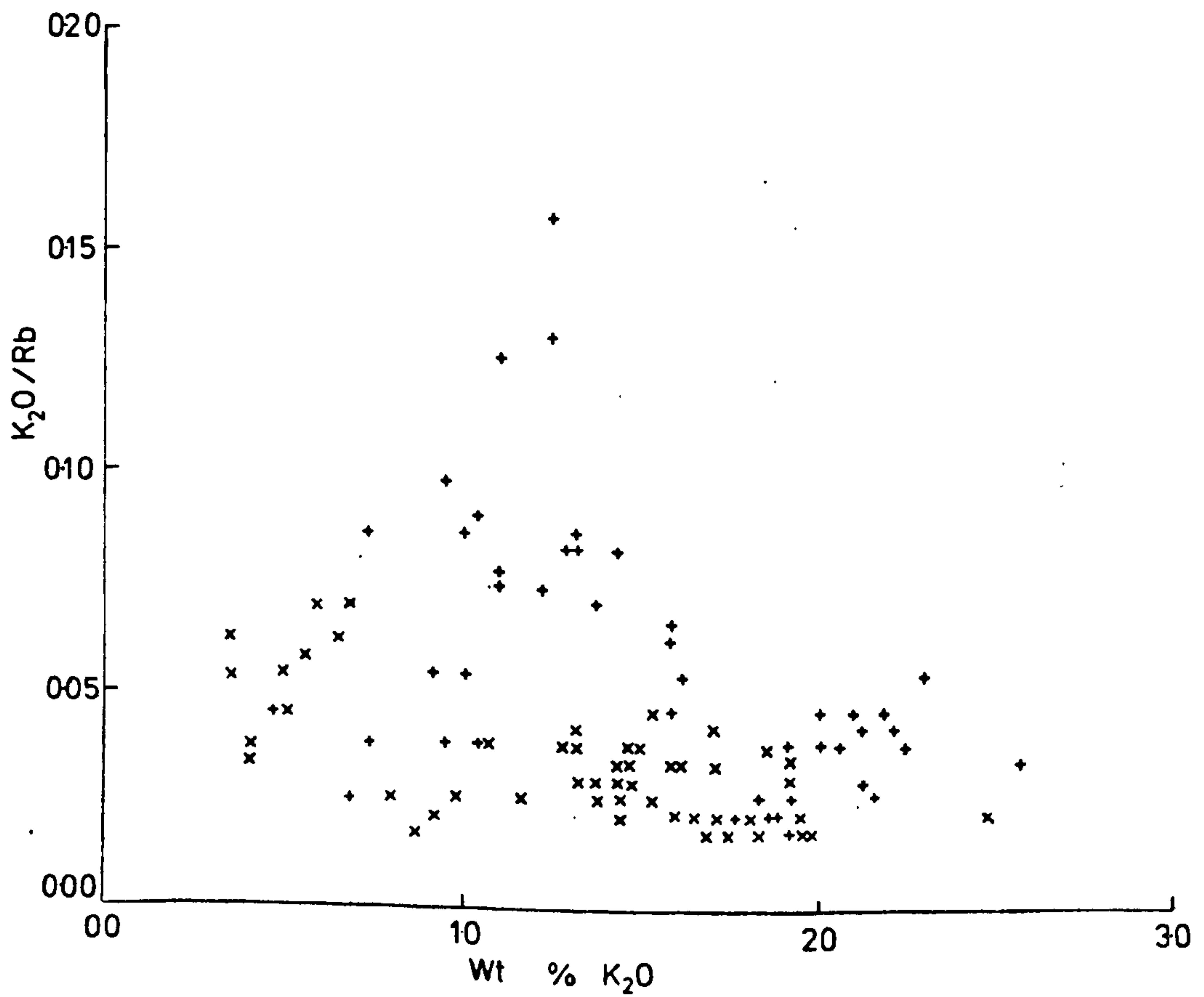
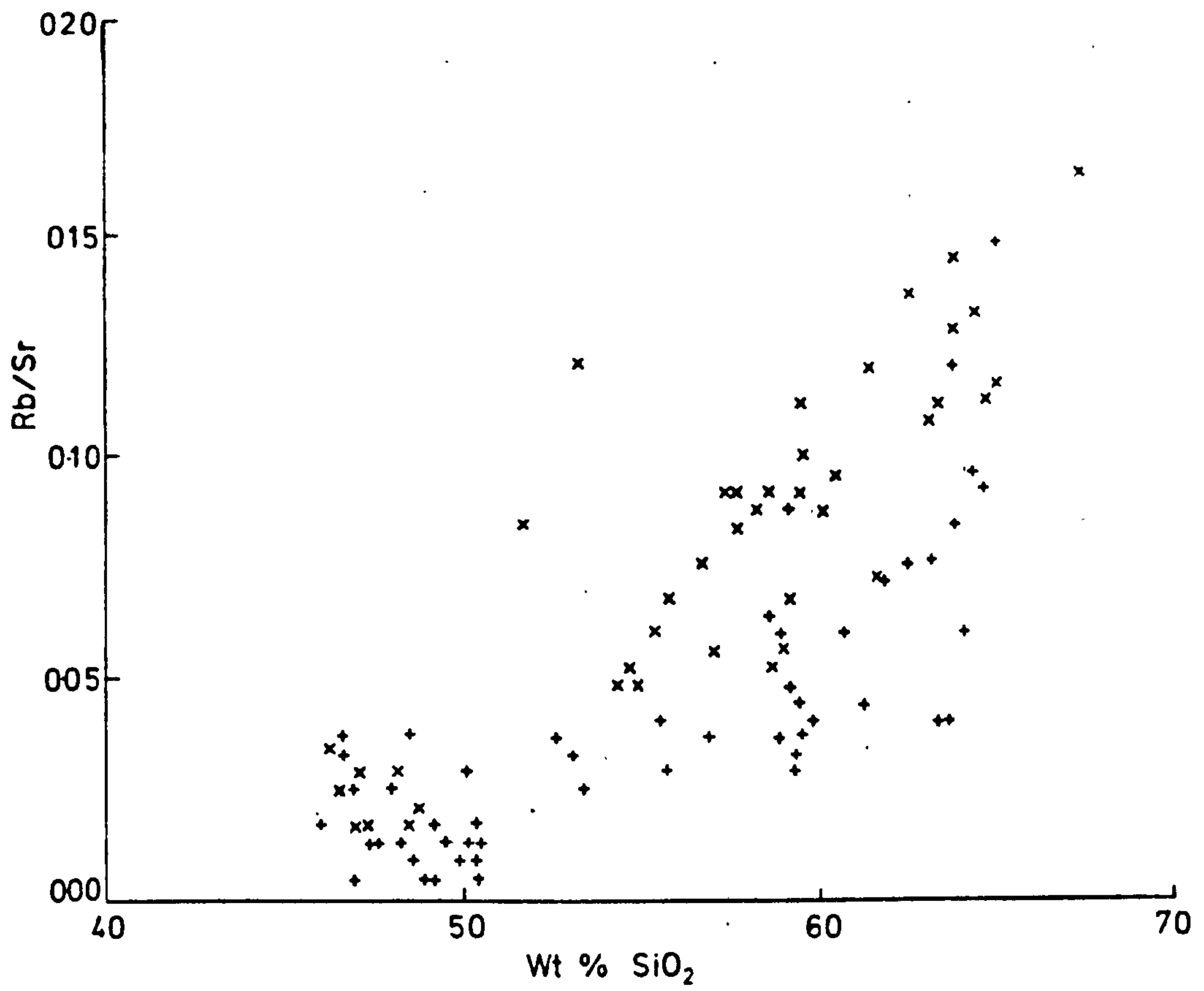


Fig. 59

Plot of Rb/Sr v  $\text{SiO}_2$  and  $\text{K}_2\text{O}$  (wt.%) v Rb (ppm)  
for the Mt. Granby-Fedon's<sup>2</sup>Camp and Mt. St.  
Catherine centres combined.

x = low-Sr series

+ = high-Sr series





in the transitional basalts of the high-Sr series suggests that only minor amphibole fractionation could have occurred in conjunction with another mineral phase or phases that generated a higher K/Rb ratio in the residual melt. It is suggested in this account that dominant olivine fractionation and retardation of plagioclase fractionation is responsible for the rapid increase of Sr in the high-Sr series of alkali and transitional basalts. The low compound partition coefficient for K/Rb between olivine and residual melt ( $\sim 0.07$ ) would result in an increased K/Rb ratio in the melt if extensive fractional crystallisation of olivine occurs. The general decline in the K/Rb ratio of the Grenada suite from basalt to dacite may be attributed to the fractional crystallisation together with olivine, of clinopyroxene ( $D^{K/Rb} \sim 1.5$ ), and subsequently plagioclase feldspar ( $D^{K/Rb} \sim 3.0$ ).

The high-Sr series are also characterised initially by a less rapid increase in Rb/Sr ratios than the low-Sr series (Fig. 59). Olivine has the highest compound partition coefficient ( $D^{Rb/Sr} \sim 0.7$ ) of the minerals listed in Table and thus extensive fractional crystallisation of this phase, combined with the delayed fractionation of plagioclase feldspar may explain the variation in the Rb/Sr as well as K/Rb ratios of the Grenada high-Sr series. In general in the Grenada suite, the increase in Rb/Sr ratios is more rapid when the bulk compositions contain more than approximately 50 wt.%  $\text{SiO}_2$ . The low compound partition coefficient of Rb/Sr between plagioclase feldspar and residual melt suggests that fractional crystallisation of this mineral phase became volumetrically more significant at this stage in the evolution of the suite.

The preferential enrichment in the residual melt of Ba by all the phenocryst minerals (Table 35 ) may explain the steady increase in concentration of this element with increasing  $\text{SiO}_2$  content of the host rock. With regard to information concerning the nature of the fractionating mineral assemblage at any stage, the variation of elements such as Ba is not very informative. However, the continuous variation in level of concentration of this element in the sequence from undersaturated to silica-saturated compositions is considerable support for a genetic link between these compositions.

The preferred hypothesis for the generation of the andesites and dacites of Grenada is by fractional crystallisation of basaltic magma. Contrary to the situation in some of the northern islands of the Lesser Antilles (e.g. Rea, 1970) basalt compositions are present in nearly all the volcanic centres of Grenada. In addition the most recent activity has been eruptions of alkali basalt compositions from Kick-em-Jenny volcano. Thus, there is evidence that basalt has been available throughout the evolution of the Grenada suite. Estimates of relative abundance of compositions are notoriously difficult to assess (Ridley, 1972) but there does appear to be a greater volume of basalt compositions in Grenada than in the other islands of the Lesser Antilles. In the older centres in the south of the island, basalt lava flows are widespread and basalt compositions probably constitute 40% of the total surface exposed volume.

In the Mt. Granby - Fedon's Camp centre, basalt flows although numerous and topographically conspicuous, probably form at most 25% of the surface exposure. In the Mt. St. Catherine and Northern



Domes centres basalt compositions are even more restricted in abundance. Basalt lava flows are only exposed in the deep valleys on the northern flanks of Mt. St. Catherine. In these two centres, basalt compositions probably only form 5 to 10% of the surface exposure with andesitic and dacitic compositions predominant. Despite the differences in surface exposure, geochemical similarities between the basalt-andesite-dacite associations of the various centres suggest that generally similar igneous processes have occurred during the formation of each centre. In view of the erupted compositions of the recent explosion craters and Kick-em-Jenny volcano, it is likely that these processes are continuing at the present time.

The major and trace element gradations, Rare Earth element and Sr-isotope similarities, and the mineralogical and petrographic relationships described in the preceeding Chapters all support the suggestion that fractional crystallisation of basalt magma is the most important process in the generation of the andesites and dacites. The cumulus plutonic blocks are direct evidence that this has occurred in some instances. However, in view of the nature of the variable partial melt model proposed in Chapter 7, and the complex variation in physical conditions that may influence magma differentiation trends, some scatter in the geochemical data is to be expected. In part these may reflect analytical uncertainties but also may represent genuine differences in magma compositions associated with unique evolutionary histories. Only by isolation of individual centres of activity has a more coherent relationship between the variety of basalt, andesite and dacite compositions emerged.

The restricted volume of erupted products on Grenada compared with some of the islands further north in the Lesser Antilles has already been mentioned (Chapter 6). To this extent, the problem concerning the volume of cumulate compositions required as the complementary fraction to the andesites and dacites as a result of fractional crystallisation of basalt magma is reduced. Only restricted surface sampling of emergent islands of the arc has been completed and a considerable submarine pile of unsampled compositions is present. The abundance of basic and ultrabasic compositions within this pile is undetermined but the high gravity anomaly over the arc (Andrew et al., 1970) suggests that they are present. The ejected cumulus blocks are direct evidence of the presence of this ultrabasic material and by the nature of their formation are unlikely to be exposed during the actual creation of the arc. In summary therefore, there is a considerable volume of evidence that suggests the calc-alkaline suite of Grenada is the result of fractional crystallisation of basalt magma, and an independent origin for the andesites and dacites seems unlikely.

#### 10:9 Discussion

Evidence has been presented in this and preceeding chapters for the evolution of the Grenada andesites and dacites by fractional crystallisation of picrite and alkali basalt magmas. The major and trace element geochemistry of the basalts suggests derivation by partial melting of a peridotite Upper Mantle source, but the variability in composition is attributed to differing degrees of partial melting of this source. It appears that this geochemical variability, although modified by fractionating mineral phases, is



inherited by the andesites and dacites. The crystallising phases likely to predominate during the early evolution of the basalt melts are olivine, clinopyroxene and spinel. Petrographic and geochemical evidence suggests that, in general, plagioclase and then amphibole are the next phases to appear. The  $P_{H_2O}$  of the magmas are predicted to be low relative to  $P_{tot}$  but higher than is generally the case in tholeiitic and alkaline suites. The early precipitation of magnetite, together with delayed fractionation of plagioclase feldspar, may explain the absence of any trend towards iron-enrichment of the magmas but increasing enrichment in silica and initially in alumina. The subsequent fractional crystallisation of plagioclase and amphibole from the melts is important in preventing a trend towards increasing alkalinity whilst accentuating the trend towards silica-enrichment in the melts.

The compositional variation of the Grenada suite is unusual in the island arc situation but is supporting evidence that the island arc calc-alkaline suite constitutes an additional magma series typical of Upper Mantle melting episodes (Brown and Schairer, 1971). In the final chapter of this study, the significance of the Grenada basalt-andesite-dacite association is discussed in relation to island-arc series elsewhere and its relevance to information concerning the nature of the Upper Mantle.

## CHAPTER 11

### MAGMA VARIATION IN ISLAND ARCS

The great volume of research completed in the Japanese island arcs has shown a polarity of magma compositions, consistently spatially related with increasing distance from the oceanic trench, in the series summarised by Kuno (1966):

tholeiitic basalt - high-alumina basalt - alkali basalt

Kuno (1950) identified two magma series in the Izu-Hakone region of Japan termed "pigeonitic" and "hypersthenic" respectively. These magma series were erupted from different volcanic centres at intervals in the period Miocene to Recent. Kuno regarded the pigeonitic series as representative of uncontaminated, Upper Mantle derived melts of tholeiitic affinities. The hypersthenic series (calc-alkaline s.s. of Kuno) was regarded as derived by sialic contamination of tholeiitic magma. In addition, Kuno (1968) after Aoki (1966) proposed that sialic contamination of alkali basalt magma could also result in a calc-alkaline (silica-enrichment as opposed to iron-enrichment) trend of differentiation. Alternative models were proposed by Kuno (1966) to account for the geochemical differences in the parental magmas:

- 1) Differing depths of magma generation
- 2) Similar depths of generation but subsequent fractional crystallisation at progressively shallower levels nearer to the volcanic front.

O'Hara (1968) and Gast (1968) have shown that alkali basalt magma is unlikely to be related to tholeiitic magma by fractional crystallisation processes, and the first model suggested by Kuno



seems to be a more probable explanation of the zoning of magma compositions in the Japanese arcs.

Variations in magma compositions have since been described in other island arcs but in some cases the significance of the near-contemporaneous eruption of contrasted magma series in the Izu-Hakone region has been misinterpreted. Jakes and Gill (1970) have suggested that the "island-arc tholeiite series" constitutes a distinct magma series associated with the near-trench, voluminous early eruptions of the island-arcs of the southwest Pacific. Jakes and Gill distinguish the island arc tholeiite series from the calc-alkaline series on the basis of major, trace and Rare Earth element differences. In addition they suggest that both temporal and spatial separation distinguishes the calc-alkaline series which is erupted later than and at a greater distance from the trench than the tholeiitic series. In contrast Kuno (1950) emphasises the spatial and temporal coincidence of the pigeonitic (tholeiitic) and hypersthenic (calc-alkaline) rock series in Japan.

An empirical relationship between the potash content of erupted lavas and depth to the Benioff Zone has been described by Dickinson and Hatherton (1967). This is essentially a re-statement of the observations of Kuno (1966) and Sigimura (1967) of the increasing alkalinity of lava types with increasing distance from the trench. Dickinson and Hatherton (1967) however, suggest that the different levels of potash content are imposed at the site of partial melting, specifically at the Benioff Zone. In order to account for this relationship it is necessary to

postulate that if the magmas are derived by partial melting of a subducted plate, then the distribution of potash between melt and solid must rise with increased pressure. This model for the zonation of island arc magmas can be criticised on the following grounds. In the subduction regime, the initial partial melt from the lithospheric plate whether it is derived from oceanic sediments, unaltered oceanic tholeiite, metamorphosed basalt compositions or a combination of any or all of these, will be enriched in the incompatible trace elements relative to their concentration in the original unmelted compositions. These incompatible trace elements will include in addition to K, Th, Ba and Rb. Fitton (1971) has suggested that the composition of these melts will be determined by the breakdown of amphibolite. The residual phases in the slab will be subjected to further heating and greater pressure during subduction deeper into the Upper Mantle. However, additional partial melt increments can only approach the bulk composition of the residual phases which Wyllie (1973) has shown to be of eclogite facies at depths greater than 100 km. In the dynamic situation, the incompatible elements will continue to be preferentially enriched into the near-trench, initial partial melts. Thus the zonation of these elements in island-arc magmas should be the reverse of that so far described.

Ninkovich and Hays (1972) have suggested that greater 'leaching' or wall-rock contamination occurs with increasing travel-path distance of the magmas en route to the surface. This would explain the zonation observed but relies on progressive release of  $H_2O$  from the subducted slab at depths up to 300 kms. Wyllie (1973) has shown



that hydrated compositions are unlikely to be present at such depths in subducted lithospheric plates, and that volatile release from the slab is probably only significant at depths less than 100 km.

Several recent studies have suggested that sediment contamination of the partial melts in a subduction regime is responsible for the anomalous abundances of the large cations such as K, Ba and Rb in island arc magmas in comparison with their probable abundances in oceanic tholeiite compositions (e.g. Jakes and Gill, 1970; Armstrong, 1971). In addition Armstrong (1971) has suggested that the similarities in lead isotope ratios between island arc volcanics and oceanic sediments indicates fusion of the sediments in the subduction zone. Opposition to the generation of andesites and dacites by fractional crystallisation of basalt magma has been based on volumetric and geochemical grounds (Jakes and Gill, 1970; Taylor, et al., 1969). The relative abundance of andesite or the local absence of basaltic compositions in island arcs is not a conclusive argument against the derivation of andesite from a more mafic parent. The original studies of Kuno (1950) and more recent studies of island arc calc-alkaline series (Brown and Schairer, 1971; Lewis, 1971) support the derivation of andesites and dacites by fractional crystallisation of basalt magma. The direct derivation of silica-saturated andesites and dacites as partial melts from subducted eclogite compositions (Fitton, 1971; Jakes and Gill, 1970) implies ascent through the overlying ultrabasic Upper Mantle as unchanged melts for distances in excess of 100 km. Complete segregation of the melts from the Upper Mantle compositions would have to occur in order for the calc-alkaline melts to be erupted unaltered.

There is considerable evidence now available that suggests the role of sediment contamination is minor if present at all. Firstly there is the experimental evidence of Wyllie (1973) that fusion of hydrated sediments would be complete at depth less than 100 km. As suggested in Chapter 10, spatial relationships of volcanicity and Benioff Zone suggest that this depth limit severely restricts the importance of hydrated sediments in island arc environments. With regard to lead isotope ratios, Oversby and Ewart (1972) has shown that mass balance considerations rule out any significant contribution of oceanic sediments to the ratios observed in the Tonga arc. The maximum amount of sediments allowed by the lead data would not have a significant petrogenetic effect. In addition the  $\text{Sr}^{87}/_{86}$  ratios reported in the present account do not support a sediment contamination model. High  $\text{Sr}^{87}/_{86}$  ratios are associated with lower abundances of incompatible trace elements which is the reverse of the contamination effects expected of sediment admixtures. Church and Tilton (1973) suggest that uniform  $\text{Sr}^{87}/_{86}$  ratios in the Cascade (U.S.A.) calc-alkaline lavas irrespective of Sr abundance argue against sediment contamination and the lead isotopes are also inconsistent with such a model.

The present study of the volcanic geology of Grenada has revealed several unusual features relevant to the problem of magma variation and zonation in island-arcs. The eruptions of silica-undersaturated alkali basalt compositions has occurred on the island at similar distances from the axis of negative gravity anomaly (defining the approximate locus of subduction, Fig. 5 , Chapter 2) as eruptions of silica-saturated high-alumina



tholeiitic basalt further north in the arc (Baker, 1968; Rea, 1970). In addition the higher level of alkalis and in particular potash in the Grenada suite is associated with a shallower depth to the Benioff Zone than is the case further north (Sigurdsson et al., 1973). This is unlike the spatial relationships discovered in other island arcs.

Variations in Sr isotope ratios and Rare Earth Element distribution has been demonstrated within individual volcanic centres of Grenada. In Table 37 published  $\text{Sr}^{87}/_{86}$  ratios from the other islands of the Lesser Antilles are listed. The inter-island variation in these ratios but similarity between basalt, andesite and dacite compositions of individual islands has previously been noted by Hedge and Lewis (1971). The Rare Earth Element distribution patterns in the Grenada calc-alkaline suite are unusual in the range of enrichment relative to chondrites displayed. Yajima et al (1972) have described a greater degree of light Rare Earth enrichment in the hypersthenic in comparison with the pigeonitic series of Izu-Hakone region. The variations in Sr isotope ratios and degree of Light Rare Earth enrichment occurs within a restricted geographical range on Grenada and are also repeated frequently in time. A model of variable partial melting has been outlined in this study to account for these variations and the range of major and trace element compositions observed. Variable partial melting has not previously been invoked to any great extent in island-arc studies in order to explain geochemical differences within a restricted geographic locality. However, the absence of conclusive evidence relating this variability to sediment contamination and

TABLE 37

Strontium isotope data for three volcanic centres  
in the Lesser Antilles island arc (from Hedge and  
Lewis, 1971).

Mt. Misery suite, St. Kitts

<u>SiO<sub>2</sub> wt.%</u>	<u>Rb/Sr</u>	<u>Sr<sup>87</sup>/86</u>
48.8	0.026	0.7036
50.3	0.028	0.7036
50.9	0.029	0.7037
53.3	0.040	0.7040
56.6	0.046	0.7037
58.6	0.053	0.7038
59.1	0.056	0.7040
59.7	0.065	0.7037
61.6	0.056	0.7039

Soufriere suite, St. Vincent

47.7	0.035	0.7040
51.3	0.049	0.7043
51.9	0.054	0.7042
52.3	0.061	0.7040
52.3	0.053	0.7040
53.6	0.071	0.7041
55.0	0.065	0.7039
55.4	0.075	0.7039

Carriacou suite

45.7	0.013	0.7052
46.7	0.027	0.7051
46.9	0.039	0.7053
56.9	0.055	0.7053
61.7	0.056	0.7054



subducted slab-derived melts suggests that the model may be applicable elsewhere. ✓

The silica-undersaturated nature of the alkaline and picritic compositions suggests that small volumes of partial melt are involved in the Grenada situation. O'Hara (1968) has stressed that considerable variation in major and trace element geochemistry can occur during the initial stages of partial melting ( $< 15\%$  total volume of partial melt), whereas with further equilibrium melting, variation is reduced relative to the differences in volume produced. The shallow ( $\sim 100$  km) nature of the proposed magma source beneath Grenada may be a factor promoting the eruption of small volumes of melt. However, the question remains as to why this does not occur in all island arcs under similar pressure and temperature conditions. The relationship of the Upper Mantle thermal regime and rate of subduction of the lithospheric plate may be an additional factor. The absence of currently observable movement along the southern boundary of the Caribbean Plate was mentioned in Chapter 2. It is possible that the rate of subduction of the Americas beneath the Caribbean Plate increases further north (Ball and Harrison, 1970) and that the volume of partial melts produced are substantially greater as a result of the greater-energy release. The comparatively minor volume of erupted volcanics in Grenada in comparison with islands such as Dominica suggests that fundamentally different proportions of melt are involved in the two areas

Allowing for differences in volumes of partial melt, it is also possible that lateral inhomogeneity in the Upper Mantle

source composition is present. Gast (1968) has proposed that the composition of oceanic tholeiite suggests considerable volumes of melt from the Upper Mantle have previously been extracted in the source regions. Schilling (1973a; 1973b) has discovered regular geochemical variation southwards along the Reykjanes ridge from Iceland and in the vicinity of the Afar triangle (Red Sea). Subbarao (1972) has recognised differences in K/Rb and  $\text{Sr}^{87}/_{86}$  ratios between ocean-ridge and abyssal-hill tholeiites in the Pacific and suggested that the differences arise through contrasted histories of magma extractions in the source regions. Thus a possible variable that has to be considered in relation to the geochemistry of the island-arc calc-alkaline associations is the previous melting histories of the source regions. Different Upper Mantle conditions are probably involved in the collision and spreading regimes of active vulcanicity.

Arculus and Curran (1972) proposed that a consequence of the plate tectonic model is the involvement of Upper Mantle zones of contrasted previous tectonic and volcanic history. The continental crust and linked rigid portion of underlying Upper Mantle are an immediate possible source of compositions contrasted in nature with the suboceanic crust and Upper Mantle. The highly alkaline nature of the erupted products of many continental rift volcanoes are very different in composition to the oceanic tholeiite produced at mid-ocean ridges. It is possible that some of the contrast in compositions is the result of melting of Upper Mantle source material that has suffered different degrees of previous magma extraction along the lines suggested by Gast (1968).



The encroachment of the Americas Plate on the Upper Mantle underlying continental South America at the southern end of the Lesser Antilles may be an example of the contrasted magma source regions possible in collision regimes. Gorshkov (1965) suggested that the transition from oceanic to continental crust in the Kurile-Kamchatka region is not marked by any strong differences in erupted calc-alkaline magma compositions that could be associated with anatexis of continental crustal material. Nevertheless Gorshkov noted the slightly increased alkalinity of the continental calc-alkaline associations. It is possible that this is an example of heterogeneity of source region.

The enrichment of the island arc tholeiitic and calc-alkaline series (Jakes and Gill, 1970) in the large cations such as K, Ba, Rb may be the result of partial melting of relatively undepleted Upper Mantle source regions in comparison with the source regions of oceanic tholeiite. Thus a comparison between island-arc and mid-ocean ridge basalts may provide a measure of the chemical composition of the underlying Upper Mantle. An additional factor suggested in this account in relation to local variation in island arc magma compositions is the possibility of variable partial melting of the Upper Mantle.

The role of the subducted plate has been minimised but is obviously essential as a physical trigger for the generation of island arc magmas. In some situations a chemical contribution from volatile and partially melted compositions is to be expected as well. The great abundance of andesitic and dacitic ignimbrites in continental calc-alkaline associations may reflect fundamentally

different conditions of magma generation. However the suggestion that the Upper Mantle is the main source region of the island-arc calc-alkaline suites receives strong support in this account of the alkali basalt-andesite association of Grenada, Lesser Antilles.



## REFERENCES

- Albarede, F. and Bottinga, Y., 1972. Kinetic disequilibrium in trace element partitioning between phenocrysts and host lava. *Geochim. et Cosmochim. Acta* 36, 141-156.
- Anderson, T., 1908. Report on the eruptions of the Soufriere in St. Vincent in 1902, and on a visit to Montagne Pelee in Martinique. *Phil. Trans. Roy. Soc. A* 208, 275-332.
- Anderson, T. and Flett, J.S., 1903. Report on the eruptions of the Soufriere in St. Vincent, in 1902, and on a visit to Montagne Pelee, in Martinique - Part 1. *Phil. Trans. R. Soc. Lond. A* 200, 353-553.
- Andrew, E.M., Masson-Smith, D. and Robson, G.R., 1970. Gravity anomalies in the Lesser Antilles. N.E.R.C. Inst. Geol. Sci. Geophysical Paper No.5.
- Aoki, K. and Oji, Y., 1966. Calc-alkaline volcanic rock series derived from alkali-olivine basalt magma. *J. Geophys. Res.* 71, 6127-6135.
- Arculus, R.J., 1973. Recent submarine pillow lavas in the Catania area, Eastern Sicily. *Phil. Trans. R. Soc. Lond. A* 274, 153-162.
- Arculus, R.J. and Curran, E.B., 1972. The Genesis of the Calc-Alkaline Rock Suite. *Earth Planet. Sci. Lett.* 15, 255-62.
- Armstrong, R.L., 1971. Isotopic and chemical constraints on models of magma genesis in volcanic ores. *Earth. Planet. Sci. Lett.* 12, 137-142.
- Atkins, F.B., 1969. Pyroxenes of the Bushveld Intrusion, South Africa. *J. Petrology* 10, 222-249.
- Baker, P.E., 1963. The geology of Mt. Misery Volcano, St. Kitts. Unpublished D.Phil. thesis, University of Oxford.
- Baker, P.E., 1968. Petrology of Mt. Misery Volcano, St. Kitts, West Indies. *Lithos* 1, 124-150.
- Ball, M.M. and Harrison, C.G.A., 1970. Crustal plates in the Central Atlantic. *Science*, 147, 1128-1129.
- Ball, M.M., Supko, P.R., Bock, W. and Maloney, N.J., 1970. Marine Geophysical Measurements on the southern boundary of the Caribbean Sea.
- Barberi, F., Bizouard, H. and Varet, J., 1971. Nature of the clinopyroxene and iron enrichment in alkali and transitional basaltic magmas. *Cont. Mineral. and Petrol.* 33, 93-107.
- Bell, P.M., Mao, H.K. and Virgo, D., 1972. Crystal Field Determinations of  $\text{Fe}^{3+}$ . *Yb. Carnegie Instn. Wash.* 71, 531-537.

- Bottinga, Y., Kudo, A. and Weill, D., 1966. Some observations on oscillatory zoning and crystallisation of magmatic plagioclase. *Am. Mineral.* 51, 792-806.
- Bowen, N.L., 1928. The evolution of the igneous rocks. Princeton University Press.
- Boyd, F.R., England, J.L. and Davis, B.T.C., 1964. Effects of pressure on the melting and polymorphism of enstatite,  $\text{MgSiO}_3$ . *J. Geophys. Res.* 69, 2101-2109.
- Brooks, C.K., 1968. On the interpretation of trends in element ratios in differentiated igneous rocks, with particular reference to strontium and calcium. *Chem. Geol.* 3, 15-20.
- Brown, G.M., 1968. Mineralogy of Basaltic Rocks. pp.103-162 in H.H. Hess, and A. Poldervaart, eds., *Basalts, The Poldervaart treatise on rocks of basaltic composition* 1, 482pp.
- Brown, G.M. and Schairer, J.F., 1971. Chemical and melting relations of some calc-alkaline volcanic rocks. *Geol. Soc. Am. Mem.* 130, 139-56.
- Brown, G.M., Emeleus, C.H., Holland, J.G. and Phillips, R., 1970. Petrographic, mineralogic and X-ray fluorescence analysis of lunar igneous-type rocks and spherules. *Science*, 167, 559-601.
- Buddington, A.F. and Lindsley, D.H., 1964. Iron-titanium oxide minerals and synthetic equivalents. *J. Petrology* 5, 310-357.
- Bultitude, R.J. and Green, D.H., 1968. Experimental study at high pressures on the origin of olivine nephelinite and olivine melilite nephelinite magmas. *Earth. Planet. Sci. Lett.* 3, 325-337.
- Cann, J.R., 1970. New model for the structure of the ocean crust. *Nature* 226, 928-930.
- Carmichael, I.S.E., 1967. Mineralogy of Thingmuli, a Tertiary volcano of Eastern Iceland. *Am. Mineral.* 52, 1815-41.
- Cawthorn, R.G., Curran, E.B. and Arculus, R.J., 1973. A petrogenetic model for the origin of the calc-alkaline suite of Grenada, Lesser Antilles. *J. Petrology* 14, 327-338.
- Chase, R.L. and Bunce, E.T., 1969. Underthrusting of the eastern margin of the Antilles by the floor of the western North Atlantic Ocean, and origin of the Barbados Ridge. *J. Geophys. Res.* 74, 1413-1420.
- Chayes, F., 1966. Alkaline and subalkaline basalts. *Am. J. Sci.* 264, 128.
- Christman, R., 1953. Geology of St. Bartholomew, St. Martin and Anguilla, Lesser Antilles. *Geol. Soc. Am. Bull.* 64, 65-96.



- Church, S.E. and Tilton, G.R., 1973. Lead and strontium isotopic studies in the Cascade Mountains: Bearing on andesite genesis. *Bull. Geol. Soc. Am.* 84, 431-454.
- Clark, S.P. and Ringwood, A.E., 1964. Density distribution and constitution of the mantle. *Rev. Geophys.* 2, 35-83.
- Cohen, L.H., Ito, K. and Kennedy, G.C., 1967. Melting and phase relations in an anhydrous basalt to 40 kb. *Am. J. Sci.* 265, 475-518.
- Coombs, D.S., 1963. Trends and affinities of basaltic magmas and pyroxenes as illustrated on the diopside-olivine-silica diagram. *Mineral. Soc. Am. Pap.* 1, 227.
- Crowe, B.M. and Fisher, R.V., 1973. Sedimentary structures in base-surge deposits with special reference to cross-bedding Ubehebe Craters, Death Valley, California. *Geol. Soc. Am. Bull.* 84, 663-682.
- Daviess, S.N., 1971. Barbados: A major submarine gravity slide. *Geol. Soc. Am. Bull.* 82, 2593-2602.
- Dickinson, W.R. and Hatherton, T., 1967. Andesitic volcanism and seismicity around the Pacific. *Science* 157, 801-803.
- Deer, W.A., Howie, R.A. and Zussman, J., 1966. An introduction to the rock forming minerals. Longmans, London, 528pp.
- Dorman, J., Ewing, M., and Oliver, J., 1968. Study of shear velocity distribution in the upper mantle by Rayleigh waves. *Seismol. Soc. Am. Bull.* 50, 87-115.
- Earle, K.W., 1924. Geological survey of Grenada and the (Grenada) Grenadines. St. George (sic), Grenada: Government Printing Office, 9pp.
- Edgar, N.T., Ewing, J.I. and Hennion, J., 1971. Seismic refraction and reflection in the Caribbean Sea. *Bull. Am. Assn. Petr. Geol.* 55, 833-870.
- Eggler, D.H., 1972. Amphibole stability in H<sub>2</sub>O-undersaturated calc-alkaline melts. *Earth Planet. Sci. Lett.* 15, 28-34.
- Eggler, D.H., 1972. Water-saturated and under-saturated melting relations in a Paracutin andesite and an estimate of water content in the natural magma. *Cont. Mineral. and Petrol.* 34, 261-271.
- Elsasser, W.M., 1971. Sea-floor spreading as thermal convection. *J. Geophys. Res.* 76, 1101-1112.
- Engel, A.E.J. and Engel, C.G., 1964. Composition of basalts from the Mid-Atlantic Ridge. *Science* 144, 1330-1333.

- Engel, A.E.J., Engel, G.G. and Havens, R.G., 1965. Chemical characteristics of oceanic basalts and the upper mantle. *Geol. Soc. Am. Bull.* 76, 719-734.
- Fenner, C.N., 1926. The Katmai magmatic province. *J. Geol.* 34, 673-772.
- Finger, L.W., 1971. The Uncertainty in the calculated ferric iron content of a microprobe analysis. *Yb. Carnegie Instn. Wash.* 71, 601-603.
- Fink, L.K. Jr., 1968. Geology of the Guadeloupe region, Lesser Antilles island arc. Unpublished D. Phil. Thesis, University of Miami.
- Fink, L.K. Jr., 1972. Bathymetric and geologic studies of the Guadeloupe region, Lesser Antilles island arc. *Marine Geology* 12, 267-288.
- Fisher, R.L., 1961. Middle America trench: topography and structure. *Geol. Soc. Am. Bull.* 72, 703-720.
- Fitton, J.G., 1971. The generation of magmas in island arcs. *Earth Planet. Sci. Lett.* 11, 63-67.
- Flanagan, F.J., 1969. U.S. Geological Survey standards - II. First compilation of data for the new U.S.G.S. rocks. *Geochim. et Cosmochim. Acta* 33, 81-120.
- Flanagan, F.J., 1973. 1972 values for international geochemical reference samples. *Geochim. et Cosmochim. Acta* 37, 1189-1200.
- Fodor, R.V., 1971. Fe content in pyroxenes from a calc-alkaline volcanic suite New Mexico U.S.A. *Earth Planet. Sci. Lett.* 11, 385-390.
- Fox, P.J., Schreiber, E. and Heezen, B.C., 1971. The geology of the Caribbean crust: Tertiary sediments, granitic and basic rocks from the Aves Ridge. *Tectonophysics* 12, 89-109.
- Freeland, G.L. and Dietz, R.S., 1971. Plate Tectonic evolution of Caribbean - Gulf of Mexico region. *Nature Phys. Sci.* 232, 20-23.
- Gast, P.W., 1968. Trace element fractionation and the origin of tholeiitic and alkaline magma types. *Geochim. et Cosmochim. Acta* 32, 1057-1086.
- Gibb, F.G.F., 1973. The zoned clinopyroxenes of the Shiant Isles Sill, Scotland. *J. Petrology* 14, 203-30.
- Gill, R.C.O., 1972. The geochemistry of the Grønnefjeld-Ika alkaline complex, South Greenland. Unpublished Ph.D. thesis, University of Durham.
- Gorshkov, G.S., 1970. Volcanism and the upper mantle. Plenum Press, New York-London, 385pp.



- Green, D.H., 1969. The origin of basaltic and nephelinitic magmas in the earth's mantle. *Tectonophysics* 7, 409-22.
- Green, D.H., 1970. The origin of basaltic and nephelinitic magmas. *Trans. Leics, Lit. and Phil. Soc.* 64, 28-54.
- Green, D.H. and Ringwood, A.E., 1963. Mineral assemblages in a model mantle composition. *J. Geophys. Res.* 68, 937-945.
- Green, D.H. and Ringwood, A.E., 1967. The genesis of basaltic magmas. *Cont. Mineral. and Petrol.* 15, 103-190.
- Green, H.W. II, 1972. A CO<sub>2</sub> charged asthenosphere. *Nature Phys. Sci.* 238, 2-5.
- Green, T.H. and Ringwood, A.E., 1968. Crystallizations of basalt and andesite under high pressure hydrous conditions. *Earth Planet. Sci. Lett.* 3, 481-489.
- Hamilton, D.L. and Anderson, G.M., 1967. Effects of water and oxygen pressures on the crystallization of basaltic magmas. pp.445-82, in H.H. Hess, and A. Poldervaart, eds., *Basalt, The Poldervaart treatise on rocks of basaltic composition* 1, 482pp.
- Hargraves, R.B., Hollister, L.S. and Otalora, G., 1970. Compositional zoning and its significance in pyroxenes from three coarse grained lunar samples. *Science* 167, 631-633.
- Harloff, C., 1927. Zonal structures in plagioclases. *Leid. Geol. Meded.* 2, 99-114.
- Harris, P.G., Reay, A., White, I.G., 1967. Chemical composition of the upper mantle. *J. Geophys. Res.* 72, 6359-6369.
- Harrison, J.B., 1896. The rocks and soils of Grenada and Carriacou. Waterlow Sons London, 59pp.
- Hart, S.R., 1971. K, Rb, Cs, Sr and Ba contents and Sr isotope ratios of ocean floor basalts. *Phil. Trans R. Soc. Lond. A.* 268, 573-588.
- Hart, R.A., 1973. Geochemical and geophysical implications of the reaction between seawater and the oceanic crust. *Nature* 243, 76-78.
- Heald, E.F., Naughton, J. and Barnes, I.L., 1963. The chemistry of volcanic gases, use of equilibrium calculations in the interpretation of volcanic gas samples. *J. geophys. Res.* 68, 545-57.
- Hedge, C.E. and Lewis, J.F., 1971. Isotopic composition of strontium in three basalt-andesite centres along the Lesser Antilles arc. *Cont. Mineral. and Petrol.* 32, 39-47.

- Helz, R.T., 1973. Phase relations of basalts in their melting range at  $P_{H_2O} = 5$  kb as a function of oxygen fugacity. *J. Petrology* 14, 249-302.
- Hill, R.E.T. and Boettcher, A.L., 1970. Water in the earth's mantle: melting curves of basalt-water and basalt-water-carbon dioxide. *Science* 167, 980.
- Holland, J.G. and Brindle, D.W., 1966. A self-consistent mass absorption correction for silicate analysis by X-ray Fluorescence. *Spectrochim. Acta* 22, 2083.
- Hollister, L.S., 1970. Origin, mechanism and consequences of compositional sector zoning in staurolite. *Amer. Mineral.* 55, 742-66.
- Holloway, J.R., 1973. The system pargasite- $H_2O$ - $CO_2$ : a model for melting of a hydrous mineral with a mixed-volatile fluid - I. Experimental results to 8 kbar. *Geochim. et Cosmochim. Acta* 37, 651-666.
- Holloway, J.R. and Burnham, C.W., 1972. Melting relations of basalt with equilibrium water pressure less than total pressure. *J. Petrology* 13, 1-29.
- Holloway, J.R., Burnham, C.W. and Millhollen, G., 1968. Generation of  $H_2O$ - $CO_2$  mixtures for use in hydrothermal experimentation. *J. Geophys. Res.* 73, 6598-6600.
- Holmes, A., 1920. The nomenclature of petrology. Murby, London. 284pp.
- Huckenholz, H.G., Schairer, J.F. and Yoder, H.S.Jr., 1969. Synthesis and stability of ferridiopside. *Mineral. Soc. Amer. spec. Pap.* 2, 163-177.
- Irvine, T.N. and Baragar, W.R.A., 1971. A guide to the chemical classification of the common volcanic rocks. *Can. Jour. Earth Sci.* 8, 523-48.
- Isacks, B., Oliver, J. and Sykes, L.R., 1968. Seismology and the new global tectonics. *J. Geophys. Res.* 73, 5855-5900.
- Ito, K. and Kennedy, G.C., 1967. Melting and phase relations in a natural peridotite to 40 kilobars. *Am. J. Sci.* 265, 519-539.
- Jakes, P. and Gill, J.B., 1970. Structure of the Melanesian arcs and correlation with distribution of magma types. *Tectonophysics* 8, 223-236.
- Kennedy, W.Q., 1933. Trends of differentiation in basaltic magmas. *Amer. J. Sci. Ser. 5* 25, 239-256.
- Kuno, H., 1950. Petrology of Hakone volcano and the adjacent areas, Japan. *Geol. Soc. Amer. Bull.* 61, 957-1020.



- Kuno, H., 1966. Lateral variation of basalt magma across continental margins and island arcs. *Bull. Volcanol.* 29, 195-222.
- Kuno, H., 1968. Differentiation of Basalt Magmas. pp.623-688 in H.H. Hess, and A. Poldervaart, eds., *Basalts, the Poldervaart treatise on rocks of basaltic composition* 2, 862.
- Kushiro, I., 1962. Clinopyroxene solid solutions, Part I, the  $\text{CaAl}_2\text{SiO}_6$  component. *Japan J. Geol. Geogr.* 33, 213-20.
- Kushiro, I., 1969. Discussion of paper "The origin of basaltic and nephelinitic magmas in the earth's mantle". *Tectonophysics*, 7, 1685-1692.
- Kushiro, I., 1972a. Partial melting of synthetic and natural peridotites at high pressures. *Yb. Carnegie Instn. Wash.* 71, 357-361.
- Kushiro, I., 1972b. Effect of water on the composition of magmas formed at high pressures. *J. Petrol.* 13, 311-334.
- Kushiro, I., Syono, Y. and Akimoto, S., 1968. Melting of a peridotite nodule at high pressures and high water pressure. *J. Geophys. Res.* 73, 6023.
- Lambert, I.B. and Wyllie, P.J. 1970. Low-velocity zone of the earth/mantle: incipient melting caused by water. *Science* 169, 764-766.
- Le Bas, M.J., 1962. The role of aluminium in igneous clinopyroxenes with relation to their parentage. *Am. Jour. Sci.* 260, 267-288.
- Leeman, W.P. and Manton, W.I., 1971. Strontium isotopic composition of basaltic lavas from the Snake River Plain, southern Idaho. *Earth Planet. Sci. Lett.* 11, 420-434.
- Leeman, W.P. and Rogers, J.J.W., 1970. Late Cenozoic alkali-olivine basalts of the Basin-Range Province, U.S.A. *Cont. Mineral. and Petrol.* 25, 1-24.
- Lewis, J.F., 1964. Mineralogical and petrological studies of plutonic blocks from the Soufriere Volcano, St. Vincent, B.W.I. Unpublished D.Phil. thesis, University of Oxford. 270pp.
- Lewis, J.F., 1971. Composition, origin and differentiation of basalt magma in the Lesser Antilles. *Geol. Soc. Am. Mem.* 130, 159-179.
- Lewis, J.F., 1973. Petrology of the ejected plutonic blocks of the Soufriere Volcano, St. Vincent, West Indies. *J. Petrology.* 14, 81-112.
- Lowder, G.G., 1970. The volcanics and caldera of Talasea, New Britain. *Mineralogy. Cont. Mineral. and Petrol.* 26, 324-340.

- MacDonald, G.A., 1972. *Volcanoes*. Prentice-Hall, Inc. New Jersey. 510pp.
- MacDonald, G.A., 1968. Composition and origin of Hawaiian lavas. *Geol. Soc. Amer. Mem.* 116, 477-522.
- MacIntyre, I.G., 1972. Submerged reefs of Eastern Caribbean. *Bull. Am. Ass. Pet. Geol.* 56, 720-758.
- Malfait, B.T., and Dinkelmann, M.G., 1972. Circum-Caribbean tectonic and igneous activity and the evolution of the Caribbean Plate. *Geol. Soc. Amer. Bull.* 83, 251-272.
- Martin-Kaye, P.H.A., 1969. A summary of the geology of the Lesser Antilles. *Overseas Geol. and Min. Res.* 10, 172-206.
- Masuda, A., Nakamura, N. and Tenaka, T., 1973. Fine structures of mutually normalised rare earth patterns of chondrites. *Geochim. et Cosmochim. Acta.* 37, 239-248.
- Merrill, R.B. and Wyllie, P.J., 1973. Absorption of iron by platinum capsules in high pressure rock melting experiments. *Am. Mineral.* 58, 16-20.
- Meyerhoff, P.A. and Meyerhoff, H.A., 1972. Continental drift IV: The Caribbean "Plate". *J. Geol.* 80, 34-60.
- Middlemost, E.A.K., 1973. A simple classification of volcanic rocks. *Bull. Volcanol.* 30, 382.
- Molnar, P. and Sykes, L.R., 1969. Tectonics of the Caribbean and Middle America regions from focal mechanisms and seismicity. *Geol. Soc. Amer. Bull.* 80, 1639-1684.
- Moore, J.G., 1967. Base-surge in recent volcanic eruptions. *Bull. volcanol.* 30, 337-63.
- Nicholls, J., Carmichael, I.S.E. and Stormer, J.C.Jr., 1971. Silica activity and  $P_{\text{total}}$  in igneous rocks. *Contr. Mineral. and Petrol.* 33, 1-20.
- Ninkovitch, D. and Hays, J.D. 1972. Mediterranean island arcs and origin of high potash volcanoes. *Earth. Planet. Sci. Lett.* 16, 331-345.
- Nockolds, S.R., 1954. Average chemical compositions of some igneous rocks. *Geol. Soc. Amer. Bull.*, 65, 1007-1032.
- Nolan, J. and Edgar, A.D., 1963. An X-ray investigation of synthetic pyroxenes in the system acmite-diopside-water at 1000 kg/cm<sup>2</sup> water vapour-pressure. *Min. Mag.* 37, 216-229.
- O'Hara, M.J., 1965. Primary magmas and the origin of basalts. *Scot. J. Geol.* 1, 19-40.



- O'Hara, M.J., 1967. Mineral paragenesis in ultrabasic rocks. pp 393-403 in P.J. Wyllie, ed., *Ultramafic and Related Rocks*. Wiley, New York. 464pp.
- O'Hara, M.J., 1968. The bearing of phase equilibria studies in synthetic and natural systems on the origin and evolution of basic and ultrabasic rocks. *Earth Sci. Reviews*. 4, 69-133.
- O'Hara, M.J. 1970. Upper mantle composition inferred from laboratory experiments and observation of volcanic products. *Phys. Earth Planet. Interiors* 3, 236-245.
- Ollier, C.D., 1967. Maars. Their characteristics, varieties and definition. *Bull. volcanol.* 31, 45-73.
- O'Nions, R.K., Pankhurst, R.J. and Arculus, R.J., in MS., Rare Earth elements and strontium isotope ratios of the calc-alkaline rock suite of Grenada.
- Onuma, N., Higuchi, H., Wakita, H. and Nagasawa, H., 1968. Trace element partition between two pyroxenes and the host lava, *Earth Planet Sci. Lett.*, 5, 47-51.
- Osborn, E.F., 1959. Role of oxygen pressure in the crystallization and differentiation of basaltic magma. *Am. J. Sci.* 257, 609-647.
- Osborn, E.F., 1969. The complementarity of orogenic andesite and alpine peridotite. *Geochim. et Cosmochim. Acta* 33, 307-324.
- Oversby, V.M. and Ewart, A., 1972. Lead isotopic compositions of Tonga-Kermadec volcanics and their petrogenetic significance. *Contr. Mineral. and Petrol.* 37, 181-210.
- Peacock, M.A., 1931. Classification of igneous rocks. *J. Geol.* 39, 54-67.
- Peterman, Z.E., Carmichael, I.S.E. and Smith, A.L., 1970.  $\text{Sr}^{87}/^{86}$  ratios of Quaternary lavas of the Cascade Range, northern California. *Geol. Soc. Am. Bull.* 81, 311-318.
- Phillips, R., 1966. Amphibole compositional space. *Min. Mag.* 35, 945-952.
- Philpotts, J.A. and Schnetzler, C.C., 1970. Phenocryst-matrix partition coefficients for K, Rb, Sr and Ba with applications to anorthosite and basalt genesis. *Geochim. et Cosmochim. Acta* 34, 307-22.
- Press, F., 1968. Earth models obtained by Monte Carlo inversion. *J. Geophys. Res.* 73, 5223-5234.
- Purgett, L., 1971. The birth of the Caribbean. *Science News* 99, 169-170.
- Rea, W.J., 1970. The geology of Montserrat, British West Indies. Unpublished D.Phil thesis. University of Oxford.

- Reeves, M.J., 1971. Geochemistry and mineralogy of British Carboniferous seatearths from northern coalfields. Unpublished Ph.D. thesis, University of Durham.
- Ridley, W.I., 1972. The field relations of the Canadas Volcanoes, Tenerife, Canary Islands. *Bull. Volcanol.* 35, 318-334.
- Ringwood, A.E., 1966. The mineralogy of the Mantle in: P.M. Hurley (Editor) *Advances in Earth Sciences*. M.I.T. Press, Boston, Mass., p.357-417.
- Ringwood, A.E., 1972. Phase transformations and mantle dynamics. *Earth Planet. Sci. Lett.* 14, 233-241.
- Robinson, E. and Jung, P., 1972. Stratigraphy and age of marine rocks, Cariacou, West Indies. *Bull. Am. Assn. Petr. Geol.* 56, 114-127.
- Robson, G.R. and Tomblin, J.F., 1966. Catalogue of the active volcanoes of the world including Solfarata fields. *Peut XX*. West Indies. International Association of Volcanology, Rome, Italy.
- Roedder, E., 1965. Liquid CO<sub>2</sub> inclusions in olivine-bearing nodules and phenocrysts from Basalts. *Am. Mineralogist.* 50, 1746-1782.
- Roeder, P.L. and Emslie, R.F., 1970. Olivine-liquid fractionation. *Contr. Mineral. and Petrol.* 29, 275-289.
- Roeder, P.L. and Osborn, E.F., 1966. Experimental data for the system MgO-FeO-Fe<sub>2</sub>O<sub>3</sub>-CaAl<sub>2</sub>Si<sub>2</sub>O<sub>8</sub>-SiO<sub>2</sub> and their petrologic implications. *Am. J. Sci.* 264, 428-480.
- Ross, M., Papike, J.J. and Shaw, K.W., 1969. Exsolution textures in amphiboles as indicators of subsolidus thermal histories. *Spec. Paper. Miner. Soc. Am.* 2, 275-299.
- Ross, M., Bence, A.E., Dwornik, E.J., Clark, J.R. and Papike, J.J. 1970. Lunar clinopyroxenes: chemical composition, structural state, and texture. *Science*, 167, 628-630.
- Sapper, K., 1903. Ein Besuch der insel Grenada. *Zentbl. Miner. Geol. Palaeont.*, 182-6.
- Schilling, J.G., 1973a. Afar mantle-plume: Rare Earth evidence. *Nature, Phys. Sci.*, 242, 2-5.
- Schilling, J.G., 1973b. Iceland mantle-plume. Geochemical study of Reykjanes Ridge. *Nature Phys. Sci.* 242, 565-571.
- Schnetzer, C.C. and Philpotts, J.A., 1970. Phenocryst-matrix partition coefficients for K, Rb, Sr and Ba with applications to anorthosite and basalt genesis. *Geochim. et Cosmochim. Acta* 34, 307-22.



- Scott, P.W., 1970. Ferromagnesian minerals from the volcanic suite of Tenerife. Unpublished D.Phil. thesis. University of London.
- Sigurdsson, H., Tomblin, J.F., Brown, G.M., Holland, J.G. and Arculus, R.J., 1973. Strongly undersaturated magmas in the Lesser Antilles island arc. *Earth Planet. Sci. Lett.* 18, 285-295.
- Subbarao, K.V., 1972. The strontium isotopic composition of basalts from the East Pacific and Chile Rises and abyssal hills in the Eastern Pacific Ocean. *Contr. Mineral. and Petrol.* 37, 111-120.
- Sugimura, A., 1967. Chemistry of volcanic rocks and seismicity of the earth's mantle in the island arcs. *Bull. Volcanol.* 30, 319-332.
- Sweatman, T.R. and Long, J.V.P., 1969. Quantitative electron probe microanalysis of rock-forming minerals. *J. Petrology.* 10, 332-379.
- Sykes, L.R., 1972. Seismicity as a guide to global tectonics and earthquake prediction. *Tectonophysics* 13, 393-414.
- Taylor, S.R. and White, A.J.R., 1965. Geochemistry of andesites and the growth of continents. *Nature* 208, 271-273.
- Taylor, S.R., Kaye, M., White, A.J.R., Duncan, A.R. and Ewart, E., 1969. Genetic significance of Co, Ni, Sc, and V content of andesites. *Geochim. et Cosmochim. Acta* 33, 1555-1557.
- Thompson, R.N., 1972a. Oscillatory and sector zoning in augite from a Vesuvian lava. *Yb. Carnegie Instn. Wash.* 71, 463-470.
- Thompson, R.N., 1972b. The atmosphere melting patterns of some basaltic volcanic series. *Am. J. Sci.* 272, 901-932.
- Tilley, C.E., 1950. Some aspects of magmatic evolution. *Quart. Jour. Geol. Soc. London* 106, 37-62.
- Toksoz, M.N., Minear, J.W. and Julian, B.R., 1971. Temperature field and geophysical affects of a down-going slab. *J. Geophys. Res.* 76, 1113-38.
- Tomblin, J.F., 1964. The volcanic history and petrology of the Soufriere region, St. Lucia. Unpublished D.Phil. thesis University of Oxford.
- Tomblin, J.F., 1971. Seismicity and plate tectonics of the eastern Caribbean Caribb. *Geol. Conf.*, 6th, Margarita, Venezuela, 1971, 11pp.
- Tuttle, C.F. and Bowen, N.L., 1958. Origin of granite in the light of experimental studies in the system  $\text{NaAlSi}_3\text{O}_8$ - $\text{KAlSi}_3\text{O}_8$ - $\text{SiO}_2$ - $\text{H}_2\text{O}$ . *Geol. Soc. Am. Mem.* 74, 153pp.

- Vogt, P.R., Avery, O.E., Schneider, E.D., Anderson, C.N. and Bracey, D.R., 1969. Discontinuities in sea-floor spreading, *Tectonophysics* 8, 285-317.
- Wager, L.R. and Brown, G.M., 1968. Layered igneous rocks. Oliver and Boyd, Edinburgh. 588pp.
- Wager, L.R. and Deer, W.A., 1939. Geological investigations in East Greenland: Part III, The Petrology of the Skaergaard intrusion, Kanderdlugssuaq, East Greenland. *Meddl. om Grønland* 105, 1-352.
- Wass, S.Y., 1973. The origin and petrogenetic significance of hour-glass zoning in titaniferous clinopyroxenes. *Mineral. Mag.* 39, 133-134.
- Wilkinson, J.F.G., 1971. The petrology of some vitrophyric calc-alkaline volcanics from the Carboniferous of New South Wales. *J. Petrology* 587-620.
- Wyllie, P.J., 1967. ed. Ultramafic and Related Rocks. Wiley, New York. 464pp.
- Wyllie, P.J., 1973. Experimental petrology and global tectonics - a preview. *Tectonophysics* 17, 189-209.
- Yagi, K. and Onuma, K., 1967. The join  $\text{CaMgSi}_2\text{O}_6$ - $\text{CaTiAl}_2\text{O}_6$  and its bearing on the titanaugites. *J. Fac.Sci.Hokkaido Univ.* Ser. 4, 13, 463-483.
- Yajima, T., Higuchi, H. and Nagasawa, H., 1972. Variation of Rare Earth concentrations in pigeonitic and hypersthene rock series from Izu-Hakone region, Japan. *Contr. Mineral. and Petrol.* 35, 235-244.
- Yoder, H.S. Jr., 1969. Calc-alkaline andesites, experimental data bearing on the origin of their assumed characteristics. *Org. Rep. Geol. Mineral. Ind. Bull.* 65, 77-89.
- Yoder, H.S. Jr., 1962. Origin of basalt magmas: an experimental study of natural and synthetic rock systems. *J. Petrology* 3, 342-532.

